frontiers | Research Topics

Proanthocyanidins and Isoflavonoids

Edited by
Deyu Xie and Li Tian

Published in
Frontiers in Plant Science

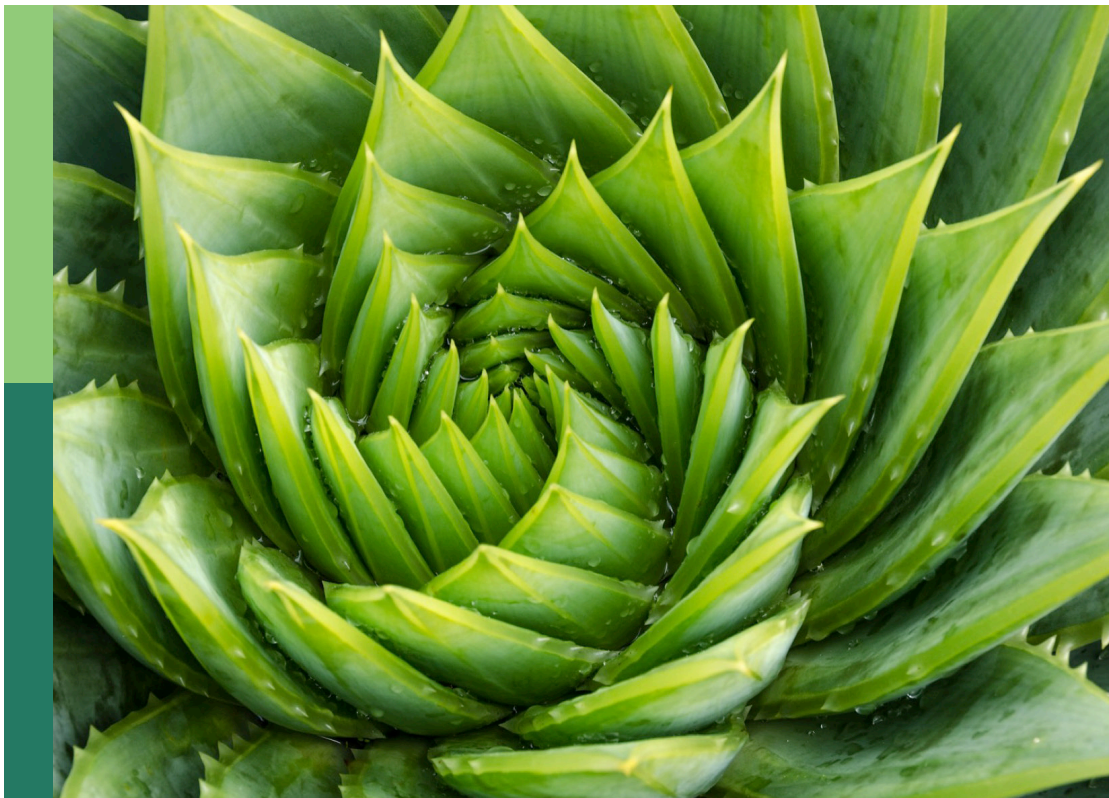

ISSN 1664-8714
ISBN 978-2-8325-5555-2
DOI 10.3389/978-2-8325-5555-2

About Frontiers

Frontiers is more than just an open access publisher of scholarly articles: it is a pioneering approach to the world of academia, radically improving the way scholarly research is managed. The grand vision of Frontiers is a world where all people have an equal opportunity to seek, share and generate knowledge. Frontiers provides immediate and permanent online open access to all its publications, but this alone is not enough to realize our grand goals.

Frontiers journal series

The Frontiers journal series is a multi-tier and interdisciplinary set of open-access, online journals, promising a paradigm shift from the current review, selection and dissemination processes in academic publishing. All Frontiers journals are driven by researchers for researchers; therefore, they constitute a service to the scholarly community. At the same time, the *Frontiers journal series* operates on a revolutionary invention, the tiered publishing system, initially addressing specific communities of scholars, and gradually climbing up to broader public understanding, thus serving the interests of the lay society, too.

Dedication to quality

Each Frontiers article is a landmark of the highest quality, thanks to genuinely collaborative interactions between authors and review editors, who include some of the world's best academicians. Research must be certified by peers before entering a stream of knowledge that may eventually reach the public - and shape society; therefore, Frontiers only applies the most rigorous and unbiased reviews. Frontiers revolutionizes research publishing by freely delivering the most outstanding research, evaluated with no bias from both the academic and social point of view. By applying the most advanced information technologies, Frontiers is catapulting scholarly publishing into a new generation.

What are Frontiers Research Topics?

Frontiers Research Topics are very popular trademarks of the *Frontiers journals series*: they are collections of at least ten articles, all centered on a particular subject. With their unique mix of varied contributions from Original Research to Review Articles, Frontiers Research Topics unify the most influential researchers, the latest key findings and historical advances in a hot research area.

Find out more on how to host your own Frontiers Research Topic or contribute to one as an author by contacting the Frontiers editorial office: frontiersin.org/about/contact

Proanthocyanidins and isoflavonoids

Topic editors

Deyu Xie — North Carolina State University, United States

Li Tian — University of California, Davis, United States

Citation

Xie, D., Tian, L., eds. (2024). *Proanthocyanidins and isoflavonoids*. Lausanne: Frontiers Media SA. doi: 10.3389/978-2-8325-5555-2

Table of contents

frontiers | Frontiers in Plant Science

TYPE Editorial
PUBLISHED 02 October 2024
DOI 10.3389/fpls.2024.1498989

OPEN ACCESS

EDITED AND REVIEWED BY
Laigeng Li,
Chinese Academy of Sciences (CAS), China

*CORRESPONDENCE
Deyu Xie
dxie@ncsu.edu

RECEIVED 19 September 2024
ACCEPTED 25 September 2024
PUBLISHED 02 October 2024

CITATION
Tian L and Xie D (2024) Editorial: Proanthocyanidins and isoflavonoids. *Front. Plant Sci.* 15:1498989. doi: 10.3389/fpls.2024.1498989

Editorial: Proanthocyanidins and isoflavonoids

Li Tian[1] and Deyu Xie[2]*

[1]Department of Plant Sciences, University of California, Davis, Davis, CA, United States, [2]Department of Plant and Microbial Biology, North Carolina State University, Raleigh, NC, United States

KEYWORDS

proanthocyanidin, condensed tannin, isoflavonoid, flavonoid, anthocyanin

Editorial on the Research Topic
Proanthocyanidins and isoflavonoids

Proanthocyanidins (PAs), also known as condensed tannins (CTs), are polyphenolic compounds produced in a wide range of plants. They are recognized for their antioxidant properties, functions in plant defense, and contributions to the astringency and nutritional quality of foods. Isoflavonoids, a subclass of flavonoids primarily found in legumes, play important roles in plant defense and symbiotic interactions with nitrogen-fixing bacteria. Recent advances have greatly enhanced our understanding of the biosynthesis of PAs and isoflavonoids. For example, studies have uncovered new roles for anthocyanidin reductase (ANR), leucoanthocyanidin reductase (LAR), and anthocyanidin synthase (ANS) in PA formation, as well as novel mechanisms governing PA polymerization and regulation. Similarly, progress in understanding enzyme structures and regulatory pathways has shed light on previously unknown aspects of isoflavonoid biosynthesis.

In collaboration with the Phytochemical Society of North America (PSNA), mentees and colleagues of Professor Richard A. Dixon have compiled this Research Topic to honor his retirement and celebrate his exceptional contributions to the study of PAs and isoflavonoids. The Research Topic includes five original research articles, two mini-reviews, and four reviews, which are organized around the following themes.

Biosynthesis, transport, and regulation of isoflavonoids

In their comprehensive review, Wang et al. highlighted major developments in understanding key enzymes, transporters, and regulatory mechanisms involved in isoflavonoid biosynthesis. They discussed strategies, technologies, and resources for enhancing isoflavonoid levels in leguminous and non-leguminous plants through metabolic engineering. Modifications such as glycosylation and methylation of core structures are important for producing unique isoflavonoids with health-promoting activities in the traditional Chinese medicinal plant *Pueraria lobata*. Li and Zhang's

review summarized recent research on these modifications and the relevant biosynthetic enzymes in *P. lobata*. In a related review, Yang and Wang focused on recent progress in isoflavonoid biosynthesis, regulation, transport, and functions in soybeans. They also suggested exploring new factors in isoflavonoid metabolism and plant-microbe interactions.

Isoflavonoids are synthesized from phenylalanine via the phenylpropanoid and downstream pathways. Clayton et al. built on earlier research on soybean AROGENATE DEHYDRATASE (*Gm*ADT) isozymes—which catalyze the final step of phenylalanine biosynthesis through the arogenate pathway—and identified additional *Gm*ADT isoforms. Their analyses of gene structure, phylogeny, expression patterns, subcellular localization, and protein interactions of these putative *Gm*ADTs suggested a role in the isoflavonoid metabolon. Interestingly, some *Gm*ADTs exhibited PREPHENATE DEHYDRATASES (PDT) activity in the prephenate pathway for phenylalanine biosynthesis in a yeast complementation assay. Future studies could explore how different *Gm*ADTs contribute to flavonoid and isoflavonoid metabolons and the extent to which tissue-specific expression determines these functions.

Flavonoids in citrus fruits and anthocyanins in mung beans

Rootstock grafting and fruit thinning are commonly adopted practices for varietal improvement in citrus, such as for increasing functional compounds including flavonoids, phenolic acids, and terpenes. Li S. et al. used high performance liquid chromatography (HPLC) to investigate the impact of different rootstocks on functional compounds, antioxidant capacity, and fruit quality at six developmental stages of 'Orah' fruit. They found that certain rootstocks significantly enhance sensory quality, functional constituents, and antioxidant properties of the fruit. They also identified key developmental stages for fruit pruning, when young fruits are abundant in functional compounds suitable for extraction. This study provided useful insights for improving orchard management practices in citrus. In parallel, Li C. et al. focused their study on mung bean, a dual-use crop valued for food and medicinal uses. Through comparative transcriptome and metabolite analysis, they identified transcripts with significantly higher accumulation in an anthocyanin-rich variety, correlating with elevated anthocyanin levels. In particular, two transcription factors, *Vr*MYB3 and *Vr*MYB90, were found to potentially increase anthocyanin levels by upregulating key biosynthetic genes. These insights into anthocyanin regulation may inform breeding efforts in mung beans.

Pigments shaping the color palette of cotton

Naturally colored cotton (NCC) varieties come in shades ranging from green to brown; their PAs contribute to both pigmentation and UV protection in fibers. These varieties also exhibit resistance to insects and diseases, as well as tolerance to salt and drought stresses. In their review, Naoumkina et al. discussed the molecular mechanisms underlying pigment production in naturally-colored brown cotton (NBC), challenges in breeding NCC with diverse colors without compromising fiber quality, and the potential of using flame-retardant NCC varieties for textile applications. To address the knowledge gap regarding the correlation between pigmentation and flame resistance in NBC, Hinchliffe et al. conducted a comparative transcript and metabolite analysis of developing fibers from brown (MC-BL) and white (MC-WL) cotton near isogenic lines differing at a single locus. Their study revealed significant differences in metabolite profiles and gene expression during key stages of fiber development. Notably, MC-BL showed higher accumulation of the phenylpropanoid pathway derivatives and organic acids from the citric acid cycle, while amino acid levels were lower compared to MC-WL. Further research is needed to understand how these differentially accumulated metabolites contribute to the flame-retardant properties of NBC fibers.

PA biosynthesis and perspectives

PAs, anthocyanins, and flavonols largely impact the nutritional and sensory qualities of grape berries and red wine. Shi et al. reviewed how environmental factors, such as water availability, light exposure, and temperature, as well as their interactions with phytohormones, affect the composition and content of these compounds, with the goal of providing a better understanding of the underlying regulatory mechanisms. While PAs are often found in the fruit peels and seeds of plants, such as grapes, they are also present in the vegetative tissues, including the roots, of woody plants. Westley et al. demonstrated that CTs (i.e., PAs) are predominantly located in younger white roots and at the tips of hybrid poplar (*Populus tremula* x *alba*) roots. They observed higher concentrations of CTs in root cap and epidermal cells, and lower levels in older roots and those with secondary growth. CTs are most concentrated in the insoluble fraction within the cork zone, and their accumulation correlates with increased ammonium (NH_4^+) uptake near the root tip, while nitrate (NO_3^-) and calcium (Ca^{2+}) uptake remains consistent. To further investigate the functional role of CTs in roots, transgenic poplar plants with modified CT profiles could be utilized for direct testing.

Lu revisited questions raised about PA biosynthesis two decades ago and provided an update on our current understanding, particularly regarding precursors, intermediates, and polymerization reactions. However, questions remain concerning the intracellular transport and deposition of PAs, as well as the subcellular localization of enzymes involved in PA biosynthesis. The mini-review also outlined future research directions, including the exploration of additional model species, other forms of PA, factors affecting PA biosynthesis, and the extent of PA polymerization.

Looking ahead, understanding the spatial distribution and intracellular dynamics of PA and isoflavonoid biosynthesis remains a priority for future research. Additionally, elucidating the interplay between environmental factors and the metabolism of

PAs and isoflavonoids could offer valuable insights for improving agricultural traits and nutritional quality. Advanced biochemical, genetic, and omics tools, combined with metabolic engineering approaches, will play a key role in bridging these research gaps and translating findings into practical applications.

Author contributions

LT: Writing – original draft, Writing – review & editing. DX: Writing – review & editing.

Acknowledgments

The Guest Editors would like to thank all the authors for their contributions to this Research Topic, as well as the reviewers, editors, and the editorial office for their support and assistance throughout the process.

Conflict of interest

The authors declare that the research was conducted in the absence of any commercial or financial relationships that could be construed as a potential conflict of interest.

The author(s) declared that they were an editorial board member of Frontiers, at the time of submission. This had no impact on the peer review process and the final decision.

Publisher's note

frontiers | Frontiers in Plant Science

TYPE Original Research
PUBLISHED 24 October 2023
DOI 10.3389/fpls.2023.1251464

OPEN ACCESS

EDITED BY
Deyu Xie,
North Carolina State University,
United States

REVIEWED BY
Yue Zhu,
North Carolina State University,
United States
Seyit Yuzuak,
Mehmet Akif Ersoy University, Türkiye

*CORRESPONDENCE
Chao Ma
machao840508@163.com

†These authors have contributed equally to this work

RECEIVED 01 July 2023
ACCEPTED 11 October 2023
PUBLISHED 24 October 2023

CITATION
Li C, Gao Z, Hu W, Zhu X, Li Y, Li N and Ma C (2023) Integration of comparative transcriptomics and WGCNA characterizes the regulation of anthocyanin biosynthesis in mung bean (*Vigna radiata* L.). *Front. Plant Sci.* 14:1251464. doi: 10.3389/fpls.2023.1251464

Integration of comparative transcriptomics and WGCNA characterizes the regulation of anthocyanin biosynthesis in mung bean (*Vigna radiata* L.)

Chunxia Li[1,2†], Zexiang Gao[1,2†], Weili Hu[3], Xu Zhu[3], Youjun Li[1,2], Na Li[1,2] and Chao Ma[1,2*]

[1]College of Agriculture, Henan University of Science and Technology, Luoyang, China, [2]Dry-land Agricultural Engineering Technology Research Center in Henan, Henan University of Science and Technology, Luoyang, Henan, China, [3]Crop Breeding Research Center, Nanyang Academy of Agricultural Science, Nanyang, Henan, China

Mung bean is a dual-use crop widely cultivated in Southeast Asia as a food and medicine resource. The development of new functional mung bean varieties demands identifying new genes regulating anthocyanidin synthesis and investigating their molecular mechanism. In this study, we used high-throughput sequencing technology to generate transcriptome sequence of leaves, petioles, and hypocotyls for investigating the anthocyanins accumulation in common mung bean variety as well as anthocyanidin rich mung bean variety, and to elucidate their molecular mechanisms. 29 kinds of anthocyanin compounds were identified. Most of the anthocyanin components contents were significantly higher in ZL23 compare with AL12. Transcriptome analysis suggested that a total of 93 structural genes encoding the anthocyanin biosynthetic pathway and 273 regulatory genes encoding the ternary complex of MYB-bHLH-WD40 were identified, of which 26 and 78 were differentially expressed in the two varieties. Weighted gene co-expression network analysis revealed that VrMYB3 and VrMYB90 might have enhanced mung bean anthocyanin content by inducing the expression of structural genes such as *PAL*, *4CL*, *F3'5'H*, *LDOX*, and *F3'H*, which was consistent with qRT-PCR results. These findings are envisaged to provide a reference for studying the molecular mechanism of anthocyanin accumulation in mung beans.

KEYWORDS

mung bean, anthocyanins, transcriptome sequencing, weighted gene co-expression analysis, differentially expressed genes

1 Introduction

Mung bean (*Vigna radiata* L.) is a cowpea (*Vigna*) plant belonging to the leguminosae family and is one of the fastest-growing edible legume crops in Asia (Han and Na, 2021; Zhao et al., 2022). Not only is it drought- and infertile-resistant, and easy to cultivate, it can also symbiotically fix nitrogen, making it a better alternative to cereals, sweet potatoes, cotton and other fruit trees. (Ilyas et al., 2018; Qian et al., 2018; Gong et al., 2020). It has a high nutritional values as it is rich in amino acids, vitamins, proteins, and minerals, and also contains many flavonoids with antioxidant and anti-aging properties. As an important source of protein supplements, mung bean has become a crucial part of human food consumption, especially in financially vulnerable regions (Luo et al., 2016; Zhu et al., 2018; Kumar and Pandey, 2020). Continuous improvement in living standards and increasing health awareness have created the need for diversified nutritious and healthy pulses, and this has also become a new target for the mung bean. More importantly, the color of cereal products has become an important indicator of the nutritional content and economic value of these products (Thakur S, et al., 2019; Li et al., 2022a).

Anthocyanins, which are water-soluble pigments found in leaves, fruits, grains, and flowers, impart various colors to plants including red, blue, or purple (Leyrer et al., 2016). Following different modifications, biosynthetic anthocyanins are transported to vesicles and other locations for storage (Masukawa et al., 2018). In plants, anthocyanins have been reported to possess diverse biological functions such as scavenging free radicals generated during physiological metabolism under biotic or abiotic stress conditions. This helps reduce cell damage and maintain normal photosynthetic activity (Li et al., 2022b). Additionally, anthocyanins contribute to the vibrant colors of plant flowers and aid in attracting insects for pollination purposes (Wim and El-Esawe, 2014). As phytonutrients with potent antioxidant and anti-mutagenic activities, they play a pivotal role in human health (Li et al., 2019b; Yousuf et al., 2016). As one of the important secondary metabolites and bioactive substances in mung beans, anthocyanins have become one of the hot spots in the current research on the development of functional mung beans (Ma et al., 2023). They are considered major antioxidants along with numerous other compounds present in mung beans (Kan et al., 2018). The biosynthesis of anthocyanins is regulated by two major groups of structural genes, namely early and late biosynthetic genes. The former comprises includes *chalcone synthase* (*CHS*), *chalcone isomerase* (*CHI*), *flavanone 3-hydroxylase* (*F3H*), *flavonoid 3'-hydroxylase* (*F3'H*), and *flavonoid 3'5'-hydroxylase* (*F3'5'H*), which are responsible for the synthesis of flavonols and flavonoids (Stotz et al., 1985; Wienand et al., 1986; Tunen et al., 1988; Meldgaard, 1992; Tanaka et al., 1996). The latter comprises *leucoanthocyanidin dioxygenase* (*LDOX*), *anthocyanidin synthase* (*ANS*), and *UDP-flavonoid glycosyltransferase* (*UFGT*) (Heller et al., 1985; Ju et al., 1995; Simoneau, 1999). Studies investigating the regulation of anthocyanins have primarily focused on MYB, bHLH, and WD40 transcription factors, which form a ternary complex that regulates the expression of structural genes involved in anthocyanin biosynthesis (Shi et al., 2019). Furthermore, various environmental factors can indirectly influence anthocyanin content (Gao et al., 2021). Several studies have demonstrated that light, temperature, low phosphorus levels, and hormones can regulate the expression of anthocyanin synthesis genes (Yang et al., 2017; Saigo et al., 2020; Mo et al., 2021).

Recent studies utilizing high-throughput sequencing technology and multi-omics research methods have revealed that transcription factors such as NAC, bZIP, MADS-box, and GRF-like are also involved in regulating anthocyanin biosynthesis besides MYB-, bHLH-, and WD40-proteins. This expanded understanding is anticipated to explain significant variations observed in anthocyanin profiles among different plant species (Rouholamin et al., 2015; Deng et al., 2020; Bao et al., 2022; Fu et al., 2022). Extensive elucidation has been made regarding the biosynthetic pathways of anthocyanins in crops, such as wheat, maize, potato, and sweet potato (Jiang et al., 2018; Hu et al., 2020; Qi et al., 2023; Fu et al., 2022). However, the accumulation and distribution patterns of anthocyanins in mung bean, as well as the gene regulatory network of biosynthesis, remain unexplored. Therefore, it is necessary to study the molecular mechanism of anthocyanin synthesis in mung bean. In this study, total anthocyanin content in leaves, petioles, and hypocotyls was analyzed using common (AL12), and anthocyanidin-rich mung bean variety (ZL23), where key genes regulating anthocyanin synthesis were identified by multiple omics combined with WGCNA analysis. The results of this study not only extend our understanding of the biosynthesis of anthocyanin-like compounds in mung beans at the molecular level but also provide valuable information for the further development of novel mung beans based nutraceuticals.

2 Materials and methods

2.1 Plant materials

AL12 (almost no anthocyanidin in the aboveground organs) and ZL23 (ZL23, anthocyanidin rich in leaves, petioles and hypocotyls) varieties of mung beans were used as plant materials whose seeds were generously provided by the Miscellaneous Grains Research Laboratory of Henan University of Science and Technology. The experiment was carried out from May to September 2022. All experimental procedures on plant materials were conducted at the experimental farm of Henan University of Science and Technology, situated at 34° 41′ N and 112° 27′ E, at an altitude of 280 m above sea level. The mean annual rainfall and temperature in the region is 578.2 mm and 14.8°C, respectively. The soil in the experimental farm is classified as fluvo-aquic soil, and has the following physicochemical characteristics: pH (H_2O) = 7.08, available nitrogen = 80.09 mg·kg^{-1}, available phosphorus = 3.31 mg·kg^{-1}, available potassium = 81.32 mg·kg^{-1}, organic matter = 14.5 g·kg^{-1}. Cultivation, and cultivation management was kept the same as for the general high-yielding fields. The leaves, petioles, and hypocotyls of both varieties were sampled after the 5-leaves stages. GL, GB, and GP stand for leaves, petioles, and hypocotyls of AL12, respectively; BL, BB, and BP stand for leaves, petioles, and hypocotyls of ZL23, respectively. Samples were snap frozen in

liquid nitrogen and stored at -80°C in a refrigerator till further use. In order to ensure the reliability and reproducibility of the experiment, physiological indexes, metabolome analysis and transcriptome analysis both use 3 biological replicates.

2.2 Total anthocyanin measurement and metabolite profiling analysis

The total anthocyanin contents were determined using the hydrochloric acid (HCl)-ethanol method (Wang et al., 2013). Briefly, an accurately weighed 0.1g of sample was taken and ground using a tissue grinder in liquid nitrogen into powder and extracted at 60°C in a water bath for 30 min with 10 ml of 0.1 mol/L HCl-ethanolic solution. The supernatant was carefully separated and transferred to a new 25 ml volumetric flask and extracted again as per the previous procedure. Both the extract fractions were combined, and the final volume was made up to 25 ml using HCl-ethanolic solution. The absorbance of the extract was then recorded at wavelengths of 530 nm, 620nm, and 650nm, respectively. The anthocyanin contents were then estimated using the following equation, and worked out their content by molecular weight of cyanidin-3-O-galactoside.

$$OD_{\lambda} = (OD530 - OD620) - 0.1(OD650 - OD620) \quad (1)$$

Where OD is optical density.

$$\text{Content (mg/g)} = \frac{OD_{\lambda}}{\varepsilon} \times \frac{V}{m} \times \frac{1}{1000} \times M \quad (2)$$

Where V is total volume of extract; ε is molar extinction coefficient of anthocyanin; m is sample weight; M is molecular weight of cyanidin-3-O-galactoside (449 g/mol).

Anthocyanin metabolome analysis was completed by Wuhan Metware Biotechnology Co., Ltd. through LC-MS/MS. Lyophilized plant tissue sample was ground into powder by a tissue grinder (MM 400, Retsch). 50 mg sample was dissolved in 500 μL extract solution (50% methanol containing 0.1% HCl). The extract solution was oscillated by vortices for 5 min, and was extracted by ultrasonic extractor for 5 min. Then, the extract solution was centrifuged for 10 min (4°C, 12000 rpm min^{-1}). The supernatant was transferred to a new centrifuge tube and repeat the extraction process. The extract was filtered with a microporous filter membrane (0.22μm pore size). The extract was then analyzed using a liquid chromatography tandem mass spectrometry system (Applied Biosystems 6500 QTRAP). The liquid chromatographic conditions were as follows: the column was C18 (ACQUITY BEH, 1.7μm, 2.1mm×100mm), and the mobile phase A was ultrapure water (containing 0.1% formic acid), B was methanol (containing 0.1% formic acid), the flow rate was 0.35 mL min^{-1}, the column temperature was 40°C, and the injection was 2 μL. Mass spectrometry conditions were as follows: electrospray ion source temperature was 550°C, mass spectrometry voltage was 5500V, curtain gas was 35psi. The acquired mass spectrometry data were then qualitatively analyzed by means of a local database. Finally, the anthocyanin components were quantitatively analyzed using the multiple reaction monitoring mode of triple quadrupole mass spectrometry.

2.3 RNA extraction, library construction, and sequencing

Total RNA was extracted from samples using TaKaRa MiniBEST Plant RNA Extraction Kit (TAKARA 9769), and cDNA libraries were constructed for samples meeting the purity, concentration, and integrity of the RNA. The mRNA was enriched with magnetic beads with Oligo (dT), and randomly interrupted by adding a fragmentation buffer. The first cDNA strand was synthesized with random hexamers using the mRNA as a template, followed by purification through AMPure XP beads. The purified double-stranded cDNA was then end-repaired, A-tailed, and ligated to sequencing junctions, followed by fragment size selection using AMPure XP beads, and finally enriched by PCR to obtain the cDNA library. The cDNA libraries were sequenced by Biomarker Technologies Ltd. (Beijing, China) using the Illumina platform. The adapter sequences and low-quality sequences of the off-machine data were filtered to obtain clean data. Sequence alignment was performed with the reference genome of mung bean, and uniq mapped genes were obtained through HISAT2 and StringTie software. Functional annotation of a single gene was performed using multiple databases including NR (Non-Redundant Protein Sequence Database), Swiss-Prot (Swiss Protein Sequence Database), GO (Gene Gntology Annotation), COG (Clusters of Orthologous Groups), KOG (EuKaryotic Orthologous Groups), Pfam (Protein Family Analysis and Modeling), and KEGG (Kyoto Encyclopedia of Genes and Genomes).

2.4 Differentially expressed genes and WGCNA

The expression levels of all genes were calculated and normalized to fragments per kilobase of transcript per million fragments mapped (FPKM). Fold Change≥1 and FDR<0.05 were used as the criteria for screening differential expression genes (DEGs). The identified DEGs were further enriched by GO, COG, and KEGG pathway analysis. Gene co-expression network analysis was constructed using the R language software WGCNA package. Since input gene expression was the result of TPM normalization, the expression was first subjected to a further log2 transformation. To ensure that the data conform to the scale-free network distribution, the weighting coefficient β value was screened and the network topology was analyzed using the pickSoftThreshold function in the WGCNA package to obtain the correlation value (R^2) corresponding to the alternative soft threshold, which is required to ensure R^2 is close to 0.8 having a certain degree of gene connectivity. A horizontal line was drawn with $R^2 = 0.8$ as the threshold, and the first-time power exceeding the threshold was found to be 15. Since power=15 was having a high degree of connectivity, the β=15 was selected to construct the co-expression network and for subsequent analysis. To quantify the co-expression similarity of the whole module, the dynamic tree cut algorithm was used to identify the co-expression modules of the transcriptome expression data, and the minimum number of variables allowed to be included in the module (minModuleSize) was set to 100. To

quantify the similarity of co-expression across modules, the characteristic genes of the modules were calculated, with unmerged modules, and other parameters were set by default. The modules are plotted below the tree using the plot dendro and colors function. The soft connectivity function was used to calculate the connectivity between genes, and the top 10 genes with kME values as the core genes of the module (hubgene) were selected. The topological overlap matrix was used to calculate the weights of the different genes in the module, where a higher weight value indicated a higher degree of association between genes. Due to the large network size, a weight value > 0.35 was set as network filtering criteria, and the reciprocal network of 10 hubgene was visualized using Cytoscape v3.6.1. Based on the results of WGCNA, the dark green gene module with the highest correlation to anthocyanins was selected, and the genes within the module were further visualized and analyzed using Cytoscape v3.6.1 for the interactions network. The top 8 genes with the highest degree of linkage were selected as the core genes (hubgene) and were focused owing to key genes affecting anthocyanin biosynthesis.

2.5 Gene expression analysis by qRT-PCR

Total RNA extraction, reverse transcription reactions, and qPCR were performed using the kit method (TaKaRa; 9769, RR047B, and RR430B), and primers were designed (Table S1). A total of 20 µl reaction volume contained 10 µl of TB Green Fast qPCR Mix (2×), 1 µl cDNA, 0.4 µl each of upstream and downstream primers (10 µmol. L^{-1}), and 8.2 µl doubled distilled water (ddH_2O). The reaction proceeded in a two-step process i.e., pre-denaturation at 95°C for 30 seconds, followed by denaturation at 95°C for 5 seconds, and annealing at 60°C for 30 seconds. A total of 40 cycles were performed, and fluorescence was determined at reversion time. The experiment was conducted in triplicates and relative expression was calculated using the $2^{-\Delta\Delta CT}$ method with *VrActin* as the internal reference gene.

2.6 Subcellular localization of MYB3 and MYB90

The CDS sequences of MYB3 and MYB90 were cloned into *pCAMBIA1300-GFP* vector without termination. Recombinant plasmid of *35S:MYB3-GFP* and *35S:MYB90-GFP* were transformed into agrobacterium GV3101 for subcellular localization. Agrobacterium (35S:VrMYB3-GFP and 35S: VrMYB90-GFP) was identified as positive clones which was cultured with liquid LB medium (50 µg mL^{-1} of kanamycin and rifampicin each) at 28°C. 1.5 mL of bacterial solution was centrifuged at 5 000 r min^{-1} for 3 min to collect bacterial cells. Then, the OD_{600} of agrobacterium suspension, including 1 mol L^{-1} MES (pH 5.6), 1 mol L^{-1} $MgCl_2$ and 20 mmol L^{-1} acetosyringone, was adjusted to about 0.7. Agrobacterium suspension was standed still at 25°C for 1 h. The bacterial solution was slowly injected into the mesophyll cells on the back of Nicotiana benthamiana leaves, and the injected plants were cultured under light for 48 h. The subcellular localization of fusion protein was observed through LSM 710 NLO confocal microscope (Zeiss, Germany).

2.7 Statistical analysis

All the data are presented as mean ± SD (standard deviation). Microsoft Excel 2016 and SPSS17.0 were used to process the data while comparing the significance between treatments was done using the LSD method.

3 Results

3.1 Analysis of phenotypes, anthocyanin content and their components of different organs of mung bean

To investigate the biosynthesis and accumulation of anthocyanins during the growth and development of AL12 and ZL23 mung bean varieties, the phenotype and anthocyanin content of leaves, petioles, and hypocotyls of both varieties were analyzed. All three parts in the common green bean variety were green in color with no anthocyanin accumulation observed during growth and development. In contrast, the leaf veins, petioles, and hypocotyls of the greenish-black bean leaves showed significant anthocyanin accumulation during the same period (Figures 1A-P). The anthocyanin content in leaves, petioles, and hypocotyls during the same period were found to be significantly lower in AL12 compared to ZL23. A substantial difference in anthocyanin contents among the two varieties was found in petioles and hypocotyls, where AL12 contained 29.3 mg g^{-1} in petioles and 4.5 mg g^{-1} in hypocotyls, while the same was found to be 90.2 mg g^{-1} and 75.2 mg g^{-1} in ZL23, respectively, showing a 3.07-fold and 16.7-fold increased anthocyanin contents in ZL23. Nevertheless, the difference in anthocyanin contents in leaves among the two varieties was relatively small i.e., 10.3 mg g^{-1} in AL12, and 17.4 mg g^{-1} in ZL23, respectively, where the contents in ZL23 were still 1.7-fold higher compared to AL12 (Figure 1Q), which could be attributed to the fact that anthocyanin in leaves is mainly accumulated in the leaf veins.

Principal component analysis (PCA) showed that there were significant differences between the two varieties and three site samples (Figure 1R). 72.16% of the differences between samples could be explained by PCA1 (47.79%) and PCA2 (24.37%), indicating that anthocyanins showed a dynamic change pattern during two varieties and three site samples. Hierarchical cluster analysis (HCA) of metabolome data exhibited low difference in biological replicates. The correlation coefficient of anthocyanin components contents was up to 0.93 among biological replicates (Figure 1S). This suggests that there was a good correlation among the bio-replicates. The above results demonstrated the results was stable and repeatable, and provided a guarantee for the reliability of the results. Seven categories, consisted of 29 kinds of anthocyanin compounds, in these three stages were identified through LC-MS/MS, including 8 kinds of cyanidin, 7 kinds of delphinidin, 7 kinds of

10.3389/fpls.2023.1251464

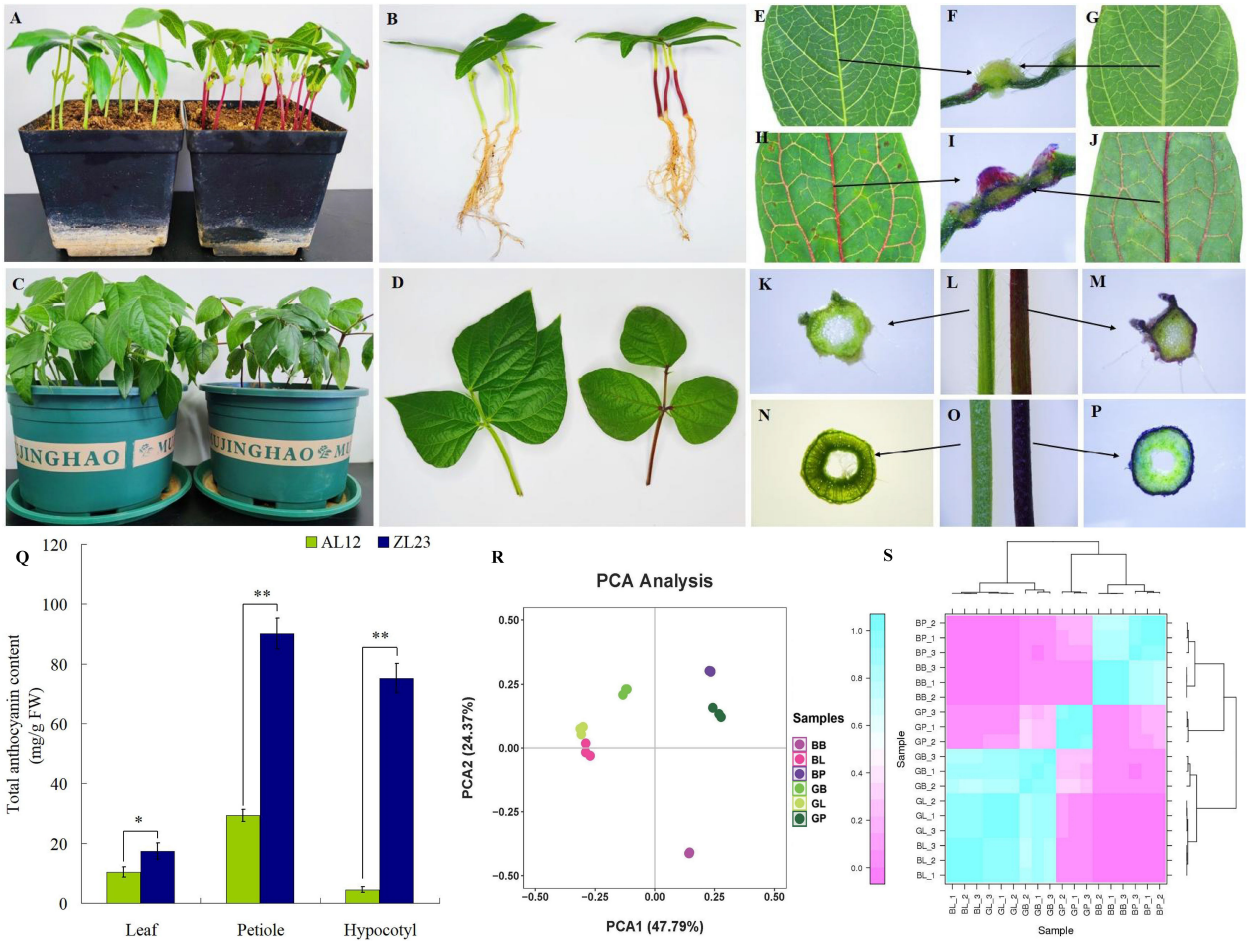

FIGURE 1
Phenotypes of AL12 (almost no anthocyanidin in the aboveground organs) and ZL23 (ZL23, anthocyanidin rich in leaves, petioles and hypocotyls) varieties of mung beans. **(A, B)** AL12 (left) and ZL23 (right) 10 days after sowing. **(C, D)** AL12 (left) and ZL23 (right) 20 days after sowing. **(E-G)** Leaf phenotype of AL12. **(H-J)** Leaf phenotype of ZL23. **(K)** Petiole crosscutting phenotype of AL12. **(L)** Petiole phenotype of AL12 (left) and ZL23 (right). **(M)** Petiole crosscutting phenotype of ZL23. **(N)** Hypocotyls crosscutting phenotype of AL12. **(O)** Hypocotyls phenotype of AL12 (left) and ZL23 (right). **(P)** Hypocotyls crosscutting phenotype of ZL23. **(Q)** Changes in total anthocyanin content in leaves, petioles and hypocotyls. The data were in the form of mean ± standard deviation. * and ** indicate significant difference at $p< 0.05$ and $p< 0.01$ levels, respectively. **(R)** PCA of metabolome data. **(S)** Metabolome data among three biological duplications. The x-axis represents principal component 1 (PC1); the y-axis represents principal component 2 (PC2); two cultivars (AL12 and ZL23) and three developmental organs (GB, GL, and GP stand for leaves, petioles, and hypocotyls of AL12; while for ZL23 as BL, BB, and BP, respectively) are distinguished by different colors.

pelargonidin, 2 kinds of malvidin, 2 kinds of peonidin, 2 kinds of petunidin, and 1 kinds of procyanidin (Figure 2, Table S2). In AL12, cyanidin was the highest proportion of anthocyanins in the leaves and petioles, accounting for 84.1% and 55.9% respectively; pelargonidin was the highest proportion of anthocyanins in the hypocotyl, accounting for 82.8%. In ZL23, cyanidin was the highest proportion of anthocyanins in the leaves, accounting for 86.5%; delphinidin was the highest proportion of anthocyanins in the petioles and hypocotyl, accounting for 95.3% and 64.3%, respectively.

3.2 Global analysis of RNA-seq

The PCA results of transcriptome data showed a clear separation between the two varieties and three site samples, relatively. A negligible variability in transcriptome expression was found in GB and GP of AL12, and BB and BP of ZL23, while the same was higher in the leaves (GL, and BL). The 47.4% of the variation between samples was explained by PCA1 (31.58%) and PCA2 (15.82%), indicating that anthocyanin accumulation showed significant differences between the two varieties and different parts (Figure 3A). Correlation coefficient analysis between biological replicates as shown in Figure 3B indicated that the correlation coefficient of gene expression levels among biological replicates of all samples was >0.91, indicating an excellent reproducibility among biological replicates and that the data could be further used to determine DEGs.

To further clarify the molecular mechanism of anthocyanin biosynthesis during the growth and development of stated organs in ZL23, 18 cDNA libraries comprising two varieties of three organs in triplicates were prepared for transcriptome analysis. As shown in

10.3389/fpls.2023.1251464

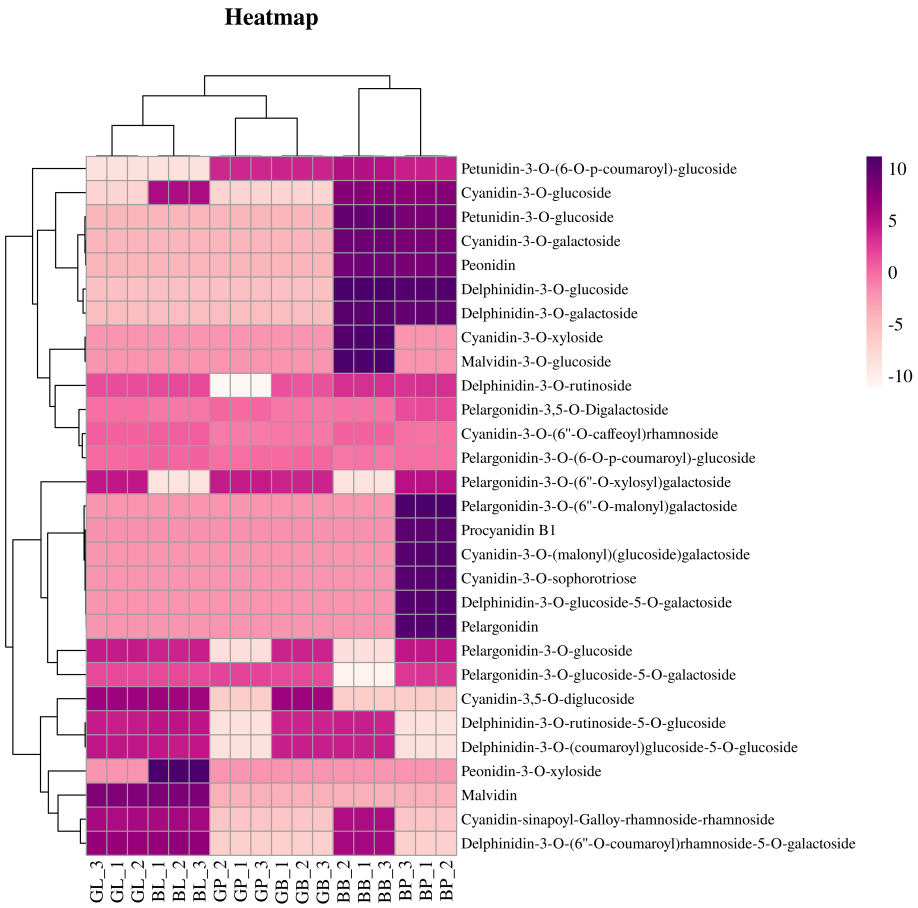

FIGURE 2
Hierarchical cluster analysis based on the anthocyanin components contents in mung bean.

Table S3, a total of 116.64 Gb of clean data was obtained after filtering, with 19, 236, 210 to 38, 429, and 484 clean reads for each library. The percentage of Q30 (sequences with a sequencing error rate<0.1%) for each library was over 92%, while GC contents of the samples ranged between 44.67 and 46.20%. The clean reads were mapped between 83.58 and 93.87% to the reference genome of each library and which was then used for further analysis.

3.3 DEGs analysis

A total of 8211 DEGs were screened in the three comparison combinations as shown in Figure 3C, among which, a total of 4921 were up-regulated and 3284 were down-regulated. Additionally, 2803 DEGs were screened in the GB-1_GB-2_GB_3_vs_BB-1_BB_2_BB_3 comparison sample, among which 1882 were up-regulated and 981 were down-regulated. The GL-1_GL-2_GL_3_vs_BL-1_BL_2_BL_3 comparison sample screened a total of 3548 DEGs, with 2007 up-regulated and 1541 down-regulated genes, while GP-1_GP-2_GP_3_vs_BP-1_BP_2_BP_3 comparison sample screened a total of 1860 DEGs, where 1098 were up-regulated and 762 were down-regulated. These results suggested that the DEGs in AL12 and ZL23 might be involved in the synthesis of anthocyanins in mung beans. As shown in the Wayne diagram (Figure 3D), the number of DEGs specific to leaves, petioles, and hypocotyls were 2053, 1167, and 535, respectively, where the number of common DEGs between leaves and petioles was 567, and between leaves and hypocotyls was 256. Similarly, the number of common DEGs between petioles and hypocotyls was 397, while 672 were among leaves, petioles, and hypocotyls. Further, 833 transcription factors were found to be differentially expressed in the two varieties (Figures 3E-F, Table S4), belonging to 15 transcription factor families, among which 109 and 92 were significantly up- and down-regulated, respectively.

3.4 GO and KEGG analysis

The GO enrichment analysis results are shown in Figure S1 and Table S5, where 52 functional components were grouped into 3 categories, including 'biological processes', 'molecular functions' and 'cellular components'. The highest number of annotations was shown for 'metabolic processes' within 'biological processes', followed by 'cellular processes'. In 'cellular components', the most numerous genes were annotated as 'cellular', 'cellular components', and 'membrane components'. Similarly, in 'molecular function', the most genes were annotated as 'binding' and 'catalytic activity'. These results indicated that many types of enzymatic pathways

10.3389/fpls.2023.1251464

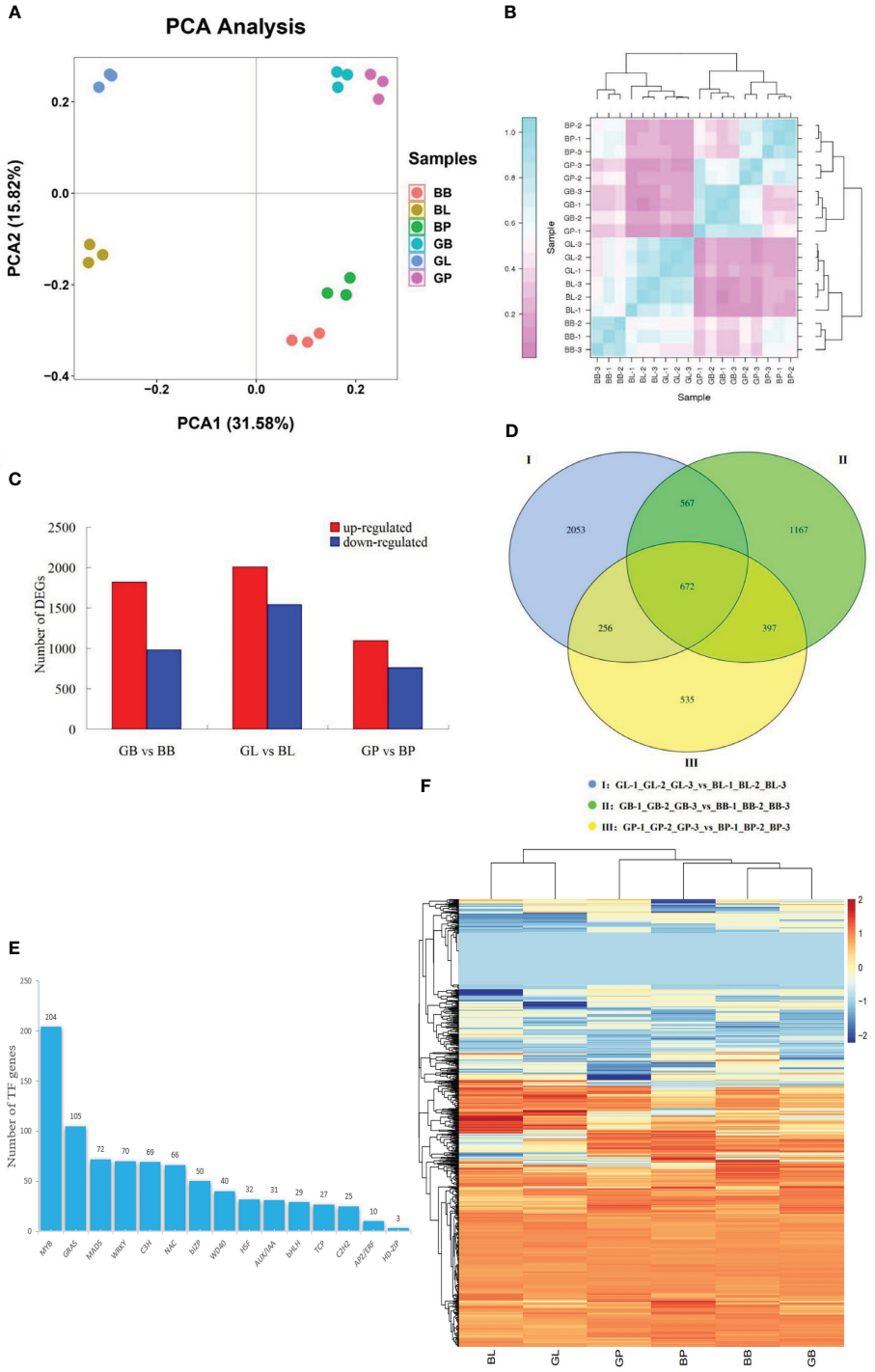

FIGURE 3
(A) PCA of transcriptome data. **(B)** transcriptome data among three biological duplications. The x-axis represents principal component 1 (PC1); the y-axis represents principal component 2 (PC2); two cultivars (AL12 and ZL23) and three developmental organs (GB, GL, and GP stand for leaves, petioles, and hypocotyls of AL12; while for ZL23 as BL, BB, and BP, respectively) are distinguished by different colors. **(C)** Number of differentially expressed genes in the same organs of AL12 and ZL23. **(D)** Wayne diagram of the number of differentially expressed genes between the same organs of AL12 and ZL23. **(E)** Number of transcription factors differentially expressed in AL12 and ZL23. **(F)** Hierarchical clustering analysis of the expression of each type of transcription factor in six different treatments (BB, BL, BP, GB, GL and GP).

were active in mung beans. To further identify the metabolic pathways of DEGs, KEGG enrichment analysis was performed. As shown in Figure S2; Table S6, the top 20 KEGG pathways with the lowest Q values were mainly concentrated in 'phytopathogen interaction', 'phenylpropane biosynthesis', 'photosynthesis', 'flavonoid biosynthesis', and 'flavonoid and flavonol biosynthesis' pathways. The 'flavonoid biosynthesis' pathway was significantly enriched in all three comparative combinations, and results

suggested that anthocyanin biosynthesis belonged to the flavonoid pathway and was also associated with the phenylalanine metabolic pathway. The large enrichment of the flavonoid biosynthesis pathway correlated with the large amount of anthocyanin synthesis in ZL23.

3.5 Analysis of structural and regulatory genes of anthocyanin synthesis in the different organs of mung bean

The published literature suggests that anthocyanins are mainly synthesized by 12 structural genes i.e., *CHI*, *CHS*, *C4H*, *CHS*, *4CL*, *DFR*, *F3'H*, *F3'5'H*, *F3H*, *LDOX*, *PAL*, *UFGT*, and three major transcriptional factors namely MYB, bHLH, and WD40, which were made into HCA (Figures 4, 5). As shown by HCA results, the reliability of the anthocyanin content and PCA results was further illustrated by the fact that the genes related to anthocyanin synthesis were significantly different between the two varieties. The HCA of structural genes is shown in Figure 5A, which were at significantly higher expression levels in the petioles and hypocotyls of ZL23 compared to AL12. However, the differences in expression in leaves were relatively small. Moreover, the three regulatory genes i.e., *MYB*, *WD40*, and *bHLH* showed similar results as shown in Figures 5B-D and Table S4.

3.6 Validation of RNA-seq data by RT-qPCR

To further characterize the expression of genes related to anthocyanin biosynthesis, the relative expression of 12 structural genes for anthocyanin biosynthesis and *MYB*, *bHLH*, and *WD40* were determined by RT-qPCR (Figure 6). The expression profile results indicated a high correlation between RNA-seq and RT-qPCR, thereby further cementing the reliability of the RNA-seq results.

3.7 Gene Co-expression Networks in the different organs of mung bean

To identify co-expressed gene modules and explore the relationship between gene networks and anthocyanin synthesis, the WGCNA was further performed, including 6415 DEGs. The correspondence between correlation coefficients and average connectivity at different thresholds (power values = 1 to 30) was measured. As shown in Figure 7, correlation coefficients, and average connectivity were guaranteed when the power value was 30. Finally, 14 modules were obtained from the clustering dendrogram (Figure 7D), where each module contained a different number of genes, with the 'BROWN' module containing the most genes at 1511 and the 'BLUE' module containing the least genes at 49, with an average of 458 genes per module. Pearson correlation analysis was performed between the genes and traits in each module according to the amount of anthocyanins in each site, and results are shown in Figure 7. The results demonstrated that seven of the 14 modules were positively correlated and seven were negatively correlated with anthocyanin synthesis. The green and dark-grey modules had the highest positive and negative correlation with anthocyanin content, respectively. The top 8 genes in the green module were selected as the core genes, including Vigna_radiata_var._radiata_newGene_3976, Vigna_radiata_var._radiata_newGene_4853, gene10693, gene25494, gene6451, gene12756, gene22866, and gene21475. These genes and their associated genes were mapped in a visual gene interaction network (Figure 8). Results showed that gene22866 and gene21475, which encode LDOX and F3'5'H respectively, were structural genes for anthocyanin synthesis, while Vigna_radiata_var._radiata_newGene_3976, Vigna_radiata_var._radiata_newGene_4853, gene10693, gene25494, gene6451, gene12756 belonged to MYB transcription factors. Due to the low expression of Vigna_radiata_var._radiata_newGene_3976, Vigna_radiata_var._radiata_newGene_4853, gene10693, gene25494 (FPKM ≤10), they will be ignored. Based on the combined analysis of the above results, gene12756 (*VrMYB3*) and gene6451 (*VrMYB90*) were found to play important roles in the regulation of anthocyanin synthesis in mung beans.

3.8 Subcellular localization analysis of VrMYB3 and VrMYB90

To confirm the location of VrMYB3 and VrMYB90 proteins in cells, the transiently expressed fusion proteins of VrMYB3 and VrMYB90 in tobacco leaves were detected by confocal laser microscopy. Figure 9 showed that there were GFP signals on both cell nucleus and cell membrane after transiently expressed *35S:GFP* vector in tobacco epidermal cells. However, transiently expressed of *35S:VrMYB3-GFP* and *35S:VrMYB30-GFP* vectors in tobacco epidermal cells, GFP signals were present on the nucleus. It suggests that VrMYB3 and VrMYB90 have potential function of transcriptional regulatory.

4 Discussion

Anthocyanins confer plants' colorful phenotype, increase their attractiveness to insects, and improve pollination efficiency, as well as improve resistance to adverse conditions and survival ability (Liu et al., 2020). They are water-soluble pigment found in plants and are generally prevalent in all types of plant organs. However, they usually stored as more stable glycosides in the vesicles of the plant's epidermal cells, accounting for the wide range of colors in plant organs (Li et al., 2021). For most plants, anthocyanins often accumulate in light-exposed locations e.g., in the seed coat of wheat (Flores et al., 2022) and maize (Paulsmeyer et al., 2022), the dextrin layer of rice (Peanparkdee et al., 2020), the seed coat of mung beans (Ma et al., 2023), etc. Moreover, some plants can also accumulate in other above-ground parts, e.g., rice (Mackon et al., 2021), wheat (Zhao et al., 2019), and maize (Lopez-Malvar et al.,

10.3389/fpls.2023.1251464

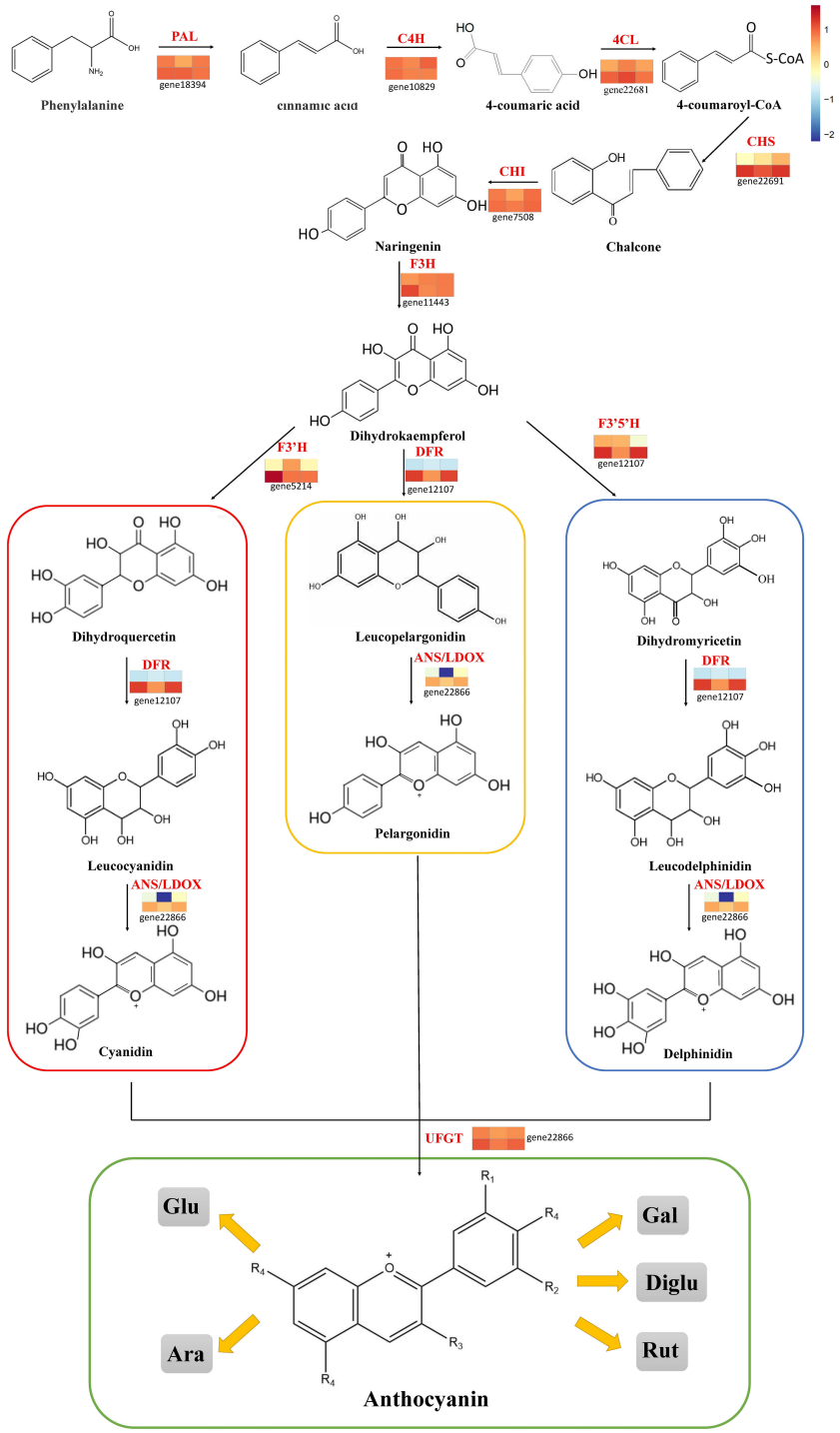

FIGURE 4
Transcript profiling of anthocyanin biosynthesis pathway in AL12 and ZL23.

2017), which suggests that light is an essential instigator for the synthesis of plant anthocyanins. Interestingly, underground plant organs such as purple potatoes, purple sweet potatoes, and black peanuts are also able to accumulate anthocyanins in large quantities (Kuang et al., 2018; Li et al., 2019a), suggesting anthocyanin accumulation is regulated by different genes in different species. In this study, the results indicated that the ZL23 mung bean variety accumulated anthocyanins mainly in the leaf veins, petioles, and hypocotyls. Though it accumulated anthocyanins in significant quantities in the above-ground plants, its seed coat remained normal for mung beans, implying the involvement of a complex regulatory mechanism for anthocyanin accumulation in mung beans. In the current study, the components and contents of anthocyanins in two varieties and three site samples were identified by using liquid chromatography-tandem mass spectrometry. A total of 7 categories and 29 kinds of

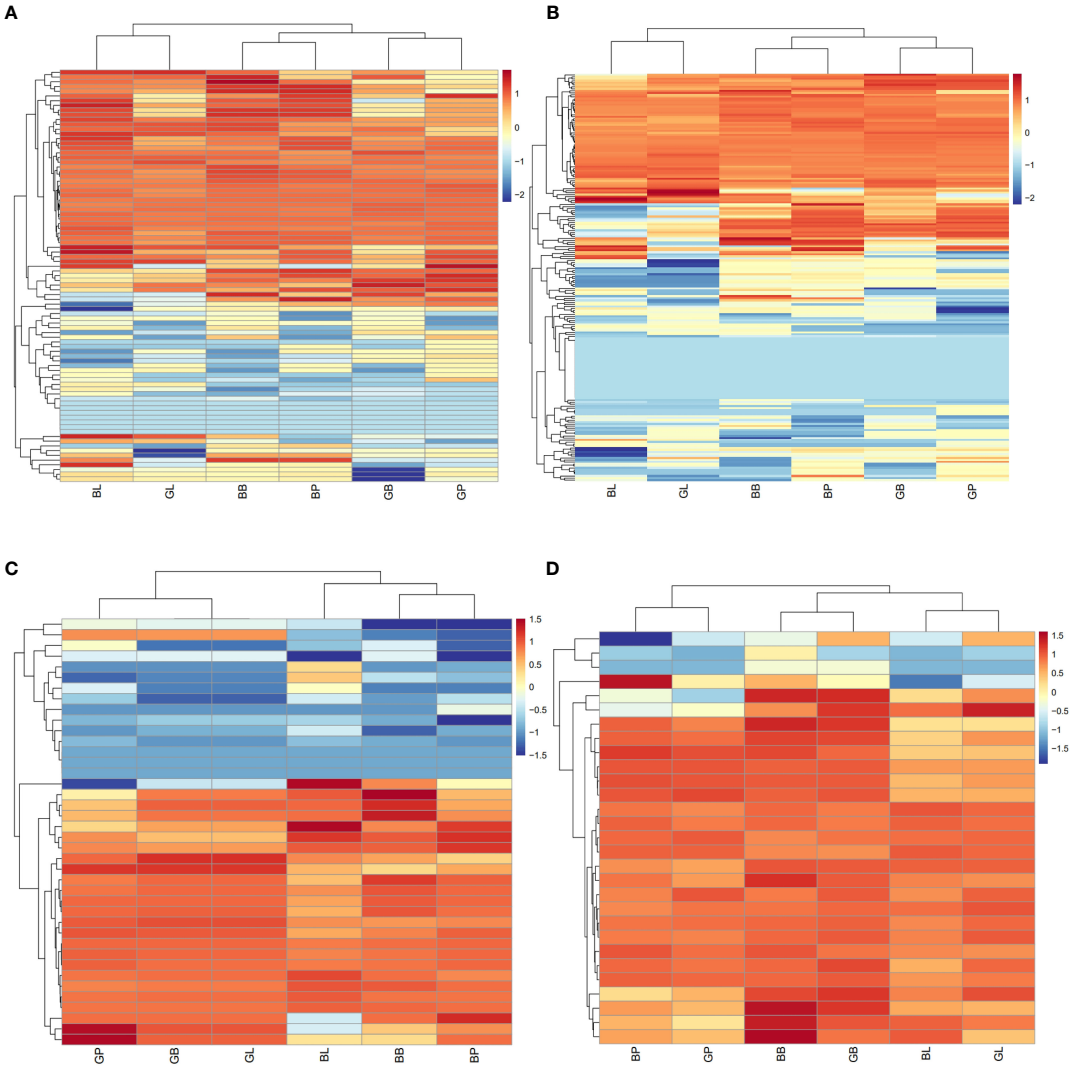

FIGURE 5
(A) HCA of structural genes for anthocyanin biosynthesis based on the RNA-Seq. **(B)** HCA of potential regulatory genes of MYB based on the RNA-Seq. **(C)** HCA of potential regulatory genes of bHLH based on the RNA-Seq. **(D)** HCA of potential regulatory genes of WD40 based on the RNA-Seq.

anthocyanins were detected. The content of most components contents were significantly higher in ZL23 compare with AL12. Interestingly, the main components of anthocyanins in three site samples were not the same. For example, in the petioles and petioles of ZL23, delphinidin-3-O-glucoside was the highest proportion of anthocyanins, accounting for 95.3% and 64.3%, respectively; however, in the leaves, cyanidin-3-O-(6''-O-caffeoyl)-rhamnoside was the highest proportion of anthocyanins, accounting for 86.5%. It suggested that the components and contents of anthocyanin varied greatly among different organs or different varieties of the same crop.

The synthesis of anthocyanins is regulated by two main groups of genes i.e., structural genes, which promote the synthesis of anthocyanins from phenylalanine by regulating a series of enzymatic reactions of phenylalanine in plants, and regulatory genes regulating anthocyanin biosynthesis by inducing or inhibiting the transcriptional levels of structural genes (Li et al., 2022c). Currently, the structural genes for anthocyanin synthesis have been relatively well studied and their biological functions were relatively clear, including *PAL*, *CHS*, *CHI*, *4CL*, *C4H*, *LDOX*, *F3H*, *F3'H*, *F3'5'H*, *DFR*, *ANS*, *UFGT*, etc (Chen et al., 2020). Similarly, a significant number of studies have focused on *MYB*, *WD40*, and *bHLH* for regulatory genes (Sharma et al., 2020). In this study, 26 structural and 78 regulatory genes were found to be differentially expressed in both varieties. Further analysis revealed that some structural and regulatory genes were significantly correlated with anthocyanin content. In addition, other transcription factors that may be involved in the regulation of anthocyanin synthesis were also identified, e.g., 18 *bZIPs*, 20 *NACs*, and 9 *MADSs* were differentially expressed in the two mung bean varieties, respectively. Notably, many studies have identified regulatory genes beyond the MYB-bHLH-WD40 ternary complex e.g., peach *PpNAC1* (Zhou et al., 2015), tomato *SlHY5* (He et al., 2023), and sweet potato *IbMADS10* (Dong et al., 2016) are all involved in the

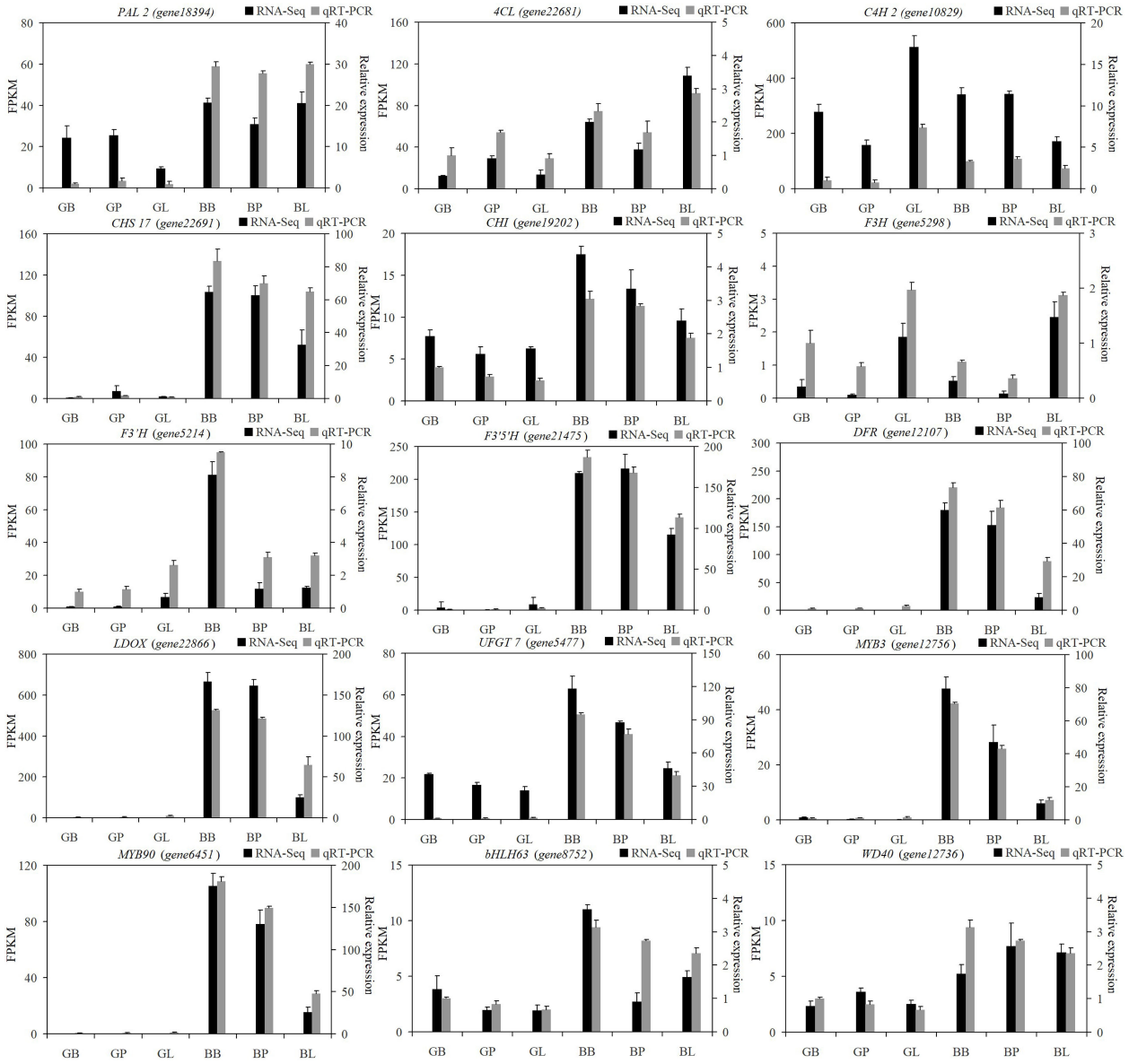

FIGURE 6
Expression analysis of fifteen genes by the RNA-Seq and qRT-PCR.

regulation of anthocyanin biosynthesis. These data suggest that plant anthocyanin biosynthesis is controlled by a complex and sophisticated regulatory network.

With the development of sequencing technology, the systematic study of massive amounts of genomic, transcriptomic, and metabolomic data using co-expression networks has gained immense attention for data processing (Xie et al., 2022). The WGCNA is an effective method for co-expression network analysis, capable of specifically screening out co-expression modules with high biological significance to the target trait, and has proven to be an efficient data mining method in a variety of plants (Sahu et al., 2019; Lu et al., 2019). In traditional methods, differential trait comparison is often focused on finding differential genes, thus neglecting the inter-genes correlation. Many genes have similar expression patterns and may have similar functions, allowing similar inter-genes interactions that regulate similar biological metabolic processes or the protein products they produce (Li et al., 2023). Through WGCNA, the clustering of genes with similar expression patterns can be used to identify co-expressed gene modules, explore the biological relevance of the modules to the target traits, and mine the core genes in the network (Wan et al., 2020). In this study, a weighted gene co-expression network was constructed by WGCNA on 18 sets of transcriptome sequencing data from the two mung bean varieties, and co-expression modules were identified that were highly significantly associated with anthocyanin expression i.e., Medarkgreen (0.97), Melightsteelblue1 (0.66), Medarkmagenta (0.64), and Melightpink4 (0.62), where Medarkgreen module showed strong correlation. The genes in the Medarkgreen module were constructed as a visual gene interaction network map, and the top eight genes with the highest

10.3389/fpls.2023.1251464

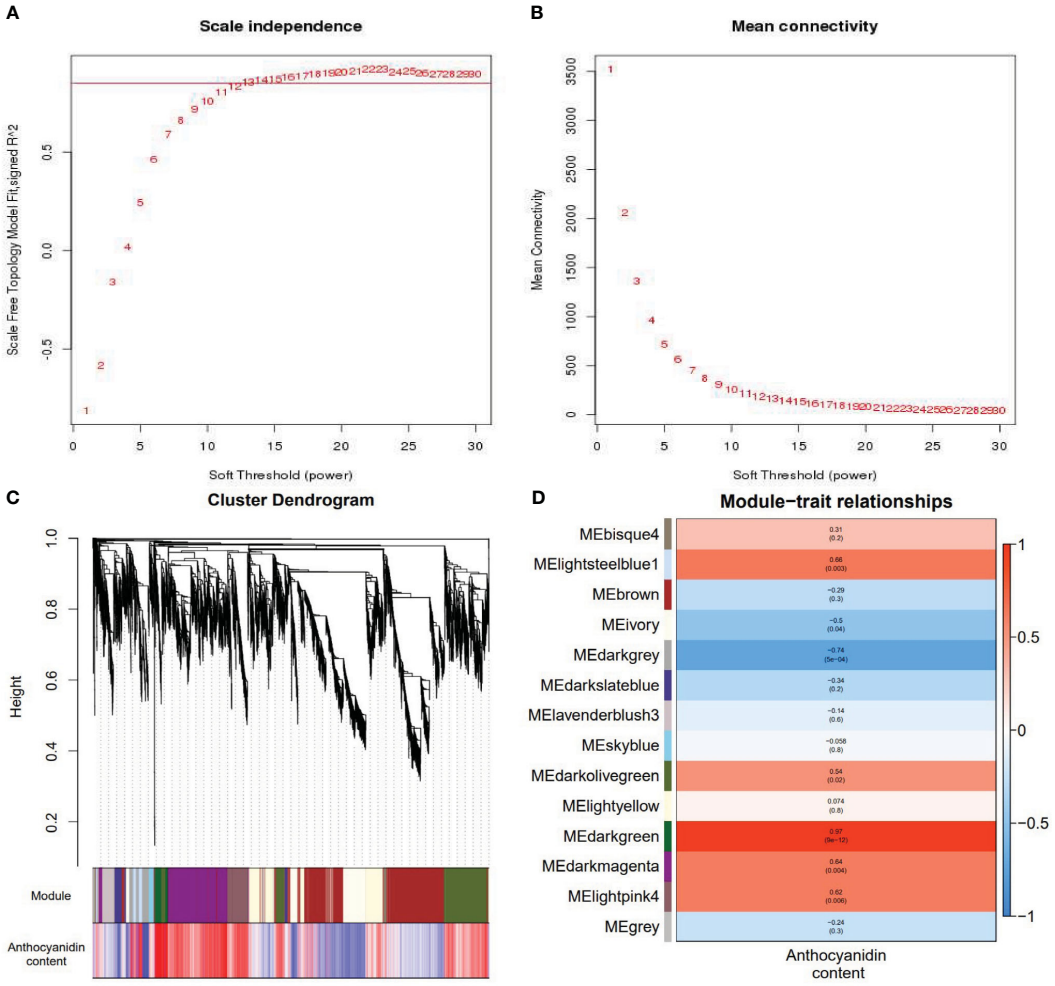

FIGURE 7
Weighted gene coexpression network analysis of metabolites and genes. **(A, B)** Analysis of network topology for various soft thresholding (power) and **(C)** construction of co-expression module. The same color represents the same module. If the module-features genes between two different modules are similar, they will be merged automatically. **(D)** Correlation heatmap between anthocyanin content and 14 gene modules. The y-axis represents each module. The x-axis represents anthocyanin content. Red and blue colors indicate up-regulated and down-regulated transcripts, respectively.

gene connectivity within the module were selected as hubgene, among which, gene22866 (*LDOX*, kME=0.9673) and gene21475 (*F3'5'H* kME=0.9709) were identified as structural genes for anthocyanin biosynthesis, while Vigna_radiata_var._radiata_newGene_3976 (*MYB*, kME=0.9685), vigna_radiata_var._radiata_newGene_4853 (*MYB*, kME= 0.9756), gene10693 (*MYB4*, kME=0.9696), gene25494 (*MYB*, kME=0.9642), gene6451 (*MYB90*, kME=0.9713), and gene12756 (*MYB3*, kME=0.9627) were found to be MYB transcription factors. These results are envisaged to indicate that the Medarkgreen module was highly associated with anthocyanin biosynthesis in ZL23. Therefore, it was speculated that the above genes may have important regulatory roles in the synthesis of anthocyanins in mung beans.

In addition to the direct involvement of structural genes, the process of anthocyanin synthesis was regulated by a protein complex formed by MYB, WD40, and bHLH, with major involvement of MYB. The MYB transcription factors can be further classified based on the number of structural domains into MYB-related, R2R3-MYB, R1R2R3-MYB, and atypical MYB, R2R3-MYB, R1R2R3-MYB, and atypical MYB, among which R1R2R3-MYB was mainly found in animals, and R2R3-MYB in plants, in addition to abundant R2R3-MYB (Shui et al., 2022). The number of atypical MYBs was relatively small and needs further exploration. A study reported that out of nearly 200 MYB *Arabidopsis* transcription factors, there were 126 R2R3-MYB class transcription factors (Li et al., 2023). Similarly, among the nearly 200 reported MYBs in rice, 109 were R2R3-MYBs. These proteins are reported to contain two MYB domains (R2, R3) at the N-terminus and are widely involved in the synthesis of plant secondary metabolites, as well as in response to various stressors and stress responses (Chen et al., 2006). R2R3-MYB transcription factors are the most important regulatory factors in the anthocyanidin biosynthesis pathway known to date. The type and content of anthocyanin were determined by regulating the expression of the structural gene of anthocyanin biosynthesis, which ultimately affects the colors of flowers, fruits, and leaves

10.3389/fpls.2023.1251464

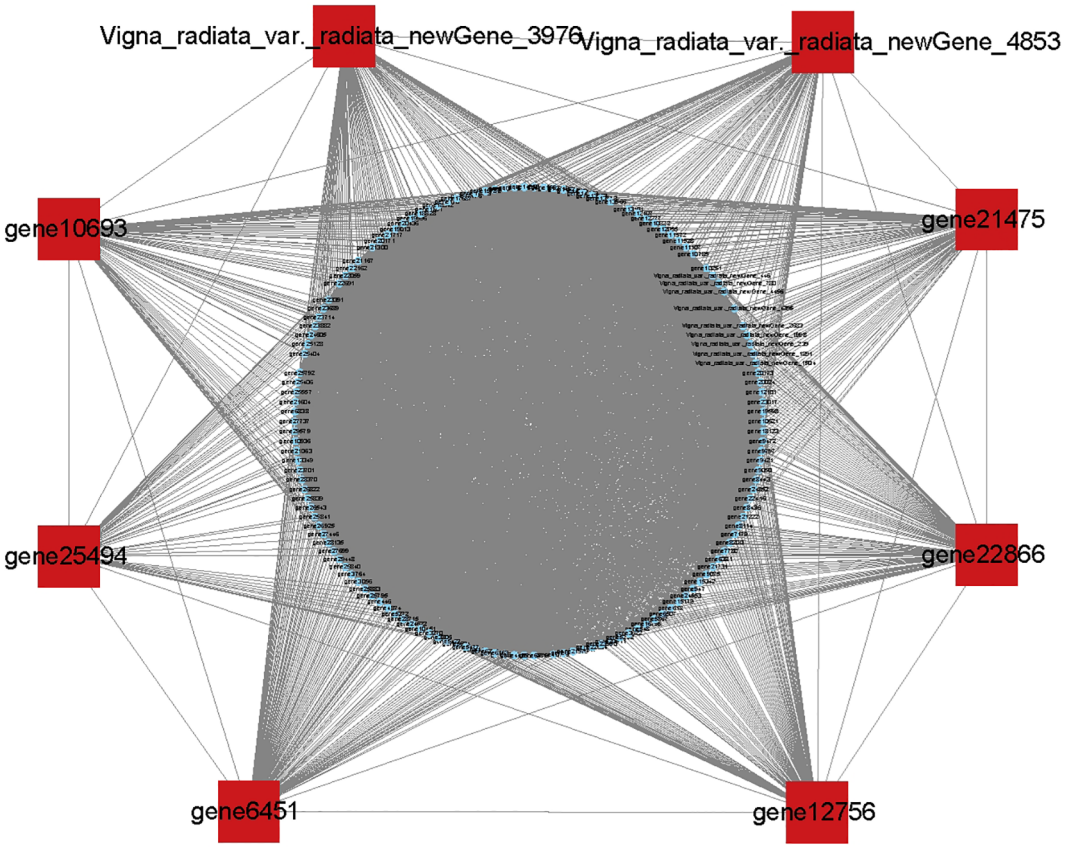

FIGURE 8
Based on the eight genes with the highest connectivity in the green module, the red dots are core genes and the blue dots are reciprocal genes.

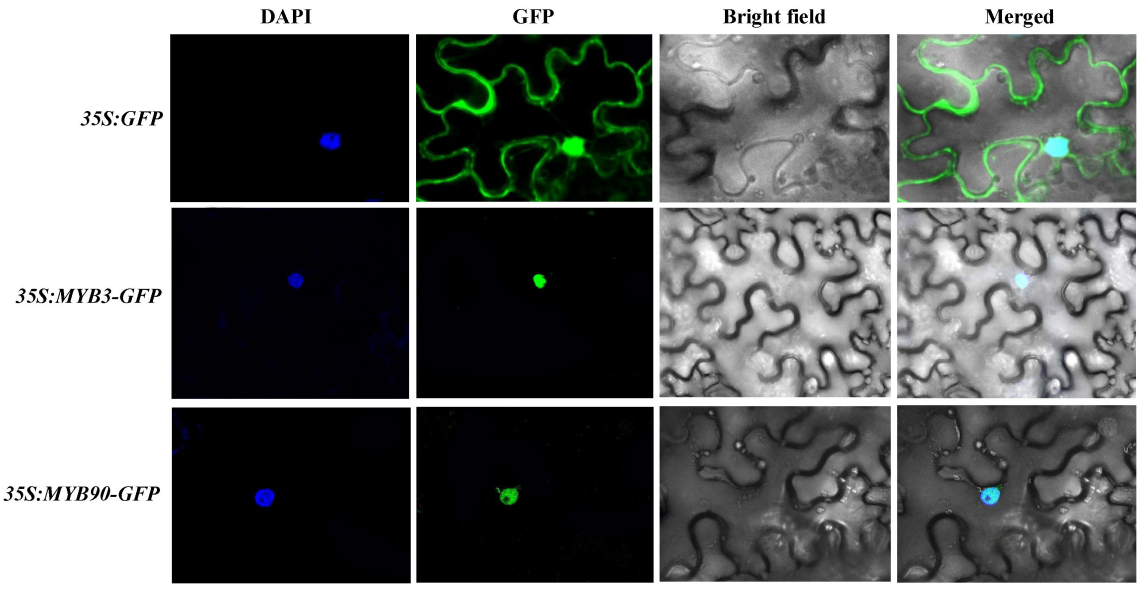

FIGURE 9
Subcellular localization analysis of VrMYB3 and VrMYB90 in *N. benthamiana* cells.

(Yin et al., 2021). The R2R3-MYB family has been further divided into 25 subfamilies based on the different conserved amino acid sequences of R2R3-MYB proteins, among which some have been shown closely related to anthocyanin biosynthesis e.g. (Zhou et al., 2020), in *Arabidopsis thaliana*, subfamily 5 AtMYB123 was involved in the accumulation of procyanidine in seeds coat, 6 AtMYB75, AtMYB90, AtMYB113, and AtMYB114 regulated the synthesis of anthocyanins in nutritional tissues, and 7 AtMYB11, AtMYB12, and AtMYB111 regulated the synthesis of anthocyanins in all *Arabidopsis* organs. In addition, most members of subclade 4 were negative regulators of the anthocyanin synthesis pathway in Arabidopsis. Our results suggested that MYB3 and MYB90, the R2R3-MYB transcription factor family members, increased the anthocyanin content by regulating the expression of structural genes such as *PAL*, *4CL*, *F3'5'H*, *LDOX*, and *F3'H*. Further, our data present a potential working model for elucidating the molecular mechanism of mung bean anthocyanin synthesis (Figure S3), however, how MYB3 and MYB90 precisely control anthocyanin synthesis required further investigation.

5 Conclusions

This study compared two different mung bean varieties with significantly different anthocyanin accumulation as test material. High-throughput sequencing analysis results showed that anthocyanin accumulation in ZL23 was mainly concentrated in the leaf veins, petioles, and hypocotyls. Transcriptome combined with WGCNA analysis indicated MYB3 and MYB90 were responsible for increasing anthocyanin content by inducing the expression of structural genes such as anthocyanin *PAL*, *4CL*, *F3'5'H*, *LDOX*, and *F3'H*. Our study further suggests that the nuclear localization of MYB3 and MYB90 were highly correlated with anthocyanin biosynthesis, which is envisaged to play a pivotal regulatory role in the biological process of anthocyanin biosynthesis in mung beans. It is envisaged to further enhance the current understanding of anthocyanin biosynthesis in mung beans and provide valuable information for breeding anthocyanin-rich cereals.

Data availability statement

The datasets presented in this study can be found in online repositories. The names of the repository/repositories and accession number(s) can be found below: BioProject, PRJNA991706.

Author contributions

CL: conceptualization, methodology, data curation, writing-original draft preparation, writing-review and editing, visualization, supervision and funding acquisition. ZG: conceptualization and writing-original draft preparation. WH: software and validation. XZ: software and validation. YL: investigation. NL: investigation. CM: conceptualization, methodology, data curation, writing-review and editing, visualization, supervision, project administration and funding acquisition. All authors contributed to the article and approved the submitted version.

Funding

The author(s) declare financial support was received for the research, authorship, and/or publication of this article. This work is supported by the National Natural Science Foundation of China (32372227), the Modern Agricultural Industry Technology System of Henan (HARS-22-04-G2), the National Natural Science Foundation of Henan Province (222300420430), the Training Program for University Young Key Teachers in Henan Province (2021GGJS050), and the Doctoral Research Foundation of Henan University of Science and Technology (13480091).

Conflict of interest

The authors declare that the research was conducted in the absence of any commercial or financial relationships that could be construed as a potential conflict of interest.

Publisher's note

Supplementary material

The Supplementary Material for this article can be found online at: https://www.frontiersin.org/articles/10.3389/fpls.2023.1251464/full#supplementary-material

SUPPLEMENTARY FIGURE 1
(A-C) Plots of GO enrichment analysis of differentially expressed genes in the combination (GBvsBB, GLvsBL and GPvsBP) of AL12 and ZL23.

SUPPLEMENTARY FIGURE 2
(A-C) KEGG pathway from TSA enriched in the combination (GBvsBB, GLvsBL and GPvsBP) of AL12 and ZL23. y-axis indicates the KEGG pathway; x-axis indicates the enrichment fraction.

SUPPLEMENTARY FIGURE 3
A possible molecular mechanism model for anthocyanin biosynthesis in mung bean.

References

Bao, Y., Nie, T., Wang, D., and Chen, Q. (2022). Anthocyanin regulatory networks in *Solanum tuberosum* L. leaves elucidated via integrated metabolomics, transcriptomics, and stan1 overexpression. *BMC Plant Biol.* 22, 1–17. doi: 10.1186/s12870-022-03557-1

Chen, L., Shi, X., and Nian, B. (2020). Alternative splicing regulation of anthocyanin biosynthesis in camellia sinensis var. assamica unveiled by pacbio iso-seq. *G3-Genes.Genom. Genet.* 10, 2713–2723. doi: 10.1534/g3.120.401451

Chen, Y., Yang, X., He, K., Liu, M., Li, J., Gao, Z., et al. (2006). The myb transcription factor superfamily of arabidopsis: expression analysis and phylogenetic comparison with the rice MYB family. *Plant Mol. Biol.* 60, 107. doi: 10.1007/s11103-005-2910-y

Deng, J., Li, J., Su, M., Lin, Z., Chen, L., and Yang, P. (2020). A BHLH gene NNTT8 of nelumbo nucifera regulates anthocyanin biosynthesis. *Plant Physiol. Bioch.* 158, 518–523. doi: 10.1016/j.plaphy.2020.11.038

Dong, W., Niu, L., Li, H., and Gao, F. (2016). Isolation and analysis of the promoter of IbMYB1 gene from storage roots of purple-fleshed sweet potato. *J. Plant Biochem. Biot.* 25, 278–284. doi: 10.1007/s13562-015-0339-1

Flores, P., Yoon, J., Kim, D., and Seo, Y. (2022). Transcriptome analysis of MYB genes and patterns of anthocyanin accumulation during seed development in wheat. *Evol. Bioinform.* 17, 1–12. doi: 10.1177/11769343221093341

Fu, D., Hui, Y., Chen, Y., Yang, S., and Gao, F. (2022). Screening of upstream transcript factors of IbMYB1-1by yeast one-hybrid in purple-fleshed sweet potato. *Trop. Plant Biol.* 15, 148–156. doi: 10.1007/s12042-022-09309-7

Gao, H., Jiang, H., Cui, J., You, C., and Li, Y. (2021). Review: The effects of hormones and environmental factors on anthocyanin biosynthesis in apple. *Plant Sci.* 312, 111024. doi: 10.1016/j.plantsci.2021.111024

Gong, X., Ferdinand, U., Dang, K., and Feng, B. (2020). Boosting proso millet yield by altering canopylight distribution in proso millet|mung bean intercropping systems. *Crop J.* 8, 365–377. doi: 10.1016/j.cj.2019.09.009

Han, I., and Na, S. (2021). Health promoting effect of tofus prepared with Mung bean and soybean. *Cereal Chem.* 98, 1175–1182. doi: 10.1002/cche.10469

He, R., Liu, K., Zhang, S., Ju, J., Hu, Y., Li, Y., et al. (2023). Omics analysis unveils the pathway involved in theanthocyanin biosynthesis in tomato seedling and fruits. *Int. J. Mol. Sci.* 24, 10. doi: 10.3390/ijms24108690

Heller, W., Britsch, L., and Grisebach, F. (1985). Leucoanthocyanidins as intermediates in anthocyanidin biosynthesis in flowers of Matthiola incana R. Br. *Planta* 163, 191–196. doi: 10.1007/BF00393505

Hu, X., Liu, Li, W., Wen, T., Li, T., Guo, X., et al. (2020). Anthocyanin accumulation, biosynthesis and antioxidant capacity of black sweet corn (*Zea mays L.*) during kernel development over two growing seasons - ScienceDirect. *J. Cereal. Sci.* 95, 103065. doi: 10.1016/j.jcs.2020.103065

Ilyas, N., Ambreen, F., Batool, N., Arshad, M., and Saeed, M. (2018). Contribution of nitrogen fixed by Mung beanto the following wheat crop. *Commun. Soil. Sci.Plan.* 49, 148–158. doi: 10.1080/00103624.2017.1421215

Jiang, W., Liu, T., Nan, W., Jeewani, D., Niu, Y., Li, C., et al. (2018). Two transcription factors TaPpm1 and TaPpb1 co-regulate anthocyanin biosynthesis in purple pericarps of wheat. *J. Exp. Bot.* 69, 2555–2567. doi: 10.1093/jxb/ery101

Ju, Z., Liu, C., and Yuan, Y. (1995). Activities of chalcone synthase and UDPGal: flavonoid-3-o-glycosyltransferase in relation to anthocyanin synthesis in apple. *Sci. Hortic.* 63, 175–185. doi: 10.1016/0304-4238(95)00807-6

Kan, L., Nie, S., Hu, J., Wang, S., Bai, Z., Wang, J., et al. (2018). Comparative study on the chemical composition, anthocyanins, tocopherols and carotenoids of selected legumes. *Food Chem.* 260, 317–326. doi: 10.1016/j.foodchem.2018.03.148

Kuang, Q., Yu, Y., Attree, R., and Xu, B. (2018). A comparative study on anthocyanin, saponin, and oil profiles of black and red seed coat peanut (*Arachis hypogacea*) grown in China. *Int. J. Food. Prop.* 20, S131–S140. doi: 10.1080/10942912.2017.1291676

Kumar, S., and Pandey, G. (2020). Biofortification of pulses and legumes to enhance nutrition. *Heliyon* 6, 3. doi: 10.1080/10942912.2017.1291676

Leyrer, J., Hunter, R., Rubilar, M., Pavez, B., and Torres, S. (2016). Development of dye-sensitized solar cells based on naturally extracted dye from the maqui berry (*Aristotelia Chilensis*). *Opt. Mater.* 60, 411–417. doi: 10.1016/j.optmat.2016.08.021

Li, A., Xiao, R., He, S., An, X., He, Y., Wang, C., et al. (2019a). Research advances of purple sweet potato anthocyanins:extraction, identification, stability, bioactivity, application, and biotransformation. *Molecules* 24, 21. doi: 10.3390/molecules24213816

Li, D., Su, X., Lei, Z., Li, M., Gong, X., Cheng, S., et al. (2022a). Proline-rich protein MdPRP6 alters low nitrogen stress tolerance by regulating lateral root formation and anthocyanin accumulation in transgenicapple (*Malus domestica*). *Environ. Exp. Bot.* 197, 104841. doi: 10.1016/j.envexpbot.2022.104841

Li, H., Lv, Q., Ma, C., Qu, J., and Chen, Q. (2019b). Metabolite profiling and transcriptome analyses provide insights into the flavonoid biosynthesis in the developing seed of tartary buckwheat (*Fagopyrum tataricum*). *J. Agr. Food Chem.* 67, 11262–11276. doi: 10.1021/acs.jafc.9b03135

Li, H., Lv, Q., Liu, A., Wang, J., Sun, X., Deng, J., et al. (2022b). Comparative metabolomics study of Tartary (*Fagopyrum tataricum (L.) Gaertn*) and common (*Fagopyrum esculentum Moench*) buckwheat seeds. *Food Chem.* 371, 131125. doi: 10.1016/j.foodchem.2021.131125

Li, M., Zhou, Y., Li, K., and Guo, H. (2023). Genome-wide comparative analysis of the r2r3-myb gene family in six ipomoea species and the identification of anthocyanin-related members in sweet potatoes. *Plants-Basel* 12, 8. doi: 10.3390/ijms23042259

Li, S., He, Y., Li, L., Li, D., and Chen, H. (2022c). New insights on the regulation of anthocyanin biosynthesis in purple Solanaceous fruit vegetables. *Sci. Hortic-amsterdam.* 297, 110917. doi: 10.1016/j.scienta.2022.110917

Li, X., Li, Y., Zhao, M., Hu, Y., Meng, F., Song, X., et al. (2021). Molecular and metabolic insights into anthocyanin biosynthesis for leaf color change in chokecherry (*Padus virginiana*). *Int. J. Mol. Sci.* 22, 19. doi: 10.3390/ijms221910697

Liu, R., Ding, L., Li, M., Cao, W., Wang, Y., Yu, Y., et al. (2020). Characterization of a rapeseed anthocyanin-more mutant with enhanced resistance to sclerotinia sclerotiorum. *J. Plant Growth. Regul.* 39, 703–716. doi: 10.1007/s00344-019-10011-4

Lopez-Malvar, A., Ordas, B., Souto, C., Encina, A., Malvar, R., and Santiago, R. (2017). Chemical changes during maize tissue aging and its relationship with mediterranean corn borer resistance. *J. Agr. Food. Chem.* 65, 9180–9185. doi: 10.1021/acs.jafc.7b02911

Lu, C., Pu, Y., Liu, Y., Li, Y., Qu, J., Huang, H., et al. (2019). Comparative transcriptomics and weighted gene co-expression correlation network analysis (WGCNA) reveal potential regulation mechanism of carotenoid accumulation in Chrysanthemum × morifolium-ScienceDirect. *Plant Physiol. Bioch.* 142, 415–428. doi: 10.1016/j.plaphy.2019.07.023

Luo, J., Cai, W., Wu, T., and Xu, B. (2016). Phytochemical distribution in hull and cotyledon of adzki bean (*Vigna angularis L.*) and Mung bean (*Vigna radiate L.*), and their contributionto antioxidant, anti-inflammatory and anti-diabetic activities. *Food Chem.* 201, 350–360. doi: 10.1016/j.foodchem.2016.01.101

Ma, C., Feng, Y., Zhou, S., Zhang, J., Guo, B., Xiong, Y., et al. (2023). Metabolomics and transcriptomics provide insights into the molecular mechanisms of anthocyanin accumulation in the seed coat of differently colored Mung bean (*Vigna radiata L.*). *Plant Physiol. Bioch.* 200, 107739. doi: 10.1016/j.plaphy.2023.107739

Mackon, E., Charlie, G., Dongho, J., Ma, Y., Kashif, M., Ali, N., et al. (2021). Recent insights into anthocyanin pigmentation, synthesis, trafficking, and regulatory mechanisms in rice (*Oryza sativa L.*) caryopsis. *Biomolecules* 11, 3. doi: 10.3390/biom11030394

Masukawa, T., Cheon, K. ,. S., Mizuta, D., Akira, N., and Nobuo, K. (2018). Insertion of a retrotransposon into a Flavonoid 3'-hydroxylase homolog confers the red root character in the Radish (*Raphanus sativus L.* var. *longipinnatus L. H. Bailey*). *Horticulture J.* 87, 1. doi: 10.2503/hortj.OKD-075

Meldgaard, M. (1992). Expression of chalcone synthase, dihydroflavonol reductase and flavanone-3-hydroxylase in mutants of barley deficient in anthocyanin and proantocyanidin biosynthesis. *Theor. Appl. Genet.* 83, 695–706. doi: 10.1007/BF00226687

Mo, X., Zhang, M., Zhang, Z., Lu, X., Liang, C., and Tian, J. (2021). Phosphate (Pi) starvation up-regulated GmCSN5A/Bparticipates in anthocyanin synthesis in Soybean (*Glycine max*) dependent on Pi availability. *Int. J. Mol. Sci.* 22, 12348. doi: 10.3390/ijms222212348

Paulsmeyer, M., Vermillion, K., and Juvik, J. (2022). Assessing the diversity of anthocyanin composition in various tissues of purple corn (*Zea mays L.*). *Phytochemistry* 201, 113263. doi: 10.1016/j.phytochem.2022.113263

Peanparkdee, M., Patrawart, J., and Iwamoto, S. (2020). Physicochemical stability and in *vitro* bioaccessibility of phenolic compounds and anthocyanins from Thai rice bran extracts. *Food Chem.* 329, 127157. doi: 10.1016/j.foodchem.2020.127157

Qi, E., Jia, X., Lv, H., Huang, W., Wen, G., Li, Z., et al. (2023). Mining genes related to anthocyanin synthesis and regulation in different potato varieties based on comparative transcriptomics. *J. Plant Biochem. Biot.* 32, 363–374. doi: 10.1007/s13562-022-00816-y

Qian, X., Zang, H., Xu, H., Hu, Y., Ren, C., Guo, L., et al. (2018). Relay strip intercropping of oat with maize, sunflowerand mung bean in semi-arid regions of northeast China: Yield advantages and economic benefits. *Field Crops Res.* 223, 33–40. doi: 10.1016/j.fcr.2018.04.004

Rouholamin, S., Zahedi, B., Nazarian-Firouzabadi, F., and Saei, A. (2015). Expression analysis of anthocyanin biosynthesis key regulatory genes involved in pomegranate (*Punica granatum L.*). *Sci. Hortic-amsterdam.* 186, 84–88. doi: 10.1016/j.scienta.2015.02.017

Sahu, J., Panda, D., Baruah, G., Patar, L., Sen, P., Borah, B., et al. (2019). Revealing shared differential co-expression profiles in rice infected by virus from reoviridae and sequiviridae group. *Gene* 698, 82–91. doi: 10.1016/j.gene.2019.02.063

Saigo, T., Wang, T., Watanabe, M., and Tohge, T. (2020). Diversity of anthocyanin and proanthocyanin biosynthesis in land plants. *Curr. Opin. Plant Biol.* 55, 93–99. doi: 10.1016/j.pbi.2020.04.001

Sharma, S., Holme, I., Dionisio, G., Kodama, M., Dzhanfezova, T., Joernsgaard, B., et al. (2020). Cyanidin based anthocyanin biosynthesis in orange carrot is restored by expression of AmRosea1 and AmDelila, MYB and bHLH transcription factors. *Plant Mol. Biol.* 103, 443–456. doi: 10.1007/s11103-020-01002-1

Shi, Q., Li, X., Du, J., and Li, X. (2019). Anthocyanin synthesis and the expression patterns of bHLH transcription factor family during development of the Chinese jujube fruit (*Ziziphus Jujuba Mill.*). *Forests* 10, 4. doi: 10.3390/f10040346

Shui, L., Li, W., Yan, M., Li, H., and Guo, F. (2022). Characterization of the R2R3-MYB transcription factor CsMYB113 regulates anthocyanin biosynthesis in Tea plants (*Camellia sinensis*). *Plant Mol. Biol. Rep.* 41, 46–58. doi: 10.1007/s11105-022-01348-4

Simoneau, I. (1999). Molecular characterization of the anthocyanidin synthase gene in Forsythia×intermedia reveals organ-specific expression during flower development. *Plant Sci.* 149, 73–79. doi: 10.1016/S0168-9452(99)00146-6

Stotz, G., Vlaming, P., Wiering., H., Schram, A., and Forkmann, G. (1985). Genetic and biochemical studies on flavonoid 3'-hydroxylation in flowers of Petunia hybrida. *Theor. Appl. Genet.* 70, 300–305. doi: 10.1007/BF00304915

Tanaka, Y., Yonekura, K., Fukuchi-Mizutani, M., Fukui, Y., Fujiwara, H., Ashikari, T., et al. (1996). Molecular and biochemical characterization of three anthocyanin synthetic enzymes from gentiana triflora. *Plant Cell Physiol.* 37, 711–716. doi: 10.1093/oxfordjournals.pcp.a029004

Thakur, S., Scanlon, M. G., Tyler, R. T., Milani, A., and Paliwal, J. (2019). Pulse flour characteristics from a wheatflour miller's perspective: a comprehensive review. *Compr. Rev. Food Sci. F.* 18, 3. doi: 10.1111/1541-4337.12413

Tunen, A., Koes, R., Spelt, C., Van, D., Stuitje, A., and Mol, J. (1988). Cloning of the two chalcone flavanone isomerase genes from Petunia hybrida: coordinate, light-regulated and differential expression of flavonoid genes. *EMBO J.* 7, 1257–1263. doi: 10.1002/j.1460-2075.1988.tb02939.x

Wan, Y., Zhang, M., Hong, A., Lan, X., Yang, H., and Liu, Y. (2020). Transcriptome and weighted correlation network analyses provide insights into inflorescence stem straightness in Paeonia lactiflora. *Plant Mol. Biol.* 102, 239–252. doi: 10.1007/s11103-019-00945-4

Wang, J., Bai, G., Li, J., Wang, Y., Leng, J., and Qin, J. (2013). Solvent extraction for determination of blueberry anthocyanins. *Chinses. J. Anal. Chem.* 40, 1952–1953. doi: 10.3724/SP.J.1096.2012.20901

Wienand, U., Weydemann, U., Niesbach-Kloesgen, U., Peterson, P., and Saedler, H. (1986). Molecular cloning of C2 locus of Zeamays, the gene coding for chalcone synthase. *Mol. Gen. Genet.* 203, 202–207. doi: 10.1007/BF00333955

Wim, V. D. E., and El-Esawe, S. K. (2014). Sucrose signaling pathways leading to fructan and anthocyanin accumulation: A dual function in abiotic and biotic stress responses? *Environ. Exp. Bot.* 108, 4–13. doi: 10.1016/j.envexpbot.2013.09.017

Xie, G., Zou, X., Liang, Z., Wu, D., He, J., Xie, K., et al. (2022). Integrated metabolomic and transcriptomic analyses reveal molecular response of anthocyanins biosynthesis in perilla to light intensity. *Front. Plant Sci.* 13, 976449. doi: 10.3389/fpls.2022.976449

Yang, L., Zhang, D., Qiu, S., Gong, Z., and Shen, H. (2017). Effects of environmental factors on seedling growthand anthocyanin content in Betula 'Royal Frost' leaves. *J. Forestry. Res.* 28, 1147–1155. doi: 10.1007/s11676-017-0487-3

Yin, X., Zhang, Y., Zhang, L., Wang, B., Zhao, Y., Irfan, M., et al. (2021). Regulation of MYB transcription factors of anthocyanin synthesis in lily flowers. *Front. Plant Sci.* 12. doi: 10.3389/fpls.2021.761668

Yousuf, B., Singh, P., Gul, K., and Wani, A. A. (2016). Health benefits of anthocyanins and their encapsulation for potential use in food systems: a review. *Crit. Rev. Food Sci.* 56, 13. doi: 10.1080/10408398.2013.805316

Zhao, Q., Chen, Z., Khalifa, M. A. S., Yin, F., Qu, X., Zhang, J., et al. (2022). DNA fingerprinting construction and genetic diversity analysis for azuki bean (*Vigna angularis*) and mung bean (*Vigna radiata L.*) germplasm resources. *Legume Res.* 2, 45. doi: 10.18805/LRF-652

Zhao, S., Xi, X., Zong, Y., Li, S., Li, Y., Cao, D., et al. (2019). Overexpression of ThMYC4E enhances anthocyanin biosynthesis in common wheat. *Int. J. Mo. Sci.* 21, 1. doi: 10.3390/ijms21010137

Zhou, H., Kui, L., Wang, H., Gu, C., Dare, A., Espley, R., et al. (2015). Molecular genetics of blood-fleshed peach reveals activation of anthocyanin biosynthesis by NAC transcription factors. *Plant J.* 82, 105–121. doi: 10.1111/tpj.12792

Zhou, L., Rajesh, Y., Longfei, J., and Cao, H. (2020). Genome-wide identification and expression analysis of MYB gene family in oil palm (*Elaeis guineensis Jacq.*) under abiotic stress conditions. *Environ. Exp. Bot.* 180, 104245. doi: 10.1007/s00709-021-01666-6

Zhu, Y. S., Sun, S., and Richard, F. G. (2018). Mung bean proteins and peptides: nutritional, functional and bioactive properties. *J. Food. Nutr. Res.* 62, 1290. doi: 10.29219/fnr.v62.1290

frontiers | Frontiers in Plant Science

TYPE Review
PUBLISHED 15 December 2023
DOI 10.3389/fpls.2023.1330586

OPEN ACCESS

EDITED BY
Deyu Xie,
North Carolina State University, United States

REVIEWED BY
Mehran Dastmalchi,
McGill University, Canada
Junbo Gou,
Hubei University of Chinese Medicine, China

*CORRESPONDENCE
Yansheng Zhang
zhangys1@shu.edu.cn

RECEIVED 31 October 2023
ACCEPTED 01 December 2023
PUBLISHED 15 December 2023

CITATION
Li C and Zhang Y (2023) Glycosylation and methylation in the biosynthesis of isoflavonoids in *Pueraria lobata*. *Front. Plant Sci.* 14:1330586. doi: 10.3389/fpls.2023.1330586

Glycosylation and methylation in the biosynthesis of isoflavonoids in *Pueraria lobata*

Changfu Li and Yansheng Zhang*

Shanghai Key Laboratory of Bio-Energy Crops, School of Life Sciences, Shanghai University, Shanghai, China

The pathway for forming isoflavonoid skeletal structure is primarily restricted to the Leguminosae family. Subsequent decorations on the compound backbone by tailoring enzymes would change their biological and medicinal properties. *Pueraria lobata* is a leguminous plant, and as a traditional Chinese medicine its roots have been ascribed a number of pharmacological activities. Glycosylation and methylation are the main modifying processes in isoflavonoid metabolism in *P. lobata* roots, resulting in the accumulation of unique glycosylated and methylated end isoflavonoid compounds. For instance, daidzein 8-*C*-glucoside (i.e., puerarin) and puerarin derivatives are produced only by the *Pueraria* genus. Puerarin has been established as a clinical drug for curing cardiovascular diseases. To better understand the characteristic isoflavonoid metabolism in *P. lobata*, this review attempts to summarize the research progress made with understanding the main glycosylation and methylation of isoflavonoids in *P. lobata* and their biosynthetic enzymes.

KEYWORDS

glycosylation, methylation, isoflavonoid, pueraria, biosynthesis

Introduction

Among the 26 *Pueraria* species listed in the plant database (www.theplantlist.org), only three species, *Pueraria lobata* (Willd.) ohwi (Figure 1A), *Pueraria thomsonii* Benth, and *Pueraria peduncularis* Benth, have been included into Chinese Pharmacopoeia (Wang et al., 2020). The dried root of *P. lobata* (Figure 1B), also called Ge-Gen in China, is used as traditional herb medicine mainly for treating cardiovascular diseases, vascular hypertension, and diabetes (Ehrman et al., 2007; Wong et al., 2011). Modern pharmacological studies have revealed hepatoprotective (Sun et al., 2019), anti-inflammatory (Xi C. et al., 2023), anti-boneloss (Yang et al., 2017), and anti-cancer effects (Ahmad et al., 2020) of *P. lobata* extracts.

Isoflavonoid compounds are considered the main bioactive components of *P. lobata* (Rong et al., 1998). A significant example is puerarin (i.e., daidzein 8-*C*-glucoside), an isoflavone that has been used as a prescribed drug in clinical practice for

the treatment of cardiovascular diseases (Zhou et al., 2021). The biosynthetic pathway for the formation of isoflavonoid backbone is predominantly conserved in legumes (Falcone Ferreyra et al., 2012). Subsequent modifications on the isoflavonoid skeleton, such as glycosylation and methylation, result in the difference in isoflavonoid composition between different leguminous species. For instance, puerarin and its glycosylated and/or methylated derivatives (e.g. 3'-methoxy puerarin, 6''-*O*-xylosylpuerarin and puerarin 4'-*O*-glucoside) are produced only by the species within the *Pueraria* genus (Wang et al., 2020), therefore conferring their unique medicinal value for human. Phytochemical studies revealed glycosylation and methylation as the two major modifications in isoflavonoid metabolism in *P. lobata* (Wang et al., 2020). As a consequence, pharmacological activities of *P. lobata* have focused mainly on the specifically glycosylated or/and methylated isoflavonoids, such as puerarin (Wang et al., 2022) and 3'-methoxy puerarin (Zhao et al., 2007). There is intense interest in identifying the enzymes responsible for the glycosylation and methylation reactions for isoflavonoid metabolism in *P. lobata*. This review considers the recent progress in understanding the biochemistry of the glycosylation and methylation for isoflavonoid metabolism in *P. lobata*.

Isoflavonoid metabolism in *Pueraria lobata*

Isoflavonoid glycosides from *Pueraria* are mainly the *C*- and *O*-glycosides (Wang et al., 2020). The glycol-conjugation towards *Pueraria* isoflavonoids occurs primarily at the positions of *O*-7, *C*-8, and *O*-4' (Wang et al., 2020) (Figure 1C). Mono-glycosylation at *C*-8 or *O*-7 seems to be prevalent in *P. lobata*, as the most abundant isoflavone glycosides in *P. lobata* include the 7-*O*-glucosides of genistein and daidzein, and the 8-*C*-glucosides of daidzein (i.e., puerarin) (Ohshima et al., 1988; Rong et al., 1998; Wang et al., 2016). *P. lobata* root also accumulates the 4'-*O*-glucosides of puerarin, genistein, and daidzein (Ohshima et al., 1988; Li et al., 2010; Wang et al., 2016), and daidzein 4',7-*O*-diglucosides (Keung et al., 1996). Glycosylation reaction is enzymatically driven by uridine diphosphate (UDP)-sugar glycosyltransferases (UGTs), and the UGTs involved in plant secondary metabolism usually belong to the family 1 UGTs, which possess the signature PSPG (plant secondary product glycosyltransferase consensus sequence) motif at their *C*-terminal (Vogt and Jones, 2000).

The common sites for methylation of *P. lobata* isoflavonoids are *O*-4', *O*-3', and *O*-7 (Figure 1D). The majority of methylated isoflavonoids in *P. lobata* are 4'-*O*-methylated isoflavones represented by formononetin (4'-*O*-methyldaidzein) and biochanin A (5-hydroxy formononetin), while the 3'- and 7-*O*-methylated isoflavones are produced in much less amounts (Rong et al., 1998). The 4'- and 7-*O*-methylated isoflavones are also produced in other leguminous plant species, including *Medicago truncatula*, *Glycyrrhiza echinata*, *Medicago sativa*, and *Lotus japonicus* (He et al., 1998; Akashi et al., 2003; Deavours et al., 2006). Interestingly, the occurrence of 3'-*O*-methylated isoflavones seems to be restricted to the *Pueraria* genus. The *O*-methylation reaction is catalyzed by an OMT which transfers a methyl from the donor SAM (S-adenosyl-L-methionine) to a hydroxyl moiety of an acceptor.

Identification of UGTS and OMTS acting on isoflavonoids in *P. Lobata*

8-*C*-glycosyltransferase

The 8-*C*-glycosylation is required for puerarin formation. There is great interest in understanding the biochemical process for the formation of the 8-*C*-glycosyl group in puerarin (Inoue and Fujita, 1977; Wang et al., 2017; Bao et al., 2022). Some data remain contradictory, particularly regarding the step at which the 8-*C*-glucosyl group is introduced (Figure 2). Early labeling studies had proposed an upstream intermediate isoliquiritigenin at the chalcone stage, but not daidzein at the isoflavone stage, as an acceptor for the 8-*C*-glycosylation (Inoue and Fujita, 1977). However, an enzyme assay using the *Pueraria* root crude protein provided an implication that the *C*-glucosyl unit in puerarin might be introduced at the isoflavanone stage (He et al., 2011). This assumption is prone to being considered because that a number of flavone *C*-GTs recognize 2-hydroxyflavanone intermediates as their natural substrates (Brazier-Hicks et al., 2009; Nagatomo et al., 2014; Hirade et al., 2015). Nonetheless, Xi et al. revealed that there are no orthologs of 2-hydroxyflavanone *C*-GTs in *P. lobata* (Xi H.T. et al., 2023), indicating that if the *C*-glycosylation for puerarin biosynthesis occurs at the isoflavanone stage, it is probably catalyzed by a phylogenetically distinct UGT. A very recent labeling study provided evidence that both isoliquiritigenin and daidzein could be incorporated into puerarin *in vivo* (Adolfo et al., 2022), suggesting that the 8-*C*-glycosylation can happen at either the chalcone or isoflavone stage, or simultaneously at both levels.

For the first time, a *P. lobata* *C*-GT (namely PlUGT43), which directly transfers a glucose group to the C-8 position of daidzein leading to puerarin, was molecularly cloned from the root of *P. lobata* by Wang et al. (Wang et al., 2017). Through the *in vitro* assays, PlUGT43 was found to have no or negligible activity with the chalcone intermediate isoliquiritigenin (Wang et al., 2017). However, its isoform (officially named UGT71T5), which shares 99.72% sequence identity with PlUGT43, was recently reported to be capable of catalyzing the *C*-glycosylation activity against both daidzein and isoliquiritigenin (Adolfo et al., 2022). Incubation of the recombinant PlUGT43 or UGT71T5 with 2-hydroxyisoflavanone did not generate a product matching the 2-hydroxyisoflavanone *C*-glycoside (Wang et al., 2017; Adolfo et al., 2022), indicating that they had no *C*-glycosylation activity with 2-hydroxyisoflavanone. The RNAi-mediated down-regulation of UGT71T5 caused a strong reduction in the levels of puerarin in *P. lobata* hairy roots (Adolfo et al., 2022), confirming that PlUGT43 (UGT71T5) functions as a *C*-GT at least partially for puerarin biosynthesis in *P. lobata*. Interestingly, when the 2-HIS (2-hydroxyisoflavanone synthase; see its place in the pathway in

C

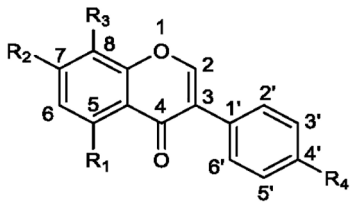

	R1	R2	R3	R4
7-*O*-Gly	H/OH	OGlc	H	OH
8-*C*-Gly	H/OH	OH	Glc	OH
4′-*O*-Gly	H/OH	OH	H	OGlc
4′,7-*O*-di-Gly	H/OH	OGlc	H	OGlc

D

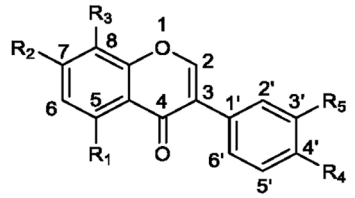

	R1	R2	R3	R4	R5
4′-*O*-Met	H/OH	OH/OGlc	H	OCH_3	H
3′-*O*-Met	H	OH	H/Glc	OH	OCH_3
7-*O*-Met	H/OH	OCH_3	H	OH	H
4′,7-di-*O*-Met	H/OH	OCH_3	H	OH	OCH_3

FIGURE 1
The medicinal plant *Pueraria lobata* and the main glycosylated and methylated isoflavonoids accumulated in it. **(A)** *P. lobata* plant. **(B)** The dried roots of *P. lobata* used in traditional Chinese medicine. **(C)** Structures of the main isoflavone glucosides. **(D)** Structures of the main *O*-methylated isoflavonoids.

Figure 2), which is the entry enzyme catalyzing the formation of isoflavonoid backbone (Steele et al., 1999; Jung et al., 2000), was down-regulated in *P. lobata* hairy roots, the potential *C*-glycosides of isoliquiritigenin and/or liquiritigenin significantly accumulated, when compared to that in the control roots (Adolfo et al., 2022). This data clearly supports that introduction of the *C*-glucosyl group can take place at the chalcone stage and then the 2-HIS would be able to accommodate the *C*-glycosides as substrates (Figure 2). Recently, another variant of PlUGT43, designated PlCGT, was identified from *P. lobata* by Ye et al. (Bao et al., 2022). PlCGT shows 97.01% amino acid identity with PlUGT43, and this variant essentially catalyzes the same *C*-glycosylation activity as PlUGT43 (Bao et al., 2022). An ortholog of PlUGT43, named PtUGT8, was also isolated from *P. thomsonii* species (Duan et al., 2022). Despite exhibiting a high sequence identity (96.52%) to PlUGT43, PtUGT8 was shown as primarily having a 7-*O*-glucosylation activity toward isoflavones whereas not catalyzing the 8-*C*-glycosylation reaction as does by PlUGT43 (Duan et al., 2022). In view of a previous finding that *O*- and *C*-GT can be easily shifted by changing only a few amino acids (Gutmann and Nidetzky, 2012), a subtle difference in the active sites of PtUGT8 and PlUGT43 may plausibly account for this discrepancy.

Taken together, combination of the published data from the *in vitro* assays using the recombinant UGTs, the *in vivo* labeling experiments, and the transgenic studies of *P. lobata* hairy roots strongly supports that during puerarin biosynthesis, the *C*-glucosylation reaction takes place most likely at either the chalcone or isoflavone stage, or both.

7-*O*-glycosyltransferase

The 7-*O*-glycosylation is common for isoflavonoid metabolism in leguminous plant species. In the 1980s, a relatively pure protein bearing the isoflavone 7-*O*-glucosylation activity was first purified from *Cicer arietinum* L (Koster and Barz, 1981). Later, genes encoding isoflavone 7-*O*-glucosyltransferases were isolated from the cell suspension cultures of *Glycyrrhiza echinata* (Nagashima et al., 2004), the roots (Noguchi et al., 2007) and seeds (Dhaubhadel et al., 2008) of *Glycine max*.

A total of six *P. lobata* UGTs, named PlUGT1(official UGT designation UGT88E12), PlUGT13(UGT88H1), PlUGT4 (UGT72Y3), PlUGT15(UGT88E23), PlUGT57(UGT84F7) and

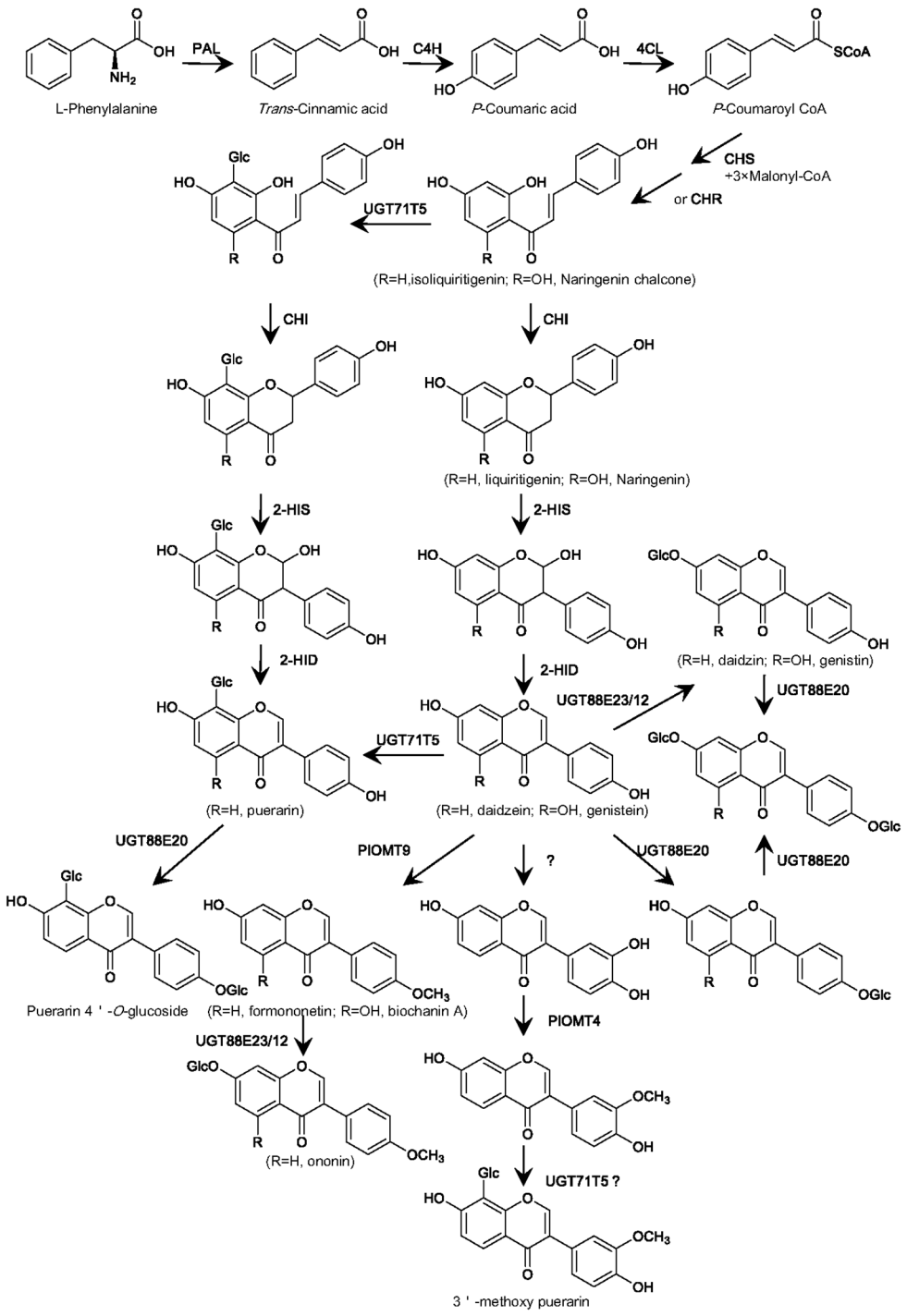

FIGURE 2
Proposed biosynthesis in *P. lobata* of the main glycosylated and methylated isoflavonoids based on the properties of the *P. lobata* UGTs and OMTs characterized so far. PAL, phenylalanine ammonialyase; C4H, cinnamate 4-hydroxylase; 4CL, 4-coumarate CoA ligase; CHS, chalcone synthase; CHR, chalcone reductase; CHI, chalcone isomerase; 2-HIS, 2-hydroxyisoflavanone synthase; 2-HID, 2-hydroxyisoflavanone dehydratase; UGT, UDP-glucosyltransferase; OMT, *O*-methyltransferase.

UGT88A40, had been characterized by *in vitro* assays as having an isoflavone 7-*O*-glucosylation activity on daidzein and genistein (Li et al., 2014; Wang et al., 2019; Adolfo et al., 2022). Analysis of the substrate conversion rate and enzymatic kinetic parameter revealed that both PlUGT1 and PlUGT15 are highly specific for isoflavones with no or little activity against other acceptors, including chalcones, flavanones, flavones, and flavonols (Li et al., 2014; Wang et al., 2019). The PlUGT13, PlUGT4, or UGT88A40 can accept relatively broad substrates and glycosylates substrates at different positions (Li et al., 2014; Adolfo et al., 2022). Although PlUGT57 also shows a strict substrate preference for isoflavone aglycones, its catalytic efficiency (K_{cat}/K_m; 2.10×10^3 $M^{-1}s^{-1}$) toward

daidzein, when UDP-glucose is used as a sugar donor, is about 20-fold lower than UGT88E12 (3.79×10^4 $M^{-1}s^{-1}$), and 80-fold lower than UGT88E23(1.75×10^5 $M^{-1}s^{-1}$) (Wang et al., 2019). Phylogenetic analysis (Li et al., 2014; Wang et al., 2019) revealed that PlUGT1 and PlUGT15 showed a close relationship with a *G. max* 7-*O*-UGT GmIF7GT (UGT88E3) that shows a substrate preference for isoflavones (Noguchi et al., 2007). Therefore, members of the UGT88E family are believed to truly contribute to the 7-*O*-glycosylation in isoflavonoid metabolism in *P. lobata*.

4′-*O*-glycosyltransferase

The presence of 4'-*O*-glucosides of daidzein, genistein, and puerarin (Ohshima et al., 1988; Fang et al., 2006), and 4',7-*O*-diglucoside of daidzein (Zhang et al., 2013) in *P. lobata* tissues suggests the occurrence of UGTs specific for 4'-*O*-glycosylating these compounds.

One full-length cDNA encoding PlUGT2 (officially assigned as UGT88E20) was identified and cloned from *P. lobata* using an RNA-sequencing approach (Wang et al., 2016). Tissue-specific expression analysis indicated that the transcript of PlUGT2 was higher in roots relative to stems and leaves. Phylogenetic analysis (Wang et al., 2016) showed that PlUGT2 was grouped into the same clade with GmUGT1 and GmUGT7 from *Glycine max*, which are the flavone 4'-*O*-UGTs (Funaki et al., 2015). The purified protein of PlUGT2 could catalyze either *O*-4'- or *O*-7-glucosylation of genistein, daidzein, liquiritigenin, and naringenin, yielding their mono-4'-*O*- or 7-*O*-glucosides. Interestingly, PlUGT2 consecutively glycosylates these mono-glucosides to di-glucosides with both *O*-4' and *O*-7 being glucosylated (Wang et al., 2016). In comparison with the mono-glycosylation, the di-glycosylation activity catalyzed by PlUGT2 is much lower, consistent with the fact that the 4',7-*O*-di-glucosides are produced at extremely low levels in *P. lobata* tissues (Zhang et al., 2013). PlUGT2 is the first 4'-*O*-glucosyltransferase identified from *P. lobata*. Recently, Adolfo et al. (Adolfo et al., 2022) reported another *P. lobata* UGT, named UGT73C42, which catalyzes either 4'- or 7-*O*-glucosylation of various polyphenolic compounds, including chalcones, flavones, and isoflavones.

PlUGT2 could also catalyze 4'- or 7-*O*-glucosylation of puerarin (Wang et al., 2016), which is currently a clinical drug for curing cardiovascular diseases (Zhou et al., 2021). Although puerarin is currently a prescribed drug, its low water solubility is still a serious drawback in clinical applications (Wang et al., 2012; Chen et al., 2021). Glycosylation is an efficient way to increase water solubility (Liu et al., 2016), thus, the identification of PlUGT2 would provide such an opportunity.

3′-*O*-methyltransferase

Many isoflavonoids are *O*-methylated with the methoxy residue improving their biological activities by increasing liposolubility (Wen et al., 2017). *P. lobata* accumulates 3'-methoxy-derivatives of isoflavones, including 3'-methoxydaidzein, 3'-methoxydaidzin, 3'-methoxypuerarin, and 3'-methoxyformononetin (Rong et al., 1998; Li et al., 2016b; Wang et al., 2020). Relative to the puerarin itself, its derivative 3'-methoxypuerarin exhibited better protective effects on cerebral ischemic-reperfusion injury in rats (Zhao et al., 2007).

One OMT, designated PlOMT4, was cloned (Li et al., 2016b) from *P. lobata* based on the *P. lobata* transcriptome database (Wang et al., 2015). Tissue-specific expression analysis revealed that PlOMT4 was expressed most highly in roots, and its transcript was up-regulated by MeJA (Li et al., 2016b). PlOMT4 was found to have the activity of methylating 3'-hydroxy daidzein to form 3'-methoxy-daidzein (Li et al., 2016b). PlOMT4 has no activity with the isoflavonoid substrates with free hydroxyl groups at either C7 or C4' (Li et al., 2016b), suggesting the methylation activity of PlOMT4 is region-specific. In addition, PlOMT4 is inactive with 3'-hydroxy puerarin (Li et al., 2016b), indicating that the 8-*C*-glucosylation of 3'-hydroxy daidzein prevents methylation at the 3'-position, and thereby the 3'-methylation should take place prior to the 8-*C*-glycosylation during 3'-methoxy-puerarin biosynthesis. PlOMT4 seems to be the only isoflavone specific 3'-*O*-methyltransferase so far identified from plant species.

4′- *O*-methyltransferase

In the early 1970s, scientists began a search for the isoflavone 4'-*O*-methyltransferase (I4'OMT) from plants. At a protein level, a methyltransferase, which catalyses the 4'-*O*-methylation of the isoflavone daidzein, was purified from *Cicer arietinum* L (Wengenmayer et al., 1974), indicating that the 4'-*O*-methylation for biosynthesis of 4'-*O*-methylated isoflavonoids can take place at the isoflavone stage. However, in alfalfa (*Medicago sativa* L.) seedlings, radiolabeled daidzein is not incorporated into 4'-*O*-methylated isoflavonoids (Dewick and Martin, 1979). Paradoxically, biosynthesis of the 4'-*O*-methylated isoflavonoids in alfalfa suspension cells strongly correlates with the isoflavone 7-*O*-methyltransferase (I7OMT) activity (Edwards and Dixon, 1991; He et al., 1998), and over-expression of the I7OMT led to enhanced levels of 4'-*O*-methylated isoflavonoids in the elicited alfalfa leaves(He and Dixon, 2000). In the elicited alfalfa leaves, the operationally soluble I7OMT re-locates to the endoplasmic reticulum where the 2-HIS naturally resides, leading to an interesting hypothesis that the association with other isoflavonoid pathway enzymes may change the region-specificity of I7OMT from the 7- to 4'-position *in vivo* (Liu and Dixon, 2001). On the other hand, an enzyme assay with the *Glycyrrhiza echinata* cell-free extract demonstrated that the 4'-*O*-methylation occurs at the level of 2,7,4'-trihydroxyisoflavanone (Akashi et al., 2000). This is supported by the molecular cloning and characterization of cDNAs encoding the 2,7, 4'-tri-hydroxyisoflavanone 4'-*O*-methyltransferase (HI4'OMT) from *Glycyrrhiza echinata* (Akashi et al., 2003), and *Medicago truncatula* (Deavours et al., 2006). The isoflavone daidzein could not be converted by HI4'OMT, and it only recognizes 2-trihydroxy-isoflavanone as the direct methyl acceptor (Akashi et al., 2003), suggesting that HI4'OMT catalyzes the 4'-*O*-methylation reaction only at the isoflavanone stage. Therefore, the history leading to the finding of isoflavonoid 4'-*O*-

methyltransferases demonstrates two alternative pathways likely involved: one is the simplest 4'-*O*-methylation occurring at the isoflavone stage, and the other is the reaction performed at the level of 2-hydroxyisoflavanones. From *P. lobata*, Li et al. identified a novel isoflavone 4'-*O*-methyltransferase (designated PlOMT9) that is capable of directly 4'-*O*-methylating isoflavones (Li et al., 2016a). Because that PlOMT9 shows the highest degree of amino acid identity with the isoflavone 7-*O*-methyltransferases (I7OMTs), PlOMT9 was initially presumed as an I7OMT. However, yeast cells expressing PlOMT9 efficiently performed the 4'-*O*-methylation of daidzein, genistein, prunetin, and isoformononetin (Li et al., 2016a), demonstrating that PlOMT9 functions actually as a I4'OMT. The I4'OMT activity catalyzed by PlOMT9 was further confirmed by *in vitro* assays using the purified recombinant PlOMT9 (Li et al., 2016a). Moreover, the recombinant PlOMT9 was not active with 2,7,4'-trihydroxy-isoflavanone, which is the natural substrate of HI4'OMT (Akashi et al., 2003). In addition to the main I4'OMT activity, PlOMT9 retains an extremely low 7-*O*-methylation activity, such as *O*-methylating daidzein at C7 position to yield trace amounts of isoformononetin. Over-expression of *PlOMT9* in *Glycine max* hairy roots increased the levels of formononetin and ononin (formononetin 7-*O*-glucoside) by 111.2% and 940.9%, respectively, in comparison with the controls. *P. lobata* contains a HI4'OMT-like enzyme (Li et al., 2016a), which shares 73% amino acid identity with the HI4'OMT from *G. echinata* (Akashi et al., 2003), but it is inactive either with 2,7,4'-trihydroxy-isoflavanone or the isoflavone daidzein (Li et al., 2016a).

Conclusion and prospects

In summary, utilizing the transcriptomic analysis, in combination with *in vitro* biochemical analysis of recombinant protein, provides a strong basis for understanding the biosynthetic mechanism of glycosylation and methylation of isoflavonoids in *P. lobata* (Figure 2). For the *O*-glycosylation of isoflavonoids in *P. lobata*, either 7-*O*- or 4'-*O*-glycosyltransferase protein is from members of the UGT88E subgroup. For the *C*-glycosylation of isoflavonoids, PlUGT43 (official designated UGT71T5) is the only isoflavone *C*-GT identified from plants so far. For the *O*-methylation of isoflavonoids in *P. lobata*, both 3'- and 4'-*O*-methyltransferases perform the methylation reactions at the isoflavone stage, directly utilizing isoflavones as the best acceptors.

Of particular value among the isoflavonoids are puerarin and its derivatives, which are produced exclusively in *Pueraria* species. Puerarin has been established as a clinical drug to deal with cardiovascular diseases (Wang et al., 2022). By expressing the *PlUGT43*, in combination with other pathway genes, the production of puerarin directly from glucose could be achieved in yeast at a concentration of 72.8 mg/L (Liu et al., 2021). The poor water solubility of puerarin is still a challenge in narrowing its treatment window in clinical usage (Liu et al., 2016). Considering that glycosylation is the most effective way to increase water solubility of small molecules (Li et al., 2004), the PlUGT2, which is capable of glucosylating puerarin, would provide an excellent template for further designing novel enzymes to increase the water solubility of puerarin.

Author contributions

CL: Writing – original draft. YZ: Funding acquisition, Writing – review & editing.

Funding

The author(s) declare financial support was received for the research, authorship, and/or publication of this article. This work was supported by the National Natural Science Foundation of China (32270416; 31870275; 31170284), and the National Key R&D Program of China (2018YFC1706200).

Conflict of interest

The authors declare that the research was conducted in the absence of any commercial or financial relationships that could be construed as a potential conflict of interest.

The author(s) declared that they were an editorial board member of Frontiers, at the time of submission. This had no impact on the peer review process and the final decision.

Publisher's note

References

Adolfo, L. M., Burks, D., Rao, X. L., Alvarez-Hernandez, A., and Dixon, R. A. (2022). Evaluation of pathways to the-glycosyl isoflavone puerarin in roots of kudzu (Pueraria montana lobata). *Plant Direct* 6 (9), e442. doi: 10.1002/pld3.442

Ahmad, B., Khan, S., Liu, Y., Xue, M. Z., Nabi, G., Kumar, S., et al. (2020). Molecular mechanisms of anticancer activities of Puerarin. *Cancer Manage. Res.* 12, 79–90. doi: 10.2147/Cmar.S233567

Akashi, T., Sawada, Y., Aoki, T., and Ayabe, S. (2000). New scheme of the biosynthesis of formononetin involving 2,7,4'-trihydroxyisoflavanone but not daidzein as the methyl acceptor. *Biosci. Biotechnol. Biochem.* 64 (10), 2276–2279. doi: 10.1271/bbb.64.2276

Akashi, T., Sawada, Y., Shimada, N., Sakurai, N., Aoki, T., and Ayabe, S. (2003). cDNA cloning and biochemical characterization of S-adenosyl-L-methionine: 2,7,4'-trihydroxyisoflavanone 4'-O-methyltransferase, a critical enzyme of the legume isoflavonoid phytoalexin pathway. *Plant Cell Physiol.* 44 (2), 103–112. doi: 10.1093/pcp/pcg034

Bao, Y. O., Zhang, M., Qiao, X., and Ye, M. (2022). Functional characterization of a *C*-glycosyltransferase from *Pueraria lobata* with dual-substrate selectivity. *Chem. Commun.* 58 (88), 12337–12340. doi: 10.1039/d2cc04279g

Brazier-Hicks, M., Evans, K. M., Gershater, M. C., Puschmann, H., Steel, P. G., and Edwards, R. (2009). The C-glycosylation of flavonoids in cereals. *J. Biol. Chem.* 284 (27), 17926–17934. doi: 10.1074/jbc.M109.009258

Chen, H., Pang, Z., Qiao, Q., Xia, Y., Wei, Y., Gao, Y., et al. (2021). Puerarin-na chelate hydrate simultaneously improves dissolution and mechanical behavior. *Mol. Pharm.* 18 (7), 2507–2520. doi: 10.1021/acs.molpharmaceut.1c00005

Deavours, B. E., Liu, C. J., Naoumkina, M. A., Tang, Y., Farag, M. A., Sumner, L. W., et al. (2006). Functional analysis of members of the isoflavone and isoflavanone *O*-methyltransferase enzyme families from the model legume Medicago truncatula. *Plant Mol. Biol.* 62 (4-5), 715–733. doi: 10.1007/s11103-006-9050-x

Dewick, P. M., and Martin, M. (1979). Biosynthesis of pterocarpan, isoflavan and coumestan metabolites of Medicago sativa: Chalcone,isoflavone and isoflavanone precursors. *Phytochemistry* 18, 597–602. doi: 10.1016/S0031-9422(00)84267-3

Dhaubhadel, S., Farhangkhoee, M., and Chapman, R. (2008). Identification and characterization of isoflavonoid specific glycosyltransferase and malonyltransferase from soybean seeds. *J. Exp. Bot.* 59 (4), 981–994. doi: 10.1093/jxb/ern046

Duan, H. Y., Wang, J., Zha, L. P., Peng, H. S., Zhao, Y. P., Yuan, Y., et al. (2022). Molecular cloning and functional characterization of an isoflavone glucosyltransferase from. *Chin. J. Nat. Med.* 20 (2), 133–138. doi: 10.1016/S1875-5364(21)60105-X

Edwards, R., and Dixon, R. A. (1991). Isoflavone *O*-methyltransferase activities in elicitor-treated cell suspension cultures of *Medicago sativa*. *Phytochemistry* 30, 2597–2606. doi: 10.1016/0031-9422(91)85107-B

Ehrman, T. M., Barlow, D. J., and Hylands, P. J. (2007). Phytochemical informatics of traditional Chinese medicine and therapeutic relevance. *J. Chem. Inf. Model.* 47 (6), 2316–2334. doi: 10.1021/ci700155t

Falcone Ferreyra, M. L., Rius, S. P., and Casati, P. (2012). Flavonoids: biosynthesis, biological functions, and biotechnological applications. *Front. Plant Sci.* 3. doi: 10.3389/fpls.2012.00222

Fang, C. B., Wan, X. C., Tan, H. R., and Jiang, C. J. (2006). Separation and determination of isoflavonoids in several kudzu samples by high-performance capillary electrophoresis (HPCE). *Annali Di Chimica* 96 (1-2), 117–124. doi: 10.1002/adic.200690002

Funaki, A., Waki, T., Noguchi, A., Kawai, Y., Yamashita, S., Takahashi, S., et al. (2015). Identification of a highly specific isoflavone 7-*O*-glucosyltransferase in the soybean (*Glycine max* (L.) Merr.). *Plant Cell Physiol.* 56 (8), 1512–1520. doi: 10.1093/pcp/pcv072

Gutmann, A., and Nidetzky, B. (2012). Switching between *O*- and *C*-Glycosyltransferase through exchange of active-site motifs. *Angewandte Chemie-International Edition* 51 (51), 12879–12883. doi: 10.1002/anie.201206141

He, X. Z., Blount, J. W., Ge, S. J., Tang, Y. H., and Dixon, R. A. (2011). A genomic approach to isoflavone biosynthesis in kudzu (*Pueraria lobata*). *Planta* 233 (4), 843–855. doi: 10.1007/s00425-010-1344-1

He, X. Z., and Dixon, R. A. (2000). Genetic manipulation of isoflavone 7-*O*-methyltransferase enhances biosynthesis of 4'-*O*-methylated isoflavonoid phytoalexins and disease resistance in alfalfa. *Plant Cell* 12 (9), 1689–1702. doi: 10.1105/tpc.12.9.1689

He, X. Z., Reddy, J. T., and Dixon, R. A. (1998). Stress responses in alfalfa (*Medicago sativa* L). XXII. cDNA cloning and characterization of an elicitor-inducible isoflavone 7-*O*-methyltransferase. *Plant Mol. Biol.* 36 (1), 43–54. doi: 10.1023/a:1005938121453

Hirade, Y., Kotoku, N., Terasaka, K., Saijo-Hamano, Y., Fukumoto, A., and Mizukami, H. (2015). Identification and functional analysis of 2-hydroxyflavanone *C*-glucosyltransferase in soybean (*Glycine max*). *FEBS Lett.* 589 (15), 1778–1786. doi: 10.1016/j.febslet.2015.05.010

Inoue, T., and Fujita, M. (1977). Biosynthesis of puerarin in *Pueraria* root. *Chem. Pharm. Bull.* 25, 3226–3231. doi: 10.1248/cpb.25.3226

Jung, W., Yu, O., Lau, S. M. C., O'Keefe, D. P., Odell, J., Fader, G., et al. (2000). Identification and expression of isoflavone synthase, the key enzyme for biosynthesis of isoflavones in legumes. *Nat. Biotechnol.* 18 (2), 208–212. doi: 10.1038/72671

Keung, W. M., Lazo, O., Kunze, L., and Vallee, B. L. (1996). Potentiation of the bioavailability of daidzin by an extract of Radix puerariae. *Proc. Natl. Acad. Sci. U.S.A.* 93 (9), 4284–4288. doi: 10.1073/pnas.93.9.4284

Koster, J., and Barz, W. (1981). UDP-glucose:isoflavone 7-*O*-glucosyltransferase from roots of chick pea (*Cicer arietinum* L.). *Arch. Biochem. Biophys.* 212 (1), 98–104. doi: 10.1016/0003-9861(81)90347-7

Li, D., Park, S. H., Shim, J. H., Lee, H. S., Tang, S. Y., Park, C. S., et al. (2004). *In vitro* enzymatic modification of puerarin to puerarin glycosides by maltogenic amylase. *Carbohydr. Res.* 339 (17), 2789–2797. doi: 10.1016/j.carres.2004.09.017

Li, G., Zhang, Q., and Wang, Y. (2010). Chemical constituents from roots of *Pueraria lobata*. *Zhongguo Zhong Yao Za Zhi* 35 (23), 3156–3160. doi: 10.4268/cjcmm20102314

Li, J., Li, C. F., Gou, J. B., Wang, X., Fan, R. Y., and Zhang, Y. S. (2016a). An alternative pathway for formononetin biosynthesis in. *Front. Plant Sci.* 7. doi: 10.3389/Fpls.2016.00861

Li, J., Li, C. F., Gou, J. B., and Zhang, Y. S. (2016b). Molecular cloning and functional characterization of a novel isoflavone 3'-*O*-methyltransferase from. *Front. Plant Sci.* 7. doi: 10.3389/Fpls.2016.00793

Li, J., Li, Z. B., Li, C. F., Gou, J. B., and Zhang, Y. S. (2014). Molecular cloning and characterization of an isoflavone 7-*O*-glucosyltransferase from. *Plant Cell Rep.* 33 (7), 1173–1185. doi: 10.1007/s00299-014-1606-7

Liu, C. J., and Dixon, R. A. (2001). Elicitor-induced association of isoflavone *O*-methyltransferase with endomembranes prevents the formation and 7-*O*-methylation of daidzein during isoflavonoid phytoalexin biosynthesis. *Plant Cell* 13 (12), 2643–2658. doi: 10.1105/tpc.13.12.2643

Liu, G., Liu, Z., and Yuan, S. (2016). Recent advances in methods of puerarin biotransformation. *Mini Rev. Med. Chem.* 16 (17), 1392–1402. doi: 10.2174/1389557516666160505114456

Liu, Q. L., Liu, Y., Li, G., Savolainen, O., Chen, Y., and Nielsen, J. (2021). *De novo* biosynthesis of bioactive isoflavonoids by engineered yeast cell factories. *Nat. Commun.* 12 (1), 6085. doi: 10.1038/S41467-021-26361-1

Nagashima, S., Inagaki, R., Kubo, A., Hirotani, M., and Yoshikawa, T. (2004). cDNA cloning and expression of isoflavonoid-specific glucosyltransferase from cell-suspension cultures. *Planta* 218 (3), 456–459. doi: 10.1007/s00425-003-1118-0

Nagatomo, Y., Usui, S., Ito, T., Kato, A., Shimosaka, M., and Taguchi, G. (2014). Purification, molecular cloning and functional characterization of flavonoid *C*-glucosyltransferases from *Fagopyrum esculentum* M. (buckwheat) cotyledon. *Plant J.* 80 (3), 437–448. doi: 10.1111/tpj.12645

Noguchi, A., Saito, A., Homma, Y., Nakao, M., Sasaki, N., Nishino, T., et al. (2007). A UDP-glucose:isoflavone 7-*O*-glucosyltransferase from the roots of soybean (*Glycine max*) seedlings. *J. Biol. Chem.* 282 (32), 23581–23590. doi: 10.1074/jbc.M702651200

Ohshima, Y., Okuyama, T., Takahashi, K., Takizawa, T., and Shibata, S. (1988). Isolation and high performance liquid chromatography (HPLC) of isoflavonoids from the *Pueraria* root. *Planta Med.* 54 (3), 250–254. doi: 10.1055/s-2006-962420

Rong, H., Stevens, J. F., Deinzer, M. L., Cooman, L. D., and Keukeleire, D. D. (1998). Identification of isoflavones in the roots of *Pueraria lobata*. *Planta Med.* 64 (7), 620–627. doi: 10.1055/s-2006-957534

Steele, C. L., Gijzen, M., Qutob, D., and Dixon, R. A. (1999). Molecular characterization of the enzyme catalyzing the aryl migration reaction of isoflavonoid biosynthesis in soybean. *Arch. Biochem. Biophys.* 367 (1), 146–150. doi: 10.1006/abbi.1999.1238

Sun, Y. J., Zhang, H. M., Cheng, M., Cao, S. J., Qiao, M., Zhang, B. L., et al. (2019). New hepatoprotective isoflavone glucosides from *Pueraria lobata* (Willd.) Ohwi. *Nat. Prod. Res.* 33 (24), 3485–3492. doi: 10.1080/14786419.2018.1484461

Vogt, T., and Jones, P. (2000). Glycosyltransferases in plant natural product synthesis: characterization of a supergene family. *Trends Plant Sci.* 5 (9), 380–386. doi: 10.1016/s1360-1385(00)01720-9

Wang, D., Bu, T., Li, Y. Q., He, Y. Y., Yang, F., and Zou, L. (2022). Pharmacological activity, pharmacokinetics, and clinical research progress of puerarin. *Antioxidants* 11 (11), 2121. doi: 10.3390/Antiox11112121

Wang, X., Fan, R., Li, J., Li, C., and Zhang, Y. (2016). Molecular cloning and functional characterization of a novel (Iso)flavone 4',7-*O*-diglucoside glucosyltransferase from Pueraria lobata. *Front. Plant Sci.* 7. doi: 10.3389/fpls.2016.00387

Wang, X., Li, S. T., Li, J., Li, C. F., and Zhang, Y. S. (2015). *De novo* transcriptome sequencing in *Pueraria lobata* to identify putative genes involved in isoflavones biosynthesis. *Plant Cell Rep.* 34 (5), 733–743. doi: 10.1007/s00299-014-1733-1

Wang, X., Li, C. F., Zhou, C., Li, J., and Zhang, Y. S. (2017). Molecular characterization of the *C*-glucosylation for puerarin biosynthesis in *Pueraria lobata*. *Plant J.* 90 (3), 535–546. doi: 10.1111/tpj.13510

Wang, X., Li, C. F., Zhou, Z. L., and Zhang, Y. S. (2019). Identification of three (Iso) flavonoid glucosyltransferases from *Pueraria lobata*. *Front. Plant Sci.* 10. doi: 10.3389/Fpls.2019.00028

Wang, Y., Ma, Y., Ma, Y., Du, Y., Liu, Z., Zhang, D., et al. (2012). Formulation and pharmacokinetics evaluation of puerarin nanocrystals for intravenous delivery. *J. Nanosci. Nanotechnol.* 12 (8), 6176–6184. doi: 10.1166/jnn.2012.6436

Wang, S. G., Zhang, S. M., Wang, S. P., Gao, P., and Dai, L. (2020). A comprehensive review on *Pueraria*: Insights on its chemistry and medicinal value. *Biomed. Pharmacother.* 131, 110734. doi: 10.1016/J.Biopha.2020.110734

Wen, L. R., Jiang, Y. M., Yang, J. L., Zhao, Y. P., Tian, M. M., and Yang, B. (2017). Structure, bioactivity, and synthesis of methylated flavonoids. *Ann. New York Acad. Sci.* 1398 (1), 120–129. doi: 10.1111/nyas.13350

Wengenmayer, H., Ebel, J., and Grisebach, H. (1974). Purification and properties of a *S*-adenosylmethionine: isoflavone 4'-*O*-methyltransferase from cell suspension cultures of Cicer arietinum L. *Eur. J. Biochem.* 50 (1), 135–143. doi: 10.1111/j.1432-1033.1974.tb03881.x

Wong, K. H., Li, G. Q., Li, K. M., Razmovski-Naumovski, V., and Chan, K. (2011). Kudzu root: Traditional uses and potential medicinal benefits in diabetes and cardiovascular diseases. *J. Ethnopharmacol.* 134 (3), 584–607. doi: 10.1016/j.jep.2011.02.001

Xi, C., Zhang, M. Y., Li, B. T., Meng, X. W., Xu, S. C., Du, H., et al. (2023). Metabolomics of the anti-inflammatory effect of *Pueraria lobata* and *Pueraria lobata* var. *Thomsonii* in rats. *J. Ethnopharmacol.* 306, 116144. doi: 10.1016/J.Jep.2023.116144

Xi, H. T., Zhu, Y. R., Sun, W. W., Tang, N., Xu, Z. Q., Shang, X. H., et al. (2023). Comparative transcriptome analysis of provides candidate genes involved in puerarin biosynthesis and its regulation. *Biomolecules* 13 (1), 170. doi: 10.3390/Biom13010170

Yang, X., Yang, Y., Zhou, S., Gong, X., Dai, Q., Zhang, P., et al. (2017). Puerarin stimulates osteogenic differentiation and bone formation through the ERK1/2 and p38-MAPK signaling pathways. *Curr. Mol. Med.* 17 (7), 488–496. doi: 10.2174/1566524018666171219101142

Zhang, Z., Lam, T. N., and Zuo, Z. (2013). Radix Puerariae: an overview of its chemistry, pharmacology, pharmacokinetics, and clinicpal use. *J. Clin. Pharmacol.* 53 (8), 787–811. doi: 10.1002/jcph.96

Zhao, T. F., Han, J., Chen, Y. Q., Wan, H. T., and Bie, X. D. (2007). The mechanism of 3-methoxy puerarin on decreasing the cerebral ischemia-reperfusion injury in rats. *Asia Pacific J. Clin. Nutr.* 16, 302–304.

Zhou, Y. X., Zhang, H., and Peng, C. (2021). Effects of puerarin on the prevention and treatment of cardiovascular diseases. *Front. Pharmacol.* 12. doi: 10.3389/fphar.2021.771793

frontiers | Frontiers in Plant Science

TYPE Original Research
PUBLISHED 23 January 2024
DOI 10.3389/fpls.2024.1307489

OPEN ACCESS

EDITED BY
Deyu Xie,
North Carolina State University, United States

REVIEWED BY
Xianzhi He,
North Carolina State University, United States
Katherine (Kate) M. Warpeha,
University of Illinois Chicago, United States

*CORRESPONDENCE
Sangeeta Dhaubhadel
sangeeta.dhaubhadel@agr.gc.ca

RECEIVED 04 October 2023
ACCEPTED 03 January 2024
PUBLISHED 23 January 2024

CITATION
Clayton EJ, Islam NS, Pannunzio K, Kuflu K, Sirjani R, Kohalmi SE and Dhaubhadel S (2024) Soybean AROGENATE DEHYDRATASES (GmADTs): involvement in the cytosolic isoflavonoid metabolon or trans-organelle continuity?
Front. Plant Sci. 15:1307489.
doi: 10.3389/fpls.2024.1307489

Soybean AROGENATE DEHYDRATASES (GmADTs): involvement in the cytosolic isoflavonoid metabolon or trans-organelle continuity?

Emily J. Clayton[1,2], Nishat S. Islam[1], Kelsey Pannunzio[1,2], Kuflom Kuflu[1], Ramtin Sirjani[1,2], Susanne E. Kohalmi[2] and Sangeeta Dhaubhadel[1,2]*

[1]London Research and Development Centre, Agriculture and Agri-Food Canada, London, ON, Canada, [2]Department of Biology, University of Western Ontario, London, ON, Canada

Soybean (*Glycine max*) produces a class of phenylalanine (Phe) derived specialized metabolites, isoflavonoids. Isoflavonoids are unique to legumes and are involved in defense responses *in planta*, and they are also necessary for nodule formation with nitrogen-fixing bacteria. Since Phe is a precursor of isoflavonoids, it stands to reason that the synthesis of Phe is coordinated with isoflavonoid production. Two putative AROGENATE DEHYDRATASE (ADT) isoforms were previously co-purified with the soybean isoflavonoid metabolon anchor ISOFLAVONE SYNTHASE2 (GmIFS2), however the *GmADT* family had not been characterized. Here, we present the identification of the nine member *GmADT* family. We determined that the GmADTs share sequences required for enzymatic activity and allosteric regulation with other characterized plant ADTs. Furthermore, the GmADTs are differentially expressed, and multiple members have dual substrate specificity, also acting as PREPHENATE DEHYDRATASES. All GmADT isoforms were detected in the stromules of chloroplasts, and they all interact with GmIFS2 in the cytosol. In addition, GmADT12A interacts with multiple other isoflavonoid metabolon members. These data substantiate the involvement of GmADT isoforms in the isoflavonoid metabolon.

KEYWORDS

soybean, arogenate dehydratase, isoflavone synthase, phenylalanine, isoflavonoid, metabolon, specialized metabolites

Introduction

Soybean (*Glycine max* [L.] Merr) is an important grain legume grown worldwide. Soybean seeds are high in oil and protein content, making them a nutrient-rich food source for both livestock and humans (Hill and Breidenbach, 1974; Messina, 2010). As one of the most cultivated oilseed crops, agricultural waste from soybean harvest has potential applications as a biofuel source (Yong and Wu, 2022). Soybeans also produce a legume unique class of specialized metabolites called isoflavonoids. Isoflavonoids are important signaling molecules, as they are essential for interaction between legumes and nitrogen-fixing bacteria (Phillips and Kapulnik, 1995; Subramanian et al., 2006; Hassan and Mathesius, 2012). Isoflavonoid glyceollins act as phytoalexins and provide defense against abiotic and biotic stress, such as resistance against the soil-borne pathogen *Phytophthora sojae* (Subramanian et al., 2006; Lozovaya et al., 2007), that cause massive crop losses (Bradley et al., 2021; Chandra et al., 2022). Furthermore, there is some evidence suggesting that isoflavonoids such as genistein and glyceollin have health benefits (Lamartiniere, 2000; Dixon and Ferreria, 2002; Sarkar and Li, 2003; Cederroth and Nef, 2009; Messina, 2010; Bhat et al., 2021). As such, isoflavonoids have been the target of traditional breeding and metabolic engineering to improve cultivar resistance to biotic and abiotic stress (Scott et al., 2021; Yousefi-Taemeh et al., 2021).

The biosynthesis of isoflavonoids is a complex process that is derived from the phenylpropanoid metabolism (Winkel, 2001), downstream from the synthesis of the aromatic amino acid phenylalanine (Phe). As shown in Figure 1, the first committed step of (iso)flavonoid biosynthesis is the action of CHALCONE SYNTHASE (CHS) to synthesize a chalcone scaffold from which all (iso)flavonoids are built (Winkel, 2006; Dastmalchi and Dhaubhadel, 2014). The key branch point of isoflavonoid synthesis from the flavonoid biosynthetic pathway is catalyzed by the cytochrome P450 enzyme ISOFLAVONE SYNTHASE (IFS) where naringenin and liquiritigenin are converted to isoflavones genistein and daidzein, respectively (Winkel, 2006; Dastmalchi and Dhaubhadel, 2014; García-Calderón et al., 2020). Many of the enzymes involved in (iso) flavonoid biosynthesis have been shown to form protein-protein interactions (Winkel, 2004; Jorgensen et al., 2005; Dastmalchi et al., 2016). The phenylpropanoid pathway was first proposed to form a multienzyme metabolon by Helen Stafford (1974) and further confirmed by Hrazdina and Wagner (1985), as an explanation for the efficiency of substrate channeling in specialized metabolite biosynthesis. Further evidence demonstrated that the metabolon includes enzymes involved in flavonoid synthesis, such as CHS, CHALCONE ISOMERASE (CHI), and FLAVONOL SYNTHASE (FLS) (Winkel, 2004; Nakayama et al., 2019). In soybean, this metabolon also includes key isoflavonoid biosynthetic enzymes CHALCONE REDUCTASE (CHR) and IFS (Figure 2) (Dastmalchi et al., 2016). The isoflavonoid biosynthetic metabolon is associated with the cytosolic surface of the endoplasmic reticulum (ER), anchored by the two ER membrane cytochrome P450 monooxygenase enzymes CINNAMATE 4-HYDROXYLASE (C4H) and IFS (Jorgensen et al., 2005; Dastmalchi et al., 2016). To date, the flavonoid metabolon has been identified in a wide range of plant species (Owens et al., 2008; Crosby et al., 2011; Waki et al., 2016; Nakayama et al., 2019), conferring a variety of advantages such as metabolic channeling of substrates, or the sequestering of toxic intermediates (Moller, 2010; Pareek et al., 2021; Zhang and Fernie, 2021).

When characterizing the soybean isoflavonoid metabolon, we detected an interaction between GmIFS2 and two putative AROGENATE DEHYDRATASES (ADTs), Glyma.12G181800.1 and Glyma.13G319000.1 (Dastmalchi et al., 2016). ADTs catalyze the final step in Phe biosynthesis via the arogenate pathway (Maeda and Dudareva, 2012) in which prephenate is converted to arogenate by a PREPHENATE AMINOTRANSFERASE (PPA-AT; (Graindorge et al., 2010; Maeda et al., 2011), followed by a decarboxylation/dehydration to Phe, catalyzed by an ADT (Jung et al., 1986; Ehlting et al., 2005; Cho et al., 2007). The interaction between ADT and IFS observed in our previous work was an unexpected finding (Dastmalchi et al., 2016), as ADTs have been shown to localize within the chloroplasts in other plant species, consistent with the chloroplastic localization of shikimate and arogenate pathway enzymes (Cho et al., 2007; Rippert et al., 2009; Maeda et al., 2010; El-Azaz et al., 2016). However, a second Phe biosynthetic route, the prephenate pathway, had been described where prephenate is first decarboxylated/dehydrated into phenylpyruvate by a PREPHENATE DEHYDRATASE (PDT; (Cotton and Gibson, 1965), which is then transaminated into Phe by the action of a PHENYLPYRUVATE AMINOTRANSFERASE (PPY-AT; (Cotton and Gibson, 1965; Fazel et al., 1980). While prephenate pathway is predominantly used by microbes, there was evidence for existence of the prephenate pathway in plants. PPY-ATs had been identified in several plant species (Watanabe et al., 2002; Kaminaga et al., 2006; Warpeha et al., 2006), and PDT activity had been reported in *Petunia hybrida*, *Arabidopsis*, *Oryza sativa* and *Pinus pinaster*, though the dual ADT/PDT enzymes have a preference for arogenate over prephenate (Cho et al., 2007; Yamada et al., 2008; Maeda et al., 2010; El-Azaz et al., 2016; El-Azaz et al., 2022). Recently, cytosolic Phe biosynthesis *via* the prephenate pathway was reported in *Petunia x hybrida* (Yoo et al., 2013; Qian et al., 2019) and is expected to act in parallel with the arogenate pathway. As the isoflavonoid metabolon is anchored to the cytosolic face of the ER, the two GmADTs identified as part of the isoflavonoid metabolon (Dastmalchi et al., 2016) could be part the cytosolic Phe synthesis route, and may have PDT activity. As most plant genomes encode at least two, if not more *ADT* genes, there are likely many more than two GmADT isoforms present in soybean as it is a paleopolyploid. These isoforms may also interact with the isoflavonoid metabolon. However, the complete GmADT family has not been characterized.

Here we identified additional ADT family members in soybean and describe their gene structure, phylogeny, tissue-specific gene expression and subcellular localization. We demonstrate that some members of the GmADT family contain PDT activity in yeast complementation analysis. Despite the fact that all GmADTs were detected in the chloroplast, we confirmed their ability to interact with GmIFS2 and multiple other isoflavonoid metabolon enzymes *in planta*. Together, these data suggest that members of the GmADT family are associating with the isoflavonoid metabolon, and those with PDT activity could be supplying Phe to the metabolon through a cytosolic prephenate pathway.

10.3389/fpls.2024.1307489

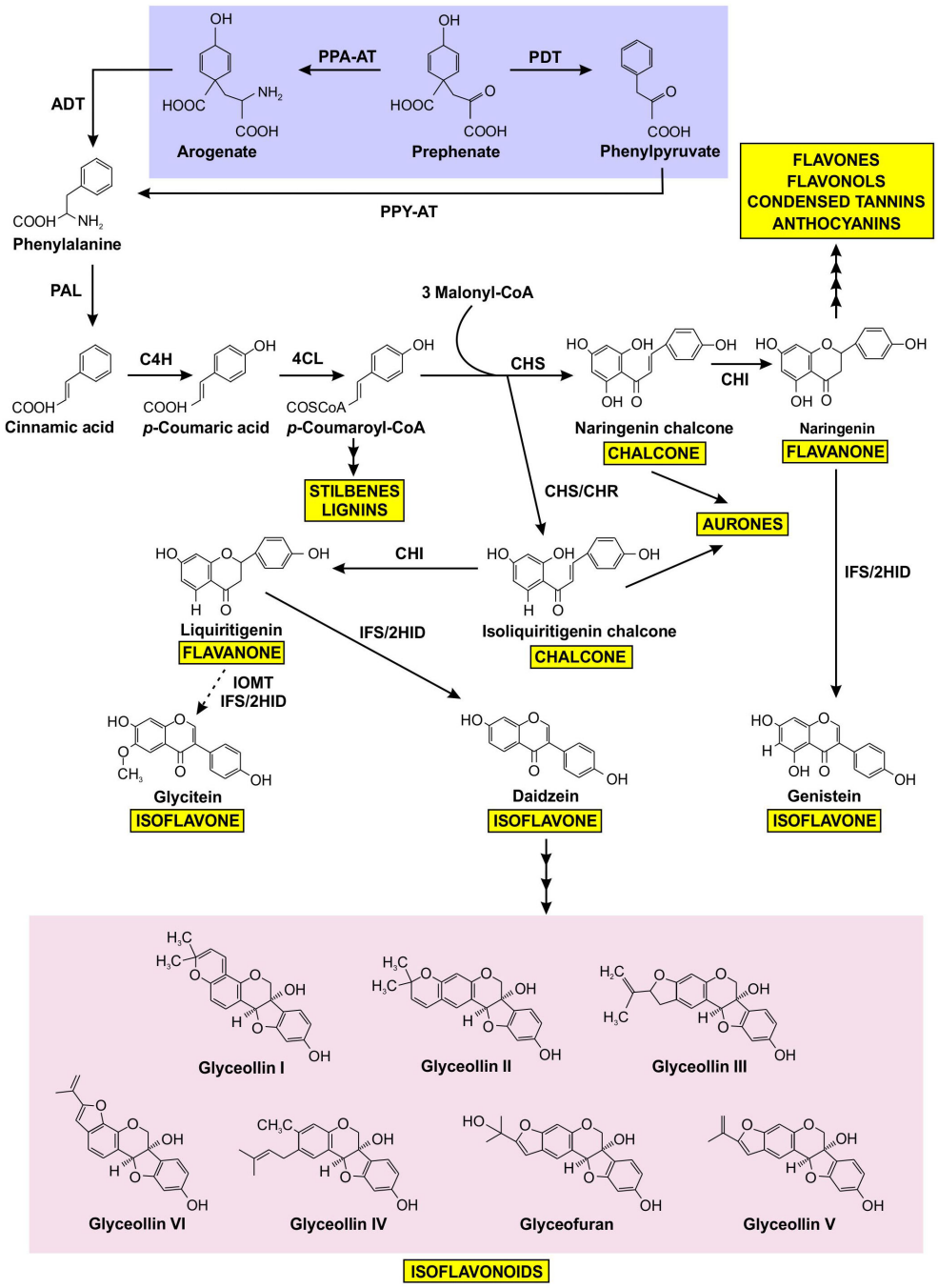

FIGURE 1
Prephenate from the shikimate pathway uses two different mechanisms to produce phenylalanine, which is subsequently channeled into the production of a variety of phenylpropanoids, including isoflavonoids. Phenylalanine produced by the arogenate and phenylpyruvate branches are highlighted in purple, isoflavonoids are highlighted in pink, and other phenylpropanoid end products are highlighted in yellow. The dotted arrow represents speculative steps, and multiple arrows indicate two or more steps in the pathway. PPA-AT, prephenate-aminotransferase; PDT, prephenate dehydratase; PPY-AT, phenylpyruvate aminotransferase; PPA-AT, prephenate aminotransferase; ADT, arogenate dehydratase; PAL, phenylalanine ammonia lyase; C4H, cinnamate 4-hydroxylase; 4CL, 4–coumarate: CoA ligase; CHS, chalcone synthase; CHR, chalcone reductase; CHI, chalcone isomerase; IFS, isoflavone synthase; 2HID, 2-hydroxyisoflavanone dehydratase; I2'H, isoflavone 2'-hydroxylase; IOMT, isoflavone O–methyltransferase.

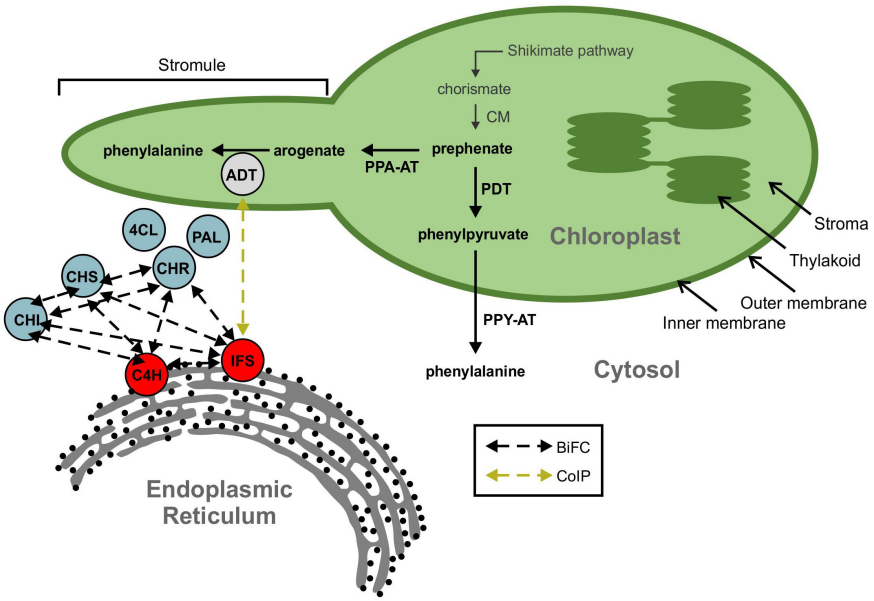

FIGURE 2
A model showing ADT interaction with the isoflavonoid metabolon. The isoflavonoid metabolon is made up of cytoplasm-localized enzymes (blue) anchored to the cytosolic face of the ER membrane through interaction with cytochrome P450 enzymes, IFS and C4H (red). Protein-protein interactions between multiple members of the isoflavonoid metabolon have been determined by BiFC (black dashed arrows). An interaction between IFS and an ADT (grey) was also detected *via* Co-IP (yellow dashed arrow). ADT enzymes are involved in phenylalanine biosynthesis and are localized to the chloroplast along with the shikimate pathway and other aromatic amino acid biosynthetic machinery. Subcellular compartments are indicated by grey fonts. ADT, arogenate dehydratase; PAL, phenylalanine ammonia lyase; 4CL, 4-coumarate-CoA ligase; C4H, cinnamate 4-hydroxylase; CHI, chalcone isomerase; CHR, chalcone reductase; CHS, chalcone synthase; CM, chorismite mutase; IFS, isoflavone synthase; PDT, prephenate dehydratase; PPA-AT, prephenate aminotransferase; PPY-A, phenylpyruvate aminotransferase.

Materials and methods

Plant materials and growth conditions

Nicotiana benthamiana was grown on PRO-MIX® BX MYCORRHIZAETM soil (Rivière-du-Loup, Canada) in a growth room set to 16 h light at 24°C and 8 h dark at 20°C with 60% relative humidity and a light intensity of 80-100 µmol $m^{-2}s^{-1}$.

Soybean cultivar Williams 82 seeds were planted in sterile pots containing PRO-MIX® BX MYCORRHIZAE™ soil (Premier Tech Home and Garden, Rivière-du-Loup, QC) and maintained in a growth room under a 16 h light and 8 h dark cycle at 24°C with 60-70% humidity and a light intensity of 250 µmol $m^{-2}s^{-1}$. The plants were watered with a fertilizer solution containing nitrogen-phosphorus-potassium (20-8-20). At the flowering stage of soybean plants, stem, leaf, root, and flower tissue were harvested, frozen in liquid nitrogen, and stored at -80°C.

In silico and phylogenetic analyses

Candidate soybean *ADTs* (*GmADTs*) were identified by mining the soybean genome in Phytozome 13 (https://phytozome-next.jgi.doe.gov/). Two previously identified soybean ADTs Glyma.13G319000.1 and Glyma.12G181800.1 (GmADT13A and GmADT12A, Table 1) (Dastmalchi et al., 2016) were used in BLAST searches against the soybean genome database (Glycine max Wm82.a4.v1). Each unique gene identified from the two initial input sequences was used in BLAST search again to look for all possible GmADTs. Multiple sequence alignments were performed using protein sequences of ADTs in Clustal Omega (Sievers et al., 2011), and visualized in boxshade using pyBoxshade (https://github.com/mdbaron42/pyBoxshade). TargetP was used for subcellular localization and cleavage site prediction (Emanuelsson et al., 2007). The gene and transcript data (in gff3 format) for *GmADT*s were retrieved from Phytozome 13 for Wm82.a4.v1 genome assembly and the gene structure model was generated using TBtools (Chen et al., 2020).

For phylogenetic analysis, the predicted transit peptide sequences were removed from plant ADTs and putative GmADTs according to Cho et al. (2007). The chorismate mutase domain of the *E. coli* P-protein was removed according to Zhang et al. (1998). The mature protein sequences were aligned using ClustalW and the tree was constructed with the bootstrap set to 1,000 replicates using MEGAX software (Kumar et al., 2018).

Gene expression analysis and heat map generation

Soybean RNA-seq data was retrieved from Phytozome 13 database with expression values in FPKM (Wang et al., 2019). A heatmap was generated using log_2-transformed normalized transcript abundance values using TBtools (Chen et al., 2020).

TABLE 1 Characteristics of putative *ADT* gene family members in soybean.

Gene name	Locus name	Locus range	Coding sequence length (bp)	Predicted protein size (kDa)	Splice variants	Predicted subcellular localization
GmADT9	Glyma.09G004200	Gm09:331514.337738	1215	44.5	2	Other
GmADT11A	Glyma.11G189100	Gm11:16210640.16212382	1287	46.9	1	Chloroplast
GmADT11B	Glyma.11G151288	Gm11:11415143.11420316	1158	42.7	1	Other
GmADT12A	Glyma.12G181800	Gm12:35716180.35718032	1278	46.2	1	Chloroplast
GmADT12B	Glyma.12G085500	Gm12:6875420.6877191	1287	46.8	1	Chloroplast
GmADT12C	Glyma.12G193000	Gm12:36904068.36910226	1155	42.8	1	Chloroplast
GmADT12D	Glyma.12G072500	Gm12:5330594.5336280	933	33.8	1	Chloroplast
GmADT13A	Glyma.13G319000	Gm13:40728761.40730567	1275	46.1	1	Chloroplast
GmADT13B	Glyma.13G309300	Gm13:39881239.39884055	645	23.1	1	Other
GmADT17	Glyma.17G012600	Gm17:970102.977629	1200	43.7	1	Chloroplast

Gene cluster in the Newick tree was generated in MEGAX and imported into the heatmap.

RNA extraction and reverse transcription-PCR

Total RNA was extracted from soybean tissues (50-70 mg) using the RNeasy plant Mini kit (Qiagen). An on column DNase I (Promega) treatment was performed prior to RNA elution from each sample. Total RNA (1 µg) was used to synthesize cDNA using oligo dT primers and SuperScript IV First Strand Synthesis System (Thermofisher) as per manufacturer's instructions.

Cloning of *GmADT*s

The coding regions of *GmADTs* were amplified using RT-PCR with gene-specific primers (Supplementary Table 1) and cloned into pDONR-Zeo (Invitrogen) using BP clonase® (Invitrogen), followed by transformation into *E. coli* DH5α via electroporation. The recombinant entry clones were confirmed by sequencing and then recombined with the destination vectors pEarleyGate101 (pEG101) for subcellular localization (Earley et al., 2006) and pEarleyGate201-YN and pEarleyGate202-YC for *in planta* protein-protein interaction assays (Lu et al., 2010) in an LR recombination reaction (Invitrogen). The expression clones were transformed into *Agrobacterium tumefaciens* GV3101. GmIFS2 (Glyma.13G173500) in pEarleyGate201-YN and pEarleyGate202-YC were obtained from Dastmalchi et al. (2016).

For the PDT assay, each of the *GmADT*s with a 6×His-C-terminal fusion was recombined into the destination vector pAG423GAL-ccdB-ECFP (Addgene plasmid # 14173; http://n2t.net/addgene:14173; RRID : Addgene_14173) using Gateway technology as described above and transformed into *Saccharomyces cerevisiae pha2* (Ackerman et al., 1992) using Frozen-EZ Yeast Transformation II™ kit (Zymo Research). Transformants were screened on minimal synthetic dextrose (SD)/-His plates.

Confocal microscopy

For subcellular localization, *A. tumefaciens* harboring pEG101 containing *GmADT*s were transformed into *N. benthamiana* leaves by infiltration as described by Sparkes et al. (2006). For protein-protein interaction by BiFC, fusions containing YN and YC fragments of YFP were co-infiltrated into *N. benthamiana* leaves in a 1:1 (v/v) mixture as described before. The protein expression was visualized 48 h post-infiltration by using the Olympus FV1000 confocal microscope under a 60× water immersion objective lens. For YFP visualization, the excitation wavelength was set to 514 nm and emission was collected at 520-550 nm. For chloroplast-visualization, the natural auto-fluorescence produced by chlorophyll was harnessed by exciting the chlorophyll at 600 nm and emission was collected at 640-700 nm.

pha2 complementation assay

For the *pha2* complementation assay (Bross et al., 2011), yeast cultures were grown in appropriately supplemented liquid raffinose media overnight at 30°C with shaking. Each culture diluted in double distilled water to a final density of 5 x 10^4 cells/mL, and 10 µL of cells were spotted on appropriate selection media. SD plates prepared with different carbon sources (glucose, galactose, and raffinose) were used. The *GAL1* promoter in the destination vectors is expressed or repressed by galactose or glucose, respectively, whereas raffinose has no influence on the regulation of the promoter (St John and Davis, 1981; Lohr et al., 1995). Plates of each carbon source were made either with a -histidine (-His), or a -histidine-phenylalanine (-His-Phe) dropout powder. The lack of His selects for the presence of the ADT expression vector, while the lack of Phe selects for PDT activity when ADT proteins are induced.

Negative (untransformed *pha2* and empty destination vector) and positive (WT AtADT2) controls were spotted on every plate, and all complementation tests were repeated at least 3 times. Images were taken with a digital camera (Canon EOS 70D) six and thirteen days after spotting, and a single representative image of each construct is shown.

Western blotting

Yeast cultures were grown overnight in glucose media, washed twice with double distilled water, then grown overnight to an OD_{600} of 0.6-0.8 in glucose media as a negative control, or in galactose media to induce ADT expression. Total protein was extracted using the yeast alkaline lysis method (Kushnirov, 2000). Protein extracts were then size separated on an SDS-PAGE gel (6% stacking gel, 12% separating gel). Following electrophoresis, the resolved proteins were visualized with Coomassie Brilliant Blue. Gels were incubated at room temperature for 30 minutes with shaking, and then destained for 2-3 hrs to remove background stain before an image was taken.

GmADT-6×His and CHR14-6xHis fusion proteins were detected using Western blot analysis with a monoclonal mouse anti-His primary antibody (1:1200, Sigma, SAB1305538). A goat anti-mouse HRP conjugate secondary antibody (BioRad, 1706516) was used in all cases, and HRP activity was visualized using the Clarity ECL kit (BioRad, 1705061).

Results

The soybean genome contains 10 putative *GmADT* genes

To identify all the members of the *GmADT* gene family, we used *Glyma.12G181800* (*GmADT12A*) and *Glyma.13G319000* (*GmADT13A*) sequences as queries in a BLAST search in the *G. max* Wm82.a4.v1 genome database. These two searches identified 10 *GmADT*s. Each of these *GmADT*s were used separately as a query sequence in the BLAST search in the soybean genome database. This process was repeated until no new *ADT* was discovered (Table 1). The following nomenclature was developed: *GmADT*s were numbered according to the chromosome on which they are encoded and a letter (A, B, etc) was added if more than one *GmADT* was located on the same chromosome.

The 10 identified *ADT* loci in the soybean genome are distributed across five different chromosomes, with chromosome 12 containing four *GmADTs* (*GmADT12A, GmADT12B, GmADT12C* and *GmADT12D*) while chromosomes 11 (*GmADT11A, GmADT11B*) and 13 (*GmADT13A, GmADT13B*) each contain two *GmADTs*. Chromosomes 9 and 17 carry only one *GmADT* each (*GmADT9 and GmADT17*, Table 1). The putative *GmADT* genes encode proteins with a calculated molecular mass ranging from 23.1 to 46.9 kDa (Table 1).

A multiple sequence alignment of previously characterized ADTs from *Arabidopsis thaliana* (AtADTs), *Petunia x hybrida* (PhADTs) and *Pinus pinaster* (PpADTs) and the deduced amino acid sequences of GmADTs revealed that, similar to other plant ADTs, GmADTs also contain a putative N-terminal transit peptide, an internal catalytic domain, and a C-terminal ACT domain (Figure 3). As expected the transit peptide regions are highly variable while the catalytic and ACT domains of the GmADT, AtADT, PhADT and PpADT proteins exhibit substantial levels of sequence conservation. Comparing GmADT sequences, GmADT9 is the most varied member of the family and shares only 49.5-63.3% sequence identity with other isoforms at the amino acid level. A pairwise percentage identity of full-length GmADTs sequences at the amino acid and nucleotide levels varied from 49.5 to 96.2% and 50.6 to 94.8%, respectively (Table 2). Most GmADTs except GmADT12C and GmADT13B contain the conserved TRF triad (Figure 3, green box) in the catalytic domain that is critical for substrate binding and prephenate/arogenate catalysis (Zhang et al., 2000; Hsu et al., 2004; Tan et al., 2008). Instead of the TRF triad, GmADT12C contains an SRY sequence instead. In addition, key ligand binding motifs (ESRP and GALV) in the ACT domain (Pohnert et al., 1999; Tan et al., 2008) are also shared by the GmADTs and other ADTs. However, the C-terminal region of the catalytic domain and the entire ACT domain from GmADT13B, and the C-terminus of the ACT domain from GmADT12D are missing. As such, GmADT12D contains the GALV but lacks the ESRP regulatory motif due to C-terminal truncation. Soybean cultivar Williams 82 whole genome sequence has been reassembled multiple times, however, this discrepancy was observed consistently including in the most recent release *Glycine max* var. Williams 82-ISU-01 (https://phytozome-next.jgi.doe.gov/info/GmaxWm82ISU_01_v2_1). As GmADT13B lacks the entirety of the ACT domain, it is likely not allosterically regulated if it is a functional protein.

Originaly ADTs were thought to be monofunctional enzymes like bacterial PDTs. However it has been demonstrated that some ADT isozymes can also act as PDTs (Cho et al., 2007; Maeda et al., 2010; Bross et al., 2011; El-Azaz et al., 2016; Qian et al., 2019). ADT and PDT enzymes catalyze the same biochemical reaction (decarboxylation/dehydration) using very similar substrates, and many key catalytic and regulatory residues are conserved between them (Cho et al., 2007; Tan et al., 2008). Previous work to determine the sequences responsible for this dual substrate recognition in *Pinus pinaster* ADTs (PpADTs) identified a 22 amino acid region at the N-terminus of the ACT domain, termed the PDT activity conferring domain, or PAC domain (El-Azaz et al., 2016). Additionally, a critical alanine residue (Ala314 in PpADT-G) was to be sufficient to define prephenate substrate recognition in the PpADTs. Five GmADTs contain this alanine residue within the PAC domain: GmADT9, GmADT11B, GmADT12C, GmADT12D and GmADT17 (Figure 3), suggesting these isoforms are ADT/PDTs.

GmADT gene structure and phylogenetic analysis

An analysis of *GmADT* gene structure indicated that four *GmADTs* (*GmADT11A, GmADT12A, GmADT12B* and *GmADT13A*) contained no introns in their open reading frame

10.3389/fpls.2024.1307489

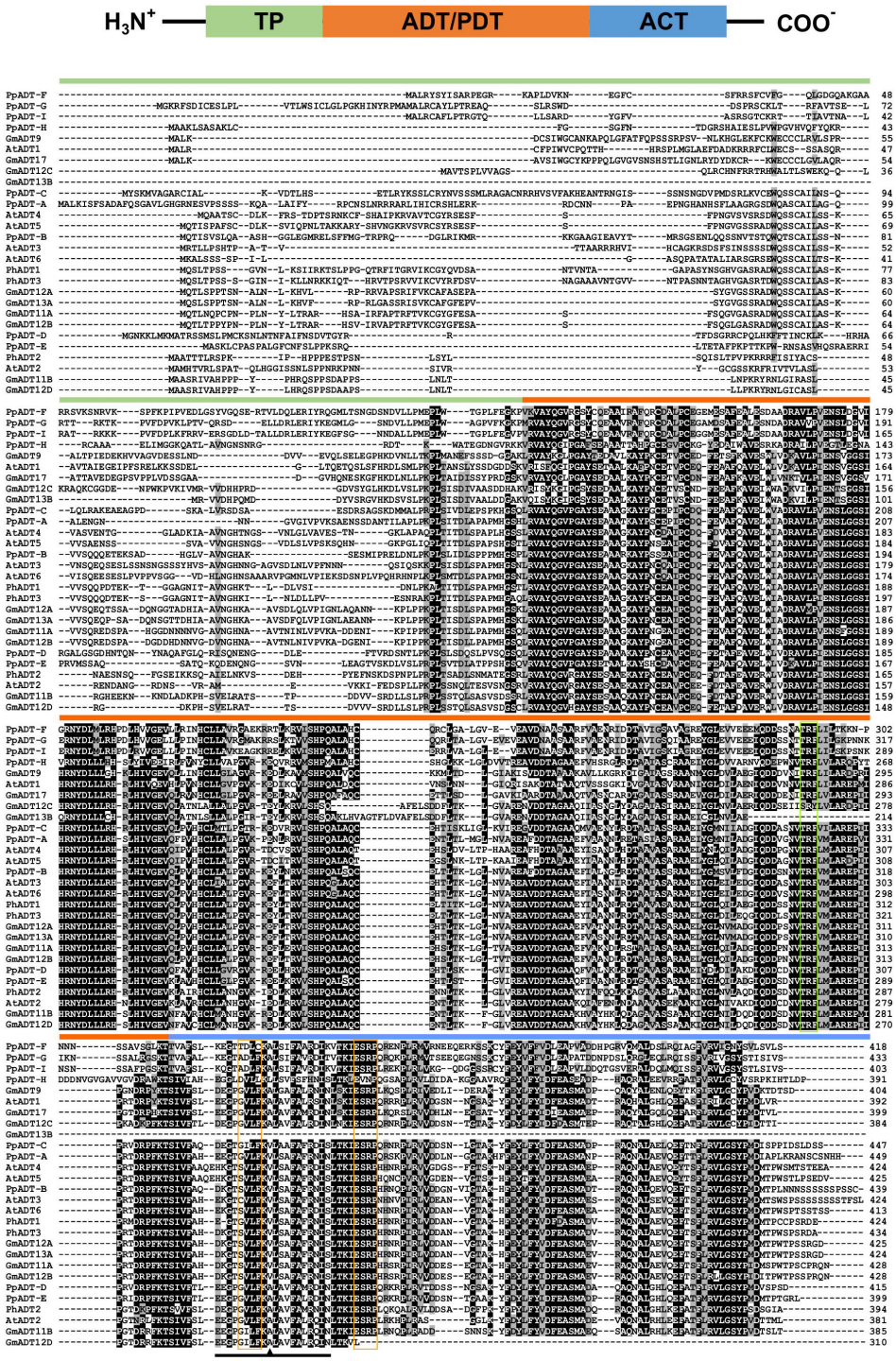

FIGURE 3
Protein domains and multiple sequence alignment of GmADTs and AtADTs. A schematic diagram (top) of predicted protein domains of ADTs include transit peptide (TP), catalytic ADT or PDT domain and regulatory ACT domain (modified from Cho et al., 2007). The amino acid sequences of the GmADTs, *Arabidopsis* ADTs (AtADT), *Petunia hybrida* (PhADTs) and *Pinus pinaster* (PpADTs) were aligned using ClustalO. Black shading indicates identical residues, grey shading indicates similar amino acid residues and dashed lines indicate gaps. Colored bars above the sequences indicate predicted protein domains color coded as shown on top. Green boxe indicate TRF motif. Conserved A (A314 in PpADT) residue conferring PDT activity is shown by the arrow head within the PAC domain (black line). Yellow boxes indicate GALV and ESRP domains.

while six contained multiple introns (Figure 4A). *GmADT9*, *GmADT11B*, *GmADT12C* and *GmADT17* contained 10 introns of varying sizes ranging from 81 to 1444 nucleotides while *GmADT12D* and *GmADT13B* contained eight and five introns, respectively. Among all the *GmADT* family members, only *GmADT11B* and *GmADT12D* contained introns in its 3`UTR.

To illustrate the evolutionary relationship among soybean ADTs and other characterized ADT proteins, a phylogenetic

10.3389/fpls.2024.1307489

TABLE 2 Pairwise coding region and amino acid sequence comparisons of the soybean *GmADT* gene family.

	Name	GmADT9	GmADT11A	GmADT11B	GmADT12A	GmADT12B	GmADT12C	GmADT12D	GmADT13A	GmADT13B	GmADT17
Amino acids	*GmADT9*		49.49	52.85	49.75	49.75	54.35	53.4	50.13	54.73	65.33
	GmADT11A	50.88		56.76	81.8	94.39	52.52	56.95	81.28	53.77	53.96
	GmADT11B	57.2	53.3		56.38	55.97	56.82	95.48	56.38	51.52	55.71
	GmADT12A	51.93	79.72	53.21		81.8	53.6	56.81	96.23	55	54.76
	GmADT12B	50.63	93.94	52.77	79.8		53.05	57.62	81.04	53.77	54.22
	GmADT12C	60.95	51.84	56.41	53.81	52.47		55.2	54.01	92.08	59.15
	GmADT12D	57.17	51.75	93.89	51.75	51.43	53.86		57.14	52.79	56.12
	GmADT13A	51.98	79.43	53.53	93.96	78.96	54.72	51.82		56	54.9
	GmADT13B	61.22	51.14	55.76	53.33	51.8	94.75	55.95	53.82		57
	GmADT17	76.72	53.46	58.67	53.37	53.55	63.85	57.85	52.91	63.71	
Nucleotides											

analysis was performed using the predicted amino acid sequences of their mature proteins. As shown in Figure 4B, similar to AtADTs (Cho et al., 2007), soybean ADTs form three distinct subgroups. GmADT9, GmADT13B, and GmADT17 grouped in 'subgroup III' with AtADT1. Three GmADTs, GmADT11B, GmADT12D, and GmADT13A grouped into 'subgroup II' with AtADT2 and PhADT2 while four GmADTs, GmADT11A, GmADT12A, GmADT12B and GmADT12C, grouped in 'Subgroup I' with AtADT3, AtADT4, AtADT5 and AtADT6. Similar to other angiosperms, at least one GmADT isoform is present in each subgroup. In addition, GmADTs in each subgroup are clustered with ADT sequences with other legume species (*Medicago truncatula, Lotus japonicus*, and *Phaseolus vulgaris*). As observed for most of the gene families in soybean, GmADTs mostly group in pairs, consistent with its recent whole genome duplication (Schmutz et al., 2010; Yuan and Song, 2023). Subgroups II and III contain other plant ADTs that have been shown to act as PDTs (eg. AtADT1, AtADT2, PpADT-G, PhADT2).

Expression analysis of *GmADT* genes

To determine the mRNA expression patterns of the *GmADT* gene family members in soybean tissues, we utilized the transcriptome dataset available in the public domain as a resource (Wang et al., 2019). As shown in Figure 5, the dataset obtained from Phytozome 13 database consisted of transcript accumulation in root, nodules, stem, leaf, flowers (open and unopen) and seed tissues collected during the development from early to mature seeds. The maximum fragments per kilobase of transcript per million mapped reads (FPKM) values of *GmADT*s varied from 0.5 (*GmADT9* in early seed development) to 36.1 (*GmADT12C* in flowers). While the majority of *GmADT*s were expressed in most of the tissue analyzed, each gene family member displayed a unique tissue-specific expression pattern. *GmADT12A* and *GmADT13A* transcripts accumulated to highest levels in root tissues while the transcripts of only *GmADT12D* and *GmADT17* were found in nodules. Transcript accumulation for *GmADT9, GmADT11B, GmADT12A, GmADT12D* and *GmADT17* was higher during early seed development whereas expression of *GmADT13B* was detected in leaf, flower and seed tissue at mid-maturation stage. Despite lacking the transit peptide and the ACT domain, the predicted *GmADT13B* transcript levels were detectable, thus potentially producing only a truncated protein (Figure 3; Table 1). Therefore, it is likely that GmADT13B is non-functional as ADT/PDT and was excluded from further characterization in this study.

GmADTs primarily localize to chloroplasts

Plant ADTs were previously reported to localize to the chloroplasts in multiple species including *Arabidopsis*, petunia and pine (Rippert et al., 2009; Maeda et al., 2010; El-Azaz et al., 2016; Bross et al., 2017). To confirm if the GmADTs also are chloroplast localized, we investigated the subcellular localization of

10.3389/fpls.2024.1307489

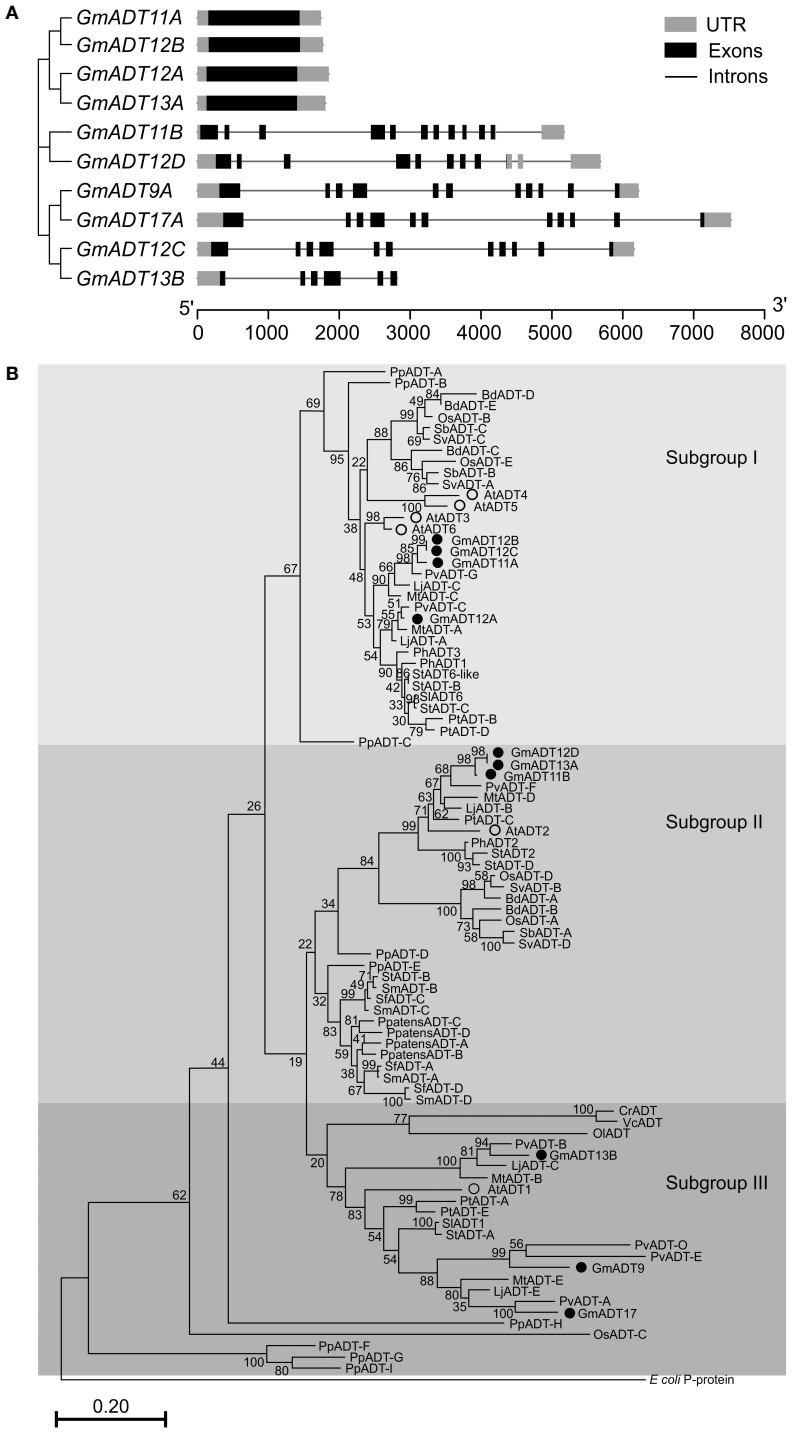

FIGURE 4
Gene structure and phylogenetic analysis of GmADTs. **(A)** Genomic structure of *GmADTs* were drawn to scale using gene models of *GmADTs*, retrieved from Phytozome 13 for soybean (*G. max* Wm82.a4.v1) genome and the gene cluster was imported from a neighbor-joining tree of *GmADTs*. **(B)** Mature protein sequences of GmADTs, AtADTs, PpADTs and PhADTs were identified using TargetP, aligned using ClustalO and a phylogenetic tree was constructed by neighbor-joining method using MEGAX. Bootstrap values (1000 replicates) are shown as percentages next to branch points. The PDT domain of the *E. coli* P-protein was included as an outgroup. At, *Arabidopsis thaliana;* Pp, *Pinus pinaster;* Ph, *Petunia hybrida.* Accession numbers: AtADT1, AT1G11790.1; AtADT2, AT3G07630.1; AtADT3, AT2G27820.1; AtADT4, AT3G44720.1; AtADT5, AT5G22630.1; AtADT6, AT1G08250.1; PhADT1, ACY79502.1; PhADT2, ACY79503.1; PhADT3, ACY79504.1; PpADTA, APA32582.1; PpADTB, APA32583.1; PpADTC, APA32584.1; PpADTD, APA32585.1; PpADTE, APA32586.1; PpADTF, APA32587.1; PpADTG, APA32588.1; PpADTH, APA32589.1; PpADTI, APA32590.1; *E. coli*, WP_115444483.1.

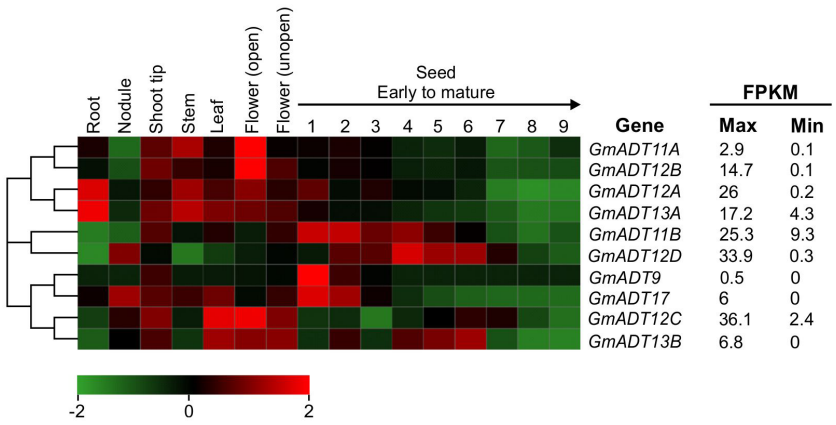

FIGURE 5
mRNA expression analysis of *GmADTs*. The transcriptome data of *GmADT* across different tissues were retrieved from Phytozome 13 database (Wang et al., 2019) for heatmap generation. The maximum (max) and minimum (min) expression values for each gene are shown and the gene cluster was imported from neighbor-joining tree generated with GmADT protein sequences in MEGAX. The black arrow on top of 1 to 9 indicates seed developmental stages from early (1) to mature (9). The color scale below the heatmap indicates transcript abundance values in log2 transformed across each row. Red and green indicating high and low levels of transcript abundance, respectively. FPKM, fragments per kilobase of transcript per million.

the nine GmADTs that were initially annotated in Phytozome as full length ADTs (as predicted truncated protein, GmADT13B was excluded from further analysis). GmADTs were translationally fused to YFP, transiently expressed in *N. benthamiana* leaves, and visualized by confocal microscopy. The red auto-fluorescence generated by chlorophyll was used as a chloroplast marker. As shown in Figure 6, all nine GmADTs showed chloroplastic localization, specifically a stromule sub-plastidial localization. Stromules resemble tail-like or bead-like protrusions from the chloroplast body (Arimura et al., 2001; Pyke and Howells, 2002; Kwok and Hanson, 2004b; Hanson and Hines, 2018). This stromule sub-plastidial localization of the GmADTs is consistent with the reports for other plant ADTs (Maeda et al., 2010; El-Azaz et al., 2016; Bross et al., 2017). Furthermore, GmADT11B displayed additional thin, elongated sub-plastidial localization at the poles of the chloroplasts (Figure 6, inset), distinct from the other GmADTs but similar to those observed for AtADT2, an AtADT likely involved in chloroplast division (Abolhassani Rad, 2017).

GmADTs interact with isoflavonoid metabolon enzymes

To determine if the GmADT and GmIFS2 interaction detected *via* Co-IP is actually occurring *in-planta*, we conducted Bimolecular Fluorescence Complementation (BiFC) assay to assess protein-protein interactions. In our BiFC system we used *N. benthamiana*, which synthesizes flavonoids but not isoflavonoids. However, we are introducing the key branch enzyme leading to isoflavonoid synthesis, GmISF2. The flavonoid synthesis machinery upstream of IFS2 is the same in both legumes and non legumes, allowing us to use the *N. benthamiana* transient expression system to assess GmADT interactions with GmIFS2. As we were expressing soybean genes in a heterologous system, all contructs were expessed using a 35S promoter to ensure comparable expression levels (Odell et al., 1985; Lu et al., 2010; Tsugama et al., 2013; Amack and Antunes, 2020; Liang et al., 2023).

Each GmADT was translationally fused to the C-terminal half of YFP (GmADT-YC) and GmIFS2 to the N-terminal half of YFP (GmIFS-YN). GmADT-YC and GmIFS2-YN constructs were co-expressed in *N. benthamiana* leaves and the protein-protein interaction was monitored using confocal microscopy (Figure 7). Co-expression of GmADT and GmIFS2 constructs were also performed in reciprocal combination (GmADT-YN and GmIFS2-YC (Supplementary Figure 1). As shown in Figure 7, the detection of YFP fluorescence indicating either close proximity or direct interaction between each of the GmADT family members and GmIFS2 was confirmed. The observed reticulate pattern of fluorescence indicated that the interaction was occurring at the ER surface where GmIFS2 is localized. We also detected an interaction between GmIFS2 and an *Arabidopsis* ADT, AtADT5. Similar results were obtained for the reciprocal combinations (Supplementary Figure 1). As negative controls, we also tested GmIFS2 with proteins unrelated to isoflavonoid synthesis and specialized metabolism: a protoanthocyanidin transporter protein from common bean (Figure 7, PvMATE8) and an *Arabidopsis* seed storage protein CRUCIFERIN1 (Figure 7, AtCRA1). No signal was detected when co-expressing GmIFS2 with PvMATE8 or AtCRA1 (Figure 7).

To investigate if GmADTs interact with the soluble enzymes of the (iso)flavonoid pathways, interaction between GmADT12A and GmCHS8, GmCHR14, GmCHI2 were also assayed by BiFC (Figure 8). GmADT12A was chosen as a representative ADT based on its putative involvement in the isoflavonoid metabolon (Dastmalchi et al., 2016). We also evaluated the interaction between GmADT12A and two other isoflavonoid ER anchors, GmC4H2 and GmIFS1 (Dastmalchi et al., 2016; Khatri et al., 2023). The interaction of GmADT12A with GmC4H2 and GmIFS1 was

10.3389/fpls.2024.1307489

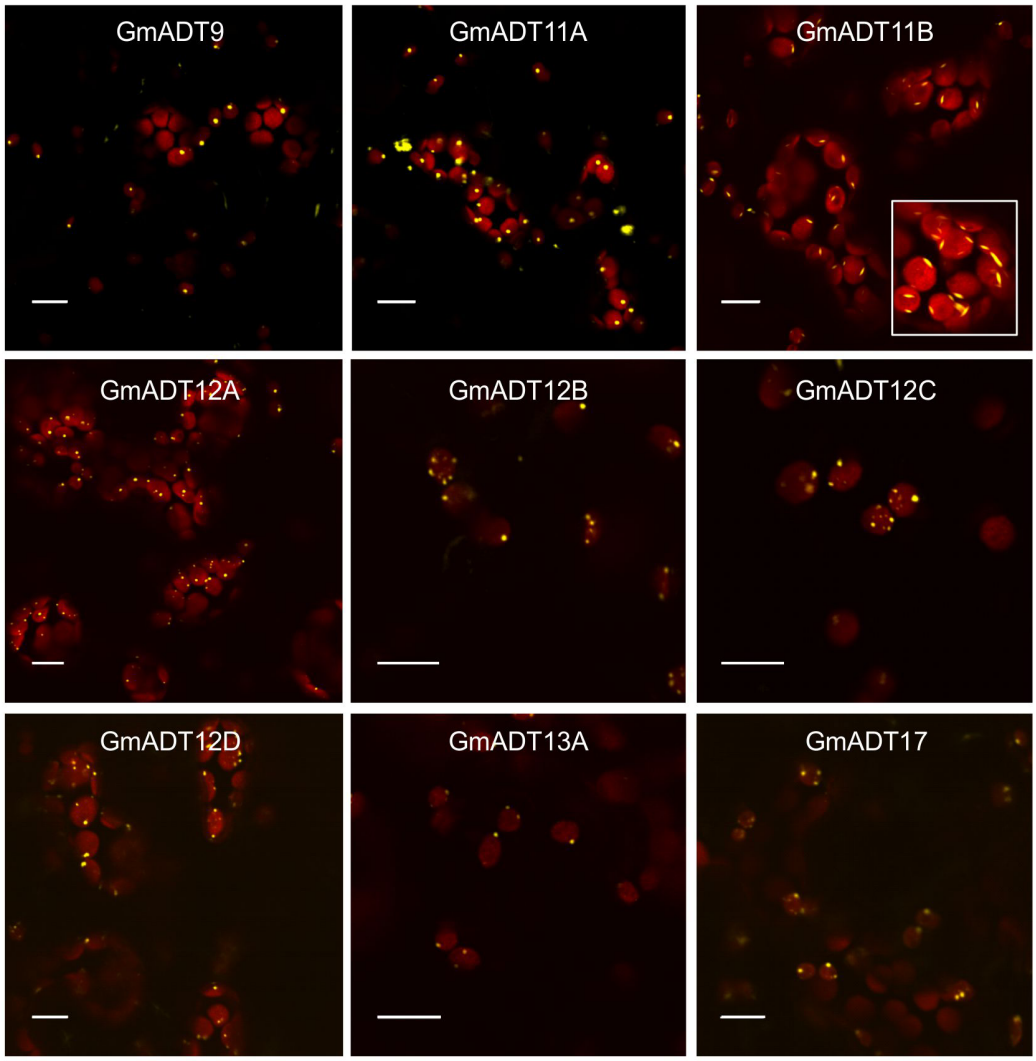

FIGURE 6
Subcellular localization of the GmADTs. A translational fusions of GmADT-YFP were transiently expressed in *N. benthamiana* leaf and visualized by confocal microscopy. Confirmation of localization was performed through co-localization of the GmADT-YFP fusion with the chloroplast autofluorescence (in red). Scale bars represent 10 μM.

restricted to the surface of the ER (Figures 8I,II). Interestingly, the interaction of GmADT12A with soluble nucleo-cytoplasmic-localized proteins GmCHS8, GmCHR14 and GmCHI2 was detected in both the nucleus and cytosol (Figures 8III-V). No interaction was observed between GmADT12A and GmCYP1, AtCRA1 or PvMATE8 (Figures 8VI–VIII). No discrepancies were observed when testing the reciprocal combinations (Supplementary Figure 2).

GmADTs with PDT activity

Sequence analysis suggested that some members of the GmADT family may have PDT activity, specifically GmADT9, GmADT11B, GmADT12C, GmADT12D and GmADT17 (Figure 3). To assess PDT activity of the GmADTs, the *pha2* yeast complementation assay (Bross et al., 2011) was performed. The *S. cerevisiae pha2* strain lacks the endogenous PDT protein, and can be complemented by a GmADT with PDT activity. Further, the *pha2* assay is inducible by galactose. Thus, only in the prescence of galactose GmADTs are expressed, and any GmADT with PDT activity will synthesize Phe and cells will grow without Phe supplementation.

The untransformed *pha2* strain and *pha2* transformed with an empty vector were used as negative controls, and they do not complement the strain (Figure 9, *pha2* and empty vector). As a positive control, AtADT2 was used as it was previously shown to have PDT activity (Cho et al., 2007; Bross et al., 2011). As expected, no growth was observed when cells were grown with glucose or raffinose as carbon sources. When induced with galactose, GmADT9, GmADT11A, GmADT11B, GmADT12A and GmADT17 complemented the *pha2* strain, indicating these GmADT isoforms have PDT activity (Figure 9).

10.3389/fpls.2024.1307489

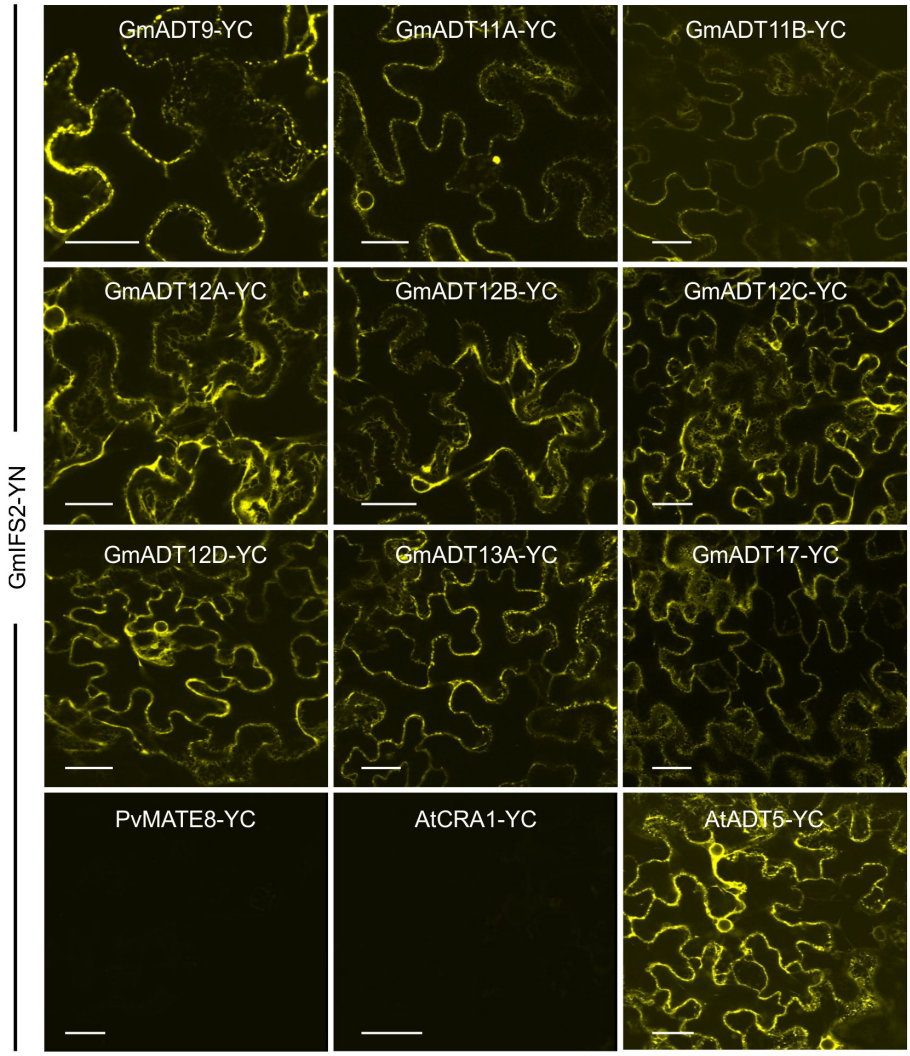

FIGURE 7
GmADTs and GmIFS2 interact *in planta* at the ER. Bi-directional interaction between GmADT isoforms and GmIFS2 by co-expression of translational fusions with N (YN)- or C (YC)- terminal fragments of YFP in *N. benthamiana* as assayed by BiFC. Proximity of the proteins results in a YFP fluorescence and localization of interaction as monitored by confocal microscopy. The interaction between chloroplast-localized GmADT and ER-localized GmIFS2 appear to be localized to the ER. As representative negative controls, GmMATE8-YC or AtCRA1-YC co-infiltrated with GmIFS2 (YN) is shown. Scale bars represent 30 μM.

Next, Western blots were performed to confirm that all 6×His-tagged GmADTs were expressed in the *pha2* yeast strain (Supplementary Figure 3). Total soluble protein was extracted (Kushnirov, 2000), and equal volumes of extract were analyzed by SDS-PAGE. Coomassie staining was performed to ensure protein was successfully extracted (Supplementary Figure 3), and purified 6×His-GmCHR14 was used as a positive control. Signals from GmADT9, GmADT11A, GmADT11B, GmADT12A and GmADT13A were observed, however the remaining GmADTs (GmADT12B, GmADT12C, GmADT12D, and GmADT17) were not detected (Supplementary Figure 3). While GmADT17 appeared to be expressed sufficiently to complement the *pha2* strain, we cannot definitively conclude that GmADT12B, GmADT12C, and GmADT12D lack PDT activity, as they do not appear to be expressed in yeast.

Discussion

Plant specialized metabolism is a tightly regulated network of overlapping pathways with many participating enzymes, all being controlled temporally during development, in response to external stimuli, and spatially in different plant tissues and subcellular organelles. Many of the enzymes involved in these biosynthetic pathways are encoded by multi-gene families (Boudet, 2007), and can direct carbon flux toward specific metabolic pathways (Cannon et al., 2004; Corea et al., 2012b). In the present study, we identified nine members of the *GmADT* family, examined their tissue-specific expression, and subcellular localization. We determined that five of the nine GmADTs possess PDT activity in the *in vivo pha2* complementation assay. We further showed that GmADTs interact with GmIFS2 *in vivo*. In particular, GmADT12A exhibits

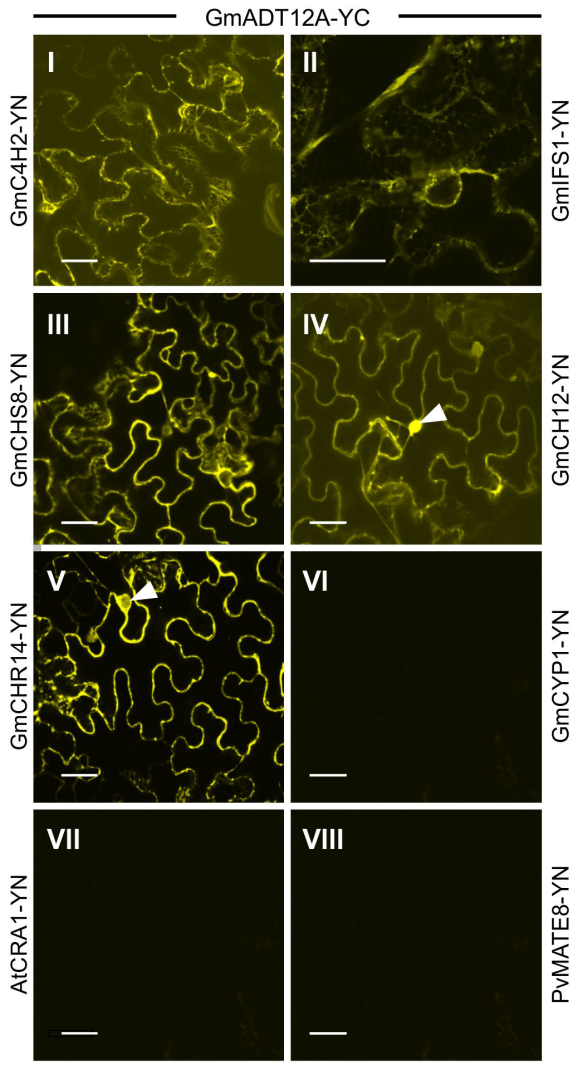

FIGURE 8
Interaction of GmADT12A with soluble and ER-localized isoflavonoid biosynthetic pathway enzymes by co-expression of translational fusions with N (YN)- or C (YC)- terminal fragments of YFP in *N. benthamiana* as assayed by BiFC. Proximity of the proteins results in a YFP fluorescence and localization of interaction as monitored by confocal microscopy. (I) and (II) The interaction between chloroplast localized GmADT12A and ER localized GmC4H2 and GmIFS1 appear to be localized to the ER. (III), (IV) and (V) GmADT12A and soluble enzymes GmCHS8, GmCHR14 and GmCHI2 appear to be localized to the cytoplasm and nucleus. White arrow heads point to nuclei. (VI), (VII) and (VIII) GmCYP1 is a nucleo-cytosolic protein (Mainali et al., 2017). No interaction was observed between GmADT12A and GmCYP1 or AtAtCRA1 or PvMATE8 (negative control). Scale bars represent 30 μM.

PDT activity, is expressed in root tissue and interacts with GmIFS2, substantiating its involvement in the isoflavonoid metabolon (Dastmalchi et al., 2016).

Paleopolyploidy and GmADTs

There have been multiple whole genome duplications (WGDs) in the evolutionary history of soybean. Aside from the ancient WGD shared by all angiosperms (Young and Bharti, 2012), soybean has undergone two more recent WGDs: one just prior to radiation of legumes (~58-59 million years ago), and one *Glycine*-specific WGD that ocurred ~13-14 million years ago (Shoemaker et al., 2006; Schmutz et al., 2010; Yuan and Song, 2023). As a result, soybean has many duplicated genes, including the *GmADT* family members. There is often a period of gene loss following WGDs leading to the pseudogenization and loss of the redundant genes, but neofunctionalization of duplicates can also occur (Lynch and Force, 2000; Young and Bharti, 2012). Our data demonstrate that most of the *GmADT*s we identified encode functional proteins, indicating the GmADT isoforms are not fully redundant. The *GmADT*s are expressed in all soybean tissues, however they have unique temporal and spatial expression patterns, suggesting they are differentially regulated, and could differentially contribute to phenylpropanoid and (iso)flavonoid biosynthesis. *GmADT9* and *GmADT17* have diverged the most in sequence, sharing only ~50-63% identity with the other GmADTs at the nucleotide level and protein levels. Generally, GmADT isoforms that share high sequence identity, such as *GmADT11A* and *GmADT12B*, had similar expression profiles reflecting their shared evolutionary history. Though *GmADT11B* and *GmADT12D* share 93% nucleotide sequence identity, their expression patterns differ in the nodules, stem and throughout seed development, suggesting differences in regulation of gene expression and perhaps different contributions to specialized metabolism between these closely related isoforms. ADT isoforms from *Arabidopsis* have also been shown to be differentially expressed and contribute uniquely to metabolism (Corea et al., 2012b; Chen et al., 2016; Muhammad et al., 2023). For example, *GmADT11A*, *GmADT12A*, *GmADT12B*, and *GmADT13A* exhibited high mRNA expression in stems (Figure 5), and these GmADTs group with AtADT4 and AtADT5 in subgroup I (Figure 4). Of the six isoforms of the AtADT family, AtADT4 and AtADT5 contributed greatly to lignin production in stem tissue (Corea et al., 2012a) suggesting a role in lignin production for *GmADT11A*, *GmADT12A*, *GmADT12B*, and *GmADT13A*. El-Azaz and colleagues (2018) demonstrated that *AtADT2* expression was crucial for normal seed development in *Arabidopsis*. Further, the *adt2* seed phenotype could be rescued by both ADT and PDT activity, by expressing either *AtADT3* or *PHA2*, the PDT from *S. cerevisiae* (El-Azaz et al., 2018). *GmADT11B* and *GmADT12D* are the highest expressed soybean isoforms in seeds that also group with AtADT2 in subgroup II, indicating they may also have an important role in seed development. GmADT12D and GmADT17 are the most highly expressed in the nodules (Figure 5), suggesting these isoforms play an important role in the nodulation process. Taken together, the soybean *GmADT* have unique expression patterns that allows the isoforms to differentially contribute to Phe biosynthesis and ultimately specialized metabolism.

A consquence of WGDs is the alteration entire genetic networks, which can provide short-term advantages to biotic and abiotic stress tolerance (Van de Peer et al., 2017). In plants, many genes involved in stress responses and development are also present as large gene families (Cannon et al., 2004; Pan et al., 2022). In addition, the legume-specific WGD is suggested to have had a profound effect on nodulation and symbiosis (Young et al., 2011).

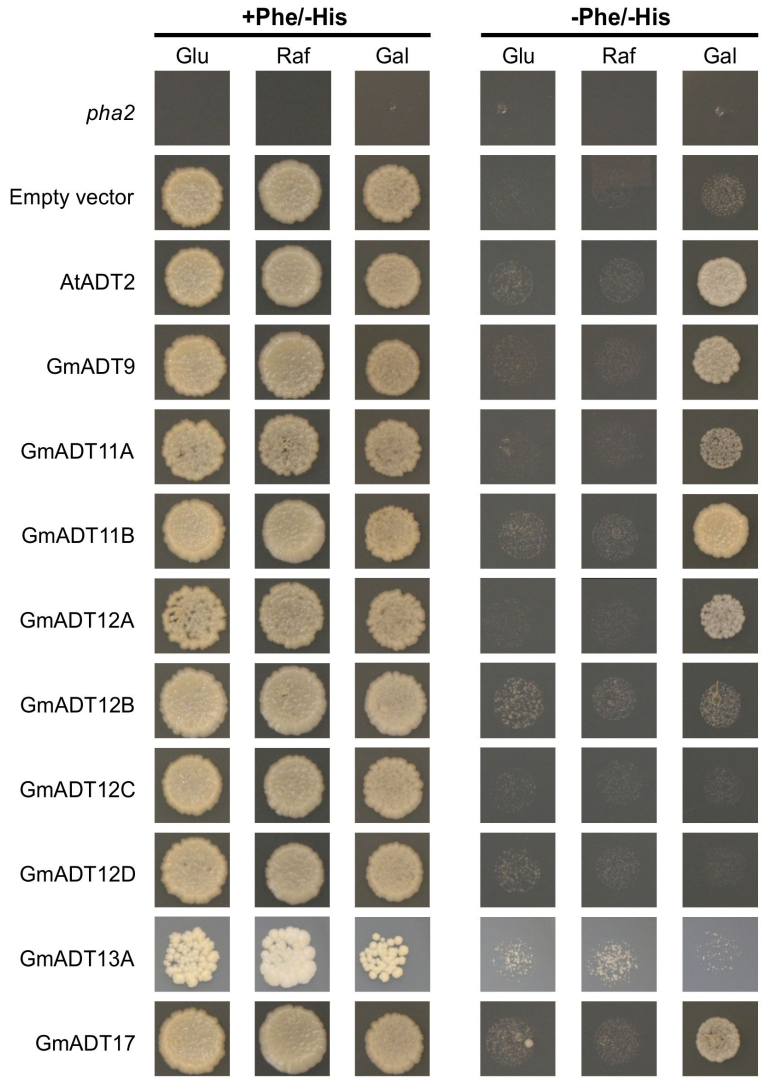

FIGURE 9
pha2 complementation analysis of GmADTs. GmADTs were expressed in the yeast *pha2* strain and spotted onto SD media supplemented with either glucose (Glu), raffinose (Raf) or galactose (Gal). Media with each carbon source were also prepared either with or without phenylalanine (Phe). *S. cerevisiae pha2* strains transformed with GmADT were diluted to a final density of 5 x 10^4 cells/mL and then equal volume of each was plated. Shown are representative growth spots, with images taken after 13 days of incubation. As negative controls, untransformed *pha2* strain and the *pha2* strain transformed with the empty expression vector were included. AtADT2 was used as a positive control. GmADT9, GmADT11A, GmADT11B, GmADT12A and GmADT17 complemented the *pha2* strain, demonstrating these GmADT enzymes possess PDT activity.

Further, duplications in the flowering plant lineage has lead to a clade of allosterically deregulated ADT enzymes (referred to as type-II), and at least one member of this clade is present in most angiosperm genomes (El-Azaz et al., 2022). Type-I ADTs are tightly allosterically regulated by Phe, and include PpADT-G, AtADT1, GmADT9, GmADT11B and GmADT17. Type-II ADTs are much more loosely regulated, and include PpADT-C, AtADT4, and the remaining GmADT isoforms. These type-II isoforms are though to contribute to the accumulation of large quantities of Phe in the cell, which can potentially be shuttled toward specialized metabolite synthesis (El-Azaz et al., 2022; Muhammad et al., 2023). As isoflavonoids are a diverse class of compounds important for establishing symbioses with *Rhizobia*, a large family of differentially regulated and loosely allosterically regulated *ADT*s may allow more flexible control over (iso)flavonoid synthesis, in addition to some degree of functional redundancy conferred by large gene families (Kafri et al., 2009; El-Azaz et al., 2022; Muhammad et al., 2023).

GmADTs interact with the isoflavonoid metabolon

Most ADT enzymes characterized to date are localized to the chloroplast, specifically to stromules (Rippert et al., 2009; Maeda et al., 2010; El-Azaz et al., 2016; Bross et al., 2017). However, some ADT isozymes localize to the nucleus or cytosol, for example, AtADT5 and AtADT6, respectively (Bross et al., 2017). We determined that the GmADTs were all localized to stromules. Since all nine GmADTs have an N-terminal chloroplast transit

peptide, this suggests all GmADTs participate in phenylalanine biosynthesis *via* the well described chloroplast localized arogenate pathway. This is not surprising, as most plants described to date have a family of plastidic ADTs to convert arogenate to Phe (Jung et al., 1986; Ehlting et al., 2005; Cho et al., 2007; Rippert et al., 2009; Maeda and Dudareva, 2012; El-Azaz et al., 2016), and the GmADTs are similar in sequence to other characterized plant ADTs.

However, we observed interactions with GmIFS2 for all nine GmADTs that occur at the ER. In addition, GmADT12A also interacts both GmC4H2 and GmIFS1 at the ER membrane, GmCHS8 in the cytosol, and with GmCHI2 and GmCHR14 in the cytosol and the nucleus (Figure 8). The interaction of GmADT12A with GmCHI2 and GmCHR14 in the nucleus adds to the growing body of evidence that has detected (iso)flavonoid synthesis enzymes in the nucleus. Nucleo-cytoplasmic localizations have previously been reported for both GmCHI2 and GmCHR14 (Dastmalchi and Dhaubhadel, 2015; Sepiol et al., 2017). In addition, nuclear localization of CHI and CHS enzymes have also been reported in *Arabidopsis* and grapevine (Saslowsky et al., 2005; Wang et al., 2016; Watkinson et al., 2018; Wang et al., 2019). Localization of the (iso)flavonoid biosynthetic machinery in nucleus would allow direct deposition of these compounds in the nucleus (Saslowsky et al., 2005), however the role of (iso)flavonoids in the nucleus is not entirely clear. As flavonoids can bind DNA and have been shown to bind histones, regulation of gene expression by binding DNA associated proteins or DNA directly have been suggested as possible roles for these compounds in the nucleus (Hodek et al., 2002; Ramadass et al., 2003). Alternatively, the GmADTs and other (iso)flavonoid synthesis enzymes in the nucleus could have a secondary role there in regulating gene expression as retrograde signals (Isemer et al., 2012).

It is unlikely that the detected interaction is due to overpression of both GmIFS2 and the GmADTs, as no interaction was detected with PvMATE8 or AtCRA1 using the same detection system, indicating the interaction is specific to the GmADTs and GmIFS2. Furthermore, the same promoter was used for both detection of subcellular localization and protein-protein interactions, indicating the difference in GmADT localization is not soley due to overexpression using the 35S promoter. In addition, it has been shown that subcellular localization patterns detected in tobacco with a 35S promoter are indicative of what happens in the native organism. For example, AtADT5 nuclear localization was first determined in tobacco and was then confirmed when expressed under its native promoter in *Arabidopsis* (Bross et al., 2017), indicating the alternate nuclear localization was not an articact of expression in tobacco.

The current data substantiate our previous investigation of the isoflavonoid metabolon that was performed using the soybean hairy roots expressing GmIFS2-YFP, and GmADT12A and GmADT13A were pulled down in Co-IP analysis (Dastmalchi et al., 2016). Among the members of GmADT family, root-specific expression was only observed for *GmADT12A* and *GmADT13A* (Figure 5) which is consistent with only these two isoforms being identified by the Co-IP analysis. As the GmADTs are differentially expressed, isoflavonoid metabolon composition may vary depending on the GmADT isoform expressed in a given tissue. It has also been suggested that there could be more than one metabolon dedicated to the synthesis of different metabolites, given the availability of enzyme isoforms and their substrate preferences (Ehlting et al., 1999; Winkel, 2004; Li et al., 2015). One also needs to consider that in addition to tissue-specific expression of isoforms, metabolons are inherently transient and dynamic in nature. Consequently, there could be a high turnover of GmADT isoforms participating in the isoflavonoid metabolon, providing flexibility in metabolon assembly, substrate sequestering, metabolic channeling potential, and stress response (Winkel, 2002; Moller, 2010; Hawes et al., 2015).

PDT activity of GmADTs

Most plant ADT families have least one isoform with predicted or demonstrated PDT activity, suggesting that both the prephenate and arogenate pathways are active in plants. It is thought that the Phe is predominantly synthesized *via* the arogenate pathway in the plastids. However, cytosolic PhPPY-AT and PhCM isoforms have been characterized (Yoo et al., 2013; Qian et al., 2019), and a cytosolic prephenate pathway has been described in *Petunia hybrida* (Qian et al., 2019). The possible advantages associated with the prephenate pathway, or the degree to which the prephenate pathway contributes to Phe synthesis is still unclear.

We determined that five GmADT isoforms had detectable PDT activity using the *pha2* complementation test: GmADT9, GmADT11A, GmADT11B, GmADT12A and GmADT17. As GmADT9 and GmADT17 fall within subgroup I, and GmADT11B in subgroup II in the ADT/PDT phylogenetic tree (Figure 4B), this result is not surprising. These three GmADT isoforms contain the critical Ala314 residue in the PAC domain that confers PDT activity to PpADT-B and PpADT-G (El-Azaz et al., 2016). Interestingly, GmADT11A and GmADT12A were also found to have PDT activity, but neither isoform contains the critical Ala314 residue. In fact, GmADT11A and GmADT12A both cluster within subgroup III, with isoforms from *Arabidopsis* and *P. pinaster* that do not have PDT activity. While some key resiudes for PDT activity have been identified in the PAC domain, it was noted that mutations in this domain had a variety of outcomes on PDT and ADT activity (El-Azaz et al., 2016; El-Azaz et al., 2022). It is possible that other unidentified amino acid residues within the PAC domain are important in defining PDT activity in soybean and other plant species. Further, by sequence alone, GmADT12C and GmADT12D were expected to act as PDTs. However, these two GmADT isoforms were among the GmADT proteins not well expressed in the *pha2* strain. As such, they could still have PDT activity if assessed using another method. We expect all the GmADTs to act as ADTs, given the sequence similarity to other plant ADTs, though we did not characterize ADT activity here. Determining the kinetics of the GmADTs with both arogenate and prephenate as a substrate should also be investigated in future, as it has been demonstrated that the *Arabidopsis* and *Petunia* ADT/PDTs prefer arogenate over prephenate as a substrate (Cho et al., 2007; Maeda et al., 2010). The proportion of phenylalanine synthesized via either pathway could also be tissue-specific,

depending on whether the *ADT* isoform expressed in a given tissue has PDT activity.

Trans-organelle continuity

As the cytoplasmic isoflavonoid metabolon assembles on the cytosolic face of the ER, we initially hypothesized that participating GmADTs are cytosolic, but no cytosolic GmADT isoforms were observed in this study when expressed alone. This begs the question, how can plastid-localized enzymes interact with a cytosolic metabolon? One possibility is that some of the *GmADT*s contain alternative transcriptional start sites, as seen for *PhADT3* (Qian et al., 2019), resulting in ADTs lacking a transit peptide that localize in the cytosoplasm (Figure 10A). Having transcript variants, with or without transit peptides, could allow differential contribution in response to various stress conditions or signaling cascades like nodulation induction. Alternatively, the full-length GmADTs could also associate with the metabolon in the cytosol prior to their transit to the chloroplast.

Another explanation for the involvement of GmADTs in the isoflavonoid metabolon is trans-organelle continuity (Figure 10B). The ER is a dynamic organelle (Allen and Brown, 1988; Bayer et al., 2017; Kriechbaumer and Brandizzi, 2020), and there is evidence that the ER can associate with various organelles in the cell, including the chloroplast (Schattat et al., 2012; Phillips and Voeltz, 2016; Barton et al., 2018). It has been demonstrated in mammalian and plant cells that the ER forms contacts with peroxisomes, mitochondria, the plasma membrane and plasmodesmata (Hawes et al., 2015; Bayer et al., 2017; Perico and

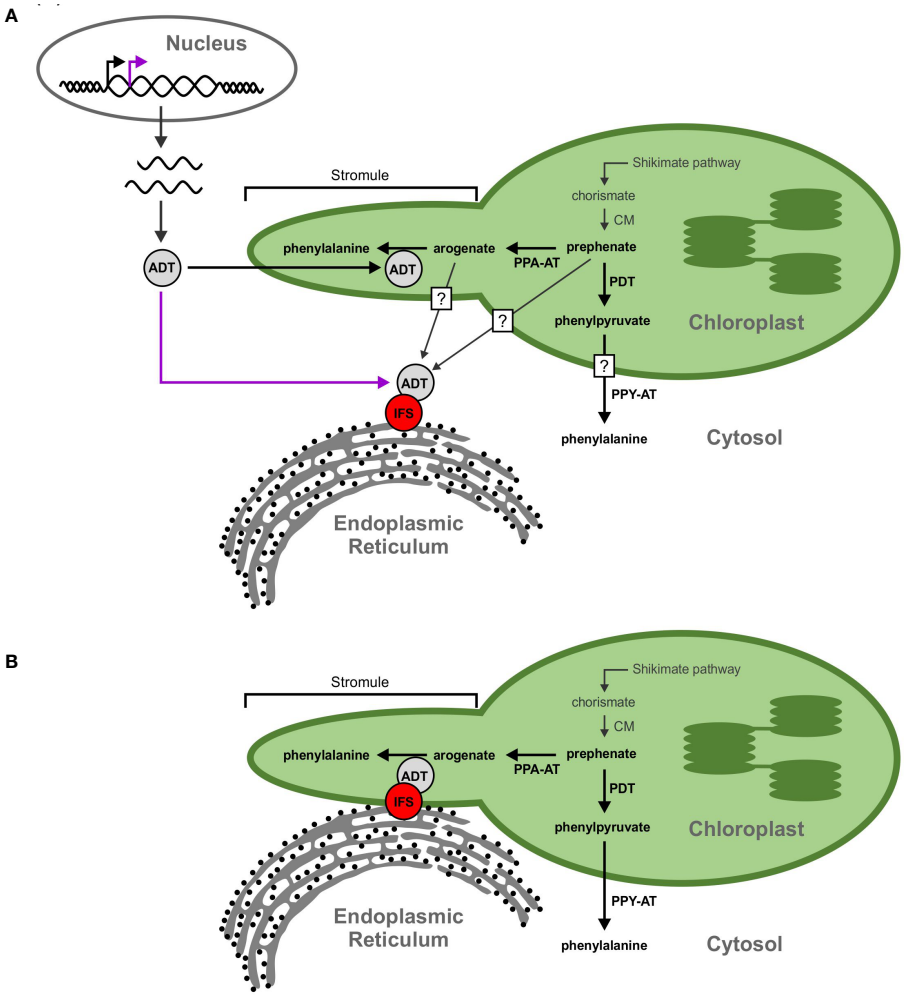

FIGURE 10
Proposed models for the GmADT-GmIFS2 interaction. **(A)** Full length ADT proteins contain an N-terminal transit peptide that directs them to the chloroplast (black arrow). However, alternate transcriptional start sites could result in a protein that lacks the transit peptide and remains in the cytosol (purple arrow). The cytosolic ADT protein would be available to interact with IFS and participate in the isoflavonoid metabolon. Substrates (prephenate, arogenate, phenylpyruvate, etc) could be transported out of the chloroplast, or they could passively diffuse across the chloroplast membrane, facilitated by the larger surface area of stromules. Prephenate could also be synthesized directly in the cytosol by cytosolic isoforms of CM. **(B)** Transorganelle continuity is another model allowing to explain the interaction between ADT and IFS proteins. The ER is a dynamic organelle that has been shown to interact with other organelles, namely the mitochondria and nucleus. Interactions between the ER and chloroplast membranes could bring the isoflavonoid metabolon and ADTs in close proximity.

Sparkes, 2018; Li et al., 2022). The ER has also been shown to be involved in nuclear envelope formation and reshaping during cell division, and may facilitate protein localization to the inner nuclear membrane (Anderson and Hetzer, 2007; Blackstone, 2017; Ungricht and Kutay, 2017).

Multiple contact sites have been demonstrated between the ER membrane and chloroplasts (Griffing, 2011; Block and Jouhet, 2015), and it has even been suggested that the ER and chloroplast membranes can become contiguous (Whatley et al., 1991). ER morphology changes have also been shown to correlate with the growth and retraction of stromules (Schattat et al., 2011). Stromules have been reported to expedite the transport and/or diffusion of small molecules and proteinsbetween the plastid and surrounding cellular compartments, and have been shown to be involved in various signaling and defense responses (Gray et al., 2001; Hanson and Hines, 2018; Perico and Sparkes, 2018), as well as plastid-to-plastid contact sites, and possible contacts with other organelles (Kwok and Hanson, 2004a; Erickson et al., 2017). It has also been demonstrated that ER lumen localized enzymes have access to tocopherol substrates at the inner plastid membrane (Mehrshahi et al., 2013), making trans-orgnalle continuity a compelling argument for GmADT access to the (iso)flavonoid metabolon. Stromule localization of GmADT proteins places them in a dynamic sub-plastidial environment, facilitating interactions with the ER, and subsequent association with the (iso)flavonoid metabolon. GmADT involvement in the (iso)flavonoid metablon would directly link flux toward Phe biosynthesis to the synthesis of specialized metabolites.

Organelle interactions offer a variety of advantages. Substrates do not need to be exported from organelles and diffused across the cytosol. Required substrates and intermediates are sequestered, limiting byproduct formation and increasing pathway efficiency (Moller, 2010; Zhang and Fernie, 2021). Regulating organelle contacts could also provide another avenue to regulate flux through pathways, in addition to transcriptional and translational regulation of enzymatic components.

Conclusions and outlook

We have identified nine *GmADT* family members and demonstrated their interaction with GmIFS2 and other (iso) flavonoid metabolon enzymes using an *N. benthamiana* BiFC expression system. While we previously reported the interaction of GmADT12A and GmADT13A with GmIFS2 in soybean roots, confirmation of the interaction between GmIFS2 and the other GmADTs in soybean tissue is still required. In addition, we have demonstrated that at least five of the nine GmADTs have PDT activity by yeast complementation analysis in the *pha2* strain. However, there are still questions surrounding the *GmADT* family members and their involvement in (iso)flavonoid synthesis. In this work, we did not assess the ADT activity of the soybean ADTs. While they appear to be homologous to other plant ADTs, and share many of the sequences defining ADT activity and regulation, quantifying the ADT activity of the GmADT family is still necessary. Further, the factors influencing flux between the arogenate pathway and the prephenate pathway, and how GmADTs contribute phenylalanine to the (iso)flavonoid metabolon are yet unknown. Finally, determining the extent to which tissue-specific expression influences the (iso)flavonoid metabolon and ADT isoform involvement would provide insights into the differential regulation and diverging functions of gene family members.

Data availability statement

The original contributions presented in the study are included in the article/Supplementary Material. Further inquiries can be directed to the corresponding author.

Author contributions

EC: Data curation, Investigation, Formal analysis, Methodology, Writing – original draft. NI: Data curation, Methodology, Software, Validation, Writing – review & editing. KP: Writing – review & editing, Investigation. KK: Investigation, Writing – review & editing, Validation. RS: Investigation, Writing – review & editing. SK: Writing – review & editing, Supervision. SD: Supervision, Writing – review & editing, Conceptualization, Data curation, Funding acquisition, Investigation, Project administration, Resources, Validation, Visualization.

Funding

The author(s) declare financial support was received for the research, authorship, and/or publication of this article. This research was supported by Agriculture and Agri-Food Canada's Genomics Research and Development Initiative Abase grants (J-001826) and a Natural Sciences and Engineering Research Council of Canada's Discovery Grant (385922-2011, 044661-2018 RGPIN) to SD.

Acknowledgments

The authors thank Ling Chen and Alex Molnar for technical assistance.

Conflict of interest

The authors declare that the research was conducted in the absence of any commercial or financial relationships that could be construed as a potential conflict of interest.

Publisher's note

that may be evaluated in this article, or claim that may be made by its manufacturer, is not guaranteed or endorsed by the publisher.

Supplementary material

The Supplementary Material for this article can be found online at: https://www.frontiersin.org/articles/10.3389/fpls.2024.1307489/full#supplementary-material

SUPPLEMENTARY FIGURE 1
GmADT and GmIFS2 interact *in planta* at the ER. Reciprocal combination of GmADT isoforms and GmIFS2 (as shown in)and their interaction by co-expression of translational fusions with N (YN)- or C (YC)- terminal fragments of YFP in *N. benthamiana* as assayed by BiFC.

SUPPLEMENTARY FIGURE 2
GmADT12A-YN and isoflavonoid biosynthetic enzymes-YC interaction (reciprocal combination of).

SUPPLEMENTARY FIGURE 3
Western blot detection of *Gm*ADTs in *S. cerevisiae pha2*. **(A)** GmADTs- his were expressed in the yeast *pha2* strain and detected by western blotting analysis using anti-his antibody. **(B)** Coomassie stained gel of total protein under non-inducing (glucose) condition. **(C)** Coomassie stained gel of total protein under inducing (galactose) condition.

References

Abolhassani Rad, S. (2017). *The mystery of nuclear localization of AROGENATE DEHYDRATASE 5 from Arabidopsis thaliana* (London, ON: The University of Western Ontario).

Ackerman, S. H., Martin, J., and Tzagoloff, A. (1992). Characterization of ATP11 and detection of the encoded protein in mitochondria of *Saccharomyces cerevisiae*. *J. Biol. Chem.* 267, 7386–7394. doi: 10.1016/S0021-9258(18)42529-X

Allen, N. S., and Brown, D. T. (1988). Dynamics of the endoplasmic reticulum in living onion epidermal cells in relation to microtubules, microfilaments, and intracellular particle movement. *Cell Motil.* 10, 153–163. doi: 10.1002/cm.970100120

Amack, S. C., and Antunes, M. S. (2020). CaMV35S promoter – A plant biology and biotechnology workhorse in the era of synthetic biology. *Curr. Plant Biol.* 24, 100179. doi: 10.1016/j.cpb.2020.100179

Anderson, D., and Hetzer, M. (2007). Nuclear envelope formation by chromatin-mediated reorganization of the endoplasmic reticulum. *Nat. Cell Biol.* 9, 1160–1166. doi: 10.1038/ncb1636

Arimura, S., Hirai, A., and Tsutsumi, N. (2001). Numerous and highly developed tubular projections from plastids observed in Tobacco epidermal cells. *Plant Sci.: an Int. J. Exp. Plant Biol.* 160, 449–454. doi: 10.1016/s0168-9452(00)00405-2

Barton, K. A., Wozny, M. R., Mathur, N., Jaipargas, E. A., and Mathur, J. (2018). Chloroplast behaviour and interactions with other organelles in *Arabidopsis thaliana* pavement cells. *J. Cell Sci.* 131, jcs202275. doi: 10.1242/jcs.202275

Bayer, E. M., Sparkes, I. A., Vanneste, S., and Rosado, A. (2017). From shaping organelles to signalling platforms: the emerging functions of plant ER–PM contact sites. *Curr. Opin. Plant Biol.* 40, 89–96. doi: 10.1016/j.pbi.2017.08.006

Bhat, S. S., Prasad, S. K., Shivamallu, C., Prasad, K. S., Syed, A., Reddy, P., et al. (2021). Genistein: A potent anti-breast cancer agent. *Curr. Issues Mol. Biol.* 43, 1502–1517. doi: 10.3390/cimb43030106

Blackstone, C. (2017). Protein targeting: ER leads the way to the inner nuclear envelope. *Curr. Biol.* 27, 1284–1286. doi: 10.1016/j.cub.2017.10.037

Block, M. A., and Jouhet, J. (2015). Lipid trafficking at endoplasmic reticulum-chloroplast membrane contact sites. *Curr. Opin. Cell Biol.* 35, 21–29. doi: 10.1016/j.ceb.2015.03.004

Boudet, A. M. (2007). Evolution and current status of research in phenolic compounds. *Phytochemistry* 68, 2722–2735. doi: 10.1016/j.phytochem.2007.06.012

Bradley, C. A., Allen, T. W., Sisson, A. J., Bergstrom, G. C., Bissonnette, K. M., Bond, J., et al. (2021). Soybean yield loss estimates due to diseases in the United States and Ontario, Canada, from 2015 to 2019. *Plant Health Prog.* 22, 483–495. doi: 10.1094/PHP-01-21-0013-RS

Bross, C. D., Corea, O. R., Kaldis, A., Menassa, R., Bernards, M. A., and Kohalmi, S. E. (2011). Complementation of the *pha2* yeast mutant suggests functional differences for arogenate dehydratases from *Arabidopsis thaliana*. *Plant Physiol. Biochem.* 49, 882–890. doi: 10.1016/j.plaphy.2011.02.010

Bross, C. D., Howes, T. R., Abolhassani Rad, S., Kljakic, O., and Kohalmi, S. E. (2017). Subcellular localization of Arabidopsis arogenate dehydratases suggests novel and non-enzymatic roles. *J. Exp. Bot.* 68, 1425–1440. doi: 10.1093/jxb/erx024

Cannon, S. B., Mitra, A., Baumgarten, A., Young, N. D., and May, G. (2004). The roles of segmental and tandem gene duplication in the evolution of large gene families in *Arabidopsis thaliana*. *BMC Plant Biol.* 4, 10. doi: 10.1186/1471-2229-4-10

Cederroth, C. R., and Nef, S. (2009). Soy, phytoestrogens and metabolism: A review. *Mol. Cell Endocrinol.* 304, 30–42. doi: 10.1016/j.mce.2009.02.027

Chandra, S., Choudhary, M., Bagaria, P. K., Nataraj, V., Kumawat, G., Choudhary, J. R., et al. (2022). Progress and prospectus in genetics and genomics of Phytophthora root and stem rot resistance in soybean (*Glycine max* L.). *Front. Genet. Nov* 14, 13. doi: 10.3389/fgene.2022.939182

Chen, C., Chen, H., Zhang, Y., Thomas, H. R., Frank, M. H., He, Y., et al. (2020). TBtools: An integrative toolkit developed for interactive analyses of big biological data. *Mol. Plant* 13, 1194–1202. doi: 10.1016/j.molp.2020.06.009

Chen, Q., Man, C., Li, D., Tan, H., Xie, Y., and Huang, J. (2016). Arogenate dehydratase isoforms differentially regulate anthocyanin biosynthesis in *Arabidopsis thaliana*. *Mol. Plant* 9, 1609–1619. doi: 10.1016/j.molp.2016.09.010

Cho, M.-H., Corea, O. R. A., Yang, H., Bedgar, D. L., Laskar, D. D., Anterola, A. M., et al. (2007). Phenylalanine biosynthesis in *Arabidopsis thaliana*. Identification and characterization of arogenate dehydratases. *J. Biol. Chem.* 282, 30827–30835. doi: 10.1074/jbc.M702662200

Corea, O. R., Bedgar, D. L., Davin, L. B., and Lewis, N. G. (2012a). The arogenate dehydratase gene family: towards understanding differential regulation of carbon flux through phenylalanine into primary versus secondary metabolic pathways. *Phytochemistry* 82, 22–37. doi: 10.1016/j.phytochem.2012.05.026

Corea, O. R. A., Ki, C., Cardenas, C. L., Kim, S. J., Brewer, S. E., Patten, A. M., et al. (2012b). Arogenate dehydratase isoenzymes profoundly and differentially modulate carbon flux into lignins. *J. Biol. Chem.* 287, 11446–11459. doi: 10.1074/jbc.M111.322164

Cotton, R. G. H., and Gibson, F. (1965). Biosynthesis of phenylalanine and tyrosine - enzymes converting chorismic acid into prephenic acid and their relationships to prephenate dehydratase and prephenate dehydrogenase. *Biochim. Biophys. Acta* 100, 76–88. doi: 10.1016/0304-4165(65)90429-0

Crosby, K. C., Pietraszewska-Bogiel, A., Gadella, T. W. J., and Winkel, B. S. J. (2011). Forster resonance energy transfer demonstrates a flavonoid metabolon in living plant cells that displays competitive interactions between enzymes. *FEBS Lett.* 585, 2193–2198. doi: 10.1016/j.febslet.2011.05.066

Dastmalchi, M., Bernards, M. A., and Dhaubhadel, S. (2016). Twin anchors of the soybean isoflavonoid metabolon: evidence for tethering of the complex to the endoplasmic reticulum by IFS and C4H. *Plant J.* 85, 689–706. doi: 10.1111/tpj.13137

Dastmalchi, M., and Dhaubhadel, S. (2014). "Soybean seed isoflavonoids: biosynthesis and regulation," in *Phytochemicals – Biosynthesis, Function and Application* (Cham: Springer International Publishing), 1–21.

Dastmalchi, M., and Dhaubhadel, S. (2015). Soybean chalcone isomerase: evolution of the fold, and the differential expression and localization of the gene family. *Planta* 241, 507–523. doi: 10.1007/s00425-014-2200-5

Dixon, R. A., and Ferreria, D. (2002). Genistein. *Phytochemistry* 60, 205–211. doi: 10.1016/S0031-9422(02)00116-4

Earley, K. W., Haag, J. R., Pontes, O., Opper, K., Juehne, T., Song, K., et al. (2006). Gateway-compatible vectors for plant functional genomics and proteomics. *Plant J.* 45, 616–629. doi: 10.1111/j.1365-313X.2005.02617.x

Ehlting, J., Büttner, D., Wang, Q., Douglas, C. J., Somssich, I. E., and Kombrink, E. (1999). Three 4-coumarate:coenzyme A ligases in *Arabidopsis thaliana* represent two evolutionarily divergent classes in angiosperms. *Plant J.: Cell Mol. Biol.* 19, 9–20. doi: 10.1046/j.1365-313X.1999.00491.x

Ehlting, J., Mattheus, N., Aeschliman, D. S., Li, E. Y., Hamberger, B., Cullis, I. F., et al. (2005). Global transcript profiling of primary stems from *Arabidopsis thaliana* identifies candidate genes for missing links in lignin biosynthesis and transcriptional regulators of fiber differentiation. *Plant J.* 42, 618–640. doi: 10.1111/j.1365-313X.2005.02403.x

El-Azaz, J., Canovas, F. M., Avila, C., and de la Torre, F. (2018). The arogenate dehydratase ADT2 is essential for seed development in Arabidopsis. *Plant Cell Physiol.* 59, 2409–2420. doi: 10.1093/pcp/pcy200

El-Azaz, J., Cánovas, F. M., Barcelona, B., Ávila, C., and de la Torre, F. (2022). Deregulation of phenylalanine biosynthesis evolved with the emergence of vascular plants. *Plant Physiol.* 188, 134–150. doi: 10.1093/plphys/kiab454

El-Azaz, J., de la Torre, F., Ávila, C., and Cánovas, F. M. (2016). Identification of a small protein domain present in all plant lineages that confers high prephenate dehydratase activity. *Plant J.* 87, 215–229. doi: 10.1111/tpj.13195

Emanuelsson, O., Brunak, S., von Heijne, G., and Nielsen, H. (2007). Locating proteins in the cell using TargetP, SignalP and related tools. *Nat. Prot.* 2, 953–971. doi: 10.1038/nprot.2007.131

Erickson, J. L., Kantek, M., and Schattat, M. H. (2017). Plastid-nucleus distance alters the behavior of stromules. *Front. Plant Sci.* 8, 1135. doi: 10.3389/fpls.2017.01135

Fazel, A. M., Bowen, J. R., and Jensen, R. A. (1980). Arogenate (pretyrosine) is an obligatory intermediate of L-tyrosine biosynthesis - confirmation in a microbial mutant. *P Natl. Acad. Sci. U.S.A.* 77, 1270–1273. doi: 10.1073/pnas.77.3.1270

García-Calderón, M., Pérez-Delgado, C. M., Palove-Balang, P., Betti, M., and Márquez, A. J. (2020). Flavonoids and isoflavonoids biosynthesis in the model legume *Lotus japonicus*; Connections to nitrogen metabolism and photorespiration. *Plants* 9, 774. doi: 10.3390/plants9060774

Graindorge, M., Giustini, C., Jacomin, A. C., Kraut, A., Curien, G., and Matringe, M. (2010). Identification of a plant gene encoding glutamate/aspartate-prephenate aminotransferase: The last homeless enzyme of aromatic amino acids biosynthesis. *FEBS Lett.* 584, 4357–4360. doi: 10.1016/j.febslet.2010.09.037

Gray, J. C., Sullivan, J. A., Hibberd, J. M., and Hansen, M. R. (2001). Stromules: Mobile protrusions and interconnections between plastids. *Plant Biol.* 3, 223–233. doi: 10.1055/s-2001-15204

Griffing, L. R. (2011). Laser stimulation of the chloroplast/endoplasmic reticulum nexus in tobacco transiently produces protein aggregates (boluses) within the endoplasmic reticulum and stimulates local er remodeling. *Mol. Plant* 4, 886–895. doi: 10.1093/mp/ssr072

Hanson, M. R., and Hines, K. M. (2018). Stromules: probing formation and function. *Plant Physiol.* 176, 128–137. doi: 10.1104/pp.17.01287

Hassan, S., and Mathesius, U. (2012). The role of flavonoids in root-rhizosphere signalling: opportunities and challenges for improving plant-microbe interactions. *J. Exp. Bot.* 63, 3429–3444. doi: 10.1093/jxb/err430

Hawes, C., Kiviniemi, P., and Kriechbaumer, V. (2015). The endoplasmic reticulum: A dynamic and well-connected organelle. *J. Integr. Plant Biol.* 57, 50–62. doi: 10.1111/jipb.12297

Hill, J. E., and Breidenbach, R. W. (1974). Proteins of soybean seeds.1. Isolation and characterization of major components. *Plant Physiol.* 53, 742–746. doi: 10.1104/pp.53.5.742

Hodek, P., Trefil, P., and Stiborová, M. (2002). Flavonoids-potent and versatile biologically active compounds interacting with cytochromes P450. *Chemico Biol. Interact.* 139, 1–21. doi: 10.1016/S0009-2797(01)00285-X

Hrazdina, G., and Wagner, G. J. (1985). Metabolic pathways as enzyme complexes: Evidence for the synthesis of phenylpropanoids and flavonoids on membrane associated enzyme complexes. *Arch. Biochem. Biophys.* 237, 88–100. doi: 10.1016/0003-9861(85)90257-7

Hsu, S. K., Lin, L. L., Lo, H. H., and Hsu, W. H. (2004). Mutational analysis of feedback inhibition and catalytic sites of prephenate dehydratase from *Corynebacterium glutamicum*. *Arch. Microbiol.* 181, 237–244. doi: 10.1007/s00203-004-0649-5

Isemer, R., Mulisch, M., Schäfer, A., Kirchner, S., Koop, H. U., and Krupinska, K. (2012). Recombinant Whirly1 translocates from transplastomic chloroplasts to the nucleus. *FEBS Lett.* 586, 85–88. doi: 10.1016/j.febslet.2011.11.029

Jorgensen, K., Rasmussen, A. V., Morant, M., Nielsen, A. H., Bjarnholt, N., Zagrobelny, M., et al. (2005). Metabolon formation and metabolic channeling in the biosynthesis of plant natural products. *Curr. Opin. Plant Biol.* 8, 280–291. doi: 10.1016/j.pbi.2005.03.014

Jung, E., Zamir, L. O., and Jensen, R. A. (1986). Chloroplasts of higher-plants synthesize L-phenylalanine via L-arogenate. *Proc. Natl. Acad. Sci. U.S.A.* 83, 7231–7235. doi: 10.1073/pnas.83.19.7231

Kafri, R., Springer, M., and Pilpel, Y. (2009). Genetic redundancy: new tricks for old genes. *Cell* 136, 389–392. doi: 10.1016/j.cell.2009.01.027

Kaminaga, Y., Schnepp, J., Peel, G., Kish, C. M., Ben-Nissan, G., Weiss, D., et al. (2006). Plant phenylacetaldehyde synthase is a bifunctional homotetrameric enzyme that catalyzes phenylalanine decarboxylation and oxidation. *J. Biol. Chem.* 281, 23357–23366. doi: 10.1074/jbc.M602708200

Khatri, P., Chen, L., Rajcan, I., and Dhaubhadel, S. (2023). Functional characterization of Cinnamate 4-hydroxylase gene family in soybean (Glycine max). *PloS One* 18, e0285698. doi: 10.1371/journal.pone.0285698

Kriechbaumer, V., and Brandizzi, F. (2020). The plant endoplasmic reticulum: an organized chaos of tubules and sheets with multiple functions. *J. Microsc.* 280, 122–133. doi: 10.1111/jmi.12909

Kumar, S., Stecher, G., Li, M., Knyaz, C., and Tamura, K. (2018). MEGA X: Molecular evolutionary genetics analysis across computing platforms. *Mol. Biol. Evol.* 35, 1547–1549. doi: 10.1093/molbev/msy096

Kushnirov, V. V. (2000). Rapid and reliable protein extraction from yeast. *Yeast* 16, 857–860. doi: 10.1002/1097-0061(20000630)16:9<857::AID-YEA561>3.0.CO;2-B

Kwok, E. Y., and Hanson, M. R. (2004a). Plastids and stromules interact with the nucleus and cell membrane in vascular plants. *Plant Cell Rep.* 23, 188–195. doi: 10.1007/s00299-004-0824-9

Kwok, E. Y., and Hanson, M. R. (2004b). Stromules and the dynamic nature of plastid morphology. *J. Microsc.* 214, 124–137. doi: 10.1111/j.0022-2720.2004.01317.x

Lamartiniere, C. A. (2000). Protection against breast cancer with genistein: a component of soy. *Am. J. Clin. Nutr.* 71, 1705S–1707S. doi: 10.1093/ajcn/71.6.1705S

Li, C., Duckney, P., Zhang, T., Fu, Y., Li, X., Kroon, J., et al. (2022). TraB family proteins are components of ER-mitochondrial contact sites and regulate ER-mitochondrial interactions and mitophagy. *Nat. Commun.* 13, 5658. doi: 10.1038/s41467-022-33402-w

Li, Y., Kim, J. I., Pysh, L., and Chapple, C. (2015). Four Isoforms of Arabidopsis 4-coumarate-CoA ligase have overlapping yet distinct roles in phenylpropanoid metabolism. *Plant Physiol.* 169, 2409–2421. doi: 10.1104/pp.15.00838

Liang, B., Cao, J., Wang, R., Fan, C., Wang, W., Hu, X., et al. (2023). ZmCIPK32 positively regulates germination of stressed seeds via gibberellin signal. *Plant Physiol. Biochem.* 199, 107716. doi: 10.1016/j.plaphy.2023.107716

Lohr, D., Venkov, P., and Zlatanova, J. (1995). Transcriptional regulation in the yeast GAL gene family: a complex genetic network. *FASEB J.* 9, 777–787. doi: 10.1096/fasebj.9.9.7601342

Lozovaya, V. V., Lygin, A. V., Zernova, O. V., Ulanov, A. V., Li, S., Hartman, G. L., et al. (2007). Modification of phenolic metabolism in soybean hairy roots through down regulation of chalcone synthase or isoflavone synthase. *Planta* 225, 665–679. doi: 10.1007/s00425-006-0368-z

Lu, Q., Tang, X., Tian, G., Wang, F., Liu, K., Nguyen, V., et al. (2010). *Arabidopsis* homolog of the yeast TREX-2 mRNA export complex: components and anchoring nucleoporin. *Plant J.* 61, 259–270. doi: 10.1111/j.1365-313X.2009.04048.x

Lynch, M., and Force, A. (2000). The probability of duplicate gene preservation by subfunctionalization. *Genetics* 154, 459–473. doi: 10.1093/genetics/154.1.459

Maeda, H., and Dudareva, N. (2012). The shikimate pathway and aromatic amino Acid biosynthesis in plants. *Annu. Rev. Plant Biol.* 63, 73–105. doi: 10.1146/annurev-arplant-042811-105439

Maeda, H., Shasany, A. K., Schnepp, J., Orlova, I., Taguchi, G., Cooper, B. R., et al. (2010). RNAi suppression of Arogenate Dehydratase1 reveals that phenylalanine is synthesized predominantly via the arogenate pathway in petunia petals. *Plant Cell.* 22, 832–849. doi: 10.1105/tpc.109.073247

Maeda, H., Yoo, H. J., and Dudareva, N. (2011). Prephenate aminotransferase directs plant phenylalanine biosynthesis *via* arogenate. *Nat. Chem. Biol.* 7, 19–21. doi: 10.1038/nchembio.485

Mainali, H. R., Vadivel, A. K. A., Li, X., Gijzen, M., and Dhaubhadel, S. (2017). Soybean cyclophilin GmCYP1 interacts with an isoflavonoid regulator GmMYB176. *Sci. Rep.* 7, 39550. doi: 10.1038/srep39550

Mehrshahi, P., Stefano, G., Andaloro, J. M., Brandizzi, F., Froehlich, J. E., and DellaPenna, D. (2013). Transorganellar complementation redefines the biochemical continuity of endoplasmic reticulum and chloroplasts. *Proc. Natl. Acad. Sci.* 110, 12126–12131. doi: 10.1073/pnas.1306331110

Messina, M. (2010). Insights gained from 20 years of soy research. *J. Nutr.* 140, 2289–2295. doi: 10.3945/jn.110.124107

Moller, B. L. (2010). Dynamic metabolons. *Science* 330, 1328–1329. doi: 10.1126/science.1194971

Muhammad, D., Alameldin, H. F., Oh, S., Montgomery, B. L., and Warpeha, K. M. (2023). Arogenate dehydratases: unique roles in light-directed development during the seed-to-seedling transition in Arabidopsis thaliana. *Front. Plant Sci.* 14. doi: 10.3389/fpls.2023.1220732

Nakayama, T., Takahashi, S., and Waki, T. (2019). Formation of flavonoid metabolons: functional significance of protein-protein interactions and impact on flavonoid chemodiversity. *Front. Plant Sci.* 10. doi: 10.3389/fpls.2019.00821

Odell, J. T., Nagy, F., and Chua, N.-H. (1985). Identification of DNA sequences required for activity of the cauliflower mosaic virus 35S promoter. *Nature* 313, 810–812. doi: 10.1038/313810a0

Owens, D. K., Alerding, A. B., Crosby, K. C., Bandara, A. B., Westwood, J. H., and Winkel, B. S. J. (2008). Functional analysis of a predicted flavonol synthase gene family in Arabidopsis. *Plant Physiol.* 147, 1046–1061. doi: 10.1104/pp.108.117457

Pan, L., Luo, Y., Wang, J., Li, X., Tang, B., Yang, H., et al. (2022). Evolution and functional diversification of catalase genes in the green lineage. *BMC Genomics* 23, 411. doi: 10.1186/s12864-022-08621-6

Pareek, V., Sha, Z., He, J., Wingreen, N. S., and Benkovic, S. J. (2021). Metabolic channeling: predictions, deductions, and evidence. *Mol. Cell.* 81, 3775–3785. doi: 10.1016/j.molcel.2021.08.030

Perico, C., and Sparkes, I. (2018). Plant organelle dynamics: cytoskeletal control and membrane contact sites. *Nat. Rev. Mol. Cell Biol.* 220, 381–394. doi: 10.1111/nph.15365

Phillips, D. A., and Kapulnik, Y. (1995). Plant isoflavonoids, pathogens and symbionts. *Trends Microbiol.* 3, 58–64. doi: 10.1016/S0966-842X(00)88876-9

Phillips, M. J., and Voeltz, G. K. (2016). Structure and function of ER membrane contact sites with other organelles. *Nat. Rev. Mol. Cell Biol.* 17, 69–82. doi: 10.1038/nrm.2015.8

Pohnert, G., Zhang, S., Husain, A., Wilson, D. B., and Ganem, B. (1999). Regulation of phenylalanine biosynthesis. Studies on the mechanism of phenylalanine binding and feedback inhibition in the Escherichia coli P-protein. *Biochemistry-Us* 38, 12212–12217. doi: 10.1021/bi991134w

Pyke, K. A., and Howells, C. A. (2002). Plastid and stromule morphogenesis in tomato. *Ann. Bot.* 90, 559–566. doi: 10.1093/aob/mcf235

Qian, Y., Lynch, J. H., Guo, L., Rhodes, D., Morgan, J. A., and Dudareva, N. (2019). Completion of the cytosolic post-chorismate phenylalanine biosynthetic pathway in plants. *Nat. Commun.* 10, 15. doi: 10.1038/s41467-018-07969-2

Ramadass, P., Meerarani, P., Toborek, M., Robertson, L. W., and Hennig, B. (2003). Dietary flavonoids modulate PCB-induced oxidative stress, CYP1A1 induction, and AhR-DNA binding activity in vascular endothelial cells. *Toxicol. Sci.* 76, 212–219. doi: 10.1093/toxsci/kfg227

Rippert, P., Puyaubert, J., Grisollet, D., Derrier, L., and Matringe, M. (2009). Tyrosine and phenylalanine are synthesized within the plastids in Arabidopsis. *Plant Physiol.* 149, 1251–1260. doi: 10.1104/pp.108.130070

Sarkar, F. H., and Li, Y. W. (2003). Soy isoflavones and cancer prevention. *Cancer Invest.* 21, 744–757. doi: 10.1081/CNV-120023773

Saslowsky, D. E., Warek, U., and Winkel, B. S. (2005). Nuclear localization of flavonoid enzymes in Arabidopsis. *J. Biol. Chem.* 280, 23735–23740. doi: 10.1074/jbc.M413506200

Schattat, M., Barton, K., Baudisch, B., Klösgen, R. B., and Mathur, J. (2011). Plastid stromule branching coincides with contiguous endoplasmic reticulum dynamics. *Plant Physiol.* 155, 1667–1677. doi: 10.1104/pp.110.170480

Schattat, M. H., Griffiths, S., Mathur, N., Barton, K., Wozny, M. R., Dunn, N., et al. (2012). Differential coloring reveals that plastids do not form networks for exchanging macromolecules. *Plant Cell.* 24, 1465–1477. doi: 10.1105/tpc.111.095398

Schmutz, J., Cannon, S. B., Schlueter, J., Ma, J., Mitros, T., Nelson, W., et al. (2010). Genome sequence of the palaeopolyploid soybean. *Nature* 463, 178–183. doi: 10.1038/nature08670

Scott, I. M., McDowell, T., Renaud, J. B., Krolikowski, S. W., Chen, L., and Dhaubhadel, S. (2021). Soybean (Glycine max L Merr) host-plant defenses and resistance to the two-spotted spider mite (Tetranychus urticae Koch). *PloS One* 16, e0258198. doi: 10.1371/journal.pone.0258198

Sepiol, C. J., Yu, J., and Dhaubhadel, S. (2017). Genome-wide identification of *chalcone reductase* gene family in soybean: insight into root-specific *GmCHR*s and *Phytophthora sojae* resistance. *Front. Plant Sci.* 8. doi: 10.3389/fpls.2017.02073

Shoemaker, R. C., Schlueter, J., and Doyle, J. J. (2006). Paleopolyploidy and gene duplication in soybean and other legumes. *Curr. Opin. Plant Biol.* 9, 104–109. doi: 10.1016/j.pbi.2006.01.007

Sievers, F., Wilm, A., Dineen, D., Gibson, T. J., Karplus, K., Li, W., et al. (2011). Fast, scalable generation of high-quality protein multiple sequence alignments using Clustal Omega. *Mol. Syst. Biol.* 7, 539–545. doi: 10.1038/msb.2011.75

Sparkes, I. A., Runions, J., Kearns, A., and Hawes, C. (2006). Rapid, transient expression of fluorescent fusion proteins in tobacco plants and generation of stably transformed plants. *Nat. Prot.* 1, 2019–2025. doi: 10.1038/nprot.2006.286

Stafford, H. A. (1974). "Possible multienzyme complexes regulating the formation of C6-C3 phenolic compounds and lignins in higher plants," in *Recent Advances in Phytochemistry* (New York: Elsevier), 53–79.

St John, T. P., and Davis, R. W. (1981). The organization and transcription of the galactose gene cluster of Saccharomyces. *J. Mol. Biol.* 152, 285–315. doi: 10.1016/0022-2836(81)90244-8

Subramanian, S., Stacey, G., and Yu, O. (2006). Endogenous isoflavones are essential for the establishment of symbiosis between soybean and *Bradyrhizobium japonicum*. *Plant J.* 48, 261–273. doi: 10.1111/j.1365-313X.2006.02874.x

Tan, K. M., Li, H., Zhang, R. G., Gu, M. Y., Clancy, S. T., and Joachimiak, A. (2008). Structures of open (R) and close (T) states of prephenate dehydratase (PDT) - Implication of allosteric regulation by L-phenylalanine. *J. Struct. Biol.* 162, 94–107. doi: 10.1016/j.jsb.2007.11.009

Tsugama, D., Liu, S., and Takano, T. (2013). A bZIP protein, VIP1, interacts with Arabidopsis heterotrimeric G protein β subunit, AGB1. *Plant Physiol. Biochem.* 71, 240–246. doi: 10.1016/j.plaphy.2013.07.024

Ungricht, R., and Kutay, U. (2017). Mechanisms and functions of nuclear envelope remodelling. *Nat. Rev. Mol. Cell Biol.* 18, 229–245. doi: 10.1038/nrm.2016.153

Van de Peer, Y., Mizrachi, E., and Marchal, K. (2017). The evolutionary significance of polyploidy. *Nat. Rev. Genet.* 18, 411–424. doi: 10.1038/nrg.2017.26

Waki, T., Yoo, D., Fujino, N., Mameda, R., Denessiouk, K., Yamashita, S., et al. (2016). Identification of protein-protein interactions of isoflavonoid biosynthetic enzymes with 2-hydroxyisoflavanone synthase in soybean (*Glycine max* (L.) Merr.). *Biochem. Bioph. Res. Co.* 469, 546–551. doi: 10.1016/j.bbrc.2015.12.038

Wang, J., Hossain, M. S., Lyu, Z., Schmutz, J., Stacey, G., Xu, D., et al. (2019). SoyCSN: Soybean context-specific network analysis and prediction based on tissue-specific transcriptome data. *Plant Direct.* 3, e00167. doi: 10.1002/pld3.167

Wang, H., Wang, W., Zhan, J., Yan, A., Sun, L., Zhang, G., et al. (2016). The accumulation and localization of chalcone synthase in grapevine (*Vitis vinifera* L.). *Plant Physiol. Biochem.* 106, 165–176. doi: 10.1016/j.plaphy.2016.04.042

Warpeha, K. M., Lateef, S. S., Lapik, Y., Anderson, M., Lee, B. S., and Kaufman, L. S. (2006). G-protein-coupled receptor 1, G-protein Galpha-subunit 1, and prephenate dehydratase 1 are required for blue light-induced production of phenylalanine in etiolated Arabidopsis. *Plant Physiol.* 140, 844–855. doi: 10.1104/pp.105.071282

Watanabe, S., Hayashi, K., Yagi, K., Asai, T., Mactavish, H., Picone, J., et al. (2002). Biogenesis of 2-Phenylethanol in Rose Flowers: Incorporation of [2H8]L-Phenylalanine into 2-Phenylethanol and its β-D-Glucopyranoside during the Flower Opening of Rosa `Hoh-Jun' and Rosa damascena Mill. *Biosci. Biotechnol. Biochem.* 66, 943–947. doi: 10.1271/bbb.66.943

Watkinson, J. I., Bowerman, P. A., Crosby, K. C., Hildreth, S. B., Helm, R. F., and Winkel, B. S. J. (2018). Identification of MOS9 as an interaction partner for chalcone synthase in the nucleus. *PeerJ* 6, e5598. doi: 10.7717/peerj.5598

Whatley, J. M., McLean, B., and Juniper, B. E. (1991). Continuity of chloroplast and endoplasmic reticulum membranes in *Phaseolus vulgaris*. *New Phytol.* 117, 209–217. doi: 10.1111/j.1469-8137.1991.tb04901.x

Winkel, B. S. J. (2001). It takes a garden. How work on diverse plant species has contributed to an understanding of flavonoid metabolism. *Plant Physiol.* 127, 1399–1404. doi: 10.1104/pp.010675

Winkel, B. S. J. (2002). Biosynthesis of flavonoids and effects of stress. *Curr. Opin. Plant Biol.* 5, 218–223. doi: 10.1016/S1369-5266(02)00256-X

Winkel, B. S. J. (2004). Metabolic channeling in plants. *Annu. Rev. Plant Biol.* 55, 85–107. doi: 10.1146/annurev.arplant.55.031903.141714

Winkel, B. S. J. (2006). "The biosynthesis of flavonoids," in *The Science of Flavonoids* (New York, NY: Springer New York), 71–95.

Yamada, T., Matsuda, F., Kasai, K., Fukuoka, S., Kitamura, K., Tozawa, Y., et al. (2008). Mutation of a rice gene encoding a phenylalanine biosynthetic enzyme results in accumulation of phenylalanine and tryptophan. *Plant Cell.* 20, 1316–1329. doi: 10.1105/tpc.107.057455

Yong, K. J., and Wu, T. Y. (2022). Second-generation bioenergy from oilseed crop residues: Recent technologies, techno-economic assessments and policies. *Energy Conversion Manag.* 267, 115869. doi: 10.1016/j.enconman.2022.115869

Yoo, H., Widhalm, J. R., Qian, Y., Maeda, H., Cooper, B. R., Jannasch, A. S., et al. (2013). An alternative pathway contributes to phenylalanine biosynthesis in plants via a cytosolic tyrosine:phenylpyruvate aminotransferase. *Nat. Commun.* 4, 2833. doi: 10.1038/ncomms3833

Young, N. D., and Bharti, A. K. (2012). Genome-enabled insights into legume biology. *Annu. Rev. Plant Biol.* 63, 283–305. doi: 10.1146/annurev-arplant-042110-103754

Young, N. D., Debellé, F., Oldroyd, G. E. D., Geurts, R., Cannon, S. B., Udvardi, M. K., et al. (2011). The Medicago genome provides insight into the evolution of rhizobial symbioses. *Nature* 480, 520–524. doi: 10.1038/nature10625

Yousefi-Taemeh, M., Lin, J., Ifa, D. R., Parrott, W., and Kovinich, N. (2021). Metabolomics differences of *Glycine max* QTLs resistant to soybean looper. *Metabolites* 11, 710. doi: 10.3390/metabo11100710

Yuan, J., and Song, Q. (2023). Polyploidy and diploidization in soybean. *Mol. Breed.* 43, 51. doi: 10.1007/s11032-023-01396-y

Zhang, Y., and Fernie, A. R. (2021). Metabolons, enzyme–enzyme assemblies that mediate substrate channeling, and their roles in plant metabolism. *Plant Commun.* 2, 100081. doi: 10.1016/j.xplc.2020.100081

Zhang, S., Pohnert, G., Kongsaeree, P., Wilson, D. B., Clardy, J., and Ganem, B. (1998). Chorismate mutase-prephenate dehydratase from *Escherichia coli*. Study of catalytic and regulatory domains using genetically engineered proteins. *J. Biol. Chem.* 273, 6248–6253. doi: 10.1074/jbc.273.11.6248

Zhang, S., Wilson, D. B., and Ganem, B. (2000). Probing the catalytic mechanism of prephenate dehydratase by site-directed mutagenesis of the *Escherichia coli* P-protein dehydratase domain. *Biochemistry-Us* 39, 4722–4728. doi: 10.1021/bi9926680

frontiers | Frontiers in Plant Science

TYPE Review
PUBLISHED 09 February 2024
DOI 10.3389/fpls.2024.1368870

OPEN ACCESS

EDITED BY
Deyu Xie,
North Carolina State University, United States

REVIEWED BY
Xianzhi He,
North Carolina State University, United States
Gaojie Hong,
Zhejiang Academy of Agricultural Sciences, China

*CORRESPONDENCE
Guodong Wang
gdwang@genetics.ac.cn

RECEIVED 11 January 2024
ACCEPTED 29 January 2024
PUBLISHED 09 February 2024

CITATION
Yang Q and Wang G (2024) Isoflavonoid metabolism in leguminous plants: an update and perspectives. *Front. Plant Sci.* 15:1368870. doi: 10.3389/fpls.2024.1368870

Isoflavonoid metabolism in leguminous plants: an update and perspectives

Qilin Yang[1,2] and Guodong Wang[1,2]*

[1]Key Laboratory of Seed Innovation, Institute of Genetics and Developmental Biology, The Innovative Academy of Seed Design, Chinese Academy of Sciences, Beijing, China, [2]College of Advanced Agricultural Sciences, Chinese Academy of Sciences, Beijing, China

Isoflavonoids constitute a well-investigated category of phenylpropanoid-derived specialized metabolites primarily found in leguminous plants. They play a crucial role in legume development and interactions with the environment. Isoflavonoids usually function as phytoalexins, acting against pathogenic microbes in nature. Additionally, they serve as signaling molecules in rhizobial symbiosis. Notably, owing to their molecular structure resembling human estrogen, they are recognized as phytoestrogens, imparting positive effects on human health. This review comprehensively outlines recent advancements in research pertaining to isoflavonoid biosynthesis, transcriptional regulation, transport, and physiological functions, with a particular emphasis on soybean plants. Additionally, we pose several questions to encourage exploration into novel contributors to isoflavonoid metabolism and their potential roles in plant-microbe interactions.

KEYWORDS

isoflavonoids, metabolism, human health, nodulation, plant-microbe interactions

Introduction

Isoflavonoids, primarily found in legumes, are recognized as phytoestrogens owing to their structural and size resemblance to human estrogens (17β-estradiol and daidzein-derived (*S*)-equol, structures see Figure 1) (Krizova et al., 2019). Soybeans and soy products are the primary source of these compounds in human diets (Rizzo and Baroni, 2018). Following ingestion, isoflavonoids especially the genistein and daidzein, exhibit the capacity to bind to estrogen receptors, thereby exerting estrogenic or anti-estrogenic effects. (Ariyani et al., 2023). They are thought to confer a protective effect against hormone-related cancers, such as prostate and breast cancer (Boutas et al., 2022; Yu et al., 2023). Besides cancer prevention, isoflavonoids are implicated in averting various diseases, including cardiovascular ailments, Alzheimer's disease, and possess anti-inflammatory and sterol-lowering properties (Li and Zhang, 2017; Xie et al., 2021; Vina et al., 2022) (Table 1). Isoflavonoids extend beyond human health benefits, crucially influencing plant-microbe interactions. They serve as signals in rhizobia-legume symbiosis, triggering nodulation gene expression in rhizobia and enhancing

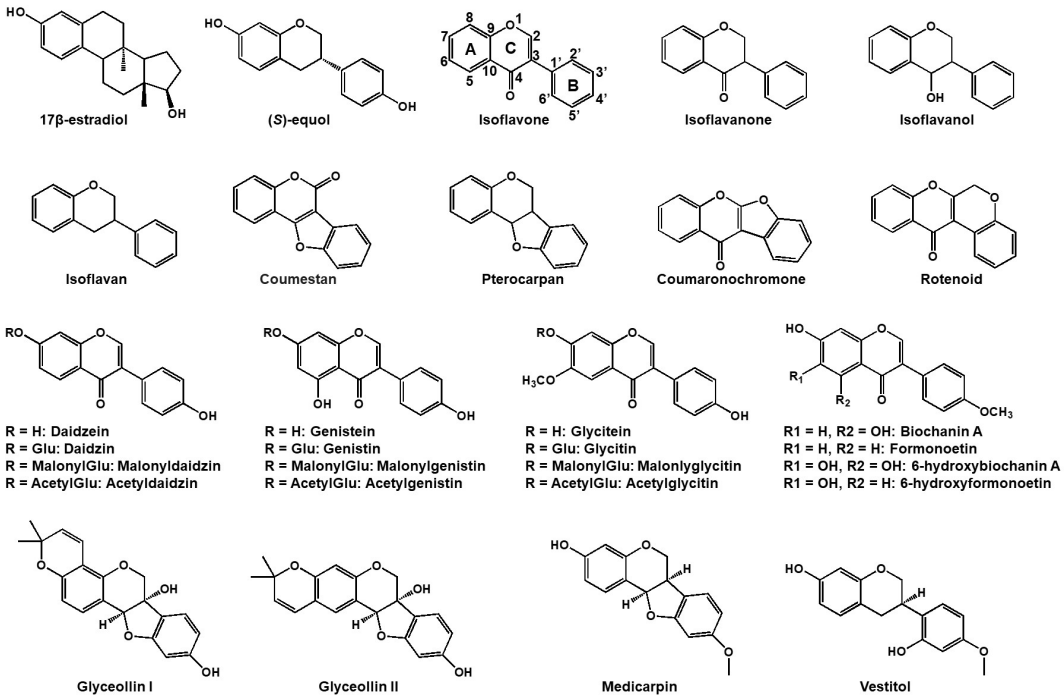

FIGURE 1
Chemical structures of representative isoflavonoids in leguminous plants. Both 17β-estradiol (estrogen) and daidzein-derived (*S*)-equol have a high affinity for estrogen receptor in human.

the nodulation process in legumes (Subramanian et al., 2006; Han et al., 2020). Notably, when investigating isoflavonoids in leguminous plants, it is crucial to consider all specialized metabolites as a whole, including other compounds such as saponins (Sugiyama, 2019; Yuan et al., 2023). This review, however, will focus on isoflavonoid distribution, biosynthesis, regulation, transport, and their pivotal roles in plant ecology.

Chemical structure and distribution of plant isoflavonoids

Isoflavonoids commonly harbor a C6-C3-C6 carbon skeleton—comprising two 6-carbon benzene rings A and C and a 3-carbon heterocyclic ring B (Figure 1) (Nabavi et al., 2020). Diverse modifications such as oxidation, glycosylation, acylation, prenylation and others, along with intra-molecular cyclization yield an array of isoflavonoids, including isoflavans, isoflavanones, isoflavanols, coumestans, coumaronochromones, rotenoids, pterocarpans and so on (see Figure 1; Veitch, 2007). Thus far, there are more than 2,000 isoflavonoids were isolated and structurally elucidated in plants (Mackova et al., 2006; Veitch, 2007; Al-Maharik, 2019, 2009; 2013). Legume isoflavonoids are comprised of aglycones and glycosides which include glucosides, malonylglucosides, or acetylglucosides. They prevail and translocate within vacuoles of plant cells (Zhao and Dixon, 2010). Different legume plant species may produce different types of isoflavonoids in response to the growing environment. Soybean produces daizein, genistein, glycitein, and derivatives, with glyceollin synthesized in response to pathogens (Ng et al., 2011), while in *Medicago truncatula* and *Lotus japonicus*, the methylated glycones, formononetin and biochanin-A are produced respectively alongside daidzein and genistein. In addition, *M. truncatula* produces medicarpin, while *L. japonicus* yields vestitol through further reduction from medicarpin (Naoumkina et al., 2007; Masunaka et al., 2011).

While isoflavonoids are prominently found in legumes, they are also reported to be isolated in numerous non-leguminous plant families (Reynaud et al., 2005). Over 200 isoflavonoids have been identified in 50+ non-leguminous plant families, spanning Bryopsida, Pinopsida, Magnoliopsida, and Liliopsida classes (Lapcík, 2007).

Isoflavonoid metabolism in leguminous plants

The biosynthetic pathway of isoflavonoids in legumes is currently well investigated, comprising three key phases: the phenylpropanoid pathway, biosynthesis of the isoflavonoid aglycone, and the final production of isoflavonoids (Dixon and Pasinetti, 2010; Sohn et al., 2021). Initially, isoflavonoids originate from the phenylpropanoid pathway, where phenylalanine undergoes a sequential three-step catalytic transformation by phenylalanine ammonia lyase (PAL), cinnamic acid 4-hydroxylase (C4H), and 4-coumaroyl-CoA ligase (4CL) to produce the flavonoid precursor, *p*-coumaroyl-CoA. Subsequently, through the catalytic action of chalcone synthase (CHS), *p*-coumaroyl-CoA condenses with three units of malonyl-CoA to yield naringenin chalcone, a crucial intermediate and the

TABLE 1 Pharmacological activities of isoflavonoids from clinical studies.

Isoflavonoid	Dose-time	Pharmacological activities	Ref.
Daidzein	1 tablet/d (6 months)	reducing **lower urinary tract symptoms (LUTS)**	(Tiscione et al., 2017)
Genistein	120 mg/d (12 months)	therapeutics to delay the onset of Alzheimer's dementia in patients with prodromal **Alzheimer's disease**	(Vina et al., 2022)
	54 mg/d (24 months)	therapeutics to **glucocorticoid-induced osteoporosis (GIO)**	(Squadrito et al., 2023)
	30 mg/d (3-6 weeks)	influencing the gene expression in **prostate cancer**	(Bilir et al., 2017)
	150 mg/d (1 month)	inhibiting pathways in **human prostate** that drive transformation to a lethal high motility phenotype	(Zhang et al., 2019)
Daidzein/ Genistein/Glycitein	136.6 mg/d (5 d/week 2 years)	reducing fibroglandular breast tissue (FGBT), protecting against **breast cancer**	(Lu et al., 2022)
	50 mg/d (8 weeks)	functioning as a complementary treatment for women with migraine to improve **migraine characteristics**	(Babapour et al., 2022)
	52 - 220 mg/d (50 days)	functioning as effective **bone**-preserving agents in **postmenopausal** women	(Pawlowski et al., 2015)
	66 mg/d (6 months)	improving **cardiovascular disease risk (CVR)** markers, and prevent against CVR	(Sathyapalan et al., 2018)

first-rate-limiting step in the flavonoid biosynthetic pathway. Simultaneously, isoliquiritigenin is also formed through the concerted activities of CHS and chalcone reductase (CHR). In soybeans, naringenin chalcone and isoliquiritigenin undergo further enzymatic transformations involving chalcone isomerase (CHI), isoflavone synthase (IFS), and 2-hydroxyisoflavanone dehydratase (HID) to generate three primary isoflavonoid aglycones: genistein, daidzein, and glycitein. However, in other leguminous species such as *M. truncatula* and *L. japonicus*, naringenin chalcone and isoliquiritigenin take an alternative route, giving rise to two distinct 4'-methoxyisoflavonoids, biochanin-A and formononetin. This diversion is facilitated by the involvement of a crucial enzyme, 2-hydroxyisoflavanone 4′-*O*-methyltransferase (HI4'OMT). Subsequently, these isoflavonoid aglycones serve as substrates for various modifying enzymes, including glycosyltransferases and acyltransferases, leading to the formation of diverse isoflavonoid derivatives (Figure 2A). Additionally, further enzymatic reactions contribute to the synthesis of intricate and biologically active isoflavonoids, such as glyceollin, medicarpin, and vestitol. Notably, two tandem P450 enzymes, C4H and IFS, localized to the endoplasmic reticulum (ER), play a pivotal role in anchoring other isoflavonoid enzymes to the ER through protein-protein interactions, thereby establishing an isoflavonoid metabolon on the ER (Dastmalchi et al., 2016).

IFS, a cytochrome P450 enzyme, is a pivotal rate-limiting determinant governing the transition of intermediates from the flavonoid pathway to the isoflavonoid pathway. This transformation involves the migration of the B-ring from the C2 to the C3 position of the C-ring, succeeded by hydroxylation at the C2 position of the C-ring (Figure 2A; Dixon and Steele, 1999; Jung et al., 2000). While IFS is prevalent in legumes, it is not exclusive to this plant family, as evidenced by its presence in non-legumes. For example, IFS has been identified in sugarbeet (*Beta vulgaris*) exhibiting substantial similarity to legume IFS (Jung et al., 2000). In addition to sugarbeet, a wheat-specific *IFS* gene, *TaCYP71F53*, has been recently identified in wheat, setting it apart from legume IFSs by utilizing artocarpanone A as a substrate instead of naringenin or liquiritigenin. The wheat IFS (TaCYP71F53) is responsible for aryl migration coupled with C-ring desaturation of artocarpanone A; however, the legume IFSs are usually responsible for aryl migration and 2-hydroxylation of naringenin or liquiritigenin. Phylogenetic analysis further elucidated that legume IFSs belong to the CYP93 family, while the wheat-specific IFS belongs to the CYP71 family (Polturak et al., 2023). This discovery underscores a parallel gain in the capacity for isoflavonoid production in both soybeans and wheat. In essence, the broad distribution of IFS across diverse plant species highlights its evolutionary significance and the adaptability of distinct plants to engage in the synthesis of bioactive isoflavonoids.

Isoflavonoids synthesized in the ER and cytoplasm often undergo subsequent transport processes, with two main possibilities identified: membrane vesicle-mediated transport and membrane transporter-mediated transport (Zhao and Dixon, 2010). Among membrane transporters, multidrug and toxic compound extrusion (MATE) transporters are considered crucial, particularly in the translocation of isoflavonoids from the cytoplasm to the vacuole. Notably, *GmMATE1* and *GmMATE2*, identified as soy isoflavonoid transporters, facilitate the accumulation of isoflavonoids in soybean seeds. However, studies using the yeast system have revealed that these transporters specifically facilitate the transport of aglycones and glycosides but not malonylglycosides (Ng et al., 2021). Similarly, GmMATE4, localized in vacuole-like membranes, plays a role in mediating the transport of isoflavonoids, including daidzein, genistein, glycitein, and glycitin, into the vacuole for storage. The uptake and efflux of isoflavonoids across the tonoplast or plasma membrane involve various transporters. It is suggested that an unknown ATP-binding cassette (ABC) transporter may be involved in the secretion of soy isoflavonoid aglycones. This inference is supported by the ATP-dependent transport of genistein with and without typical ABC transporter inhibitors (Sugiyama et al., 2007). The intricate interplay of these transport mechanisms adds another layer of complexity to the regulation of isoflavonoid compartmentalization and function within plant cells.

Although the isoflavonoid biosynthesis pathway has been well-investigated in plants, little research focuses on the catabolism of

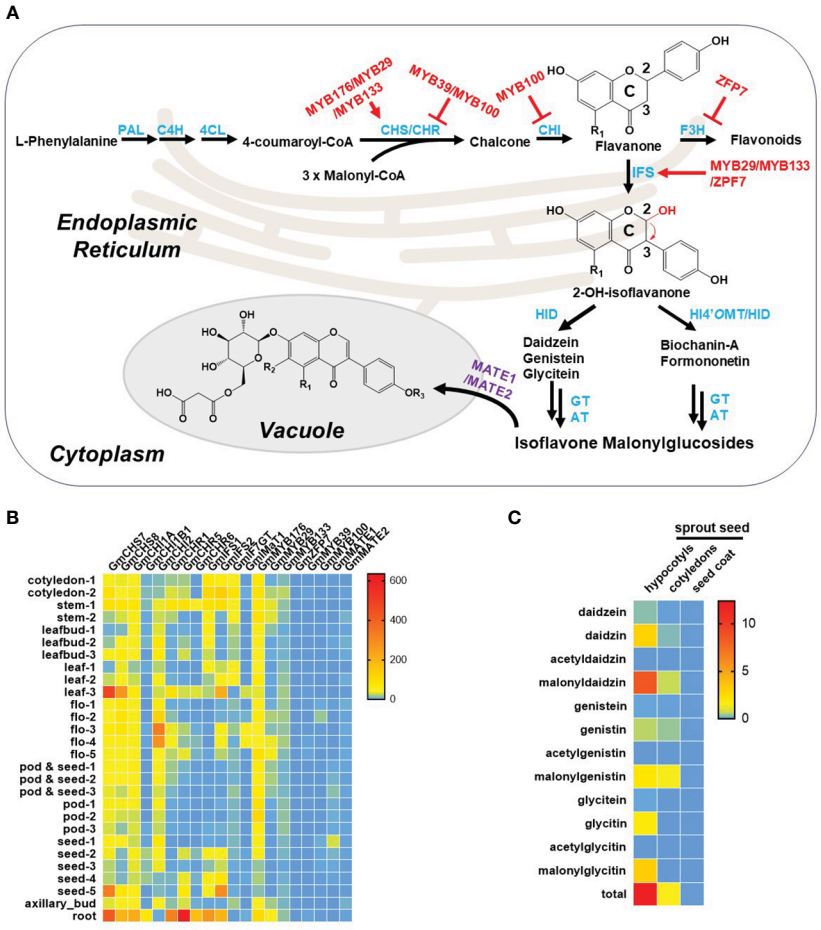

FIGURE 2
Isoflavonoid metabolism in soybean plants. **(A)** Summary of isoflavonoid metabolism in soybean plant. Notably, R_1 and R_2 represent either −H or −OH, and R_3 represents either −H or $-CH_3$ in the chemical structures here. The biosynthetic enzymes, transporters, and transcript factors are highlighted in blue, purple, and red, respectively. Abbreviations: PAL, phenylalanine ammonia lyase; C4H, cinnamic acid 4-hydroxylase; 4CL, 4-coumaroyl-CoA ligase; CHS, chalcone synthase; CHR, chalcone reductase; CHI, chalcone isomerase; F3H, flavanone 3-hydroxylase; IFS, isoflavone synthase; HID, 2-hydroxyisoflavanone dehydratase; HI4′OMT, 2-hydroxyisoflavanone 4′-*O*-methyltransferase; GT, glucosyltransferase; AT, acyltransferase. **(B)** Tissue specificity of isoflavonoid known genes in soybean plants. Transcriptome data are extracted from SoyOmics database (https://ngdc.cncb.ac.cn/soyomics/index). **(C)** Distribution of isoflavonoids in seeds. Data are extracted from the work by Yuan et al. (Yuan et al., 2009).

isoflavonoids. Recently, Aoki et al. discovered an isoflavone oxidative catabolic gene cluster in legume root bacteria (*Variovorax* sp.), which belongs to *Comamonadaceae*. The identified catabolism (*ifc*) gene cluster includes at least four functional genes, and the final catabolic products of isoflavones eventually enter the tricarboxylic acid cycle in bacteria. The authors further demonstrated that *ifc* genes are frequently found in bacterial strains isolated from legume plants (Aoki et al., 2023). It can be foreseen that more isoflavone degradation gene clusters will be discovered in near future, especially in plant rhizosphere bacteria.

Isoflavonoid regulation in leguminous plants

Isoflavonoid biosynthetic enzymes and transporters definitely play a crucial role in determining the production of isoflavonoids. However, the regulatory network involves transcription factors which can directly/indirectly control the expression of isoflavonoid biosynthetic genes, and consequently altering isoflavonoid content. Numerous studies have identified MYB transcription factors as pivotal regulators in the isoflavonoid biosynthesis. For instance, the R1 MYB transcription factor *GmMYB176* was reported to bind with the promoter of *CHS8*, activating *CHS8* expression and enhancing isoflavonoid accumulation (Yi et al., 2010). Similarly, positive regulators like *GmMYB29* (R2R3 MYB) and *GmMYB133* (CCA1-like MYB) were found to activate the expression of *CHS8* and *IFS2*, leading to increased isoflavonoid content (Chu et al., 2017; Bian et al., 2018). However, not all MYB transcription factors exhibit positive regulation; some, such as *GmMYB39* and *GmMYB100*, act as repressors by inhibiting (iso)flavonoid biosynthesis through the repression of upstream genes such as *CHS*, *CHR*, and *CHI* (Liu et al., 2013; Yan et al., 2015). Moreover, some MYB transcription factors do not act alone. They can interact with other

transcription factors to regulate the isoflavonoid biosynthesis. For example, GmMYB176 can interact with GmbZIP5, and the co-overexpression of these two genes was shown to increase isoflavonoid content (Anguraj Vadivel et al., 2021). Additionally, other transcription factors, such as the C2H2-type zinc finger protein *GmZFP7*, accelerate isoflavonoid synthesis by promoting the expression of *GmIFS2* and inhibiting the expression of *GmF3H1*, thereby increasing the metabolic flux of isoflavonoids and enhancing their levels (Feng et al., 2023). *GmNAC42-1* was identified as an essential positive regulator of glyceollin biosynthesis, directly binding to the promoters of *IFS2* and *G4DT*, promoting the expression of these two genes, and increasing glyceollin content (Jahan et al., 2019).

In addition to transcription factors, microRNAs might also play a role in mediating the isoflavonoid biosynthetic pathway to regulate isoflavonoid production. *Gma-miR26* and *Gma-miRNA28*, along with their corresponding target genes (*Glyma.10G197900* and *Glyma.09G127200*), were found to be directly related to isoflavonoid content (Gupta et al., 2017). Furthermore, *Gma-miR5030* was identified as a mediator of the expression of the target gene *GmMYB176*, affecting isoflavonoid biosynthesis (Gupta et al., 2019). This intricate regulatory network involving transcription factors and microRNAs adds a layer of complexity to the modulation of isoflavonoid biosynthesis in plants. Notably, the role of microRNAs involved in the regulation of (iso) flavonoid in plants need further experimental validation.

The publicly available transcriptome reveals that genes involved in isoflavone metabolism exhibit higher expression levels in roots and mature seeds compared to other organs, as illustrated in Figure 2B. This heightened expression corresponds to increased accumulation of isoflavonoids in these specific tissues. Notably, seeds play a crucial role as a significant source of soy isoflavones for human consumption through direct intake or soy products. The distribution of soy isoflavones within the mature soy seed varies significantly among its different parts. The highest concentration of all isoflavones is observed in the hypocotyl, followed by the cotyledons, while the seed coat contains almost negligible amounts of isoflavones. Furthermore, within the hypocotyl, daidzein and its derivatives exhibit higher levels compared to the other two isoflavones. In the cotyledons, there is an enrichment of genistein and its derivatives (Yuan et al., 2009) (Figure 2C).

Physiological functions of isoflavonoid

Isoflavonoids play pivotal roles in plant ecology, particularly in plant-microbe interactions, functioning as phytoalexins to combat various diseases caused by nematode, oomycete, fungi, bacteria and virus (Lin et al., 2022), and fostering root-rhizobia symbiosis to regulate nodulation (Hammerschmidt, 1999). Notably, transgenic rice expressing the *GmIFS1* gene demonstrated enhanced resistance to the rice blast pathogen, indicating that isoflavonoid biosynthesis, particularly genistein, serves as a phytoalexin in transgenic rice (Pokhrel et al., 2021). In soybeans, glyceollin acts as a crucial phytoalexin induced by cell wall glucan elicitors to resist *Phytophthora sojae*. The silencing of upstream synthesis genes (*IFS* and *CHR*) impairs soybean resistance to *P. sojae* (Ayers et al., 1976; Graham et al., 2007). Glyceollins also exhibit anti-bacterial, anti-nematode and anti-fungal activities besides anti-oomycetes (*P. sojae*) (Ng et al., 2011). Also, the soybean plants with 2-fold increased isoflavonoids through simultaneous knockout of three flavanone genes (*GmF3H1*, *GmF3H2* and *GmFNSII-1*) enhanced the leaf resistance to soya bean mosaic virus (Zhang et al., 2020). In *M. truncatula*, medicarpin synergizes with SA to combat powdery mildew *Erysiphe pisi* and *Rhizoctonia solani* (Gupta et al., 2022).

Isoflavonoids also serve as signals to mediate a symbiotic relationship between legumes and nitrogen-fixing bacteria, primarily Rhizobium, converting atmospheric nitrogen into ammonia for direct plant utilization through the process of biological nitrogen fixation (Yang et al., 2022). Subramanian et al. demonstrated the crucial role of isoflavonoids in nodulation formation, revealing that endogenous production of genistein is sufficient to support nodulation in the soybean hairy root system through RNAi-mediated silencing of the *IFS* and *CHR* genes (Subramanian et al., 2006). During nodulation formation, cells transport (iso)flavonoids, mainly aglycones and glycosides, directly into the apoplast (Biala-Leonhard et al., 2021). In the apoplast, isoflavonoid conjugate-hydrolyzing β-glucosidase (ICHG) hydrolyzes isoflavonoid glycosides, forming aglycones (Matsuda et al., 2023). Subsequently, in the soil, legume roots release these (iso)flavonoid aglycones to attract rhizobia to the rhizosphere. Following this, (iso)flavonoids form a complex by binding to the transcriptional activator NodD protein, activating the transcription of rhizobial nod genes (*nodA*, *nodB*, and *nodC*), and inducing rhizobia to synthesize and secrete the Nod factors, like lipo-chitooligosaccharides (Peck et al., 2006; Del Cerro et al., 2019; Rush et al., 2020).

Perspectives

In light of the evident of the beneficial impact of isoflavonoids on human health, numerous endeavors have been undertaken to produce isoflavonoids in various chassis, like *Saccharomyces cerevisiae*, *Escherichia coli* and plants (Sajid et al., 2021). Recently, Liu et al. engineered the metabolism of *S. cerevisiae* for *de novo* production of isoflavonoid from glucose. The final optimized strain produces up to 85.4 mg L^{-1} of daidzein and 72.8 mg L^{-1} puerarin (Liu et al., 2021). The efficient synthesis of isoflavonoids using synthetic biology strategies is expected to be a prominent research focus in this field.

The exploration of customized soybean seeds with enhanced nutrition and the investigation of the physiological functions of isoflavonoids in plant-microbe interactions offer other exciting avenues for future research (Figure 3). Both future researches rely on the comprehensive understanding the biosynthesis and regulation of isoflavonoids and the use of loss-of-function plant materials. Recent years have witnessed the identification of key enzymes in the isoflavonoid biosynthetic pathway, facilitating the

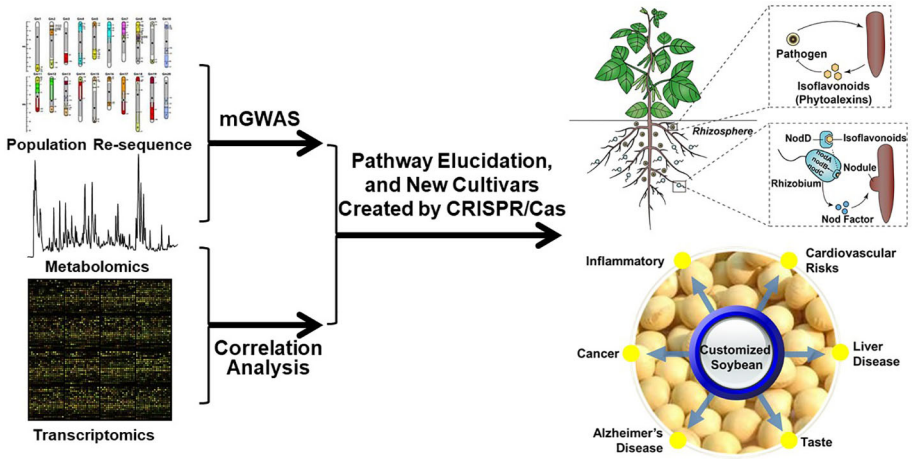

FIGURE 3
Workflow for isoflavonoid pathway elucidation and their applications in either rhizosphere or seeds.

utilization of metabolic engineering techniques to expedite the production of higher levels of isoflavonoids for application in the prevention and treatment of associated diseases. Despite the substantial progress, certain isoflavonoid biosynthetic enzymes remain uncharacterized. For instance, although it has been suggested that flavonoid 6-hydroxylase (F6H, a cytochrome P450 monooxygenase belonging to the CYP71D subfamily) may play a role in glycitein synthesis, there is a lack of relevant genetic evidence to substantiate this claim (LatundeDada et al., 2001; Artigot et al., 2013). Continued exploration of these uncharted enzymatic territories holds promise for advancing our understanding and harnessing the full potential of isoflavonoids. Metabolic genome-wide association studies (mGWAS) and quantitative trait locus (QTL), together with co-expression analysis, have emerged as powerful tools in unraveling the complex genetic architecture underlying various biological pathways (Luo, 2015). Given the public availability of soybean-omics databases, these approaches provide a novel and insightful avenue for identifying previously unknown contributors to the isoflavonoid metabolic pathway (Grant et al., 2010; Zheng et al., 2022; Azam et al., 2023; Chu et al., 2023; Liu et al., 2023). The customized soybean seeds thus could be reached by genetic engineering for optimizing isoflavonoid composition and quantity. This process will focus on manipulating key genes involved in the biosynthesis of isoflavonoids and the nutritional knowledge of specific isoflavonoids (Table 2). Finally, investing the potential health benefits of customized soybean seeds enriched with specific isoflavonoids could have impact on human health, such as their antioxidant properties, anti-inflammatory

TABLE 2 Major QTLs and mGWAS determined for soybean isoflavonoids.

Isoflavonoids	Method	Chromosome	Position	Related Gene	Reference
Total	GWAS	20	43458721[a]	GmMYB29	(Chu et al., 2017)
Glycitein	GWAS	5	36904003	-[c]	(Chu et al., 2017)
Daidzein Total	GWAS	6	41283321	–	(Chu et al., 2017)
Glycitein	GWAS	11	8262066	–	(Chu et al., 2017)
Daidzein Total	GWAS	8	42737801	GmMPK1	(Wu et al., 2020)
Malonylglycitin	GWAS	11	8147595-8315102	–	(Azam et al., 2023)
Total	GWAS	5	41760764-42234431	–	(Azam et al., 2023)
Genistein Malonylgenitin	GWAS	5	38940662	–	(Kim et al., 2022)
Genistein	GWAS	5	35170270	–	(Kim et al., 2022)
Total	QTL	20	1[b]	GmZFP7	(Feng et al., 2023)
Total	QTL	5	236.4	–	(Cai et al., 2018)
Total	QTL	5	237.1	–	(Cai et al., 2018)
Malonylgenistin	QTL	14	23	GmCHR1	(Pei et al., 2018)

(Continued)

TABLE 2 Continued

Isoflavonoids	Method	Chromosome	Position	Related Gene	Reference
Genistin	QTL	8	0	–	(Pei et al., 2018)
Malonyldaidzin	QTL	19	14	–	(Pei et al., 2018)
Malonylgenistin	QTL	18	158	–	(Pei et al., 2018)
Total	QTL	19	14	–	(Pei et al., 2018)
Malonylglycitin	QTL	11	37	–	(Watanabe et al., 2019)

[a]unit for mGWAS, base pair (bp).
[b]unit for QTL, centimorgan (cM).
[c]-, not determined yet.

effects, and potential role in preventing chronic diseases. For instance, increasing the metabolic flux to daidzein by reducing glycitein branch might be a good target for customized soybean seeds (Zaheer and Humayoun Akhtar, 2017; Alshehri et al., 2021).

As above-mentioned, isoflavonoids play a crucial role as signals mediating plant-microbe symbiosis, particularly in the context of rhizobial interactions. This symbiotic relationship is essential for the ability of legumes to thrive in nitrogen-poor soils, offering a distinct advantage over non-leguminous plants that rely on chemical fertilizers for normal development in low-nitrogen environments. Modifying key enzymes involved in isoflavonoid synthesis in non-leguminous plants holds the potential to promote the establishment of this symbiosis, thereby reducing the dependence on nitrogen fertilizers. The overexpression of *IFS* in transgenic rice has been shown to induce nod gene expression in rhizobia, opening up the possibility of symbiosis (Sreevidya et al., 2006). Furthermore, isoflavonoids can influence the bacterial community composition in the soil. For instance, the bacterial communities in daidzein-treated soils more closely resemble those in the soybean rhizosphere (Okutani et al., 2020). The addition of daidzein enriches the abundance of bacteria in *Comamonadaceae*, a predominant bacterial family in soybean roots. This suggests that manipulating isoflavonoid and other type of plant specialized metabolites could be a strategic approach to change the soil environment, potentially improving crop yields in non-leguminous plants through methods such as crop rotations in nitrogen-deficient conditions (Chen et al., 2019; Sugiyama, 2019; Wang et al., 2023). Understanding the regulation of isoflavonoids in the context of legume-rhizobial symbiosis allows for the development of crops with improved nitrogen fixation capabilities, which is essential for sustainable agriculture by reducing the need for synthetic fertilizers.

Author contributions

QY: Writing – original draft, Conceptualization. GW: Conceptualization, Funding acquisition, Writing – review & editing.

Funding

The author(s) declare financial support was received for the research, authorship, and/or publication of this article. This work was financially supported by National Key Research and Development Projects (2018YFA0900603 to GW).

Conflict of interest

The authors declare that the research was conducted in the absence of any commercial or financial relationships that could be construed as a potential conflict of interest.

The author(s) declared that they were an editorial board member of Frontiers, at the time of submission. This had no impact on the peer review process and the final decision.

Publisher's note

References

Al-Maharik, N. (2019). Isolation of naturally occurring novel isoflavonoids: an update. *Nat. Prod. Rep.* 36 (8), 1156–1195. doi: 10.1039/c8np00069g

Alshehri, M. M., Sharifi-Rad, J., Herrera-Bravo, J., Jara, E. L., Salazar, L. A., Kregiel, D., et al. (2021). Therapeutic potential of isoflavones with an emphasis on daidzein. *Oxid. Med. Cell Longev.* 2021, 6331630. doi: 10.1155/2021/6331630

Anguraj Vadivel, A. K., McDowell, T., Renaud, J. B., and Dhaubhadel, S. (2021). A combinatorial action of *GmMYB176* and *GmbZIP5* controls isoflavonoid biosynthesis in soybean (*Glycine max*). *Commun. Biol.* 4 (1), 356. doi: 10.1038/s42003-021-01889-6

Aoki, N., Shimasaki, T., Yazaki, W., Sato, T., Nakayasu, M., Ando, A., et al. (2023). Discovery of an isoflavone oxidative catabolic pathway in legume root microbiota. *bioRxiv*. doi: 10.1101/2023.08.07.552369

Ariyani, W., Amano, I., and Koibuchi, N. (2023). Isoflavones mediate dendritogenesis mainly through estrogen receptor α. *Int. J. Mol. Sci.* 24 (10), 9011. doi: 10.3390/ijms24109011

Artigot, M. P., Baes, M., Dayde, J., and Berger, M. (2013). Expression of flavonoid 6-hydroxylase candidate genes in normal and mutant soybean genotypes for glycitein content. *Mol. Biol. Rep.* 40 (7), 4361–4369. doi: 10.1007/s11033-013-2526-2

Ayers, A. R., Ebel, J., Valent, B., and Albersheim, P. (1976). Host-pathogen interactions: X. fractionation and biological activity of an elicitor isolated from the mycelial walls of *Phytophthora megasperma* var. sojae. *Plant Physiol.* 57 (5), 760–765. doi: 10.1104/pp.57.5.760

Azam, M., Zhang, S., Li, J., Ahsan, M., Agyenim-Boateng, K. G., Qi, J., et al. (2023). Identification of hub genes regulating isoflavone accumulation in soybean seeds *via* GWAS and WGCNA approaches. *Front. Plant Sci.* 14. doi: 10.3389/fpls.2023.1120498

Babapour, M., Khorvash, F., Rouhani, M. H., Ghavami, A., Ghasemi-Tehrani, H., Heidari, Z., et al. (2022). Effect of soy isoflavones supplementation on migraine characteristics, mental status and calcitonin gene-related peptide (CGRP) levels in women with migraine: results of randomised controlled trial. *Nutr. J.* 21 (1), 50. doi: 10.1186/s12937-022-00802-z

Biala-Leonhard, W., Zanin, L., Gottardi, S., de Brito Francisco, R., Venuti, S., Valentinuzzi, F., et al. (2021). Identification of an isoflavonoid transporter required for the nodule establishment of the *Rhizobium-Fabaceae* symbiotic interaction. *Front. Plant Sci.* 12. doi: 10.3389/fpls.2021.758213

Bian, S., Li, R., Xia, S., Liu, Y., Jin, D., Xie, X., et al. (2018). Soybean CCA1-like MYB transcription factor GmMYB133 modulates isoflavonoid biosynthesis. *Biochem. Biophys. Res. Commun.* 507 (1-4), 324–329. doi: 10.1016/j.bbrc.2018.11.033

Bilir, B., Sharma, N. V., Lee, J., Hammarstrom, B., Svindland, A., Kucuk, O., et al. (2017). Effects of genistein supplementation on genome-wide DNA methylation and gene expression in patients with localized prostate cancer. *Int. J. Oncol.* 51 (1), 223–234. doi: 10.3892/ijo.2017.4017

Boutas, I., Kontogeorgi, A., Dimitrakakis, C., and Kalantaridou, S. N. (2022). Soy isoflavones and breast cancer risk: a meta-analysis. *Vivo* 36 (2), 556–562. doi: 10.21873/invivo.12737

Cai, Z., Cheng, Y., Ma, Z., Liu, X., Ma, Q., Xia, Q., et al. (2018). Fine-mapping of QTLs for individual and total isoflavone content in soybean (*Glycine max* L.) using a high-density genetic map. *Theor. Appl. Genet.* 131 (3), 555–568. doi: 10.1007/s00122-017-3018-x

Chen, Q., Jiang, T., Liu, Y. X., Liu, H., Zhao, T., Liu, Z., et al. (2019). Recently duplicated sesterterpene (C25) gene clusters in Arabidopsis thaliana modulate root microbiota. *Sci. China Life Sci* 62 (7), 947–958. doi: 10.1007/s11427-019-9521-2

Chu, D., Zhang, Z., Hu, Y., Fang, C., Xu, X., Yuan, J., et al. (2023). Genome-wide scan for oil quality reveals a coregulation mechanism of tocopherols and fatty acids in soybean seeds. *Plant Commun.* 4 (5), 100598. doi: 10.1016/j.xplc.2023.100598

Chu, S., Wang, J., Zhu, Y., Liu, S., Zhou, X., Zhang, H., et al. (2017). An R2R3-type MYB transcription factor, GmMYB29, regulates isoflavone biosynthesis in soybean. *PloS Genet.* 13 (5), e1006770. doi: 10.1371/journal.pgen.1006770

Dastmalchi, M., Bernards, M. A., and Dhaubhadel, S. (2016). Twin anchors of the soybean isoflavonoid metabolon: evidence for tethering of the complex to the endoplasmic reticulum by IFS and C4H. *Plant J.* 85 (6), 689–706. doi: 10.1111/tpj.13137

Del Cerro, P., Megias, M., Lopez-Baena, F. J., Gil-Serrano, A., Perez-Montano, F., and Ollero, F. J. (2019). Osmotic stress activates nif and fix genes and induces the Rhizobium tropici CIAT 899 Nod factor production *via* NodD2 by up-regulation of the nodA2 operon and the nodA3 gene. *PloS One* 14 (3), e0213298. doi: 10.1371/journal.pone.0213298

Dixon, R. A., and Pasinetti, G. M. (2010). Flavonoids and isoflavonoids: from plant biology to agriculture and neuroscience. *Plant Physiol.* 154 (2), 453–457. doi: 10.1104/pp.110.161430

Dixon, R. A., and Steele, C. L. (1999). Flavonoids and isoflavonoids - a gold mine for metabolic engineering. *Trends Plant Sci.* 4 (10), 394–400. doi: 10.1016/s1360-1385(99)01471-5

Feng, Y., Zhang, S., Li, J., Pei, R., Tian, L., Qi, J., et al. (2023). Dual-function C2H2-type zinc-finger transcription factor GmZFP7 contributes to isoflavone accumulation in soybean. *New Phytol.* 237 (5), 1794–1809. doi: 10.1111/nph.18610

Graham, T. L., Graham, M. Y., Subramanian, S., and Yu, O. (2007). RNAi silencing of genes for elicitation or biosynthesis of 5-deoxyisoflavonoids suppresses race-specific resistance and hypersensitive cell death in Phytophthora sojae infected tissues. *Plant Physiol.* 144 (2), 728–740. doi: 10.1104/pp.107.097865

Grant, D., Nelson, R. T., Cannon, S. B., and Shoemaker, R. C. (2010). SoyBase, the USDA-ARS soybean genetics and genomics database. *Nucleic Acids Res.* 38 (Database issue), D843–D846. doi: 10.1093/nar/gkp798

Gupta, A., Awasthi, P., Sharma, N., Parveen, S., Vats, R. P., Singh, N., et al. (2022). Medicarpin confers powdery mildew resistance in *Medicago truncatula* and activates the salicylic acid signalling pathway. *Mol. Plant Pathol.* 23 (7), 966–983. doi: 10.1111/mpp.13202

Gupta, O. P., Dahuja, A., Sachdev, A., Kumari, S., Jain, P. K., Vinutha, T., et al. (2019). Conserved miRNAs modulate the expression of potential transcription factors of isoflavonoid biosynthetic pathway in soybean seeds. *Mol. Biol. Rep.* 46 (4), 3713–3730. doi: 10.1007/s11033-019-04814-7

Gupta, O. P., Nigam, D., Dahuja, A., Kumar, S., Vinutha, T., Sachdev, A., et al. (2017). Regulation of isoflavone biosynthesis by miRNAs in two contrasting soybean genotypes at different seed developmental stages. *Front. Plant Sci.* 8. doi: 10.3389/fpls.2017.00567

Hammerschmidt, R. (1999). Phytoalexins: What have we learned after 60 years? *Annu. Rev. Phytopathol.* 37, 285–306. doi: 10.1146/annurev.phyto.37.1.285

Han, F., He, X., Chen, W., Gai, H., Bai, X., He, Y., et al. (2020). Involvement of a novel tetR-like regulator (*BdtR*) of *Bradyrhizobium diazoefficiens* in the efflux of isoflavonoid genistein. *Mol. Plant Microbe Interact.* 33 (12), 1411–1423. doi: 10.1094/MPMI-08-20-0243-R

Jahan, M. A., Harris, B., Lowery, M., Coburn, K., Infante, A. M., Percifield, R. J., et al. (2019). The NAC family transcription factor GmNAC42-1 regulates biosynthesis of the anticancer and neuroprotective glyceollins in soybean. *BMC Genomics* 20 (1), 149. doi: 10.1186/s12864-019-5524-5

Jung, W., Yu, O., Lau, S. M., O'Keefe, D. P., Odell, J., Fader, G., et al. (2000). Identification and expression of isoflavone synthase, the key enzyme for biosynthesis of isoflavones in legumes. *Nat. Biotechnol.* 18 (2), 208–212. doi: 10.1038/72671

Kim, J. M., Lyu, J. I., Kim, D., Hung, N. N., Seo, J. S., Ahn, J., et al. (2022). Genome wide association study to detect genetic regions related to isoflavone content in a mutant soybean population derived from radiation breeding. *Front. Plant Sci.* 13. doi: 10.3389/fpls.2022.968466

Krizova, L., Dadakova, K., Kasparovska, J., and Kasparovsky, T. (2019). Isoflavones. *Molecules* 24 (6), 1076. doi: 10.3390/molecules24061076

Lapcík, O. (2007). Isoflavonoids in non-leguminous taxa: a rarity or a rule? *Phytochemistry* 68 (22-24), 2909–2916. doi: 10.1016/j.phytochem.2007.08.006

LatundeDada, A. O., CabelloHurtado, F., Czittrich, N., Didierjean, L., Schopfer, C., Hertkorn, N., et al. (2001). Flavonoid 6-hydroxylase from soybean (*Glycine max* L.), a novel plant P-450 monooxygenase. *J. Biol. Chem.* 276 (3), 1688–1695. doi: 10.1074/jbc.M006277200

Li, Y., and Zhang, H. (2017). Soybean isoflavones ameliorate ischemic cardiomyopathy by activating Nrf2-mediated antioxidant responses. *Food Funct.* 8 (8), 2935–2944. doi: 10.1039/c7fo00342k

Lin, F., Chhapekar, S. S., Vieira, C. C., Da Silva, M. P., Rojas, A., Lee, D., et al. (2022). Breeding for disease resistance in soybean: a global perspective. *Theor. Appl. Genet.* 135 (11), 3773–3872. doi: 10.1007/s00122-022-04101-3

Liu, Q., Liu, Y., Li, G., Savolainen, O., Chen, Y., and Nielsen, J. (2021). *De novo* biosynthesis of bioactive isoflavonoids by engineered yeast cell factories. *Nat. Commun.* 12 (1), 6085. doi: 10.1038/s41467-021-26361-1

Liu, X. Q., Yuan, L. L., Xu, L., Xu, Z. L., Huang, Y. H., He, X. L., et al. (2013). Over-expression of GmMYB39 leads to an inhibition of the isoflavonoid biosynthesis in soybean (*Glycine max.* L). *Plant Biotechnol. Rep.* 7 (4), 445–455. doi: 10.1007/s11816-013-0283-2

Liu, Y., Zhang, Y., Liu, X., Shen, Y., Tian, D., Yang, X., et al. (2023). SoyOmics: A deeply integrated database on soybean multi-omics. *Mol. Plant* 16 (5), 794–797. doi: 10.1016/j.molp.2023.03.011

Lu, L. W., Chen, N., Brunder, D. G., Nayeem, F., Nagamani, M., Nishino, T. K., et al. (2022). Soy isoflavones decrease fibroglandular breast tissue measured by magnetic resonance imaging in premenopausal women: a 2-year randomized double-blind placebo controlled clinical trial. *Clin. Nutr. ESPEN* 52, 158–168. doi: 10.1016/j.clnesp.2022.10.007

Luo, J. (2015). Metabolite-based genome-wide association studies in plants. *Curr. Opin. Plant Biol.* 24, 31–38. doi: 10.1016/j.pbi.2015.01.006

Mackova, Z., Koblovska, R., and Lapcik, O. (2006). Distribution of isoflavonoids in non-leguminous taxa - an update. *Phytochemistry* 67 (9), 849–855. doi: 10.1016/j.phytochem.2006.01.020

Masunaka, A., Hyakumachi, M., and Takenaka, S. (2011). Plant growth-promoting fungus, *Trichoderma koningi* suppresses isoflavonoid phytoalexin vestitol production for colonization on/in the roots of *Lotus japonicus*. *Microbes Environments* 26 (2), 128–134. doi: 10.1264/jsme2.me10176

Matsuda, H., Yamazaki, Y., Moriyoshi, E., Nakayasu, M., Yamazaki, S., Aoki, Y., et al. (2023). Apoplast-localized beta-glucosidase elevates isoflavone accumulation in the soybean rhizosphere. *Plant Cell Physiol.* 64 (5), 486–500. doi: 10.1093/pcp/pcad012

Nabavi, S. M., Samec, D., Tomczyk, M., Milella, L., Russo, D., Habtemariam, S., et al. (2020). Flavonoid biosynthetic pathways in plants: Versatile targets for metabolic engineering. *Biotechnol. Adv.* 38, 107316. doi: 10.1016/j.bioteChadv.2018.11.005

Naoumkina, M., Farag, M. A., Sumner, L. W., Tang, Y., Liu, C. J., and Dixon, R. A. (2007). Different mechanisms for phytoalexin induction by pathogen and wound signals in *Medicago truncatula*. *Proc. Natl. Acad. Sci. U.S.A.* 104 (46), 17909–17915. doi: 10.1073/pnas.0708697104

Ng, M. S., Ku, Y. S., Yung, W. S., Cheng, S. S., Man, C. K., Yang, L., et al. (2021). MATE-type proteins are responsible for isoflavone transportation and accumulation in soybean seeds. *Int. J. Mol. Sci.* 22 (21), 12017. doi: 10.3390/ijms222112017

Ng, T. B., Ye, X. J., Wong, J. H., Fang, E. F., Chan, Y. S., Pan, W., et al. (2011). Glyceollin, a soybean phytoalexin with medicinal properties. *Appl. Microbiol. Biotechnol.* 90 (1), 59–68. doi: 10.1007/s00253-011-3169-7

Okutani, F., Hamamoto, S., Aoki, Y., Nakayasu, M., Nihei, N., Nishimura, T., et al. (2020). Rhizosphere modelling reveals spatiotemporal distribution of daidzein shaping

soybean rhizosphere bacterial community. *Plant Cell Environ.* 43 (4), 1036–1046. doi: 10.1111/pce.13708

Pawlowski, J. W., Martin, B. R., McCabe, G. P., McCabe, L., Jackson, G. S., Peacock, M., et al. (2015). Impact of equol-producing capacity and soy-isoflavone profiles of supplements on bone calcium retention in postmenopausal women: a randomized crossover trial. *Am. J. Clin. Nutr.* 102 (3), 695–703. doi: 10.3945/ajcn.114.093906

Peck, M. C., Fisher, R. F., and Long, S. R. (2006). Diverse flavonoids stimulate NodD1 binding to nod gene promoters in *Sinorhizobium meliloti*. *J. Bacteriol.* 188 (15), 5417–5427. doi: 10.1128/JB.00376-06

Pei, R., Zhang, J., Tian, L., Zhang, S., Han, F., Yan, S., et al. (2018). Identification of novel QTL associated with soybean isoflavone content. *Crop J.* 6 (3), 244–252. doi: 10.1016/j.cj.2017.10.004

Pokhrel, S., Ponniah, S. K., Jia, Y. L., Yu, O., and Manoharan, M. (2021). Transgenic rice expressing isoflavone synthase gene from soybean shows resistance against blast fungus (*Magnaporthe oryzae*). *Plant Dis.* 105 (10), 3141–3146. doi: 10.1094/Pdis-08-20-1777-Re

Polturak, G., Misra, R. C., El-Demerdash, A., Owen, C., Steed, A., McDonald, H. P., et al. (2023). Discovery of isoflavone phytoalexins in wheat reveals an alternative route to isoflavonoid biosynthesis. *Nat. Commun.* 14 (1), 6977. doi: 10.1038/s41467-023-42464-3

Reynaud, J., Guilet, D., Terreux, R., Lussignol, M., and Walchshofer, N. (2005). Isoflavonoids in non-leguminous families: an update. *Nat. Prod. Rep.* 22 (4), 504–515. doi: 10.1039/b416248j

Rizzo, G., and Baroni, L. (2018). Soy, soy foods and their role in vegetarian diets. *Nutrients* 10 (1), 43. doi: 10.3390/nu10010043

Rush, T. A., Puech-Pages, V., Bascaules, A., Jargeat, P., Maillet, F., Haouy, A., et al. (2020). Lipo-chitooligosaccharides as regulatory signals of fungal growth and development. *Nat. Commun.* 11 (1), 3897. doi: 10.1038/s41467-020-17615-5

Sajid, M., Stone, S. R., and Kaur, P. (2021). Recent advances in heterologous synthesis paving way for future green-modular bioindustries: a review with special reference to isoflavonoids. *Front. Bioeng. Biotechnol.* 9. doi: 10.3389/fbioe.2021.673270

Sathyapalan, T., Aye, M., Rigby, A. S., Thatcher, N. J., Dargham, S. R., Kilpatrick, E. S., et al. (2018). Soy isoflavones improve cardiovascular disease risk markers in women during the early menopause. *Nutr. Metab. Cardiovasc. Dis.* 28 (7), 691–697. doi: 10.1016/j.numecd.2018.03.007

Sohn, S. I., Pandian, S., Oh, Y. J., Kang, H. J., Cho, W. S., and Cho, Y. S. (2021). Metabolic engineering of isoflavones: an updated overview. *Front. Plant Sci.* 12. doi: 10.3389/fpls.2021.670103

Squadrito, F., Imbalzano, E., Rottura, M., Arcoraci, V., Pallio, G., Catalano, A., et al. (2023). Effects of genistein aglycone in glucocorticoid induced osteoporosis: a randomized clinical trial in comparison with alendronate. *BioMed. Pharmacother.* 163, 114821. doi: 10.1016/j.biopha.2023.114821

Sreevidya, V. S., Srinivasa Rao, C., Sullia, S. B., Ladha, J. K., and Reddy, P. M. (2006). Metabolic engineering of rice with soybean isoflavone synthase for promoting nodulation gene expression in rhizobia. *J. Exp. Bot.* 57 (9), 1957–1969. doi: 10.1093/jxb/erj143

Subramanian, S., Stacey, G., and Yu, O. (2006). Endogenous isoflavones are essential for the establishment of symbiosis between soybean and *Bradyrhizobium japonicum*. *Plant J.* 48 (2), 261–273. doi: 10.1111/j.1365-313X.2006.02874.x

Sugiyama, A. (2019). The soybean rhizosphere: Metabolites, microbes, and beyond-A review. *J. Adv. Res.* 19, 67–73. doi: 10.1016/j.jare.2019.03.005

Sugiyama, A., Shitan, N., and Yazaki, K. (2007). Involvement of a soybean ATP-binding cassette-type transporter in the secretion of genistein, a signal flavonoid in legume-Rhizobium symbiosis. *Plant Physiol.* 144 (4), 2000–2008. doi: 10.1104/pp.107.096727

Tiscione, D., Gallelli, L., Tamanini, I., Luciani, L. G., Verze, P., Palmieri, A., et al. (2017). Daidzein plus isolase associated with zinc improves clinical symptoms and quality of life in patients with LUTS due to benign prostatic hyperplasia: results from a phase I-II study. *Arch. Ital Urol. Androl.* 89 (1), 12–16. doi: 10.4081/aiua.2017.1.12

Veitch, N. C. (2007). Isoflavonoids of the leguminosae. *Nat. Prod. Rep.* 24 (2), 417–464. doi: 10.1039/b511238a

Veitch, N. C. (2009). Isoflavonoids of the leguminosae. *Nat. Prod. Rep.* 26 (6), 776–802. doi: 10.1039/b616809b

Veitch, N. C. (2013). Isoflavonoids of the leguminosae. *Nat. Prod. Rep.* 30 (7), 988–1027. doi: 10.1039/c3np70024k

Vina, J., Escudero, J., Baquero, M., Cebrian, M., Carbonell-Asins, J. A., Munoz, J. E., et al. (2022). Genistein effect on cognition in prodromal Alzheimer's disease patients. *Genial Clin. Trial Alzheimers Res. Ther.* 14 (1), 164. doi: 10.1186/s13195-022-01097-2

Wang, X., Zhang, J., Lu, X., Bai, Y., and Wang, G. (2023). Two diversities meet in the rhizosphere: root specialized metabolites and microbiome. *J. Genet. Genomics*. doi: 10.1016/j.jgg.2023.10.004

Watanabe, S., Yamada, R., Kanetake, H., Kaga, A., and Anai, T. (2019). Identification and characterization of a major QTL underlying soybean isoflavone malonylglycitin content. *Breed Sci.* 69 (4), 564–572. doi: 10.1270/jsbbs.19027

Wu, D., Li, D., Zhao, X., Zhan, Y., Teng, W., Qiu, L., et al. (2020). Identification of a candidate gene associated with isoflavone content in soybean seeds using genome-wide association and linkage mapping. *Plant J.* 104 (4), 950–963. doi: 10.1111/tpj.14972

Xie, C. L., Park, K. H., Kang, S. S., Cho, K. M., and Lee, D. H. (2021). Isoflavone-enriched soybean leaves attenuate ovariectomy-induced osteoporosis in rats by anti-inflammatory activity. *J. Sci. Food Agric.* 101 (4), 1499–1506. doi: 10.1002/jsfa.10763

Yan, J. H., Wang, B., Zhong, Y. P., Yao, L. M., Cheng, L. J., and Wu, T. L. (2015). The soybean R2R3 MYB transcription factor GmMYB100 negatively regulates plant flavonoid biosynthesis. *Plant Mol. Biol.* 89 (1-2), 35–48. doi: 10.1007/s11103-015-0349-3

Yang, J., Lan, L., Jin, Y., Yu, N., Wang, D., and Wang, E. (2022). Mechanisms underlying legume-rhizobium symbioses. *J. Integr. Plant Biol.* 64 (2), 244–267. doi: 10.1111/jipb.13207

Yi, J., Derynck, M. R., Li, X., Telmer, P., Marsolais, F., and Dhaubhadel, S. (2010). A single-repeat MYB transcription factor, GmMYB176, regulates CHS8 gene expression and affects isoflavonoid biosynthesis in soybean. *Plant J.* 62 (6), 1019–1034. doi: 10.1111/j.1365-313X.2010.04214.x

Yu, X., Yan, J., Li, Y., Cheng, J., Zheng, L., Fu, T., et al. (2023). Inhibition of castration-resistant prostate cancer growth by genistein through suppression of AKR1C3. *Food Nutr. Res.* 67, 9024. doi: 10.29219/fnr.v67.9024

Yuan, J., Ma, L., Wang, Y., Xu, X., Zhang, R., Wang, C., et al. (2023). A recently evolved BAHD acetyltransferase, responsible for bitter soyasaponin A production, is indispensable for soybean seed germination. *J. Integr. Plant Biol.* 65 (11), 2490–2504. doi: 10.1111/jipb.13553

Yuan, J. P., Liu, Y. B., Peng, J., Wang, J. H., and Liu, X. (2009). Changes of isoflavone profile in the hypocotyls and cotyledons of soybeans during dry heating and germination. *J. Agric. Food Chem.* 57 (19), 9002–9010. doi: 10.1021/jf902248b

Zaheer, K., and Humayoun Akhtar, M. (2017). An updated review of dietary isoflavones: Nutrition, processing, bioavailability and impacts on human health. *Crit. Rev. Food Sci. Nutr.* 57 (6), 1280–1293. doi: 10.1080/10408398.2014.989958

Zhang, P., Du, H., Wang, J., Pu, Y., Yang, C., Yan, R., et al. (2020). Multiplex CRISPR/Cas9-mediated metabolic engineering increases soya bean isoflavone content and resistance to soya bean mosaic virus. *Plant Biotechnol. J.* 18 (6), 1384–1395. doi: 10.1111/pbi.13302

Zhang, H., Gordon, R., Li, W., Yang, X., Pattanayak, A., Fowler, G., et al. (2019). Genistein treatment duration effects biomarkers of cell motility in human prostate. *PloS One* 14 (3), e0214078. doi: 10.1371/journal.pone.0214078

Zhao, J., and Dixon, R. A. (2010). The 'ins' and 'outs' of flavonoid transport. *Trends Plant Sci.* 15 (2), 72–80. doi: 10.1016/j.tplants.2009.11.006

Zheng, T., Li, Y., Li, Y., Zhang, S., Ge, T., Wang, C., et al. (2022). A general model for "germplasm-omics" data sharing and mining: a case study of SoyFGB v2.0. *Sci. Bull.* 67 (17), 1716–1719. doi: 10.1016/j.scib.2022.08.001

frontiers | Frontiers in Plant Science

TYPE Original Research
PUBLISHED 13 March 2024
DOI 10.3389/fpls.2024.1372232

OPEN ACCESS

EDITED BY
Deyu Xie,
North Carolina State University, United States

REVIEWED BY
Junshan Gao,
Anhui Agricultural University, China
Jia-He Wu,
Chinese Academy of Sciences (CAS), China

*CORRESPONDENCE
Doug J. Hinchliffe
doug.hinchliffe@usda.gov
Marina Naoumkina
marina.naoumkina@usda.gov

RECEIVED 17 January 2024
ACCEPTED 22 February 2024
PUBLISHED 13 March 2024

CITATION
Hinchliffe DJ, Naoumkina M, Thyssen GN, Nam S, Chang S, McCarty JC and Jenkins JN (2024) Multi-omics analysis of pigmentation related to proanthocyanidin biosynthesis in brown cotton (*Gossypium hirsutum* L.). *Front. Plant Sci.* 15:1372232. doi: 10.3389/fpls.2024.1372232

Multi-omics analysis of pigmentation related to proanthocyanidin biosynthesis in brown cotton (*Gossypium hirsutum* L.)

Doug J. Hinchliffe[1,2*], Marina Naoumkina[1*], Gregory N. Thyssen[1], Sunghyun Nam[1], SeChin Chang[2], Jack C. McCarty[3] and Johnie N. Jenkins[3]

[1]Cotton Fiber Bioscience and Utilization Research Unit, United States Department of Agriculture (USDA), Agricultural Research Service (ARS), New Orleans, LA, United States, [2]Cotton Quality and Innovation Research Unit, USDA-ARS, New Orleans, LA, United States, [3]Genetics and Sustainable Agriculture Research Unit, USDA-ARS, Mississippi State, MS, United States

Naturally-colored brown cotton (NBC) fiber is an environmentally friendly raw source of fiber for textile applications. The fiber of some NBC cultivars exhibits flame-retardant properties, which can be used in textiles that require flame resistance. Proanthocyanidins or their derivatives are responsible for the brown pigment in NBC; however, how flame retardancy is related to pigmentation in NBC is poorly understood. To gain insight into brown pigment biosynthesis, we conducted comparative transcripts and metabolites profiling analysis of developing cotton fibers between the brown (MC-BL) and white (MC-WL) cotton near-isogenic lines (NILs), genetically different only in the *Lc1* locus. In this study, mass spectrometry was used to detect metabolites in BL and WL developing fibers at 8, 12, 16, 20, 24, 36, and 40 days post anthesis (DPA) and mature fibers. Transcripts analysis was performed at two critical fiber developmental points, 8 DPA (fiber elongation) and 20 DPA (secondary cell wall deposition). We found 5836 (ESI MS positive mode) and 4541 (ESI MS negative mode) metabolites significantly different accumulated between BL and WL. Among them, 142 were known non-redundant metabolites, including organic acids, amino acids, and derivatives of the phenylpropanoid pathway. Transcript analysis determined 1691 (8 DPA) and 5073 (20 DPA) differentially expressed genes (DEGs) between BL and WL, with the majority of DEGs down-regulated at 20 DPA. Organic acids of the citric acid cycle were induced, while most of the detected amino acids were reduced in the MC-BL line. Both *cis*- and *trans*-stereoisomers of flavan-3-ols were detected in developing MC-WL and MC-BL fibers; however, the gallocatechin and catechin accumulated multiple times higher. Gas chromatography-mass spectrometry (GC-MS) analysis of fatty acids determined that palmitic acid long-chain alcohols were the main

constituents of waxes of mature fibers. Energy-dispersive X-ray spectrometry (EDS) analysis of mature fibers revealed that potassium accumulated three times greater in MC-BL than in MC-WL mature fibers. This study provides novel insights into the biosynthesis of pigments and its association with flame retardancy in NBC fibers.

KEYWORDS

brown cotton, proanthocyanidins, metabolites, mass spectrometry, *Gossypium hirsutum*, flame-retardant

1 Introduction

Environmentally friendly fibers of naturally-colored brown cotton (NBC) varieties are most commonly used for fabrics. Due to pigments, clothes from NBC fibers resist fading colors during laundry and protect the skin from ultraviolet radiation. Fibers of some NBC varieties exhibited flame retardant (FR) properties that can offer an eco-friendly alternative to synthetic FR additives in textiles.

Pigments responsible for the color of NBC are proanthocyanidins (PAs), also called condensed tannins. PAs are polymeric flavan-3-ols whose chemical structure consists of benzopyran (A and C rings) linked with another aromatic ring (B ring) at the C2 position (Yu et al., 2023). The common PA subunits are catechin and epicatechin with the gallate modification of the hydroxyl group at the C3' position on the B-ring (Dixon et al., 2005; Xie and Dixon, 2005). The difference between catechin and epicatechin is the stereochemistry around the 2 and 3 positions of the C-ring; catechin is 2,3-*trans*-2R,3S-flavan-3-ol, while epicatechin is 2,3-*cis*-2R,3R-flavan-3-ol. Flavan-3-ols are synthesized from leucoanthocyanidins or anthocyanidins through the flavonoid pathway. Catechin is produced from leucoanthocyanidin by removing the hydroxyl group at the C4 position catalyzed by the leucoanthocyanidin reductase (LAR). Epicatechin is converted from anthocyanidins by anthocyanidin reductase (ANR) (Xie et al., 2003; Zhu et al., 2015).

Initially, PAs were detected in NBC fibers with DMACA (*p*-Dimethylaminocinnamaldehyde) staining (Xiao et al., 2007; Li et al., 2012). A small amount of PAs was also detected in early-developing white fibers, which gradually disappeared at the later stage of development (Li et al., 2012). Both isoforms of PA subunits, catechin and epicatechin, were detected in NBC by using liquid-chromatography mass spectrometry (LC-MS), nuclear magnetic resonance (NMR), and a matrix-assisted laser desorption/ionization-time of flight mass spectrometry (MALDI-TOF MS). Using LC-MS analyses, one study detected catechin and gallocatechin as the most abundant PAs in NBC fibers (Xiao et al., 2014). Another study determined by NMR and MALDI-TOF MS analyses that epicatechin and epigallocatechin were the most predominant PAs in NBC fibers (Feng et al., 2014). The dimeric PAs, procyanidin (PC) and prodelphidin (PD) were detected in white and NBC fibers; however, their ratios were different: the amount of PC and PD was equal in white fibers, whereas NBC fibers contained mainly PD units (Feng et al., 2014). The oxidation products of PAs, quinones, are responsible for color development in NBC fiber since developing fibers do not show distinct coloration until maturation (Feng et al., 2014).

Transcription factors, including TT2 (MYB123), TT8 (bHLH42), and TTG1 (WD40 family), are primary regulators of PA biosynthesis (Yu et al., 2023). In cotton, at least six incompletely dominant genetic loci (*Lc1* – *Lc6*) have been associated with brown fiber (Kohel, 1985). The *Lc1* was mapped to a 1.4 Mb inversion on chromosome A07 upstream of a TT2 homologous gene (*Gh_A07G2341*) (Hinchliffe et al., 2016). An independent mapping study determined that two QTLs in the *Lc1* locus regulate the shades of brown color in fibers. The *qBF-A07-1* (*Gh_A07G2341* - TT2) contributes to the brown color, while the *qBF-A07-1* and *qBF-A07-2* (*Gh_A07G0100* - TTG1) regulate the shades of brown fiber (Wen et al., 2018). A recent study demonstrated that the *Gh_A07G2341 (GhTT2-3A)* overexpression in cotton activated PA structural genes and PA biosynthesis that resulted in brown mature fiber in transgenic lines (Yan et al., 2018).

The source of FR in the NBC remains unclear and is not entirely correlated with the intensity of color in different NBC cultivars (Hinchliffe et al., 2015). One study suggested that higher FR in NBC is linked to condensed tannins and sodium content; authors demonstrated sequestration of inorganic salts such as sodium through ionic interactions with the partial negative charges generated by adjacent hydroxyl units on the B-ring of flavonoid units in PAs and the possible formation of flavonoid–metal complexes in NBC (Nam et al., 2016). Another study argued that condensed tannin is not the source of FR in brown cotton since enhanced FR and anthocyanin precursors appear in developing fibers well before the brown color is detectable; authors suggested that the unknown FR component is probably sequestered by PAs or PA precursors via metal-flavonoid complexes (Hinchliffe et al., 2016).

The current study aims to understand the relationship between pigmentation and FR in NBC. To gain insight into PA biosynthesis in NBC, we conducted comparative metabolite profiling analyses of developing cotton fibers between the brown (MC-BL) and white

(MC-WL) near-isogenic lines (NILs). We found significant changes in metabolite accumulation not only in secondary but in primary metabolism as well. Both isoforms of PA subunits, (+)-catechin and (-)-epicatechin, were detected in NBC and white fibers, with the relative amount of catechin greater than epicatechin. Gas chromatography-mass spectrometry (GC-MS) analysis of fatty acids determined that palmitic acid and long-chain alcohols, 1-Octacosanol and 1-Triacontanol, were predominant in cotton fiber waxes. Scanning electron microscopy and elemental mapping analysis of mature fibers revealed potassium accumulation three times greater in NBC than in white fibers.

2 Materials and methods

2.1 Plant materials

A spontaneous mutation that changed fiber color from white to brown on one branch of the same plant was observed in a cotton (*G. hirsutum* L.) line of unknown background in Starkville, MS (Hinchliffe et al., 2016). The seeds from white and brown cotton bolls from this single plant were collected and designated as MC-WL and MC-BL. The lines differ in *Lc1* locus only; therefore, they are near-isogenic lines (NILs). Both lines continued to maintain their corresponding fiber color through the following generations. The lines were further advanced by self-pollination single seed descent for three generations in New Orleans, LA. Pure lines of MC-WL and MC-BL were planted in the field in New Orleans, LA, in 2017 and grown using standard agricultural practices. Seeds for each cotton line were planted in rows measuring 20 m x 1 m with approximately 50 plants per row. Three rows were planted for each line, with each row used as a biological replicate for sample harvest. Developing cotton fibers were collected from the MC-WL and MC-BL cotton lines at 8, 12, 16, 20, 24, 32, 40 DPA, and mature fibers from open bolls. Mature seed cotton was hand-harvested and ginned using a laboratory roller gin.

2.2 Ultra high performance liquid chromatography-mass spectrometry analysis

Developing (8, 12, 16, 20, 24, 32, and 40 DPA) and mature (~50 DPA) cotton fibers in three biological replicates from MC-WL and MC-BL were used for metabolomic analysis. Fiber samples (15 mg each) were extracted using 8:1:1 acetonitrile: methanol: acetone ratio. Southeast Center for Integrated Metabolomics University of Florida performed sample extraction and metabolome analysis. Global metabolomics profiling was performed on a Thermo Q-Exactive Orbitrap mass spectrometer with Dionex UHPLC and autosampler. Catechins standards were run along with the samples to confirm their presence in the samples. All samples were analyzed in positive and negative heated electrospray ionization with a mass resolution of 35,000 at m/z 200 as separate injections. Separation was achieved on an ACE 18-pfp 100 x 2.1 mm, 2 µM column with mobile phase A as 0.1% formic acid in water and mobile phase B as acetonitrile. The flow rate was 350 µL/min with a column temperature of 25°C. Aliquot of 4 µL was injected for negative ions and 2 µL for positive ions.

2.3 GC-MS analysis of fatty acids

Long chain alcohol standards, 1-Octacosanol and 1-Triacontanol, and Supelco 37-component FAME mix (C4 – C24) were obtained from Sigma-Aldrich (St. Louis, MO); MSTFA+1% TMCS was purchased from Thermo Scientific (Bellefonte, PA). Cotton waxes were extracted from 1 g of mature fibers with dichloromethane using an Dionex ASE 350 Accelerated Solvent Extractor (Thermo Fisher Scientific, (Waltham, MA). Extracts were taken to dryness under a nitrogen stream.

Esterification of fatty acids was performed as follows: 1 mg of dry extract was dissolved in 1 ml of diethyl ether and mixed with 20 µl of methyl acetate and 40 µl of 0.5M sodium methoxide in anhydrous methanol and incubated for 5 min; 30 µl of saturated oxalic acid in ether was added to precipitate glycerides; samples were centrifuged for 7 min and supernatants were transferred to new glass vials, dried in SpeedVac and diluted in 200 µl hexane; injection volume was 1 µl.

Derivatization of long chain alcohols was performed as follows: 10 µl of MSTFA + 1% TMCS were added to 1 mg of dry extracts; incubated at 50°C for 1 hour; 200 ul of hexane was added, mixed, and transferred into a vial for GC automatic sampling; injection volume was 100 split of 1 µl.

The fatty acids and long chain alcohols were analyzed by GC-MS using an Agilent 6890 GC, 5973 MS, and Gerstel MACH (Agilent LTM) fast GC adaptation, using an HP-88 LTM column (30 m × 0.18 mm, 0.18 µM; Agilent). The column heat gradient was 50°C (1 min hold) to 140°C at 25°C/min, followed by a 4°C/min gradient to 177°C and a 2°C/min gradient to 210°C (1.65 min hold). A pressure ramp program was set up as 29.2 psi (1 min hold) to 39.3 at 2.81 psi/min, followed by a 0.44 psi/min gradient to 43.4 psi and a 0.22 psi/min gradient to 47.1 psi (1.65 min hold), which kept a 1 mL/min helium flow rate. The inlet was set to a 50:1 split at 220°C, using an insert with glass wool (Agilent 5062-3587). The GC oven and MS transfer were set at 250°C. A 5 µL syringe was used in a 7683 autosampler. A mass range of m/z 35–500 was acquired.

Concentrations of wax components were determined using standard curves of commercially available FAMEs and long chain alcohols; the peak areas of target ions were used for concentration calculation; the peak areas were normalized by the area of the internal standard C19:0 for a specific sample. Analysis was performed in five technical replicates from two independent isolations of waxes from mature cotton fibers.

2.4 RNA isolation and RNAseq

Total RNA was extracted using the Sigma Spectrum Plant Total RNA Kit (Sigma-Aldrich, St Louis, MO, USA) with on-column DNase I digestion following the manufacturer's protocol. RNA quantity and integrity were evaluated as previously described (Hinchliffe et al., 2011).

Total RNA from 8 and 20 DPA developing fibers of MC-BL and MC-WL in two biological replicates were used for library preparation and RNAseq (LC Sciences, Houston, TX, USA). Sample preparation and library constructions were performed using TruSeq Stranded mRNA Library Prep Kit (Illumina Inc., San Diego, CA, USA) following the manufacturer's protocols. Samples were sequenced using a HiSeq 2000 (Illumina Inc.) with 100 bp paired-end reads. Raw sequence reads were filtered for quality and trimmed by SICKLE (Joshi and Fass, 2011) and aligned to the draft *G. hirsutum* TM-1 reference genome (Zhang et al., 2015) with GSNAP software (Wu and Nacu, 2010). Reads mapping to annotated genes were counted using BEDTools software (Quinlan and Hall, 2010).

2.5 Energy-dispersive X-ray spectroscopy

EDS and elemental mapping analyses of fiber surfaces in scanning electron micrographs (SEM) were conducted with an accelerating voltage of 15 kV using a Phenom G6 ProX SEM (Nanoscience Instruments, Phoenix, AZ, USA) equipped with an EDS detector. The sample was mounted on a stub using double-sided carbon tape, and then a seven nm-thick gold coating was placed onto the sample using a LUXOR gold sputter coater (Aptco Technologies, Nazareth, Belgium).

2.6 Statistical analyses

Statistical analyses of UHPLC-MS and RNAseq data of cotton fiber samples were performed using JMP Genomics 10 software (SAS Institute Inc. Cary, NC, USA). An ANOVA was conducted to find differentially accumulated metabolites or expressed genes between MC-BL and MC-WL as previously described (Naoumkina et al., 2013, 2014). The metabolites or genes that accumulated or expressed differently between two lines by at least 2-fold with a false discovery rate < 0.05 (Benjamini and Yekutieli, 2001) were considered significant. A two-way ANOVA of fatty acids was conducted with Prism 9 (GraphPad Software, Inc.).

3 Results

3.1 Global metabolite changes in NBC fibers

Figure 1A shows images of open bolls of MC-WL and MC-BL near-isogenic lines (NILs). The mature fiber length of MC-BL was about 14 mm, whereas MC-WL fiber was about 27 mm. Developing (8, 12, 16, 20, 24, 32, and 40 DPA) and mature (50 DPA) fibers of white (MC-WL) and brown (MC-BL) cotton were used for metabolite analysis. Each sample (in three biological replicates) was analyzed in positive and negative heated electrospray ionization on a Thermo Q-Exactive Orbitrap mass spectrometer. A total number of detected peaks, 9140 (positive) and 5895 (negative), were used for principal component analysis (PCA) to explore the relationship between brown and white fiber samples in metabolite pools (Figure 1B). According to PCA, samples from developing fibers (8, 12, 16, 20, 24, 32, and 40 DPA) separated between white and brown cotton, while samples from mature fibers formed a distinct cluster (Figure 1B). Therefore, a substantial difference in metabolite composition (in the detectable range of molecular weights by the UHPLC-MS) was observed between MC-WL and MC-BL in developing fibers.

A two-way ANOVA determined that 5836 (ESI MS positive mode) and 4541 (ESI MS negative mode) metabolites were significantly different in accumulation between brown and white fibers (Supplementary Data 1). Figure 2A shows the distribution of up-regulated and down-regulated compounds in MC-BL vs. MC-WL developing and mature fiber samples. The highest number of peaks was detected by both methods at 40 DPA and the lowest at 24 DPA of fiber development. There were significantly more up-regulated than down-regulated metabolites at each developmental time point.

Among detected peaks, 142 were non-redundant known metabolites, 70 of which were significantly (FDR < 0.05) up-regulated and 48 down-regulated (Supplementary Tables 1, 2). Amino acids and their derivatives were the main category among down-regulated metabolites, whereas phenylpropanoids, organic acids, and sugars were the major categories among up-regulated metabolites (Figure 2B).

3.2 Global transcript changes in NBC fibers

We analyzed RNAseq data between the NBC and white NILs from developing fibers at 8 and 20 DPA. Two strategically essential time points, including the peak of elongation (8 DPA) and secondary cell wall (SCW) biosynthesis (20 DPA), were selected for RNAseq due to cost efficiency, with two biological replicates minimally required for statistical analysis. A two-way ANOVA determined that 1691 (8 DPA) and 5073 (20 DPA) genes were significantly (FDR < 0.05) differentially expressed (DEGs) between NILs (Supplementary Data 2). The count of up-regulated and down-regulated DEGs was 986 and 705, correspondingly, at 8 DPA (Figure 3A). However, at 20 DPA, almost all of the DEGs were down-regulated, 4993 genes (Figure 3A).

We used an integrated web-based Gene Ontology (GO) analysis toolkit agriGO to analyze the GO enrichment of DEGs (Tian et al., 2017). The GO analysis showed that the up-regulated genes at 8 DPA in the NBC fibers were enriched in secondary metabolism, phenylpropanoid, flavonoid, nucleotide, oxidoreduction, organic acid, carbohydrate, etc. biological processes, cell wall, plasmodesmata, vacuole, apoplast, cytosol, etc. cellular components, and oxidoreductase activity, heme and tetrapyrrole binding molecular functions, whereas down-regulated genes were enriched in plastid ribosome, plastoglobule, photosystem cellular components and chlorophyll binding molecular function (Figure 3B). At 20 DPA, the up-regulated DEGs in NBC fibers were enriched in secondary metabolic and oxidation biological processes, oxidoreductase activity,

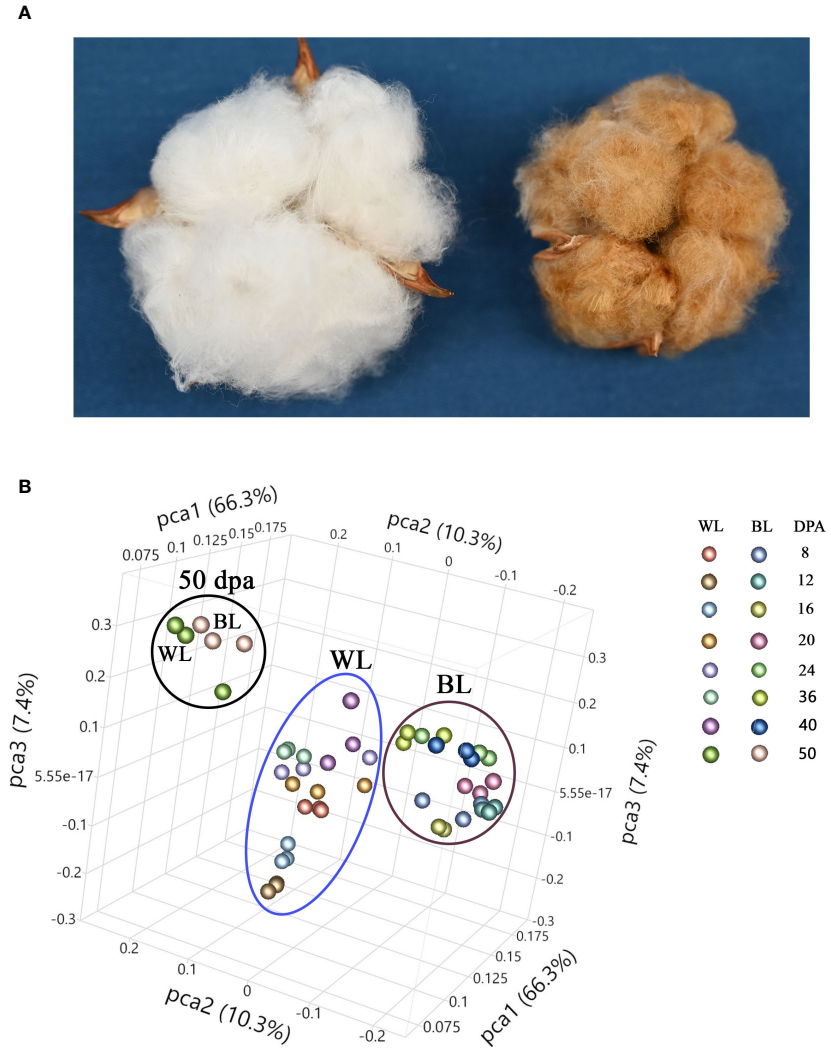

FIGURE 1
Phenotype and principal component analysis (PCA) of white and NBC fiber samples. **(A)** Images of open bolls of MC-WL and MC-BL NILs. **(B)** PCA of fiber samples based on UHPLC-MS metabolome data. WL, white line MC-WL fiber samples, and BL, brown line MC-BL fiber samples. Each fiber developmental time-point is represented by three biological replicates (annotation on the right).

and transmembrane transported activity molecular function. In contrast, down-regulated genes were enriched in nucleic acid, chromosome, cell cycle, etc. biological processes, nucleus, cytoskeleton, nucleoplasm, etc. cellular components, and nucleic acid binding molecular function (Figure 3B).

Organic acids are synthesized as intermediates of metabolic pathways, representing fixed carbon's transitory or stored forms. The citric acid cycle (TCA cycle) connects most metabolic pathways and is essential for energy production. Figure 4 shows changes in the MC-BL fibers in detected metabolites and transcripts of genes encoding enzymes involved in glycolysis and TCA pathways. Most genes from both pathways were up-regulated in MC-BL fibers at 8 DPA and down-regulated at 20 DPA. Genes encoding three enzymes from TCA pathway were significantly differentially expressed between fibers of MC-BL and MC-WL NILs, including aconitase (ACO), isocitrate dehydrogenase (IDH), and malate dehydrogenase (MDH); among them, the MDH was shown to control flux of TCA cycle (Zhang and Fernie, 2018). Glycerol-3-P and detected organic acids from TCA, including citrate, 2-ketoglutarate, succinate, and malate, were significantly (FDR < 0.05) increased in MC-BL compared to MC-WL fibers. In contrast, in MC-BL fibers, shikimate and most amino acids, including phenylalanine, were significantly decreased (Figure 4). Thus, the data indicate that significant changes occurred in the primary metabolism of the brown compared to its white NIL.

3.3 Proanthocyanidin content in MC-BL and MC-WL fibers

Substantial carbon flux from primary metabolism was directed into the PA pathway. Both isoforms of flavan-3-ols, (+)-catechin

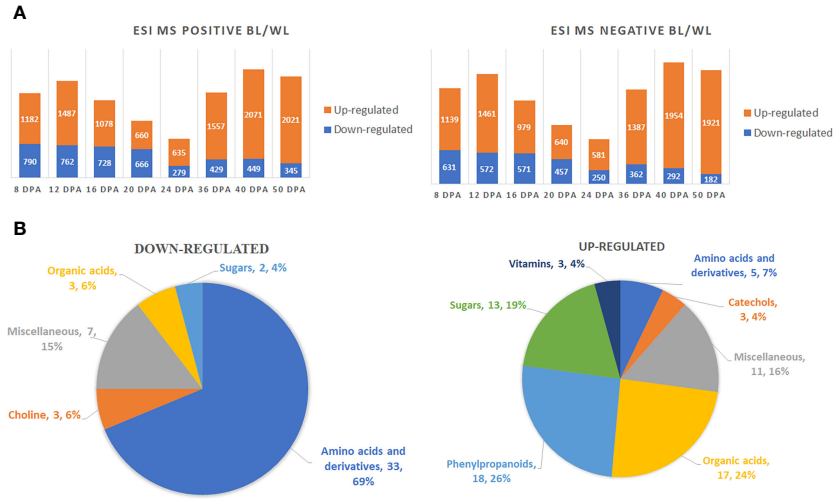

FIGURE 2
Global metabolite changes in developing fibers of brown vs. white cotton lines. **(A)** Bar charts of up-regulated and down-regulated metabolites in brown fibers according to ESI MS positive and negative detection modes. Digits on the bars represent the number of detected metabolites by two detection modes, significantly accumulated at least 2-fold differently between brown and white cotton lines. Fiber development time points are 8, 12, 16, 20, 24, 36, 40 and 50 DPA. BL, brown cotton line MC-BL, and WL, white cotton line MC-WL. **(B)** Pie chart of down-regulated and up-regulated metabolites in brown fibers. Quantity and percentage of metabolites are shown in each category.

and (-)-epicatechin, were detected in NBC and white developing and mature fibers. Figure 5A shows the structures of catechins and epicatechins with gallate modifications detected in fibers of both NILs. A representative total ion chromatogram of extract from fibers at 20 DPA reveals that detected catechins are present in brown and white fibers; the relative amount of catechin is multiple times greater than epicatechin and their corresponding gallate modifications (Figure 5B).

Figure 6 presents relative (based on peak areas) quantifications of catechins, epicatechins, and their gallate modifications in developing and mature fibers of NILs. Catechin and gallocatechin were the most abundant compounds among detected PA subunits. Gallocatechin-3-gallate and Epcatechin-3-gallate accumulated in small amounts, mainly in 8-12 DPA fibers, gradually decreasing during fiber maturation. Catechin, gallocatechin, epicatechin, and epigallocatechin accumulated the most during 16-24 DPA of fiber development in the NBC fibers and substantially less in white fibers. Concentrations of all detected PA subunits were significantly reduced in mature fibers, indicating that they converted into condensed tannins.

3.4 GC-MS analyses of fatty acids and long chain alcohols in waxes of mature fibers

The composition of waxes extracted from mature fibers was compared between NBC and white NILs. Figure 7 shows a total ion chromatogram and quantification of ester derivatives of fatty acids extracted from NBC fibers. Palmitic acid (C16:0) and long-chain alcohols, 1-Octcosanol and 1-Triacontanol, were the main components of cotton fiber waxes. Palmitic acid is the building block for many other fatty acids and phospholipids and is widely present in different classes of plant lipids. Palmitic acid and 1-Triacontanol were significantly (FDR < 0.05) higher accumulated in NBC than white fiber waxes (Figure 7B). Expression levels of genes involved in biosynthesis fatty acids, including acetyl-CoA carboxylase, acyl-carrier protein, acyl CoA ligase, and 3-ketoacyl-CoA synthase, were significantly up-regulated in NBC developing fibers at 8 DPA but down-regulated at 20 DPA (Supplementary Table 4).

3.5 EDS analysis of mature fibers

It has been previously shown that the presence of various inorganics in raw cotton fibers can alter the thermal properties of cellulose (Nam et al., 2014; Hinchliffe et al., 2015; Nam et al., 2016, 2017). Elemental analysis of the surfaces of NBC and white mature fibers in SEM was conducted using EDS. Figure 8 shows the EDS results including color-coded elemental maps, EDS spectra, and elemental compositions in atomic percent. Among inorganic elements, only potassium was detected by EDS. The EDS spectra showed that potassium measured in NBC was three times greater than in white fibers (Figures 8B, C). To explain the increased potassium level in NBC fibers, we searched transcript data to identify DEGs involved in potassium transport. Two *G. hirsutum* genes homologous to *Arabidopsis*, the two-pore potassium (K+) channel (TPK3), were significantly (FDR < 0.05) up-regulated in NBC developing fiber at 8 DPA (Figure 8D). In *Arabidopsis*, the TPK3 regulates the proton gradient in the thylakoid membrane and, therefore, photosynthetic light utilization (Carraretto et al., 2013).

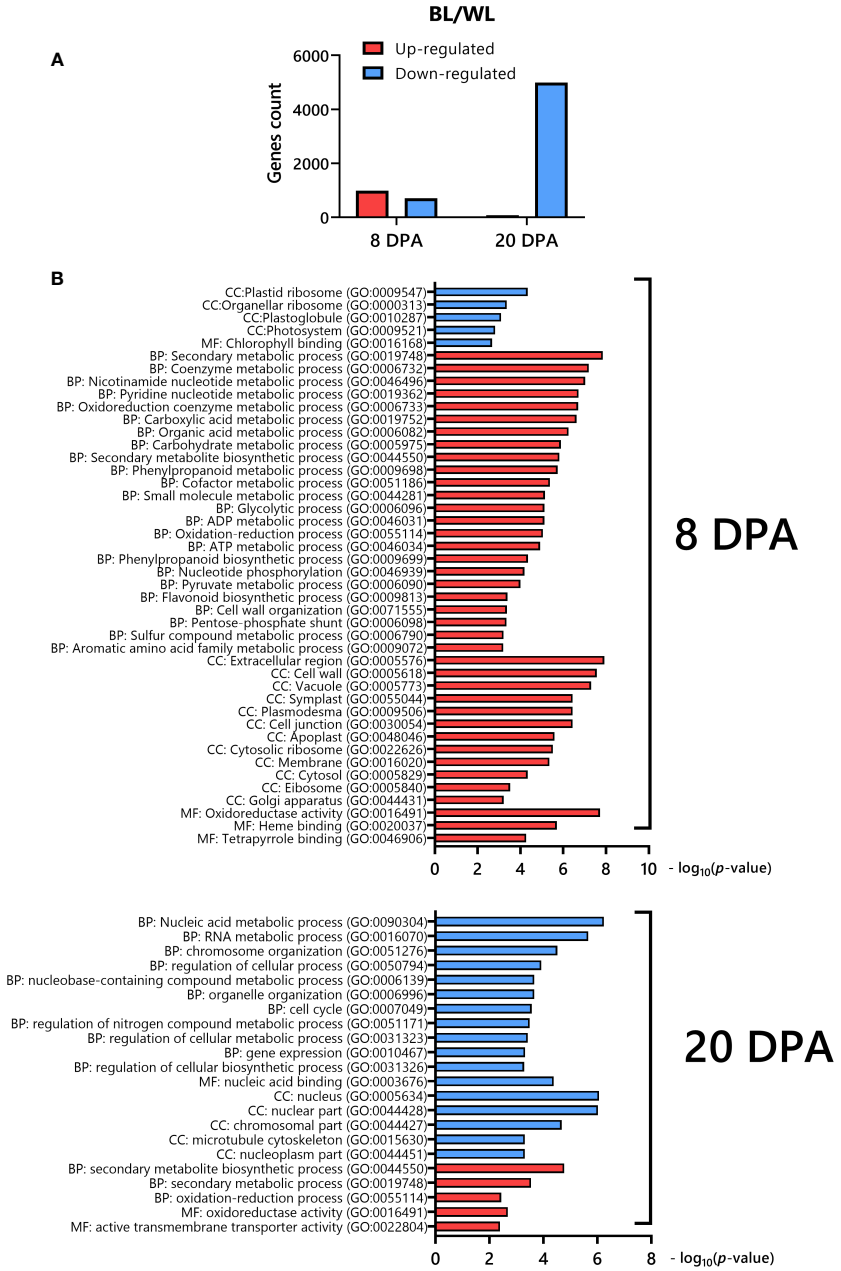

FIGURE 3
Differentially expressed genes in fibers of NBC compared to its white near-isogenic line. **(A)** Distribution of up-regulated and down-regulated DEGs in NBC. **(B)** Gene ontology (GO) enrichment analysis of DEGs down-regulated (blue) or up-regulated (red) in NBC. The GO terms include those representing cellular components (CC), molecular function (MF), and biological processes (BP).

4 Discussion

We performed comparative metabolite analyses of developing and mature MC-BL and MC-WL fibers to understand pigmentation processes in NBC and its relationship to FR. The spontaneous mutation occurred in the *Lc1* locus, turning white fiber on the same plant into brown fiber, from which MC-BL and MC-WL NILs originated (Hinchliffe et al., 2016). A 1.4 Mb inversion on chromosome A07 upstream of a TT2 homologous gene (*Gh_A07G2341*) most likely caused up-regulation of the *Gh_A07G2341*, which induced the expression of structural genes in the PA pathway (Hinchliffe et al., 2016).

Previously, independent studies revealed predominance in the accumulation of catechin and gallocatechin (Xiao et al., 2014) or epicatechin and epigallocatechin (Feng et al., 2014) in NBC fibers. Here, we detected both isoforms of flavan-3-ols, (+)-catechin and

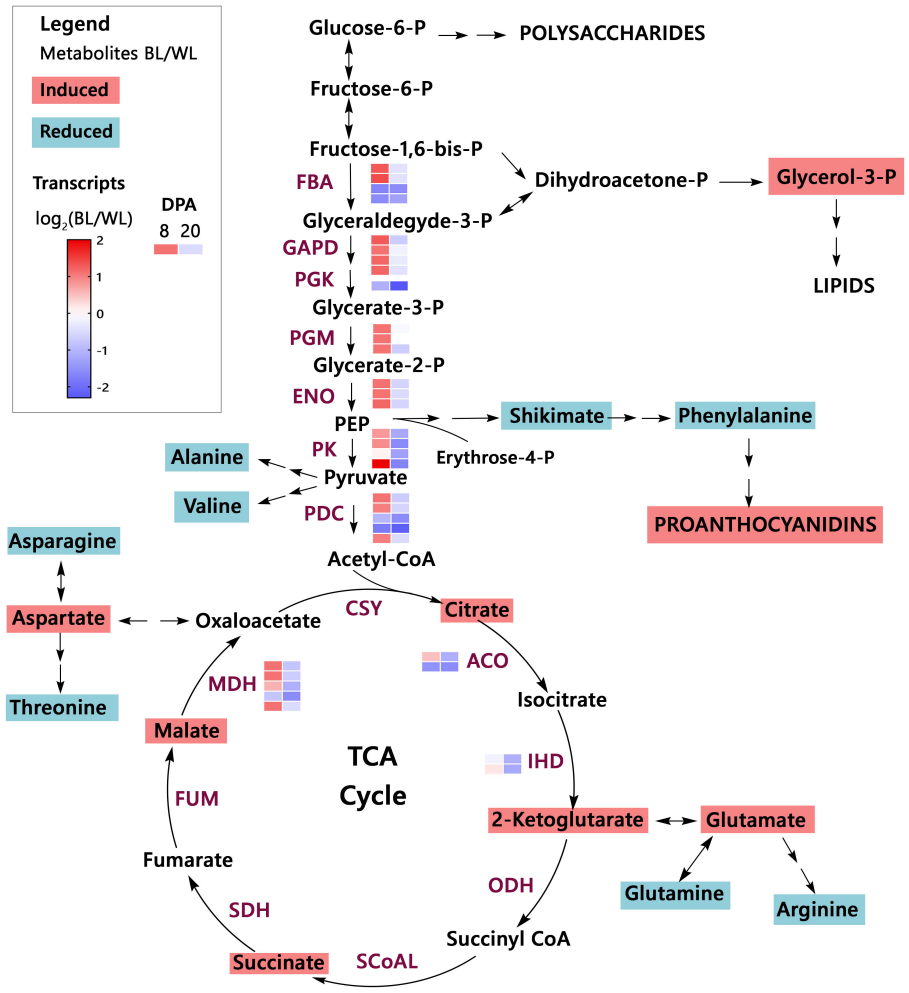

FIGURE 4
Primary metabolism overview in brown cotton. Metabolites highlighted by magenta color are significantly up-regulated, whereas metabolites highlighted by teal color are down-regulated in MC-BL fibers (Supplementary Tables 1, 2). PEP, phosphoenolpyruvate; TCA cycle, the citric acid cycle. Abbreviations of the enzymes (maroon color): FBA, fructose-bisphosphate aldolase; GAPD, glyceraldehyde 3-phosphate dehydrogenase; PGK, phosphoglycerate kinase; PGM, phosphoglycerate mutase; ENO, enolase; PK, pyruvate kinase; PDC, pyruvate dehydrogenase complex; CSY, citrate synthase; ACO, aconitase; IHD, isocitrate dehydrogenase; ODH, 2-Oxoglutarate Dehydrogenase complex; SCoAL, Succinyl-CoA Ligase; SDH, succinate dehydrogenase; FUM, fumarase; MDH, malate dehydrogenase. The heat map represents the log_2 ratio of transcripts from fibers (8 and 20 DPA) of brown and white NILs (Supplementary Table 3).

(-)-epicatechin and their derivatives, in MC-BL and MC-WL fibers; however, catechin and gallocatechin were accumulated multiple times higher than epicatechin and epigallocatechin (Figures 5, 6). What is guiding the PA pathway into the prevalence of *trans*-flavan-3-ols in MC-BL fibers is unclear. Transcript profiling of structural PA genes showed that anthocyanidin synthase (ANS) and anthocyanidin reductase (ANR) were induced in MC-BL much higher than leucoanthocyanidin reductase (LAR) (Hinchliffe et al., 2016; Figure 5), expecting higher accumulation of *cis*-flavan-3-ols isoforms. One of the explanations for the higher abundance of *cis*-stereoisomers in MC-BL fibers can be provided by *in vitro* studies that showed ANRs from different species can produce both *cis*- and *trans*-stereoisomers (Xie and Dixon, 2005; Gargouri et al., 2009; Pang et al., 2013; Dixon and Sarnala, 2020); however, this remains to be confirmed *in vivo*.

Induction of the PA pathway in the *Lc1* mutant, MC-BL, leads to condensed tannin accumulation in mature fibers, which reduces fiber length and also affects the primary metabolism during fiber development. At 8 DPA fiber development, up-regulated DEGs involved in metabolic processes such as secondary, nucleotide, oxidoreduction, organic acid, and carbohydrate metabolic processes were significantly enriched in MC-BL (Figure 3B). Metabolite analyses revealed that organic acids (TCA cycle) were increased, while most amino acids decreased in MC-BL fibers (Figure 4; Supplementary Tables 1, 2). TCA metabolic pathway is part of the mitochondrial respiratory apparatus and is responsible for oxidative decarboxylation

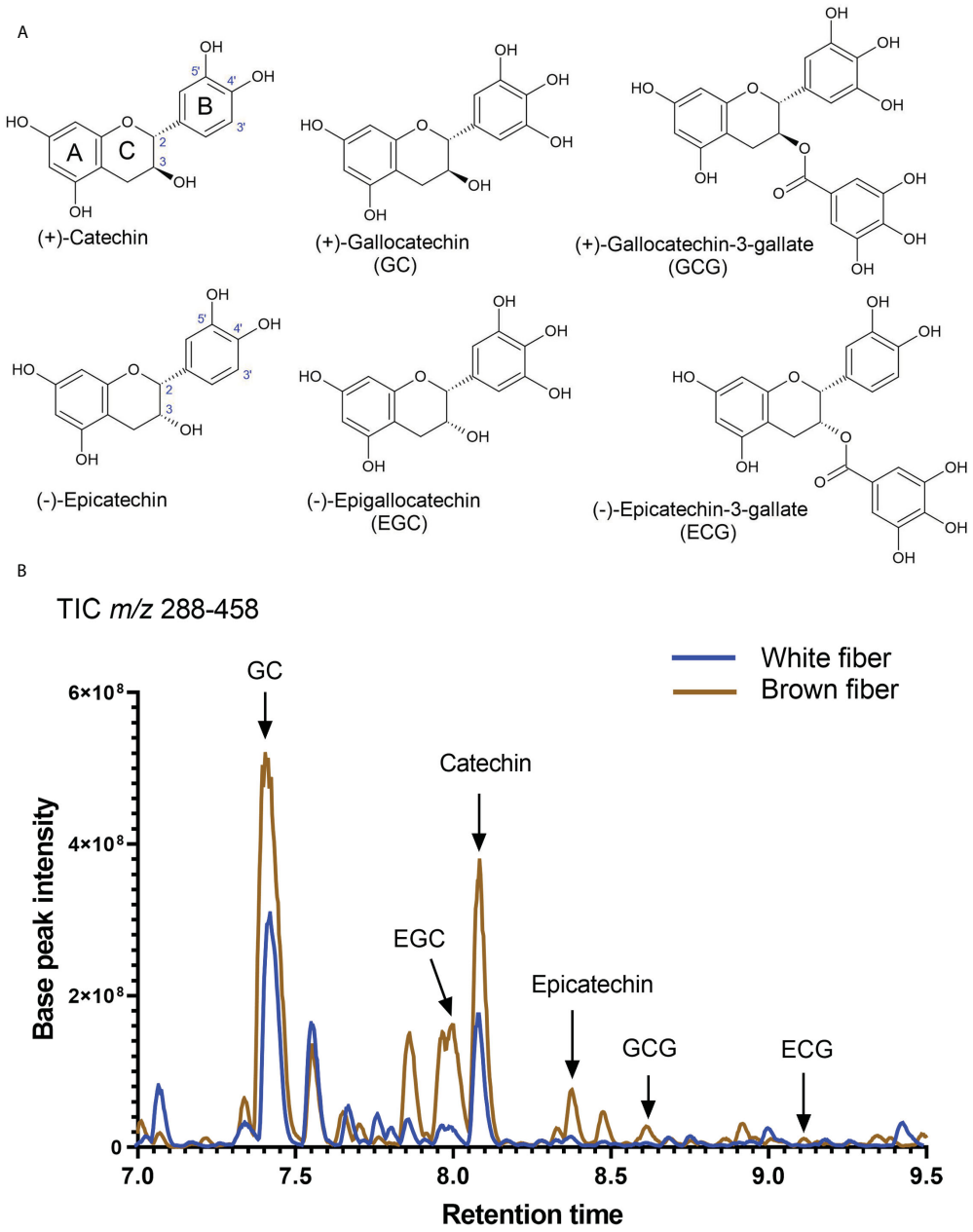

FIGURE 5
Detection of catechins in brown and white cotton fibers. **(A)** Structures of detected catechins in cotton fibers. **(B)** Total negative-ion UHPLC-MS chromatogram (*m/z* 288-458) from the fiber extract at 20 DPA. A brown line shows chromatograms of compounds detected in the brown fiber sample, whereas the blue line is in the white fiber sample. Arrows indicate the peaks of identified catechins. Abbreviations of catechins are indicated in **(A)**.

of organic acids to produce energy in the form of ATP (Millar et al., 2011). TCA connects many metabolic pathways, including carbohydrate, fat, secondary metabolism, and protein biosynthesis. Increasing activity in TCA cycle provides extra energy and carbon sources for PA biosynthesis in MC-BL fibers. We observed a higher accumulation of palmitic acid and 1-triacontanol in MC-BL than in MC-WL, possibly due to increased activity in the TCA cycle.

The source of FR in brown fibers is still a mystery. The condensed tannins are unlikely to be the cause since enhanced FR properties occur in developing fibers before the brown color is detectable. It has been speculated that the unknown FR compound is synthesized in developing fibers and segregated by PA precursors via metal-flavonoid complexes (Hinchliffe et al., 2016). Here, we detected thousands of unknown metabolites accumulated significantly differently between MC-BL and MC-WL fibers; however, which one (or multiple compounds) is responsible for FR in cotton fibers will determine future studies. From another perspective, it has been experimentally

10.3389/fpls.2024.1372232

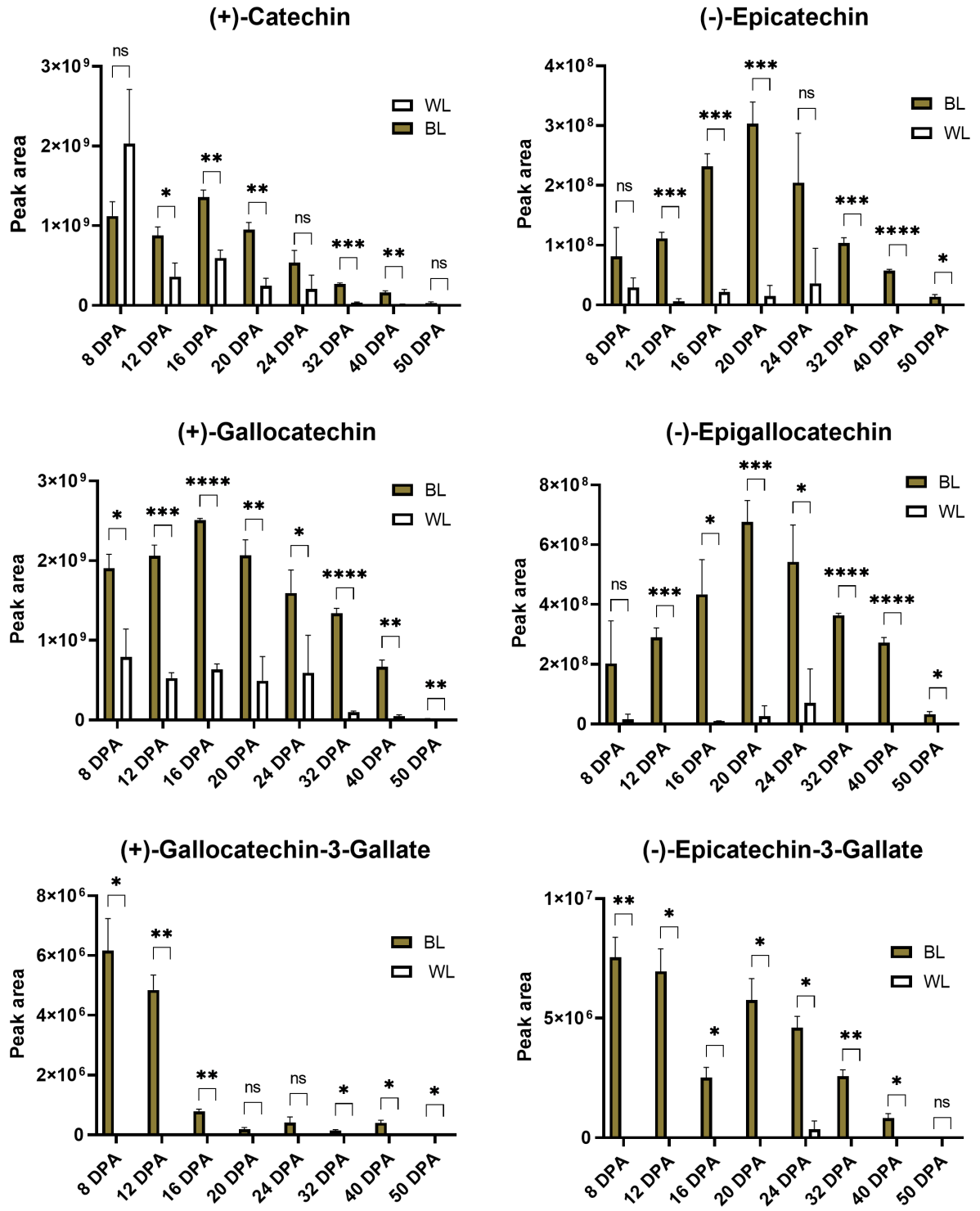

FIGURE 6
Relative content of catechins based on peak areas in brown and white cotton fibers. Error bars represent standard deviations from three independent biological samples. Asterisks indicate the level of statistical significance determined by multiple comparisons test (Abdi, 2007). *p-value < 0.05, **p-value < 0.01, ***p-value < 0.001, ****p-value < 0.0001, ns, not significant.

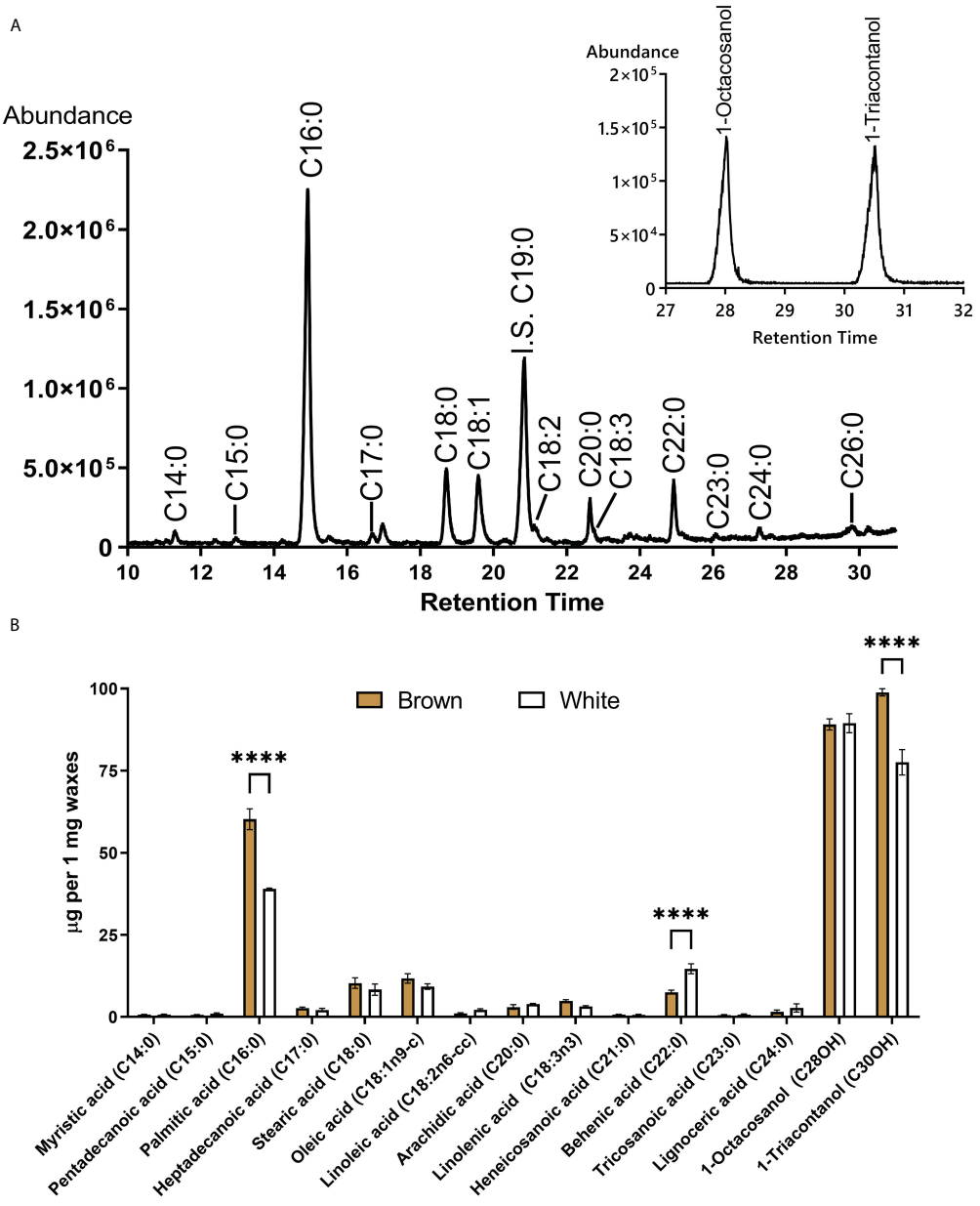

FIGURE 7
GC-MS of fatty acids and long-chain alcohols from waxes of mature cotton fibers. **(A)** The central panel shows a total ion chromatogram of ester derivatives of fatty acids (from brown fibers). IS an internal standard. Inset represents the base peak chromatogram (m/z 467 + 495) of TMS derivatives of long-chain alcohols. **(B)** Waxes composition from mature fiber of brown and white NILs. Asterisks indicate the level of statistical significance determined by the Mixed model with Bonferroni correction (****p-value < 0.0001).

demonstrated that different metal ions alter the thermal properties of cotton fibers (Nam et al., 2014; Hinchliffe et al., 2015; Nam et al., 2016, 2017). Among metal ions previously detected, only potassium, the most prevalent inorganic element in cotton fibers, was detected by EDS. Potassium accumulated three times more in brown than white fibers (Figure 8). The higher potassium level in brown fibers could be supplied by two up-regulated *G. hirsutum* genes, *Gh_A09G0068* and *Gh_D09G0065*, homologous to *Arabidopsis* TPK3 (the two-pore K+ channel).

5 Conclusions

This study found significant changes in thousands of metabolites and transcripts accumulated in MC-WL and MC-BL developing and mature fibers. Organic acids of TCA cycle were induced, while many amino acids were reduced in MC-BL fibers. Both *cis*- and *trans*-stereoisomers of flavan-3-ols were detected in MC-WL and MC-BL fibers. Gene Ontology of up-regulated genes in the MC-BL fibers revealed significant enrichment of genes involved in secondary metabolism, phenylpropanoid, and flavonoid pathways. The

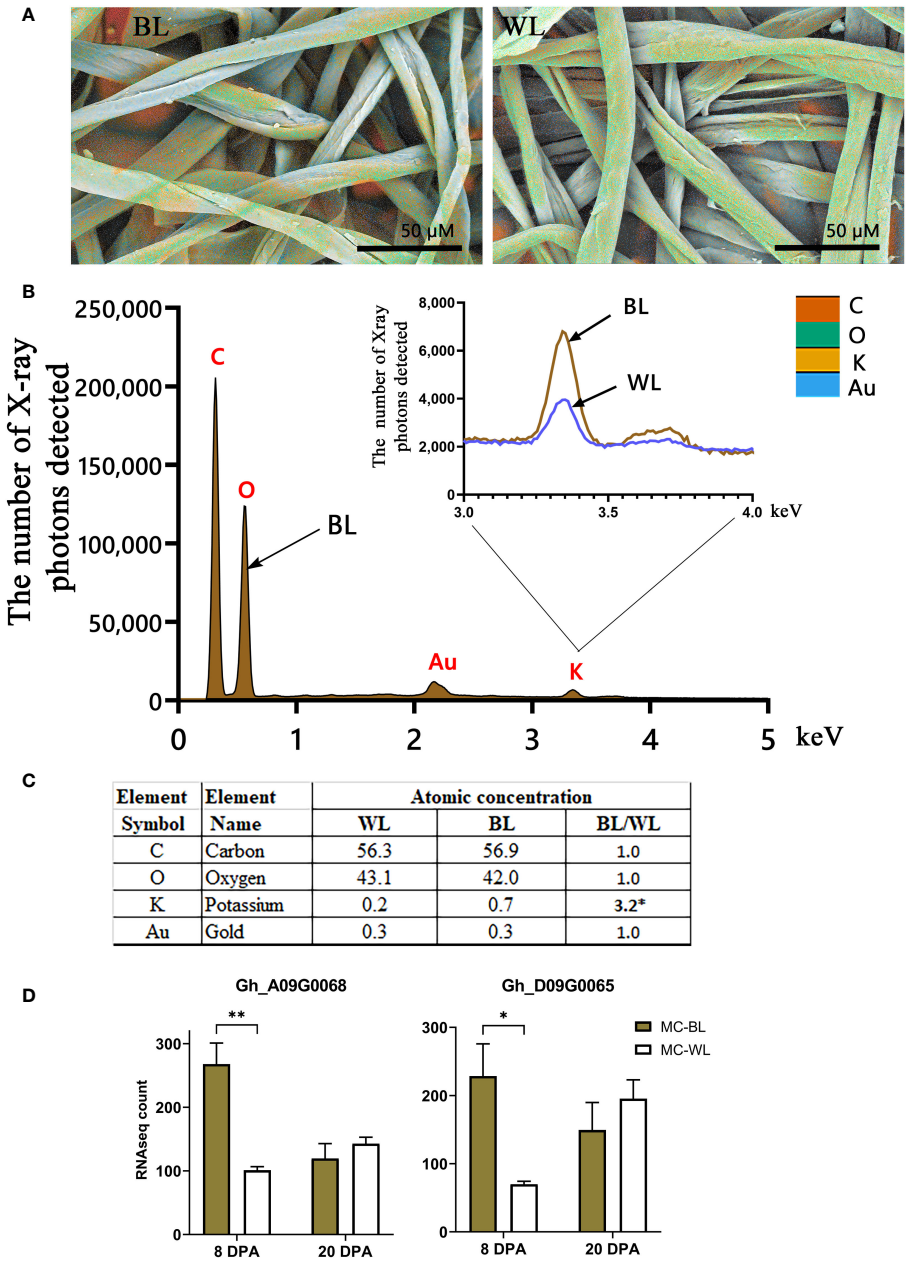

FIGURE 8
EDS analysis of mature NBC and white fibers. **(A)** EDS color-coded elemental maps embedded in SEM micrographs of mature brown (BL) and white (WL) fibers of NILs. The color code of detected elements is below, on the right. **(B)** EDS spectra for BL mature fibers with inset of magnified potassium peaks from BL and WL fibers. Each element symbol is shown on top of the peak. **(C)** Elemental compositions of BL and WL fibers quantified in atomic percent. The detection limit is approximately 0.1 wt %. The presence of gold resulted from the sputter coating of samples. **(D)** RNAseq expression of two *G hirsutum* genes homologous to *Arabidopsis* TPK3, the two-pore potassium channel. Error bars represent standard deviations from two biological replicates. Asterisks indicate the level of statistical significance determined by multiple comparisons test (Abdi, 2007). *p-value < 0.05, **p-value < 0.01.

gallocatechin and catechin were the main constituents of PA precursors in developing fibers. GC-MS analysis of fatty acids determined that palmitic acid and long-chain alcohols, 1-Octacosanol and 1-Triacontanol, were predominant in cotton fiber waxes. EDS analysis of mature fibers revealed that potassium accumulation was three times greater in MC-BL than in MC-WL fibers.

Data availability statement

The datasets presented in this study can be found in online repositories. The names of the repository/repositories and accession number(s) can be found below: BioProject, PRJNA326737.

Author contributions

DH: Conceptualization, Funding acquisition, Investigation, Methodology, Project administration, Resources, Supervision, Writing – review and editing. MN: Data curation, Formal analysis, Software, Validation, Visualization, Writing – original draft, Writing – review and editing. GT: Data curation, Writing – review and editing, Investigation. SN: Data curation, Writing – review and editing, Investigation. SC: Data curation, Writing – review and editing, Investigation. JM: Resources, Writing – review and editing. JJ: Resources, Writing – review and editing.

Funding

The author(s) declare financial support was received for the research, authorship, and/or publication of this article. This research was supported by the US Department of Agriculture (USDA), Agricultural Research Service. This research received no specific grant from any funding agency in the public, commercial, or not-for-profit sectors.

Acknowledgments

We appreciate Southeast Center for Integrated Metabolomics University of Florida for metabolome analysis. Special thanks to Dr. John Bland from the Food and Feed Safety Research Unit (New Orleans, LA) for GC-MS analysis of fatty acids. The mention of trade names or commercial products is solely for the purpose of providing specific information and does not imply recommendation or endorsement by USDA. USDA is an equal opportunity provider and employer.

Conflict of interest

The authors declare that the research was conducted in the absence of any commercial or financial relationships that could be construed as a potential conflict of interest.

The author(s) declared that they were an editorial board member of Frontiers, at the time of submission. This had no impact on the peer review process and the final decision.

Publisher's note

Supplementary material

The Supplementary Material for this article can be found online at: https://www.frontiersin.org/articles/10.3389/fpls.2024.1372232/full#supplementary-material

SUPPLEMENTARY DATA SHEET 1
A two-way ANOVA analysis of ESI MS Positive and Negative data.

SUPPLEMENTARY DATA SHEET 2
A two-way ANOVA analysis of transcript data.

References

Abdi, H. (2007). The Bonferonni and Šidák Corrections for Multiple Comparisons. In N.J. Salkind (Ed.), Encyclopedia of Measurement and Statistics. Thousand Oaks (CA): Sage. pp. 103–107.

Benjamini, Y., and Yekutieli, D. (2001). The control of the false discovery rate in multiple testing under dependency. *Ann. Stat.* 29, 1165–1188. doi: 10.1214/aos/1013699998

Carraretto, L., Formentin, E., Teardo, E., Checchetto, V., Tomizioli, M., Morosinotto, T., et al. (2013). A thylakoid-located two-pore K+ channel controls photosynthetic light utilization in plants. *Science* 342, 114–118. doi: 10.1126/science.1242113

Dixon, R. A., and Sarnala, S. (2020). Proanthocyanidin biosynthesis-a matter of protection. *Plant Physiol.* 184, 579–591. doi: 10.1104/pp.20.00973

Dixon, R. A., Xie, D.-Y., and Sharma, S. B. (2005). Proanthocyanidins: A final frontier in flavonoid research? *New Phytol.* 165, 9–28. doi: 10.1111/j.1469-8137.2004.01

Feng, H., Li, Y., Wang, S., Zhang, L., Liu, Y., Xue, F., et al. (2014). Molecular analysis of proanthocyanidins related to pigmentation in brown cotton fibre (Gossypium hirsutum L.). *J. Exp. Bot.* 65, 5759–5769. doi: 10.1093/jxb/eru286

Gargouri, M., Manigand, C., Mauge, C., Granier, T., Langlois d'Estaintot, B., Cala, O., et al. (2009). Structure and epimerase activity of anthocyanidin reductase from Vitis vinifera. *Acta Crystallogr. Sect. D* 65, 989–1000. doi: 10.1107/S0907444909025013

Hinchliffe, D., Condon, B., Delhom, C. D., Chang, S., Montalvo, J., Madison, C., et al. (2015). Physical and combustion properties of nonwoven fabrics produced from conventional and naturally colored cottons. *Text. Res. J.* 85, 1666–1680. doi: 10.1177/0040517515573410

Hinchliffe, D. J., Condon, B. D., Thyssen, G., Naoumkina, M., Madison, C. A., Reynolds, M., et al. (2016). The GhTT2_A07 gene is linked to the brown colour and natural flame retardancy phenotypes of Lc1 cotton (Gossypium hirsutum L.) fibres. *J. Exp. Bot.* 67, 5461–5471. doi: 10.1093/jxb/erw312

Hinchliffe, D. J., Turley, R. B., Naoumkina, M., Kim, H. J., Tang, Y., Yeater, K. M., et al. (2011). A combined functional and structural genomics approach identified an EST-SSR marker with complete linkage to the Ligon lintless-2 genetic locus in cotton (*Gossypium hirsutum* L.). *BMC Genomics* 12, 445. doi: 10.1186/1471-2164-12-445

Joshi, N. A., and Fass, J. N. (2011) *Sickle: A sliding-window, adaptive, quality-based trimming tool for FastQ files (Version 1.33)*. Available online at: https://github.com/najoshi/sickle.

Kohel, R. J. (1985). Genetic analysis of fiber color variants in cotton. *Crop Sci.* 25, 793–797. doi: 10.2135/cropsci1985.0011183X0025000500017x

Li, T., Fan, H., Li, Z., Wei, J., Lin, Y., and Cai, Y. (2012). The accumulation of pigment in fiber related to proanthocyanidins synthesis for brown cotton. *Acta Physiol. Plant.* 34, 813–818. doi: 10.1007/s11738-011-0858-x

Millar, A. H., Whelan, J., Soole, K. L., and Day, D. A. (2011). Organization and regulation of mitochondrial respiration in plants. *Annu. Rev. Plant Biol.* 62, 79–104. doi: 10.1146/annurev-arplant-042110-103857

Nam, S., Condon, B. D., Foston, M. B., and Chang, S. (2014). Enhanced thermal and combustion resistance of cotton linked to natural inorganic salt components. *Cellulose*. 21:791–802. doi: 10.1007/s10570-013-0133-y

Nam, S., Condon, B. D., Xia, Z., Nagarajan, R., Hinchliffe, D. J., and Madison, C. A. (2017). Intumescent flame-retardant cotton produced by tannic acid and sodium hydroxide. *J. Anal. Appl. Pyrol.* 126, 239–246. doi: 10.1016/j.jaap.2017.06.003

Nam, S., Kim, H. J., Condon, B. D., Hinchliffe, D. J., Chang, S., McCarty, J. C., et al. (2016). High resistance to thermal decomposition in brown cotton is linked to tannins and sodium content. *Cellulose* 23, 1137–1152. doi: 10.1007/s10570-016-0871-8

Naoumkina, M., Hinchliffe, D. J., Turley, R. B., Bland, J. M., and Fang, D. D. (2013). Integrated metabolomics and genomics analysis provides new insights into the fiber

elongation process in Ligon lintless-2 mutant cotton (Gossypium hirsutumL.). *BMC Genomics* 14, 155. doi: 10.1186/1471-2164-14-155

Naoumkina, M., Thyssen, G., Fang, D. D., Hinchliffe, D. J., Florane, C., Yeater, K. M., et al. (2014). The Li_2 mutation results in reduced subgenome expression bias in elongating fibers of allotetraploid cotton (*Gossypium hirsutum* L.). *PloS One* 9, e90830. doi: 10.1371/journal.pone.0090830

Pang, Y., Abeysinghe, I. S., He, J., He, X., Huhman, D., Mewan, K. M., et al. (2013). Functional characterization of proanthocyanidin pathway enzymes from tea and their application for metabolic engineering. *Plant Physiol.* 161, 1103–1116. doi: 10.1104/pp.112.212050

Quinlan, A. R., and Hall, I. M. (2010). BEDTools: a flexible suite of utilities for comparing genomic features. *Bioinformatics* 26, 841–842. doi: 10.1093/bioinformatics/btq033

Tian, T., Liu, Y., Yan, H., You, Q., Yi, X., Du, Z., et al. (2017). agriGO v2.0: a GO analysis toolkit for the agricultural community 2017 update. *Nucleic Acids Res.* 45, W122–W129. doi: 10.1093/nar/gkx382

Wen, T., Wu, M., Shen, C., Gao, B., Zhu, D., Zhang, X., et al. (2018). Linkage and association mapping reveals the genetic basis of brown fibre (Gossypium hirsutum). *Plant Biotechnol. J.* 16, 1654–1666. doi: 10.1111/pbi.12902

Wu, T. D., and Nacu, S. (2010). Fast and SNP-tolerant detection of complex variants and splicing in short reads. *Bioinformatics* 26, 873–881. doi: 10.1093/bioinformatics/btq057

Xiao, Y.-H., Yan, Q., Ding, H., Luo, M., Hou, L., Zhang, M., et al. (2014). Transcriptome and biochemical analyses revealed a detailed proanthocyanidin biosynthesis pathway in brown cotton fiber. *PloS One* 9, e86344. doi: 10.1371/journal.pone.0086344

Xiao, Y.-H., Zhang, Z.-S., Yin, M.-H., Luo, M., Li, X.-B., Hou, L., et al. (2007). Cotton flavonoid structural genes related to the pigmentation in brown fibers. *Biochem. Biophys. Res. Commun.* 358, 73–78. doi: 10.1016/j.bbrc.2007.04.084

Xie, D.-Y., and Dixon, R. A. (2005). Proanthocyanidin biosynthesis – still more questions than answers? *Phytochemistry* 66, 2127–2144. doi: 10.1016/j.phytochem.2005.01.008

Xie, D.-Y., Sharma, S. B., Paiva, N. L., Ferreira, D., and Dixon, R. A. (2003). Role of anthocyanidin reductase, encoded by *BANYULS* in plant flavonoid biosynthesis. *Science* 299, 396–399. doi: 10.1126/science.1078540

Yan, Q., Wang, Y., Li, Q., Zhang, Z., Ding, H., Zhang, Y., et al. (2018). Up-regulation of Gh TT 2-3A in cotton fibres during secondary wall thickening results in brown fibres with improved quality. *Plant Biotechnol. J.* 16, 1735–1747. doi: 10.1111/pbi.12910

Yu, K., Song, Y., Lin, J., and Dixon, R. A. (2023). The complexities of proanthocyanidin biosynthesis and its regulation in plants. *Plant Commun.* 4, 100498. doi: 10.1016/j.xplc.2022.100498

Zhang, T., Hu, Y., Jiang, W., Fang, L., Guan, X., Chen, J., et al. (2015). Sequencing of allotetraploid cotton (*Gossypium hirsutum* L. acc. TM-1) provides a resource for fiber improvement. *Nat. Biotechnol.* 33, 531–537. doi: 10.1038/nbt.3207nbt

Zhang, Y., and Fernie, A. R. (2018). On the role of the tricarboxylic acid cycle in plant productivity. *J. Integr. Plant Biol.* 60, 1199–1216. doi: 10.1111/jipb.12690

Zhu, Y., Wang, H., Peng, Q., Tang, Y., Xia, G., Wu, J., et al. (2015). Functional characterization of an anthocyanidin reductase gene from the fibers of upland cotton (Gossypium hirsutum). *Planta* 241, 1075–1089. doi: 10.1007/s00425-014-2238-4

frontiers | Frontiers in Plant Science

TYPE Mini Review
PUBLISHED 21 March 2024
DOI 10.3389/fpls.2024.1350405

OPEN ACCESS

EDITED BY
Li Tian,
University of California, Davis, United States

REVIEWED BY
Guoli Song,
Chinese Academy of Agricultural Sciences, China
Yue Zhu,
North Carolina State University, United States

*CORRESPONDENCE
Marina Naoumkina
marina.naoumkina@usda.gov

RECEIVED 05 December 2023
ACCEPTED 11 March 2024
PUBLISHED 21 March 2024

CITATION
Naoumkina M, Hinchliffe DJ and Thyssen GN (2024) Naturally colored cotton for wearable applications. *Front. Plant Sci.* 15:1350405. doi: 10.3389/fpls.2024.1350405

Naturally colored cotton for wearable applications

Marina Naoumkina*, Doug J. Hinchliffe and Gregory N. Thyssen

Cotton Fiber Bioscience and Utilization Research Unit, United States Department of Agriculture (USDA), Agricultural Research Service (ARS), Southern Regional Research Center (SRRC), New Orleans, LA, United States

Naturally colored cotton (NCC) offers an environmentally friendly fiber for textile applications. Processing white cotton fiber into textiles requires extensive energy, water, and chemicals, whereas processing of NCC skips the most polluting activity, scouring-bleaching and dyeing; therefore, NCC provides an avenue to minimize the harmful impacts of textile production. NCC varieties are suitable for organic agriculture since they are naturally insect and disease-resistant, salt and drought-tolerant. Various fiber shades, ranging from light green to tan and brown, are available in the cultivated NCC (*Gossypium hirsutum* L.) species. The pigments responsible for the color of brown cotton fiber are proanthocyanidins or their derivatives synthesized by the flavonoid pathway. Due to pigments, the NCC has excellent ultraviolet protection properties. Some brown cotton varieties exhibited superior thermal resistance of fiber that can be used to make fabrics with enhanced flame retardancy. Here, we review molecular mechanisms involved in the pigment production of brown cotton and challenges in breeding NCC varieties with a wide range of colors but without penalty in fiber quality. Also, we discuss opportunities for NCC with flame-retarding properties in textile applications.

KEYWORDS

naturally colored cotton, proanthocyanidin pigments, flame retardance, condensed tannin, flavan-3-ols

Introduction

Naturally colored cotton (NCC) fibers exist in different hues of brown, red, rust, and green and can be used as eco-friendly alternatives to white cotton (Figure 1). The conventional process of dyeing white cotton requires extensive water, energy, and chemicals and contributes about 15% to the cost of the finished garment (Nimon and Beghin, 1999). NCC fabrics resist fading since colors become stronger after laundering (Günaydin et al., 2019). Due to pigments, the clothes made from NCC fibers protect the skin from ultraviolet radiation. Fibers of some brown cotton varieties exhibited flame retardant (FR) properties, making them suitable for specific end-use applications, such as

FIGURE 1
Open bolls of brown and white cotton.

automotive interiors (Parmar and Chakraborty, 2001; Hinchliffe et al., 2015, 2016; Nam et al., 2016, 2017).

Despite these advantages, typical NCC fibers are weaker and shorter than cultivated white cotton fibers, deeming them unsuitable for high-speed woven textile machinery. The breeding efforts in the 1990s resulted in the release of improved brown fiber germplasm lines (May et al., 1994). However, the major obstacle to expanding NCC production is not marketing but regulations to protect white cotton from contamination during ginning and the cost associated with cleaning equipment (Funk and Gamble, 2009). Limited color diversity is another hindrance to expanding the NCC to commercial textile production (Dutt et al., 2004; Yuan et al., 2013). Currently, NCC occupies a textile market niche promoting environmentally friendly clothing production.

Nevertheless, the use of NCC has great merit and should be expanded since global textile production generates toxic chemical waste with a negative impact on the environment. A recent forum article reviewed molecular mechanisms underlying pigmentation in brown and green cotton and suggested "omics-driven breeding" for better fiber quality NCC (Sun et al., 2021). Here, we review the regulation of pigment development in brown cotton and possible biotechnological strategies to increase hue diversity and improve fiber yield and quality. Also, we discuss the source of FR in brown cotton.

Pigments in brown cotton fibers

Brown cotton varieties are most commonly used for NCC fabrics. Proanthocyanidins (PAs) are the primary pigments responsible for brown fibers. PAs, also called condensed tannins, are polymeric flavan-3-ols with the diphenylpropane typical chemical structure (C6-C3-C6), which includes a benzopyran (A and C rings) linked with another aromatic ring (B ring) at C2 position (Figure 2) (Yu et al., 2023). The adjacent subunits of PA are linked by C4-C8 or C4-C6 carbon-carbon bonds (Xie et al., 2004). PAs were initially detected in brown fibers with DMACA (*p*-Dimethylaminocinnamaldehyde) staining. A comparative study of the treatment of mature white, green, and brown fibers with DMACA determined that only brown fibers turned blue, while white and green fibers did not change color (Xiao et al., 2007). However, PAs in minimal quantities were detected in developing white fibers from 5 to 15 days post-anthesis (DPA) and, after that, gradually disappeared (Li et al., 2012). In contrast, PAs were detected as early as 3 DPA in developing brown fibers and were synthesized in high quantities up to maturation (Li et al., 2012).

The common flavan-3-ols are (+)-catechin (2,3-*trans*) and (-)-epicatechin (2,3-*cis*) with the gallate modification of the hydroxyl group at the C3' position on the B-ring (Figure 2) (Dixon et al., 2005; Xie and Dixon, 2005). The structure variability of PAs depends on the 2,3- stereochemistry of the starter and extension units and additional derivatizations such as O-methylation, O-acylation, C- and O-glycosylation (Dixon and Sarnala, 2020). The structure of PA units in brown fibers was studied with nuclear magnetic resonance (NMR), a matrix-assisted laser desorption/ionization-time of flight mass spectrometry (MALDI-TOF MS), and liquid-chromatography mass spectrometry (LC-MS) (Feng et al., 2014; Xiao et al., 2014). In one study, LC-MS analyses determined that the most abundant flavan-3-ols in brown fiber were in 2,3-*trans* form (catechin and gallocatechin), and leucoanthocyanidin reductase (LAR) was highly expressed (Xiao et al., 2014). Another work showed by NMR and MALDI-TOF MS analyses that the most predominant PA units were 2,3-*cis* form (epicatechin and epigallocatechin), and anthocyanidin reductase (ANR) was a key gene in brown fiber pigment biosynthesis (Feng et al., 2014). Therefore, both flavan-3-ols forms, 2,3-*trans* and 2,3-*cis* units, can be produced in brown cotton. The dimeric PAs, procyanidin (PC) and prodelphidin (PD) were detected in white and brown fibers; however, acylation modified some PAs in white fibers (Feng et al., 2014). The ratio of PC and PD was equal in white fibers, whereas brown cotton fibers contained mainly PD units with a relative ratio of 9:1. Feng et al. (2014) suggested that quinones, the oxidation products of proanthocyanidins, directly contribute to color development in brown fiber because developing fibers do not show distinct coloration until maturation.

10.3389/fpls.2024.1350405

PA biosynthesis in brown cotton

PAs are synthesized through the flavonoid pathway, a branch of the phenylpropanoid pathway (Yu et al., 2023). Phenylalanine is converted into 4-Coumaroyl-CoA through a few enzymatic steps by phenylalanine ammonia-lyase (PAL), cinnamate 4-hydroxylase (C4H), and 4-coumarate CoA ligase (4CL) (Figure 2). Chalcone synthase (CHS) then catalyzes chalcone from one molecule of 4-coumaroyl-CoA and three molecules of malonyl-CoA. Chalcone isomerase (CHI) catalyzes the cyclization of chalcone into flavanone naringenin. Flavanone 3/3'/3'5'hydroxylases (F3H/F3'H/F3'5'H) add hydroxyl groups to the C-3, C-3', and C-5' of the

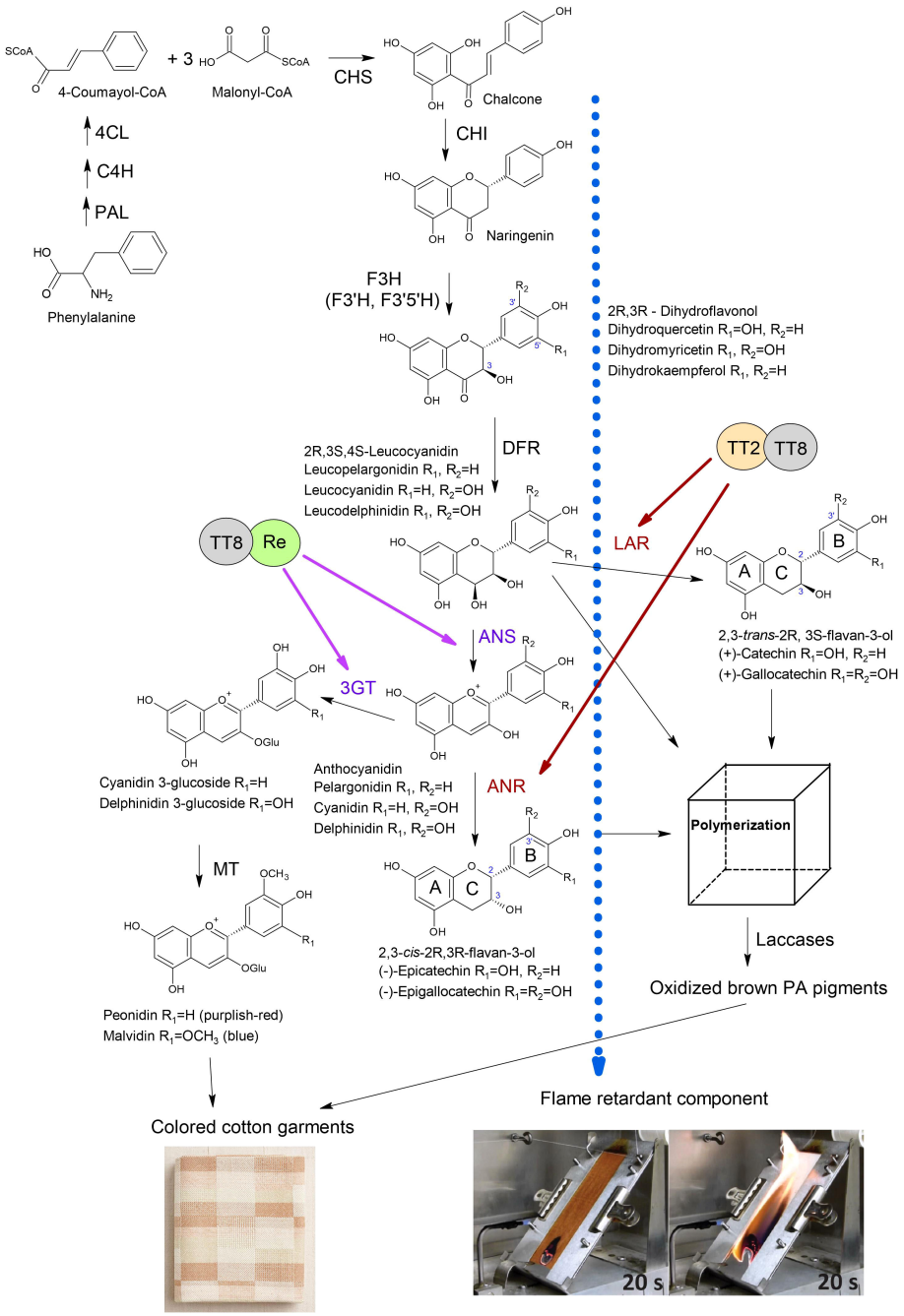

FIGURE 2
Anthocyanidin and proanthocyanidin biosynthesis in brown cotton. PAL, phenylalanine ammonia-lyase; C4H, cinnamate 4-hydroxylase; 4CL, 4-coumarate CoA ligase; CHS, chalcone synthase; CHI, chalcone isomerase; F3H, flavanone 3-hydroxylase; F3'H, flavonoid 3'-hydroxylase; F3'5'H, flavonoid 3',5'-hydroxylase; DFR, dihydroflavonol 4-reductase; LAR, leucoanthocyanidin reductase; ANS, anthocyanidin synthase; 3GT, 3-O-glucosyltransferase; ANR, anthocyanidin reductase; MT, methyltransferase. The Blue dotted arrow indicates the transport of an unknown FR compound. Images of the flammability test of brown and white cotton fabrics were adopted from the report (Hinchliffe et al., 2016). Brown arrows indicate the activation of LAR and ANR by the TT2-TT8 complex reported by (Yan et al., 2018). Purple arrows indicate activation of ANS and 3GT by Re-TT8 complex reported by (Wang et al., 2022).

naringenin, generating dihydrokaempferol, dihydroquercetin, or dihydromyricetin. Dihydroflavonol 4-reductase (DFR) reduces the carbonyl group at the C4 position to a hydroxyl group, producing leucoanthocyanidins (Figure 2). Leucoanthocyanidins are converted into flavan-3-ols in two ways: 1) LAR catalases the reductive removal of the hydroxyl at the C4 position producing 2,3-*trans* isoforms; 2) anthocyanidin synthase (ANS) catalases production of anthocyanidins, which are converted by ANR into 2,3-*cis* flavan-3-ol monomers (Xie et al., 2003). It has been demonstrated by *in vitro* enzyme assays and virus-induced gene silencing (VIGS) that the ANR pathway contributes to the biosynthesis of 2,3-*cis* flavan-3-ol in cotton (Zhu et al., 2015).

Transcriptomic and proteomic studies in cotton identified that a set of structural genes of the flavonoid pathway, including *PAL*, *C4H*, *4CL*, *CHS*, *CHI*, *F3H, F3'H*, *DFR*, *LAR*, *ANS*, *ANR*, were up-regulated in brown fibers (Li et al., 2013; Feng et al., 2014; Xiao et al., 2014; Hinchliffe et al., 2016; Gao et al., 2019; Peng et al., 2020; Canavar and Rausher, 2021). Several structural genes of the flavonoid pathway were characterized in brown cotton. VIGS of *GhCHS2*, *GhLAR1*, and *GhANR* significantly reduced intensity of the color of brown fibers and anthocyanidin content (Gao et al., 2019). RNAi silencing of *GhCHI-1* in brown cotton resulted in three fiber phenotypes of transgenic plants: brown, almost white, and green (Liu et al., 2018). In transgenic lines with almost white fibers, the *GhCHI-1* and *GhCHI-2* were significantly suppressed, whereas in transgenic lines with brown and green fibers were not. Interestingly, an anthocyanidin 3-O-glucosyltransferase (*Gh3GT*) that glucosylates the 3-position of the flavonoid C-ring was significantly up-regulated in green fiber transgenic lines. Furthermore, it was confirmed that the overexpression of the *Gh3GT* or *At3GT* gene in brown cotton lines produced green fiber. The green color of fibers could be due to the increased amount of anthocyanidins caused by the upregulation of *Gh3GT* that redirected the flux toward anthocyanidins (Liu et al., 2018; Canavar and Rausher, 2021). RNAi suppression of *GhF3H* in white cotton significantly increased naringenin content and reduced the length and micronaire of mature fibers (Tan et al., 2013). The even greater negative effect of naringenin on fiber properties was observed in brown cotton with introduced RNAi *GhF3H* copy by a cross. However, the overexpression of the *GhF3H* caused no noticeable effects on fiber phenotype (Tan et al., 2013).

Three classes of proteins, including TT2 (MYB123), TT8 (bHLH42), and TTG1 (WD40 family), often referred to as MBW complex, are primary regulators of PA biosynthesis. Experimental studies showed that TT2 and TT8 activate PA pathway genes while TTG1 stabilizes the MBW complex and is essential in maintaining MBW activity genes (Baudry et al., 2004; Yu et al., 2023). Two TT2-type MYB transcription factors (*GhMYB36* and *GhMYB10*) isolated from cotton were able to activate promoters of LAR and ANR as well as recover the seed phenotype of *Arabidopsis tt2* mutant, confirming their role in PA biosynthesis (Lu et al., 2017). In cotton, genetic studies identified at least six incompletely dominant genetic loci (*Lc1* – *Lc6*) linked to brown fiber (Kohel, 1985). The *Lc1* was linked to a 1.4 Mb inversion on chromosome A07 upstream of a TT2 homologous gene (*Gh_A07G2341*), which this inversion could activate (Hinchliffe et al., 2016). A fine-mapping study determined that two QTLs in the *Lc1* locus regulate the shades of brown color in fibers. The *qBF-A07-1* (*Gh_A07G2341* - TT2) is responsible for the brown color, whereas interaction between the *qBF-A07-1* and *qBF-A07-2* (*Gh_A07G0100* - TTG1) regulates the shades of brown fiber (Wen et al., 2018). A genome-wide association study (GWAS) revealed that epistatic interaction between *qBF-A07-1* and *qBF-A07-2* negatively impacts fiber yield and quality traits (Wen et al., 2018).

Progress on research to enhance color diversity in NCC

The first report that inadvertently shifted the carbon flow from colorless PAs into colorful anthocyanidins in brown fibers was trying to suppress *GhCHI-1* (Liu et al., 2018). The transgenic line that failed to suppress the *GhCHI* produced green-colored cotton due to the activation of *Gh3GT*, further confirmed by transgenic overexpression of *Gh3GT* and *At3GT* in cotton. Whatever activated *3GT* in brown cotton during *CHI* suppression is unclear; nonetheless, Liu et al. (2018) showed an experimental enhancement of the anthocyanidin biosynthesis in NCC.

Another study has exploited color diversity in NCC by modulating the expression of transcription factors controlling anthocyanin biosynthesis genes. The transcription factor *GhMYB113* (*Re*), which regulates anthocyanin biosynthesis, has been overexpressed in cotton under fiber-specific promoter (Wang et al., 2022). A clear purple-red color was produced in developing fibers (5-10 DPA) of transgenic lines; however, the mature fiber turned brown. The anthocyanins content was high at 5-10 DPA and then gradually decreased, whereas PA content was low at 20 DPA and gradually increased at 25 DPA (Wang et al., 2022). The expression levels of *UFGT* (*3GT*) and *ANR* were elevated in transgenic lines. Authors suggested that anthocyanins accumulated during the early fiber developmental stage converted into PAs during the maturation and dehydration process (Wang et al., 2022).

How do we prevent the conversion of anthocyanins into PAs during the late stage of fiber development? One possible approach is activating anthocyanin biosynthesis during the later stage of fiber development, and a recent study demonstrated that it is feasible. The *GhTT2-3A* (*Gh_A07G2341)* was overexpressed under the secondary cell wall (SCW) specific promoter (*FbL2A*) in cotton; PA structural genes and PA biosynthesis were activated during the SCW stage in transgenic plants that resulted in brown mature fiber with lint percentage and fiber quality comparable to white fiber control (Yan et al., 2018). This study tried to reduce the adverse effects of pigment production on fiber cell development due to the known PA subunit's cellular toxicity and the inhibitory role of naringenin on fiber elongation (Tan et al., 2013; Dixon and Sarnala, 2020). Yan et al. (2018) achieved the goal of producing brown fiber with improved quality. They demonstrated that the SCW stage can be used for biotechnological manipulations of PAs and other flavonoids in cotton fiber.

Enhanced flame retardancy of NCC

What is causing the flame retardancy (FR) of NCC still remains unclear. Few studies have been published on NCC fabrics' thermal and burning behavior. The earlier work detected a higher value of limited oxygen index for brown than for white cotton fabric (Parmar and Chakraborty, 2001). The same study suggested that heavy metal ions and color compounds could be responsible for higher FR in brown cotton (Parmar and Chakraborty, 2001). Another study tested FR properties of needle-punched (NP) and hydroentangled (H-E) nonwoven fabrics produced from fibers of brown and white cotton (Hinchliffe et al., 2015). NP is a process for manufacturing nonwoven fabrics using barbed needles, whereas H-E is high-pressure water jets for interlocking fibers together. The NP fabrics showed significantly higher FR than H-E fabrics of brown cotton. The study suggested that the unknown FR component in the brown cotton fibers is water-soluble and was removed by water during the H-E process; the higher levels of phosphorous and boron in brown cotton corresponded with enhanced FR (Hinchliffe et al., 2015).

More recent studies suggested that PA biosynthesis plays a vital role in the natural FR of brown cotton (Figure 2). Nam et al. (2016) demonstrated by washing fibers in water and a low concentration of sodium hydroxide solution that the condensed tannins and higher sodium content in brown cotton are responsible for the FR property. Authors suggested that condensed tannins significantly enhanced the adsorption of sodium ions to the fiber, contributing to FR (Nam et al., 2016). Another study argued that condensed tannin is not the source of FR in brown cotton since enhanced FR and anthocyanin precursors appear in developing fibers well before the brown color is detectable (Hinchliffe et al., 2016). Authors suggested that enhanced FR can be developed in white cotton by activating biosynthesis of flavonoids or PA precursors but preventing PA polymerization (source of brown color); the unknown FR component is probably sequestered by PAs or PA precursors via metal-flavonoid complexes (Figure 2) (Hinchliffe et al., 2016). As proof of concept, the follow-up study found four recombinant inbred lines (RILs) with enhanced FR in the multi-parent advanced generation intercross (MAGIC) population (Thyssen et al., 2023). All four RILs have white cotton fibers and enhanced FR. Authors suggested that the accumulation of colorless flavonoids might contribute to FR in these RILs; however, metabolite analysis of developing fibers has yet to confirm this hypothesis (Thyssen et al., 2023). Identifying the natural FR compound from cotton could help minimize the use of synthetic FR additives in textiles.

Utilization of NCC

NCC has been cultivated and used for thousands of years; however, with the Industrial Revolution and the development of synthetic dyes, NCC varieties became less common as white cotton became the standard. Recently, interest in NCC has resurged due to its sustainability and environmental benefits since NCC cultivation is adaptable to dry land and organic farming (Günaydin et al., 2019; Rathinamoorthy and Parthiban, 2019). Organic NCC is softer, more breathable, and less likely to cause allergies than conventional cotton.

NCC is primarily used in high-end fashion, home textiles, upholstery fabrics, etc (Günaydin et al., 2019; Rathinamoorthy and Parthiban, 2019). The unique colors of NCC, ranging from light beige to red, rust, and brown, are highly sought by designers and consumers looking for sustainable and environmentally friendly products. These cotton varieties create a wide range of products, including clothing, bedding, and towels. Using NCC in these products adds a unique and natural element that is impossible with conventionally dyed cotton. One of the challenges of using NCC in textiles is its limited availability compared to conventional cotton. While there are efforts to increase the production of NCC, it remains a niche product in the textile industry. However, as consumer demand for sustainable and environmentally friendly products grows, the use of NCC will likely continue to increase.

Some NCC varieties possess flame-retardant properties which can be used in various applications. For example, flame-retardant textiles can be used as protective clothing for firefighters, gear for soldiers, automobile interiors, matrasses, house upholsteries, and drapes. Currently, cotton-based textiles are chemically modified to introduce multifunctional groups, making them flame-retardant. The most common method is to merge N, S, P, and Si-based polymeric, non-polymeric, polymeric/non-polymeric hybrids, inorganic, and organic/inorganic hybrids with cellulose to fabricate flame-retardant cotton textiles (Islam and van de Ven, 2021). As an eco-friendlier approach, biomass tannin and phytic acid are applied to the cotton fabric surface as a flame-retardant modification (Nam et al., 2017; Yang et al., 2023). Researchers at the U.S. Department of Agriculture's Agricultural Research Service have recently reported studies on the FR properties of brown and four white cotton lines (Hinchliffe et al., 2015, 2016; Thyssen et al., 2023). These lines reduce the need for flame-retardant chemicals embedded in consumer products. These advancements demonstrate the potential of naturally colored cotton in creating safer and more sustainable textiles.

Concluding remarks

The biosynthesis of PAs in brown cotton has been well characterized through transgenic analysis of structural flavonoid genes. However, little is known about how PA units are modified and transported into the vacuole and how PAs are polymerized. It has been experimentally demonstrated that the SCW biosynthesis stage of fiber development is the most suitable time for biotechnological modification of the flavonoid pathway. The anthocyanin pathway can be induced in cotton fibers by overexpressing *Re* (*GhMYB113*). In future studies, it would be interesting to overexpress *Re* and anthocyanidin modifiers during the SCW stage of fiber development to see the effects on the color of fibers. The FR has been detected in brown and white cotton fibers. The FR compound, which is yet to be identified, could be an eco-friendly alternative to synthetic FR additives in textiles. The utilization of NCC remains a niche in the textile industry.

However, usage of NCC will likely continue to increase as consumer demand for sustainable and environmentally friendly products grows.

Author contributions

MN: Writing – original draft; Writing – review & editing. DH: Writing – review & editing. GT: Writing – review & editing.

Funding

The author(s) declare that financial support was received for the research, authorship, and/or publication of this article. The United States Department of Agriculture, Agricultural Research Service financially supported the research (CRIS project 6054-21000-019-00D). The mention of trade names or commercial products is solely for the purpose of providing specific information and does not imply recommendation or endorsement by USDA. USDA is an equal opportunity provider and employer.

Conflict of interest

The authors declare that the research was conducted in the absence of any commercial or financial relationships that could be construed as a potential conflict of interest.

Publisher's note

All claims expressed in this article are solely those of the authors and do not necessarily represent those of their affiliated organizations, or those of the publisher, the editors and the reviewers. Any product that may be evaluated in this article, or claim that may be made by its manufacturer, is not guaranteed or endorsed by the publisher.

References

Baudry, A., Heim, M. A., Dubreucq, B., Caboche, M., Weisshaar, B., and Lepiniec, L. (2004). TT2, TT8, and TTG1 synergistically specify the expression of BANYULS and proanthocyanidin biosynthesis in Arabidopsis thaliana. *Plant J.* 39, 366–380. doi: 10.1111/j.1365-313X.2004.02138.x

Canavar, Ö., and Rausher, M. D. (2021). Molecular analysis of structural genes involved in flavonoids biosynthesis in naturally colored cotton. *Crop Sci.* 61, 1117–1126. doi: 10.1002/csc2.20410

Dixon, R. A., and Sarnala, S. (2020). Proanthocyanidin biosynthesis-a matter of protection. *Plant Physiol.* 184, 579–591. doi: 10.1104/pp.20.00973

Dixon, R. A., Xie, D.-Y., and Sharma, S. B. (2005). Proanthocyanidins: A final frontier in flavonoid research? *New Phytol.* 165, 9–28. doi: 10.11 1 1 /j.1469-8137.2004.012

Dutt, Y., Wang, X. D., Zhu, Y. G., and Li, Y. Y. (2004). Breeding for high yield and fiber quality in colored cotton. *Plant Breed.* 123, 145–151. doi: 10.1046/j.1439-0523.2003.00938.x

Feng, H., Li, Y., Wang, S., Zhang, L., Liu, Y., Xue, F., et al. (2014). Molecular analysis of proanthocyanidins related to pigmentation in brown cotton fiber (Gossypium hirsutum L.). *J. Exp. Bot.* 65, 5759–5769. doi: 10.1093/jxb/eru286

Funk, P., and Gamble, G. R. (2009). Fiber properties of saw and roller ginned naturally colored cottons. *J. Cotton. Sci.* 13, 166–173.

Gao, J., Shen, L., Yuan, J., Zheng, H., Su, Q., Yang, W., et al. (2019). Functional analysis of GhCHS, GhANR and GhLAR in colored fiber formation of Gossypium hirsutum L. *BMC Plant Biol.* 19, 1–18. doi: 10.1186/s12870-019-2065-7

Günaydin, G. K., Avinc, O., Palamutcu, S., Yavas, A., and Soydan, A. S. (2019). "Naturally colored organic Cotton and Naturally Colored Cotton Fiber Production," in *Organic Cotton: Is it a Sustainable Solution*? Eds. M. A. Gardetti and S. S. Muthu (Springer Singapore, Singapore), 81–99.

Hinchliffe, D., Condon, B., Delhom, C. D., Chang, S., Montalvo, J., Madison, C., et al. (2015). Physical and combustion properties of nonwoven fabrics produced from conventional and naturally colored cottons. *Textile. Res. J.* 85, 1666–1680. doi: 10.1177/0040517515573410

Hinchliffe, D. J., Condon, B. D., Thyssen, G., Naoumkina, M., Madison, C. A., Reynolds, M., et al. (2016). The GhTT2_A07 gene is linked to the brown color and natural flame retardancy phenotypes of Lc1 cotton (Gossypium hirsutum L.) fibers. *J. Exp. Bot.* 67, 5461–5471. doi: 10.1093/jxb/erw312

Islam, M. S., and van de Ven, T. G. M. (2021). Cotton-based flame-retardant textiles: A review. *BioResources* 16, 4354–4381.

Kohel, R. J. (1985). Genetic analysis of fiber color variants in cotton1. *Crop Sci.* 25, cropsci1985.0011183X0025000500017x. doi: 10.2135/cropsci1985.0011183X0025000500017x

Li, T., Fan, H., Li, Z., Wei, J., Lin, Y., and Cai, Y. (2012). The accumulation of pigment in fiber related to proanthocyanidins synthesis for brown cotton. *Acta Physiol. Plant.* 34, 813–818. doi: 10.1007/s11738-011-0858-x

Li, Y.-J., Zhang, X.-Y., Wang, F.-X., Yang, C.-L., Liu, F., Xia, G.-X., et al. (2013). A comparative proteomic analysis provides insights into pigment biosynthesis in brown color fiber. *J. Proteomics* 78, 374–388. doi: 10.1016/j.jprot.2012.10.005

Liu, H.-F., Luo, C., Song, W., Shen, H., Li, G., He, Z.-G., et al. (2018). Flavonoid biosynthesis controls fiber color in naturally colored cotton. *PeerJ* 6, e4537. doi: 10.7717/peerj.4537

Lu, N., Roldan, M., and Dixon, R. A. (2017). Characterization of two TT2-type MYB transcription factors regulating proanthocyanidin biosynthesis in tetraploid cotton, Gossypium hirsutum. *Planta* 246, 323–335. doi: 10.1007/s00425-017-2682-z

May, O. L., Green, C. C., Roach, S. H., and Kittrell, B. U. (1994). Registration of PD 93001, PD 93002, PD 93003, and PD 93004 germplasm lines of upland cotton with brown lint and high fiber quality. *Crop Sci.* 34, 542–542.

Nam, S., Condon, B. D., Xia, Z., Nagarajan, R., Hinchliffe, D. J., and Madison, C. A. (2017). Intumescent flame-retardant cotton produced by tannic acid and sodium hydroxide. *J. Analytical. Appl. Pyrolysis.* 126, 239–246. doi: 10.1016/j.jaap.2017.06.003

Nam, S., Kim, H. J., Condon, B. D., Hinchliffe, D. J., Chang, S., McCarty, J. C., et al. (2016). High resistance to thermal decomposition in brown cotton is linked to tannins and sodium content. *Cellulose* 23, 1137–1152. doi: 10.1007/s10570-016-0871-8

Nimon, W., and Beghin, J. (1999). Are eco-labels valuable? Evidence from the apparel industry. *Am. J. Agric. Econ.* 81, 801–811. doi: 10.2307/1244325

Parmar, M. S., and Chakraborty, M. (2001). Thermal and burning behavior of naturally colored cotton. *Textile. Res. J.* 71, 1099–1102. doi: 10.1177/004051750107101211

Peng, Z., Gao, Q., Luo, C., Gong, W., Tang, S., Zhang, X., et al. (2020). Flavonoid biosynthetic and starch and sucrose metabolic pathways are involved in the pigmentation of naturally brown-colored cotton fibers. *Ind. Crops Products.* 158, 113045. doi: 10.1016/j.indcrop.2020.113045

Rathinamoorthy, R., and Parthiban, M. (2019). "Colored Cotton: Novel Eco-friendly Textile Material for the Future," in *Handbook of Ecomaterials*. Eds. L. M. T. Martínez, O. V. Kharissova and B. I. Kharisov (Springer International Publishing, Cham), 1499–1519.

Sun, J., Sun, Y., and Zhu, Q.-H. (2021). Breeding next-generation naturally colored cotton. *Trends Plant Sci.* 26, 539–542. doi: 10.1016/j.tplants.2021.03.007

Tan, J., Tu, L., Deng, F., Hu, H., Nie, Y., and Zhang, X. (2013). A genetic and metabolic analysis revealed that cotton fiber cell development was retarded by flavonoid naringenin. *Plant Physiol.* 162, 86–95. doi: 10.1104/pp.112.212142

Thyssen, G. N., Condon, B. D., Hinchliffe, D. J., Zeng, L., Naoumkina, M., Jenkins, J. N., et al. (2023). Flame resistant cotton lines generated by synergistic epistasis in a MAGIC population. *PloS One* 18, e0278696. doi: 10.1371/journal.pone.0278696

Wang, N., Zhang, B., Yao, T., Shen, C., Wen, T., Zhang, R., et al. (2022). Re enhances anthocyanin and proanthocyanidin accumulation to produce red foliated cotton and brown fiber. *Plant Physiol.* 189, 1466–1481. doi: 10.1093/plphys/kiac118

Wen, T., Wu, M., Shen, C., Gao, B., Zhu, D., Zhang, X., et al. (2018). Linkage and association mapping reveals the genetic basis of brown fiber (Gossypium hirsutum). *Plant Biotechnol. J.* 16, 1654–1666. doi: 10.1111/pbi.12902

Xiao, Y.-H., Yan, Q., Ding, H., Luo, M., Hou, L., Zhang, M., et al. (2014). Transcriptome and biochemical analyses revealed a detailed proanthocyanidin biosynthesis pathway in brown cotton fiber. *PloS One* 9, e86344. doi: 10.1371/journal.pone.0086344

Xiao, Y.-H., Zhang, Z.-S., Yin, M.-H., Luo, M., Li, X.-B., Hou, L., et al. (2007). Cotton flavonoid structural genes related to the pigmentation in brown fibers. *Biochem. Biophys. Res. Commun.* 358, 73–78. doi: 10.1016/j.bbrc.2007.04.084

Xie, D.-Y., and Dixon, R. A. (2005). Proanthocyanidin biosynthesis – still more questions than answers? *Phytochemistry* 66, 2127–2144. doi: 10.1016/j.phytochem.2005.01.008

Xie, D. Y., Sharma, S. B., and Dixon, R. A. (2004). Anthocyanidin reductases from Medicago truncatula and Arabidopsis thaliana. *Arch. Biochem. Biophys.* 422, 91–102. doi: 10.1016/j.abb.2003.12.011

Xie, D.-Y., Sharma, S. B., Paiva, N. L., Ferreira, D., and Dixon, R. A. (2003). Role of anthocyanidin reductase, encoded by *BANYULS* in plant flavonoid biosynthesis. *Science* 299, 396–399. doi: 10.1126/science.1078540

Yan, Q., Wang, Y., Li, Q., Zhang, Z., Ding, H., Zhang, Y., et al. (2018). Up-regulation of Gh TT 2-3A in cotton fibers during secondary wall thickening results in brown fibers with improved quality. *Plant Biotechnol. J.* 16, 1735–1747. doi: 10.1111/pbi.12910

Yang, M., Yang, Y., Shi, J., and Rao, W. (2023). Fabrication of eco-friendly flame-retardant and hydrophobic coating for cotton fabric. *Cellulose* 30, 3267–3280. doi: 10.1007/s10570-023-05051-9

Yu, K., Song, Y., Lin, J., and Dixon, R. A. (2023). The complexities of proanthocyanidin biosynthesis and its regulation in plants. *Plant Commun.* 4, 100498. doi: 10.1016/j.xplc.2022.100498

Yuan, S. N., Malik, W., Bibi, N., Wen, G. J., Ni, M., and Wang, X. D. (2013). Modulation of morphological and biochemical traits using heterosis breeding in colored cotton. *J. Agric. Sci.* 151, 57–71. doi: 10.1017/S0021859612000172

Zhu, Y., Wang, H., Peng, Q., Tang, Y., Xia, G., Wu, J., et al. (2015). Functional characterization of an anthocyanidin reductase gene from the fibers of upland cotton (Gossypium hirsutum). *Planta* 241, 1075–1089. doi: 10.1007/s00425-014-2238-4

frontiers | Frontiers in Plant Science

TYPE Mini Review
PUBLISHED 26 March 2024
DOI 10.3389/fpls.2024.1373975

OPEN ACCESS

EDITED BY
Deyu Xie,
North Carolina State University, United States

REVIEWED BY
Valentina Passeri,
National Research Council (CNR), Italy
Boas Pucker,
Technical University of Braunschweig, Germany
Yue Zhu,
North Carolina State University, United States

*CORRESPONDENCE
Nan Lu
Nan.Lu@unt.edu

RECEIVED 21 January 2024
ACCEPTED 18 March 2024
PUBLISHED 26 March 2024

CITATION
Lu N (2024) Revisiting decade-old questions in proanthocyanidin biosynthesis: current understanding and new challenges.
Front. Plant Sci. 15:1373975.
doi: 10.3389/fpls.2024.1373975

Revisiting decade-old questions in proanthocyanidin biosynthesis: current understanding and new challenges

Nan Lu*

BioDiscovery Institute and Department of Biological Sciences, University of North Texas, Denton, TX, United States

Proanthocyanidins (PAs), one of the most abundant natural polymers found in plants, are gaining increasing attention because of their beneficial effects for agriculture and human health. The study of PA biosynthesis has been active for decades, and progress has been drastically accelerated since the discovery of key enzymes such as Anthocyanidin Reductase (ANR), Leucoanthocyanidin Reductase (LAR), and key transcription factors such as Transparent Testa 2 (TT2) and Transparent Testa 8 (TT8) in the early 2000s. Scientists raised some compelling questions regarding PA biosynthesis about two decades ago in the hope that addressing these questions would lead to an enhanced understanding of PA biosynthesis in plants. These questions focus on the nature of starter and extension units for PA biosynthesis, the stereochemistry of PA monomers and intermediates, and how and where the polymerization or condensation steps work subcellularly. Here, I revisit these long-standing questions and provide an update on progress made toward answering them. Because of advanced technologies in genomics, bioinformatics and metabolomics, we now have a much-improved understanding of functionalities of key enzymes and identities of key intermediates in the PA biosynthesis and polymerization pathway. Still, several questions, particularly the ones related to intracellular PA transportation and deposition, as well as enzyme subcellular localization, largely remain to be explored. Our increasing understanding of PA biosynthesis in various plant species has led to a new set of compelling open questions, suggesting future research directions to gain a more comprehensive understanding of PA biosynthesis.

KEYWORDS

proanthocyanidins, condensed tannins, anthocyanin, anthocyanidin reductase, leucocyanidin reductase

1 Introduction

Proanthocyanidins (PAs), or condensed tannins (CTs), are oligomers of flavan 3-ols naturally produced in plants. Like other polyphenols, PAs have shown promise of health benefits because of their antioxidant activity. PAs, in particular, are believed to have antidiabetic and anticancer functions and have beneficial effects in preventing cardiovascular disease and reducing inflammation (Cos et al., 2004). Many plant-based foods and drinks, such as rice, sorghum, soybean, persimmon, grapes, tea and fruit juice, are rich in PAs, making plants an important dietary source of PAs for humans (Bhagwat and Haytowitz, 2015). PAs, while mostly accumulated in seed coats, are found in almost all tissues, including flowers, leaves, stems and roots, where they play a pivotal role in protecting plants from UV damage, abiotic stresses, as well as pest and fungal attack (Dixon and Sarnala, 2020; Figure 1). In agriculture, animal feeds are often supplemented with PAs to reduce ruminal bloat, a lethal and costly disease, and to decrease methane emissions from ruminants, a contributing factor to global warming (Waghorn, 2008; Jonker and Yu, 2016).

The beneficial effects of PAs in human and animal health, as well as their role in plant stress responses, have made decoding the PA biosynthesis pathways a research area of interest. Initial progress was made mainly by characterizing mutants with disrupted PA accumulation in PA-rich plants such as barley (*Hordeum vulgare*) and *Arabidopsis thaliana*. The first breakthrough discovery came when Anthocyanidin Reductase (ANR), the enzyme that converts anthocyanidins to flavan 3-ols, was identified and characterized by Xie et al. (2003) in Arabidopsis, which specified the PA-specific branch in the general flavonoid biosynthesis pathway. Shortly after, two review papers (Dixon et al., 2005; Xie and Dixon, 2005) raised a series of open questions that were critical for advancing our understanding of PA biosynthesis. These questions range from functions of some key enzymes in the pathway to the stereochemistry of PA precursors, as well as how and where PAs are transported.

Now, almost two decades since these PA review papers were published, I revisit the original questions, summarize major advances made since then, and come up with a new set of compelling questions, hoping to shed light on future studies toward a better understanding of the regulation and mechanism of PA biosynthesis in plants.

2 Milestones in understanding PA biosynthesis

2.1 The extended functions of key enzymes in PA biosynthesis in diverse plant species

In PA-rich plant species, ANR is fundamental in making the building blocks (i.e., flavan 3-ols) for PA biosynthesis (Figure 1). Loss of activity of ANR results in loss of PAs and increase of anthocyanins in Arabidopsis, *Medicago truncatula*, cotton (*Gossypium hirsutum*) and soybean (*Glycine max*) (Xie et al., 2003; Kovinich et al., 2012; Zhu et al., 2015). Further studies of PA biosynthesis demonstrated that the starter and extension units for PA polymerization are actually generated by two parallel

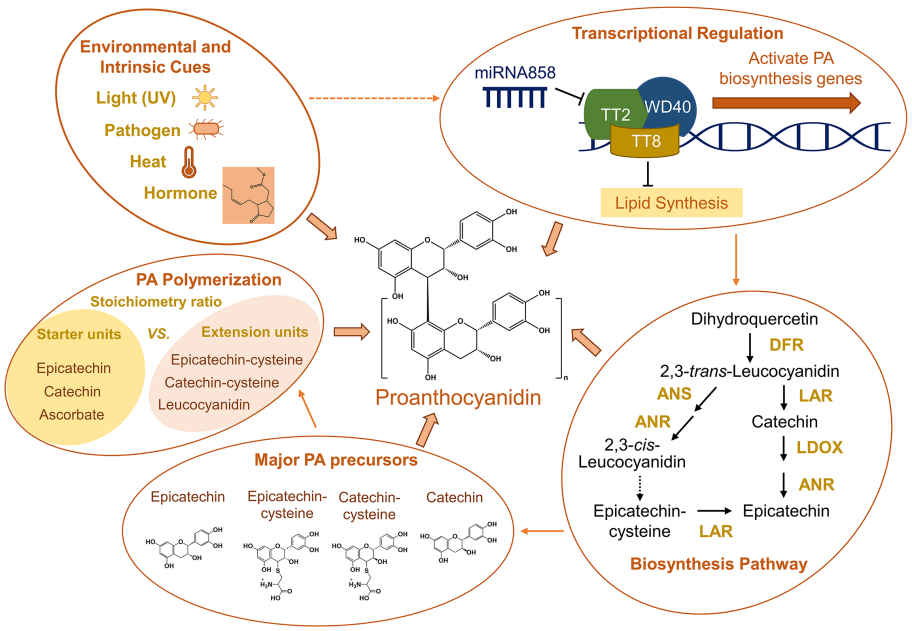

FIGURE 1
Summary of environmental and intrinsic cues for PA biosynthesis, transcriptional regulation of PA biosynthesis, simplified conventional PA biosynthesis pathway based on studies in Medicago, major PA precursors, and factors affecting PA polymerization. Arrows between groups indicate cause-and-effect relationships. Dashed arrows between groups and in the PA biosynthesis pathway indicate processes that remain unclear. The hormone structure in the "Environmental and Intrinsic Cues" group represents methyl jasmonate. ANR, anthocyanidin reductase; ANS, anthocyanidin synthase; DFR, dihydroflavonol-4-reductase; LAR, leucoanthocyanidin reductase; LDOX, leucoanthocyanidin dioxygenase.

pathways, both of which require the participation of ANR (Jun et al., 2021). In Medicago, the branch leading to epicatechin starter units also involves Leucoanthocyanidin Reductase (LAR) and Leucoanthocyanidin Dioxygenase (LDOX), while the other branch leading to PA extension units requires Anthocyanidin Synthase (ANS) (Jun et al., 2018; Figure 1). Intriguingly, many plant species, such as Arabidopsis, seem to only have ANS or LDOX (i.e. LAR is not present), suggesting the complexity and diversity of the PA biosynthesis pathway in various plant species.

In wheat (*Triticum aestivum*) and maize (*Zea mays*), two species that do not accumulate PAs, ANRs preferably produce (+)-epicatechin rather than the (-)-epicatechin stereoisomer commonly found in PA-rich plants, suggesting that ANRs in wheat and maize may have evolved distinct functions and may contribute to the lack of PA oligomers in these two species (Jun et al., 2021; Lu et al., 2023).

As mentioned before, one of the key enzymes at the branch point of PA biosynthesis is LAR, which was initially known for catalyzing the synthesis of catechin, a starter unit for PA polymerization (Bogs et al., 2005). A decade later, a study of PA biosynthesis in Medicago suggested a role of LAR in balancing the ratio of PA starter and extension units (Liu et al., 2016; Figure 1). Loss of LAR activity in Medicago seeds led to significantly increased levels of insoluble (highly polymerized) PAs and reduced levels of soluble PAs, indicating that the LAR-dependent ratio of starter and extension units is a crucial factor for determining the degree of PA polymerization. However, as mentioned above, there is no evidence so far suggesting the existence of any LAR-like enzymes in some PA-rich plant species like Arabidopsis, raising the question of how PA chain length is controlled in these species.

2.2 Identification of key intermediates in PA biosynthesis

Identification and characterization of intermediates in the biosynthesis of PA monomers has been a focal point of research interest, as the reaction intermediates are key to understanding the mechanistic details of PA biosynthesis. While much effort has been made to search for intermediates in PA biosynthesis, only a few compounds, such as 4β-(S-cysteinyl)-epicatechin and 2,3-*cis*-leucocyanidin, have been identified so far as possible intermediates in PA monomer biosynthesis and PA polymerization (Liu et al., 2016; Wang et al., 2020; Jun et al., 2021; Yu et al., 2022; Figure 1). Identifying intermediates in PA biosynthesis reactions can be challenging, because of the instability of flavonoid carbocations. Thus, developing new approaches that can effectively "capture" these compounds will be key to elucidating the mechanisms of PA biosynthesis in plants.

2.3 The role of TT19 (AtGSTF12) beyond anthocyanin deposition

While TT19 has long been considered involved in both anthocyanin and PA biosynthesis, the exact function of TT19 beyond the role in anthocyanin deposition has been a mystery ever since its homologous genes were first discovered in maize (McLaughlin and Walbot, 1987) and petunia (Alfenito et al., 1998). It was proposed the oxidized anthocyanins were the reason for the bronze phenotype in maize seeds (Marrs et al., 1995). In Arabidopsis *tt19* mutant, besides the loss of anthocyanins in the stem tissue, its seeds show small vacuoles, and the mechanism causing this phenotype is not clear (Kitamura et al., 2010). In the last few years, progresses have been achieved in understanding the role of TT19 in PA biosynthesis. Loss of TT19 activity in Arabidopsis seeds leads to significant reduction of PA starter units (i.e., epicatechin), but not PA extension units (i.e., epicatechin-cysteine), which consequently results in disrupted ratio of soluble and insoluble PAs (Lu et al., 2022). Another study suggests that TT19-like enzymes possess catalytic functions *in vitro* (Eichenberger et al., 2023). It will be interesting to further investigate how this new role helps explain the TT19 function in PA biosynthesis, and how this mechanism is correlated with the altered vacuole phenotype in the *tt19* mutant.

2.4 Engineering PAs in crops

The beneficial effects of PAs in health and agriculture have attracted increasing attention of plant scientists to engineering PAs in crops. As more regulatory factors and key enzymes of the PA biosynthesis pathway are identified and characterized, a number of strategies have been developed to engineer economic crops for enhanced PA production. The most straightforward approach to increase PA production is manipulating master transcription factors regulating the expression of PA biosynthesis genes. Similar to the regulatory machinery controlling anthocyanin biosynthesis, a conserved complex involving multiple classes (MYB, bHLH, WD40 etc.) of transcription factors activates PA biosynthesis genes and initiates PA biosynthesis by binding to promoters of genes in both early and late stages of the pathway (Figure 1). Besides, WRKY family of TFs have been shown to involve in the transport of PAs in Arabidopsis and grape (Gonzalez et al., 2016; Amato et al., 2017). Other transcriptional activators and repressors can influence the stability of the complex or its ability to bind on promoters, determining when and where PAs are synthesized in plants (Jun et al., 2015).

Ectopic expression of TaMYB14-1, a TT2-type transcription factor from *Trifolium arvense* (Hancock et al., 2012), in white clover (*Trifolium repens*) significantly improved the level of soluble PAs to over 2% of dry matter, and the PAs in white clover leaves were able to bind to forage proteins and reduce ammonia and methane emissions (Roldan et al., 2022). Cotton plants over-expressing *GhTT2L-3A* produced brown-colored fibers accumulating substantial amounts of PAs, and the fiber quality was also improved in transgenic plants compared to wild-type control plants (Yan et al., 2018). Given that the increased accumulation of PAs in some tissues may cause negative effects on plant growth and development, new approaches using tissue-specific promotors have been proposed for precisely controlled accumulation of PAs (Cui et al., 2022). These achievements in engineering PAs will likely

inspire future studies to develop novel strategies for improving PA production in other economically useful crops.

3 Rising questions to be addressed and future perspectives

3.1 What is the next model species for studying PA biosynthesis?

Arabidopsis and Medicago have long been used as model species to study anthocyanin and PA biosynthesis. This was driven by the early release of their genomes, the generation of tens-of-thousands of mutants, and the easy-to-observe PA phenotype since the wild-type plants naturally accumulate colored PAs in seeds. However, it has come to our attention that there is no one-model-fits-all for PA biosynthesis. Getting knowledge from more species is key to better understanding the "core" enzymes and the "expendable" enzymes in the pathway. With more genomes becoming available on a monthly basis and the transformation efficiency dramatically increasing with new technology emerging, the pool for finding the next model plant species is getting larger. As previously mentioned by Dixon and Sarnala (2020), poplar (*Populus tremula*) is one good candidate model species, because, among other reasons listed, PAs naturally accumulate in various tissues rather than being limited in seeds. Another candidate would be cotton, which is an economically important crop worldwide. Similar to poplar, cotton accumulates PAs in various tissues, including seeds, fibers, leaves, and stems (Lu et al., 2017). In addition, a highly efficient Virus-Induced-Gene-Silencing (VIGS) system makes it easy to test the function of PA-related genes in a timely manner (Zhu et al., 2015). These technologies could also apply to major fruit crops with PA and/or anthocyanin presence such as strawberry and grape (Xie et al., 2020; Yang et al., 2022).

In contrast to the extensively studied PA biosynthesis in dicots, details about the PA biosynthesis pathway and its regulatory mechanism in monocots remain largely unknown with only a few candidate genes identified so far. In rice (*Oryza sativa*), *Rc* and *Rd* were identified as genes encoding a bHLH-type transcription factor and a dihydroflavonol-4-reductase (DFR), respectively (Furukawa et al., 2007). The *tannin1* locus in sorghum encodes a WD40 protein that belongs to the transcription factor ternary complex necessary for activating PA biosynthesis in sorghum (Wu et al., 2012). In barley (*Hordeum vulgare*), the *ant13*, *ant17* and *ant18* loci encode WD40, flavanone 3-hydroxylase (F3H), and DFR, respectively (Olsen et al., 1993; Himi and Taketa, 2015; Shoeva et al., 2023). Notably, those genes identified from mutants with significant PA deficiency phenotypes are either major transcriptional regulators or enzymes at relatively early steps of the PA biosynthetic pathway. Despite these discoveries, the lack of an accessible and saturated mutant pool is still the bottleneck for studying PA biosynthesis in monocots. A recent release of an ethyl methane sulfonate (EMS)-induced sorghum mutant library (Jiao et al., 2023) offers another promising opportunity for studying PA biosynthesis and regulation in monocots.

3.2 Will PAs exist in other non-traditional forms?

Because of the reactive nature of the PA precursors, it is not surprising that PAs exist in various forms of oligomers and conjugates. In maize, some purple-colored seeds accumulate anthocyanin-catechin conjugates (Lu et al., 2023). In Arabidopsis *ans* mutant seeds, *trans*-leucocyanidin, as extension units, attacks ascorbate to form catechin-ascorbate oligomers (Yu et al., 2022). Recently, a new form of PA-like oligomers involving flavan 3-ols, named papanridin, was discovered by Zhu et al. (2023). It will be interesting to find out whether additional non-traditional PA-like oligomers or polymers exist in different plant species, and more importantly, to demonstrate the role of these compounds in plants and their beneficial bioactivities.

3.3 What determines the level of PA polymerization?

PA polymerization in Arabidopsis and Medicago is currently considered as a spontaneous process that does not require enzyme catalyzation. However, the level of PA polymerization can be affected by many factors, such as the stoichiometry of starter and extension units and the stereochemistry of PA monomers (Liu et al., 2016; Lu et al., 2023). It will be a necessary next step to learn how PA polymerization is determined and how to regulate the level of PA polymerization for different application purposes. Since the PA starter units and extension units are generated in two separate pathways, it would be interesting to know whether it is possible to manipulate enzymes in one branch of the pathway but not the other branch, and whether it is possible to control how and when extension units "find" starter units.

3.4 What are other factors affecting PA biosynthesis?

Some well-studied transcription factors (e.g., TT2, TTG1, TT8) can activate or repress the expression of PA-related genes and subsequently affect PA and/or anthocyanin biosynthesis (Lu et al., 2021). Are there other factors that can turn on or off these transcription factors? Recently, several microRNAs that target PA-related transcription factors or enzymes have been identified in grape berry (Vale et al., 2021), apple (*Malus domestica*) (Zhang et al., 2022), persimmon (Yang et al., 2020), kiwifruit (*Actinidia deliciosa*) (Wang et al., 2023) and cotton (Mei et al., 2023). Notably, the miR858 family members target TT2-type MYBs, a key activating regulator of PA biosynthesis functionally conserved in many plant species (Figure 1). The involvement of these small RNAs in PA biosynthesis opens a new avenue for PA engineering in crops.

Plant hormones participate in almost all aspects of plant growth and development, but whether or not they play a role in PA biosynthesis remain largely unknown. Recent studies indicated that plant hormones could affect PA biosynthesis. Applying methyl jasmonate induced PA accumulations in apple calli by influencing the interactions between Jasmonate ZIM-domain (MdJAZ) proteins and the MYB-bHLH-WD40 transcription factor complex that regulates PA biosynthesis (An et al., 2015; Figure 1). It will be interesting to find out whether and how other families of plant hormones might be involved in regulating PA accumulation in plants.

3.5 How is PA biosynthesis related to lipid metabolism?

TT8 has been known for its role in the transcriptional regulation of PA biosynthesis, as disruption of TT8 results in loss of PA in Arabidopsis seed coats (Nesi et al., 2000). A study of lipids in the Arabidopsis *tt8* mutant showed that the accumulation of fatty acids was significantly enhanced in *tt8* seeds, and further transcript analysis showed that TT8 might function as a repressor to down-regulate genes required for lipid biosynthesis (Chen et al., 2014; Figure 1). Later on, similar enhanced lipid accumulation phenotypes were observed in seeds of *Brassica napus* and tobacco (*Nicotiana tabacum*) when TT8-like genes were disrupted (Zhai et al., 2020; Tian et al., 2021). These findings suggest crosstalk between flavonoid biosynthesis and central metabolism pathways. Future studies of the crosstalk between PA and lipid biosynthesis may focus on deciphering the regulatory mechanism for maintaining the homeostasis of PAs and lipids, exploring its biological significance in plant growth and development, and developing new strategies for PA and lipid engineering in crops.

4 Concluding remarks

Unlike many other metabolite biosynthesis pathways that are conserved among plants, the pathways of PA biosynthesis are complex and divergent in different plant species. Substantial progresses have been made over the past two decades in advancing our understanding of the PA biosynthesis pathway, particularly in proposed diverse and expanded roles of key enzymes branching from anthocyanin pathway and in successful isolation of extension units for PA polymerization, but questions still need to be addressed to elucidate the mechanistical details of how PAs are synthesized, transported and regulated in various plant species. I envision that this will stimulate more studies and lead to new discoveries in this area.

Author contributions

NL: Writing – original draft, Writing – review & editing.

Funding

The author(s) declare financial support was received for the research, authorship, and/or publication of this article. The author's work is supported by grant from Grasslanz Technology Limited, Palmerston North, New Zealand to Richard A. Dixon.

Conflict of interest

The author declares that the research was conducted in the absence of any commercial or financial relationships that could be construed as a potential conflict of interest.

Publisher's note

References

Alfenito, M. R., Souer, E., Goodman, C. D., Buell, R., Mol, J., Koes, R., et al. (1998). Functional complementation of anthocyanin sequestration in the vacuole by widely divergent glutathione S-transferases. *Plant Cell.* 10, 1135–1149. doi: 10.1105/tpc.10.7.1135

Amato, A., Cavallini, E., Zenoni, S., Finezzo, L., Begheldo, M., Ruperti, B., et al. (2017). A grapevine TTG2-like WRKY transcription factor is involved in regulating vacuolar transport and flavonoid biosynthesis. *Front. Plant Sci.* 7, 1979. doi: 10.3389/fpls.2016.01979

An, X. H., Tian, Y., Chen, K. Q., Liu, X. J., Liu, D. D., Xie, X. B., et al. (2015). MdMYB9 and MdMYB11 are involved in the regulation of the JA-induced biosynthesis of anthocyanin and proanthocyanidin in apples. *Plant Cell Physiol.* 56, 650–662. doi: 10.1093/pcp/pcu205

Bhagwat, S., and Haytowitz, D. B. (2015). *USDA database for the proanthocyanidin content of selected foods, release 2* (Nutrient Data Laboratory, Beltsville Human Nutrition Research Center, ARS, USDA). doi: 10.15482/USDA.ADC/1324621

Bogs, J., Downey, M. O., Harvey, J. S., Ashton, A. R., Tanner, G. J., and Robinson, S. P. (2005). Proanthocyanidin synthesis and expression of genes encoding leucoanthocyanidin reductase and anthocyanidin reductase in developing grape berries and grapevine leaves. *Plant Physiol.* 139, 652–663. doi: 10.1104/pp.105.064238

Chen, M., Xuan, L., Wang, Z., Zhou, L., Li, Z., Du, X., et al. (2014). TRANSPARENT TESTA 8 inhibits seed fatty acid accumulation by targeting several seed development regulators in Arabidopsis. *Plant Physiol.* 165, 905–916. doi: 10.1104/pp.114.235507

Cos, P., De Bruyne, T., Hermans, N., Apers, S., Berghe, D. V., and Vlietinck, A. J. (2004). Proanthocyanidins in health care: current and new trends. *Curr. Med. Chem.* 11, 1345–1359. doi: 10.2174/0929867043365288

Cui, X., Jun, J. H., Rao, X., Bahr, C., Chapman, E., Temple, S., et al. (2022). Leaf layer-based transcriptome profiling for discovery of epidermal-selective promoters in *Medicago truncatula*. *Planta* 256, 31. doi: 10.1007/s00425-022-03920-4

Dixon, R. A., and Sarnala, S. (2020). Proanthocyanidin biosynthesis—a matter of protection. *Plant Physiol.* 184, 579–591. doi: 10.1104/pp.20.00973

Dixon, R. A., Xie, D. Y., and Sharma, S. B. (2005). Proanthocyanidins–a final frontier in flavonoid research? *New Phytol.* 165, 9–28. doi: 10.1111/j.1469-8137.2004.01217.x

Eichenberger, M., Schwander, T., Hüppi, S., Kreuzer, J., Mittl, P. R. E., Peccati, F., et al. (2023). The catalytic role of glutathione transferases in heterologous anthocyanin biosynthesis. *Nat. Catal.* 6, 927–938. doi: 10.1038/s41929-023-01018-y

Furukawa, T., Maekawa, M., Oki, T., Suda, I., Iida, S., Shimada, H., et al. (2007). The *Rc* and *Rd* genes are involved in proanthocyanidin synthesis in rice pericarp. *Plant J.* 49, 91–102. doi: 10.1111/j.1365-313X.2006.02958.x

Gonzalez, A., Brown, M., Hatlestad, G., Akhavan, N., Smith, T., Hembd, A., et al. (2016). TTG2 controls the developmental regulation of seed coat tannins in Arabidopsis by regulating vacuolar transport steps in the proanthocyanidin pathway. *Dev. Biol.* 419, 54–63. doi: 10.1016/j.ydbio.2016.03.031

Hancock, K. R., Collette, V., Fraser, K., Greig, M., Xue, H., Richardson, K., et al. (2012). Expression of the R2R3-MYB transcription factor TaMYB14 from *Trifolium arvense* activates proanthocyanidin biosynthesis in the legumes *Trifolium repens* and *Medicago sativa*. *Plant Physiol.* 159, 1204–1220. doi: 10.1104/pp.112.195420

Himi, E., and Taketa, S. (2015). Barley Ant17, encoding flavanone 3-hydroxylase (F3H), is a promising target locus for attaining anthocyanin/proanthocyanidin-free plants without pleiotropic reduction of grain dormancy. *Genome* 58, 43–53. doi: 10.1139/gen-2014-0189

Jiao, Y., Nigam, D., Barry, K., Daum, C., Yoshinaga, Y., Lipzen, A., et al. (2023). A large sequenced mutant library - valuable reverse genetic resource that covers 98% of sorghum genes. *Plant J.* 117 (5), 1543–1557. doi: 10.1111/tpj.16582

Jonker, A., and Yu, P. (2016). The role of proanthocyanidins complex in structure and nutrition interaction in alfalfa forage. *Int. J. Mol. Sci.* 17, 793. doi: 10.3390/ijms17050793

Jun, J. H., Liu, C., Xiao, X., and Dixon, R. A. (2015). The transcriptional repressor MYB2 regulates both spatial and temporal patterns of proanthocyanidin and anthocyanin pigmentation in *Medicago truncatula*. *Plant Cell* 27, 2860–2879. doi: 10.1105/tpc.15.00476

Jun, J. H., Lu, N., Docampo-Palacios, M., Wang, X., and Dixon, R. A. (2021). Dual activity of anthocyanidin reductase supports the dominant plant proanthocyanidin extension unit pathway. *Sci. Adv.* 7, eabg4682. doi: 10.1126/sciadv.abg4682

Jun, J. H., Xiao, X., Rao, X., and Dixon, R. A. (2018). Proanthocyanidin subunit composition determined by functionally diverged dioxygenases. *Nat. Plants* 4, 1034–1043. doi: 10.1038/s41477-018-0292-9

Kitamura, S., Matsuda, F., Tohge, T., Yonekura-Sakakibara, K., Yamazaki, M., Saito, K., et al. (2010). Metabolic profiling and cytological analysis of proanthocyanidins in immature seeds of *Arabidopsis thaliana* flavonoid accumulation mutants. *Plant J.* 62, 549–559. doi: 10.1111/tpj.2010.62.issue-4

Kovinich, N., Saleem, A., Arnason, J. T., and Miki, B. (2012). Identification of two anthocyanidin reductase genes and three red-brown soybean accessions with reduced anthocyanidin reductase 1 mRNA, activity, and seed coat proanthocyanidin amounts. *J. Agric. Food Chem.* 60, 574–584. doi: 10.1021/jf2033939

Liu, C., Wang, X., Shulaev, V., and Dixon, R. A. (2016). A role for leucoanthocyanidin reductase in the extension of proanthocyanidins. *Nat. Plants* 2, 16182. doi: 10.1038/nplants.2016.182

Lu, N., Jun, J. H., Li, Y., and Dixon, R. A. (2023). An unconventional proanthocyanidin pathway in maize. *Nat. Commun.* 14, 4349. doi: 10.1038/s41467-023-40014-5

Lu, N., Jun, J. H., Liu, C. G., and Dixon, R. A. (2022). The flexibility of proanthocyanidin biosynthesis in plants. *Plant Physiol.* 190, 202–205. doi: 10.1093/plphys/kiac274

Lu, N., Rao, X., Li, Y., Jun, J. H., and Dixon, R. A. (2021). Dissecting the transcriptional regulation of proanthocyanidin and anthocyanin biosynthesis in soybean (*Glycine max*). *Plant Biotech. J.* 19, 1429–1442. doi: 10.1111/pbi.13562

Lu, N., Roldan, M., and Dixon, R. A. (2017). Characterization of two TT2-type MYB transcription factors regulating proanthocyanidin biosynthesis in tetraploid cotton, *Gossypium hirsutum*. *Planta* 246, 323–335. doi: 10.1007/s00425-017-2682-z

Marrs, K. A., Alfenito, M. R., Lloyd, A. M., and Walbot, V. (1995). A glutathione S-transferase involved in vacuolar transfer encoded by the maize gene Bronze-2. *Nature* 375, 397–400. doi: 10.1038/375397a0

McLaughlin, M., and Walbot, V. (1987). Cloning of a mutable *bz2* allele of maize by transposon tagging and differential hybridization. *Genetics* 117, 771–776. doi: 10.1093/genetics/117.4.771

Mei, J., Niu, Q., Xu, K., Huang, Y., Bai, S., Zhu, J., et al. (2023). GhmiR858 inhibits the accumulation of proanthocyanidins by targeting *GhTT2L* in cotton (*Gossypium hirsutum*). *J. Agric. Food Chem.* 71, 15341–15351. doi: 10.1021/acs.jafc.3c03884

Nesi, N., Debeaujon, I., Jond, C., Pelletier, G., Caboche, M., and Lepiniec, L. (2000). The *TT8* gene encodes a basic helix-loop-helix domain protein required for expression of *DFR* and *BAN* genes in Arabidopsis siliques. *Plant Cell* 12, 1863–1878. doi: 10.1105/tpc.12.10.1863

Olsen, O., Wang, X., and von Wettstein, D. (1993). Sodium azide mutagenesis: preferential generation of A.T–>G.C transitions in the barley Ant18 gene. *Proc. Natl. Acad. Sci. U.S.A.* 90, 8043–8047. doi: 10.1073/pnas.90.17.8043

Roldan, M. B., Cousins, G., Muetzel, S., Zeller, W. E., Fraser, K., Salminen, J. P., et al. (2022). Condensed tannins in white clover (*Trifolium repens*) foliar tissues expressing the transcription factor TaMYB14-1 bind to forage protein and reduce ammonia and methane emissions in *vitro*. *Front. Plant Sci.* 12, 777354. doi: 10.3389/fpls.2021.777354

Shoeva, O. Y., Mukhanova, M. A., Zakhrabekova, S., and Hansson, M. (2023). Ant13 encodes regulatory factor WD40 controlling anthocyanin and proanthocyanidin synthesis in barley (*Hordeum vulgare* L.). *J. Agric. Food Chem.* 71, 6967–6977. doi: 10.1021/acs.jafc.2c09051

Tian, Y., Liu, X., Fan, C., Li, T., Qin, H., Li, X., et al. (2021). Enhancement of tobacco (*Nicotiana tabacum* L.) seed lipid content for biodiesel production by CRISPR-Cas9-mediated knockout of NtAn1. *Front. Plant Sci.* 11, 599474. doi: 10.3389/fpls.2020.599474

Vale, M., Rodrigues, J., Badim, H., Gerós, H., and Conde, A. (2021). Exogenous application of non-mature miRNA-encoded miPEP164c inhibits proanthocyanidin synthesis and stimulates anthocyanin accumulation in grape berry cells. *Front. Plant Sci.* 12, 706679. doi: 10.3389/fpls.2021.706679

Waghorn, G. (2008). Beneficial and detrimental effects of dietary condensed tannins for sustainable sheep and goat production—Progress and challenges. *Anim. Feed Sci. Technol.* 147, 116–139. doi: 10.1016/j.anifeedsci.2007.09.013

Wang, P., Liu, Y., Zhang, L., Wang, W., Hou, H., Zhao, Y., et al. (2020). Functional demonstration of plant flavonoid carbocations proposed to be involved in the biosynthesis of proanthocyanidins. *Plant J.* 101, 18–36. doi: 10.1111/tpj.14515

Wang, W. Q., Liu, X. F., Zhu, Y. J., Zhu, J. Z., Liu, C., Wang, Z. Y., et al. (2023). Identification of miRNA858 long-loop precursors in seed plants. *Plant Cell*, koad315. doi: 10.1093/plcell/koad315

Wu, Y., Li, X., Xiang, W., Zhu, C., Lin, Z., Wu, Y., et al. (2012). Presence of tannins in sorghum grains is conditioned by different natural alleles of *Tannin1*. *Proc. Natl. Acad. Sci. U.S.A.* 109, 10281–10286. doi: 10.1073/pnas.1201700109

Xie, D. Y., Sharma, S. B., Paiva, N. L., Ferreira, D., and Dixon, R. A. (2003). Role of anthocyanidin reductase, encoded by BANYULS in plant flavonoid biosynthesis. *Science* 299, 396–399. doi: 10.1126/science.1078540

Xie, D. Y., and Dixon, R. A. (2005). Proanthocyanidin biosynthesis–still more questions than answers? *Phytochemistry* 66, 2127–2144. doi: 10.1016/j.phytochem.2005.01.008

Xie, Y., Ma, Y., Bi, P., Wei, W., Liu, J., Hu, Y., et al. (2020). Transcription factor FvTCP9 promotes strawberry fruit ripening by regulating the biosynthesis of abscisic acid and anthocyanins. *Plant Physiol. Biochem.* 146, 374–383. doi: 10.1016/j.plaphy.2019.11.004

Yan, Q., Wang, Y., Li, Q., Zhang, Z., Ding, H., Zhang, Y., et al. (2018). Up-regulation of GhTT2-3A in cotton fibres during secondary wall thickening results in brown fibres with improved quality. *Plant Biotechnol. J.* 16, 1735–1747. doi: 10.1111/pbi.12910

Yang, B., Wei, Y., Liang, C., Guo, J., Niu, T., Zhang, P., et al. (2022). VvANR silencing promotes expression of VvANS and accumulation of anthocyanin in grape berries. *Protoplasma* 259, 743–753. doi: 10.1007/s00709-021-01698-y

Yang, S., Zhang, M., Xu, L., Luo, Z., and Zhang, Q. (2020). MiR858b Inhibits proanthocyanidin accumulation by the repression of *DkMYB19* and *DkMYB20* in persimmon. *Front. Plant Sci.* 11, 576378. doi: 10.3389/fpls.2020.576378

Yu, K., Dixon, R. A., and Duan, C. (2022). A role for ascorbate conjugates of (+)-catechin in proanthocyanidin polymerization. *Nat. Commun.* 13, 3425. doi: 10.1038/s41467-022-31153-2

Zhai, Y., Yu, K., Cai, S., Hu, L., Amoo, O., Xu, L., et al. (2020). Targeted mutagenesis of *BnTT8* homologs controls yellow seed coat development for effective oil production in *Brassica napus* L. *Plant Biotechnol. J.* 18, 1153–1168. doi: 10.1111/pbi.13281

Zhang, B., Yang, H. J., Qu, D., Zhu, Z. Z., Yang, Y. Z., and Zhao, Z. Y. (2022). The MdBBX22-miR858-MdMYB9/11/12 module regulates proanthocyanidin biosynthesis in apple peel. *Plant Biotechnol. J.* 20, 1683–1700. doi: 10.1111/pbi.13839

Zhu, Y., Wang, H., Peng, Q., Tang, Y., Xia, G., Wu, J., et al. (2015). Functional characterization of an anthocyanidin reductase gene from the fibers of upland cotton (*Gossypium hirsutum*). *Planta* 241, 1075–1089. doi: 10.1007/s00425-014-2238-4

Zhu, Y., Yuzuak, S., Sun, X., and Xie, D. Y. (2023). Identification and biosynthesis of plant papanridins, a group of novel oligomeric flavonoids. *Mol. Plant* 16, 1773–1793. doi: 10.1016/j.molp.2023.09.015

frontiers | Frontiers in Plant Science

TYPE Original Research
PUBLISHED 24 April 2024
DOI 10.3389/fpls.2024.1388549

OPEN ACCESS

EDITED BY
Deyu Xie,
North Carolina State University, United States

REVIEWED BY
Maarit Karonen,
University of Turku, Finland
Axel Schmidt,
Max Planck Institute for Chemical Ecology, Germany

*CORRESPONDENCE
C. Peter Constabel
cpc@uvic.ca

RECEIVED 20 February 2024
ACCEPTED 28 March 2024
PUBLISHED 24 April 2024

CITATION
Westley R, Ma D, Hawkins BJ and Constabel CP (2024) Tissue and cellular localization of condensed tannins in poplar roots and potential association with nitrogen uptake.
Front. Plant Sci. 15:1388549.
doi: 10.3389/fpls.2024.1388549

Tissue and cellular localization of condensed tannins in poplar roots and potential association with nitrogen uptake

Rebecca Westley, Dawei Ma, Barbara J. Hawkins and C. Peter Constabel*

Biology Department and Center for Forest Biology, University of Victoria, Victoria, BC, Canada

Condensed tannins are common in vegetative tissues of woody plants, including in roots. In hybrid poplar (*Populus tremula x alba;* also known as *P. x canescens*) CT assays indicated they were most concentrated in younger white roots and at the root tip. Furthermore, CT-specific staining of embedded tissue sections demonstrated accumulation in root cap cells and adjacent epidermal cells, as well as a more sporadic presence in cortex cells. In older, brown roots as well as roots with secondary growth (cork zone), CT concentration was significantly lower. The insoluble fraction of CTs was greatest in the cork zone. To determine if CT accumulation correlates with nutrient uptake in poplar roots, a microelectrode ion flux measurement (MIFE™) system was used to measure flux along the root axis. Greatest NH_4^+ uptake was measured near the root tip, but NO_3^- and Ca^{2+} did not vary along the root length. In agreement with earlier work, providing poplars with ample nitrogen led to higher accumulation of CTs across root zones. To test the functional importance of CTs in roots directly, CT-modified transgenic plants could be important tools.

KEYWORDS

***Populus*, proanthocyanidin, microelectrode ion flux measurement (MIFE), root cap, 4-dimethylaminocinnamaldehyde (DMACA), flavonoid**

1 Introduction

Condensed tannins, (CTs, syn. proanthocyanidins) are the most widely distributed specialized plant metabolites in the plant kingdom. While in herbaceous plants they are typically restricted to the seed coat and other specialized tissues, CTs are highly prevalent and widespread in trees and woody plants and accumulate in all tissues, including leaves, bark and roots. CTs are typically high-molecular weight polyphenols synthesized from a branch of the well-known flavonoid pathway and are biosynthetically related to the anthocyanins. They consist of polymerized chains of 2-30 or more flavan-3-ol monomers, most commonly catechin and epicatechin, but also including gallocatechin

and epigallocatechin (Barbehenn and Constabel, 2011). Like most other phenolic specialized metabolites, CTs are generally stored as soluble compounds in plant vacuoles. Nevertheless, depending on plant species and tissue, a significant fraction of CTs is not extractable and thus considered insoluble. It is assumed that CTs can become crosslinked to the cell wall or other structures, though mechanisms are unclear and exact structures are often undefined (Tarascou et al., 2010).

Condensed tannins can interact with diverse molecules via their numerous hydroxyl groups or via hydrophobic interactions of the phenolic rings (Quideau et al., 2011). This characteristic gives rise to the many potential molecular interactions of the CTs. Most commonly, they are known to bind proteins in solutions at neutral to low pH (Hagerman and Robbins, 1987; Barbehenn and Constabel, 2011). However, they can also bind to other polymers, including carbohydrate such as pectin, or chitin from fungal cell walls (Adamczyk et al., 2019). CTs also chelate positively charged ions including Fe^{2+} (Kimura and Wada, 1989; Elessawy et al., 2021) and Al^{3+} (Osawa et al., 2011; Schmidt et al., 2013). Furthermore, CTs have strong *in vitro* antioxidant capacity (Hagerman et al., 1998); by contrast under some conditions such as high pH, they can also act as pro-oxidants (Barbehenn and Constabel, 2011). Thus they have the potential for diverse biological effects (Constabel et al., 2014).

Leaf CTs are often believed to be general defenses against folivorous insect herbivores; however, for lepidopterans this is unlikely due to their high gut pH (Barbehenn and Constabel, 2011). Vertebrates and other animals with acidic guts can be negatively impacted by high concentrations of CTs, which bind and precipitate protein (Barbehenn and Constabel, 2011). CTs also have broad antimicrobial activity (Scalbert, 1991). *In planta*, this effect is demonstrated in experiments where high CT concentrations are associated with reduced disease intensity or infection (Ullah et al., 2017; Holeski et al., 2009). Other adaptive functions of CTs include their antioxidant capacity. We recently demonstrated their protective effects against oxidative stress in leaves caused by drought, UV-B, and herbicide exposure (Gourlay et al., 2022; Gourlay and Constabel, 2019).

The high CT content of woody plants also leads to CT accumulation in forest soils. Here they are known to modulate metabolic activities of soil microorganisms and alter the soil microbiome. This has direct impacts on nutrient cycling, and thus has important effects for forest carbon and nitrogen budgets (Hättenschwiler and Vitousek, 2000; Kraus et al., 2003; Coq et al., 2022). Recently, Adamczyk et al. (2019) demonstrated a role of tannins in stabilizing forest soil carbon by forming stable interactions with fungal necromass. Given the ecological dominance of forest ecosystems globally, the CTs are significant at the ecosystem scale (Whitham et al., 2006).

CTs are found in roots of many species of trees and woody plants (Endo et al., 2021), often at substantial concentration. For example, Dong et al. (2016) reported 6-16% CT content in a survey of roots of 15 Chinese temperate forest trees. Kraus et al. (2004) measured 1-3.2%DW in roots of ericaceous and coniferous shrubs and trees in the pygmy forest of coastal California. In *Populus tremuloides*, root CT concentration is reported between 1-5% DW depending on the study (Kosola et al., 2006; Stevens et al., 2014; Dettlaff et al., 2018). While the impacts of CTs when released into the soil have been well documented as outlined above, very little is known about functions of CTs within living roots and root systems. Similar to above-ground roles, CTs in roots may be important for defense against soil-borne pathogens and other microbes, or protect against herbivory. Furthermore, by virtue of their ability to chelate metal ions, in some species CTs are able to protect against toxicity from excess Al^{3+} (Osawa et al., 2011) or Fe^{2+} (Kimura and Wada, 1989) in the environment. It is also plausible that CTs can interact with nutrient cations, in particular NH_4^+, although this has not yet been investigated experimentally. Interestingly, low N availability has been observed to repress accumulation of CTs in a variety of species (Kraus et al., 2004; Stevens et al., 2014). These connections motivated us to investigate potential interactions of root CTs with nitrogen uptake.

Determining the distribution and localization of CTs in root tissues and cells is a critical first step for understanding potential functions of these compounds. Fine woody roots are typically composed of a white zone adjacent to the root tip, beyond which a brown zone as well as a cork zone can be distinguished (Peterson et al., 1999). The cork zone is formed by secondary growth, where the cortex is disrupted, and secondary xylem and a periderm are formed. The root tips and youngest regions of the root system are most active in water and mineral absorption (Hawkins et al., 2008), with older roots functioning in transport. Previous studies have localized CTs to various cell types of roots undergoing primary growth using 4-dimethylaminocinnamaldehyde (DMACA) staining (Kao et al., 2002; Hoffmann et al., 2012; Endo et al., 2021) and generally find CTs in root cap and epidermal cells near the root tips, with more sporadic localization in distal cortical cells.

Poplars, aspens, and cottonwoods (*Populus* spp., here collectively called poplars) are widely used for tree research, as they grow rapidly and can be clonally propagated. *Populus* has also become a molecular model system for tree molecular biology, genomics, and phenolic metabolism (Jansson and Douglas, 2007). Here, we systematically measured CT content, distribution and cellular localization along a developmental axis in hybrid *P. tremula x alba (syn. P. x canescens)* roots. In parallel, we measured NH_4^+, NO_3^- and the cation Ca^{2+} net flux along the root axis using a microelectrode ion flux measurement (MIFE™) system, which allowed us to test for a correlation of CTs with N uptake.

2 Materials and methods

2.1 Plant material and growth conditions

Populus tremula x *alba* (clone INRA 717-1B4) plants were propagated from ~1 cm cuttings of *in vitro* plantlets and grown in half-strength Murashige-Skoog medium (Caisson Laboratories, UT, USA) supplemented with 0.5 µM indole-3-butyric acid (IBA). Plantlets were grown in culture in Magenta boxes for a minimum of eight weeks until they were approximately 8 cm in height. Plantlets were then transplanted into small seedling pots containing vermiculite, covered, and acclimated for three weeks in a mist-chamber. They were then repotted into vermiculite-filled, one-gallon round pots and moved into the greenhouse and grown for

approximately 8 weeks. Plants used for histochemistry were fertilized three times per week with 100 mL of general purpose 20-20-20 Plant Prod® NPK fertilizer (100 ppm nitrogen, phosphorus and potassium; Plant Products Co. Ltd, Brampton, ON, Canada), and watered with an equal volume of distilled H_2O. Plants used for quantitative CT analysis and the nitrogen experiment were fertilized three times per week with a modified Long Ashton's solution optimized for poplar growth (1 mM NH_4NO_3, 0.9 mM CaSO · $2H_2O$, 0.6 mM KH_2PO_4, 0.5 mM KCl, 0.04 mM K_2PO_4, 0.33 mM $MgCl_2$ · 7 H_2O, and 0.03 g L-1 standard micronutrient mix (Plant Products Co. Ltd, Brampton, CT ON, Canada), pH 5.6).

For N manipulation experiments, a *P. tremula x tremuloides* hybrid (clone INRA 353-38) was used. Plants propagated as above were grown in Sunshine Basic Mix #2 (Sungro, Seba Beach, AB, Canada) under three nitrogen fertilization treatments. Three plants were assigned to each nitrogen condition: 0.1 mM, 1 mM or 10 mM NH_4NO_3 considered to be low, medium (normal) and high nitrogen treatments, respectively. The plants were fertilized on alternate days with 100 mL of the desired NH_4NO_3 concentration within modified Long Ashton's nutrient solution (0.9 mM $CaCl_2$, 0.6 mM KH_2PO_4, 0.5 mM KCl, 0.04 mM K_2HPO_4, 0.3 mM $MgSO_4$ x $7H_2O$ and 0.03 g L^{-1} standard micronutrient mix (Plant Products Co. Ltd, Brampton, ON, Canada), pH 5.6). All other concentrations of nutrients were standardized in these solution. Plants were grown in greenhouse conditions for 12 weeks and watered with dH_2O as necessary.

2.2 Quantification of condensed tannins

Roots were harvested after eight weeks of growth, divided into segments according to distance from root tip and root color, and then pooled into groups for each plant (n>30). Samples were frozen immediately in liquid nitrogen and then freeze-dried for three days. An aliquot of 8 mg was weighed from each pooled sample. For some samples (mainly root tips) where material was limited, the entire sample was weighed and extracted and the precise weight used in final calculations. Pooled root samples were extracted thrice in 100% MeOH by grinding freeze-dried samples in a PreCellys 24 homogenizer for two minutes using three 2 mm steel beads per sample, sonicating for ten minutes and centrifuging for five minutes at 1500 rpm. This procedure was followed using 1 x 1.5 mL, and 2 x 1 mL of 100% MeOH resulting in 3.5 mL of extract. The extract volume was made up to 5 mL to ensure it was within the linear range for soluble CT quantification. Soluble CTs were measured using the butanol-HCl assay (Porter et al., 1986) as described previously (Gourlay and Constabel, 2019). CTs purified from *P. tremula x tremuloides* leaf tissue (mean degree of polymerization ~9) was used as a standard, isolated and characterized as described by Preston and Trofymow (2015).

Insoluble CTs were quantified by depolymerizing CTs directly in the previously-extracted pellet. Six mL of 1-butanol:HCl (95:5) and 200 µL Fe reagent (Porter et al., 1986) were added directly to the dried pellet and heated to 95 oC for 40 minutes. 400 µL of MeOH was added to each sample before heating to correct for the volume of soluble extract used in the standard curve. Spectrophotometer readings were converted to CT concentration (µg mL-1) for the total sample using a standard curve prepared using purified Populus CTs (Mellway et al., 2009).

2.3 Histochemical analysis

Roots were carefully removed from plants, washed to remove potting soil, and cut into 1 cm sequential segments beginning at the root tip. Samples were immediately fixed at room temperature in modified Karnovsky's fixative (25% glutaraldehyde and 16%) paraformaldehyde in 0.5 mM sodium phosphate buffer (PBS), pH 7.4). Samples were stored in fixative at 4 °C for up to four weeks before embedding. Samples were then rinsed three times for 30 minutes each with 0.5 mM PBS, pH 7.4, and dehydrated in sequential ethanol rinses (30%, 50%, 70%, 95%, and 100%) over the course of one day. Throughout the following week, plants were infiltrated with increasing concentrations of Technovit® 7100 Glyco Methycrylate (Electron Microscopy Sciences) in 100% ethanol, before being cured.

Longitudinal sections (5 µm) were cut using a glass blade microtome (Sorval JB-4). Sections were dried onto slides and stained with 0.1% 4-dimethylaminocinnamaldehyde (DMACA) (w/v) in 0.5 M sulphuric acid in 1-butanol according to the method of Gutmann and Feucht (1991). The slides were covered in 1 mL of stain solution and heated on a Thermolyne Type 1000 hot plate (setting 2.5) for two minutes or until the stain began to evaporate and discolor. The slides were removed from the heat before bubbling occurred in the resin, rinsed three times for 30 s in 1- butanol or until all unbound stain was removed, and cover slips were then secured with PermountTM mounting medium. Sections were imaged within 24 hours on a transmitted light microscope (Zeiss [47-30-12-9902], Germany) fitted with a SPOT RTKE diagnostic 7.2 Color Mosaic camera. A deep burgundy stain indicated the presence of CTs, consistent with other reports of DMACA stained CTs in embedded samples hydrolyzed by hot sulphuric acid (Abeynayake et al., 2011; Gutmann, 1993).

2.4 Micro-electrode ion flux measurement analysis

Five clonal *P. tremula x alba* plants were grown for nutrient ion flux analysis. The Long Ashton's solution was altered from previous experiments to match the measuring solution used during MIFE™ analysis, with overall concentrations of each ion similar to previous studies (Hawkins et al., 2014; 1 mM NH_4NO_3, 0.9 mM $CaSO_4$ · $2H_2O$, 0.6 mM KH_2PO_4, 0.5 mM KCl, 0.04 mM K_2PO_4, 0.3 mM $MgCl_2$ · 7 H_2O and 0.03 g L^{-1} standard micronutrient mix, Plant Products Co. Ltd, Brampton, ON, Canada, pH 5.6). Plants were grown in pairs in a continuous rotation to ensure that they were all the same age when harvested after six weeks of growth. Healthy, individual roots were excised from the plant, and placed in aerated solution containing 500 µM NH_4NO_3 and 500 µM $CaSO_4$ for 30 minutes prior to measurement to allow the roots to acclimate.

Borosilicate glass capillaries (1.5 mm diameter) were pulled, dried at 200 °C for five hours and silanized with tributylchlorosilane to make sterile, measuring electrodes. Once cooled, electrodes were backfilled with 200 mM NH_4Cl for NH_4^+, 500 mM $CaCl_2$ $2H_2O$ for Ca^{2+}, and 500 mM KNO_3 100 mM KCl for NO_3^-. Electrode tips were then filled with ion-selective resins: NH_4^+ and Ca^{2+} -selective cocktails (Fluka), and NO_3^-selective cocktail containing 0.5% methyltridodecylammoniumnitrate (MTDDA NO_3^-), 0.084% methyltriphenylphosphonium (MTPPB) and 99.4% n-phenyloctylether (NPOE) (Plassard et al., 2002). Electrodes were calibrated using a set of standards at pH 5.6. A reference electrode filled with 100 mM KCl in 1% agar and electrolyzed, chloride silver wire was placed in the solution for each measurement to complete the electrical current. Calibration was conducted at the beginning and end of each day to ensure readings were representative and reliable.

The electrodes were mounted in a specialized holder (MMT-5, Narishige, Tokyo, Japan) providing three-dimensional positioning. A maximum distance of 20 µm was recorded between the electrodes and the root surface, and 4 µm between the electrode tips. Roots were secured and placed in the measuring chamber with fresh measuring solution (500 µM NH_4NO_3 and 500 µM $CaSO_4$). The chamber was moved by a computer-controlled manipulator (PatchMan NP2, Eppendorf AG, Hamburg, Germany). During flux measurements, the MIFE™ computer caused the chamber to gently oscillate over a distance of 40 µm, back and forth from the root surface in a 10 s square-wave cycle. The concentration of each ion was calculated from its electrochemical potential at the two positions and ion net flux calculated from the difference in concentration between the two positions (Shabala et al., 1997).

Flux measurements were taken at four discrete positions along the root in the white zone: at the root tip (<2 mm), and three positions within the maturation zone of the white root zone (0.5 cm, 1.5 cm and 3.5 cm from the root tip). These root distances were chosen as they included the zones where uptake is expected to be highest (Hawkins et al., 2008; 2014).

2.5 Statistical analysis

Data was analyzed and graphed using R v.3.0.3. Once model assumptions and normality were checked, data was statistically analyzed using a two-sample T-test or one-way analysis of variance (ANOVA) with Tukey's Honestly Significant Difference (HSD) test.

3 Results

3.1 Condensed tannin content is greatest at the root tip and within the white zone of roots

In order to determine the overall distribution of CTs in roots, root systems from greenhouse-grown poplar were carefully removed from pots and soil and root zones separated and dissected. Root systems were white at the actively growing regions, with older sections becoming brown, and developing obvious secondary growth towards the crown (Figure 1). We used both color and root diameter to divide root systems into four zones similar to the classification of Peterson et al. (1999): root tips (meristematic and elongation zone; <0.5 cm), white zone (maturation zone; 1.0-12 cm), brown zone (without periderm; 13-20 cm), and cork zone (with periderm; >20 cm). Any root tips that showed necrosis were excluded.

The sum of soluble and insoluble CT concentration was highest in the root tips and within the white zone, and then decreased with increasing distance from the root tip (Figure 2). In the youngest parts of the roots (< 5 cm from the root tip), CTs accumulated to more than 100 mg/g DW; this is as much as 20-fold greater than the CT concentration in leaves of greenhouse grown plants. Older parts of the root system contained approximately 25-50 mg/g DW. The lowest CT content was found in the oldest zone, which showed secondary growth - the cork zone. Soluble CTs comprised the predominant fraction of CTs in all regions except in the cork zone, where insoluble CTs were predominant (Figure 2).

3.2 Histochemical analysis indicates a distinct pattern of CT accumulation in epidermal and subepidermal tissues

To further define areas of CT accumulation at the cellular level, embedded tissues from excised root samples from different root zones were stained with 4-dimethylaminocinnamaldehyde (DMACA). In embedded tissue sections, this stain colors CTs reddish brown rather than blue (Abeynayake et al., 2011). In our root sections, CTs were strongly stained in several cell layers of the root cap, but not in the underlying smaller meristematic cells (Figure 3A). In the white zone immediately adjacent (~ 1 cm from tip), CTs were detected in the epidermal cell layers just behind the root cap. Staining was also seen sporadically in cortical cells (Figure 3B). Some DMACA positive staining was observed in the endodermis, but not within vascular tissue of the stele. In older roots, where secondary xylem expands laterally and begins to disrupt the cortex, only very low levels of staining were observed (Figure 3C). Overall, the pattern of DMACA staining was consistent with the chemical analysis: the most intense staining of CTs was seen in the tips and younger sections of the roots, predominantly in epidermal and subepidermal regions around the tip.

At higher magnification, distinct patterns of CT accumulation distribution were visible within different cell types within the white zone. In the outer epidermal layer of the young white root, CT staining was typically observed in large vacuoles filling most of the intracellular space (Figure 4). By contrast, in cortical cells below the epidermal layer, CTs tended to occur in smaller, more concentrated vacuole-like structures. In many cases, these CT-containing structures were arranged around the periphery of the cells, possibly around a central zone or structure, or were found throughout the cell. CTs were not present in all cortical cells but occurred somewhat sporadically, as we had noted at lower magnification (Figure 3). This pattern was observed consistently in multiple sections observed within this region.

10.3389/fpls.2024.1388549

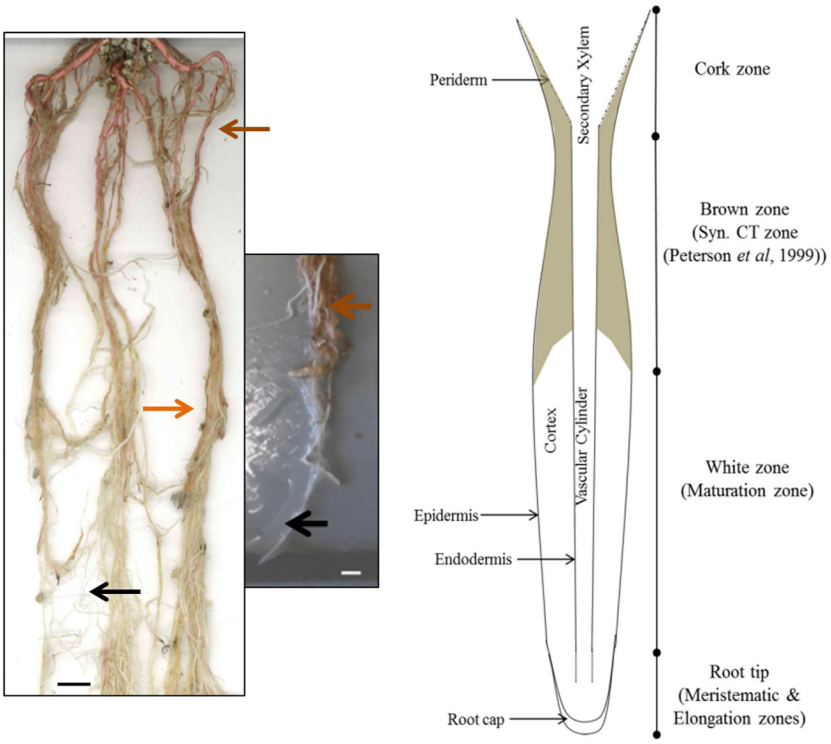

FIGURE 1
Images and cartoon of typical *Populus tremula* x *alba* roots after eight weeks of growth showing white zone and transition to brown zone. Black arrows indicates typical white zone; orange arrows show brown zone of roots prior to secondary growth. Brown arrow indicates the cork zone. Scale bar = 1 cm.

3.3 Interactions of N uptake and nutrition with CT accumulation in different root zones

MIFE™ technology is a non-invasive method to measure net fluxes of specific nutrient ions at precise root locations (Shabala and Newman, 1997; Shabala et al., 1997). To determine if there is a potential interaction of CTs with N uptake, we looked for correlations of N fluxes with CT accumulation. We measured the net flux of NO_3- and NH_4+ along the longitudinal axis of young poplar roots using a MIFE system. Since the root tip and youngest part of the root is most active in nutrient acquisition (Hawkins et al., 2014), we focused on the white zone and root tip. Ion net fluxes were measured for eight minutes at each of four positions along the root axis to ensure that a reliable average flux measurement was gained for each replicate. Five plants were grown and three roots were measured per plant. The highest NH_4^+ net fluxes were observed at the root tip, which were significantly greater than fluxes at more distal positions (Figure 5). NO_3- uptake was lower than NH_4^+ flux at the root tip and did not vary significantly along the length of the root. We also measured the net fluxes of another cation, Ca^{2+}, at the three positions, and these also did not vary with distance from the root tip.

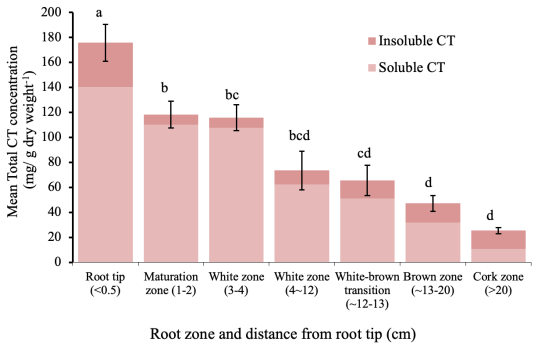

FIGURE 2
Mean soluble and insoluble CT concentrations in zones along the root axis in *P. tremula* x *alba*. Root zone samples were pooled individually by plant for each of five plants. Different letters indicated significant differences (Tukey HSD p<0.05). Error bars indicate SE (n=5) for total CT concentration.

We next tested if CT concentration in the different root zones is influenced by external N supply. Young potted poplar plants were fertilized with a modified Long Ashton nutrient solution that provided 0.1, 1.0 or 10 mM NH_4NO_3 (low, medium, and high N). After the six-week experimental period, the impact of N limitation at the lowest N level was shown by reduced plant growth and a lighter leaf color compared to plants grown at medium and high N availability. Roots were excised and samples taken from the tip, white, and brown zones for CT assays. Under all three N treatments, we observed the same pattern: highest CT concentration at the root

10.3389/fpls.2024.1388549

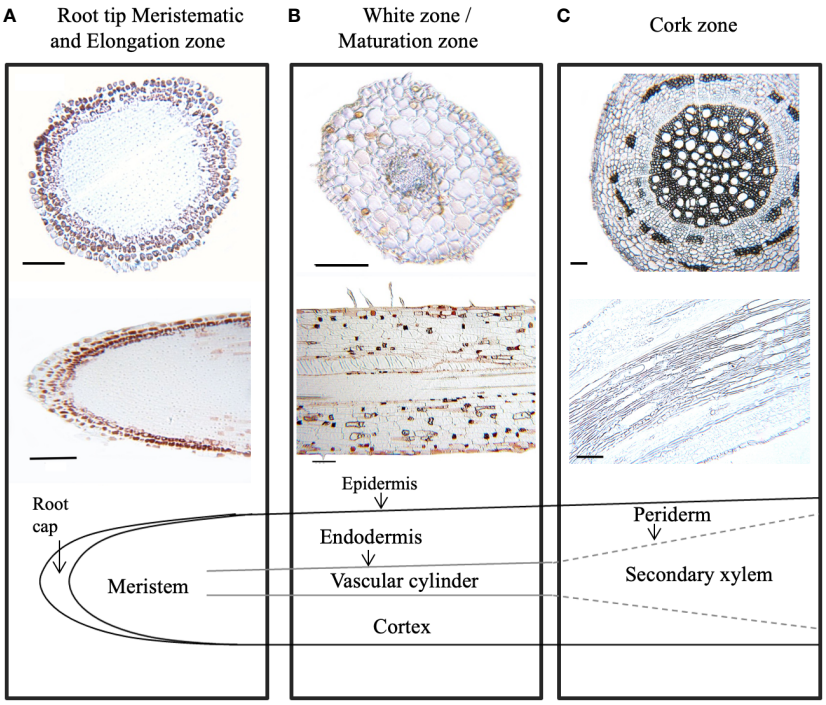

FIGURE 3
Localization of condensed tannins in *P. tremula x alba* roots visualized by DMACA staining of longitudinal and cross root sections. CTs stain with reddish-brown color under these conditions. **(A)** Root tip (< 2 mm from root). **(B)** White zone/maturation zone (1cm back from root tip). **(C)** cork zone (> 20 cm back from root tip). Scale bar = 100μm.

tip, which decreased with increasing distance from the tip in the white and brown zones (Figure 6). Within each root zone, the highest CT concentration was measured in roots grown with 0.1mM NH_4NO_3; roots of plants grown under intermediate N levels showed intermediate CT concentration, and the lowest CT concentration was measured for all three root zones in plants supplied with 10 mM NH_4NO_3. In the white zone, CT concentration was two-fold lower at the highest compared to lowest N availability. This confirmed the repressive effect of N on CT metabolism, and demonstrated this effect across all three root zones.

4 Discussion

The importance of CTs as flexible adaptations of woody plants to biotic and abiotic stresses has emerged in recent years (Constabel et al., 2014; Gourlay et al., 2022), but their functions in roots are not well understood. As a first step in a functional analysis of root CTs, we studied CT localization and distribution in the poplar hybrid *P. tremula* x *alba*. Based on both CT assays and DMACA staining, our work demonstrates the greatest concentration of CTs in the root tip and proximal regions of the white zone, decreasing with increasing

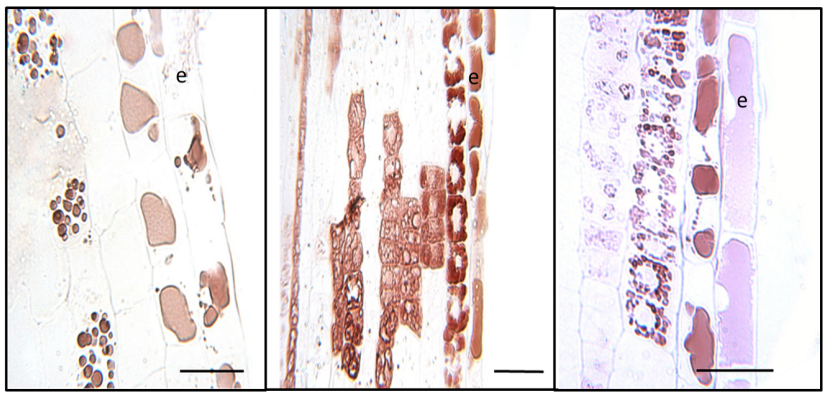

FIGURE 4
Cellular localization of condensed tannins of *P. tremula x alba*. Longitudinal sections of roots 5-10mm from root tip in the white zone were embedded, sectioned and stained with DMACA as described under Materials and Methods. CTs stain with reddish-brown color under these conditions. Epidermal cells are indicated by 'e'. Scale bars=25μm.

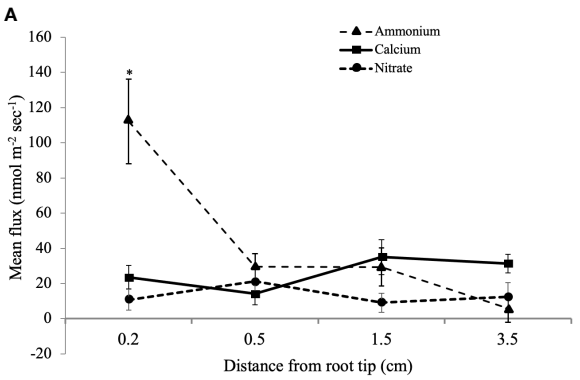

FIGURE 5
Mean influx of NH_4^+, Ca^{2+}, and NO_3^- ions into white zone roots of *P. tremula x alba* at defined distances from the root tip. Mean ion fluxes (+/- SE) were measured in young poplar roots at a defined distance from root tip using a MIFE system as described in Materials and Methods. *indicates significantly different means from other measurements for the same ion ($p<0.001$).

distance from the apex. This gradient of decreasing CTs along the root axis was not influenced by altered N-availability, although overall CT concentrations were reduced with the highest N treatment. In embedded sections, CT-specific staining showed a distinct localization of CTs to cells of the root cap and immediately adjacent epidermal cells, with some sporadic accumulation in cortical cells. Using a microelectrode ion flux measurement (MIFE^{TM}) system, we also found the root tip to be the most active zone for NH_4+ uptake; by contrast, NO3- and Ca^{2+} uptake did not vary significantly along the root axis. To our knowledge, this is the first report testing for a correlation of CT localization in roots with nutrient uptake.

The localization of CTs in the root apical region in the white root zone observed here is consistent with reports from other species.

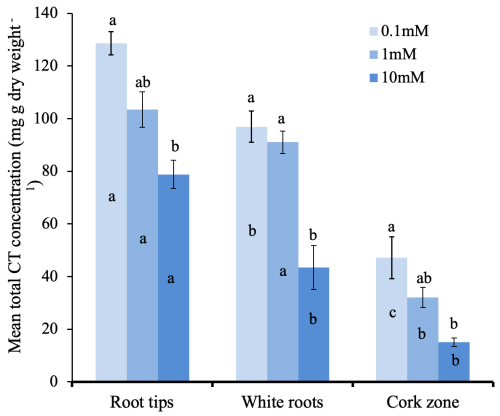

FIGURE 6
Total CT concentrations in distinct growth zones of *P. tremula x P. tremuloides* roots grown with 0.1, 1.0, or 10 mM N. Small letters indicate significantly different means (Tukey HSD, $P<0.05$). Bars show means ± SE (n=3). Letters above bars are Tukey pairwise comparisons for differing nitrogen treatments within each root zone. Letters within bars are pairwise comparison between different root sections with the same nitrogen treatment.

Early work with woody species in the *Rosaceae* also suggested that root tips have particularly high CT content, with accumulation in the root cap and epidermal layers of the elongation zone (Weiss et al., 1997; Hoffmann et al., 2012). Likewise, in *Populus tremuloides* roots, Kao et al. (2002) previously reported CTs in the root cap and epidermal layers near the root tip, as well as in randomly distributed cortical cells closer to the apex and cell division zone. By contrast, in other species a CT distribution in older parts of the root was reported. For example, in *Pinus* and *Eucalyptus* roots, CTs were reported primarily from older, brown regions of the root system (McKenzie and Peterson 1995). The authors named this the 'tannin zone'; however, this is not consistent with our findings and others that report the highest CT levels in the tip and adjacent regions. Endo et al. (2021) analyzed root cross-sections from primary and higher order roots from 20 different temperate woody plants, and found a diverse distribution of CTs. Most species studied stained for DMACA most consistently in the first order (youngest) roots in different cell types including epidermal, phloem and cortex cells. Since mostly older roots were used in that work, it is difficult to compare directly without taking into consideration developmental stages or tissue age; importantly, our work does demonstrate the breadth of cell types and diversity of CT accumulation patterns in different species. Endo et al. (2021) also concluded that trees with ectomycorrhizal associations tended to have higher CT content than those with arbuscular mycorrhizal associations.

The intracellular patterns of CT accumulation as visualized by DMACA at higher magnification is intriguing. In the epidermal cells near the root tip, stain is observed throughout the large central vacuole, whereas in other cells we see mini-vacuoles. The vacuolar accumulation of CTs is broadly known, and has been observed directly using osmium-stained transmission electron microscopy (Lees et al., 1993; 1995). These studies investigated CT localization in apple seeds and peel, as well as leaves and other tissues in sainfoin, a forage crop. All show a diversity of vacuolar accumulation patterns that includes reticulated, net-like patterns, round globules, or a band of CTs that accumulates around the tonoplast. While these studies do not report on CTs in roots, the diversity of CT accumulation patterns in different cells is intriguing and consistent with CT accumulation patterns we detected here. How these accumulation patterns relate, and if they represent different stages in CT synthesis and accumulation, are interesting questions that merit further study.

It should be noted that recently developed fluorescence-based DMACA localization methods in poplar roots provide direct evidence of CT accumulation in cell walls (CW), as well as within the cells (Chowdhury et al., 2023). The CW signal likely represents the unextractable CT fraction often observed in plant tissues (Tarascou et al., 2010). Our CT assays confirm that a substantial proportion of CTs are insoluble. Interestingly, Chowdhury et al. (2023) also show a tissue-age related accumulation of CT. Likewise, our chemical data demonstrate a greater proportion of insoluble vs soluble CTs in the older, cork zone roots. This could be the result of gradual cross-linking with cell walls during root development. Taken together, this pattern suggests that CT accumulation are more dynamic than previously thought.

The negative effect of N supply on CT accumulation we observed in roots is consistent with the pattern observed in other species, including in poplar (Stevens et al., 2014). Our observation of this negative association in all three root zones further underlines that this reflects a fundamental metabolic adaptation. However, to date no consistent physiological function or adaptive function of CT induction under low N supply (or repression of CT synthesis under high N) has emerged. The carbon-nutrient balance hypothesis proposes that CTs act as an internal carbon sink under nutrient limiting conditions and has been much discussed, but has not received broad experimental support (Bryant et al., 1983; Stamp, 2003). Alternative explanations invoke the antioxidant potential of CTs. For example, in leaves low N availability may lead to a reduced capacity for photosynthetic electron transport, and thus lead to a greater production of reactive oxygen species. Together with the ability of CTs to protect against oxidative stresses in leaves (Gourlay et al., 2022), this could explain the stimulation of leaf CT synthesis under N stress. How this could apply to below-ground effects is not clear, but oxidative stress can also be caused by heavy metals in soil. We speculate that ample N supply can facilitate enzymatic and protein-based adaptations to below ground oxidative stress. In the absence of N, carbon-rich phenolics such as tannins may provide alternative anti-oxidant mechanisms.

Although preliminary, the correlation of CT content and NH_4+ uptake could be suggestive of a role of CTs in modulating some cation movement into the root. However, additional work is needed to better understand how these patterns may vary seasonally or under other environmental conditions. Plants with modified root CT content (Liu et al., 2023) would be useful tools in testing this as well as other potential functions of CTs in roots. Since mycorrhizae are critical components of nutrient availability for many forest trees, future work will include studies of the roles of CTs in regulating these ecological interactions.

Data availability statement

The original contributions presented in the study are included in the article/supplementary materials, further inquiries can be directed to the corresponding author/s.

Author contributions

RW: Conceptualization, Methodology, Visualization, Writing – original draft, Writing – review & editing, Formal analysis, Investigation. DM: Investigation, Methodology, Resources, Writing – review & editing. BJH: Methodology, Writing – review & editing, Funding acquisition. CPC: Conceptualization, Funding acquisition, Methodology, Resources, Supervision, Visualization, Writing – original draft, Writing – review & editing.

Funding

The author(s) declare financial support was received for the research, authorship, and/or publication of this article. This work was funded by NSERC Discovery Grants to CPC and BJH as well as the NSERC CREATE Program for Forests and Climate Change at the Centre for Forest Biology, University of Victoria.

Acknowledgments

We thank Samantha Robbins for help with the MIFE system and Brad Binges for expert greenhouse support. We also thank Brent Gowen for expert help with embedding and sectioning techniques.

Conflict of interest

The authors declare that the research was conducted in the absence of any commercial or financial relationships that could be construed as a potential conflict of interest.

Publisher's note

References

Abeynayake, S. W., Panter, S., Mouradov, A., and Spangenberg, G. (2011). A high-resolution method for the localization of proanthocyanidins in plant tissues. *Plant Methods* 7. doi: 10.1186/1746-4811-7-13

Adamczyk, B., Sietiö, O. M., Biasi, C., and Heinonsalo, J. (2019). Interaction between tannins and fungal necromass stabilizes fungal residues in boreal forest soils. *New Phytol.* 223, 16–21. doi: 10.1111/nph.15729

Barbehenn, R. V., and Constabel, C. P. (2011). Tannins in plant-herbivore interactions. *Phytochemistry* 72, 1551–1565. doi: 10.1016/j.phytochem.2011.01.040

Bryant, J. P., Chapin, F. S., and Klein, D. R. (1983). Carbon nutrient balance of boreal plants in relation to vertebrate herbivory. *Oikos* 40, 357–368. doi: 10.2307/3544308

Chowdhury, J., Ferdous, J., Lihavainen, J., Albrectsen, B. R., and Lundberg-Felten, J. (2023). Fluorogenic properties of 4-dimethylaminocinnamaldehyde (DMACA) enable high resolution imaging of cell-wall-bound proanthocyanidins in plant root tissues. *Front. Plant Sci.* 13. doi: 10.3389/fpls.2022.1060804

Constabel, C. P., Yoshida, K., and Walker, V. (2014). Diverse ecological roles of plant tannins: plant defense and beyond. *Recent Adv. Polyphenol Res.* A. Romani, V. Lattanzio and S. Quideau 4, pp. 115-142. doi: 10.1002/9781118329634.ch5

Coq, S., Cardenas, R. E., Mousain, D., et al. (2022). Acquisition of nitrogen from tannin protein complexes in ectomycorrhizal pine seedlings. *Pedobiologia*, 93–94. doi: 10.1016/j.pedobi.2022.150817

Dettlaff, M. A., Marshall, V., Erbilgin, N., and Cahill, J. F. (2018). Root condensed tannins vary over time, but are unrelated to leaf tannins. *AOB Plants* 10. doi: 10.1093/aobpla/ply044

Dong, L. L., Mao, Z. J., and Sun, T. (2016). Condensed tannin effects on decomposition of very fine roots among temperate tree species. *Soil Biol. Biochem.* 103, 489–492. doi: 10.1016/j.soilbio.2016.10.003

Elessawy, F. M., Vandenberg, A., El-Aneed, A., and Purves, R. W. (2021). An untargeted metabolomics approach for correlating pulse crop seed coat polyphenol profiles with antioxidant capacity and iron chelation ability. *Molecules* 26, , 3833. doi: 10.3390/molecules26133833

Endo, I., Kobatake, M., Tanikawa, N., et al. (2021). Anatomical patterns of condensed tannin in fine roots of tree species from a cool-temperate forest. *Ann. Bot.* 128, 59–71. doi: 10.1093/aob/mcab022

Gourlay, G., and Constabel, C. P. (2019). Condensed tannins are inducible antioxidants and protect hybrid poplar against oxidative stress. *Tree Physiol.* 39, 345–355. doi: 10.1093/treephys/tpy143

Gourlay, G., Hawkins, B. J., Albert, A., Schnitzler, J. P., and Constabel, C. P. (2022). Condensed tannins as antioxidants that protect poplar against oxidative stress from drought and UV-B. *Plant Cell Environ.* 45, 362–377. doi: 10.1111/pce.14242

Gutmann, M., and Feucht, W. (1991). A new method for selective localization of flavan-3-ols in plant-tissues involving glycolmethacrylate embedding and microwave irradiation. *Histochemistry* 96, 83–86. doi: 10.1007/BF00266765

Hagerman, A. E., Riedl, K. M., Jones, G. A., et al. (1998). High molecular weight plant polyphenolics (tannins) as biological antioxidants. *J. Agric. Food Chem.* 46, 1887–1892. doi: 10.1021/jf970975b

Hagerman, A. E., and Robbins, C. T. (1987). Implications of soluble tannin-protein complexes for tannin analysis and plant defense mechanisms. *J. Chem. Ecol.* 13, 1243–1259. doi: 10.1007/BF01020552

Hättenschwiler, S., and Vitousek, P. M. (2000). The role of polyphenols in terrestrial ecosystem nutrient cycling. *Trends Ecol. Evol.* 15, 238–243. doi: 10.1016/S0169-5347(00)01861-9

Hawkins, B. J., Boukcim, H., and Plassard, C. (2008). A comparison of ammonium, nitrate and proton net fluxes along seedling roots of Douglas-fir and lodgepole pine grown and measured with different inorganic nitrogen sources. *Plant Cell Environ.* 31, 278–287. doi: 10.1111/j.1365-3040.2007.01760.x

Hawkins, B. J., Robbins, S., and Porter, R. B. (2014). Nitrogen uptake over entire root systems of tree seedlings. *Tree Physiol.* 34, 334–342. doi: 10.1093/treephys/tpu005

Hoffmann, T., Friedlhuber, R., Steinhauser, C., et al. (2012). Histochemical screening, metabolite profiling and expression analysis reveal Rosaceae roots as the site of flavan-3-ol biosynthesis. *Plant Biol.* 14, 33–40. doi: 10.1111/j.1438-8677.2011.00462.x

Holeski, L. M., Vogelzang, A., Stanosz, G., and Lindroth, R. L. (2009). Incidence of Venturia shoot blight in aspen (*Populus tremuloides* Michx.) varies with tree chemistry and genotype. *Biochem. Systematics Ecol.* 37, 139–145. doi: 10.1016/j.bse.2009.02.003

Jansson, S., and Douglas, C. J. (2007). Populus: A model system for plant biology. *Annu. Rev. Plant Biol* 39, 657-669. doi: 10.1146/annurev.arplant.58.032806.103956

Kao, Y. Y., Harding, S. A., and Tsai, C. J. (2002). Differential expression of two distinct phenylalanine ammonia-lyase genes in condensed tannin-accumulating and lignifying cells of quaking aspen. *Plant Physiol.* 130, 796–807. doi: 10.1104/pp.006262

Kimura, M., and Wada, H. (1989). Tannins in mangrove tree roots and their role in the root environment. *Soil Sci. Plant Nutr.* 35, 101–108. doi: 10.1080/00380768.1989.10434741

Kosola, K. R., Parry, D., and Workmaster, B. (2006). Responses of condensed tannins in poplar roots to fertilization and gypsy moth defoliation. *Tree Physiol.* 26, 1607–1611. doi: 10.1093/treephys/26.12.1607

Kraus, T. E. C., Dahlgren, R. A., and Zasoski, R. J. (2003). Tannins in nutrient dynamics of forest ecosystems - a review. *Plant Soil* 256, 41–66. doi: 10.1023/A:1026206511084

Kraus, T. E. C., Zasoski, R. J., and Dahlgren, R. A. (2004). Fertility and pH effects on polyphenol and condensed tannin concentrations in foliage and roots. *Plant Soil* 262, 95–109. doi: 10.1023/B:PLSO.0000037021.41066.79

Lees, G. L., Suttill, N. H., and Gruber, M. Y. (1993). Condensed tannins in sainfoin 1. A histological and cytological survey of plant-tissues. *Can. J. Bot.* 71, 1147–1152. doi: 10.1139/b93-135

Lees, G. L., Suttill, N. H., Wall, K. M., and Beveridge, T. H. (1995). Localization of condensed tannins in apple fruit peel, pulp, and seeds. *Can. J. Bot.* 73, 1897–1904. doi: 10.1139/b95-202

Liu, Y. L., Ma, D. W., and Constabel, C. P. (2023). CRISPR/Cas9 disruption of MYB134 and MYB115 in transgenic poplar leads to differential reduction of proanthocyanidin synthesis in roots and leaves. *Plant Cell Physiol.* 64, 1189–1203. doi: 10.1093/pcp/pcad086

McKenzie, B. E., and Peterson, C. A. (1995). Root browning in *Pinus banksiana* Lamb. and *Eucalyptus pilularis*. *Botanica Acta* 108, 127-137. doi: 10.1111/j.1438-8677.1995.tb00842.x

Mellway, R. D., Tran, L. T., Prouse, M. B., Campbell, M. M., and Constabel, C. P. (2009). The wound-, pathogen-, and ultraviolet B-responsive MYB134 gene encodes an R2R3 MYB transcription factor that regulates proanthocyanidin synthesis in poplar. *Plant Physiol.* 150, 924–941. doi: 10.1104/pp.109.139071

Osawa, H., Endo, I., Hara, Y., Matsushima, Y., and Tange, T. (2011). Transient proliferation of proanthocyanidin-accumulating cells on the epidermal apex contributes to highly aluminum-resistant root elongation in camphor tree. *Plant Physiol.* 155, 433–446. doi: 10.1104/pp.110.166967

Peterson, C.A., Enstone, D.E., and Taylor, J.H. (2011). Pine root structure and its potential significance for root function. *Plant and Soil* 217, 205–213. doi: 10.1104/pp.110.166967

Plassard, C., Guérin-Laguette, A., Véry, A.-A., Casarin, V., and Thibaud, J.-B. (2002). Local measurements of nitrate and potassium fluxes along roots of maritime pine. Effects of ectomycorrhizal symbiosis. *Plant, Cell & Environment* 25, 75–84. doi: 10.1046/j.0016-8025.2001.00810.x

Porter, L. J., Hrstich, L. N., and Chan, B. G. (1986). The conversion of procyanidins and prodelphinidins to cyanidin and delphidin. *Phytochemistry* 25, 223–230. doi: 10.1016/S0031-9422(00)94533-3

Preston, C. M., and Trofymow, J. A. (2015). The chemistry of some foliar litters and their sequential proximate analysis fractions. *Biogeochemistry* 126, 197–209. doi: 10.1007/s10533-015-0152-x

Quideau, S., Deffieux, D., Douat-Casassus, C., and Pouysegu, L. (2011). Plant polyphenols: chemical properties, biological activities, and synthesis. *Angewandte Chemie* 50, 586–621. doi: 10.1002/anie.201000044

Scalbert, A. (1991). Antimicrobial properties of tannins. *Phytochemistry* 30, 3875–3883. doi: 10.1016/0031-9422(91)83426-L

Schmidt, M. A., Gonzalez, J. M., Halvorson, J. J., and Hagerman, A. E. (2013). Metal mobilization in soil by two structurally defined polyphenols. *Chemosphere* 90, 1870–1877. doi: 10.1016/j.chemosphere.2012.10.010

Shabala, S. N., and Newman, I. A. (1997). Proton and calcium flux oscillations in the elongation region correlate with root nutation. *Physiol. Plantarum* 100, 917–926. doi: 10.1111/j.1399-3054.1997.tb00018.x

Shabala, S. N., Newman, I. A., and Morris, J. (1997). Oscillations in H+ and Ca2+ ion fluxes around the elongation region of corn roots and effects of external pH. *Plant Physiol.* 113, 111–118. doi: 10.1104/pp.113.1.111

Stamp, N. (2003). Out of the quagmire of plant defense hypotheses. *Q. Rev. Biol.* 78, 23–55. doi: 10.1086/367580

Stevens, M. T., Gusse, A. C., and Lindroth, R. L. (2014). Root chemistry in *Populus tremuloides*: effects of soil nutrients, defoliation, and genotype. *J. Chem. Ecol.* 40, 31–38. doi: 10.1007/s10886-013-0371-3

Tarascou, I., Souquet, J. M., Mazauric, J. P., et al. (2010). The hidden face of food phenolic composition. *Arch. Biochem. Biophysics* 501, 16–22. doi: 10.1016/j.abb.2010.03.018

Ullah, C., Unsicker, S. B., Fellenberg, C., et al. (2017). Flavan-3-ols are an effective chemical defense against rust infection. *Plant Physiol.* 175, 1560–1578. doi: 10.1104/pp.17.00842

Weiss, M., Mikolajewski, S., Peipp, H., et al. (1997). Tissue-specific and development-dependent accumulation of phenylpropanoids in larch mycorrhizas. *Plant Physiol.* 114, 15–27. doi: 10.1104/pp.114.1.15

Whitham, T. G., Bailey, J. K., Schweitzer, J. A., et al. (2006). A framework for community and ecosystem genetics: from genes to ecosystems. *Nat. Rev. Genet.* 7, 510–523. doi: 10.1038/nrg1877

frontiers | Frontiers in Plant Science

TYPE Review
PUBLISHED 25 June 2024
DOI 10.3389/fpls.2024.1384091

OPEN ACCESS

EDITED BY
Deyu Xie,
North Carolina State University, United States

REVIEWED BY
Juan Guo,
Chinese Academy of Medical Sciences and Peking Union Medical College, China
Hiroshi A. Maeda,
University of Wisconsin-Madison, United States

*CORRESPONDENCE
Chaofeng Li
cfli1988cas@swu.edu.cn
Keming Luo
kemingl@swu.edu.cn

RECEIVED 08 February 2024
ACCEPTED 10 June 2024
PUBLISHED 25 June 2024

CITATION
Wang L, Li C and Luo K (2024) Biosynthesis and metabolic engineering of isoflavonoids in model plants and crops: a review.
Front. Plant Sci. 15:1384091.
doi: 10.3389/fpls.2024.1384091

Biosynthesis and metabolic engineering of isoflavonoids in model plants and crops: a review

Lijun Wang[1], Chaofeng Li[2,3]* and Keming Luo[4,5]*

[1]School of Life Science and Engineering, Southwest University of Science and Technology, Mianyang, China, [2]Maize Research Institute, Southwest University, Chongqing, China, [3]Engineering Research Center of South Upland Agriculture, Ministry of Education, Chongqing, China, [4]Chongqing Key Laboratory of Plant Resource Conservation and Germplasm Innovation, Integrative Science Center of Germplasm Creation in Western China (Chongqing) Science City, School of Life Sciences, Southwest University, Chongqing, China, [5]Key Laboratory of Eco-environments of Three Gorges Reservoir Region, Ministry of Education, School of Life Sciences, Southwest University, Chongqing, China

Isoflavonoids, the major secondary metabolites within the flavonoid biosynthetic pathway, play important roles in plant defense and exhibit free radical scavenging properties in mammals. Recent advancements in understanding the synthesis, transport, and regulation of isoflavonoids have identified their biosynthetic pathways as promising targets for metabolic engineering, offering potential benefits such as enhanced plant resistance, improved biomass, and restoration of soil fertility. This review provides an overview of recent breakthroughs in isoflavonoid biosynthesis, encompassing key enzymes in the biosynthetic pathway, transporters influencing their subcellular localization, molecular mechanisms regulating the metabolic pathway (including transcriptional and post-transcriptional regulation, as well as epigenetic modifications). Metabolic engineering strategies aimed at boosting isoflavonoid content in both leguminous and non-leguminous plants. Additionally, we discuss emerging technologies and resources for precise isoflavonoid regulation. This comprehensive review primarily focuses on model plants and crops, offering insights for more effective and sustainable metabolic engineering approaches to enhance nutritional quality and stress tolerance.

KEYWORDS

isoflavonoids, biosynthesis, metabolic engineering, bio-function, regulation

Introduction

Isoflavonoids, a major subclass of flavonoids, play pivotal roles in plant growth, development, and stress defense, with recognized implications for human health (Dixon, 1999; Veitch, 2013; Wang et al., 2022). In plant-microbe interactions, isoflavonoids function as signal molecules perceived by microorganisms (Biala-Leonhard et al., 2021).

They act as phytoalexins, inhibiting the growth and reproduction of bacteria and fungi, fortifying plant defense against pathogens. Simultaneously, isoflavonoids attract rhizobia to legume root nodules, establishing symbiotic relationships that enhance plant growth, reduce nitrogen fertilizer use, and improve soil fertility (Abd-Alla et al., 2023). Furthermore, the synthesis and accumulation of isoflavonoids in plants are induced by various biotic and abiotic stresses, enhancing overall adaptability (Dixon and Paiva, 1995). Due to their structural and functional resemblance to endogenous estrogen, isoflavonoids and their derivatives are recognized as phytoestrogens, finding applications in functional foods, nutraceuticals, and medicine for disease prevention and treatment (Dixon, 2004; Griffiths et al., 2014; Yu et al., 2021).

With a profound understanding of the significance of isoflavonoid compounds, current research has increasingly emphasized the biosynthesis, transport, and regulation processes in plants. This emphasis has significantly propelled advancements in metabolic engineering and *de novo* synthesis studies. While isoflavonoids are predominantly found in leguminous plants, their scarcity in other plants has led researchers to explore metabolic engineering and synthetic biology as promising strategies. These approaches address the challenges posed by the low abundance and difficulty in obtaining large quantities through conventional crop-based manufacturing or chemical synthesis. Prior reviews have provided detailed reviews of the synthesis, regulation, and metabolic engineering of isoflavones (Yu and McGonigle, 2005; Sohn et al., 2021). However, as time progresses, the functions of an increasing number of genes are being reported, and the application of newer technologies are spurring additional breakthroughs in the study of isoflavonoid synthesis and metabolic engineering. This review will focus on a wider variety of isoflavonoid compounds.

The chemical structures and functions of various isoflavonoids

Isoflavonoids, along with flavonoids, lignins, coumarins, and stilbenes, all belong to the class of phenylpropanoid compounds, which are crucial for plant adaptation to terrestrial environments, enabling plants to withstand gravity and offering protection against UV radiation, desiccation, pathogens, and herbivores (Muro-Villanueva et al., 2019; Yadav et al., 2020; Dong and Lin, 2021). Isoflavonoids, also known as 3-phenylchromanes, feature a C_6-C_3-C_6 backbone with the phenyl B-ring attached to position 3 of the heterocyclic pyran ring (the C ring). Based on structural characteristics, they are classified into isoflavones, isoflavans, pterocarpans, rotenoids, coumestans, and derivatives formed through methylation, glycosylation, and acylation (Figure 1).

Isoflavones, as shown in Figure 2, such as genistein, daidzein, biochanin A, formononetin, daidzin, ononin, etc., are found in various plants, with particularly high amounts in legumes like soybeans, chickpeas (*Cicer arietinum*), fava beans (*Vicia faba* L.), alfalfa (*Medicago sativa*), and medicinal plants like red clover (*Trifolium pratense*), *Glycyrrhiza uralensis*, and *Astragalus membranaceus* (Paiva et al., 1991; Kaufman et al., 1997; Tsao et al., 2006; Gao et al., 2015; Zhang et al., 2018). Almost all isoflavones exhibit antibacterial effects, aiding plants in resisting pathogens. Among them, genistein and daidzein serve as broad-spectrum antimicrobial agents, inhibiting the growth and

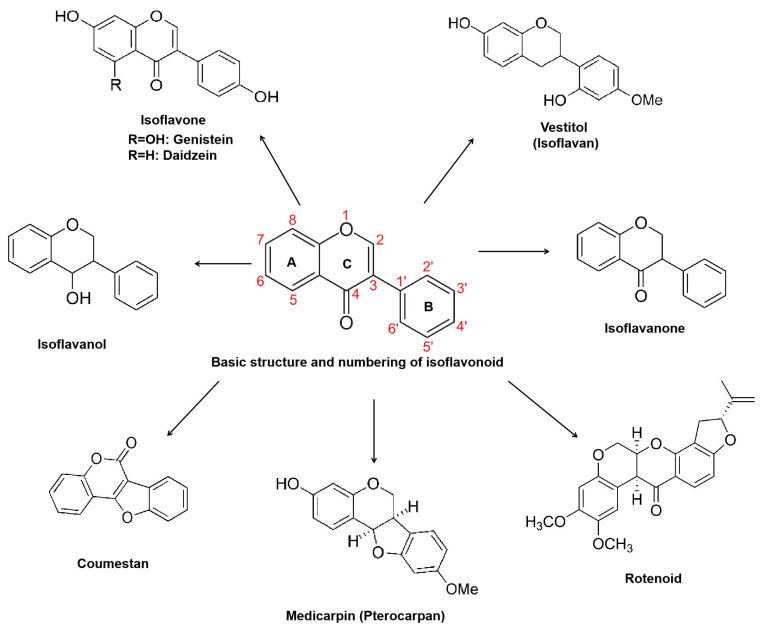

FIGURE 1
Structures and classification of isoflavonoids. This basic C6-C3-C6 structure consists of a benzene ring (A-ring), a pyran ring (C-ring), and a phenyl group (B-ring).

10.3389/fpls.2024.1384091

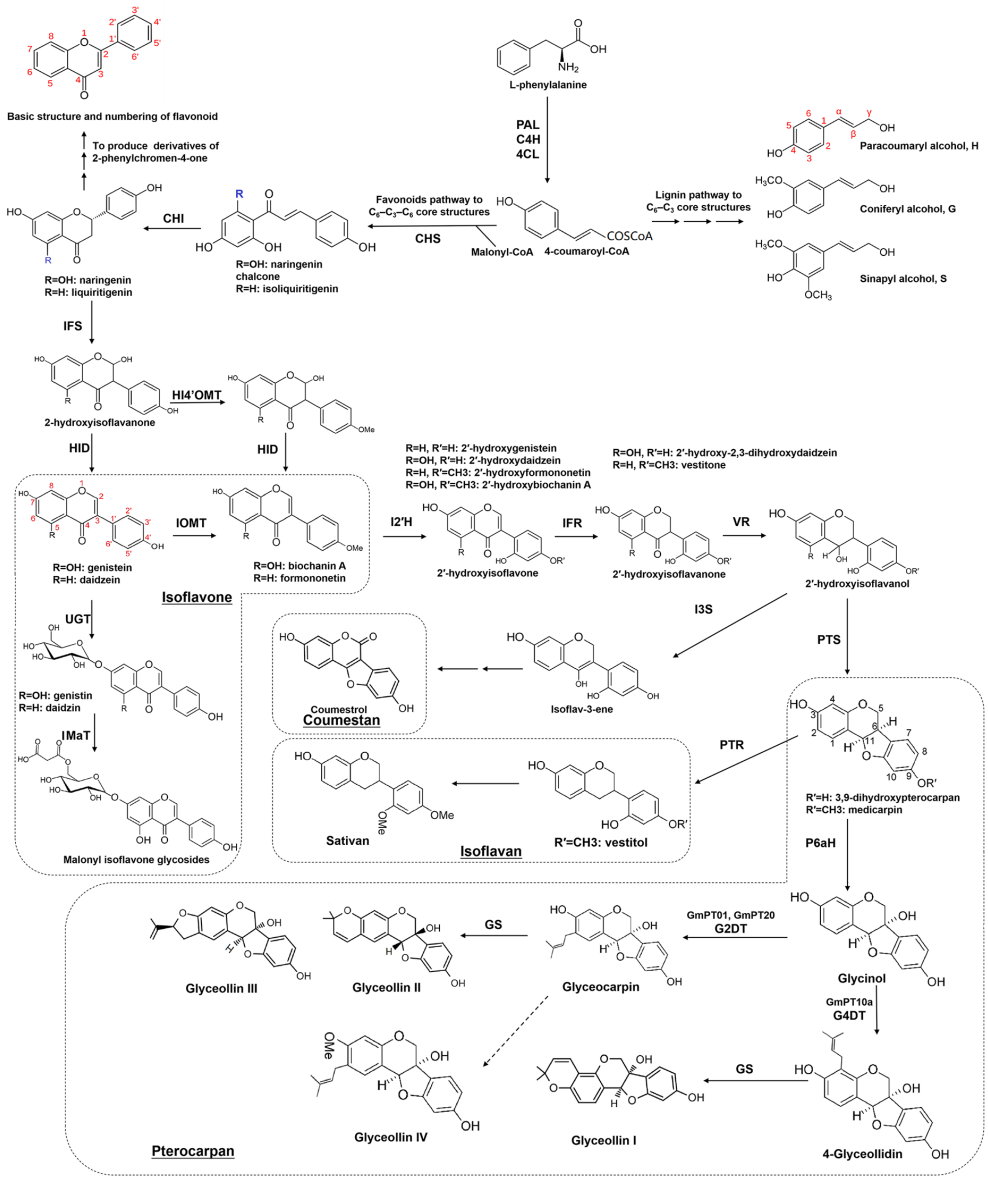

FIGURE 2
Biosynthetic pathways of isoflavonoids. PAL, phenylalanine ammonia-lyase; C4H, cinnamate 4-hydroxylase; 4CL, 4-coumarate CoA ligase; CHS, chalcone synthase; CHI, chalcone isomerase; IFS, isoflavone synthase; HI4′OMT, 2-hydroxyisoflavanone 4′-O-methyltransferase; HID/IFD, 2-hydroxyisoflavanone dehydratase; IOMT, isoflavonoid O-methyltransferase; UGT, glycosyltransferases; IMaT, isoflavone glucoside malonyltransferase; I2′H, isoflavone 2′-hydroxylase; IFR, isoflavone reductase; VR, vestitone reductase; PTS, pterocarpan synthase; PTR, Pterocarpan reductase; I3S, isoflav-3-ene synthase ; P6aH, pterocarpan 6a-hydroxylase; G2DT, glycinol 2-dimethylallyl transferase; G4DT, glycinol 4-dimethylallyl transferase; GS, glyceollin synthase.

reproduction of bacteria and fungi, thereby enhancing plant defense against pathogens (Dixon and Ferreira, 2002; Araya-Cloutier et al., 2017).

Pterocarpans, as shown in Figure 2, alongside isoflavones, are prevalent isoflavonoids found in various plants, including bitucarpin (A, B) and erybraedin C from *Bituminaria morisiana* and *Bituminaria. bituminosa*, medicarpin from *Medicago truncatula* and alfalfa, glycinol, and glyceollin from soybean, among others (Higgins, 1972; Paiva et al., 1991; Dixon, 1999; Pistelli et al., 2003; Naoumkina et al., 2007; Yoneyama et al., 2016; Sukumaran et al., 2018). In *M. truncatula*, medicarpin acts as an inducible "phytoalexin," accumulating during defense responses (Naoumkina et al., 2007; Farag et al., 2008). In soybean, glycinol is formed through the cyclization of daidzein and serves as a precursor to glyceollin. Glyceollin is synthesized via the prenylation of glycinol in response to pathogen infection, enhancing resistance against soybean pathogens like *Phytophthora sojae*, *Diaporthe phaseolorum* var. *meridionales*, *Macrophomina phaseolina*, and *Sclerotinia sclerotiorum* (Akashi et al., 2009; Lygin et al., 2010; Yoneyama et al., 2016; Sukumaran et al., 2018). In *B.*

bituminosa, the accumulation of pterocarpans (bitucarpin A and erybraedin C) significantly increases with treatment using arbuscular mycorrhizal fungi, offering a viable method for medicinal pterocarpan production (Pistelli et al., 2003, 2017).

Coumestrol, the principal coumestan compound, is derived from the conversion of unstable precursors isoflav-3-enes (Figure 2). It functions as both a phytoalexin and phytoestrogen, contributing to the well-being of both plants and humans (Martin and Dewick, 1980; Boue et al., 2000; Yuk et al., 2011; Ha et al., 2019; Uchida et al., 2020; Mun et al., 2021). For instance, the accumulation of coumestrol and the expression of genes involved in soybean coumestrol biosynthesis increase during leaf development, senescence, pathogen infection, nodulation, various stress treatments, and hormone treatments such as salicylic acid (SA), methyl jasmonate (MeJA), and ethylene (ET). This suggests that coumestans, including coumestrol, play crucial roles in plant development and stress defense (Boue et al., 2000; Lee et al., 2012; Tripathi et al., 2016; Ha et al., 2019; Mun et al., 2021; Ohta et al., 2021; Lee et al., 2022). Other coumestan compounds, like wedelolactone and psoralidin, exhibit similar functions. However, the key enzymes and regulators involved in their biosynthesis still require further exploration (Perez Rojo et al., 2023; Wang et al., 2023b).

Isoflavans, a specific subclass of isoflavonoids, are 5-deoxyisoflavonoids first discovered in legumes (Figure 2). This category includes glabridin from licorice (*Glycyrrhiza glabra*), vestitol, and sativan from *Lotus japonicus*, alfalfa, and others (Dewick and Martin, 1979; Hayashi et al., 1996; Shimada et al., 2000; Akashi et al., 2006; Veitch, 2009, 2013). The synthesis of vestitol in *Lotus* sp. is notably induced by ultraviolet (UV) radiation and the attachment of the root parasitic plant *Striga hermonthica*. Pterocarpan reductase (PTR) catalyzes this process, utilizing medicarpin as a substrate (Akashi et al., 2006; Ueda and Sugimoto, 2010; Kaducova et al., 2019; Kaducová et al., 2022). Subsequently, vestitol undergoes methylation by O-methyltransferase to produce sativan, another phytoalexin that accumulates significantly upon fungal pathogen infection in alfalfa and *Lotus* sp (Ingham and Harborne, 1976; Dewick and Martin, 1979; Saunders and O'neill, 2004; Trush et al., 2023). Glabridin, a prenylated isoflavan found in licorice plants, exhibits notable fungicidal activity against various phytopathogenic fungi such as *Fusarium graminearum*, *Sclerotinia sclerotiorum*, and *Corynospora cassiicola* (Simmler et al., 2013; Yang et al., 2021; Li et al., 2021a).

Rotenone and its derivative deguelin, the most common rotenoid compounds in *Derris* sp., are extensively employed as insecticides due to their capability to inhibit electron transport in the respiratory chain (Anzeveno, 1979; Hail and Lotan, 2004; Preston et al., 2017; Russell et al., 2020);. Additionally, rotenone exhibits anticancer activity *in vitro* but its application is limited due to neurotoxicity associated with its ability to cross the blood-brain barrier (Cannon et al., 2009; Deng et al., 2010). However, hydroxylated rotenoids are more hydrophilic and less likely to readily cross the blood-brain barrier, potentially acting as cell-selective killers to inhibit the proliferation of cancer cells (Naguib et al., 2018; Zhang et al., 2022a).

Indeed, the diversity and complexity of isoflavonoid compounds are largely due to chemical modifications such as methylation, glycosylation, and acylation. Differences in modification sites, types, and numbers of modifying groups can lead to changes in the physicochemical properties and biological activities of these derivatives. Therefore, studying the structure-function relationships of isoflavonoid derivatives and the related enzymes will contribute significantly to the efficient targeted synthesis of complex isoflavonoids in synthetic biology.

Biosynthesis of isoflavonoids in plants

The biosynthesis of isoflavonoids begins with L-phenylalanine and forms compounds with a classical C6-C3 core, which is called phenylpropanoid because of containing a benzene ring (phenyl) and a propionic acid side chain. The chemical intermediate p-coumaroyl-CoA catalyzed by 4-coumarate: CoA ligase (4CL) is a highly activated molecule, which acts as a key hub to determine the metabolic flow in response to developmental or environmental signals (Figure 2). One is to form molecules with a C6-C3 core structures, such as lignin monomers (including paracoumaryl alcohol, coniferyl alcohol, and sinapyl alcohol), and the other is to combine with Malonyl-CoA to form molecules with a C6-C3-C6 core, such as flavonoids (2-phenylchromen-4-one and derivatives) and isoflavonoids (3-phenylchromen-4-one and derivatives) (Figure 2).

Isoflavonoids can be divided into "phytoanticipins," which are pre-existing compounds, including genistein, daidzein, formononetin, lupin, etc., or inducible "phytoalexins," which are produced upon infection by pathogens or insects, such as medicarpin, pisatin, sativan, vestitol, glyceollin, and coumestrol (Dixon and Ferreira, 2002). While predominantly found in leguminous plants, isoflavonoids have been identified in various plant species beyond the legume family, including iridaceous, compositous, moraceous plants, barley (*Hordeum vulgare*), and others (Reynaud et al., 2005; Mackova et al., 2006; Darbour et al., 2007; Abderamane et al., 2011; Picmanov et al., 2012; Polturak et al., 2023). A recent study in wheat unveiled a pathogen-induced biosynthetic gene cluster with seven enzymes, including chalcone synthase (CHS1), non-induced chalcone isomerase (CHI), two cytochrome P450s, and three O-methyltransferases (OMTs), resulting in the production of a wheat-specific isoflavonoid named triticein (Polturak et al., 2023). This breakthrough provides new opportunities for isoflavonoid synthesis in non-legume crop plants.

As shown in Figure 2, the isoflavonoid biosynthetic pathway initiates with isoflavone synthase (IFS), catalyzing the migration of the B-ring from the 2- to the 3-position of the C ring, yielding 2-hydroxyisoflavanone (Jung et al., 2000; Subramanian et al., 2006). Subsequent dehydration by 2-hydroxyisoflavanone dehydratase (HID/IFD) results in isoflavones like genistein and daidzein (Hakamatsuka et al., 1998; Akashi et al., 2005; Shimamura et al., 2007). In soybeans (*Glycine max*), another HID/IFD converts 4′-methoxylated 2-hydroxyisoflavanones into formononetin or biochanin A (Akashi et al., 2005). Diverse isoflavonoid

compounds result from multiple O-methyltransferases (OMTs) methylating at the C3′-,4′, 3-, or 7-hydroxyl group. Various derivatives, such as 3'-methoxy-puerarin, 4′-O-methylated isoflavonoid formononetin, and 7-O-methylated isoflavone isoformononetin, are formed (He and Dixon, 2000; Liu and Dixon, 2001; Zubieta et al., 2001; Akashi et al., 2003; Liu et al., 2006; Li et al., 2016a). Subsequently, methylated formononetin transforms into medicarpin through isoflavone reductase (IFR), vestitone reductase (VR), and pterocarpan synthase (PTS) (Paiva et al., 1991; Oommen et al., 1994; Dixon et al., 1995; Guo and Paiva, 1995; Nakamura et al., 1999; Uchida et al., 2017). Glycosyltransferases (UGTs) further contribute to derivatives synthesis, e.g., 7-O-glucosyltransferase converting daidzein to daidzin and 8-C-glucosyltransferase forming puerarin from daidzein (He and Dixon, 2000; Noguchi et al., 2007; Li et al., 2014; Funaki et al., 2015; Wang et al., 2017). Acyltransferases add acyl groups (prenyl or acetyl) to produce prenylated or acetylated isoflavonoids, enhancing antimicrobial activities (Dixon, 1999; Mukne et al., 2011; Shen et al., 2012; Ahmad et al., 2017; Araya-Cloutier et al., 2017; Mouffouk et al., 2017; Araya-Cloutier et al., 2018; Kalli et al., 2021).

A large number of isoflavonoid compounds are produced in plants during specific developmental stages or in response to environmental signals, which are accompanied by re-distribution of substrates and induced phytoalexin synthesis (Piślewska et al., 2002; Gutierrez-Gonzalez et al., 2009, 2010). In many times, the encoding genes of these enzymes only function after being induced by speific factors (Shimada et al., 2007; Shelton et al., 2012). Therefore, key enzymes in the isoflavonoid biosynthetic pathway, especially those involved in the modification of isoflavonoids such as glycosyltransferases and methyltransferases for the modification of -OH groups at C-7, C-5, or C-4', glycosidases for hydrolysis glycosylated isoflavonoids, and acyltransferase for malonylation or acetylation of isoflavonoids are still not fully characterized, and their functions require further elucidation (Figures 2, 3). To comprehensively explore these biosynthetic pathways and regulatory mechanisms, germplasm resources of legumes can be collected or established, and integrated approaches such as genome resequencing techniques, transcriptomics, and metabolomics can be applied to identify the genes responsible for synthesizing key enzymes.

Transport of isoflavonoids in legumes

Extensive studies have indicated that glycosylation and acylation modifications of isoflavonoids not only enhance transporter affinity and efficiency, but also improve water solubility and stability, facilitating storage in vacuoles or extracellular secretion (Dixon, 1999; Zhao et al., 2011; Le Roy et al., 2016; Ahmad et al., 2017; Ku et al., 2020; Ahmad et al., 2021). Additionally, isoflavonoids can act as signaling molecules by translocating to the nucleus and influencing the expression of downstream genes (Naoumkina et al., 2007; Naoumkina and Dixon, 2008; Yu et al., 2008; Zhao and Dixon, 2010). As shown in Figure 3, various transport mechanisms, including vesicle trafficking, ATP-binding cassette (ABC) transporters, multidrug and toxic compound extrusion (MATE) transporters, and glutathione S-transferase (GST), located in the vacuolar membrane or plasma membrane, have been reported to play roles in the transport and distribution of isoflavonoids (Li et al., 1997; Naoumkina et al., 2007; Naoumkina and Dixon, 2008; Zhao and

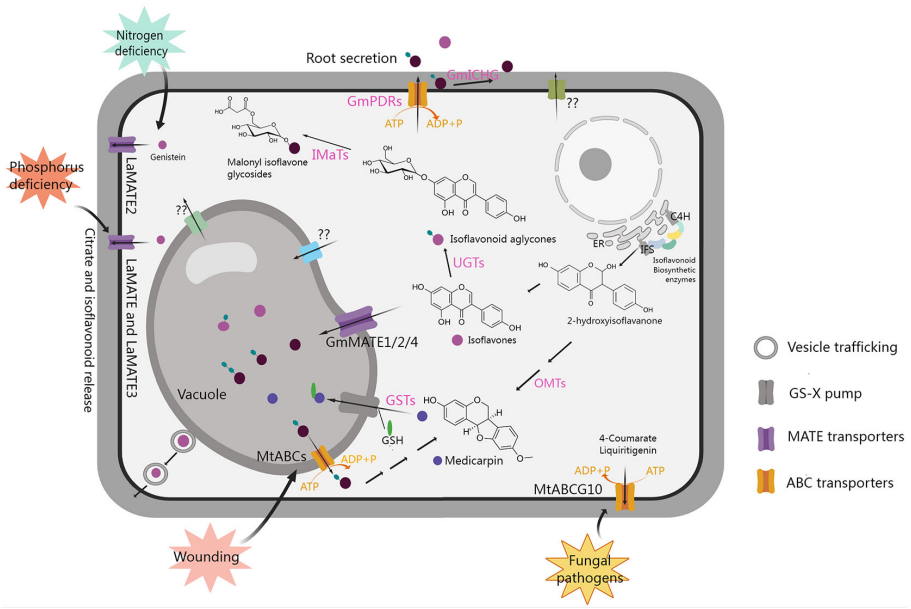

FIGURE 3
Transport and accumulation of isoflavonoids in legumes. GS-X pump, glutathione conjugates pump; PDRs, pleiotropic drug resistance transporters belonging to the ABCG subfamily; GSTs, glutathione S-transferases; ER, endoplasmic reticulum. The figure was created with Medpeer (https://image.medpeer.cn/).

Dixon, 2010; Zhao et al., 2011; Banasiak et al., 2013; Zhao, 2015; Biala-Leonhard et al., 2021).

In leguminous plants, isoflavonoids released by the roots serve as signaling molecules, influencing rhizobia to promote symbiosis. Identified transporters play crucial roles in the release of isoflavonoids from roots. For instance, in *Lupinus albus*, phosphorus deficiency induces the expression of *LaMATE*, *LaMATE2*, and *LaMATE3*, as well as the release of genistein from roots. The individual silencing of these genes reduces genistein release. Among them, LaMATE2 has been confirmed to transport genistein using yeast microsomal membrane vesicles, while the isoflavone transport functions of LaMATE and LaMATE3 require further exploration (Figure 3). Additionally, *LaMATE2* is induced by nitrogen deficiency, and its silencing also reduces the number of nodules, indicating that LaMATE2 facilitates the export of isoflavonoids into the rhizosphere, fostering nodule formation (Biala-Leonhard et al., 2021; Zhou et al., 2021). In *M. truncatula*, a plasma membrane-localized ABC transporter MtABCG10, which belongs to the G subfamily, is involved in medicarpin precursor transport, modulates the distribution of 4-coumarate and liquiritigenin during nodule formation and plant defense against fungal pathogens (Jasinski et al., 2009; Banasiak et al., 2013; Biala et al., 2017). LjABCG1, which is homologous to the MtABCG10 in *L. japonicus*, is associated with pathogenesis rather than symbiosis, but the substrate remains unclear and requires further investigation (Sugiyama et al., 2015). In soybean, 13 pleiotropic drug resistance genes (*PDRs*) encoding ABCG transporters were found to be expressed in roots. One of them was confirmed to participate in membrane transport of genistein, daidzein, and other isoflavonoid aglycones, initiating legume-rhizobium symbiosis formation (Sugiyama et al., 2007, 2008). Additionally, the β-glucosidase GmICHG in soybean cell walls hydrolyzes genistin, contributing to isoflavone secretion in roots (Suzuki et al., 2006).

Transporters also play a crucial role in directing isoflavonoids into the vacuole for storage. In soybean, GmMATE1, GmMATE2, and GmMATE4, localized in the vacuolar membrane, are implicated in transporting isoflavones for accumulation through yeast uptake assay. In addition, it has also been confirmed that the total isoflavone content in seeds is significantly increased due to the overexpression of *GmMATE1* in transgenic soybean, while it is significantly decreased due to *GmMATE1* mutation (Ng et al., 2021; Ku et al., 2022). The utilization of maize GST-mediated conjugation with GSH (medicarpin-GS) significantly enhances the uptake of isoflavonoids by vacuoles (Li et al., 1997). When plants are exposed to stress-induced signals, they utilize store isoflavonoids to synthesize phytoalexin to enhance their resistance. For example, wound signal MeJA induces a decrease in the content of isoflavone glycosides, while it can also induce the accumulation of medicarpin in alfalfa, which is accompanied by the up-regulation the expression of multiple ABC transporter genes and β-glucosidase genes, suggesting that ABC transporters may be involved in transport of isoflavone glycosides from the vacuole to the cytoplasm for the synthesis of medicarpin, thereby increasing plant resistance to wounding (Naoumkina et al., 2007). However, the specific ABC transporters involved in this process remain unclear and require further exploration.

As shown in Figure 3, the transporters that have been reported so far are mainly involved in the transport of isoflavones such as genistein, while there is scarce research on proteins that transport other types of isoflavonoids. Among them, although MtABCs may be involved in the transport of medicarpin, it is still unclear which ABC protein is responsible. There are also some transporter proteins whose encoding gene expression levels can affect the change in isoflavone content, but whether they have a direct transport function needs further confirmation. Overall, a more in-depth understanding of the transporters involved in their conveyance, accumulation, and extracellular secretion is essential for unraveling their physiological and pathological actions in plants.

Regulation of isoflavonoid biosynthesis

The biosynthesis of isoflavonoids in plants is intricately regulated by diverse environmental factors (such as UV radiation, fungal infection, nitrogen, and phosphorus deficiencies), through transcriptional regulation, post-translational modifications, and epigenetic changes (Dastmalchi et al., 2017; Su et al., 2021; Wang et al., 2023a).

Numerous studies have demonstrated the accumulation of isoflavonoid in plants is also induced by hormonal signals (Ng et al., 2015; Boivin et al., 2016; Yuk et al., 2016; Jeong et al., 2018; Kurepa et al., 2023). The dynamic presence or absence of isoflavonoids significantly influences plant resistance to fungi and environmental stresses, shaping plant growth and development through intricate modulation of auxin transport *in vivo* (Mathesius, 2001; Wasson et al., 2006; Gao et al., 2021; Zhang et al., 2022b). For instance, in alfalfa, exposure to a fungal elicitor promptly triggers the accumulation of the phytoalexin medicarpin, subsequently undergoing glycosylation and malonylation to form isoflavonoid conjugates (Kessmann et al., 1990). In *M. truncatula*, fungal infection triggers *de novo* medicarpin biosynthesis, while wound signals induce the downstream genes converting formononetin and isoflavone glycosides into medicarpin (Naoumkina et al., 2007; Farag et al., 2008). RNA interference-induced silencing of chalcone synthase gene (*CHS*) in *M. truncatula* amplifies auxin transport, leading to an impaired ability to form nodules and a deficiency in (iso)flavonoids, particularly formononetin, daidzein and medicarpin (Wasson et al., 2006). When using these compounds and their glycoside forms to treat the wild-type roots, only the free formononetin significantly inhibited auxin transport. However, compared to the wild type, *CHS* silencing increased auxin transport in roots, indicating that isoflavonoid acts as an auxin transport inhibitor in *M. truncatula* (Laffont et al., 2010). Additionally, transcriptome analysis of *M. truncatula* root hairs during rhizobial infection reveals the induction of genes associated with auxin signaling, strigolactone (SL), gibberellic acid (GA), brassinosteroid (BR), and medicarpin biosynthesis, accompanied by the repression of genes involved in lignin biosynthesis. This emphasizes the pivotal roles of (iso) flavonoids and plant hormones, particularly auxin, in the context of rhizobial infection (Breakspear et al., 2014).

An optimal auxin gradient is required for the formation and development of legume nodule primordia (Benkova et al., 2003; Kohlen et al., 2018). In soybean, the involvement of the PIN-FORMED auxin transporter GmPIN1 in nodulation has been elucidated. This process is mediated by two nodulation regulators, (iso)flavonoids (genistein and 7,4′-dihydroxyflavone), which expand GmPIN1 distribution, and cytokinin, which rearranges the cellular polarity of GmPIN1. This orchestration establishes an appropriate auxin gradient, fostering soybean nodulation (Gao et al., 2021). Furthermore, GmPIN1 is involved in the polar transport of auxin from the leaf to the petiole base, resulting in an asymmetric distribution of auxin in the upper and lower petiole cells. This asymmetry significantly impacts cell expansion and the leaf petiole angle. Light-induced (iso)flavonoids accumulate more in the upper petiole cells, inhibiting GmPIN1 expression and disrupting its distribution, leading to reduced auxin in the upper petiole cells. Conversely, lower petiole cells, with lower (iso) flavonoid levels, accumulate more auxin, promoting cell expansion (Zhang et al., 2022b). In addition, cytokinin signaling induces the expression of (iso)flavonoid synthesis genes, influencing the accumulation of (iso)flavonoids and auxin transport, thereby impacting nodule formation (Goyal and Ramawat, 2008; Ng et al., 2015).

As previously discussed, (iso)flavonoid accumulation is induced in response to light or UV radiation, a process mediated by proteins engaged in light signal transduction pathways. As shown in Figure 4, these include UV-A and blue-light photoreceptors cryptochromes (CRYs) and phototropins (PHOTs), along with CONSTITUTIVELY PHOTOMORPHOGENIC 1 (COP1, an E3 ubiquitin ligase), ELONGATED HYPOCOTYL 5 (HY5, a basic leucine-zipper transcription factor), and B-BOX CONTAINING PROTEINs (BBXs) (Xu, 2020; Liu et al., 2023). A recent study confirmed that the photoreceptors–COP1–HY5-BBX4 regulatory module could regulate the isoflavonoid biosynthesis in soybean (Song et al., 2023). GmSTF1 and GmSTF2 (HY5 orthologs) serve as positive regulators of isoflavonoid synthesis, activating the expression of *GmPAL2.1*, *GmPAL2.3*, and *GmUGT2* while repressing *GmBBX4* expression. GmBBX4, in turn, inhibits the transcriptional activation activity of GmSTF1/2 through direct interaction. Photoreceptors CRYs and PHOTs play positive regulatory roles in light-signal-mediated isoflavonoid biosynthesis. Conversely, COP1, acting as their genetically downstream component, negatively regulates isoflavonoid synthesis by promoting the degradation of GmSTF1/2. Furthermore, GmSTF3/4 are involved in UV-mediated isoflavonoid synthesis, responding to UV-B light through the UV-B photoreceptor (UVR8) in shoots.

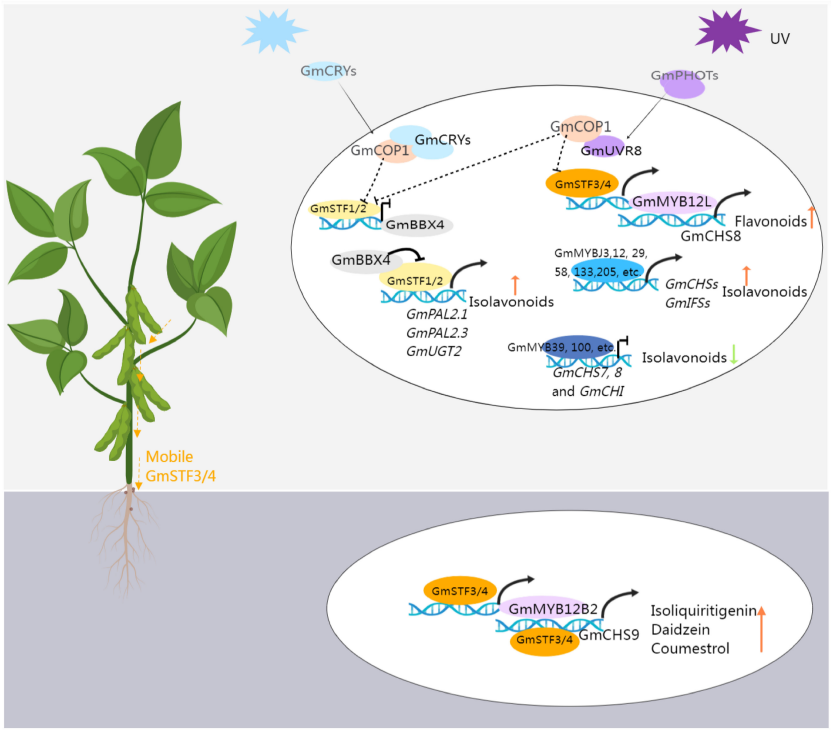

FIGURE 4
The transcriptional regulation pattern of isoflavonoid biosynthesis in soybean. Blue light activates the GmCRVs receptors, which interacts with GmCOP1, releasing GmSTF1/2 from the STF-COP1 complex. This activation leads to the expression of *GmPAL2* and *GmUGT2* by GmSTF1/2, promoting the accumulation of isoflavonoids. Additionally, at the transcriptional level, GmSTF1/2 can inhibit the expression of *GmBBX4*. At the protein level, GmBBX4 interacts with GmSTFs and suppresses their ability to activate target genes related to isoflavonoid synthesis, creating a negative feedback loop. UV activation of the URV receptor allows it to interact with COP1, releasing STF3/4 from the STF-COP1 complex. STF3/4 then activates *GmMYB12L*, which in turn activates the expression of *GmCHS8*, promoting the synthesis of flavonoids. Moreover, STF3/4 can move from the shoot to the soybean root, activating the expression of *GmMYB12B2* and *GmCHS9*, promoting the synthesis of (iso)flavonoid. The figure was created with Medpeer (https://image.medpeer.cn/).

This signal is then transmitted to the roots, activating the expression of *GmMYB12B2* and *GmCHS9*, subsequently increasing the isoflavone content (Chen et al., 2024). Investigating the impact of light on isoflavone accumulation provides both a theoretical basis and technical support for intercropping. For instance, in maize-soybean intercropping, shading effects from maize growth, limiting photosynthesis, were found to decrease mildew incidence on soybean pods, attributed to the accumulation of isoflavones in soybean under shading conditions, particularly during the vegetative stage (Li et al., 2021b).

Key enzymes in isoflavonoid biosynthesis, such as CHS, CHI, and IFS, are regulated by specific transcription factors (TFs). Notably, MYB TFs have emerged as direct regulators of isoflavonoid biosynthesis genes. As shown in Table 1, GmMYB29, GmMYB58, GmMYB205, GmMYBJ3, GmMYB12, GmMYB133, and GmMYB502 act as activators to increase the expression of *CHS* and *IFS* genes, thereby promoting the accumulation of isoflavonoids in soybean, while GmMYB39 and GmMYB100 are repressors. It is worth mentioning that GmMYB176, an R1 MYB TF, plays a dual role in isoflavonoid biosynthesis. And it decreases the isoflavonoids accumulation by down-regulating the expression of GmIFS, and increases the flavanone liquiritigenin content by activating the expression of GmCHS8, respectively. In the presence of GmbZIP5, however, GmMYB176 acts as a positive regulator to enhance the accumulation of some other isoflavonoids, such as glyceollin, isowighteone and a unique O-methylhydroxy isoflavone (Anguraj Vadivel et al., 2019, 2021). Besides, the intracellular localization of GmMYB176 or GmMYB133 can be modulated through interactions with 14–3-3 proteins, such as GmSGF14. This interaction subsequently hinders their regulatory role in isoflavonoid biosynthesis (Li and Dhaubhadel, 2012; Li et al., 2012; Bian et al., 2018). In other plant species, various MYB TFs have been documented, including positive regulators LjMYB14 and LjMYB36 in *L. japonicus*, CaMYB39 in chickpea, and a negative regulator MtPAR in *M. truncatula* (Table 1). MtPAR serves as a switch for proanthocyanidin synthesis, capable of directly inhibiting the expression of *IFS2*. Conversely, it activates the expression of anthocyanidin reductase (ANR) encoding gene in the presence of MtTT8 and MtWD40–1, leading to a reduction in isoflavone and anthocyanidin levels, thereby channeling metabolic flux towards proanthocyanidin biosynthesis (Verdier et al., 2012; Li et al., 2016b, c).

Additional regulators, including NAC and C2H2-type zinc-finger TFs, are also implicated in isoflavonoid biosynthesis. For instance, the expression of *GmNAC42–1* responds to both abiotic and biotic elicitors, stimulating the synthesis of pterocarpan glyceollin by activating *IFS2* and *G4DT* (encoding glycinol 4-dimethylallyl transferase) in soybean (Jahan et al., 2019). Notably, GmNAC42–1 is under positive regulation by GmMYB29A2, which itself acts as a positive regulator in the glyceollin biosynthetic

TABLE 1 Regulators involved in isoflavonoid biosynthesis.

Regulators		Regulatory effect	Target genes/proteins	References
Category	Name			
R2R3 MYB TF	GmMYB29	Activator	*GmIFS2* and *GmCHS8*	(Chu et al., 2017)
	GmMYB29A2	Activator	*IFS2* and *G4DT*	(Jahan et al., 2020)
	GmMYB58 and GmMYB205	Activator	*GmCHS*, *GmIFS2*, and *GmHID*	(Han et al., 2017)
	GmMYBJ3	Activator	*GmCHS8* and *GmCHI1A*	(Zhao et al., 2017)
	GmMYB1	Activator	*GmCHS8* and *GmIFS2*	(Bian et al., 2018)
	GmMYB502	Activator	*GmCHS8*, *GmIFS1*, and *GmIFS2*	(Sarkar et al., 2019)
	GmMYB12	Activator	*GmCHS8* and *GmCHS9*	(Chen et al., 2024)
	GmMYB39	Repressor	*GmCHS8*	(Liu et al., 2013)
	GmMYB100	Repressor	*Gm*CHS7 and GmCHI	(Yan et al., 2015)
	MtPAR	Inhibitor	*IFS2* and *ANR*	(Li et al., 2016c)
	LjMYB14	Activator	It is likely to be *IFS* and *IFR*.	(Shelton et al., 2012)
	LjMYB36	Activator	Unconfirmed	(Monje-Rueda et al., 2023)
	AtMYB12	Activator	*GmIFS1*	(Pandey et al., 2014)
	CaMYB39	Activator	*CHS*, *CHI*, *F3H*, F3' H, and FLS.	(Saxena et al., 2023)
R1 MYB TF	GmMYB176	Dual functions	Activate *GmCHS8* but down-regulate *GmIFS*, while interact with GmbZIP5 to enhance the level of isoflavonoids	(Yi et al., 2010; Anguraj Vadivel et al., 2019, 2021)

(Continued)

TABLE 1 Continued

Regulators		Regulatory effect	Target genes/proteins	References
Category	Name			
14–3-3 protein	GmSGF14	A negative regulator	Inhibit the function of GmMYB176.	(Li and Dhaubhadel, 2012; Li et al., 2012)
NAC	GmNAC42–1	Activator	*IFS2* and *G4DT*	(Jahan et al., 2019)
C2H2-type zinc-finger	GmZFP7	Activator	*GmIFS2* and *GmF3H1*	(Feng et al., 2023)
E3 ubiquitin ligase	GmCOP1b	A negative regulator	Promote the degradation of GmSTF1/2.	(Song et al., 2023; Chen et al., 2024)
HY5	GmSTF1/2	Activator	*GmPAL2.1*, *GmPAL2.3*, *GmUGT2* and *GmBBX4*	
	GmSTF3/4	Activator	*GmMYB12L*, *GmMYB12B2*, and *GmCHS9*	
B-BOX PROTEIN	GmBBX4	A negative regulator	Inhibit the transcriptional activation activity of GmSTF1 and GmSTF2.	
MicroRNA	*Gma-miRNA393*	A positive regulator	Unconfirmed	(Wong et al., 2014)
	Gma-miRNA5030	A negative regulator	It is likely to be *GmMYB176*.	(Gupta et al., 2019b)
	Gma-miRNA 12/24/29	A negative regulator	Correspond to *Glyma.08G181000*, *Glyma.10G224000*, and *Glyma.02G279600*, encoding different UGTs	(Gupta et al., 2017)
	Gma-miRNA26	A negative regulator	It is likely to be *Glyma.10G197900*, encoding a 4-coumarate-CoA ligase	(Gupta et al., 2019a; Elseehy, 2020)
	Gma-miRNA28	A negative regulator	It is likely to be *Glyma.09G127200*, encoding an isoflavone 7-OMT.	
DNA methyltransferase	Unconfirmed	Cytosine methylation	IFS genes	(Gupta et al., 2019a; Elseehy, 2020)

pathway (Jahan et al., 2020). Another player, GmZFP7, a C2H2 zinc-finger TF, has been reported to modulate isoflavone accumulation by activating *GmIFS2* and *Flavanone 3 β-hydroxylase 1* (*GmF3H1*) in soybean (Feng et al., 2023).

Recent studies also reveal the involvement of microRNAs (miRNAs) in post-transcriptional regulation of isoflavonoid biosynthesis. In soybean, *P. sojae* infection induced the expression of *Gma-miRNA393* in roots. Knockdown of *Gma-miRNA393* reduced isoflavonoid content and downregulated the gene expression of *GmHID1* and *GmIFS1*, while increasing susceptibility to *P. sojae*. This suggests that Gma-miRNA393 acts as a positive regulator of isoflavonoid biosynthesis; however, its downstream target genes remain unidentified (Wong et al., 2014). Table 1 delineates additional miRNAs, including Gma-miRNA12, Gma-miRNA24, Gma-miRNA29, Gma-miRNA26, and Gma-miRNA28, acting as negative regulators by interfering with the expression of their target genes. These target genes encode key enzymes or transcription factors crucial in isoflavonoid biosynthesis (Gupta et al., 2017; Gupta et al., 2019b).

Moreover, epigenetic regulation, including DNA methylation and histone modifications, has been implicated in the control of isoflavonoid accumulation (Baulcombe and Dean, 2014; Chang et al., 2020). A comprehensive comparative analysis across various soybean genotypes exhibiting distinct isoflavone contents revealed a positive correlation between the expression of the *IFS* gene and the cytosine methylation level within its coding region (Gupta et al., 2019a). This finding underscores the potential positive regulatory impact of epigenetic modifications on the intricate process of isoflavonoid biosynthesis. In the first generation (T1) of transgenic wheat (*Triticum aestivum*) overexpressing *IFS*, methylation levels in the exogenous promoter region exhibited a negative correlation with *IFS* expression (Elseehy, 2020), implying that T1 plants can reconstitute gene expression by altering the methylation status of the exogenous promoter.

Collectively, as shown in Figure 4 and Table 1, although many genes involved in the regulation of isoflavonoid synthesis and their target genes have been reported, some regulatory mechanisms are still unclear. These regulatory genes often affect the synthesis of multiple isoflavonoid compounds simultaneously. Therefore, in future, more specific factors need to be explored, such as those that uniquely control the synthesis of the subclass of isoflavonoids. In addition, as mentioned earlier, environmental factors and hormone signals play a significant role in isoflavonoid synthesis, regulation, and transport, which is also an important direction for future exploration.

Metabolic engineering of isoflavonoids biosynthesis

Isoflavonoids, recognized for their benefits in plants, livestock, and human health, have spurred research in metabolic engineering.

As shown in Table 2, strategies like antisense RNA, RNA interference, CRISPR/Cas9-mediated gene editing, co-expression, and heterologous expression have been employed for isoflavonoid engineering in legumes, non-legume plants, and microorganisms (Dixon and Steele, 1999; Zhang et al., 2020; Liu et al., 2021).

The main strategies for forage legumes breeding to increase the nutritional value and digestibility of forage include reducing anti-nutritional factors, such as lectins, saponins, oxalic acid, and condensed tannins, increasing crude protein concentrations, enhancing stress tolerance, and changing cell wall structure and composition to improve the degradability of cell wall polysaccharides (Kumar, 2011; Kulkarni et al., 2018; Katoch, 2022). Interestingly, most of these breeding goals can be achieved through metabolic engineering of phenylpropanoid biosynthesis (Dixon and Steele, 1999; Du et al., 2010). In alfalfa, overexpression of the encoding gene of isoflavone O-methyltransferase (IOMT) results in heightened levels of formononetin and medicarpin, enhancing disease resistance to *Phoma medicaginis* in transgenic plants (He and Dixon, 2000). Heterologous expression of *MtIFS1* can lead to the enhanced accumulation of medicarpin in transgenic alfalfa plants upon *P. medicaginis* infection, indicating that this modification is beneficial for plant response to stress (Deavours and Dixon, 2005). Moreover, Gou et al. disrupted the limitation of precursors by simultaneously overexpressing of *GmIFS1*, *GmCHS7* and *GmCHI1* in *M. truncatula*, promoted both isoflavone and proanthocyanidin accumulation, which are beneficial for ruminant animals (Gou et al., 2016). As shown in Table 2, the key enzyme genes involved in isoflavonoid biosynthesis are important target genes for metabolic engineering, *Caffeoyl-CoA O-methyltransferase* (*CCoAOMT*) encoding a key enzyme of lignin pathway also has an important impact on isoflavonoid synthesis. Down-regulated of *CCoAOMT* via antisense RNA technology, leading to a decrease in the content of guaiacyl (G) lignin and an increase in syringyl to guaiacyl ratio (S/G) (Guo et al., 2001). When wild-type and *CCoAOMT* downregulated plants are infected with fungi, the expression of medicarpin biosynthesis genes is upregulated in both, but more significantly in the *CCoAOMT* downregulated plants. This leads the lignin modified alfalfa to

TABLE 2 Metabolic engineering of isoflavonoid biosynthesis in model plants and microbial hosts.

Strategy	Target genes	Results	Species	References
Overexpression	*GmMYB176* and *GmbZIP5*	Accumulation of multiple isoflavonoids	Soybean	(Anguraj Vadivel et al., 2021)
Antisense RNA	*CCoAOMT*	Accumulation of medicarpin upon fungi infection	Alfalfa	(Gill et al., 2018)
RNA interference	*GmFNSII-1* and *GmFNSII-2*	Accumulation of isoflavone	Soybean	(Jiang et al., 2010)
	GmF3H and *GmFNSII*	Accumulation of isoflavone	Soybean	(Jiang et al., 2014)
Heterologous expression	*GmIFS*	Accumulation of genistein	Arabidopsis mutant (tt6/tt3)	(Liu et al., 2002)
	Co-verexpression of *CRC* and *F3H*	Accumulation of total isoflavone	Soybean	(Yu et al., 2003)
	MtIFS1	Accumulation of isoflavonoid	Alfalfa	(Deavours and Dixon, 2005)
	Fusion of *GmIFS2* and alfalfa *CHI*	Accumulation of isoflavonoid	Yeast and tobacco	(Tian and Dixon, 2006)
	GmIFS	Accumulation of genistein	Transgenic tobacco with antisense of F3H	(Liu et al., 2007)
	GmIFS	Accumulation of genistein derivatives	Rice	(Sreevidya et al., 2006)
	GmIFS2	Accumulation of genistin	Tomato	(Shih et al., 2008)
	GmIFS2	Accumulation of genistein derivatives	Brassica napus	(Li et al., 2011)
	AtMYB12 and *GmIFS1*	Accumulation of genistein glycoconjugates	Tobacco	(Pandey et al., 2014)
	GmIFS1, *GmCHS7* and *GmCHI1*	Both isoflavone and proanthocyanidin accumulation	M. truncatula	(Gou et al., 2016)
	GmCHIs and *GmIFS*	Transformation of chalcones into isoflavonoids	Yeast	(Ralston et al., 2005)
CRISPR/Cas9-mediated gene-editing	*GmF3H1*, *GmF3H2* and *GmFNSII-1*	Improvement of isoflavone content and resistance to mosaic virus	Soybean	(Zhang et al., 2020)
De novo biosynthesis	*At4CL1*, *GmCHR5*, *GmCHS8*, *GmCHI1B2*, *Ge2-HIS*, *GmHID* and *GmUGT4*	De novo biosynthesis of isoflavonoids	Yeast	(Liu et al., 2021)

redirect metabolic flux towards the medicarpin pathway upon fungal infection, thereby improving the availability of cell wall polysaccharides and resistance against fungal disease (Guo et al., 2001; Gill et al., 2018).

In soybean, the overexpression of *F3H* alone does not significantly affect the total isoflavone content. However, the overexpression of a fusion gene of the maize *C1* and *R* (*CRC*) increases the total isoflavone content in transgenic soybean seeds by approximately 2-fold. Co-verexpression of *CRC* and *F3H* can enhance the total isoflavone content by about 4-fold (Yu et al., 2003). RNA interference was used to generate silence *FNSs* (encoding flavone synthases) in soybean, which reduced the synthesis of apigenins and anthocyanins from naringenin, thus promoting the accumulation of isoflavones (Jiang et al., 2010). Notably, silencing alone of *FNSII* or *F3H* results in a ~1.3- or ~1.9-fold increase in isoflavone content, while double silencing of *FNSII* and *F3H* can result in a ~2.2-fold increase in isoflavone production compared to transgenic soybean hairy roots containing empty vectors (Jiang et al., 2014). Co-overexpression of *GmMYB176* and *GmbZIP5* results in an approximate 1.4-fold increase in the total isoflavonoid content in hairy roots (Anguraj Vadivel et al., 2021).

Non-legume plants and microorganisms can also synthesize large amounts of isoflavonoids through metabolic engineering, which involves utilizing the existing flavonoid biosynthesis pathway to provide precursors and introducing the key enzyme genes for isoflavonoid biosynthesis. For example, heterologous expression *GmIFS* in *Arabidopsis thaliana* could accumulate a small amount of genistein glycosides while introducing the GmIFS gene into *tt6/tt3* double mutant, where expression of *F3H* and *dihydroflavonol reductase* (*DFR*) was abolished, resulted in a large accumulation of genistein, which provides an important idea for the isoflavonoid accumulation via metabolic engineering (Liu et al., 2002). Heterologous expression of the IFS/CHI fusion gene in tobacco results in higher levels of genistein and its glycoside compounds compared to expressing IFS alone (Tian and Dixon, 2006). When *AtMYB12* and *GmIFS1* are co-overexpressed in tobacco, the expression of key enzyme genes in the flavonoid pathway is significantly upregulated, leading to a substantial increase in the content of flavonoid compounds and synthesizing approximately 0.05 mg/g of genistein in the fresh tissues (Pandey et al., 2014). In addition, isoflavonoids could be synthesized and accumulated in non-legume plants through the heterologous expression of *GmIFSs* in rice, tomato and *Brassica napus* (Sreevidya et al., 2006; Tian and Dixon, 2006; Liu et al., 2007; Shih et al., 2008; Li et al., 2011; Pandey et al., 2014). These results indicate that heterologous expression of key enzyme genes can achieve the synthesis of isoflavones in non-leguminous plants. However, to achieve high content, a strategy of co-expressing multiple structural genes or a combination of transcription factors with structural genes can be employed. Additionally, the activity of key isoflavone biosynthetic enzymes may vary in different non-leguminous plants, which may potentially affect the yields. For example, CHIs are divided into two groups (type I and type II). Type I CHIs, which are found in both legumes and non-legumes, function to isomerize only 6′-hydroxychalcone to 5-hydroxyflavanone (naringenin). Whereas, type II CHIs belong to a legume-specific group that are active on both 6′-deoxychalcone and 6′-hydroxychalcone, yielding 5-deoxyflavanone (liquiritigenin) and 5-hydroxyflavanone, respectively (Shimada et al., 2003). The experiments in yeast or *E. coli* strains successfully demonstrate that they have significant differences in enzymatic activity (Shimada et al., 2003; Tian and Dixon, 2006).

Recently, microorganisms such as *Saccharomyces cerevisiae* and *Escherichia coli* have been adapted and engineered for heterologous isoflavonoid synthesis, overcoming the complexity associated with biosynthesis and accumulation in non-endogenous plants through advancements in synthetic biology. The *de novo* synthesis of parent isoflavonoids, such as genistein and quercetin, has been achieved in engineered yeast strains by overexpressing at least seven enzymes (PAL/TAL, 4CL, CHS, CHI, CHR, IFS, and IFD) (Trantas et al., 2009; Rodriguez et al., 2017). Co-cultivation of an IFS-expressing *S. cerevisiae* strain with a naringenin-producing *E. coli* strain resulted in the accumulation of genistein (6 mg/L) (Katsuyama et al., 2007). Additionally, *de novo* biosynthesis of bioactive isoflavonoids and the hops bioactive flavonoid xanthohumol has been achieved in yeast (Liu et al., 2021; Yang et al., 2024). These studies demonstrate that the optimal combination of key enzyme genes from various plants, the copy number of these genes, the physical distance between adjacent key enzymes, and the accommodation of membrane proteins by the endoplasmic reticulum are factors influencing the efficient synthesis of isoflavonoids. These are all important considerations for future *de novo* synthesis of (iso) flavonoidand other complex natural products.

New technologies and resources

The CRISPR/Cas systems, known for their high efficiency and versatility, have found extensive applications in various plant genome editing and metabolic engineering endeavors (Wada et al., 2022). In *Fagopyrum tataricum*, the CRISPR/Cas9-mediated knockout of *FtMYB45* resulted in a reduction of flavonoids (Wen et al., 2022). In soybean, precise editing of key enzymes involved in isoflavonoid biosynthesis, including GmF3H1, GmF3H2, GmFNS-1, and Gm-IFS, was achieved through CRISPR/Cas9-directed mutagenesis (Zhang et al., 2020). This targeted mutagenesis led to a 2-fold increase in isoflavone content in soybean leaves and enhanced resistance to soybean mosaic virus. The study emphasized the roles of genes in isoflavonoid biosynthesis and phytohormones influencing growth effects (Mipeshwaree Devi et al., 2023).

Machine learning and multiomics approaches have also been incorporated into isoflavonoid research. Nearly thirty flavor molecule databases and various models have been identified (Kou et al., 2023). Over 1200 natural flavonoid compounds have been cataloged in the customized Flavonoid Astringency Prediction Database (FAPD, Guo et al., 2023). The establishment of this database facilitates an understanding of the relationship between the molecular structure of flavonoid compounds and their astringency in foods. Key genes in crops that influence astringency can be screened by integrating transcriptomic and

metabolomic analyses. Subsequently, transgenic or gene editing approaches are utilized to verify the functions of these genes, facilitating the breeding of superior crop varieties that are both healthy and flavorful (Qin et al., 2022; Qiu et al., 2023). Given that the distribution of isoflavonoids and the genes involved in biosynthesis, regulation and transport are strongly induced by environmental factors, and exhibit tissue specificity and developmental stage specificity in leguminous plants. The integration of single-cell sequencing and spatial transcriptomics is poised to provide robust support for further elucidation and metabolic engineering of the isoflavonoid biosynthetic pathway. For instance, the iflavonoids in the roots of leguminous plants are closely related to the formation of root nodules. Through single-cell sequencing technology, researchers can analyze the gene expression patterns of specific cell types during the root nodule formation process at the single-cell level. Combined with transcriptomic sequencing, it is possible to further explore the gene expression patterns related to isoflavonoid synthesis, regulation, transport, and secretion.

Conclusion and future prospects

Isoflavonoids play a crucial role in plant adaptation to complex environmental stimuli, with leguminous plant roots utilizing them to regulate nodule formation and influence overall growth. Consequently, exploring isoflavonoid metabolic engineering holds promise for genetic improvements in both legume and non-legume crops. However, it is important to note that changes in the composition and content of flavonoids, isoflavonoids, and lignin, which are interconnected through the phenylpropanoid pathway, could potentially have adverse effects on plants, such as reduced biomass, an imbalance between disease resistance and stress tolerance, and altered flavor. Therefore, it is necessary to consider the entire growth and developmental state of the plant, rather than focusing solely on changes in isoflavonoid content. Recent innovative approaches, exemplified by Sulis et al.'s work using a multiscale model of lignin biosynthesis, showcase effective multiplex CRISPR-editing strategies (Sulis et al., 2023). This enables the reduction of lignin levels in poplar without compromising growth, enhancing cell wall degradability, promoting cellulose utilization for papermaking and bioenergy production, and minimizing environmental impact. These advances provide valuable insights for precise and efficient crop genetic breeding.

What is the relationship between the molecular structure of isoflavonoid compounds and their bioactivity and flavor? Which genes determine the production of specific isoflavonoids? Which genes influence the transformation between free isoflavonoids and their modifications? What is the connection between the accumulation or secretion of plant isoflavonoids and the environment? Can the synthesis of isoflavonoids in non-leguminous plants achieve symbiosis with rhizobia to enhance nitrogen fixation? These are all subjects that require further research and exploration. Further exploration of diverse isoflavonoids and derivatives through metabolic engineering or synthetic biology requires the identification of key enzyme genes and regulators. Integration of machine learning and database predictions may expedite the discovery of additional enzymes and compounds. The future lies in the collaborative efforts of synthetic biology and metabolic engineering for efficient and sustainable isoflavonoid production. Advancements in multi-omics technologies are anticipated to unravel key insights into isoflavonoid biosynthesis, transport, and accumulation.

Author contributions

LW: Funding acquisition, Resources, Writing – original draft, Data curation, Writing – review & editing. CL: Funding acquisition, Writing – original draft, Resources, Writing – review & editing. KL: Writing – original draft, Writing – review & editing.

Funding

The author(s) declare financial support was received for the research, authorship, and/or publication of this article. This work was supported by the Natural Science Foundation of China (31901333, 32372040), the Natural Science Foundation of Southwest University of Science and Technology (19zx7120), the Fundamental Research Funds for the Central Universities of Southwest University (SWU-KQ22074).

Conflict of interest

The authors declare that the research was conducted in the absence of any commercial or financial relationships that could be construed as a potential conflict of interest.

Publisher's note

References

Abd-Alla, M. H., Al-Amri, S. M., and El-Enany, A.-W. E. (2023). Enhancing rhizobium–legume symbiosis and reducing nitrogen fertilizer use are potential options for mitigating climate change. *Agriculture* 13, 2092. doi: 10.3390/agriculture13112092

Abderamane, B., Tih, A. E., Ghogomu, R. T., Blond, A., and Bodo, B. (2011). Isoflavonoid derivatives from Lophira alata stem heartwood. *Z Naturforsch. C J. Biosci.* 66, 87–92. doi: 10.1515/znc-2011-3-401

Ahmad, M. Z., Li, P., Wang, J., Rehman, N. U., and Zhao, J. (2017). Isoflavone malonyltransferases GmIMaT1 and GmIMaT3 differently modify isoflavone glucosides in soybean (*Glycine max*) under various stresses. *Front. Plant Sci.* 8. doi: 10.3389/fpls.2017.00735

Ahmad, M. Z., Zhang, Y., Zeng, X., Li, P., Wang, X., Benedito, V. A., et al. (2021). Isoflavone malonyl-CoA acyltransferase GmMaT2 is involved in nodulation of soybean by modifying synthesis and secretion of isoflavones. *J. Exp. Bot.* 72, 1349–1369. doi: 10.1093/jxb/eraa511

Akashi, T., Aoki, T., and Ayabe, S. (2005). Molecular and biochemical characterization of 2-hydroxyisoflavanone dehydratase. Involvement of carboxylesterase-like proteins in leguminous isoflavone biosynthesis. *Plant Physiol.* 137, 882–891. doi: 10.1104/pp.104.056747

Akashi, T., Koshimizu, S., Aoki, T., and Ayabe, S. (2006). Identification of cDNAs encoding pterocarpan reductase involved in isoflavan phytoalexin biosynthesis in *Lotus japonicus* by EST mining. *FEBS Lett.* 580, 5666–5670. doi: 10.1016/j.febslet.2006.09.016

Akashi, T., Sasaki, K., Aoki, T., Ayabe, S., and Yazaki, K. (2009). Molecular cloning and characterization of a cDNA for pterocarpan 4-dimethylallyltransferase catalyzing the key prenylation step in the biosynthesis of glyceollin, a soybean phytoalexin. *Plant Physiol.* 149, 683–693. doi: 10.1104/pp.108.123679

Akashi, T., Sawada, Y., Shimada, N., Sakurai, N., Aoki, T., and Ayabe, S. (2003). cDNA cloning and biochemical characterization of S-adenosyl-L-methionine: 2,7,4'-trihydroxyisoflavanone 4'-O-methyltransferase, a critical enzyme of the legume isoflavonoid phytoalexin pathway. *Plant Cell Physiol.* 44, 103–112. doi: 10.1093/pcp/pcg034

Anguraj Vadivel, A. K., McDowell, T., Renaud, J. B., and Dhaubhadel, S. (2021). A combinatorial action of GmMYB176 and GmbZIP5 controls isoflavonoid biosynthesis in soybean (*Glycine max*). *Commun. Biol.* 4, 356. doi: 10.1038/s42003–021-01889–6

Anguraj Vadivel, A. K., Renaud, J., Kagale, S., and Dhaubhadel, S. (2019). GmMYB176 regulates multiple steps in isoflavonoid biosynthesis in soybean. *Front. Plant Sci.* 10. doi: 10.3389/fpls.2019.00562

Anzeveno, P. B. (1979). Rotenoid interconversion. Synthesis of deguelin from rotenone. *J. Organic Chem.* 44, 2578–2580. doi: 10.1021/jo01328a056

Araya-Cloutier, C., den Besten, H. M., Aisyah, S., Gruppen, H., and Vincken, J. P. (2017). The position of prenylation of isoflavonoids and stilbenoids from legumes (Fabaceae) modulates the antimicrobial activity against Gram positive pathogens. *Food Chem.* 226, 193–201. doi: 10.1016/j.foodchem.2017.01.026

Araya-Cloutier, C., Vincken, J. P., van de Schans, M. G. M., Hageman, J., Schaftenaar, G., den Besten, H. M. W., et al. (2018). QSAR-based molecular signatures of prenylated (iso)flavonoids underlying antimicrobial potency against and membrane-disruption in Gram positive and Gram negative bacteria. *Sci. Rep.* 8, 9267. doi: 10.1038/s41598–018-27545–4

Banasiak, J., Biala, W., Staszkow, A., Swarcewicz, B., Kepczynska, E., Figlerowicz, M., et al. (2013). A *Medicago truncatula* ABC transporter belonging to subfamily G modulates the level of isoflavonoids. *J. Exp. Bot.* 64, 1005–1015. doi: 10.1093/jxb/ers380

Baulcombe, D. C., and Dean, C. (2014). Epigenetic regulation in plant responses to the environment. *Cold Spring Harb. Perspect. Biol.* 6, a019471. doi: 10.1101/cshperspect.a019471

Benkova, E., Michniewicz, M., Sauer, M., Teichmann, T., Seifertova, D., Jurgens, G., et al. (2003). Local, efflux-dependent auxin gradients as a common module for plant organ formation. *Cell* 115, 591–602. doi: 10.1016/S0092-8674(03)00924-3

Biala, W., Banasiak, J., Jarzyniak, K., Pawela, A., and Jasinski, M. (2017). *Medicago truncatula* ABCG10 is a transporter of 4-coumarate and liquiritigenin in the medicarpin biosynthetic pathway. *J. Exp. Bot.* 68, 3231–3241. doi: 10.1093/jxb/erx059

Biala-Leonhard, W., Zanin, L., Gottardi, S., de Brito Francisco, R., Venuti, S., Valentinuzzi, F., et al. (2021). Identification of an isoflavonoid transporter required for the nodule establishment of the rhizobium-fabaceae symbiotic interaction. *Front. Plant Sci.* 12. doi: 10.3389/fpls.2021.758213

Bian, S., Li, R., Xia, S., Liu, Y., Jin, D., Xie, X., et al. (2018). Soybean CCA1-like MYB transcription factor GmMYB133 modulates isoflavonoid biosynthesis. *Biochem. Biophys. Res. Commun.* 507, 324–329. doi: 10.1016/j.bbrc.2018.11.033

Boivin, S., Fonouni-Farde, C., and Frugier, F. (2016). How auxin and cytokinin phytohormones modulate root microbe interactions. *Front. Plant Sci.* 7 1240. doi: 10.3389/fpls.2016.01240

Boue, S. M., Carter, C. H., Ehrlich, K. C., and Cleveland, T. E. (2000). Induction of the soybean phytoalexins coumestrol and glyceollin by Aspergillus. *J. Agric. Food Chem.* 48, 2167–2172. doi: 10.1021/jf9912809

Breakspear, A., Liu, C., Roy, S., Stacey, N., Rogers, C., Trick, M., et al. (2014). The root hair "infectome" of *Medicago truncatula* uncovers changes in cell cycle genes and reveals a requirement for Auxin signaling in rhizobial infection. *Plant Cell* 26, 4680–4701. doi: 10.1105/tpc.114.133496

Cannon, J. R., Tapias, V., Na, H. M., Honick, A. S., Drolet, R. E., and Greenamyre, J. T. (2009). A highly reproducible rotenone model of Parkinson's disease. *Neurobiol. Dis.* 34, 279–290. doi: 10.1016/j.nbd.2009.01.016

Chang, Y. N., Zhu, C., Jiang, J., Zhang, H., Zhu, J. K., and Duan, C. G. (2020). Epigenetic regulation in plant abiotic stress responses. *J. Integr. Plant Biol.* 62, 563–580. doi: 10.1111/jipb.12901

Chen, J., Xu, H., Liu, Q., Ke, M., Zhang, Z., Wang, X., et al. (2024). Shoot-to-root communication via GmUVR8-GmSTF3 photosignaling and flavonoid biosynthesis fine-tunes soybean nodulation under UV-B light. *New Phytol.* 241, 209–226. doi: 10.1111/nph.19353

Chu, S., Wang, J., Zhu, Y., Liu, S., Zhou, X., Zhang, H., et al. (2017). An R2R3-type MYB transcription factor, GmMYB29, regulates isoflavone biosynthesis in soybean. *PloS Genet.* 13, e1006770. doi: 10.1371/journal.pgen.1006770

Darbour, N., Bayet, C., Rodin-Bercion, S., Elkhomsi, Z., Lurel, F., Chaboud, A., et al. (2007). Isoflavones from ficus nymphaefolia. *Nat. Prod Res.* 21, 461–464. doi: 10.1080/14786410601086871

Dastmalchi, M., Chapman, P., Yu, J., Austin, R. S., and Dhaubhadel, S. (2017). Transcriptomic evidence for the control of soybean root isoflavonoid content by regulation of overlapping phenylpropanoid pathways. *BMC Genomics* 18, 70. doi: 10.1186/s12864-016-3463-y

Deavours, B. E., and Dixon, R. A. (2005). Metabolic engineering of isoflavonoid biosynthesis in alfalfa. *Plant Physiol.* 138, 2245–2259. doi: 10.1104/pp.105.062539

Deng, Y. T., Huang, H. C., and Lin, J. K. (2010). Rotenone induces apoptosis in MCF-7 human breast cancer cell-mediated ROS through JNK and p38 signaling. *Mol. Carcinogenesis: Published cooperation Univ. Texas MD Anderson Cancer Center* 49, 141–151. doi: 10.1002/mc.20583

Dewick, P. M., and Martin, M. (1979). Biosynthesis of pterocarpan and isoflavan phytoalexins in *Medicago sativa*: the biochemical interconversion of pterocarpans and 2′-hydroxyisoflavans. *Phytochemistry* 18, 591–596. doi: 10.1016/S0031-9422(00)84266-1

Dixon, R. A. (1999). Isoflavonoids: biochemistry, molecular biology and biological functions. *Compr. Natural products Chem.* 1, 773–823. doi: 10.1016/B978-0-08-091283-7.00030-8

Dixon, R. A. (2004). Phytoestrogens. *Annu. Rev. Plant Biol.* 55, 225–261. doi: 10.1146/annurev.arplant.55.031903.141729

Dixon, R. A., and Ferreira, D. (2002). Genistein. *Phytochemistry* 60, 205–211. doi: 10.1016/S0031-9422(02)00116-4

Dixon, R. A., Harrison, M. J., and Paiva, N. L. (1995). The isoflavonoid phytoalexin pathway: from enzymes to genes to transcription factors. *Physiologia Plantarum* 93, 385–392. doi: 10.1111/j.1399-3054.1995.tb02243.x

Dixon, R. A., and Paiva, N. L. (1995). Stress-induced phenylpropanoid metabolism. *Plant Cell* 7, 1085–1097. doi: 10.2307/3870059

Dixon, R. A., and Steele, C. L. (1999). Flavonoids and isoflavonoids - a gold mine for metabolic engineering. *Trends Plant Sci.* 4, 394–400. doi: 10.1016/S1360-1385(99)01471-5

Dong, N. Q., and Lin, H. X. (2021). Contribution of phenylpropanoid metabolism to plant development and plant-environment interactions. *J. Integr. Plant Biol.* 63, 180–209. doi: 10.1111/jipb.13054

Du, H., Huang, Y., and Tang, Y. (2010). Genetic and metabolic engineering of isoflavonoid biosynthesis. *Appl. Microbiol. Biotechnol.* 86, 1293–1312. doi: 10.1007/s00253-010-2512-8

Elseehy, M. M. (2020). Differential transgeneration methylation of exogenous promoters in T1 transgenic wheat (*Triticum aestivum*). *Cytol. Genet.* 54, 493–504. doi: 10.3103/S0095452720050151

Farag, M. A., Huhman, D. V., Dixon, R. A., and Sumner, L. W. (2008). Metabolomics reveals novel pathways and differential mechanistic and elicitor-specific responses in phenylpropanoid and isoflavonoid biosynthesis in *Medicago truncatula* cell cultures. *Plant Physiol.* 146, 387–402. doi: 10.1104/pp.107.108431

Feng, Y., Zhang, S., Li, J., Pei, R., Tian, L., Qi, J., et al. (2023). Dual-function C2H2-type zinc-finger transcription factor GmZFP7 contributes to isoflavone accumulation in soybean. *New Phytol.* 237, 1794–1809. doi: 10.1111/nph.18610

Funaki, A., Waki, T., Noguchi, A., Kawai, Y., Yamashita, S., Takahashi, S., et al. (2015). Identification of a highly specific isoflavone 7-O-glucosyltransferase in the soybean (*Glycine max* (L.) Merr.). *Plant Cell Physiol.* 56, 1512–1520. doi: 10.1093/pcp/pcv072

Gao, Z., Chen, Z., Cui, Y., Ke, M., Xu, H., Xu, Q., et al. (2021). GmPIN-dependent polar auxin transport is involved in soybean nodule development. *Plant Cell* 33, 2981–3003. doi: 10.1093/plcell/koab183

Gao, Y., Yao, Y., Zhu, Y., and Ren, G. (2015). Isoflavone content and composition in chickpea (*Cicer arietinum* L.) sprouts germinated under different conditions. *J. Agric. Food Chem.* 63, 2701–2707. doi: 10.1021/jf5057524

Gill, U. S., Uppalapati, S. R., Gallego-Giraldo, L., Ishiga, Y., Dixon, R. A., and Mysore, K. S. (2018). Metabolic flux towards the (iso)flavonoid pathway in lignin modified alfalfa lines induces resistance against *Fusarium oxysporum* f. sp. *medicaginis*. *Plant Cell Environ.* 41, 1997–2007. doi: 10.1111/pce.13093

Gou, L., Zhang, R., Ma, L., Zhu, F., Dong, J., and Wang, T. (2016). Multigene synergism increases the isoflavone and proanthocyanidin contents of *Medicago truncatula*. *Plant Biotechnol. J.* 14, 915–925. doi: 10.1111/pbi.12445

Goyal, S., and Ramawat, K. (2008). Synergistic effect of morphactin on cytokinin-induced production of isoflavonoids in cell cultures of *Pueraria tuberosa* (Roxb. ex. Willd.) DC. *Plant Growth Regul.* 55, 175–181. doi: 10.1007/s10725-008-9271-x

Griffiths, K., Wilson, D. W., Singh, R. B., and De Meester, F. (2014). Effect of dietary phytoestrogens on human growth regulation: imprinting in health & disease. *Indian J. Med. Res.* 140 Suppl, S82–S90.

Guo, D., Chen, F., Inoue, K., Blount, J. W., and Dixon, R. A. (2001). Downregulation of caffeic acid 3-O-methyltransferase and caffeoyl CoA 3-O-methyltransferase in transgenic alfalfa. Impacts on lignin structure and implications for the biosynthesis of G and S lignin. *Plant Cell* 13, 73–88. doi: 10.1105/tpc.13.1.73

Guo, L., and Paiva, N. L. (1995). Molecular cloning and expression of alfalfa (*Medicago sativa* L.) vestitone reductase, the penultimate enzyme in medicarpin biosynthesis. *Arch. Biochem. biophys.* 320, 353–360. doi: 10.1016/0003-9861(95)90019-5

Guo, T., Pan, F., Cui, Z., Yang, Z., Chen, Q., Zhao, L., et al. (2023). FAPD: an astringency threshold and astringency type prediction database for flavonoid compounds based on machine learning. *J. Agric. Food Chem.* 71, 4172–4183. doi: 10.1021/acs.jafc.2c08822

Gupta, O. P., Dahuja, A., Sachdev, A., Jain, P. K., Kumari, S., Vinutha, T., et al. (2019a). Cytosine methylation of isoflavone synthase gene in the genic region positively regulates its expression and isoflavone biosynthesis in soybean seeds. *DNA Cell Biol.* 38, 510–520. doi: 10.1089/dna.2018.4584

Gupta, O. P., Dahuja, A., Sachdev, A., Kumari, S., Jain, P. K., Vinutha, T., et al. (2019b). Conserved miRNAs modulate the expression of potential transcription factors of isoflavonoid biosynthetic pathway in soybean seeds. *Mol. Biol. Rep.* 46, 3713–3730. doi: 10.1007/s11033-019-04814-7

Gupta, O. P., Nigam, D., Dahuja, A., Kumar, S., Vinutha, T., Sachdev, A., et al. (2017). Regulation of isoflavone biosynthesis by miRNAs in two contrasting soybean genotypes at different seed developmental stages. *Front. Plant Sci.* 8. doi: 10.3389/fpls.2017.00567

Gutierrez-Gonzalez, J. J., Guttikonda, S. K., Tran, L.-S. P., Aldrich, D. L., Zhong, R., Yu, O., et al. (2010). Differential expression of isoflavone biosynthetic genes in soybean during water deficits. *Plant Cell Physiol.* 51, 936–948. doi: 10.1093/pcp/pcq065

Gutierrez-Gonzalez, J. J., Wu, X., Zhang, J., Lee, J.-D., Ellersieck, M., Shannon, J. G., et al. (2009). Genetic control of soybean seed isoflavone content: importance of statistical model and epistasis in complex traits. *Theor. Appl. Genet.* 119, 1069–1083. doi: 10.1007/s00122-009-1109-z

Ha, J., Kang, Y. G., Lee, T., Kim, M., Yoon, M. Y., Lee, E., et al. (2019). Comprehensive RNA sequencing and co-expression network analysis to complete the biosynthetic pathway of coumestrol, a phytoestrogen. *Sci. Rep.* 9, 1934. doi: 10.1038/s41598–018-38219–6

Hail, N. Jr., and Lotan, R. (2004). Apoptosis induction by the natural product cancer chemopreventive agent deguelin is mediated through the inhibition of mitochondrial bioenergetics. *Apoptosis* 9, 437–447. doi: 10.1023/B:APPT.0000031449.57551.e1

Hakamatsuka, T., Mori, K., Ishida, S., Ebizuka, Y., and Sankawa, U. (1998). Purification of 2-hydroxyisoflavanone dehydratase from the cell cultures of Pueraria lobata in honour of Professor GH Neil Towers 75th birthday. *Phytochemistry* 49, 497–505. doi: 10.1016/S0031-9422(98)00266-0

Han, X., Yin, Q., Liu, J., Jiang, W., Di, S., and Pang, Y. (2017). GmMYB58 and GmMYB205 are seed-specific activators for isoflavonoid biosynthesis in *Glycine max*. *Plant Cell Rep.* 36, 1889–1902. doi: 10.1007/s00299-017-2203-3

Hayashi, H., Hiraoka, N., Ikeshiro, Y., and Yamamoto, H. (1996). Organ specific localization of flavonoids in *Glycyrrhiza glabra* L. *Plant Sci.* 116, 233–238. doi: 10.1016/0168-9452(96)04387-7

He, X. Z., and Dixon, R. A. (2000). Genetic manipulation of isoflavone 7-O-methyltransferase enhances biosynthesis of 4'-O-methylated isoflavonoid phytoalexins and disease resistance in alfalfa. *Plant Cell* 12, 1689–1702. doi: 10.1105/tpc.12.9.1689

Higgins, V. J. (1972). Role of the phytoalexin medicarpin in three leaf spot diseases of alfalfa. *Physiol. Plant Pathol.* 2, 289–300. doi: 10.1016/0048-4059(72)90012-4

Ingham, J. L., and Harborne, J. B. (1976). Phytoalexin induction as a new dynamic approach to the study of systematic relationships among higher plants. *Nature* 260, 241–243. doi: 10.1038/260241a0

Jahan, M. A., Harris, B., Lowery, M., Coburn, K., Infante, A. M., Percifield, R. J., et al. (2019). The NAC family transcription factor GmNAC42–1 regulates biosynthesis of the anticancer and neuroprotective glyceollins in soybean. *BMC Genomics* 20, 149. doi: 10.1186/s12864-019-5524-5

Jahan, M. A., Harris, B., Lowery, M., Infante, A. M., Percifield, R. J., and Kovinich, N. (2020). Glyceollin transcription factor GmMYB29A2 regulates soybean resistance to *Phytophthora sojae*. *Plant Physiol.* 183, 530–546. doi: 10.1104/pp.19.01293

Jasinski, M., Banasiak, J., Radom, M., Kalitkiewicz, A., and Figlerowicz, M. (2009). Full-size ABC transporters from the ABCG subfamily in *Medicago truncatula*. *Mol. Plant Microbe Interact.* 22, 921–931. doi: 10.1094/MPMI-22-8-0921

Jeong, Y. J., An, C. H., Park, S. C., Pyun, J. W., Lee, J., Kim, S. W., et al. (2018). Methyl jasmonate increases isoflavone production in soybean cell cultures by activating structural genes involved in isoflavonoid biosynthesis. *J. Agric. Food Chem.* 66, 4099–4105. doi: 10.1021/acs.jafc.8b00350

Jiang, Y., Hu, Y., Wang, B., and Wu, T. (2014). Bivalent RNA interference to increase isoflavone biosynthesis in soybean (*Glycine max*). *Braz. Arch. Biol. Technol.* 57, 163–170. doi: 10.1590/S1516-89132013005000018

Jiang, Y. N., Wang, B., Li, H., Yao, L. M., and Wu, T. L. (2010). Flavonoid production is effectively regulated by RNAi interference of two flavone synthase genes from *Glycine max*. *J. Plant Biol.* 53, 425–432. doi: 10.1007/s12374-010-9132-9

Jung, W., Yu, O., Lau, S. M., O'Keefe, D. P., Odell, J., Fader, G., et al. (2000). Identification and expression of isoflavone synthase, the key enzyme for biosynthesis of isoflavones in legumes. *Nat. Biotechnol.* 18, 208–212. doi: 10.1038/72671

Kaducová, M., Eliašová, A., Trush, K., Bačovčinová, M., Sklenková, K., and Pal'ove-Balang, P. (2022). Accumulation of isoflavonoids in *Lotus* corniculatus after UV-B irradiation. *Theor. Exp. Plant Physiol.* 34, 53–62. doi: 10.1007/s40626-021-00228-8

Kaducova, M., Monje-Rueda, M. D., Garcia-Calderon, M., Perez-Delgado, C. M., Eliasova, A., Gajdosova, S., et al. (2019). Induction of isoflavonoid biosynthesis in *Lotus japonicus* after UV-B irradiation. *J. Plant Physiol.* 236, 88–95. doi: 10.1016/j.jplph.2019.03.003

Kalli, S., Araya-Cloutier, C., Hageman, J., and Vincken, J. P. (2021). Insights into the molecular properties underlying antibacterial activity of prenylated (iso)flavonoids against MRSA. *Sci. Rep.* 11, 14180. doi: 10.1038/s41598–021-92964–9

Katoch, R. (2022). "Approaches for Nutritional Quality Improvement in Forages," in *Nutritional Quality Management of Forages in the Himalayan Region* (Singapore: Springer Singapore), 167–192. doi: 10.1007/978-981-16-5437-4

Katsuyama, Y., Miyahisa, I., Funa, N., and Horinouchi, S. (2007). One-pot synthesis of genistein from tyrosine by coincubation of genetically engineered Escherichia coli and Saccharomyces cerevisiae cells. *Appl. Microbiol. Biotechnol.* 73, 1143–1149. doi: 10.1007/s00253-006-0568-2

Kaufman, P. B., Duke, J. A., Brielmann, H., Boik, J., and Hoyt, J. E. (1997). A comparative survey of leguminous plants as sources of the isoflavones, genistein and daidzein: implications for human nutrition and health. *J. Altern. Complement Med.* 3, 7–12. doi: 10.1089/acm.1997.3.7

Kessmann, H., Edwards, R., Geno, P. W., and Dixon, R. A. (1990). Stress responses in alfalfa (*Medicago sativa* L.): V. Constitutive and elicitor-induced accumulation of isoflavonoid conjugates in cell suspension cultures. *Plant Physiol.* 94, 227–232. doi: 10.1104/pp.94.1.227

Kohlen, W., Ng, J. L. P., Deinum, E. E., and Mathesius, U. (2018). Auxin transport, metabolism, and signalling during nodule initiation: indeterminate and determinate nodules. *J. Exp. Bot.* 69, 229–244. doi: 10.1093/jxb/erx308

Kou, X., Shi, P., Gao, C., Ma, P., Xing, H., Ke, Q., et al. (2023). Data-driven elucidation of flavor chemistry. *J. Agric. Food Chem.* 71, 6789–6802. doi: 10.1021/acs.jafc.3c00909

Ku, Y. S., Cheng, S. S., Cheung, M. Y., Niu, Y., Liu, A., Chung, G., et al. (2022). The poly-glutamate motif of GmMATE4 regulates its isoflavone transport activity. *Membranes (Basel)* 12, 206. doi: 10.3390/membranes12020206

Ku, Y. S., Ng, M. S., Cheng, S. S., Lo, A. W., Xiao, Z., Shin, T. S., et al. (2020). Understanding the composition, biosynthesis, accumulation and transport of flavonoids in crops for the promotion of crops as healthy sources of flavonoids for human consumption. *Nutrients* 12, 1717. doi: 10.3390/nu12061717

Kulkarni, K. P., Tayade, R., Asekova, S., Song, J. T., Shannon, J. G., and Lee, J. D. (2018). Harnessing the potential of forage legumes, alfalfa, soybean, and cowpea for sustainable agriculture and global food security. *Front. Plant Sci.* 9. doi: 10.3389/fpls.2018.01314

Kumar, S. (2011). Biotechnological advancements in alfalfa improvement. *J. Appl. Genet.* 52, 111–124. doi: 10.1007/s13353-011-0028-2

Kurepa, J., Shull, T. E., and Smalle, J. A. (2023). Friends in arms: Flavonoids and the auxin/cytokinin balance in terrestrialization. *Plants (Basel)* 12, 517. doi: 10.3390/plants12030517

Laffont, C., Blanchet, S., Lapierre, C., Brocard, L., Ratet, P., Crespi, M., et al. (2010). The compact root architecture1 gene regulates lignification, flavonoid production, and polar auxin transport in medicago truncatula. *Plant Physiol.* 153, 1597–1607. doi: 10.1104/pp.110.156620

Lee, H. I., Lee, J. H., Park, K. H., Sangurdekar, D., and Chang, W. S. (2012). Effect of soybean coumestrol on Bradyrhizobium japonicum nodulation ability, biofilm formation, and transcriptional profile. *Appl. Environ. Microbiol.* 78, 2896–2903. doi: 10.1128/AEM.07336-11

Lee, E. J., Song, M. C., and Rha, C. S. (2022). Mass biosynthesis of coumestrol derivatives and their isomers via soybean adventitious root cultivation in bioreactors. *Front. Plant Sci.* 13. doi: 10.3389/fpls.2022.923163

Le Roy, J., Huss, B., Creach, A., Hawkins, S., and Neutelings, G. (2016). Glycosylation is a major regulator of phenylpropanoid availability and biological activity in plants. *Front. Plant Sci.* 7. doi: 10.3389/fpls.2016.00735

Li, Z. S., Alfenito, M., Rea, P. A., Walbot, V., and Dixon, R. A. (1997). Vacuolar uptake of the phytoalexin medicarpin by the glutathione conjugate pump. *Phytochemistry* 45, 689–693. doi: 10.1016/S0031-9422(97)00031-9

Li, X., Chen, L., and Dhaubhadel, S. (2012). 14–3-3 proteins regulate the intracellular localization of the transcriptional activator GmMYB176 and affect isoflavonoid synthesis in soybean. *Plant J.* 71, 239–250. doi: 10.1111/j.1365-313X.2012.04986.x

Li, P., Chen, B., Zhang, G., Chen, L., Dong, Q., Wen, J., et al. (2016b). Regulation of anthocyanin and proanthocyanidin biosynthesis by *Medicago truncatula* bHLH transcription factor MtTT8. *New Phytol.* 210, 905–921. doi: 10.1111/nph.13816

Li, X., and Dhaubhadel, S. (2012). 14–3-3 proteins act as scaffolds for GmMYB62 and GmMYB176 and regulate their intracellular localization in soybean. *Plant Signal Behav.* 7, 965–968. doi: 10.4161/psb.20940

Li, P., Dong, Q., Ge, S., He, X., Verdier, J., Li, D., et al. (2016c). Metabolic engineering of proanthocyanidin production by repressing the isoflavone pathways and redirecting anthocyanidin precursor flux in legume. *Plant Biotechnol. J.* 14, 1604–1618. doi: 10.1111/pbi.12524

Li, J., Li, C., Gou, J., and Zhang, Y. (2016a). Molecular cloning and functional characterization of a novel isoflavone 3'-O-methyltransferase from *Pueraria lobata*. *Front. Plant Sci.* 7. doi: 10.3389/fpls.2016.00793

Li, J., Li, Z., Li, C., Gou, J., and Zhang, Y. (2014). Molecular cloning and characterization of an isoflavone 7-O-glucosyltransferase from *Pueraria lobata*. *Plant Cell Rep.* 33, 1173–1185. doi: 10.1007/s00299-014-1606-7

Li, X., Qin, J. C., Wang, Q. Y., Wu, X., Lang, C. Y., Pan, H. Y., et al. (2011). Metabolic engineering of isoflavone genistein in Brassica napus with soybean isoflavone synthase. *Plant Cell Rep.* 30, 1435–1442. doi: 10.1007/s00299-011-1052-8

Li, X., Yang, C., Chen, J., He, Y., Deng, J., Xie, C., et al. (2021b). Changing light promotes isoflavone biosynthesis in soybean pods and enhances their resistance to mildew infection. *Plant Cell Environ.* 44, 2536–2550. doi: 10.1111/pce.14128

Li, A., Zhao, Z., Zhang, S., Zhang, Z., and Shi, Y. (2021a). Fungicidal activity and mechanism of action of glabridin from *Glycyrrhiza glabra* L. *Int. J. Mol. Sci.* 22, 10966. doi: 10.3390/ijms222010966

Liu, C. J., Blount, J. W., Steele, C. L., and Dixon, R. A. (2002). Bottlenecks for metabolic engineering of isoflavone glycoconjugates in *Arabidopsis*. *Proc. Natl. Acad. Sci. U.S.A.* 99, 14578–14583. doi: 10.1073/pnas.212522099

Liu, C. J., Deavours, B. E., Richard, S. B., Ferrer, J. L., Blount, J. W., Huhman, D., et al. (2006). Structural basis for dual functionality of isoflavonoid O-methyltransferases in the evolution of plant defense responses. *Plant Cell* 18, 3656–3669. doi: 10.1105/tpc.106.041376

Liu, C. J., and Dixon, R. A. (2001). Elicitor-induced association of isoflavone O-methyltransferase with endomembranes prevents the formation and 7-O-methylation of daidzein during isoflavonoid phytoalexin biosynthesis. *Plant Cell* 13, 2643–2658. doi: 10.1105/tpc.010382

Liu, R., Hu, Y., Li, J., and Lin, Z. (2007). Production of soybean isoflavone genistein in non-legume plants via genetically modified secondary metabolism pathway. *Metab. Eng.* 9, 1–7. doi: 10.1016/j.ymben.2006.08.003

Liu, Q., Liu, Y., Li, G., Savolainen, O., Chen, Y., and Nielsen, J. (2021). *De novo* biosynthesis of bioactive isoflavonoids by engineered yeast cell factories. *Nat. Commun.* 12, 6085. doi: 10.1038/s41467-021-26361-1

Liu, Y., Singh, S. K., Pattanaik, S., Wang, H., and Yuan, L. (2023). Light regulation of the biosynthesis of phenolics, terpenoids, and alkaloids in plants. *Commun. Biol.* 6, 1055. doi: 10.1038/s42003-023-05435-4

Liu, X., Yuan, L., Xu, L., Xu, Z., Huang, Y., He, X., et al. (2013). Over-expression of GmMYB39 leads to an inhibition of the isoflavonoid biosynthesis in soybean (*Glycine max*. L). *Plant Biotechnol. Rep.* 7, 445–455. doi: 10.1007/s11816-013-0283-2

Lygin, A. V., Hill, C. B., Zernova, O. V., Crull, L., Widholm, J. M., Hartman, G. L., et al. (2010). Response of soybean pathogens to glyceollin. *Phytopathology* 100, 897–903. doi: 10.1094/PHYTO-100-9-0897

Mackova, Z., Koblovska, R., and Lapcik, O. (2006). Distribution of isoflavonoids in non-leguminous taxa - an update. *Phytochemistry* 67, 849–855. doi: 10.1016/j.phytochem.2006.01.020

Martin, M., and Dewick, P. M. (1980). Biosynthesis of pterocarpan, isoflavan and coumestan metabolites of *Medicago sativa*: The role of an isoflav-3-ene. *Phytochemistry* 19, 2341–2346. doi: 10.1016/S0031-9422(00)91023-9

Mathesius, U. (2001). Flavonoids induced in cells undergoing nodule organogenesis in white clover are regulators of auxin breakdown by peroxidase. *J. Exp. Bot.* 52, 419–426. doi: 10.1093/jexbot/52.suppl_1.419

Mipeshwaree Devi, A., Khedashwori Devi, K., Premi Devi, P., Lakshmipriyari Devi, M., and Das, S. (2023). Metabolic engineering of plant secondary metabolites: prospects and its technological challenges. *Front. Plant Sci.* 14. doi: 10.3389/fpls.2023.1171154

Monje-Rueda, M. D., Pal'ove-Balang, P., Trush, K., Marquez, A. J., Betti, M., and Garcia-Calderon, M. (2023). Mutation of MYB36 affects isoflavonoid metabolism, growth, and stress responses in *Lotus japonicus*. *Physiol. Plant* 175, e14084. doi: 10.1111/ppl.14084

Mouffouk, S., Marcourt, L., Benkhaled, M., Boudiaf, K., Wolfender, J.-L., and Haba, H. (2017). Two new prenylated isoflavonoids from *Erinacea anthyllis* with antioxidant and antibacterial activities. *Natural Product Commun.* 12, 1934578X1701200716. doi: 10.1177/1934578X1701200716

Mukne, A. P., Viswanathan, V., and Phadatare, A. G. (2011). Structure pre-requisites for isoflavones as effective antibacterial agents. *Pharmacogn Rev.* 5, 13–18. doi: 10.4103/0973-7847.79095

Mun, B. G., Kim, H. H., Yuk, H. J., Hussain, A., Loake, G. J., and Yun, B. W. (2021). A potential role of coumestrol in soybean leaf senescence and its interaction with phytohormones. *Front. Plant Sci.* 12. doi: 10.3389/fpls.2021.756308

Muro-Villanueva, F., Mao, X., and Chapple, C. (2019). Linking phenylpropanoid metabolism, lignin deposition, and plant growth inhibition. *Curr. Opin. Biotechnol.* 56, 202–208. doi: 10.1016/j.copbio.2018.12.008

Naguib, A., Mathew, G., Reczek, C. R., Watrud, K., Ambrico, A., Herzka, T., et al. (2018). Mitochondrial complex I inhibitors expose a vulnerability for selective killing of PTEN-null cells. *Cell Rep.* 23, 58–67. doi: 10.1016/j.celrep.2018.03.032

Nakamura, K., Akashi, T., Aoki, T., Kawaguchi, K., and Ayabe, S. (1999). Induction of isoflavonoid and retrochalcone branches of the flavonoid pathway in cultured *Glycyrrhiza eChinata* cells treated with yeast extract. *Biosci. Biotechnol. Biochem.* 63, 1618–1620. doi: 10.1271/bbb.63.1618

Naoumkina, M., and Dixon, R. A. (2008). Subcellular localization of flavonoid natural products: a signaling function? *Plant Signaling Behav.* 3, 573–575. doi: 10.4161/psb.3.8.5731

Naoumkina, M., Farag, M. A., Sumner, L. W., Tang, Y., Liu, C. J., and Dixon, R. A. (2007). Different mechanisms for phytoalexin induction by pathogen and wound signals in *Medicago truncatula*. *Proc. Natl. Acad. Sci. U.S.A.* 104, 17909–17915. doi: 10.1073/pnas.0708697104

Ng, J. L., Hassan, S., Truong, T. T., Hocart, C. H., Laffont, C., Frugier, F., et al. (2015). Flavonoids and auxin transport inhibitors rescue symbiotic nodulation in the *Medicago truncatula* cytokinin perception mutant *cre1*. *Plant Cell* 27, 2210–2226. doi: 10.1105/tpc.15.00231

Ng, M. S., Ku, Y. S., Yung, W. S., Cheng, S. S., Man, C. K., Yang, L., et al. (2021). MATE-type proteins are responsible for isoflavone transportation and accumulation in soybean seeds. *Int. J. Mol. Sci.* 22, 12017. doi: 10.3390/ijms222112017

Noguchi, A., Saito, A., Homma, Y., Nakao, M., Sasaki, N., Nishino, T., et al. (2007). A UDP-glucose:isoflavone 7-O-glucosyltransferase from the roots of soybean (*Glycine max*) seedlings. Purification, gene cloning, phylogenetics, and an implication for an alternative strategy of enzyme catalysis. *J. Biol. Chem.* 282, 23581–23590. doi: 10.1074/jbc.M702651200

Ohta, T., Uto, T., and Tanaka, H. (2021). Effective methods for increasing coumestrol in soybean sprouts. *PloS One* 16, e0260147. doi: 10.1371/journal.pone.0260147

Oommen, A., Dixon, R. A., and Paiva, N. L. (1994). The elicitor-inducible alfalfa isoflavone reductase promoter confers different patterns of developmental expression in homologous and heterologous transgenic plants. *Plant Cell* 6, 1789–1803. doi: 10.1105/tpc.6.12.1789

Paiva, N. L., Edwards, R., Sun, Y. J., Hrazdina, G., and Dixon, R. A. (1991). Stress responses in alfalfa (*Medicago sativa* L.) 11. Molecular cloning and expression of alfalfa isoflavone reductase, a key enzyme of isoflavonoid phytoalexin biosynthesis. *Plant Mol. Biol.* 17, 653–667. doi: 10.1007/BF00037051

Pandey, A., Misra, P., Khan, M. P., Swarnkar, G., Tewari, M. C., Bhambhani, S., et al. (2014). Co-expression of *Arabidopsis* transcription factor, *AtMYB12*, and soybean isoflavone synthase, *GmIFS1*, genes in tobacco leads to enhanced biosynthesis of isoflavones and flavonols resulting in osteoprotective activity. *Plant Biotechnol. J.* 12, 69–80. doi: 10.1111/pbi.12118

Perez Rojo, F., Pillow, J. J., and Kaur, P. (2023). Bioprospecting microbes and enzymes for the production of pterocarpans and coumestans. *Front. Bioeng. Biotechnol.* 11. doi: 10.3389/fbioe.2023.1154779

Piślewska, M., Bednarek, P., Stobiecki, M., Zieliśska, M., and Wojtaszek, P. (2002). Cell wall-associated isoflavonoids and β-glucosidase activity in Lupinus albus plants responding to environmental stimuli. *Plant Cell Environ.* 25, 20–40. doi: 10.1046/j.0016-8025.2001.00808.x

Picmanov, M., Honys, D., Koblovsk, R., and Lapcik, O. (2012). "Isoflavone synthase genes in legumes and non-leguminous plants: isoflavone synthase," in *2012 International Conference on Biomedical Engineering and Biotechnology*. (Macau, Macao: IEEE). 344–347. doi: 10.1109/iCBEB.2012.257

Pistelli, L., Noccioli, C., Appendino, G., Bianchi, F., Sterner, O., and Ballero, M. (2003). Pterocarpans from *Bituminaria morisiana* and *Bituminaria bituminosa*. *Phytochemistry* 64, 595–598. doi: 10.1016/S0031-9422(03)00190-0

Pistelli, L., Ulivieri, V., Giovanelli, S., Avio, L., Giovannetti, M., and Pistelli, L. (2017). Arbuscular mycorrhizal fungi alter the content and composition of secondary metabolites in *Bituminaria bituminosa* L. *Plant Biol. (Stuttg)* 19, 926–933. doi: 10.1111/plb.12608

Polturak, G., Misra, R. C., El-Demerdash, A., Owen, C., Steed, A., McDonald, H. P., et al. (2023). Discovery of isoflavone phytoalexins in wheat reveals an alternative route to isoflavonoid biosynthesis. *Nat. Commun.* 14, 6977. doi: 10.1038/s41467-023-42464-3

Preston, S., Korhonen, P. K., Mouchiroud, L., Cornaglia, M., McGee, S. L., Young, N. D., et al. (2017). Deguelin exerts potent nematocidal activity via the mitochondrial respiratory chain. *FASEB J.* 31, 4515–4532. doi: 10.1096/fj.201700288R

Qin, W., Yang, Y., Wang, Y., Zhang, X., and Liu, X. (2022). Transcriptomic and metabolomic analysis reveals the difference between large and small flower taxa of *Herba Epimedii* during flavonoid accumulation. *Sci. Rep.* 12, 2762. doi: 10.1038/s41598–022-06761-z

Qiu, S., Cai, Y., Yao, H., Lin, C., Xie, Y., Tang, S., et al. (2023). Small molecule metabolites: discovery of biomarkers and therapeutic targets. *Signal Transduct Target Ther.* 8, 132. doi: 10.1038/s41392-023-01399-3

Ralston, L., Subramanian, S., Matsuno, M., and Yu, O. (2005). Partial reconstruction of flavonoid and isoflavonoid biosynthesis in yeast using soybean type I and type II chalcone isomerases. *Plant Physiol.* 137, 1375–1388. doi: 10.1104/pp.104.054502

Reynaud, J., Guilet, D., Terreux, R., Lussignol, M., and Walchshofer, N. (2005). Isoflavonoids in non-leguminous families: an update. *Nat. Prod Rep.* 22, 504–515. doi: 10.1039/b416248j

Rodriguez, A., Strucko, T., Stahlhut, S. G., Kristensen, M., Svenssen, D. K., Forster, J., et al. (2017). Metabolic engineering of yeast for fermentative production of flavonoids. *Bioresour Technol.* 245, 1645–1654. doi: 10.1016/j.biortech.2017.06.043

Russell, D. A., Bridges, H. R., Serreli, R., Kidd, S. L., Mateu, N., Osberger, T. J., et al. (2020). Hydroxylated rotenoids selectively inhibit the proliferation of prostate cancer cells. *J. Nat. Prod* 83, 1829–1845. doi: 10.1021/acs.jnatprod.9b01224

Sarkar, M. A. R., Watanabe, S., Suzuki, A., Hashimoto, F., and Anai, T. (2019). Identification of novel MYB transcription factors involved in the isoflavone biosynthetic pathway by using the combination screening system with agroinfiltration and hairy root transformation. *Plant Biotechnol. (Tokyo)* 36, 241–251. doi: 10.5511/plantbiotechnology.19.1025a

Saunders, J., and O'neill, N. (2004). The characterization of defense responses to fungal infection in alfalfa. *BioControl* 49, 715–728. doi: 10.1007/s10526-004-5281-4

Saxena, S., Pal, L., Naik, J., Singh, Y., Verma, P. K., Chattopadhyay, D., et al. (2023). The R2R3-MYB-SG7 transcription factor CaMYB39 orchestrates surface phenylpropanoid metabolism and pathogen resistance in chickpea. *New Phytol.* 238, 798–816. doi: 10.1111/nph.18758

Shelton, D., Stranne, M., Mikkelsen, L., Pakseresht, N., Welham, T., Hiraka, H., et al. (2012). Transcription factors of Lotus: regulation of isoflavonoid biosynthesis requires coordinated changes in transcription factor activity. *Plant Physiol.* 159, 531–547. doi: 10.1104/pp.112.194753

Shen, G., Huhman, D., Lei, Z., Snyder, J., Sumner, L. W., and Dixon, R. A. (2012). Characterization of an isoflavonoid-specific prenyltransferase from *Lupinus albus*. *Plant Physiol.* 159, 70–80. doi: 10.1104/pp.112.195271

Shih, C. H., Chen, Y., Wang, M., Chu, I. K., and Lo, C. (2008). Accumulation of isoflavone genistin in transgenic tomato plants overexpressing a soybean isoflavone synthase gene. *J. Agric. Food Chem.* 56, 5655–5661. doi: 10.1021/jf800423u

Shimada, N., Akashi, T., Aoki, T., and Ayabe, S. (2000). Induction of isoflavonoid pathway in the model legume *Lotus japonicus*: molecular characterization of enzymes involved in phytoalexin biosynthesis. *Plant Sci.* 160, 37–47. doi: 10.1016/S0168-9452(00)00355-1

Shimada, N., Aoki, T., Sato, S., Nakamura, Y., Tabata, S., and Ayabe, S. (2003). A cluster of genes encodes the two types of chalcone isomerase involved in the biosynthesis of general flavonoids and legume-specific 5-deoxy(iso)flavonoids in Lotus japonicus. *Plant Physiol.* 131, 941–951. doi: 10.1104/pp.004820

Shimada, N., Sato, S., Akashi, T., Nakamura, Y., Tabata, S., Ayabe, S.-i., et al. (2007). Genome-wide analyses of the structural gene families involved in the legume-specific 5-deoxyisoflavonoid biosynthesis of Lotus japonicus. *DNA Res.* 14, 25–36. doi: 10.1093/dnares/dsm004

Shimamura, M., Akashi, T., Sakurai, N., Suzuki, H., Saito, K., Shibata, D., et al. (2007). 2-Hydroxyisoflavanone dehydratase is a critical determinant of isoflavone productivity in hairy root cultures of *Lotus japonicus*. *Plant Cell Physiol.* 48, 1652–1657. doi: 10.1093/pcp/pcm125

Simmler, C., Pauli, G. F., and Chen, S.-N. (2013). Phytochemistry and biological properties of glabridin. *Fitoterapia* 90, 160–184. doi: 10.1016/j.fitote.2013.07.003

Sohn, S. I., Pandian, S., Oh, Y. J., Kang, H. J., Cho, W. S., and Cho, Y. S. (2021). Metabolic engineering of isoflavones: an updated overview. *Front. Plant Sci.* 12, 670103. doi: 10.3389/fpls.2021.670103

Song, Z., Zhao, F., Chu, L., Lin, H., Xiao, Y., Fang, Z., et al. (2023). The GmSTF1/2-GmBBX4 negative feedback loop acts downstream of blue-light photoreceptors to regulate isoflavonoid biosynthesis in soybean. *Plant Commun.* 5, 100730. doi: 10.1016/j.xplc.2023.100730

Sreevidya, V. S., Srinivasa Rao, C., Sullia, S. B., Ladha, J. K., and Reddy, P. M. (2006). Metabolic engineering of rice with soybean isoflavone synthase for promoting nodulation gene expression in rhizobia. *J. Exp. Bot.* 57, 1957–1969. doi: 10.1093/jxb/erj143

Su, L., Liu, S., Liu, X., Zhang, B., Li, M., Zeng, L., et al. (2021). Transcriptome profiling reveals histone deacetylase 1 gene overexpression improves flavonoid, isoflavonoid, and phenylpropanoid metabolism in Arachis hypogaea hairy roots. *PeerJ* 9, e10976. doi: 10.7717/peerj.10976

Subramanian, S., Stacey, G., and Yu, O. (2006). Endogenous isoflavones are essential for the establishment of symbiosis between soybean and *Bradyrhizobium japonicum*. *Plant J.* 48, 261–273. doi: 10.1111/j.1365-313X.2006.02874.x

Sugiyama, A., Fukuda, S., Takanashi, K., Yoshioka, M., Yoshioka, H., Narusaka, Y., et al. (2015). Molecular characterization of LjABCG1, an ATP-binding cassette protein in *Lotus japonicus*. *PloS One* 10, e0139127. doi: 10.1371/journal.pone.0139127

Sugiyama, A., Shitan, N., and Yazaki, K. (2007). Involvement of a soybean ATP-binding cassette-type transporter in the secretion of genistein, a signal flavonoid in legume-rhizobium symbiosis. *Plant Physiol.* 144, 2000–2008. doi: 10.1104/pp.107.096727

Sugiyama, A., Shitan, N., and Yazaki, K. (2008). Signaling from soybean roots to Rhizobium: An ATP-binding cassette-type transporter mediates genistein secretion. *Plant Signaling Behav.* 3, 38–40. doi: 10.4161/psb.3.1.4819

Sukumaran, A., McDowell, T., Chen, L., Renaud, J., and Dhaubhadel, S. (2018). Isoflavonoid-specific prenyltransferase gene family in soybean: GmPT01, a pterocarpan 2-dimethylallyltransferase involved in glyceollin biosynthesis. *Plant J.* 96, 966–981. doi: 10.1111/tpj.14083

Sulis, D. B., Jiang, X., Yang, C., Marques, B. M., Matthews, M. L., Miller, Z., et al. (2023). Multiplex CRISPR editing of wood for sustainable fiber production. *Science* 381, 216–221. doi: 10.1126/science.add4514

Suzuki, H., Takahashi, S., Watanabe, R., Fukushima, Y., Fujita, N., Noguchi, A., et al. (2006). An isoflavone conjugate-hydrolyzing beta-glucosidase from the roots of soybean (*Glycine max*) seedlings: purification, gene cloning, phylogenetics, and cellular localization. *J. Biol. Chem.* 281, 30251–30259. doi: 10.1074/jbc.M605726200

Tian, L., and Dixon, R. A. (2006). Engineering isoflavone metabolism with an artificial bifunctional enzyme. *Planta* 224, 496–507. doi: 10.1007/s00425-006-0233-0

Trantas, E., Panopoulos, N., and Ververidis, F. (2009). Metabolic engineering of the complete pathway leading to heterologous biosynthesis of various flavonoids and stilbenoids in *Saccharomyces cerevisiae*. *Metab. Eng.* 11, 355–366. doi: 10.1016/j.ymben.2009.07.004

Tripathi, P., Rabara, R. C., Reese, R. N., Miller, M. A., Rohila, J. S., Subramanian, S., et al. (2016). A toolbox of genes, proteins, metabolites and promoters for improving drought tolerance in soybean includes the metabolite coumestrol and stomatal development genes. *BMC Genomics* 17, 102. doi: 10.1186/s12864-016-2420-0

Trush, K., Eliašová, A., Monje-Rueda, M., Kolarčík, V., Betti, M., and Pašlove-Balang, P. (2023). Chitosan is involved in elicitation of vestitol production in *Lotus japonicus*. *Biol. plantarum* 67, 75–86. doi: 10.32615/bp.2023.007

Tsao, R., Papadopoulos, Y., Yang, R., Young, J. C., and McRae, K. (2006). Isoflavone profiles of red clovers and their distribution in different parts harvested at different growing stages. *J. Agric. Food Chem.* 54, 5797–5805. doi: 10.1021/jf0614589

Uchida, K., Akashi, T., and Aoki, T. (2017). The missing link in leguminous pterocarpan biosynthesis is a dirigent domain-containing protein with isoflavanol dehydratase activity. *Plant Cell Physiol.* 58, 398–408. doi: 10.1093/pcp/pcw213

Uchida, K., Aoki, T., Suzuki, H., and Akashi, T. (2020). Molecular cloning and biochemical characterization of isoflav-3-ene synthase, a key enzyme of the biosyntheses of (+)-pisatin and coumestrol. *Plant Biotechnol. (Tokyo)* 37, 301–310. doi: 10.5511/plantbiotechnology.20.0421a

Ueda, H., and Sugimoto, Y. (2010). Vestitol as a chemical barrier against intrusion of parasitic plant *Striga hermonthica* into *Lotus japonicus* roots. *Biosci. biotechnol. Biochem.* 74, 1662–1667. doi: 10.1271/bbb.100285

Veitch, N. C. (2009). Isoflavonoids of the leguminosae. *Natural Product Rep.* 26, 776–802. doi: 10.1039/b616809b

Veitch, N. C. (2013). Isoflavonoids of the leguminosae. *Nat. Prod Rep.* 30, 988–1027. doi: 10.1039/c3np70024k

Verdier, J., Zhao, J., Torres-Jerez, I., Ge, S., Liu, C., He, X., et al. (2012). MtPAR MYB transcription factor acts as an on switch for proanthocyanidin biosynthesis in *Medicago truncatula*. *Proc. Natl. Acad. Sci. U.S.A.* 109, 1766–1771. doi: 10.1073/pnas.1120916109

Wada, N., Osakabe, K., and Osakabe, Y. (2022). Expanding the plant genome editing toolbox with recently developed CRISPR-Cas systems. *Plant Physiol.* 188, 1825–1837. doi: 10.1093/plphys/kiac027

Wang, J., Li, L., Wang, Z., Feng, A., Li, H., Qaseem, M. F., et al. (2023a). Integrative analysis of the metabolome and transcriptome reveals the molecular regulatory mechanism of isoflavonoid biosynthesis in *Ormosia henryi Prain*. *Int. J. Biol. Macromol.* 246, 125601. doi: 10.1016/j.ijbiomac.2023.125601

Wang, X., Li, C., Zhou, C., Li, J., and Zhang, Y. (2017). Molecular characterization of the C-glucosylation for puerarin biosynthesis in *Pueraria lobata*. *Plant J.* 90, 535–546. doi: 10.1111/tpj.13510

Wang, Y., Luo, Y., Zhang, Y., Xu, C., Yao, Y., Gu, J., et al. (2023b). A novel flavonoid prenyltransferase gene P*cPT11* with broad substrate promiscuity in *Psoralea corylifolia* L. *Ind. Crops Products* 199, 116746. doi: 10.1016/j.indcrop.2023.116746

Wang, X., Pan, H., Sagurthi, S., Paris, V., Zhuo, C., and Dixon, R. A. (2022). The protein conformational basis of isoflavone biosynthesis. *Commun. Biol.* 5, 1249. doi: 10.1038/s42003-022-04222-x

Wasson, A. P., Pellerone, F. I., and Mathesius, U. (2006). Silencing the flavonoid pathway in *Medicago truncatula* inhibits root nodule formation and prevents auxin transport regulation by rhizobia. *Plant Cell* 18, 1617–1629. doi: 10.1105/tpc.105.038232

Wen, D., Wu, L., Wang, M., Yang, W., Wang, X., Ma, W., et al. (2022). CRISPR/Cas9-mediated targeted mutagenesis of *FtMYB45* promotes flavonoid biosynthesis in tartary buckwheat (*Fagopyrum tataricum*). *Front. Plant Sci.* 13. doi: 10.3389/fpls.2022.879390

Wong, J., Gao, L., Yang, Y., Zhai, J., Arikit, S., Yu, Y., et al. (2014). Roles of small RNAs in soybean defense against *Phytophthora sojae* infection. *Plant J.* 79, 928–940. doi: 10.1111/tpj.12590

Xu, D. (2020). COP1 and BBXs-HY5-mediated light signal transduction in plants. *New Phytol.* 228, 1748–1753. doi: 10.1111/nph.16296

Yadav, V., Wang, Z., Wei, C., Amo, A., Ahmed, B., Yang, X., et al. (2020). Phenylpropanoid pathway engineering: an emerging approach towards plant defense. *Pathogens* 9, 312. doi: 10.3390/pathogens9040312

Yan, J., Wang, B., Zhong, Y., Yao, L., Cheng, L., and Wu, T. (2015). The soybean R2R3 MYB transcription factor GmMYB100 negatively regulates plant flavonoid biosynthesis. *Plant Mol. Biol.* 89, 35–48. doi: 10.1007/s11103-015-0349-3

Yang, S., Chen, R., Cao, X., Wang, G., and Zhou, Y. J. (2024). *De novo* biosynthesis of the hops bioactive flavonoid xanthohumol in yeast. *Nat. Commun.* 15, 253. doi: 10.1038/s41467-023-44654-5

Yang, C., Xie, L., Ma, Y., Cai, X., Yue, G., Qin, G., et al. (2021). Study on the fungicidal mechanism of glabridin against *Fusarium graminearum*. *Pesticide Biochem. Physiol.* 179, 104963. doi: 10.1016/j.pestbp.2021.104963

Yi, J., Derynck, M. R., Li, X., Telmer, P., Marsolais, F., and Dhaubhadel, S. (2010). A single-repeat MYB transcription factor, GmMYB176, regulates *CHS8* gene expression and affects isoflavonoid biosynthesis in soybean. *Plant J.* 62, 1019–1034. doi: 10.1111/j.1365-313X.2010.04214.x

Yoneyama, K., Akashi, T., and Aoki, T. (2016). Molecular characterization of soybean pterocarpan 2-dimethylallyltransferase in glyceollin biosynthesis: Local gene and whole-genome duplications of prenyltransferase genes led to the structural diversity of soybean prenylated isoflavonoids. *Plant Cell Physiol.* 57, 2497–2509. doi: 10.1093/pcp/pcw178

Yu, X. H., Chen, M. H., and Liu, C. J. (2008). Nucleocytoplasmic-localized acyltransferases catalyze the malonylation of 7-O-glycosidic (iso) flavones in *Medicago truncatula*. *Plant J.* 55, 382–396. doi: 10.1111/j.1365-313X.2008.03509.x

Yu, O., and McGonigle, B. (2005). Metabolic engineering of isoflavone biosynthesis. *Adv. Agron.* 86, 147–190. doi: 10.1016/S0065-2113(05)86003-1

Yu, L., Rios, E., Castro, L., Liu, J., Yan, Y., and Dixon, D. (2021). Genistein: dual role in women's health. *Nutrients* 13, 3048. doi: 10.3390/nu13093048

Yu, O., Shi, J., Hession, A. O., Maxwell, C. A., McGonigle, B., and Odell, J. T. (2003). Metabolic engineering to increase isoflavone biosynthesis in soybean seed. *Phytochemistry* 63, 753–763. doi: 10.1016/S0031-9422(03)00345-5

Yuk, H. J., Lee, J. H., Curtis-Long, M. J., Lee, J. W., Kim, Y. S., Ryu, H. W., et al. (2011). The most abundant polyphenol of soy leaves, coumestrol, displays potent α-glucosidase inhibitory activity. *Food Chem.* 126, 1057–1063. doi: 10.1016/j.foodchem.2010.11.125

Yuk, H. J., Song, Y. H., Curtis-Long, M. J., Kim, D. W., Woo, S. G., Lee, Y. B., et al. (2016). Ethylene induced a high accumulation of dietary isoflavones and expression of isoflavonoid biosynthetic genes in soybean (*Glycine max*) leaves. *J. Agric. Food Chem.* 64, 7315–7324. doi: 10.1021/acs.jafc.6b02543

Zhang, P., Du, H., Wang, J., Pu, Y., Yang, C., Yan, R., et al. (2020). Multiplex CRISPR/Cas9-mediated metabolic engineering increases soya bean isoflavone content and resistance to soyabean mosaic virus. *Plant Biotechnol. J.* 18, 1384–1395. doi: 10.1111/pbi.13302

Zhang, Z., Gao, L., Ke, M., Gao, Z., Tu, T., Huang, L., et al. (2022b). GmPIN1-mediated auxin asymmetry regulates leaf petiole angle and plant architecture in soybean. *J. Integr. Plant Biol.* 64, 1325–1338. doi: 10.1111/jipb.13269

Zhang, J., Liu, L., Wang, J., Ren, B., Zhang, L., and Li, W. (2018). Formononetin, an isoflavone from *Astragalus membranaceus* inhibits proliferation and metastasis of ovarian cancer cells. *J. Ethnopharmacol.* 221, 91–99. doi: 10.1016/j.jep.2018.04.014

Zhang, P., Zhang, M., Mellich, T. A., Pearson, B. J., Chen, J., and Zhang, Z. (2022a). Variation in rotenone and deguelin contents among strains across four tephrosia species and their activities against aphids and whiteflies. *Toxins (Basel)* 14, 339. doi: 10.3390/toxins14050339

Zhao, J. (2015). Flavonoid transport mechanisms: how to go, and with whom. *Trends Plant Sci.* 20, 576–585. doi: 10.1016/j.tplants.2015.06.007

Zhao, J., and Dixon, R. A. (2010). The 'ins' and 'outs' of flavonoid transport. *Trends Plant Sci.* 15, 72–80. doi: 10.1016/j.tplants.2009.11.006

Zhao, J., Huhman, D., Shadle, G., He, X. Z., Sumner, L. W., Tang, Y., et al. (2011). MATE2 mediates vacuolar sequestration of flavonoid glycosides and glycoside malonates in *Medicago truncatula*. *Plant Cell* 23, 1536–1555. doi: 10.1105/tpc.110.080804

Zhao, M., Wang, T., Wu, P., Guo, W., Su, L., Wang, Y., et al. (2017). Isolation and characterization of GmMYBJ3, an R2R3-MYB transcription factor that affects isoflavonoids biosynthesis in soybean. *PloS One* 12, e0179990. doi: 10.1371/journal.pone.0179990

Zhou, Y., Olt, P., Neuhäuser, B., Moradtalab, N., Bautista, W., Uhde-Stone, C., et al. (2021). Loss of LaMATE impairs isoflavonoid release from cluster roots of phosphorus-deficient white lupin. *Physiol. Plant* 173, 1207–1220. doi: 10.1111/ppl.13515

Zubieta, C., He, X. Z., Dixon, R. A., and Noel, J. P. (2001). Structures of two natural product methyltransferases reveal the basis for substrate specificity in plant O-methyltransferases. *Nat. Struct. Biol.* 8, 271–279. doi: 10.1038/85029

frontiers | Frontiers in Plant Science

TYPE Review
PUBLISHED 27 August 2024
DOI 10.3389/fpls.2024.1441893

OPEN ACCESS

EDITED BY
Deyu Xie,
North Carolina State University, United States

REVIEWED BY
Nan Lu,
University of North Texas, United States
Chaofeng Li,
Southwest University, China
Xinlong Dai,
Guizhou University, China

*CORRESPONDENCE
Keji Yu
yukeji@cau.edu.cn

RECEIVED 31 May 2024
ACCEPTED 08 August 2024
PUBLISHED 27 August 2024

CITATION
Shi T, Su Y, Lan Y, Duan C and Yu K (2024) The molecular basis of flavonoid biosynthesis response to water, light, and temperature in grape berries. *Front. Plant Sci.* 15:1441893. doi: 10.3389/fpls.2024.1441893

The molecular basis of flavonoid biosynthesis response to water, light, and temperature in grape berries

Tianci Shi[1,2], Yue Su[1,2], Yibin Lan[1,2], Changqing Duan[1,2] and Keji Yu[1,2]*

[1]Center for Viticulture and Enology, College of Food Science and Nutritional Engineering, China Agricultural University, Beijing, China, [2]Key Laboratory of Viticulture and Enology, Ministry of Agriculture and Rural Affairs, Beijing, China

Flavonoids, including proanthocyanidins (PAs), anthocyanins and flavonols are essential secondary metabolites that contribute to the nutritional value and sensory quality of grape berry and red wine. Advances in molecular biology technology have led to substantial progress in understanding the regulation of flavonoid biosynthesis. The influence of terroir on grape berries and wine has garnered increasing attention, yet its comprehensive regulatory network remains underexplored. In terms of application, environmental factors such as water, light, and temperature are more easily regulated in grapevines compared to soil conditions. Therefore, we summarize their effects on flavonoid content and composition, constructing a network that links environmental factors, hormones, and metabolites to provide a deeper understanding of the underlying mechanisms. This review enriches the knowledge of the regulatory network mechanisms governing flavonoid responses to environmental factors in grapes.

KEYWORDS

proanthocyanidin, anthocyanin, flavonoid, water, light, temperature, phytohormones, grape

1 Introduction

Grapevine (*Vitis vinifera*) is one of the most widely cultivated and consumed fruits in the world, and its use in wine production is attracting more interest due to its economic and health benefits (Beres et al., 2017; Wei et al., 2023). Proanthocyanidins (PAs, polymers of flavan-3-ols), anthocyanins and flavonols are abundant flavonoids in grapes. These compounds not only protect grapes from UV rays, pests and diseases, but also determine the color, astringency, and stability of red wine (Winkel-Shirley, 2002; Flamini et al., 2013). Flavonoids, characterized by a C6-C3-C6 backbone, are classified into anthocyanins, flavonols, and flavan-3-ols in grape depending on the oxidation and substitution state of the pyran ring in the carbon skeleton (Ferreyra et al., 2012; Gouot et al., 2019a). Anthocyanins are primarily located in the skin of grape, accumulating significantly

at the veraison stage and peaking around the harvest stage. Flavonols are also mainly distributed in the skin, with their synthesis starting at the flowering stage, slowing down in the early stages of fruit development, and resuming during fruit ripening. Flavan-3-ols are detected in both the grape skin and seeds, and their synthesis occurs from anthesis until the onset of ripening (Downey et al., 2004; Bogs et al., 2005; He et al., 2010).

The flavonoid pathway in grapevine, derived from the shikimate and phenylpropanoid pathways, has been well-characterized (Ferreira et al., 2018; Gouot et al., 2019a). As shown in Figure 1, phenylalanine, a product of shikimate pathway, is catalyzed by a series of enzymes, including phenylalanine ammonia-lyase (PAL), cinnamate 4-hydroxylase (C4H) and 4-coumarate coenzyme A ligase (4CL), to form 4-coumaroyl-CoA, a precursor in the flavonoid pathway. Subsequently, 4-coumaroyl-CoA and malonyl-CoA are catalyzed by chalcone synthase (CHS) and chalcone isomerase (CHI) to form chalcone, a 15-carbon flavonoid skeleton, and then naringenin, an intermediate product of flavonoid metabolism, which enters various flavonoid metabolic branches (Holton and Cornish, 1995). With the catalysis of flavanone hydroxylases (F3H, F3'H or F3'5'H), naringenin is converted to dihydroflavonols including dihydrokaempferol, dihydromyricetin and dihydroquercetin (Bogs et al., 2006). The next stage involves branching: one branch produces flavonols from dihydrokaempferol by flavonol synthase (FLS), while the other, controlled by dihydroflavonol 4-reductase (DFR), converts dihydromyricetin and dihydroquercetin into leucodelphinidin and leucocyanidin (possessing 2,3-*trans* conformation), respectively (Martens et al., 2002). Leucodelphinidin and leucocyanidin are then converted to delphinidin and cyanidin via the combined activities of anthocyanidin synthase (ANS) and glutathione-*S*-transferase (GST) (Eichenberger et al., 2023). They also can be catalyzed by leucoanthocyanidin reductase (LAR) producing 2,3-*trans* flavan-3-ol (e.g. (+)-catechin) (Yu et al., 2019). Additionally, the delphinidin and cyanidin are converted to 2,3-*cis* flavan-3-ol (e.g. (-)-epicatechin) with the catalysis of anthocyanidin reductase (ANR) (Xie et al., 2003; Bogs et al., 2005; Jun et al., 2021; Yu et al., 2022). These flavan-3-ol monomers participate in the condensation process of PA as starter units (Dixon et al., 2005; Yu et al., 2023). Flavan-3-ol carbocations, derived either from 2,3-*trans*-leucoanthocyanidins or from 2,3-*cis*-leucoanthocyanidins produced by ANR, serve as the direct extension units that form

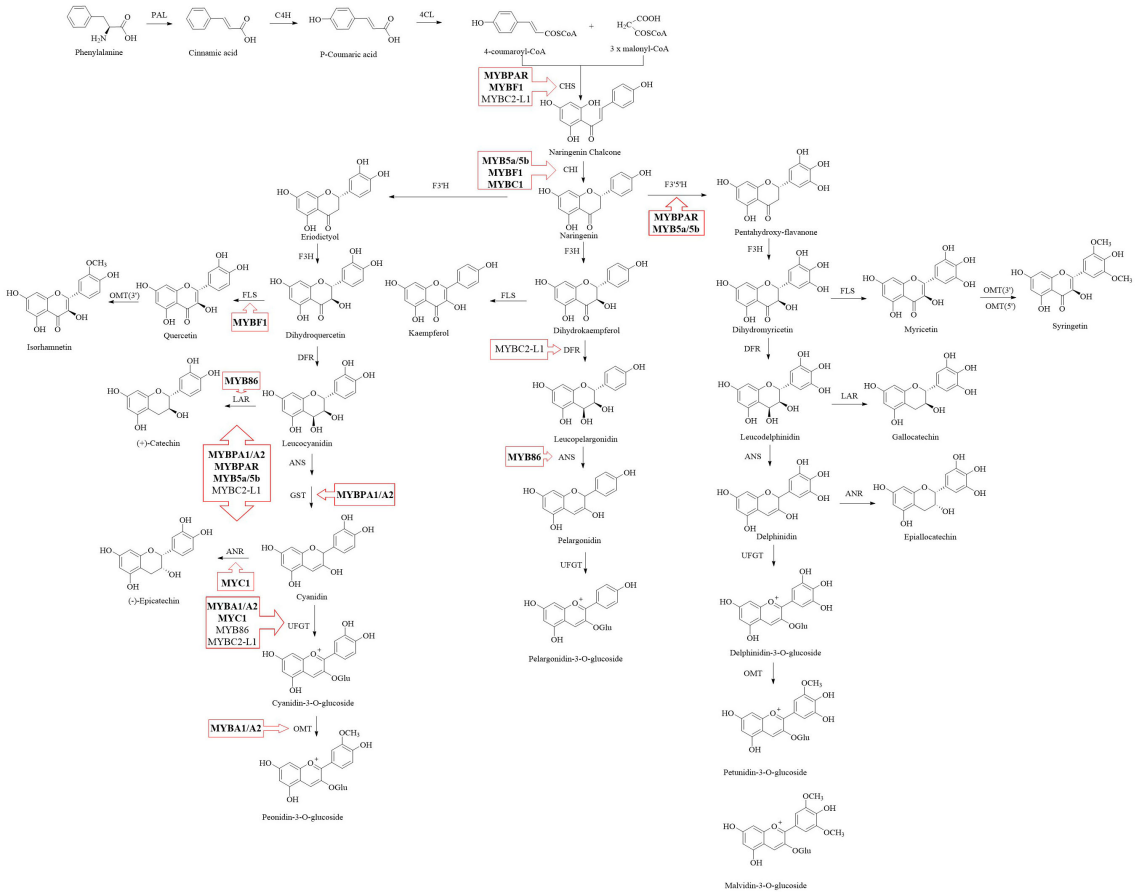

FIGURE 1
The metabolic pathway of flavonoid in grape. Positive regulators are indicated in bold text, while negative regulators are shown in normal text. PAL, phenylalanine ammonia-lyase; C4H, cinnamate-4-hydroxylase; 4CL, 4-coumarate, CoA-ligase; CHS, chalcone synthase; CHI, chalcone isomerase; F3H, flavanone 3-hydroxylase; F3'H, flavanone 3'-hydroxylase; F3'5'H, flavanone 3'5'-hydroxylase; DFR, dihydroflavonol 4-reductase; ANR, anthocyanidin reductase; ANS, anthocyanidin synthase; FLS, flavonol synthase; UFGT, UDP-glucose, flavonoid 3-*O*-glucosyltransferase; OMT, *O*-methyltransferase.

C4-C8 or C4-C6 bonds with the upper unit in non-enzymatic PA polymerization (Wang et al., 2020a; Jun et al., 2018, Jun et al., 2021; Yu et al., 2022, Yu et al., 2023). For another branch, anthocyanidins can further undergo modifications such as glycosylation, acylation, and methylation mediated by UDP-glucose (UFGT), acyltransferases and *O*-methyltransferase (OMT) respectively, to produce anthocyanins (He et al., 2008). Finally, flavonoids synthesized on the endoplasmic reticulum are typically transported by transporter proteins, including GST and multidrug and toxic extrusion transporter (MATE), to vesicles for storage (Castellarin et al., 2007a).

It is believed that flavonoid synthesis is mainly controlled by the MYB-bHLH-WD40 (MBW) complex, with the MYB protein playing a central role (Xu et al., 2015). Among the R2R3-MYB transcription factors, several of them have been identified in grapevine for their roles in flavonoid metabolism. *VvMYB5a*, expressed in the early stages of berry development, and *VvMYB5b*, expressed throughout berry development, activate the promoters of upstream flavonoid pathway genes (*VvCHI*, *VvF3'5'H*) and the PA biosynthesis pathway-related structural genes including *VvLAR1* and *VvANR* (Deluc et al., 2006, Deluc et al., 2008). Overexpression of *VvMYB5a* and *VvMYB5b* in tobacco (*Nicotiana tabacum*) leads to high accumulation of anthocyanins and PAs via upregulating the expression of genes involved in the flavonoid biosynthetic pathway, such as *VvCHS*, *VvCHI*, *VvF3H*, and *VvDFR*. Moreover, *VvCHS* and *VvCHI* can also be regulated by VvMYBF1, but VvMYBF1 mainly regulates *VvFLS* to produce flavonols, which compete with PAs and anthocyanins synthesis (Czemmel et al., 2009). VvMYBA1 and VvMYBA2 are the key positive regulators of anthocyanin synthesis in grape berries, promoting the expression of *VvUFGT*, *VvGST*, *VvOMT* and *Vv3AT* genes at the pre-veraison. stage (Kobayashi et al., 2004; Cutanda-Perez et al., 2009; Rinaldo et al., 2015). Matus et al. (2017) reported that VvMYBA1, VvMYBA6.1 and VvMYBA7 regulate the synthesis of anthocyanins in young leaves and tendrils of 'Pinot Noir' and buds of 'Corvina Veronese' by activating the promoter of *VvUFGT*, *VvOMT* and *VvF3'5'H* genes, with only VvMYBA1 inducing *VvF3'5'H*. VvMYBPA1 and VvMYBPA2, mainly expressed in seeds and skin in grapevine respectively, result in the accumulation of PAs by significantly upregulating transcript levels of *VvANR* and *VvLAR1* (Bogs et al., 2006; Terrier et al., 2009). Koyama et al. (2014) suggested that VvMYBPAR also regulate PAs content via controlling *VvLAR2* expression. Additionally, there are transcription repressors involved in flavonoid synthesis. VvMYBC2-L1/2/3 negatively regulate anthocyanin biosynthesis by inhibiting the expression of *VvCHI*, *VvCHS*, *VvDFR*, and *VvUFGT* (Cavallini et al., 2015; Zhu et al., 2019). VvMYBC2-L1 also down-regulates *VvMYBPA1*, *VvMYBPA2*, *VvDFR*, *VvLDOX*, *VvANR*, *VvLAR1* and *VvLAR2* expression to suppress the PAs synthesis (Huang et al., 2014). Cheng et al. (2021) found VvMYB86 promotes PAs synthesis through the up-regulation of *VvLAR* transcription and inhibits anthocyanin biosynthesis via the down-regulation of *VvANS* and *VvUFGT* expression. Among bHLH regulators, it has been confirmed that VvMYC1 can interact with VvMYB5a, VvMYB5b, VvMYBA1/A2, and VvMYBPA1, resulting in the induction of the promoter activities of *VvUFGT*, *VvANR*, and *VvCHI* (Hichri et al., 2010). The studies from Matus et al. (2010) and Jiu et al. (2021) reported that WDR1 enhances the anthocyanin accumulation, by forming the complex with VvMYBA2 and VvMYCA1.

The accumulation of flavonoid is affected by both macro- and micro-climates in vineyard (Downey et al., 2006; Gutierrez-Gamboa et al., 2017; Martinez-Gil et al., 2018). In a specific vineyard, environmental factors such as water, light, and temperature can be adjusted through viticulture practices to regulate the qualities of grape berries and wines (Mori et al., 2007a; Azuma et al., 2012; Rienth et al., 2021). A comprehensive understanding of the mechanisms that regulate flavonoid accumulation in response to environmental factors can contribute to the precise control of fruit traits through cultivation. The enzymes and transcription factors responsible for the biosynthesis of anthocyanins and PAs in grapevine have been extensively studied in the context of spatio-temporal accumulation of metabolites, providing the basis for interpreting how gene expression patterns cause grape berry traits under various environmental conditions. However, the lack of suitable working models to understand conflicting results from field experiment reflects the fact that the interaction between genetic background of grapevine and environmental factors has not been fully resolved. In terms of the remodeling of flavonoid biosynthesis network under various abiotic stresses, the essential roles of phytohormones (e.g. abscisic acid (ABA), ethylene, melatonin, gibberellin GA, brassinolide(BR)) in mediating the accumulation of anthocyanins and PAs in grapevine has been revealed by metabolomics and transcriptomic studies in recent years (Mori et al., 2005a; Loreti et al., 2008; Sun et al., 2017).

2 The ABA-centered flavonoid biosynthesis regulation network under water deficit

The current understandings of the effects of water condition on berry qualities are mainly from the practice of regulated deficit irrigation (RDI), a strategy to balance the water usage and the yield (Costa et al., 2007). The modulation of flavonoid biosynthesis in grape berry under water deficit is a complex process, as it may be affected by at least macro climate, grape variety, rootstock, drought timing and even berry size (Roby and Matthews, 2004; Kuhn et al., 2014; Gambetta et al., 2020; Afifi et al., 2021). Moreover, the parameter for representing the water deficit extent varies among studies, such as evapotranspiration (usually ranged from 30% to 80%) and water potentials of leaves or stems (usually ranged from -1.4 to -0.6). It is therefore plausible to observe conflict conclusions drawn from different experiments. By revisiting the existing studies, we here summarized the general molecular mechanism regarding the response of PA and anthocyanin pathways to water deficit, and proposed the omitted aspects that hinder answering the lingering questions from various studies. The commonly used RDI strategies in field studies include the early deficit (from berry setting to veraison), the late deficit (from verasion to harvest) and the seasonal deficit (from berry setting to harvest). It has repeatedly

been shown that water deficit has no effect on flavonols, although increases anthocyanin level in red grape skins at harvest, regardless the timing of RDI (Castellarin et al., 2007a; Castellarin et al., 2007b; Deluc et al., 2009; Caceres-Mella et al., 2017; Yang et al., 2020a). This is in line with the increased transcription levels of *VvPAL*, *VvCHS*, *VvF3H*, *VvF3'H*, *VvDFR*, *VvANS*, *VvGST* and *VvUFGT* responsible for anthocyanin biosynthesis in the corresponding RDI treatments (Castellarin et al., 2007a; Deluc et al., 2009; Yang et al., 2020a) (Figure 2). All three RDI strategies enhance the methylation of anthocyanins, while the late and seasonal RDI but not the early water deficit significantly increases the levels of delphindin-based and acylated anthocyanins in grape berries (Castellarin et al., 2007a; Olle et al., 2011; Yang et al., 2020a). This suggests that *VvOMT* is essentially responsive to water deficit across the berry development, while *VvF3'5'H* and *Vv3AT* are mainly sensitive to water status post-veraison. However, the patterns of the detected *VvF3'5'H* transcript levels are not always well-correlated with delphindin derivates accumulations among different RDI treatments (Castellarin et al., 2007a). It is noteworthy that *VvF3'5'H* gene family in grapevine possess more than ten isoforms, and the levels of 3'5'-OH anthocyanins are dependent on the abundance of *VvF3'5'H* transcripts pool in grapes (Falginella et al., 2010). Thus, it will be more informative to include the expression data of multiple *VvF3'5'H* gene isoforms when aiming at clarifying the mechanism about the response of anthocyanin hydroxylation extent to water deficit timing. Under both early and late water deficit treatments, the enhanced anthocyanin accumulation in grape berry associates with ripening acceleration, the process mainly regulated by ABA (Castellarin et al., 2007a). Transcriptome and metabolite data both showed that seasonal water deficit can promote ABA synthesis in red grape berries, especially at veraison (Deluc et al., 2009). And the effect of seasonal RDI on anthocyanin accumulation can be diminished by applying ABA synthesis inhibitor nordihydroguaiaretic acid (NDGA) (Guo et al., 2021). These findings suggest the pivotal role of ABA to enhance anthocyanin biosynthesis in grape berries under water deficit stress. The exogenous ABA application studies showed that most of flavonoid genes activated by ABA in grape berries are overlapped with that triggered by water deficit, including three flavonoid activators VvMYBA1, VvMYBA2 and VvMYBPA1 (Koyama et al., 2010; Caceres-Mella et al., 2017; Sun et al., 2019; Guo et al., 2021). Genetic evidence showed that VvMYBA1/2 target to genes in the entire anthocyanin pathway except *VvF3H* and *VvF3'H*, while VvMYBPA1 activates *VvF3H*, *VvF3'H* and two PA branch genes *VvLAR*1 and *VvANR* (Terrier et al., 2009; Rinaldo et al., 2015). Thus, it is likely that VvMYBA1/2 and VvMYBPA1 complement with each other for channeling the flux to anthocyanins regulated by ABA in grape berries under water deficit stress (Figure 2).

Although *VvMYBPA1* is crucial for PA accumulation in the context of grape berry development (Bogs et al., 2007), its enhanced expression seems not effectively promote PA biosynthesis under water deficit stress. Numerous studies have shown that water deficit has little effect on PA accumulation in grape berries at harvest, or its effect on grape PA content does not show a stable trend among different years (Castellarin et al., 2007a; Bucchetti et al., 2011; Olle et al., 2011; Genebra et al., 2014; Herrera et al., 2015; Yu et al., 2016; Caceres-Mella et al., 2017). Compositional analysis suggests that it is the mDP of PA, but not the gallyollation extent of PA, increases in grape skins under long term or late water deficit (Caceres-Mella et al., 2017) (Figure 2). At the transcription level, *VvANR* expression in grape skins is not responsive to late RDI but can be down-regulated by early RDI, while *VvLAR2* transcript level is affected by neither of these two treatments (Castellarin et al., 2007a). With seasonal RDI, *VvLAR2* transcript abundance can be transiently elevated before veraison, and the similar response is also observed in the grape berries sprayed with ABA (Lacampagne et al., 2010; Villalobos-González et al., 2016; Caceres-Mella et al., 2017). Moreover, pre-veraison ABA application delayed the expression

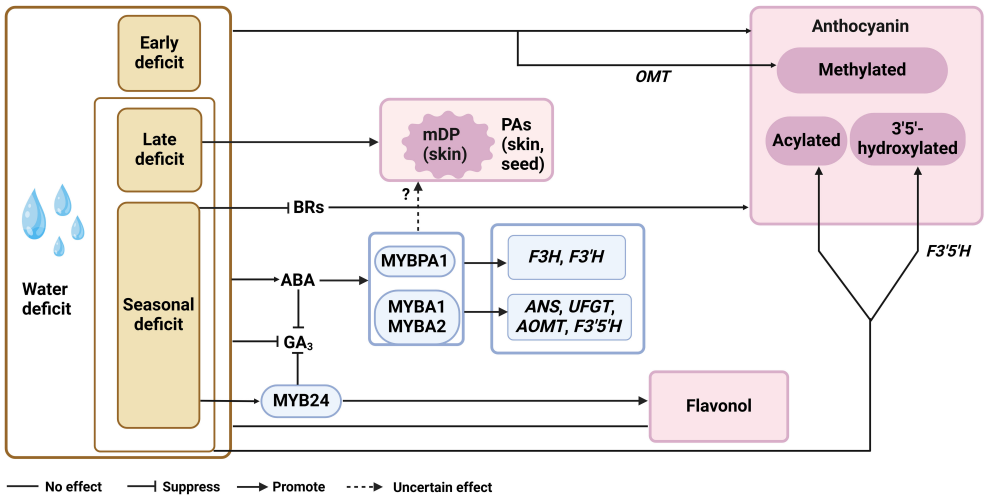

FIGURE 2
The ABA-centered flavonoid regulation network under water deficit. mDP, mean polymerization degrees; ABA, abscisic acid; GA_3, gibberellin, BRs, brassinolide; F3H, flavanone 3-hydroxylase; F3'H, flavanone 3'-hydroxylase; F3'5'H, flavanone 3'5'-hydroxylase; ANS, anthocyanidin synthase; UFGT, UDP-glucose, flavonoid 3-*O*-glucosyltransferase; OMT, *O*-methyltransferase.

of *VvANR* and *VvLAR1*, which consistent with the lower *VvANR* and *VvLAR* enzymatic activities during PA biosynthesis active stage in grape berries (Lacampagne et al., 2010). Although exogenous ABA application to large extent resemble the PA gene expression patterns under water deficit, to how much extent ABA involves in the regulation of PA structural genes expression remains to be answered, and the missing components that disturb the effects of VvMYBPA1 on the expression PA structural genes under water deficit need to be further discovered.

Accompanied with the increased ABA concentration during pre-veraison under seasonal water deficit treatments, BR and GA_3 levels are slightly decreased in grape berries in consecutive years (Yang et al., 2020b; Guo et al., 2021) (Figure 2). It has been shown that the spraying of BR before veraison enhanced the accumulation of anthocyanins and PAs in berry skins (Luan et al., 2013; Xi et al., 2013; Vergara et al., 2018), while exogenous application of GA_3 does not significantly affect the levels of anthocyanins and PAs (Reynolds et al., 2016; Murcia et al., 2017; Kaplan et al., 2019; Gao et al., 2020; Tyagi et al., 2021), except for that the long-term 80 mg/L GA_3 application on 'Red globe' promotes anthocyanin biosynthesis (Dong et al., 2023). The trade-off of ABA and BR levels has been proposed as the strategy to balance the stress response and development in plants (Wang et al., 2020b), which might also contribute to tuning the flux between PA and anthocyanin pathways under water deficit. In addition, ABA inhibits GA biosynthesis and induces GA degradation to increase drought tolerance of plants (Shohat et al., 2021; Mukherjee et al., 2023). Recently, VyMYB24 is found to confer the drought tolerance in Chinese wild *Vitis* species *V. yanshanesis* and negatively regulate GA_3 level under drought stress (Zhu et al., 2022), and its homolog in *V. vinifera* is responsible for the enhanced flavone and terpenoid accumulation under drought and high light/UV conditions (Savoi et al., 2016; Lu et al., 2021; Zhang et al., 2023). Then further answering whether and how MYB24 participates in the interaction of phytohormone levels and flavonoid gene expression can help with understanding ABA-centered anthocyanins and PAs regulation network under water deficit (Figure 2).

3 The interaction of light and phytohormones in regulating the accumulation of flavonoid

In the viticulture practice, bagging, net-shading, and canopy managements (leaf removal and shoot thinning) are effective approaches to adjust both quantity and quality of sunlight around grape berry clusters. Exposure of grape berries to sunlight generally increases anthocyanin and flavonol levels in skins, mainly by activating the expression of phenylpropanoid genes (*VvPAL*, *Vv4CL*), flavonoid genes (*VvCHS*, *VvCHI*, *VvF3'H*, *VvF3'5'H*, *VvUFGT*), flavonol gene (*VvFLS*) and the relevant transcription regulators (*VvMYBA1*, *VvMYB5b*, *VvMYBF1 and VvHY5*) (Matsuyama et al., 2014; Guan et al., 2016; Czemmel et al., 2017; Li et al., 2023) (Figure 3). However, excessive sunlight exposure can result in the sunburn of berry clusters, which induces the degradation of anthocyanins, PAs and flavonols (Sun et al., 2017; Reshef et al., 2018; Torres et al., 2020). Flavonol biosynthesis is particularly

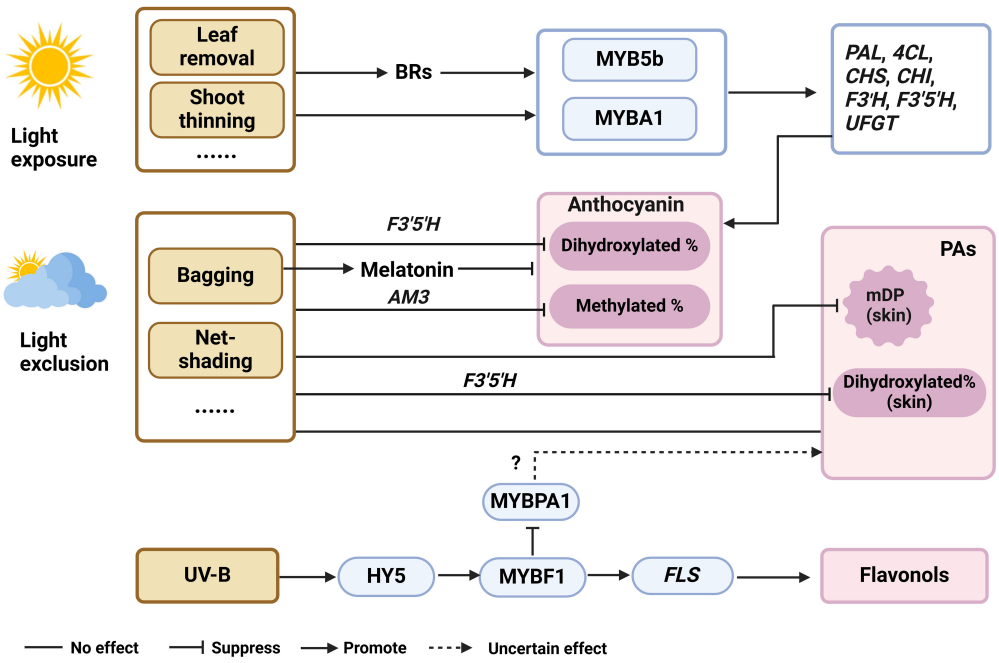

FIGURE 3
The roles of phytohormones in mediating the biosynthesis of flavonoid under various light conditions. mDP, mean polymerization degrees, BRs, brassinolide, ABA, abscisic acid, UV-B, ultraviolet-B, F3'5'H, flavanone 3'5'-hydroxylase, AM3, MATE3, PAL, phenylalanine ammonia-lyase; 4CL, 4-coumarate, CoA-ligase; CHS, chalcone synthase; CHI, chalcone isomerase; F3'H, flavanone 3'-hydroxylase; UFGT, UDP-glucose, flavonoid 3-*O*-glucosyltransferase; FLS, flavonol synthase.

sensitive to UV-B light and can be significantly inhibited in berries subjected to light exclusion using light-proof box (Koyama et al., 2012; Loyola et al., 2016). It was found that VvHY5 activated *VvMYBF1* transcript level under UV-B, which in turn regulated the expression of *VvFLS1*, *VvGT3* (encoding a glycosyltransferase) and *VvRHaT1* (encoding a rhamnosyltransferase), to promote flavonol accumulation. Additionally, VvMYBF1 negatively regulated the expression of *VvMYBPA1*, indicating a competition between the flavonol and PA branches (Czemmel et al., 2017). Under light exclusion, the proportion of dihydroxylated anthocyanins increased due to the down-regulation of *F3'5'H* expression (Downey et al., 2004; Azuma et al., 2012; Koyama et al., 2012; Matsuyama et al., 2014; Guan et al., 2016). Guan et al. (2016) also found the proportion of methylated anthocyanins increased. Light exposed and exclusion had little effect on PA content at harvest (Downey et al., 2004; Fujita et al., 2007; Koyama and Goto Yamamoto, 2008; Liu et al., 2015; VanderWeide et al., 2022) (Figure 3). This may be because the treatments are applied at the onset of veraison, while PAs are mainly synthesized in large quantities at the flowering stage. Shading grape clusters during the pre-veraison period, decreased PA levels in berry skins by down-regulating the expression of *VvLAR1* and *VvANR* before ripening (Downey et al., 2004; Jeong et al., 2004; Fujita et al., 2007; Koyama and Goto-Yamamoto, 2008; Liu et al., 2015) (Figure 3). Researchers speculate that extractable PAs decreased more markedly in sunlight-exposed conditions than in shaded berry skins during ripening, suggesting that light promotes the synthesis of insoluble PAs. Downey et al. (2004) and Fujita et al. (2007) also discovered there is no significant effect of light exclusion on the level of PAs in the seeds. While the proportion of the dihydroxylated subunits increased in berry skins, which agreed with the down-regulation of *VvF3'5'H* levels Koyama and Goto-Yamamoto, 2008). By Shading with light-proof boxes, this group further confirm that light exclusion decreased the mean degree of polymerization (mDP) of PAs in grape skin (Koyama et al., 2012).

Several studies have focused on endogenous hormones in grapes under light conditions. Guo et al. (2020) bagged two wine grape varieties, 'Cabernet Sauvignon' and 'Carignane', from fruit set until harvest and found the cluster bagging induced the melatonin synthesis. Meng et al. (2019) found the application of melatonin during the pre-veraison period at the concentration of 100 mg/L decreased the anthocyanin accumulation, while increasing the content of (+)-catechin and (-)-epicatechin in 'Merlot' berry skin. This suggests that light exclusion reduces anthocyanin accumulation by increasing melatonin levels (Figure 3). Previous research in our laboratory found that the transcriptional changes of genes required for the biosynthesis and signal transduction of auxin, ethylene, BR and ABA were in accordance with the flavonoid accumulation in light-exposed berries during development, indicating the importance of phytohormones on berry flavonoid biosynthesis in response to light (Sun et al., 2017). Guan et al. (2016) bagged the grapes from fruit set to maturity, and found that total anthocyanin levels were lower under light-exposed conditions, but ABA concentration was elevated at fruit setting stage, then the difference diminished. UV-B irradiation of grapes from pre-flowering until harvest had no effect on endogenous ABA levels (Berli et al., 2011), suggesting that ABA plays a limited role in mediating the light and UV-B effects on anthocyanin biosynthesis (Figure 3). Liu et al. (2016) analyzed endogenous ethylene biosynthetic and signal-transduction pathways under light and dark condition, and found no significant difference in the expression of genes involved during the grape development, suggesting that ethylene is not responsive to light. When grape clusters are sprayed with exogenous 24-epibrassinolide (a type of BR) under both light and dark conditions, the increase in anthocyanin levels is significantly greater under light condition. Correspondingly, the application of BR up-regulated the expression of flavonoid genes (*VvCHI1*, *VvCHS2*, *VvCHS3*, *VvDFR*, *VvANS*, *VvMYBA1*) under light conditions (Zhou et al., 2018) (Figure 3). Throughout grape development, light increases *VvBZR1* transcript, a key transcription factor positively regulating BR, suggesting that light likely increases endogenous BR content. Moreover, it has been repeatedly reported that exogenous supplement of BR enhances anthocyanin accumulation in grape skin (Luan et al., 2013; Xi et al., 2013; Vergara et al., 2018). These findings together indicate that BR and light have synergistic effects on anthocyanin biosynthesis in grapes. Additionally, BR signaling through BRI1-EMS-SUPPRESSOR 1 (BES1) typically inhibits flavonol synthesis to promote plant growth. However, under UV-B stress, this inhibition is lifted, leading to increased flavonol production in Arabidopsis (Liang et al., 2020). This BR-UV-flavonoid interaction network may also help with understanding the flux control between flavonols and anthocyanins/PAs, but it remains to be testified in grapevine in further studies.

4 The limited understanding of phytohormones in mediating the response of the flavonoid pathway to temperature changes

Climate models predict an increase in both average and extreme atmospheric temperatures (Santos et al., 2020; Gashu et al., 2023). The effect of elevated temperatures on flavonoids metabolism has been a focal point in grape research area. Most studies have demonstrated the inhibitory impact of high temperature (equal to or above 30°C) on anthocyanin. Molecular analysis has revealed decreased transcription of phenylpropanoid and flavonoid structural genes, including *VvPAL*, *VvCHS*, *VvCHI*, and *VvUFGT*, as well as transcription factor genes such as *VvMYBA1* and *VvMYBA2* under high temperature (Yamane et al., 2006; Mori et al., 2007b; Lecourieux et al., 2017; Pastore et al., 2017; Yan et al., 2020) (Figure 4). In addition to repressing anthocyanin-related genes, high temperatures have been shown to increase peroxidase activity in cells, promoting anthocyanin degradation (Mori et al., 2007b; Yan et al., 2020). High temperatures also alter anthocyanin composition, increasing the proportion of acylated and tri-hydroxylated anthocyanins, which is accompanied by enhanced expression of *Vv3AT* (Lecourieux et al., 2017; Pastore et al., 2017; Yan et al., 2020). Elevated temperatures reduce endogenous ABA levels, as well as the expression levels of *VvMYBA1* and most flavonoid structural genes, suggesting that ABA may play a role

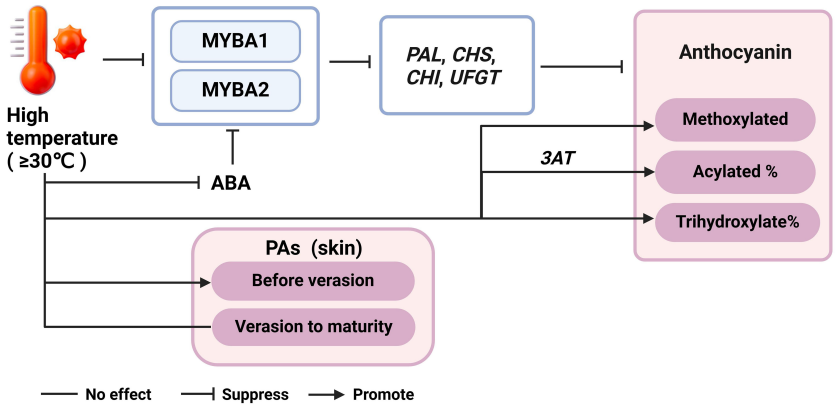

FIGURE 4
The regulatory network of temperature, phytohormones and flavonoid accumulation. ABA, abscisic acid; PAL, phenylalanine ammonia-lyase; CHS, chalcone synthase; CHI, chalcone isomerase; UFGT, UDP-glucose, flavonoid 3-*O*-glucosyltransferase.

in mediating the response of the flavonoid pathway to temperature changes (Yamane et al., 2006; Koshita et al., 2007; Azuma et al., 2012) (Figure 4). Mori et al. (2005a); Mori et al. (2005b) demonstrated that application of 250 ppm ABA through spraying almost diminished the adverse impact of night-time high temperature treatment on the reduction of anthocyanin levels in grape berries. Furthermore, Mori et al. (2005a) reported that high night temperatures (30°C) from veraison to maturity, compared to low night temperatures (15°C), reduced anthocyanin concentration in grape berry skins by inhibiting the expression of *VvCHS*, *VvF3H*, *VvDFR*, and *VvUFGT*, while flavonol levels remained unchanged. Gaiotti et al. (2018) also found low night temperature (10°C) during veraison favors the accumulation of anthocyanin by upregulating *VvCHS*, *VvF3H*, *VvUFGT* and *VvMYBA1*. Furthermore, Yan et al. (2020) observed that day temperature exerts a stronger influence on anthocyanin accumulation than night temperature. Their study, which involved setting different day and night temperature regimes, revealed that higher day temperatures led to a more pronounced decrease in anthocyanin concentration compared to variations in night temperatures.

The effect of temperature on PAs and flavonols accumulation is still not well understood. High night temperatures (above 8°C compared to environmental temperatures) during PA biosynthesis stages promoted flavan-3-ols synthesis in grape skins, while these differences were no longer significant after veraison until maturity, and no effect on flavonols regardless of the period of treatment (Cohen et al., 2012a; Cohen et al., 2012b). Pastore et al. (2017) found that PAs were not affected by heat stress (average temperature 26°C), while flavonols were decreased in Sangiovese grape skins. Similarly, studies by Gouot et al. (2019b) and Wu et al. (2019) observed no significant effect on flavan-3-ol monomer and PA levels in grape skins and seeds. In the study by Wu et al. (2019), a moderate increase in grape temperature was achieved by creating a local greenhouse effect, which led to an increase in PA levels before veraison but a decrease thereafter (Figure 4). This indicates that the timing and duration of heat exposure (at least 1.5°C higher than the ambient temperature) are crucial in determining the impact on PA accumulation. Overall, these findings highlight the nuanced and complex nature of temperature effects on grape phenolic compounds, emphasizing the need for further research to fully understand these interactions and their implications for viticulture under changing climatic conditions (Cohen et al., 2012a; Cohen et al., 2012b; Pastore et al., 2017; Gouot et al., 2019b; Wu et al., 2019).

5 Conclusion and prospect

In general, flavonoid metabolism constitute a complex process in grape. Environmental factors including water, light and temperature, significantly affect their biosynthesis. It is worth noting that there are interactions between these factors in field practice. For instance, bagging not only affects the light intensity, but also impacts on the temperature of grape. Therefore, the investigation of the interaction of various environmental factors on flavonoid metabolism is crucial for future research. Moreover, PAs is mainly synthesized at the flowering stage, so treatment of environmental factors at flowering stage may be more significant for the study of PAs regulation mechanism. Phytohormones signal network is complex and interactive during grape development. They play an important role as a medium in the process of studying environmental regulation of flavonoid. But there are limited studies that have conducted in-depth research, especially for temperature and light.

Additionally, although gene editing technology has been applied to optimize crop traits in other species such as rice and tomato, its implementation in grapes remains challenging due to the inhibition of polyphenols and other related antioxidant pathways (Osakabe et al., 2018). Consequently, scientists are focusing on more traditional hybridization methods to achieve the desired flavonoid characteristics in grapes (Yu et al., 2019). In the short term, adjusting the microclimate (water, light, and temperature) and hormone levels in

grapes may be the most valuable strategy in the field. Furthermore, these cultivation treatments can help identify genes related to environmental factors and plant hormones, which can serve as breeding markers for regulating flavonoid traits.

Author contributions

TS: Writing – original draft, Writing – review & editing, Conceptualization, Investigation. YS: Writing – review & editing. YL: Supervision, Writing – review & editing. CD: Funding acquisition, Supervision, Writing – review & editing. KY: Conceptualization, Funding acquisition, Investigation, Supervision, Writing – review & editing.

Funding

The author(s) declare financial support was received for the research, authorship, and/or publication of this article. This research was supported by the National Natural Science Foundation of China (32202452 and U20A2042); Science and Technology Major Project of Xinjiang Uygur Autonomous Region (2022A02002).

Conflict of interest

The authors declare that the research was conducted in the absence of any commercial or financial relationships that could be construed as a potential conflict of interest.

Publisher's note

References

Afifi, M., Obenland, D., and El-kereamy, A. (2021). The complexity of modulating anthocyanin biosynthesis pathway by deficit irrigation in table grapes. *Front. Plant Sci.* 12, 713277. doi: 10.3389/fpls.2021.713277

Azuma, A., Yakushiji, H., Koshita, Y., and Kobayashi, S. (2012). Flavonoid biosynthesis-related genes in grape skin are differentially regulated by temperature and light conditions. *Planta* 236, 1067–1080. doi: 10.1007/s00425-012-1650-x

Beres, C., Costa, G. N. S., Cabezudo, I., da Silva-James, N. K., Teles, A. S. C., Cruz, A. P. G., et al. (2017). Towards integral utilization of grape pomace from winemaking process: A review. *Waste Manage.* 68, 581–594. doi: 10.1016/j.wasman.2017.07.017

Berli, F. J., Fanzone, M., Piccoli, P., and Bottini, R. (2011). Solar UV-B and ABA are involved in phenol metabolism of *Vitis vinifera* L. increasing biosynthesis of berry skin polyphenols. *J. Agric. Food Chem.* 59, 4874–4884. doi: 10.1021/jf200040z

Bogs, J., Downey, M. O., Harvey, J. S., Ashton, A. R., Tanner, G. J., and Robinson, S. P. (2005). Proanthocyanidin synthesis and expression of genes encoding leucoanthocyanidin reductase and anthocyanidin reductase in developing grape berries and grapevine leaves. *Plant Physiol.* 139, 652–663. doi: 10.1104/pp.105.064238

Bogs, J., Ebadi, A., McDavid, D., and Robinson, S. P. (2006). Identification of the flavonoid hydroxylases from grapevine and their regulation during fruit development. *Plant Physiol.* 140, 279–291. doi: 10.1104/pp.105.073262

Bogs, J., Jaffé, F. W., Takos, A. M., Walker, A. R., and Robinson, S. P. (2007). The grapevine transcription factor VvMYBPA1 regulates proanthocyanidin synthesis during fruit development. *Plant Physiol.* 143, 1347–1361. doi: 10.1104/pp.106.093203

Bucchetti, B., Matthews, M. A., Falginella, L., Peterlunger, E., and Castellarin, S. D. (2011). Effect of water deficit on Merlot grape tannins and anthocyanins across four seasons. *Scientia Hortic.* 128, 297–305. doi: 10.1016/j.scienta.2011.02.003

Caceres-Mella, A., Inmaculada Talaverano, M., Villalobos-Gonzalez, L., Ribalta-Pizarro, C., and Pastenes, C. (2017). Controlled water deficit during ripening affects proanthocyanidin synthesis, concentration and composition in Cabernet Sauvignon grape skins. *Plant Physiol. Biochem.* 117, 34–41. doi: 10.1016/j.plaphy.2017.05.015

Castellarin, S. D., Matthews, M. A., Di Gaspero, G., and Gambetta, G. A. (2007a). Water deficits accelerate ripening and induce changes in gene expression regulating flavonoid biosynthesis in grape berries. *Planta* 227, 101–112. doi: 10.1007/s00425-007-0598-8

Castellarin, S. D., Pfeiffer, A., Sivilotti, P., Degan, M., Peterlunger, E., and Di Gaspero, G. (2007b). Transcriptional regulation of anthocyanin biosynthesis in ripening fruits of grapevine under seasonal water deficit. *Plant Cell Environ.* 30, 1381–1399. doi: 10.1111/j.1365-3040.2007.01716.x

Cavallini, E., Tomas Matus, J., Finezzo, L., Zenoni, S., Loyola, R., Guzzo, F., et al. (2015). The phenylpropanoid pathway is controlled at different branches by a set of R2R3-MYB C2 repressors in grapevine. *Plant Physiol.* 167, 1448–U1552. doi: 10.1104/pp.114.256172

Cheng, J., Yu, K. J., Shi, Y., Wang, J., and Duan, C. Q. (2021). Transcription factor VviMYB86 oppositely regulates proanthocyanidin and anthocyanin biosynthesis in grape berries. *Front. Plant Sci.* 11, 613677. doi: 10.3389/fpls.2020.613677

Cohen, S. D., Tarara, J. M., Gambetta, G. A., Matthews, M. A., and Kennedy, J. A. (2012a). Impact of diurnal temperature variation on grape berry development, proanthocyanidin accumulation, and the expression of flavonoid pathway genes. *J. Exp. Bot.* 63, 2655–2665. doi: 10.1093/jxb/err449

Cohen, S. D., Tarara, J. M., and Kennedy, J. A. (2012b). Diurnal temperature range compression hastens berry development and modifies flavonoid partitioning in grapes. *Am. J. Enol. Vitic.* 63, 112–120. doi: 10.5344/ajev.2011.11015

Costa, J. M., Ortuno, M. F., and Chaves, M. M. (2007). Deficit irrigation as a strategy to save water: Physiology and potential application to horticulture. *J. Integr. Plant Biol.* 49, 1421–1434. doi: 10.1111/j.1672-9072.2007.00556.x

Cutanda-Perez, M. C., Ageorges, A., Gomez, C., Vialet, S., Terrier, N., Romieu, C., et al. (2009). Ectopic expression of VlmybA1 in grapevine activates a narrow set of genes involved in anthocyanin synthesis and transport. *Plant Mol. Biol.* 69, 633–648. doi: 10.1007/s11103-008-9446-x

Czemmel, S., Hoell, J., Loyola, R., Arce-Johnson, P., Antonio Alcalde, J., Tomas Matus, J., et al. (2017). Transcriptome-wide identification of novel UV-B- and light modulated flavonol pathway genes controlled by VviMYBF1. *Front. Plant Sci.* 8, 1084. doi: 10.3389/fpls.2017.01084

Czemmel, S., Stracke, R., Weisshaar, B., Cordon, N., Harris, N. N., Walker, A. R., et al. (2009). The grapevine R2R3-MYB transcription factor VvMYBF1 regulates flavonol synthesis in developing grape berries. *Plant Physiol.* 151, 1513–1530. doi: 10.1104/pp.109.142059

Deluc, L., Barrieu, F., Marchive, C., Lauvergeat, V., Decendit, A., Richard, T., et al. (2006). Characterization of a grapevine R2R3-MYB transcription factor that regulates the phenylpropanoid pathway. *Plant Physiol.* 140, 499–511. doi: 10.1104/pp.105.067231

Deluc, L., Bogs, J., Walker, A. R., Ferrier, T., Decendit, A., Merillon, J. M., et al. (2008). The transcription factor VvMYB5b contributes to the regulation of anthocyanin and proanthocyanidin biosynthesis in developing grape berries. *Plant Physiol.* 147, 2041–2053. doi: 10.1104/pp.108.118919

Deluc, L. G., Quilici, D. R., Decendit, A., Grimplet, J., Wheatley, M. D., Schlauch, K. A., et al. (2009). Water deficit alters differentially metabolic pathways affecting important flavor and quality traits in grape berries of Cabernet Sauvignon and Chardonnay. *BMC Genomics* 10, 212. doi: 10.1186/1471-2164-10-212

Dixon, R. A., Xie, D. Y., and Sharma, S. B. (2005). Proanthocyanidins - a final frontier in flavonoid research? *New Phytol.* 165, 9–28. doi: 10.1111/j.1469-8137.2004.01217.x

Dong, Y. J., Wu, Y. X., Zhang, Z. X., Wang, S. C., Cheng, J., Gao, Y. L., et al. (2023). Transcriptomic analysis reveals GA_3 is involved in regulating flavonoid metabolism in

grape development for facility cultivation. *Mol. Genet. Genomics* 298, 845–855. doi: 10.1007/s00438-023-02019-z

Downey, M. O., Dokoozlian, N. K., and Krstic, M. P. (2006). Cultural practice and environmental impacts on the flavonoid composition of grapes and wine: a review of recent research. *Am. J. Enol. Vitic.* 57, 257–268. doi: 10.5344/ajev.2006.57.3.257

Downey, M. O., Harvey, J. S., and Robinson, S. P. (2004). The effect of bunch shading on berry development and flavonoid accumulation in Shiraz grapes. *Aust. J. Grape Wine Res.* 10, 55–73. doi: 10.1111/j.1755-0238.2004.tb00008.x

Eichenberger, M., Schwander, T., Hüppi, S., Kreuzer, J., Mittl, P. R. E., Peccati, F., et al. (2023). The catalytic role of glutathione transferases in heterologous anthocyanin biosynthesis. *Nat. Catalysis* 6, 924-938. doi: 10.1038/s41929-023-01018-y

Falginella, L., Castellarin, S. D., Testolin, R., Gambetta, G. A., Morgante, M., and Di Gaspero, G. (2010). Expansion and subfunctionalisation of flavonoid 3′, 5′-hydroxylases in the grapevine lineage. *BMC Genomics* 11, 562. doi: 10.1186/1471-2164-11-562

Ferreira, V., Pinto-Carnide, O., Arroyo-Garcia, R., and Castro, I. (2018). Berry color variation in grapevine as a source of diversity. *Plant Physiol. Biochem.* 132, 696–707. doi: 10.1016/j.plaphy.2018.08.021

Ferreyra, M. L. F., Rius, S. P., and Casati, P. (2012). Flavonoids: biosynthesis, biological functions, and biotechnological applications. *Front. Plant Sci.* 3, 222. doi: 10.3389/fpls.2012.00222

Flamini, R., Mattivi, F., De Rosso, M., Arapitsas, P., and Bavaresco, L. (2013). Advanced knowledge of three important classes of grape phenolics: anthocyanins, stilbenes and flavonols. *Int. J. Mol. Sci.* 14, 19651–19669. doi: 10.3390/ijms141019651

Fujita, A., Soma, N., Goto-Yamamoto, N., Mizuno, A., Kiso, K., and Hashizume, K. (2007). Effect of shading on proanthocyanidin biosynthesis in the grape berry. *J. Jpn. Soc Hortic. Sci.* 76, 112–119. doi: 10.2503/jjshs.76.112

Gaiotti, F., Pastore, C., Filippetti, I., Lovat, L., Belfiore, N., and Tomasi, D. (2018). Low night temperature at veraison enhances the accumulation of anthocyanins in Corvina grapes (*Vitis Vinifera* L.). *Sci. Rep.* 8, 8719. doi: 10.1038/s41598-018-26921-4

Gambetta, G. A., Herrera, J. C., Dayer, S., Feng, Q. S., Hochberg, U., and Castellarin, S. D. (2020). The physiology of drought stress in grapevine: towards an integrative definition of drought tolerance. *J. Exp. Bot.* 71, 4658–4676. doi: 10.1093/jxb/eraa245

Gao, X. T., Wu, M. H., Sun, D., Li, H. Q., Chen, W. K., Yang, H. Y., et al. (2020). Effects of gibberellic acid (GA_3) application before anthesis on rachis elongation and berry quality and aroma and flavour compounds in *Vitis vinifera* L. 'Cabernet Franc' and 'Cabernet Sauvignon' grapes. *J. Sci. Food Agric.* 100, 3729–3740. doi: 10.1002/jsfa.10412

Gashu, K., Verma, P. K., Acuña, T., Agam, N., Bustan, A., and Fait, A. (2023). Temperature differences between sites lead to altered phenylpropanoid metabolism in a varietal dependent manner. *Front. Plant Sci.* 14. doi: 10.3389/fpls.2023.1239852

Genebra, T., Santos, R. R., Francisco, R., Pinto-Marijuan, M., Brossa, R., Serra, A. T., et al. (2014). Proanthocyanidin accumulation and biosynthesis are modulated by the irrigation regime in tempranillo seeds. *Int. J. Mol. Sci.* 15, 11862–11877. doi: 10.3390/ijms150711862

Gouot, J. C., Smith, J. P., Holzapfel, B. P., Walker, A. R., and Barril, C. (2019a). Grape berry flavonoids: a review of their biochemical responses to high and extreme high temperatures. *J. Exp. Bot.* 70(2), 397-423. doi: 10.1093/jxb/ery392

Gouot, J. C., Smith, J. P., Holzapfel, B. P., and Barril, C. (2019b). Impact of short temperature exposure of *Vitis vinifera* L. cv. Shiraz grapevine bunches on berry development, primary metabolism and tannin accumulation. *Environ. Exp. Bot.* 168, 103886. doi: 10.1016/j.envexpbot.2019.103866

Guan, L., Dai, Z., Wu, B.-H., Wu, J., Merlin, I., Hilbert, G., et al. (2016). Anthocyanin biosynthesis is differentially regulated by light in the skin and flesh of white-fleshed and teinturier grape berries. *Planta* 243, 23–41. doi: 10.1007/s00425-015-2391-4

Guo, S.-H., Xu, T.-F., Shi, T.-C., Jin, X.-Q., Feng, M.-X., Zhao, X.-H., et al. (2020). Cluster bagging promotes melatonin biosynthesis in the berry skins of *Vitis vinifera* cv. Cabernet Sauvignon and Carignan during development and ripening. *Food Chem.* 305, 125502. doi: 10.1016/j.foodchem.2019.125502

Guo, S.-H., Yang, B.-H., Wang, X.-W., Li, J.-N., Li, S., Yang, X., et al. (2021). ABA signaling plays a key role in regulated deficit irrigation-driven anthocyanins accumulation in 'Cabernet Sauvignon ' grape berries. *Environ. Exp. Bot.* 181, 104290. doi: 10.1016/j.envexpbot.2020.104290

Gutierrez-Gamboa, G., Garde-Cerdan, T., Portu, J., Moreno-Simunovic, Y., and Martinez-Gil, A. M. (2017). Foliar nitrogen application in Cabernet Sauvignon vines: Effects on wine flavonoid and amino acid content. *Food Res. Int.* 96, 46–53. doi: 10.1016/j.foodres.2017.03.025

He, F., Mu, L., Yan, G. L., Liang, N. N., Pan, Q. H., Wang, J., et al. (2010). Biosynthesis of anthocyanins and their regulation in colored grapes. *Molecules* 15, 9057–9091. doi: 10.3390/molecules15129057

He, F., Pan, Q.-H., Shi, Y., and Duan, C.-Q. (2008). Biosynthesis and genetic regulation of proanthocyanidins in plants. *Molecules* 13, 2674–2703. doi: 10.3390/molecules13102674

Herrera, J. C., Bucchetti, B., Sabbatini, P., Comuzzo, P., Zulini, L., Vecchione, A., et al. (2015). Effect of water deficit and severe shoot trimming on the composition of *Vitis vinifera* L. Merlot grapes and wines. *Aust. J. Grape Wine Res.* 21, 254–265. doi: 10.1111/ajgw.12143

Hichri, I., Heppel, S. C., Pillet, J., Leon, C., Czemmel, S., Delrot, S., et al. (2010). The basic helix-loop-helix transcription factor MYC1 is involved in the regulation of the flavonoid biosynthesis pathway in grapevine. *Mol. Plant* 3, 509–523. doi: 10.1093/mp/ssp118

Holton, T. A., and Cornish, E. C. (1995). Genetics and biochemistry of anthocyanin biosynthesis. *Plant Cell* 7, 1071–1083. doi: 10.1105/tpc.7.7.1071

Huang, Y.-F., Vialet, S., Guiraud, J.-L., Torregrosa, L., Bertrand, Y., Cheynier, V., et al. (2014). A negative MYB regulator of proanthocyanidin accumulation, identified through expression quantitative locus mapping in the grape berry. *New Phytol.* 201, 795–809. doi: 10.1111/nph.12557

Jeong, S. T., Goto-Yamamoto, N., Kobayashi, S., and Esaka, A. (2004). Effects of plant hormones and shading on the accumulation of anthocyanins and the expression of anthocyanin biosynthetic genes in grape berry skins. *Plant Sci.* 167, 247–252. doi: 10.1016/j.plantsci.2004.03.021

Jiu, S., Guan, L., Leng, X., Zhang, K., Haider, M. S., Yu, X., et al. (2021). The role of *VvMYBA2r* and *VvMYBA2w* alleles of the MYBA2 locus in the regulation of anthocyanin biosynthesis for molecular breeding of grape (*Vitis* spp.) skin coloration. *Plant Biotechnol. J.* 19, 1216–1239. doi: 10.1111/pbi.13543

Jun, J. H., Lu, N., Docampo-Palacios, M., Wang, X., and Dixon, R. A. (2021). Dual activity of anthocyanidin reductase supports the dominant plant proanthocyanidin extension unit pathway. *Sci. Adv.* 7, eabg4682. doi: 10.1126/sciadv.abg4682

Jun, J. H., Xiao, X. R., Rao, X. L., and Dixon, R. A. (2018). Proanthocyanidin subunit composition determined by functionally diverged dioxygenases. *Nat. Plant* 4, 1034–1043. doi: 10.1038/s41477-018-0292-9

Kaplan, M., Najda, A., Klimek, K., and Borowy, A. (2019). Effect of gibberellic acid (GA_3) inflorescence application on content of bioactive compounds and antioxidant potential of grape (*Vitis* L.) 'Einset seedless' Berries. *S. Afr. J. Enol. Vitic.* 40, 1-10. doi: 10.21548/40-1-3004

Kobayashi, S., Goto-Yamamoto, N., and Hirochika, H. (2004). Retrotransposon-induced mutations in grape skin color. *Science* 304, 982–982. doi: 10.1126/science.1095011

Koshita, Y., Asakura, T., Fukuda, H., and Tsuchida, Y. (2007). Nighttime temperature treatment of fruit clusters of 'Aki Queen' grapes during maturation and its effect on the skin color and abscisic acid content. *Vitis* 46, 208–209.

Koyama, K., and Goto-Yamamoto, N. (2008). Bunch shading during different developmental stages affects the phenolic biosynthesis in berry skins of 'Cabernet sauvignon' Grapes. *J. Am. Soc Hortic. Sci.* 133, 743–753. doi: 10.21273/jashs.133.6.743

Koyama, K., Ikeda, H., Poudel, P. R., and Goto-Yamamoto, N. (2012). Light quality affects flavonoid biosynthesis in young berries of Cabernet Sauvignon grape. *Phytochemistry* 78, 54–64. doi: 10.1016/j.phytochem.2012.02.026

Koyama, K., Numata, M., Nakajima, I., Goto-Yamamoto, N., Matsumura, H., and Tanaka, N. (2014). Functional characterization of a new grapevine MYB transcription factor and regulation of proanthocyanidin biosynthesis in grapes. *J. Exp. Bot.* 65, 4433–4449. doi: 10.1093/jxb/eru213

Koyama, K., Sadamatsu, K., and Goto-Yamamoto, N. (2010). Abscisic acid stimulated ripening and gene expression in berry skins of the Cabernet Sauvignon grape. *Funct. Integr. Genomics* 10, 367–381. doi: 10.1007/s10142-009-0145-8

Kuhn, N., Guan, L., Dai, Z. W., Wu, B. H., Lauvergeat, V., Gomès, E., et al. (2014). Berry ripening: recently heard through the grapevine. *J. Exp. Bot.* 65, 4543–4559. doi: 10.1093/jxb/ert395

Lacampagne, S., Gagné, S., and Gény, L. (2010). Involvement of abscisic acid in controlling the proanthocyanidin biosynthesis pathway in grape skin: new elements regarding the regulation of tannin composition and leucoanthocyanidin reductase (LAR) and anthocyanidin reductase (ANR) activities and expression. *J. Plant Growth Regul.* 29, 81–90. doi: 10.1007/s00344-009-9115-6

Lecourieux, F., Kappel, C., Pieri, P., Charon, J., Pillet, J., Hilbert, G., et al. (2017). Dissecting the biochemical and transcriptomic effects of a locally applied heat treatment on developing cabernet sauvignon grape berries. *Front. Plant Sci.* 8, 53. doi: 10.3389/fpls.2017.00053

Li, H., Bai, Y., Yang, Y., Zheng, H., Xu, X., Li, H., et al. (2023). Transcriptomic analyses reveal light-regulated anthocyanin accumulation in 'ZhongShan-HongYu' grape berries. *Scientia Hortic.* 309, 111669. doi: 10.1016/j.scienta.2022.111669

Liang, T., Shi, C., Peng, Y., Tan, H., Xin, P., Yang, Y., et al. (2020). Brassinosteroid-activated BRI1-EMS-SUPPRESSOR 1 inhibits flavonoid biosynthesis and coordinates growth and UV-B stress responses in plants. *Plant Cell* 32, 3224–3239. doi: 10.1105/tpc.20.00048

Liu, L., Gregan, S., Winefield, C., and Jordan, B. (2015). From UVR8 to flavonol synthase: UV-B-induced gene expression in Sauvignon blanc grape berry. *Plant Cell Environ.* 38, 905–919. doi: 10.1111/pce.12349

Liu, M.-y., Song, C. Z., Chi, M., Wang, T. M., Zuo, L. L., Li, X. L., et al. (2016). The effects of light and ethylene and their interaction on the regulation of proanthocyanidin and anthocyanin synthesis in the skins of *Vitis vinifera* berries. *Plant Growth Regul.* 79, 377–390. doi: 10.1007/s10725-015-0141-z

Loreti, E., Povero, G., Novi, G., Solfanelli, C., Alpi, A., and Perata, P. (2008). Gibberellins, jasmonate and abscisic acid modulate the sucrose-induced expression of anthocyanin biosynthetic genes in Arabidopsis. *New Phytol.* 179, 1004–1016. doi: 10.1111/j.1469-8137.2008.02511.x

Loyola, R., Herrera, D., Mas, A., Wong, D. C. J., Hoell, J., Cavallini, E., et al. (2016). The photomorphogenic factors UV-B RECEPTOR 1, ELONGATED HYPOCOTYL 5, and HY5 HOMOLOGUE are part of the UV-B signalling pathway in grapevine and mediate flavonol accumulation in response to the environment. *J. Exp. Bot.* 67, 5429–5445. doi: 10.1093/jxb/erw307

Lu, S., Wang, J., Zhuge, Y., Zhang, M., Liu, C., Jia, H., et al. (2021). Integrative analyses of metabolomes and transcriptomes provide insights into flavonoid variation in grape berries. *J. Agric. Food Chem.* 69, 12354–12367. doi: 10.1021/acs.jafc.1c02703

Luan, L. Y., Zhang, Z. W., Xi, Z. M., Huo, S. S., and Ma, L. N. (2013). Brassinosteroids regulate anthocyanin biosynthesis in the ripening of grape berries. *S. Afr. J. Enol. Vitic.* 34, 196–203. doi: 10.21548/34-2-1094

Martens, S., Teeri, T., and Forkmann, G. (2002). Heterologous expression of dihydroflavonol 4-reductases from various plants. *FEBS Lett.* 531, 453–458. doi: 10.1016/s0014-5793(02)03583-4

Martinez-Gil, A. M., Gutierrez-Gamboa, G., Garde-Cerdan, T., Perez-Alvarez, E. P., and Moreno-Simunovic, Y. (2018). Characterization of phenolic composition in Carignan noir grapes (*Vitis vinifera* L.) from six wine-growing sites in Maule Valley, Chile. *J. Sci. Food Agric.* 98, 274–282. doi: 10.1002/jsfa.8468

Matsuyama, S., Tanzawa, F., Kobayashi, H., Suzuki, S., Takata, R., and Saito, H. (2014). Leaf Removal Accelerated Accumulation of Delphinidin-based Anthocyanins in 'Muscat Bailey A' *Vitis x labruscana* (Bailey) and *Vitis vinifera* (Muscat Hamburg) Grape Skin. *J. Jpn. Soc Hortic. Sci.* 83, 17–22. doi: 10.2503/jjshs1.CH-062

Matus, J. T., Cavallini, E., Loyola, R., Höll, J., Finezzo, L., Dal Santo, S., et al. (2017). A group of grapevine MYBA transcription factors located in chromosome 14 control anthocyanin synthesis in vegetative organs with different specificities compared with the berry color locus. *Plant J.* 91, 220–236. doi: 10.1111/tpj.13558

Matus, J. T., Poupin, M. J., Canon, P., Bordeu, E., Alcalde, J. A., and Arce-Johnson, P. (2010). Isolation of WDR and bHLH genes related to flavonoid synthesis in grapevine (*Vitis vinifera* L.). *Plant Mol. Biol.* 72, 607–620. doi: 10.1007/s11103-010-9597-4

Meng, J.-F., Yu, Y., Shi, T.-C., Fu, Y.-S., Zhao, T., and Zhang, Z.-W. (2019). Melatonin treatment of pre-veraison grape berries modifies phenolic components and antioxidant activity of grapes and wine. *Food Sci. Technol.* 39, 35–42. doi: 10.1590/1678-457x.24517

Mori, K., Goto-Yamamoto, N., Kitayama, M., and Hashizume, K. (2007a). Loss of anthocyanins in red-wine grape under high temperature. *J. Exp. Bot.* 58, 1935–1945. doi: 10.1093/jxb/erm055

Mori, K., Goto-Yamamoto, N., Kitayama, M., and Hashizume, K. (2007b). Effect of high temperature on anthocyanin composition and transcription of flavonoid hydroxylase genes in 'Pinot noir' grapes (*Vitis vinifera*). *J. Horticult. Sci. Biotechnol.* 82, 199–206. doi: 10.1080/14620316.2007.11512220

Mori, K., Saito, H., Goto-Yamamoto, N., Kitayama, M., Kobayashi, S., Sugaya, S., et al. (2005a). Effects of abscisic acid treatment and night temperatures on anthocyanin composition in Pinot noir grapes. *Vitis* 44, 161–165. doi: 10.1016/j.pnpbp.2004.11.023

Mori, K., Sugaya, S., and Gemma, H. (2005b). Decreased anthocyanin biosynthesis in grape berries grown under elevated night temperature condition. *Scientia Hortic.* 105, 319–330. doi: 10.1016/j.scienta.2005.01.032

Mukherjee, A., Dwivedi, S., Bhagavatula, L., and Datta, S. (2023). Integration of light and ABA signaling pathways to combat drought stress in plants. *Plant Cell Rep.* 42, 829–841. doi: 10.1007/s00299-023-02999-7

Murcia, G., Fontana, A., Pontin, M., Baraldi, R., Bertazza, G., and Piccoli, P. N. (2017). ABA and GA_3 regulate the synthesis of primary and secondary metabolites related to alleviation from biotic and abiotic stresses in grapevine. *Phytochemistry* 135, 34–52. doi: 10.1016/j.phytochem.2016.12.007

Olle, D., Guiraud, J. L., Souquet, J. M., Terrier, N., Ageorges, A., Cheynier, V., et al. (2011). Effect of pre- and post-veraison water deficit on proanthocyanidin and anthocyanin accumulation during Shiraz berry development. *Aust. J. Grape Wine Res.* 17, 90–100. doi: 10.1111/j.1755-0238.2010.00121.x

Osakabe, Y., Liang, Z. C., Ren, C., Nishitani, C., Osakabe, K., Wada, M., et al. (2018). CRISPR-Cas9-mediated genome editing in apple and grapevine. *Nat. Protoc.* 13, 2844–2863. doi: 10.1038/s41596-018-0067-9

Pastore, C., Dal Santo, S., Zenoni, S., Movahed, N., Allegro, G., Valentini, G., et al. (2017). Whole plant temperature manipulation affects flavonoid metabolism and the transcriptome of grapevine berries. *Front. Plant Sci.* 8, 929. doi: 10.3389/fpls.2017.00929

Reshef, N., Agam, N., and Fait, A. (2018). Grape berry acclimation to excessive solar irradiance leads to repartitioning between major flavonoid groups. *J. Agric. Food Chem.* 66, 3624–3636. doi: 10.1021/acs.jafc.7b04881

Reynolds, A., Robbins, N., Lee, H. S., and Kotsaki, E. (2016). Impacts and interactions of abscisic acid and gibberellic acid on sovereign coronation and skookum seedless table grapes. *Am. J. Enol. Vitic.* 67, 327–338. doi: 10.5344/ajev.2016.15108

Rienth, M., Vigneron, N., Darriet, P., Sweetman, C., Burbidge, C., Bonghi, C., et al. (2021). Grape berry secondary metabolites and their modulation by abiotic factors in a climate change scenario-A review. *Front. Plant Sci.* 12, 643258. doi: 10.3389/fpls.2021.643258

Rinaldo, A. R., Cavallini, E., Jia, Y., Moss, S. M. A., McDavid, D. A. J., Hooper, L. C., et al. (2015). A grapevine anthocyanin acyltransferase, transcriptionally regulated by VvMYBA, can produce most acylated anthocyanins present in grape skins. *Plant Physiol.* 169, 1897–1916. doi: 10.1104/pp.15.01255

Roby, G., and Matthews, M. A. (2004). Relative proportions of seed, skin and flesh, in ripe berries from Cabernet Sauvignon grapevines grown in a vineyard either well irrigated or under water deficit. *Aust. J. Grape Wine Res.* 10, 74–82. doi: 10.1111/j.1755-0238.2004.tb00009.x

Santos, J. A., Fraga, H., Malheiro, A. C., Moutinho-Pereira, J., Dinis, L. T., Correia, C., et al. (2020). A review of the potential climate change impacts and adaptation options for european viticulture. *Appl. Sciences-Basel* 10, 3092. doi: 10.3390/app10093092

Savoi, S., Wong, D. C. J., Arapitsas, P., Miculan, M., Bucchetti, B., Peterlunger, E., et al. (2016). Transcriptome and metabolite profiling reveals that prolonged drought modulates the phenylpropanoid and terpenoid pathway in white grapes (*Vitis vinifera* L.). *BMC Plant Biol.* 16, 67. doi: 10.1186/s12870-016-0760-1

Shohat, H., Eliaz, N. I., and Weiss, D. (2021). Gibberellin in tomato: metabolism, signaling and role in drought responses. *Mol. horticulture* 1, 15–15. doi: 10.1186/s43897-021-00019-4

Sun, R.-Z., Cheng, G., Li, Q., He, Y.-N., Wang, Y., Lan, Y.-B., et al. (2017). Light-induced variation in phenolic compounds in cabernet sauvignon grapes (*Vitis vinifera* L.) involves extensive transcriptome reprogramming of biosynthetic enzymes, transcription factors, and phytohormonal regulators. *Front. Plant Sci.* 8, 547. doi: 10.3389/fpls.2017.00547

Sun, Y., Liu, Q., Xi, B., and Dai, H. (2019). Study on the regulation of anthocyanin biosynthesis by exogenous abscisic acid in grapevine. *Scientia Hortic.* 250, 294–301. doi: 10.1016/j.scienta.2019.02.054

Terrier, N., Torregrosa, L., Ageorges, A., Vialet, S., Verries, C., Cheynier, V., et al. (2009). Ectopic expression of VvMybPA2 promotes proanthocyanidin biosynthesis in grapevine and suggests additional targets in the pathway. *Plant Physiol.* 149, 1028–1041. doi: 10.1104/pp.108.131862

Torres, N., Martinez-Luscher, J., Porte, E., and Kurtural, S. K. (2020). Optimal ranges and thresholds of grape berry solar radiation for flavonoid biosynthesis in warm climates. *Front. Plant Sci.* 11. doi: 10.3389/fpls.2020.00931

Tyagi, K., Maoz, I., Kochanek, B., Sela, N., Lerno, L., Ebeler, S. E., et al. (2021). Cytokinin but not gibberellin application had major impact on the phenylpropanoid pathway in grape. *Horticulture Res.* 8, 51. doi: 10.1038/s41438-021-00488-0

VanderWeide, J., Falchi, R., Calderan, A., Peterlunger, E., Vrhovsek, U., Sivilotti, P., et al. (2022). Juxtaposition of the Source-to-Sink Ratio and Fruit Exposure to Solar Radiation on cv. Merlot (*Vitis vinifera* L.) Berry Phenolics in a Cool versus Warm Growing Region. *J. Agric. Food Chem.* 70, 10429-10442. doi: 10.1021/acs.jafc.2c01528

Vergara, A. E., Díaz, K., Carvajal, R., Espinoza, L., Alcalde, J. A., and Pérez-Donoso, A. G. (2018). Exogenous applications of brassinosteroids improve color of red table grape (*Vitis vinifera* L. Cv. "Redglobe") berries. *Front. Plant Sci.* 9, 363. doi: 10.3389/fpls.2018.00363

Villalobos-González, L., Peña-Neira, A., Ibáñez, F., and Pastenes, C. (2016). Long-term effects of abscisic acid (ABA) on the grape berry phenylpropanoid pathway: Gene expression and metabolite content. *Plant Physiol. Biochem.* 105, 213–223. doi: 10.1016/j.plaphy.2016.04.012

Wang, P. Q., Liu, Y. J., Zhang, L. J., Wang, W. Z., Hou, H., Zhao, Y., et al. (2020a). Functional demonstration of plant flavonoid carbocations proposed to be involved in the biosynthesis of proanthocyanidins. *Plant J.* 101, 18–36. doi: 10.1111/tpj.14515

Wang, Q., Yu, F., and Xie, Q. (2020b). Balancing growth and adaptation to stress: Crosstalk between brassinosteroid and abscisic acid signaling. *Plant Cell Environ.* 43, 2325–2335. doi: 10.1111/pce.13846

Wei, X. F., Wang, W. Y., Min, Z., Li, Z. Y., Ouyang, Y. N., Ruan, X. R., et al. (2023). Transcriptomics combined with metabolisms reveals the effect of light-exclusive films on the quality and polyphenols of 'Cabernet Sauvignon' grapes. *Food Res. Int.* 170, 112754. doi: 10.1016/j.foodres.2023.112754

Winkel-Shirley, B. (2002). Biosynthesis of flavonoids and effects of stress. *Curr. Opin. Plant Biol.* 5, 218–223. doi: 10.1016/s1369-5266(02)00256-x

Wu, J., Drappier, J., Hilbert, G., Guillaumie, S., Dai, Z. W., Geny, L., et al. (2019). The effects of a moderate grape temperature increase on berry secondary metabolites. *Oeno One* 53, 321–333. doi: 10.20870/oeno-one.2019.53.2.2434

Xi, Z. M., Zhang, Z. W., Huo, S. S., Luan, L. Y., Gao, X., Ma, L. N., et al. (2013). Regulating the secondary metabolism in grape berry using exogenous 24-epibrassinolide for enhanced phenolics content and antioxidant capacity. *Food Chem.* 141, 3056–3065. doi: 10.1016/j.foodchem.2013.05.137

Xie, D. Y., Sharma, S. B., Paiva, N. L., Ferreira, D., and Dixon, R. A. (2003). Role of anthocyanidin reductase, encoded by *BANYULS* in plant flavonoid biosynthesis. *Science* 299, 396–399. doi: 10.1126/science.1078540

Xu, W. J., Dubos, C., and Lepiniec, L. (2015). Transcriptional control of flavonoid biosynthesis by MYB-bHLH-WDR complexes. *Trends Plant Sci.* 20, 176–185. doi: 10.1016/j.tplants.2014.12.001

Yamane, T., Jeong, S. T., Goto-Yamamoto, N., Koshita, Y., and Kobayashi, S. (2006). Effects of temperature on anthocyanin biosynthesis in grape berry skins. *Am. J. Enol. Vitic.* 57, 54–59. doi: 10.5344/ajev.2006.57.1.54

Yan, Y. F., Song, C. Z., Falginella, L., and Castellarin, S. D. (2020). Day temperature has a stronger effect than night temperature on anthocyanin and flavonol accumulation in 'Merlot' (*Vitis vinifera* L.) grapes during ripening. *Front. Plant Sci.* 11. doi: 10.3389/fpls.2020.01095

Yang, B., He, S., Liu, Y., Liu, B. C., Ju, Y. L., Kang, D. Z., et al. (2020a). Transcriptomics integrated with metabolomics reveals the effect of regulated deficit

irrigation on anthocyanin biosynthesis in Cabernet Sauvignon grape berries. *Food Chem.* 314, 126170. doi: 10.1016/j.foodchem.2020.126170

Yang, B., Yao, H., Zhang, J., Li, Y., Ju, Y., Zhao, X., et al. (2020b). Effect of regulated deficit irrigation on the content of soluble sugars, organic acids and endogenous hormones in Cabernet Sauvignon in the Ningxia region of China. *Food Chem.* 312, 126020. doi: 10.1016/j.foodchem.2019.126020

Yu, K., Dixon, R. A., and Duan, C. (2022). A role for ascorbate conjugates of (+)-catechin in proanthocyanidin polymerization. *Nat. Commun.* 13, 3425. doi: 10.1038/s41467-022-31153-2

Yu, K., Jun, J. H., Duan, C., and Dixon, R. A. (2019). VvLAR1 and VvLAR2 are bifunctional enzymes for proanthocyanidin biosynthesis in grapevine. *Plant Physiol.* 180, 1362–1374. doi: 10.1104/pp.19.00447

Yu, K., Song, Y., Lin, J., and Dixon, R. A. (2023). The complexities of proanthocyanidin biosynthesis and its regulation in plants. *Plant Commun.* 4, 100498. doi: 10.1016/j.xplc.2022.100498

Yu, R., Cook, M. G., Yacco, R. S., Watrelot, A. A., Gambetta, G., Kennedy, J. A., et al. (2016). Effects of Leaf Removal and Applied Water on Flavonoid Accumulation in Grapevine (*Vitis vinifera* L. cv. Merlot) Berry in a Hot Climate. *J. Agric. Food Chem.* 64, 8118–8127. doi: 10.1021/acs.jafc.6b03748

Zhang, C., Dai, Z., Ferrier, T., Orduna, L., Santiago, A., Peris, A., et al. (2023). MYB24 orchestrates terpene and flavonol metabolism as light responses to anthocyanin depletion in variegated grape berries. *Plant Cell.* 35, 4238-4265. doi: 10.1093/plcell/koad228

Zhou, Y., Yuan, C., Ruan, S., Zhang, Z., Meng, J., and Xi, Z. (2018). Exogenous 24-epibrassinolide interacts with light to regulate anthocyanin and proanthocyanidin biosynthesis in cabernet sauvignon (*Vitis vinifera* L.). *Molecules* 23, 93. doi: 10.3390/molecules23010093

Zhu, Z., Li, G., Liu, L., Zhang, Q., Han, Z., Chen, X., et al. (2019). A R2R3-MYB transcription factor, VvMYBC2L2, functions as a transcriptional repressor of anthocyanin biosynthesis in grapevine (*Vitis vinifera* L.). *Molecules* 24, 92. doi: 10.3390/molecules24010092

Zhu, Z., Quan, R., Chen, G., Yu, G., Li, X., Han, Z., et al. (2022). An R2R3-MYB transcription factor *VyMYB24*, isolated from wild grape *Vitis yanshanesis* J. X. Chen., regulates the plant development and confers the tolerance to drought. *Front. Plant Sci.* 13, 966641. doi: 10.3389/fpls.2022.966641

frontiers | Frontiers in Plant Science

TYPE Original Research
PUBLISHED 27 August 2024
DOI 10.3389/fpls.2024.1382768

OPEN ACCESS

EDITED BY
Li Tian,
University of California, Davis, United States

REVIEWED BY
Simona Fabroni,
Council for Agricultural Research and Economics, Italy
Yue Zhu,
Zhuhai College of Science and Technology, China

*CORRESPONDENCE
Lin Hong
loquatvalue@163.com

†These authors have contributed equally to this work

RECEIVED 06 February 2024
ACCEPTED 08 August 2024
PUBLISHED 27 August 2024

CITATION
Li S, Yang L, Wang M, Chen Y, Yu J, Chen H, Yang H, Wang W, Cai Z and Hong L (2024) Effects of rootstocks and developmental time on the dynamic changes of main functional substances in 'Orah' (*Citrus reticulata* Blanco) by HPLC coupled with UV detection. *Front. Plant Sci.* 15:1382768. doi: 10.3389/fpls.2024.1382768

Effects of rootstocks and developmental time on the dynamic changes of main functional substances in 'Orah' (*Citrus reticulata* Blanco) by HPLC coupled with UV detection

Shuang Li†, Lei Yang†, Min Wang, Yang Chen, Jianjun Yu, Hao Chen, Haijian Yang, Wu Wang, Zhiyong Cai and Lin Hong*

Research Institute of Pomology, Chongqing Academy of Agricultural Sciences, Chongqing, China

Introduction: Citrus fruit is rich in important functional constituents such as flavonoids, phenolic acids terpenes and other functional substances that play an important role for treating clinical diseases or controlling major agricultural diseases and pests. Plant secondary metabolites have become one of the most important resources of novel lead compounds, especially young citrus fruits contain multiple functional substances. 'Orah', a type of citrus reticulata, is known for its fine appearance, productivity, delicious sweetness, late-maturing characteristics, and is widely cultivated in China. Fruit thinning and rootstock selection are commonly used agronomic measures in its production to ensure its quality and tree vigor. However, few studies have demonstrated the effects of these agronomic measures on the functional substances of 'Orah'.

Methods: In this study, we used HPLC coupled with UV to detect the dynamic changes of fruit quality, 13 main flavonoids, 7 phenolic acids, 2 terpenes, synephrine and antioxidant capacity in both peel and pulp of citrus fruits grafted on four rootstocks (Red orange *Citrus reticulata* Blanco cv. red tangerine, Ziyang xiangcheng *Citrus junos* Sieb. ex Tanaka, Trifoliate orange *Poncirus trifoliata* L. Raf, and Carrizo citrange *Citrus sinensis* Osb.×*P.trifoliate* Raf) at six different developmental stages (from 90 DAF to 240 DAF).

Results: The results indicated that rootstock can significantly affect the contents of functional constituents and antioxidant capacity in 'Orah'. Additionally, it was found that pruning at either 90 DAF (days after flowering) or 150 DAF produced the most favorable outcomes for extracting functional substances. We also identified rootstock 'Trifoliate orange' has the highest total soluble solids (TSS) and 'Ziyang xiangcheng' to be the optimal in terms of comprehensive sensory of fruit quality, while 'Red orange' and 'Ziyang xiangcheng' are optimal in terms of functional substance quality, and 'Red orange' excels in antioxidant capacity.

10.3389/fpls.2024.1382768

Discussion: Overall, the findings demonstrate the important role of rootstocks and developmental stage in shaping fruit sensory quality and functional substance synthesis, providing valuable insights for guiding rootstock selection, determining thinning time, and utilizing pruned fruits in a more informed manner.

KEYWORDS

mandarin, phenolic compounds, bioactive compounds, antioxidant activity, fruit quality

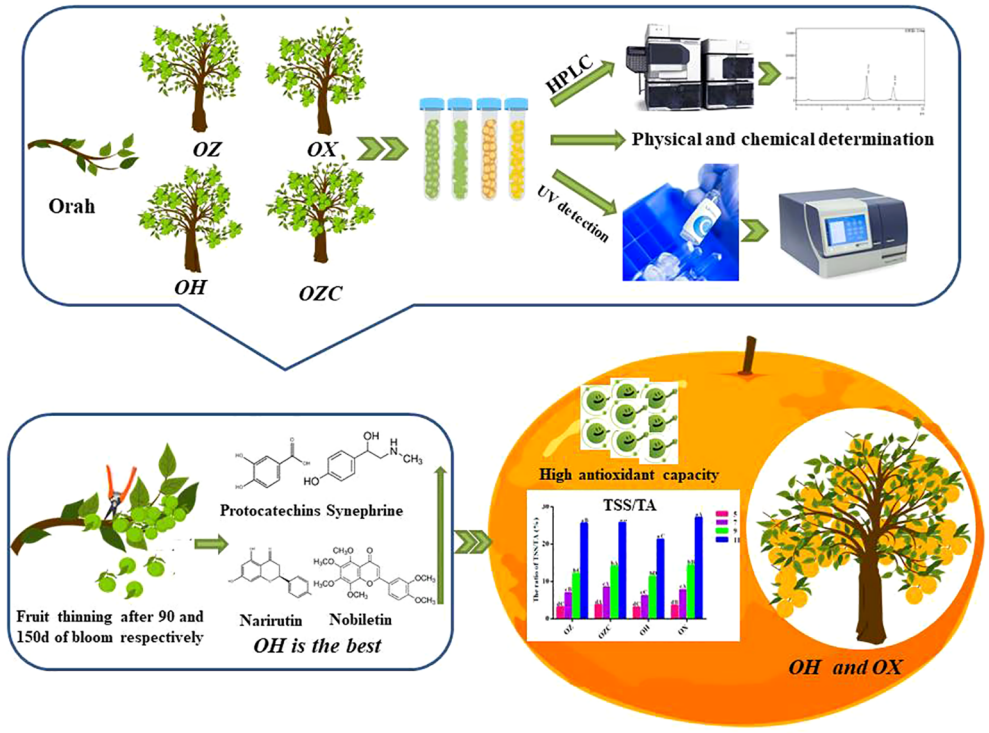

GRAPHICAL ABSTRACT

Introduction

Most natural products of medicament come from plants, animals, and microorganisms. According to records, the history of humans using plants as pharmaceuticals could be traced back to at least 60000 years ago (Shi et al., 2010). After millions of years of evolution, natural products have unique chemical diversity, leading to a diversity of their biological activity and medical properties, with great potential for treating human diseases, especially critical illnesses (Simmonds, 2003; Lattanzio et al., 2006; Galm and Shen, 2007). As early as the 1930s, many scholars discovered that citrus serves as a natural source of multiple antioxidants and bioactive substances (Robbins, 1980), rich not only in primary metabolites such as organic acids, sugars and amino acids (Shi et al., 2010; Benjamin et al., 2013), but also in valuable secondary metabolites such as carotene, polyphenols (particularly flavanones and flavonoids, phenolic acids, normilin and limonin) (Tanaka et al., 2000; Goldenberg et al., 2018), which can treat and alleviate human cardiovascular, cerebrovascular, tumor, blood and other diseases. Among them, citrus flavonoids also can be used to control various pests such as grashoppers, *Spodoptera litura*, etc (Aboshi et al., 2018; Cui et al., 2019). Naringin, naringenin, and hesperidin have insecticidal activity (Franceschini Sarria et al., 2022). The pharmacological mechanism of naringin to play an anti-cancer role in blocking tumor cell cycle, inhibiting tumor cell proliferation, alleviate Adverse drug reaction of chemotherapy, activate and strengthen immunity (He and Zhang, 2023). Citrus fruits also contain a numerous phenolic acids such as ferulic acid, p-coumaric acid, sinapic acid, and caffeic acid, vanillic acid, etc., all of which serve

as antioxidants that coordinate and stimulate metabolic transformations to protect tissues and body fluids from damages associated with the presence of reactive oxygen species (Silva et al., 2000; Czech et al., 2021). Therefore, planting citrus crops with high phenolic compounds can not only control human diseases, but also prevent and control pests, providing materials for the preparation of pesticides and medicine.

The chemical composition and biological activity of citrus fruits are influenced by various factors, including cultivation methods (water and fertilizer management, grafting), growing environment, and fruit ripeness (Li et al., 2022). Traditionally, using rootstocks to improve varieties is a normal practice in citrus cultivation, including good compatibility and adaptability, vigorous and healthy rootstocks are essential to improving fruit yield, functional substance content, overall quality, resistance, as well as the nutritional status of grafted plants. These factors ultimately affect the economic outcomes of orchards (Albrecht et al., 2018; Morales et al., 2023). Different rootstocks, citrus varieties, and even different combinations of rootstock strains exhibit significant differences, ultimately affecting their chemical compositions (Benjamin et al., 2013). For example, the scion variety Fremont mandarin, exhibited superior plant growth and fruit yield on common rootstocks (rough lemon or Karna khatta). Similarly, Pectinifera rootstock not only increases yield but also exhibited environmental stress (Albrecht et al., 2018). 'Rough lemon'-1 (scion *C. Nobilis*× *C. deliciosa*) provided the necessary concentrations of sugars, acids, phenols, vitamins, and low limonin. Furthermore, rootstocks like 'Lime' and 'Shekwasha' induced high production of limonin in 'Kinnow', while the rootstocks such as 'Shekwasha', 'Sour Orange', and 'Pectinifera' led to higher concentrations of flavonoids, quercetin, and hesperidin in 'Kinnow' fruits (Albrecht et al., 2018; Saini et al., 2019). However, the distribution and content of these compounds are not uniform in the peel and pulp of fruit at different stages of development. A study has found that the concentration of individual functional substances is higher in the pulp than in the peel (Ordóñez-Díaz et al., 2020). While other scholars believe that antioxidants in citrus peel are higher than those in other fruits and the pulp of the citrus fruit (Singh et al., 2020). It is puzzling that the distribution of functional substances in the peel and pulp of citrus fruit is not clear at different stages of fruit development.

Introduced to China in 2004, 'Orah' is a variety bred by crossing 'Temple' tangor and 'Dancy' mandarin in Israel. 'Orah' possess the characteristics such as strong tree vigor, early fruiting and maximum yield, late ripening and storage capabilities, transportation resistance, crisp and sweet pulp, a rich and juicy flavor. These qualities significantly increased the income of fruit farmers in the region (Jiang and Cao, 2011). The rootstocks commonly used for grafting 'Orah' in China include Red orange (*Citrus reticulata* Blanco cv. Red tangerine) representing *'H'* (Liu et al., 2017), Ziyang xiangcheng (Citrus junos Sieb. ex Tanaka) representing '*X* ' (He et al., 2022), Trifoliate orange (*Poncirus trifoliata* (L.) Raf)) representing '*Z* ' (Sheng et al., 2009) and Carrizo citrange (*Citrus.sinensis* Osb.×*P.trifoliate* Raf) representing '*ZC*' (Morales et al., 2021), most of which have achieved significant success in the field of applied research. For example, '*Z*' is one of the most common traditional Chinese medicines, and various new anti-tumor drugs have been explored through the development and utilization of its active ingredients (Zhang et al., 2015). In 2012, 'Orah' had been widely planted and developed into the main variety of late-maturing mandarin oranges in China (Wu et al., 2021). In our preliminary research, UPLC-MS/MS (ultra-performance liquid chromatography-tandem mass spectrometry) was performed to analyze the metabolites of Orah' grafted on four rootstocks ('Trifoliate orange', 'Carrizo citrange', 'Red tangerine' and 'Ziyang Xiangcheng'), and a considerable difference between the different rootstocks was also observed in the accumulation of lipids, phenolic acids and flavonoids (Wang et al., 2024). Unfortunately, the lack of knowledge on the functional components of 'Orah's pulp and peel grafted on different rootstocks at each developmental stages obstructs the utilization of functional substances in young fruits. Furthermore, the inner qualities resulting from grafting onto different rootstocks, especially the chemical composition of 'Orah' such as its phenolic acids, flavones, limonin, and antioxidant capacity, have not been studied thoroughly. Previous studies have shown that multiple citrus varieties, especially citrus hybrids, require thinning during the young fruit stage to improve the quality of mature fruits and tree vigor (Ouma, 2012). As a citrus hybrid, the optimal thinning time of 'Orah' was still unclear.

Although research on rootstock-scion interactions has seen gradual progress in recent years (Tietel et al., 2020), our understanding of the extent on the functional substances content of 'Orah' at different developmental stages remains limited. Vitamins, polyphenols, and limonin, etc. are key metabolites that affect the quality of citrus (Gong et al., 2015). The selection of suitable rootstocks can promote fruit quality and functional components. So far, no study has been conducted on the influence of the rootstocks of '*H*', '*X*', '*Z*', and '*ZC*' on the content of functional substances and antioxidant activity in the fruit and peel of citrus. On the other hand, the amount of fruit planted in 'Orah' is huge, thinning is necessary to ensure the normal growth of the tree and improve the fruit quality, but the optimal time of fruit-thinning has not been determined yet. Therefore, this study employs HPLC coupled with UV to evaluate the effects of rootstock on flavor, functional substances and antioxidant activity of 'Orah' fruits at different developmental stages. It aims to analyze the changes in functional and nutritional components of rootstock-scion combinations at different developmental stages, determine the suitable rootstock and fruit thinning time, and propose optimized utilization strategies for pruning fruits, providing direction for the acquisition of natural medicinal materials. At the same time, it also provides guidance for improving the the yield of 'Orah' by increasing income and reducing expenditure.

Materials and methods

Fruit sample and study site

From July 2019 to February 2020, fresh fruit samples of 'Orah' (*C.reticulata Blanco*) grafted onto '*H*', '*X*', '*Z*', '*ZC*' rootstocks were obtained from a 5-year old experimental orchard located in the Jiangjin district of Chongqing. This area is one of the most suitable regions for citrus cultivation in Southwest China (N: 29°13′36.65″, E: 106°18′37.50″). Each rootstock was grafted with 'Orah' trees, there were 9 sample trees of each rootstock-scion. Fruits from each of the three trees was collected for a biological treatment, and this was repeated thrice. The experimental orchard's soil type was a sandy and red soil, and a drip-irrigation system was used. According to the Chinese climate classification system, the local climate in the Xianfeng district is subtropical monsoon, with an annual rainfall of 1030.7 mm, primarily occurring from May to November. The temperature range varies widely throughout the year, with average temperatures of 7.7°C in winter and 28.5°C during spring and summer (https://czqxj.net.cn/qihou_814343).

Sampling of plants commenced on July 8, 2020, following the described and published protocol (Huang et al., 2009). Samples were collected at 90, 120, 150, 180, 210 and 240 days after full flower. Five samples were gathered from five different directions (East, South, West, North, and the middle of the crown periphery) in each plant. A total of 15 medium sized fruits without pests and diseases were collected from 3 sample trees as a biological replicate, and repeated 3 times. The collected samples were stored in an icebox and promptly transported to the laboratory. The peels (P) and pulps (R) were then separated using a sterilized blade, chopped and mixed, and then placed in a -80 °C ultra-low temperature refrigerator.

Standards and reagents

The glassware and consumables used in the experiments included Eppendorf 100ml single channel pipette gun, Eppendorf 50-200 μL single channel pipette gun, dry nitrogen blowing instrument (Wuxi Woxin Instrument, China), a Shimadzu LC-20AT high performance liquid chromatograph, a Wufeng LC-100 high performance liquid chromatograph, a C18 column (250 mm×4.6 mm, 5 μm), and a cryogenic centrifuge TLG-16 (Hunan Xiangyi, China). The chemical standards and reagents used in the experiment included methanol (chromatographic grade, Shanghai Ampei), acetonitrile (chromatographic grade, Shanghai Amppo), acetic acid (chromatographic grade, Aladdin), sodium lauryl sulfonate (chromatographic grade, Shanghai Yuanye Co., Ltd.), phosphoric acid (chromatographic grade, Aladdin), formic acid (chromatographic grade, Aladdin), and potassium dihydrogen phosphate (analytical pure, Shanghai Yuanye Co., Ltd). Nomelin, limonin, synephrine, protocatechuic acid, p-hydroxbenzoic, vanillic acid, caffeic acid, sinapic acid, p-coumaric, ferulic acid, sinensetin, nobiletin, hesperidin, narirutin, tangeretin, eriocitrin, naringin, rhoifolin, vanillin, naringenin, hesperetin, neohesperidin and poncirin obtained from Sigma Corporation, USA were also used. The kit including amino acids, total phenols, total flavonoid, and free radical clearance ability (FRAP, ABTS, and DPPH), was procured from Suzhou Grace Biotechnology Co., Ltd. China.

Physical and chemical determinations

Thirty 'Orah' were selected to determine their functional composition. Ten fruits served as one replicate, with the pulp and peel separated using a disinfected blade. Their weights were measured on an electronic balance (OHAUS AX223ZH/E) with 1mg accuracy. BRAun 4161 juicer was used to extract the juice for later use. The total soluble solids (TSS) and titratable acidity (TA) of 'Orah' mandarin fruit were determined using a digital refractometer (PAL-1; Atago, Tokyo, Japan) and volumetric neutralization, respectively, following the methods described by He and Zhang (2023). The TA and vitamin C contents were determined following GB8210-87 Chinese National Standard. Similarly, phenolic compounds, flavonoids, limonin, nomirin and synephrine were quantified using HPLC (Shimadzu LC-20AT and Wufeng LC-100).

Limonin and nomeline

Fresh samples of peel and pulp were separated using a sterilized blade. Portions of the samples were weighed (0.5 g), soaked in 1mL of acetonitrile, and subjected to 30 minutes of the ultrasonic treatment at 60°C using a 300 W ultrasonic equipment. The resultant supernatants were obtained, followed by centrifugation at 12,000 rpm for 10 minutes. This process was repeated 3 times and the supernatants were combined. The samples were then dried using nitrogen, after which 1mL of acetonitrile was added for proper dissolution. The obtained supernatant was filtered over a 0.22 μm organic filter membrane. The analysis was performed using HPLC (Shimadzu LC-20AT) on a C18 reverse phase chromatographic column (250 mm×4.6 mm, 5 μm). The running conditions consisted of phase A (methanol), and phase B (0.1% acetic acid water), at a ratio of A:B =35:65. The injection volume was 10 μL, with a flow rate of 1 mL min^{-1}. The column temperature was maintained at 35°C, and the running time were 30 min. The UV detection was conducted at 210 nm.

Synephrine

Fresh samples of peel and pulp (0.5g each) were taken and soaked in 1 mL of 80% methanol water solution. The samples were then subjected to sonication at 300 W for 40 minutes, followed by centrifugation at 12,000 rpm for 10 minutes. The obtained supernatant was filtered with a 0.22 μm organic filter membrane. Analysis was performed using HPLC (Wufeng LC-100) with a C18 reverse-phase chromatography column (250 mm×4.6 mm, 5 μm). The running conditions consisted mobile phase A (methanol) and mobile phase B (0.1% potassium dihydrogen phosphate aqueous solution, containing 1% sodium dodecyl sulfonate and 2 mL acetic acid, at a ratio of A:B:=50:50. The column temperature was kept at 25°C. The running time was 30 minutes, and the wavelength of the UV detector wavelength was set at 275 nm.

Protocatechuic acid, p-hydroxbenzoic and vanillic acid

Fresh samples (0.5g) of peel and pulp were taken and soaked in 1mL of 60% methanol. The samples were extracted by ultrasonication at 60 °C for 30 minutes, heated at 80°C for 1.5 hours, then diluted to 1ml with 60% methanol water. Finally, they were centrifuged at 4°C, 12,000 rpm for 10 minutes. The resultant supernatant was filtered through a 0.22 µm filter membrane. The analysis was performed using HPLC (Wufeng LC-100) with a C18 reverse phase chromatography column (250 mm×4.6 mm, 5 µm). The running conditions included mobile phase A: (methanol) and mobile phase B: (0.1% phosphoric acid water), at a ratio of A: B=20:80. The injection volume was 10 µL and the flow rate was 1 mL min^{-1}. The column temperature was kept at 25°C. The running time was 50 minutes, and UV detection maintained at 320 nm.

Caffeic acid, sinapic, acid ferulic acid and p-coumaric acid

Fresh samples (0.5 g) of peel and pulp were taken and soaked in 1 mL of 80% methanol. The samples were extracted by ultrasonication at 300 W for 40minutes. Samples were then centrifuged at 4°C, 12000 rpm for 10 minutes, to obtain supernatants. The resultant supernatants were filtered through a 0.22 µm filter membrane and analyzed using HPLC (Wufeng LC-100) following the same running conditions as explained for protocatechuic acid.

Sinensetin, nobiletin and tangeretin

Obtained fresh samples (0.5 g) of peel and pulp were mixed with 1 mL methanol DMSO (V/V=50:50) and placed at room temperature for 10 minutes. The samples were then centrifuged at 4°C, 9000 rpm for 15 minutes. This process was repeated 3 times and the resulting supernatants were combined. Subsequently, the samples were reduced under nitrogen to 0.5mL, after which 1mL of methanol was added. They were then filtered through a 0.22 µm filter membrane and analyzed using HPLC (Wufeng LC-100) on a C18 reverse phase chromatography column (250 mm×4.6 mm, 5 µm). The running conditions consisted of mobile phase A: (methanol) and mobile phase B: (0.1% formic acid water), at a ratio of A:B=45:55. The injection volume was 10µL and the flow rate was 1 mL min^{-1}. The column temperature was kept at 25°C, running time of 60 minutes, and the UV detector's wavelength of 330 nm.

Narirutin, hesperidin, neohesperidin, poncirin, hesperetin, eriocitrin, naringin, rhoifolin, vanillin and naringenin

Fresh peel and pulp samples (0.5 g) were dissolved in 1mL of 80% methanol water, and subjected to sonication at 300 W. The samples were then centrifuged at 4 °C, 12,000 rpm for 10 minutes. The supernatants were then filtered through a 0.22 µm filter membrane and analyzed using HPLC (Wufeng LC-100) following the same running conditions as those set for sinensetin, with UV detection at 283 nm.

Total phenols and flavonoids

First 0.1 g of fresh samples were obtained and ground on ice. Next, 1.5 mL of 60% ethanol was added and shaken for 2 hours at 60°C (when evaporated, it was diluted back to 1.5 mL with 60% ethanol). The detection method followed the instructions provided with the kit (Suzhou Geruisi Biotechnology Co., Ltd, for total phenols (G0117W), and flavonoids (G0118W) test kit respectively).

FRAP free radical clearance capacity

Firstly, 0.1g of fresh sample was weighed and ground in 1mL of 80% ethanol (provided). It was then transferred to a 2 mL centrifuge tube and subjected to ultrasonication at 60°C for 30 minutes at 200-300 W (with 5 min intervals of shaking and mixing). The resulting supernatant was subsequently centrifuged at 12,000 rpm for 10 minutes, cooled on ice, and assayed according to the provided.

ABTS free radical clearance ability and DPPH free radical clearing ability

A fresh sample weighing 0.1 g was obtained and uniformly ground with 1ml of methanol. Ultrasonic extraction was performed at 60°C, for 30 minutes (shaken and mixed every 5 minutes) using a 200-300W ultrasonic device. In case of any loss, the sample volume was adjusted with 80% methanol to 1mL. The samples were centrifuged at 12000 rpm for 10 minutes at room temperature to obtain the supernatant. Detection was carried out following the provided instructions with the ABTS free radical clearance ability (G0127W) kit of Suzhou Grace Biotechnology Co., Ltd. China, and DPPH free radical clearing ability (G0128W) test kit respectively).

Amino acid

0.1 g of fresh sample was weighed, to which 1mL of extract solution was added and homogenized at room temperature. Samples were then centrifuged at 12,000 rpm for 10 minutes at 4°C. The supernatant was placed on ice for detection, following the kit's instructions for Amino acid (G0415W) of Suzhou Grace Biotechnology Co., Ltd. China.

Titratable acidity, TSS and vitamin C

The development of citrus fruits includes five stages: flowering, physiological fruit drop stage (0d-89d after flowering (DAF)), fruit enlargement stage (90-149 DAF), color transformation stage, and ripe stage (Singh et al., 2015). Citrus enters the fruit-expansion stage at 90 DAF, and the fruit diameter at 120 DAF is 3-4cm, with very little juice and cannot be detected. At 150 DAF, the fruit-expansion stage ends, and the fruit diameter is 5-6cm (Mo et al., 2019). Therefore, we start testing the main fruit quality assay of TSS, Acid and VC etc., from 150 DAF. The content of soluble solids (TSS) was measured by Atago digital practice saccharimeter (PAL-1, Atago, Japan). Similarly, titrable acids were determined by NaOH neutralization titration method (Titrette digital bottle neck titrator, Germany). The Vitamin C (VC) content (mg per 100mL by weight) was determined using 2,6-dichloroindophenol sodium titration method for VC content determination.

Data analysis

Titratable acid content was calculated using citric acid with the formula = (V × M × 0.064) × 100, where 'V' representing the volume of 0.1 mol/L NaOH standard solution used to titrate the sample (mL), 'M' was the concentration of the NaOH standard solution (0.1 mol/L), and the factor '0.064' represented the grams of citric acid required to neutralize 1 mL of 0.1 mol/L NaOH. The solid acid ratio (RTT) was determined by the ratio of soluble solid content to titratable acid content. The confidence test method of the binomial normal distribution was used to establish confidence intervals for the means of the main chemical substances. The Pearson correlation coefficient was employed to analyze correlations between the parameters of 'Orah' in different rootstock-scion combinations. Principal Component Analysis (PCA) was calculated using the 'prcomp' function within the 'stat' R package, and PCA results were visualized using the R package 'factoextra'. All tests were conducted in triplicate, and the data was expressed as the mean ± standard deviation (SD) of the absolute content for each substance. Analysis of variance (Tukey method of ANOVA analysis) was performed using SPSS version 17.0, with statistical significance set at $P<0.05$.

Results

Influence of different rootstocks and development time on the quality of 'Orah'

In this study, we detected Indicators total soluble solids (TSS), titratable acid (TA), vitamin C, fruit weight and edible rate, for measuring the external quality of fruits. Based on the fruit development stage, we start testing the main fruit quality assay of TSS, Acid and VC etc., from 150 DAF. Results showed that the proportion of peel weight of 'Orah' on different rootstocks significantly decreased with the extension of developmental time ($F= 92.13$, $P<0.05$) in the early stage of fruit development. The proportion of peel weight of all rootstock-scion combinations tended to stabilize after 180 DAF except for '*ZC*', while the proportion of pulp was opposite to the trend of peel proportion. As fruit development time extended, the proportion of fruit pulp increased significantly ($F=56.63$, $P<0.05$). The fruits ofon rootstock '*H*' and '*X*' were significantly heavier than those of '*Z*' and '*ZC*', while the pulp percentage of '*ZCR*' was significantly heavier than the other threes (Figures 1A, B).

The TSS of the '*H*' and '*X*' were the lowest at 120 DAF, while that of the other rootstock continued to increase with fruits development. The TSS of the four rootstocks ('*Z*', '*ZC*', '*H*', '*X*') reached its peak at 240 DAF, with values of 13.20%, 12.30%, 12.05%, and 12.90%, respectively. Therefore, the TSS of '*Z*' was the highest in the same developmental period, significantly higher than the others (Figure 1C). And the trend of RTT was consistent with TSS, while that of total acid was opposite (Figures 1C–E).

The VC content under different rootstock grafting increased continuously with the fruit development. The highest content was observed at 210 DAF, with that of rootstock '*Z*' (44.82 mg/100ml) was significantly higher than other rootstocks ($P<0.05$) (Figure 1F).

Influence of different rootstocks and development time on the 3 types of total functional substances of 'Orah'

Phenolics are the most abundant secondary metabolites in plants. We detected the contents of total phenolic acid, total flavonoids and amino acid content in 'Orah' fruits under different development stages and rootstocks. Analysis of changes in the functional substances of the peel and pulp of 'Orah' grafted onto the four rootstocks, showed that the total phenol content of the peel in four rootstocks was relatively higher during the early stage of development (Figure 2). Among these, '*HP*' had the highest total phenolic content of 9.8 mg/g at 90 DAF, which decreased with the extension of the developmental period, reaching its the lowest point in the later stage. The total phenol content in '*HP*', '*XP*', '*ZP*', and '*ZCP*' did not exhibit significant differences. However, except for '*ZCR*', the total phenol content of the pulp in the other three combinations gradually increased with the extension of the developmental period. Among them, the rootstock '*ZCR*' and '*HR*' showed the highest levels at 120 DAF, with 1.7 mg/g and 1.51 mg/g, respectively (Figure 2A).

The changes in total flavonoid contents in the peel of the four rootstocks were consistent with the changes in total phenols. All decreased as the developmental period extended, with the highest total flavonoid content observed in '*HP*' at 4.42 mg/g. The highest total flavonoid content in the pulp of all four rootstocks was recorded at 120 DAF. Among these, the flavonoid content in '*HR*' had the highest value of 0.94 mg/g, which gradually decreased with the extension of developmental time (Figure 2B).

The results indicated that the changes in the total amino acid contents of the peel followed a pattern consistent with the changes in the total phenol content as the developmental period extended. The highest values were recorded in the early stages of development, gradually decreasing as time progressed. Of these, the total amino acid content of '*ZP*' was the highest at 50.77 μmol/g. Except for the total amino acid content of '*HP*' at its lowest point at 180 DAF, the rest were at their the lowest at 240 DAF. In the case of 'Orah' development, the total amino acid content in the pulp of 'Orah' grafted onto the four rootstocks showed an initial increasing trend, followed by a decreasing trend, with the highest levels at 150 DAF, 18.88 μmol/g, 18.29 μmol/g, 19.17 μmol/g and 20.97 μmol/g, respectively (Figure 2C).

Influence of different rootstocks and development time on the 3 kinds of special functional substances of 'Orah'

Limonin is a secondary metabolite of triterpenoids and widely exists in citrus plants. As shown in Figure 3A; Supplementary Figure S3, the change in limonin content in the peel of different rootstocks varied with the fruit development stage. '*HP*' exhibited

10.3389/fpls.2024.1382768

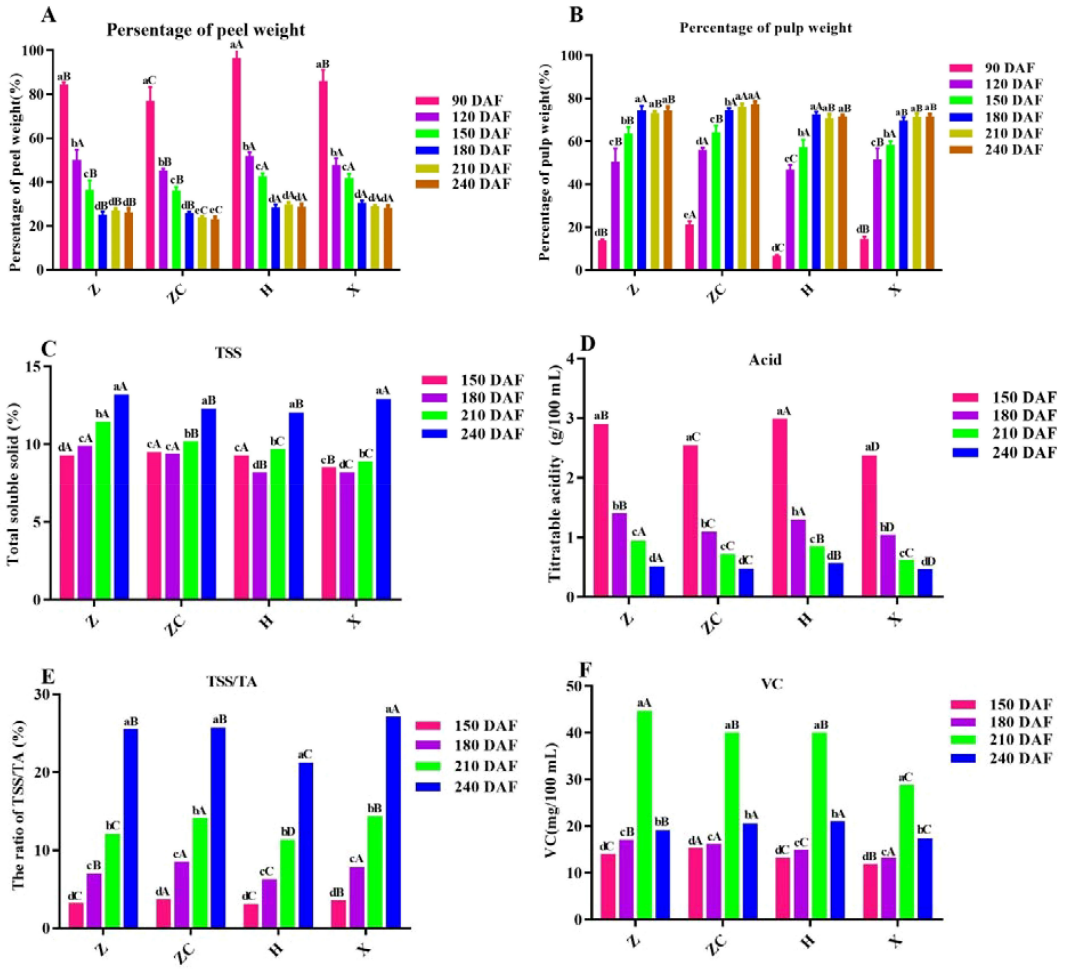

FIGURE 1
Effect of different rootstocks on fruit and quality of 'Orah'. **(A)** persentage of peel weight. **(B)** persentage of pulp weight. **(C)** TSS. **(D)** Acid. **(E)** RTT. **(F)** VC. Z: *P. trifoliata* (L.) Raf, ZC: *C. sinensis* Osb.× *P. trifoliate* Raf. H: *C. reticulata* Blanco cv. Red tangerine, X: *C. junos* Sieb. ex Tanaka, 90, 120, 150, 180, 210, 240 DAF: Fruit at 90d, 120d, 150d, 180d, 210d, 240d after flowering. The samples in panels (**C–F**) were from the fruit pulp from 150 to 240 DAF. Different lowercase letters in the same rootstock at different times represented significant difference ($P<0.05$), while capital letters represent significant differences in the different rootstocks at the same time period ($P<0.05$).

the highest content of 405.5 μg/g at 120 DAF, while '*ZP*' had the highest content of 364.49 μg/g at 90 DAF. The limonin content in the pulp initially increased and then decreased as the developmental time prolonged. It reached the lowest point at 240 DAF, with values of 2.11 μg/g, 2.54 μg/g, 2.23 μg/g, and 2.01 μg/g, respectively. Of these, '*ZR*' and '*ZCR*' reached their highest levels at 150 DAF (307.89 μg/g) and 120 DAF (374.86 μg/g), respectively (Figure 3A).

As the main limonin found in citrus fruits, nomilin has many pharmacological and health effects. Different rootstocks and developmental stages had different effects on the nomilin content in peel and pulp. The content of nomilin in '*HP*' and '*XP*' exhibited a trend of decreasing followed by increasing, and was significantly lower at 150 DAF compared to other developmental periods ($F=12.53$, $P<0.05$; $F=32.21$, $P<0.05$). The nomilin content of the '*ZCP*' was significantly higher at 120 DAF (1093.59 μg/g) and 240 DAF (938.78 μg/g) respectively, compared to the other rootstocks at the same developmental stage. However, '*ZP*' reached its highest content at 180 DAF, significantly surpassing that of the other three rootstocks at the same developmental stage with 635.79 μg/g. The normilin content in the pulp of the four rootstocks initially increased, and then decreased, being significantly higher at 120 DAF, with '*ZCR*' recording the highest at 565.59 μg/g (Figure 3B).

As an active ingredient with various biomedical functions, synephrine was found to be highly abundant in young citrus fruits. The synephrine content in the peel of the four rootstocks was significantly higher during the early stages of fruit development. '*XP*' displayed the highest value of 12807.75 μg/g after 90 DAF. All values decreased to the lowest level at 210 DAF, with values of 334.87 μg/g, 293.83 μg/g, 294.95 μg/g, and 233.71 μg/g, respectively. The content of synephrine in both '*HR*' and '*ZR*' showed an initial increase, followed by a decrease during fruit development. Both reached their highest level at 120 DAF, with values 2484.56 μg/g and 2229.25 μg/g, respectively. '*ZR*' and '*XR*' exhibited consistent changes, with synephrine content decreasing at 120 DAF and being significantly lower at 240 DAF ($F=45.76$, $P<0.05$) (Figure 3C; Supplementary Figure S4).

10.3389/fpls.2024.1382768

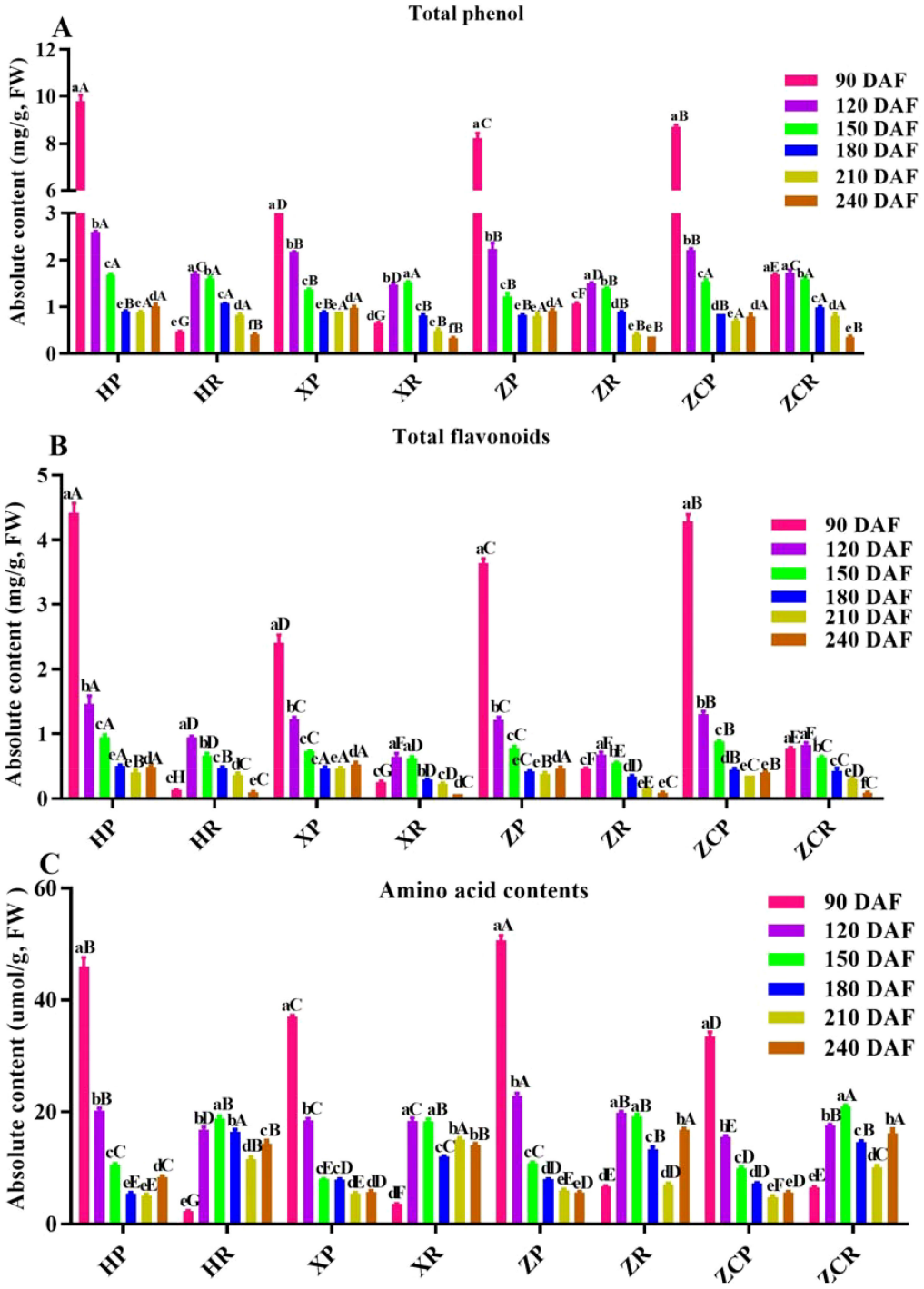

FIGURE 2
Changes in the content of functional substances in 'Orah' under grafting on different rootstocks. HP: Peel of 'Orah' grafted on *C. reticulata* Blanco cv. Red tangerine, HR: Pulp of 'Orah' grafted on *C. reticulata* Blanco cv. Red tangerine, XP: Peel of 'Orah' grafted on *C. junos* Sieb. ex Tanaka, XR: Pulp of 'Orah' grafted on *C. junos* Sieb. ex Tanaka, ZP: Peel of 'Orah' grafted on *P. trifoliata* (L.) Raf, ZR: Pulp of 'Orah' grafted on *P. trifoliata* (L.) Raf, ZCP: Peel of 'Orah' grafted on *C. sinensis* Osb.× *P. trifoliate* Raf, ZCR: Pulp of 'Orah' grafted on *C. sinensis* Osb.× *P. trifoliate* Raf. 90, 120, 150, 180, 210, 240 DAF: Fruit at 90d, 120d, 150d, 180d, 210d, 240d after flowering. All samples were fresh samples. Different lowercase letters in the same rootstock at different times represented significant difference ($P<0.05$), while capital letters represent significant differences in the different rootstocks at the same time period ($P<0.05$). **(A)** Total phenol. **(B)** Tatol flavonoids. **(C)** Tatole amino acid contents.

10.3389/fpls.2024.1382768

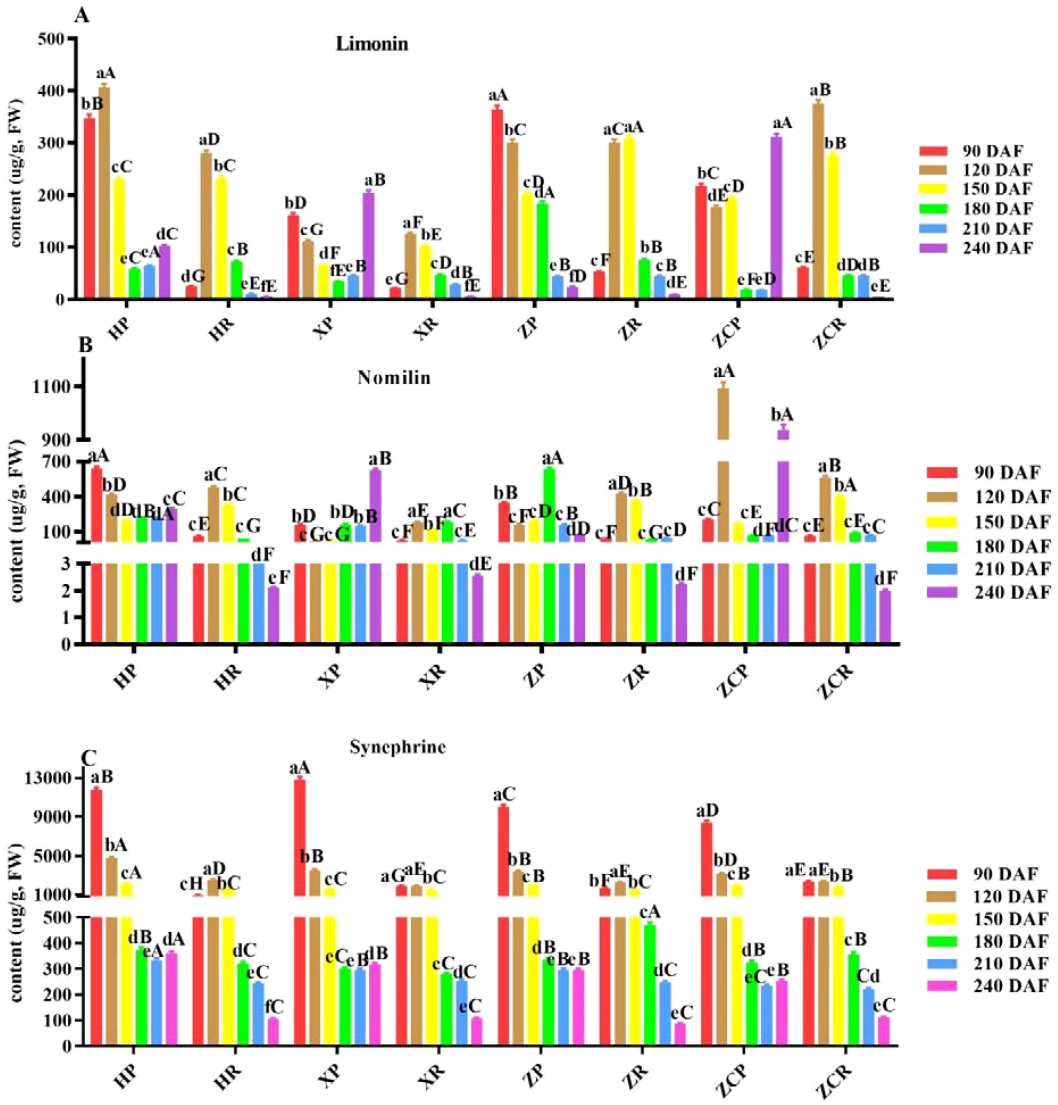

FIGURE 3
Changes of limonin, nomilin and synephrine content in 'Orah' under grafting of different rootstocks-scion combinations. HP: Peel of 'Orah' grafted on *C. reticulata* Blanco cv. Red tangerine, HR: Pulp of 'Orah' grafted on *C. reticulata* Blanco cv. Red tangerine, XP: Peel of 'Orah' grafted on *C. junos* Sieb. ex Tanaka, XR: Pulp of 'Orah' grafted on *C. junos* Sieb. ex Tanaka, ZP: Peel of 'Orah' grafted on *P. trifoliata* (L.) Raf, ZR: Pulp of 'Orah' grafted on *P. trifoliata* (L.) Raf, ZCP: Peel of 'Orah' grafted on *C. sinensis* Osb.× *P. trifoliate* Raf, ZCR: Pulp of 'Orah' grafted on *C. sinensis* Osb.× *P. trifoliate* Raf. 90, 120, 150, 180, 210, 240 DAF: Fruit at 90d, 120d, 150d, 180d, 210d, 240d after flowering. FW: Fresh weight. Different lowercase letters in the same rootstock at different times represented significant difference ($P<0.05$), while capital letters represent significant differences in the different rootstocks at the same time period ($P<0.05$). **(A)** Limonin. **(B)** Nomilin. **(C)** Synephrine.

Influence of different rootstocks and development time on the seven kinds of phenolic acid of 'Orah'

The dynamic changes of 7 main phenolic acids including protocatechuic acid, p-hydroxybenzoic acid, vanillic acid, caffeic acid, caprylic acid, ferulic acid and p-coumaric acid were quantitatively determined. The content of phenolic acids in young fruits grafting on different rootstocks was significantly different during the developmental stages.

As shown in Figure 4; Supplementary Figures S1, S6, the four phenolic acids include protocatechin, caffeic acid, ferulic acid, sinapic acid had higher content and more consistent. The content of protocatechins in peel was higher than that in pulp at all developmental stages, and reached the maximum at 90 DAF (F=45.87, $P<0.05$). It gradually decreased as the developmental time extended. Of these, '*XP*' and '*ZCR*' exhibited the highest values (Figure 4A). Caffeic acid was detected in all four rootstocks after 180 DAF, with '*HP*' having the highest content at 12.35 μg/g, surpassing that of the other rootstocks across all development stages (Figure 4B). The content of ferulic acid in the peel of the four rootstocks showed the highest level in the early stage of development, which continued to decrease as the developmental time extended. The highest ferulic acid content was measured in the pulp at 150 DAF, at 22.05μg/g, 23.13 μg/g, 22.27 μg/g, and 27.45 μg/g, respectively (Figure 4C).

10.3389/fpls.2024.1382768

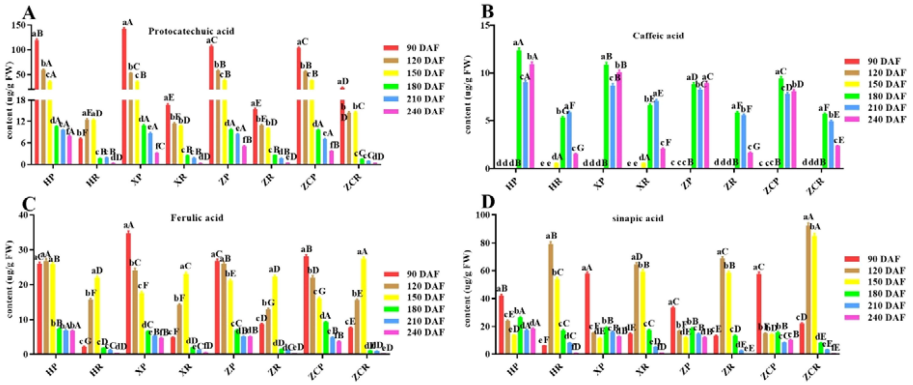

FIGURE 4
Changes in the content of four phenolic acid in 'Orah' under grafting on different rootstocks. HP: Peel of 'Orah' grafted on *C. reticulata* Blanco cv. Red tangerine, HR: Pulp of 'Orah' grafted on *C. reticulata* Blanco cv. Red tangerine, XP: Peel of 'Orah' grafted on *C. junos* Sieb. ex Tanaka,XR: Pulp of 'Orah' grafted on *C. junos* Sieb. ex Tanaka, ZP: Peel of 'Orah' grafted on *P. trifoliata* (L.) Raf, ZR: Pulp of 'Orah' grafted on *P. trifoliata* (L.) Raf, ZCP: Peel of 'Orah' grafted on *C. sinensis* Osb.× *P. trifoliate* Raf, ZCR: Pulp of 'Orah' grafted on *C. sinensis* Osb.× *P. trifoliate* Raf. 90, 120, 150, 180, 210, 240 DAF: Fruit at 90d, 120d, 150d, 180d, 210d, 240d after flowering. FW, Fresh weight. Different lowercase letters in the same rootstock at different times represented significant difference ($P<0.05$), while capital letters represent significant differences in the different rootstocks at the same time period ($P<0.05$). **(A)** Protocatechin. **(B)** Caffeic acid. **(C)** Ferulic acid. **(D)** Sinapic acid.

The sinapic acid content in pulp was significantly higher than that in peel from 120 to 150 DAF, reaching its peak at 120 DAF. '*ZCR*' exhibited a significantly higher content compared to the remaining three rootstocks, with a value of 92.37 μg/g. In the peel, it was significantly higher within 90 DAF. Among these, '*XP*' exhibited a significantly higher sinapic acid content at 57.86 μg/g (Figure 4D). The content of other three kinds phenolic acids (p-hydroxbenzoic, vanillic acid and p-Coumaric acid) in the peel and pulp of 'Orah' grafted on four rootstocks was below 12 μg/g, which increased at 180 DAF (Supplementary Figure S1).

Influence of different rootstocks and development time on the 13 kinds of flavonoids of 'Orah'

Thirteen vital flavonoids (sinensetin, nobiletin, hesperidin, narirutin, tangeretin, eriocitrin, naringin, rhoifolin, vanillin, naringenin, hesperetin, neohesperidin and poncirin) in citrus were selected for detection in this study to provide reference for flavonoid utilization after fruit thinning. Among them, six main substances were selected for analysis according to the principle similar with phenolic acids (Figure 5; Supplementary Figures S2, S5). Under the same rootstock, the sinensetin content in the peel was generally higher than that in the pulp during the same period. The sinensetin content in the peel of 'Orah' decreased as the fruit developed. Except for '*XP*', the content in the peels had lower levels at 210 DAF (58.52 μg/g, 47.92 μg/g, 51.72 μg/g). The sinensetin level of '*XR*' and '*ZCR*' was significantly higher than that of '*HR*' and '*ZR*'. The sinensetin content in pulp was the lowest at 240 DAF, measuring 0.29 μg/g, 0.26 μg/g, 0.25 μg/g, and 0.27 μg/g, respectively (Figure 5A).

The content distribution of nobiletin in peel and pulp was similar to that of sinensetin. Nobiletin in the peel and pulp of the four rootstocks showed higher levels during the early stage, which decreased to the lowest during later developmental stages. The '*XP*'stock had the highest content of 110.95 μg/g at 90 DAF. Except for '*ZR*', the level of nobiletin in the pulp of the other grafts was initially lower, then increased and and finally decreased (Figure 5B).

The narirutin content in '*HP*' and '*ZP*' decreased with the extension of developmental time, stabilizing at 150 DAF. That of '*HR*' and '*ZR*' was significantly lower at 240 DAF than in other developmental periods, with recorded levels of 2.06 μg/g, 2.0 μg/g. '*XP*' and '*ZP*' had significantly higher at 90 DAF than in other developmental stages, while that of *XR* and *ZR* was significantly higher levels at 150 DAF compared to other developmental stages ($F=37.82$, $P<0.05$). The narirutin content of *ZCR* was significantly higher at 120 and 150 DAF than other rootstock-scion combinations, with recorded values of 1356.04 μg/g and 1298.85 μg/g, respectively (Figure 5C).

The content of hesperidin in the peel of the four rootstocks was significantly higher during the early stage of development than that in the late stages. '*ZP*' showed the highest value at 311.81 μg/g. The hesperidin content in the pulp of the four rootstocks reached its peak at 180 DAF (1149.22 μg/g, 1382.42 μg/g, 1894.64 μg/g, and 1439.6 μg/g, respectively). The content was lowest at 90 DAF, with '*HR*' (20.49 μg/g) significantly lower than the other three rootstocks (Figure 5D).

The neohesperidin content in the peel and pulp of the four rootstocks increased significantly after 150 DAF. Except for '*ZCP*', the other rootstocks showed higher levels at 240 DAF, measuring 3192.35 μg/g, 3306.55 μg/g, and 2904.64 μg/g, respectively. The neohesperidin content in '*HR*' and '*ZCR*' reached the highest at 210 DAF (1217.67 μg/g and 3192.35 μg/g, respectively). While '*XR*' and '*ZR*' reached the highest level at 180 DAF (981.84 μg/g, and 1387.94 μg/g, respectively) (Figure 5E).

Except for the '*ZCP*', the poncirin contents in the peels of three rootstocks were highest during the late developmental phase, measuring 125.65 μg/g, 119.79 μg/g, and 102.96 μg/g,

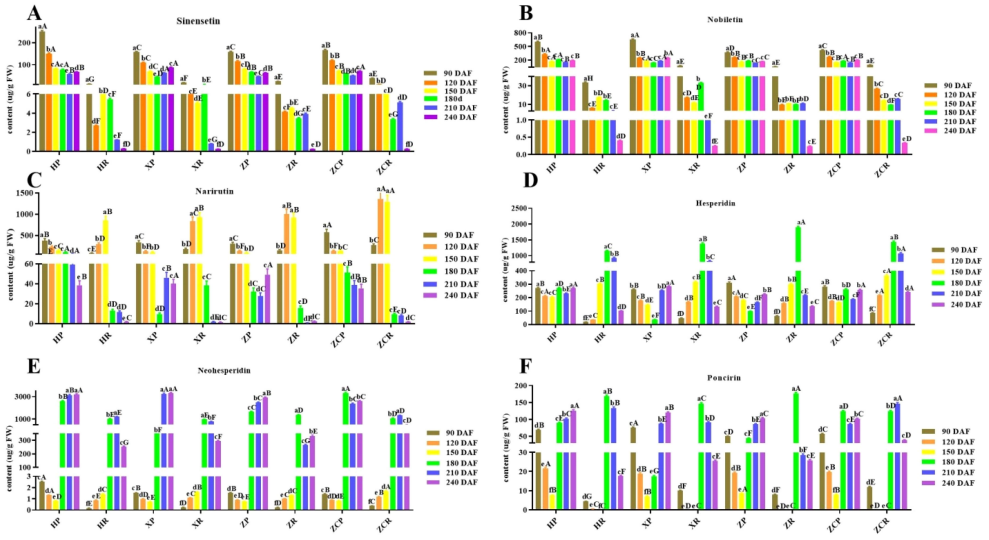

FIGURE 5
Changes in the content of six main flavonoids in 'Orah' under grafting on different rootstocks. HP: Peel of 'Orah' grafted on *C. reticulata* Blanco cv. Red tangerine, HR: Pulp of 'Orah' grafted on *C. reticulata* Blanco cv. Red tangerine, XP: Peel of 'Orah' grafted on *C. junos* Sieb. ex Tanaka,XR: Pulp of 'Orah' grafted on *C. junos* Sieb. ex Tanaka, ZP: Peel of 'Orah' grafted on *P. trifoliata* (L.) Raf, ZR: Pulp of 'Orah' grafted on *P. trifoliata* (L.) Raf, ZCP: Peel of 'Orah' grafted on *C. sinensis* Osb.× *P. trifoliate* Raf, ZCR: Pulp of 'Orah' grafted on *C. sinensis* Osb.× *P. trifoliate* Raf. 90, 120, 150, 180, 210, 240 DAF: Fruit at 90d, 120d, 150d, 180d, 210d, 240d after flowering. FW, Fresh weight. Different lowercase letters in the same rootstock at different times represented significant difference ($P<0.05$), while capital letters represent significant differences in the different rootstocks at the same time period ($P<0.05$). **(A)** sinensetin. **(B)** Nobiletin. **(C)** Narirutin. **(D)** Hesperidin. **(E)** Neohesperidin. **(F)** Poncirin.

respectively. The levels in the pulp were highest in the four rootstocks at 150 DAF, measuring 168.43 μg/g, 146.35 μg/g, 175.84 μg/g, and 123.78 μg/g, respectively (Figure 5F).

The tangeretin, hesperetin, eriocitrin, naringin, rhoifolin, vanillin and naringenin content in the peel and pulp of the four rootstocks was below 180μg/g (Supplementary Figure S2). There were no significant differences in multiple flavonoids content in the peel and pulp of the four rootstocks at the same developmental time period (Supplementary Figures S2A–C, S2F, G). Even more interestingly, with the exception of vanillin, the content of the other six kinds of flavonoids was higher in the peel and lower in the pulp (Supplementary Figure S2).

The antioxidant activity in 'Orah'fruits under four rootstock-scion combinations and development time

In order to evaluated the antioxidant capacity *in vitro* of citrus, we employed the DPPH, FRAP and ABTS method, which were relatively simple and feasible. The results showed that the antioxidant capacity of peel was significantly higher than that of pulp. FRAP free radical scavenging capacity in the peels was the highest at 90 DAF (Figure 6). Among these, '*HP*' showed the strongest antioxidant capacity at 10.7 μmol Trolox/g, which then decreased with the extension of developmental time, reaching the lowest point at 210 DAF ($F=234.21$, $P<0.05$). The FRAP free radical scavenging capacity in the pulp was initially higher which later dropped. Overall, the antioxidant was the strongest at 150 DAF, except for '*ZC*'. The highest recorded value was for '*HR*' at 4.12 μmol Trolox/g (Figure 6A).

The DPPH free radical scavenging activity in the peel showed an initial peak followed by a gradual decline. However, the scavenging activity in the pulp presented tendency of rising initially to the peak and then falling, where it was higher initially and then decreased, with the highest values at 150 DAF (1439.49 μg Trolox/g, 1317.95 μg Trolox/g, and 1395.04 μg Trolox/g, respectively), except for '*ZCR*' (Figure 6B).

Results indicated that changes in ABTS free radical scavenging activity of 'Orah' grafted onto the other three rootstocks were consistent with the changes in DPPH free radicals activity, except for '*ZCR*' (Figure 6C). Of these, '*XR*' recorded the highest value at 1927.39 μg Trolox/g, while *HR*' had the highest value at 90 DAF at 607.81 μg Trolox/g (Figure 6C).

Correlation analysis of main functional substances in the fruits of 'Orah' under four rootstock-scion combinations and development time

Considering the dynamic changes of functional substances during different developmental periods of citrus fruits, the functional substances and antioxidant activities of each developmental period were individually subjected to principal component analysis and subordinate function analysis in this study, which could more scientifically reflect the optimal young fruit thinning time. The result showed a significant positive

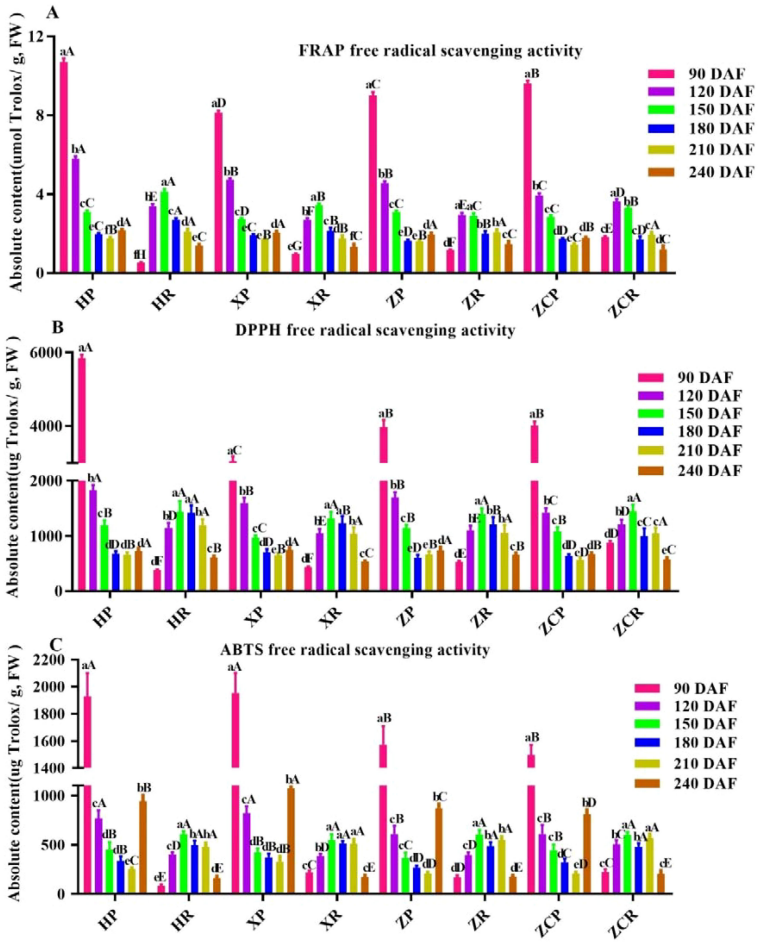

FIGURE 6
Changes in antioxidant capacity of 'Orah' under under grafting on different rootstocks. HP: Peel of 'Orah' grafted on *C. reticulata* Blanco cv. Red tangerine, HR: Pulp of 'Orah' grafted on *C. reticulata* Blanco cv. Red tangerine, XP: Peel of 'Orah' grafted on *C. junos* Sieb. ex Tanaka,XR: Pulp of 'Orah' grafted on *C. junos* Sieb. ex Tanaka, ZP: Peel of 'Orah' grafted on *P. trifoliata* (L.) Raf, ZR: Pulp of 'Orah' grafted on *P. trifoliata* (L.) Raf, ZCP: Peel of 'Orah' grafted on *C. sinensis* Osb.× *P. trifoliate* Raf, ZCR: Pulp of 'Orah' grafted on *C. sinensis* Osb.× *P. trifoliate* Raf. 90, 120, 150, 180, 210, 240 DAF: Fruit at 90d, 120d, 150d, 180d, 210d, 240d after flowering; FW, Fresh weight. Different lowercase letters in the same rootstock at different times represented significant difference ($P<0.05$), while capital letters represent significant differences in the different rootstocks at the same time period ($P<0.05$). **(A)** FRAP free radical scavenging capacity. **(B)** DPPH free radical scavenging activity. **(C)** ABTS free radical scavenging activity.

correlation (F=45.85, $P<0.01$) among the activities of antioxidant enzymes activities, as demonstrated by the FRAP, DPPH, and ABTS values (Supplementary Table S1). Additionally, a significant positive correlation was observed among three limonins (linimon, nomilin, and synephrine) and three phenolic acids (protocatechuic, sinapic, and ferulic) (F=37.92, $P<0.01$). A notable correlation was also found among the other substances (F=65.36, $P<0.05$), including 6 flavonoids. However, no significant correlations were observed between protocatechuic, sinenselin, narirutin, or between nobiletin, hesperidin, and the 3 antioxidant enzymes (FRAP, DPPH, and ABTS), as well as between nomilin, sinenselin, nobiletin hesperidin, or between poncirin and FRAP, DPPH, sinenselin, and nobiletin. Yet, a significant correlation was identified among the other substances (F=103.25, $P<0.05$).

The results of the principal component analysis revealed a high level of consistency in the functional substances of the 'Orah' grafted onto the four rootstocks (Supplementary Table S2). It is evident that the comprehensive evaluation outcomes from the principal component analysis and membership function for the functional substances of the fruits in the four rootstock-scion combinations were highly consistent. This consistency underscores the validity of the methods and indicators selected for this study.

To further analyze the variations among the tested rootstocks in terms of metabolite production, a multifactorial analysis was performed using data collected over two years. For the phenotyping (Figure 7A) conducted on July 8, 2020 (fruit at 90 DAF), the first two principal components accounted for 95.39% of the cumulative phenotypic variability (Dim1 = 88.76%, Dim2 = 6.63%). Dim1 primarily correlated with the quantity of functional metabolites produced (with Dim1>0 indicating higher production, as observed for nomilin, sinapic and neohesperiklin; Figures 4–6). Dim2 allowed a more precise differentiation based on various classes of metabolites. Rootstocks exhibiting high production of limonin, flavonoids, and antioxidant activity such as 1*ZP* and 1*HP* clustered in the upper-right quadrant (Dim1>0 and

10.3389/fpls.2024.1382768

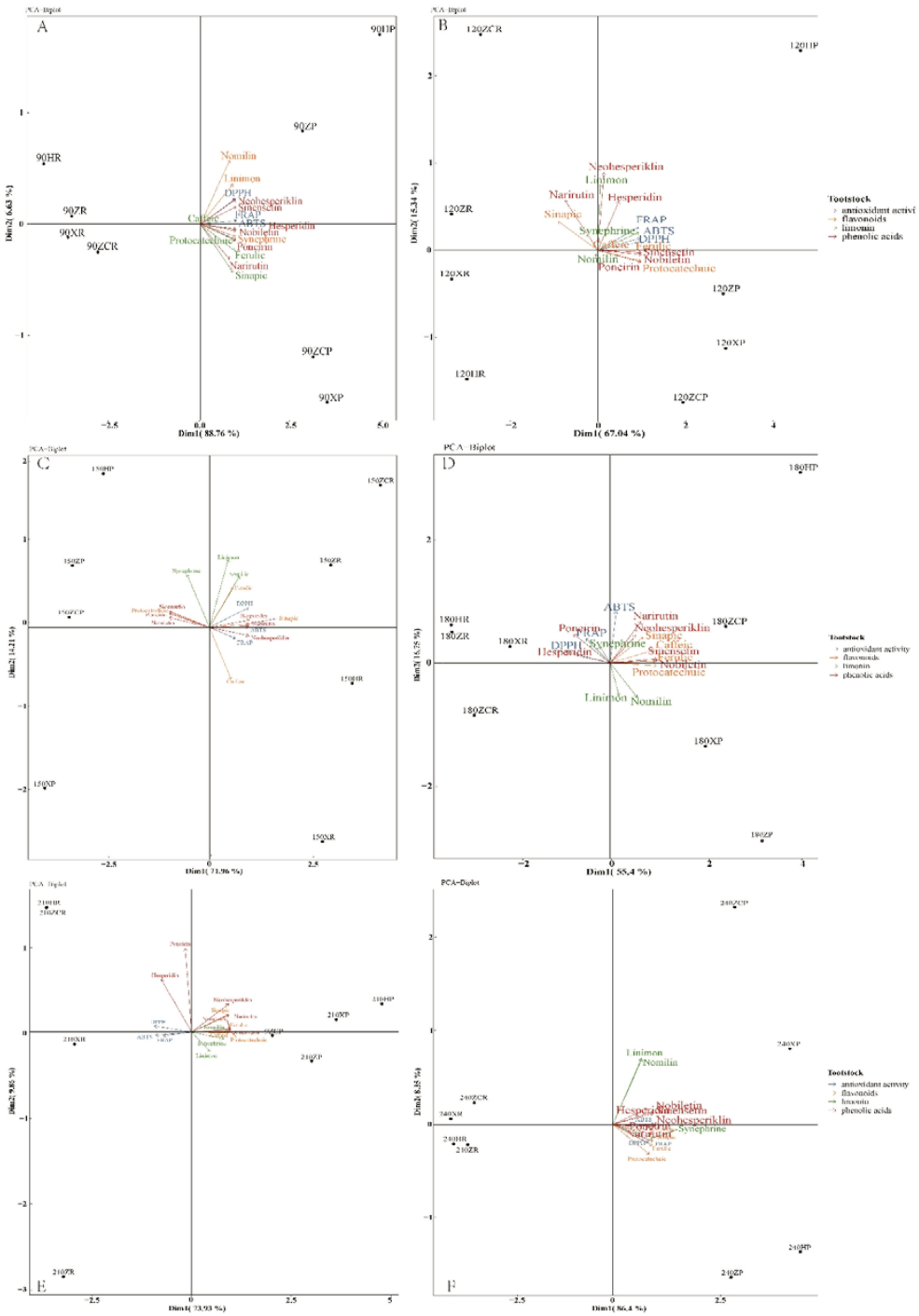

FIGURE 7
Principal component analysis (PCA) of the 16 parameters analyzed for 'Orah'. **(A)**, fruit at 90d after flowering. **(B)**, fruit at120 d after flowering. **(C)**, fruit at 150d after flowering. **(D)**, fruit at 180d after flowering. **(E)** fruit at 210d after flowering. **(F)**, fruit at 240d after flowering. Antioxidant activity, limonin, flavone compounds and phenolic compounds are coloured as categories as specified in the figure legend.

Dim2>0). Meanwhile, samples showing higher synthesis of phenolic compounds were situated (Figure 7A) in the lower-right quadrant (Dim1<0 and Dim2>0).

For the analysis performed 120 DAF, the first two principal components explained 82.38% of the total phenotypic variability. However, poncirin, sinentin, protocatechuic, nobiletin, and ferulic accessions showed a showing high accumulation of metabolites characterized by negative Dim1 values (Figures 5, 6, 7B). Moreover, at 120 DAF, the loadings related to the antioxidant activity exhibited strong consistency, all projecting towards the same PCA quadrant (upper-right). Specifically, '*HP*' exhibited both high antioxidant capacity and high flavonoid content (Figure 7B).

Further analysis revealed that after 150 DAF, the first two principal components explained 86.17% of the cumulative

phenotypic variability (Dim1 = 71.96%, Dim2 = 14.21%). Except for caffeic and neohesperiklin, the rest of the flavonoids and phenolic acids were characterized by positive Dim1 values (Figures 5, 7C). Notably, synephrine stood out, being orthogonally projected compared to the linimon and nomilin (Figure 7C). Interestingly, '*ZR*' and '*ZCR*' exhibited neohesperiklin, linimon, nomilin, sinapic, and ferulic contents, clustering in the upper-right quadrant (Dim1>0 and Dim2>0) as portrayed (Figures 5, 6, 7C).

The first two principal components explained 72.15% of the cumulative phenotypic variability (Dim1 = 55.40%, Dim2 = 16.75%). Dim1 was mainly associated with the quantity of functional metabolites produced and strongly activated the antioxidant enzymes (with Dim1>0 associated with higher production, as observed for 3 phenolic acids and 7 flavonoeds excluding protocatechuic; Figures 5–7D). Notably, synephrine was characterized by a backward projection compared to the linimon and nomilin (Figure 7D). Rootstocks characterized by high production of flavonoids (narirutin, neohesperiklin, sinensetin, and nobiletin), phenolic acids (ferulic and caffeic) and a high ABTS free radical clearance ability (Figure 7D) in '180*ZCP*' and '180*HP*' clustered in the upper-right quadrant (Dim1>0 and Dim2>0).

For the analysis performed 210 DAF, the first two principal components (Figure 7E) explained 83.79% of the total phenotypic variability (Dim1 = 73.93%, Dim2 = 9.86%). Dim2 facilitated a more precise differentiation based on antioxidant activity (Dim2<0, Figure 7E). Notably, the upper-left quadrant (Dim1<0 and Dim2>0) exhibited high contents of poncirin and hesperidin (Figures 6, 7E). Moreover, at 210 DAF, the loadings related to the '*XP*' and '*HP*' projected towards the same PCA quadrant (upper-right) (Figure 7E).

The first two principal components explain 94.75% of the cumulative phenotypic variability (Dim1 = 86.4%, Dim2 = 8.35%). The functional compounds and antioxidant activities were mainly located on the right of the PCA quadrant. Rootstocks characterized by high production of limonin, nomilin, flavonoids (sinensetin, nobiletin and hesperidin), as well as high ABTS free radical clearance ability in '240*XP*' and '240*ZCP*', clustered in the upper-right quadrant (Dim1>0 and Dim2>0), as shown (Figures 4, 6, 7F). Samples demonstrating higher synthesis of phenolic compounds (Figure 6F) were plotted in the lower-right quadrant (Dim1<0 and Dim2>0).

Discussion

Rootstocks can significantly influence both internal and external quality parameters of citrus fruits, including bioactive compounds, shortened juvenile period, and improved fruit quality (Saini et al., 2019). Choosing rootstocks is an important tool for adapt crops to adverse environmental conditions or biotic (diseases, pests) and abiotic (drought, alkalinity, cold, etc) stresses, in order to improve fruit quality (Morales et al., 2023). In this study, we evaluated the impact of rootstocks of '*H*', '*X*', '*Z*' and '*ZC*' rootstocks on the quality and functional content of 'Orah' citrus. The results showed that the rootstocks affected the sugar and acid contents of the scion fruits. Similarly, the rootstock of the 'sour' orange increased the total soluble solids (TSS) and titratable acidity (TA) levels of different citrus varieties grafted onto the rootstock, thereby delaying fruit maturity in comparison to other rootstocks (Bassal, 2009; Singh et al., 2020). The effects of different rootstocks on 'Marsh' grapefruit indicated that citrus fruits grafted onto '*ZC*' had the lowest TA content, while citrus fruits grafted onto the putative hybrid of *Citrus aurantium* had the lowest TSS content (McCollum and Bowman, 2002). It was also observed that the '*ZC*' rootstock could reduce the TSS of scion (Clementine) fruits (Hussain et al., 2013). However, the effects of the four rootstocks on 'Marisol' clementine (*H*), with fruits grafted onto '*ZC*', showed higher TSS and TA than those grafted onto 'Sour' orange (Bassal, 2009). Our results showed that the TSS and VC content of these four rootstocks continued to increase with the extension of developmental time, reaching the highest levels at maturity. In contrast, the trend of TA change was opposite, presumably due to environmental factors. The TSS/TA ratio serves as an important indicator of both citrus commercial maturity and sensory maturity (Goldenberg et al., 2018). Vitamin C is considered one of the most important nutrients in citrus fruits. It has been reported that rootstocks affect the production of vitamin C in citrus fruits (Magwaza et al., 2017). Studies have shown that rootstock '*H*' (Khalifa and Hamdy, 2015) and '*ZC*' (Cardeñosa et al., 2015) could not increase the VC content of citrus fruits. The rootstock '*Z*' having was significantly higher content than the rest of the rootstock-scion combinations in our study. Qureshi et al. had also found that rootstock '*Z*' was also superior to rootstock '*ZC*' in improving the VC content of scion 'Kinnow' fruit (Qureshi et al., 2021). Our results indicated that all four rootstocks were suitable for 'Orah', with the '*X*' being the optimal rootstock in this study.

Citrus fruits serve as natural sources of antioxidants and bioactive compounds, including organic acids, phenolic compounds, and flavonoids (Sicari et al., 2017). Phenolic compounds not only enhance antioxidant capacity, inhibit some pests feeding, but also contribute to reduced risks of cardiovascular disease and certain cancers (Lattanzio et al., 2006; Sdiri et al., 2014). Studies have shown that the 'Tavarini' rootstock affects fruit quality through interactions between water, soil nutrients, and the synthesis of compounds like phenolic compounds (Tavarini et al., 2011). In our study, multiple phenols were identified in 'Orah' grafted onto the four rootstock-scion combinations, including the protocatechins, caffeic acid, ferulic acid, and sinapic acid, among others, most of which be used as pharmaceuticals. Changes in polyphenol content followed a trend consistent with 'Kinnow' citrus grafted on different rootstocks (Singh et al., 2020). We found that ferulic acid and protocatechins were abundant in the pre-development phase (before 150 DAF), while sinapic acid was higher between 120-150 DAF. Results showed that sinapic acid and protocatechins were widely present in citrus (Nićiforović and Abramovič, 2014). A small amount of caffeic acid was produced in 'Orah' grafted onto the four rootstocks after 180 DAF. Importantly, '*ZC*' stood out as the best rootstock for 'Orah' in terms of phenolic compounds. This suggests that '*ZC*' was selected as being tolerant, which might trigger the tree's antioxidant defense system and, leading to higher phenol accumulation and providing raw

materials for pharmaceuticals (Zandalinas et al., 2017). More importantly, our principal component analysis of the fruits after 90 DAF and 150 DAF also confirmed the hypothesis (Figures 7A, C).

Flavonoids are the primary class of phenolic substances that have granted special attention due to their potential health benefits. Studies have enlightened that 'Osbeck' citrus fruit grafted onto the rootstock *C. sinensis* [L.] exhibited flavonoid biosynthetic activity, while scion leaves on 'Cleopatra mandarin' citrus demonstrated stronger flavonoid biosynthesis activity (Souza et al., 2017). Our results indicate that the qualitative characteristics of 'Orah' grafted onto the four rootstocks were similar with significant changes in contents between 500-2000 μg/g. Flavonoid content in different species varied greatly with developmental time extension. The total flavonoid content of fruits grafted onto '*H*' was higher than other rootstocks. Other studies have also reported higher phenolic content in lemon fruits grafted onto 'sour' orange rootstock (*Citrus aurantium* L.), while lemons on high-yielding 'Volkamer' rootstock have lower phenolic content (Emmanouilidou and Kyriacou, 2017). Overall, the total concentration of phenolic compounds in the four rootstocks ranged between 15 to 115 mg/100g fresh weight. These results align with previous research trends for other cultivars grafted onto the same four rootstocks (Li et al., 2022). Our research results also confirmed that the content of flavonoids and antioxidant capacity have higher content during the young fruit stage (90 and 150 DAF) especially in the '*Z*'. From the perspective of functional substances utilization, the 'Orah' fruit of 90 DAF and 150 DAF were the optimal thinning times. In practical production, fruit farmers often prethin many times from July to September. Previous study has also found that flavonoids and antioxidant capacity in grapefruit and lemon also exhibit higher levels at 90 DAF (Castillo et al., 1992; Zhu et al., 2020). Therefore, our results provide guidance for the fruits thinning, which could be carried out twice at 90 DAF and 150 DAF, reducing labor costs.

Citrus scion on the four rootstocks suggested that 'Var. Shelmahalleh' (*C. sinensis*) had the highest hesperidin content in the peel, followed by 'Swingle' citrus (Hemmati et al., 2018). In our study, '*Z*' exhibited the highest hesperidin content among the four rootstock-scion combinations, followed by '*ZC*', which is consistent with the research findings of Babazadeh-Darjazi et al (Babazadeh-Darjazi, 2018). Another study discussed the influence of six rootstocks on 'Kinnow' *Citrus Lour.* x *Citrus Deliciosa* Ten. & Pasq.) (Singh et al., 2020), and found that the highest levels of flavanones (hesperidin, naringin, pectin rutin, naringenin, and neocitric acid) and dihydroxy B-faravanol (rutin and quercetin) were induced by the 'Sour' orange rootstock. In comparision with the rootstocks '*H*', '*Z*' and '*ZC*', the fruits of rough lemon rootstocks contained higher levels of naringenin, hesperitin, and eriodyctol (Feng et al., 2018). Most of them can be used as pest control agents and raw materials for treating human diseases (Lattanzio et al., 2006; Khalifa and Hamdy, 2015; Shi et al., 2021). Our study also identified naringenin and hesperetin as functional constituents of the above rootstocks, with naringenin content significantly lower than that of hesperidin. Additionally, consistent with the previous study (Zhu et al., 2020), the hesperidin and neohesperidin contents were significantly higher than other flavonoids in the later stage of development (after 180 DAF). Overall, our results showed that the '*Z*' rootstock induced higher flavonoid content in both peel and pulp.

In addition to phenolic compounds, citrus also contains various functional substances, such as synephrine, which is the main alkaloid in *Citrus aurantium* L. extracts and the main component of traditional Chinese medicine for treating indigestion and pharyngeal diseases (Arbo et al., 2008). And citrus fruits using '*Z*' rootstocks can produce synephrine (Zhang et al., 2011). The content of synephrine in both rootstocks '*H*' and '*Z*' showed an initial increase, followed by a decrease during fruit development in our study. Citrus limonoids, the precursor for limonoids, are ascribed to fruit bitterness, but also possess favorable health properties including anti-oxidative, hypocholesterolemic and anti-carcinogenic effects (Manners, 2007). Interestingly, rootstocks could affect their content in citrus fruits. A study has found that the fruits of '*ZC*' rootstocks could produce limonin and normilin (Tietel et al., 2020). Compared with other rootstocks, we also found that the content of normilin was highest in the early stage of fruit development (120 DAF) of '*ZC*', while limonin performed the best on '*H*' rootstock.

Rootstocks also play a role in regulating the antioxidant activity of scion fruits. Our results indicate that free radical scavenging activity in 'Orah' grafted onto the four different rootstocks was higher in the early stages of development compared to later stages, with higher activity observed in the peels compared to the pulp. In terms of antioxidant capacity, the '*H*' rootstock was optimal. A study also indicated that grafting FA 'Cleopatra mandarin' on '*ZC*'. increased the concentration of several bioactive compounds, such as VC, diphenylamine, and naringenin, thus enhancing the antioxidant capacity (DPPH) of citrus fruits (Li et al., 2022).

Conclusions

The citrus variety 'Orah' has garnered consumer interest due to its high yield and rich nutritional components. In this study, we determined the fruit quality, functional constituents and antioxidant capacity in both peel and pulp of 'Orah' at 90, 120, 150, 180, 210 and 240 DAF. Results showed that the content of functional constituents was highest 150 DAF, indicating that it could utilized as a suitable fruit thinning period. In terms of TSS, rootstock '*Z*' was demonstrated the highest performance. With regarding to TSS/TA, rootstock '*X*' emerged as the optimal choice. Then, '*ZC*' proved to be the most effective for VC. The highest levels of phenolic acid and flavonoids were observed at 90 DAF with the rootstock '*H*' showing superior results, suggesting its potential use as an additional fruit thinning period. Moreover, high levels of sinensetin, nobiletin, protocatechins and ferulic acid were detected during the early stage of development. Furthermore, rootstock '*H*' and '*X*' exhibited the highest levels of functional substances, noteworthy some functional substances displayed higher content in the pulp than that in the peel. Our results also indicated that the greatest antioxidant capacity were recorded in the early stage of development, with the rootstock '*H*' identified as superior in this regard. In summary, our results suggested that

rootstocks could significantly affect the functional constituents accumulating and antioxidant capability in fruit of 'Orah'. We identified 90d and 150 DAF as the best time for fruit thinning, which can be used for the extraction of functional substances. Additionally, We identified '*X*' as the most commercially viable option, '*ZC*' in terms of functionality, '*H*' in terms of antioxidant ability. These findings can be used to determine the optimal rootstock and fruit thinning for 'Orah', based on the expected effect.

Data availability statement

The original contributions presented in the study are included in the article/Supplementary Material. Further inquiries can be directed to the corresponding author.

Author contributions

SL: Project administration, Writing – review & editing, Writing – original draft, Funding acquisition, Data curation. LY: Conceptualization, Writing – review & editing, Investigation, Data curation. MW: Writing – review & editing, Methodology, Investigation, Data curation. YC: Writing – original draft, Software, Methodology, Formal analysis. JY: Writing – original draft, Software, Data curation. HC: Writing – original draft, Software, Methodology. HY: Writing – review & editing, Validation, Resources. WW: Writing – review & editing, Visualization, Investigation. ZC: Writing – review & editing, Validation, Resources. LH: Writing – review & editing, Supervision, Project administration, Funding acquisition, Conceptualization.

Funding

The author(s) declare financial support was received for theresearch, authorship, and/or publication of this article. This research was funded by Natural Science Foundation of Chongqing Municipality (Postdoctoral Fund) (CSTB2023NSCQ-BHX0198), P.R. China, Special Funds for Agricultural Development of Chongqing (cqaas2023sjczqn013), and Chongqing Research Program of Technological Innovation and Application Demonstration (cstc2018jscx-msybX0245), P.R. China.

Conflict of interest

The authors declare that the research was conducted in the absence of any commercial or financial relationships that could be construed as a potential conflict of interest.

Publisher's note

Supplementary material

The Supplementary Material for this article can be found online at: https://www.frontiersin.org/articles/10.3389/fpls.2024.1382768/full#supplementary-material

SUPPLEMENTARY FIGURE 1
Changes in the content of three kinds of phenolic acid in 'Orah' under grafting of different rootstocks-scion combinations. HP: Peel of 'Orah' grafted on C. reticulata Blanco cv. Red tangerine, HR: Pulp of 'Orah' grafted on C. reticulata Blanco cv. Red tangerine, XP: Peel of 'Orah' grafted on C. junos Sieb. ex Tanaka,XR: Pulp of 'Orah' grafted on C. junos Sieb. ex Tanaka, ZP: Peel of 'Orah' grafted on P. trifoliata (L.) Raf, ZR: Pulp of 'Orah' grafted on P. trifoliata (L.) Raf, ZCP: Peel of 'Orah' grafted on C. sinensis Osb.× P. trifoliate Raf, ZCR: Pulp of 'Orah' grafted on C. sinensis Osb.× P. trifoliate Raf. 90, 120, 150, 180, 210, 240 DAF: Fruit at 90d, 120d, 150d, 180d, 210d, 240d after flowering, FW: Fresh weight. FW: Fresh weight. Different lowercase letters in the same rootstock at different times represented significant difference ($P<0.05$), while capital letters represent significant differences in the different rootstocks at the same time period ($P<0.05$).

SUPPLEMENTARY FIGURE 2
Changes in the content of 7 flavonoids in 'Orah' under grafting of different rootstocks. HP: Peel of 'Orah' grafted on C. reticulata Blanco cv. Red tangerine, HR: Pulp of 'Orah' grafted on C. reticulata Blanco cv. Red tangerine, XP: Peel of 'Orah' grafted on C. junos Sieb. ex Tanaka,XR: Pulp of 'Orah' grafted on C. junos Sieb. ex Tanaka, ZP: Peel of 'Orah' grafted on P. trifoliata (L.) Raf, ZR: Pulp of 'Orah' grafted on P. trifoliata (L.) Raf, ZCP: Peel of 'Orah' grafted on C. sinensis Osb.× P. trifoliate Raf, ZCR: Pulp of 'Orah' grafted on C. sinensis Osb.× P. trifoliate Raf. 90, 120, 150, 180, 210, 240 DAF: Fruit at 90d, 120d, 150d, 180d, 210d, 240d after flowering, FW: Fresh weight. FW: Fresh weight. Different lowercase letters in the same rootstock at different times represented significant difference ($P<0.05$), while capital letters represent significant differences in the different rootstocks at the same time period ($P<0.05$).

References

Aboshi, T., Ishiguri, S., Shiono, Y., and Murayama, T. (2018). Flavonoid glycosides in Malabar spinach Basella alba inhibit the growth of Spodoptera litura larvae. *Biosci. Biotechnol. Biochem.* 82, 9–14. doi: 10.1080/09168451.2017.1406301

Albrecht, U., Alferez, F., and Zekri, M. (2018). Citrus production guide: rootstock and scion selection. *IFAS Extension* 1308, 69–71. doi: 10.32473/edis-hs1308-2017

Arbo, M. D., Larentis, E. R., Linck, V. M., Aboy, A. L., Pimentel, A. L., Henriques, A. T., et al. (2008). Concentrations of p-synephrine in fruits and leaves of citrus species (Rutaceae) and the acute toxicity testing of *Citrus aurantium* extract and p-synephrine. *Food Chem. T oxicol.* 46, 2770–2775. doi: 10.1016/j.fct.2008.04.037

Babazadeh-Darjazi, B. (2018). The effect of rootstocks on the peel phenolic compounds, cartenoids, chlorophylls and ethylene of Younesi tangerine (*Citrus reticulata*). *Plant Physiol.* 8, 2371–2379. doi: 10.22034/IJPP.2

Bassal, M. A. (2009). Growth yield and fruit quality of 'Marisol' Clementine grown on four rootstocks in Egypt. *Sci. Hortic.* 119, 132–137. doi: 10.1016/j.scienta.2008.07.020

Benjamin, G., Tietel, Z., and Porat, R. (2013). Effects of rootstock/scion combinations on the flavor of citrus fruit. *J. Agric. Food Chem.* 61, 11286–11294. doi: 10.1021/jf402892p

Cardeñosa, V., Barros, L., Barreira, J. C., Arenas, F., Moreno-Rojas, J. M., and Ferreira, I. C. (2015). Different citrus rootstocks present high dissimilarities in their antioxidant activity and vitamins content according to the ripening stage. *J. Plant Physiol.* 174, 124–130. doi: 10.1016/j.jplph.2014.10.013

Castillo, J., Benavente, O., and del Rio, J. A. (1992). Naringin and neohesperidin levels during development of leaves, flower buds, and fruits of Citrus aurantium. *Plant Physi.* 99, 67–73. doi: 10.1104/pp.99.1.67

Cui, B., Huang, X., Li, S., Hao, K., Chang, B. H., Tu, X. B., et al. (2019). Quercetin affects the growth and development of the grasshopper *Oedaleus asiaticus* (Orthoptera: Acrididae). *J. Econ. Entomol.* 112, 1175–1182. doi: 10.1093/jee/toz050

Czech, A., Malik, A., Sosnowska, B., and Domaradzki, P. (2021). Bioactive substances, heavy metals, and antioxidant activity in whole fruit, peel, and pulp of citrus fruits. *Int. J. Food Sci.* 2021, 1–14. doi: 10.1155/2021/6662259

Emmanouilidou, M. G., and Kyriacou, M. C. (2017). Rootstock-modulated yield performance, fruit maturation and phytochemical quality of 'Lane Late' and 'Delta' sweet orange. *Sci. Horticul.* 225, 112–121. doi: 10.1016/j.scienta.2017.06.056

Feng, S., Niu, L., Suh, J. H., Hung, W. L., and Wang, Y. (2018). Comprehensive metabolomics analysis of mandarins (*Citrus Reticulata*) as a tool for variety, rootstock, and grove discrimination. *J. Agric. F. Chem.* 66, 10317–10326. doi: 10.1021/acs.jafc.8b03877

Franceschini Sarria, A. L., Matos, A. P., Volante, A. C., Bernardo, A. R., Sabbag Cunha, G. O., Fernandes, J. B., et al. (2022). das G.F. Insecticidal activity of copper (II) complexes with flavanone derivatives. *Nat. Prod. Res.* 36, 1342–1345. doi: 10.1080/14786419.2020.1868465

Galm, U., and Shen, B. (2007). Natural product drug discovery: The times have never been better. *Chem. Biol.* 14, 1098–1104. doi: 10.1016/j.chembiol.2007.10.004

Goldenberg, L., Yaniv, Y., Porat, R., and Carmi, N. (2018). Mandarin fruit quality: a review. *J. Agric. Food Chem.* 98, 18–26. doi: 10.1002/jsfa.8495

Gong, R. G., Wei, Y., Wang, Z. H., Liao, M. G., and Liang, G. L. (2015). Study on the sugar-acid ratio and relevant metabolizing enzyme activities in navel orange fruits from different eco-regions. *Rev. Bras. Frutic.* 37, 835–844. doi: 10.1590/0100-2945-210/14

He, Y., Li, W., Zhu, P., Wang, M., Qiu, J., Sun, H. Q., et al. (2022). Comparison between the vegetative and fruit characteristics of 'Orah' (*Citrus reticulata* Blanco) mandarin under different climatic conditions. *Sci. Hortic.* 300, 111064. doi: 10.1016/j.scienta.2022.111064

He, J., and Zhang, H. P. (2023). Research progress on the anti-tumor effect of Naringin. *Front. Pharmacol.* 14. doi: 10.3389/fphar.2023.1217001

Hemmati, N., Ghasemnezhad, A., Moghaddam, J. F., and Ebrahimi, P. (2018). Variation in the content of bioflavonoids of orange as affected by scion, rootstock, and fruit part. *Acta Physiol. Plant* 40, 83. doi: 10.1007/s11738-018-2648-1

Huang, R. H., Lu, Y. M., and Xia, R. X. (2009). Study on the active oxygen metabolism during the development and storage process of citrus unshiu fruits. *J. Anhui Agric. Sci.* 37, 1914–1916, 1921. doi: 10.3969/j.issn.0517-6611.2009.05.024

Hussain, S., Curk, F., Anjum, M. A., Pailly, O., and Tison, G. (2013). Performance evaluation of common clementine on various citrus rootstocks. *Sci. Horticul* 150, 278–282. doi: 10.1016/j.scienta.2012.11.010

Jiang, D., and Cao, L. (2011). Introduction performance of late maturing high sugar hybrid citrus variety wogan in Chongqing. S. *China Fruit* 40, 33–34.

Khalifa, S. M., and Hamdy, A. E. (2015). "Effect of some citrus rootstocks on yield and fruit quality of two mandarin varieties," in *Sixth International Scientific Agricultural Symposium" Agrosym 2015", Jahorina, Bosnia and Herzegovina October 15-18, 2015*, Proceedings, University of East Sarajevo, Lukavica, Serbia. pp.182–190.

Lattanzio, V., Lattanzio, V. M. T., and Cardinali, A. (2006). Role of phenolics in the resistance mechanisms of plants against fungal pathogens and insects. *Phytochemistry: Adv. Res.* 661, 23–67. Available at: https://www.researchgate.net/publication/303270594.

Li, C. L., Cai, Q. Y., Wu, X. Y., Tan, Z., Huang, S. H., Wei, C. Q., et al. (2022). Variation in Compositions and Biological Activities of Essential Oils from Four Citrus Species: Citrus limon, Citrus sinensis, Citrus paradisi, and. *Citrus reticulata*. *Chem. Biodivers.* 19, e202100910. doi: 10.1002/cbdv.202100910

Liu, X. Y., Li, J., Liu, M. M., Yao, Q., and Chen, J. Z. (2017). Transcriptome profiling to understand the effect of citrus rootstocks on the growth of 'shatangju' mandarin. *PLoS One* 12, e0169897. doi: 10.1371/journal.pone.0169897

Magwaza, L. S., Mditshwa, A., Tesfay, S. Z., and Opara, U. L. (2017). An overview of preharvest factors affecting vitamin C content of citrus fruit. *Sci. Hortic.* 216, 12–21. doi: 10.1016/j.scienta.2016.12.021

Manners, G. D. (2007). Citrus limonoids: analysis, bioactivity, and biomedical prospects. *J. Agr. Food Chem.* 55, 8285–8294. doi: 10.1021/jf071797h

McCollum, T. G., and Bowman, K. D. (2002). Castle, W.S. Effects of rootstock on fruit quality and postharvest behavior of 'Marsh' Grapefruit. *Proc. Florida State Hortic. Soc.* 115, 44–46.

Mo, J. S., Zhang, S. N., Ou, S. H., Mei, Z. M., Li, S. H., Liang, R. Z., et al. (2019). Observation on the law of flowers and fruits dropping of late-maturing citrus Orah. *J. South Agri* 50, 104–109. doi: 10.3969/j.issn.2095-1191.2019.01.15

Morales, A. J., Bermejo, A., Navarro, P., Quiñones, A., and Salvador, A. (2023). Effect of rootstock on citrus fruit quality: A review. *Food Rev. Int.* 39, 2835–2853. doi: 10.1080/87559129.2021.1978093

Morales, J., Salvador, A., Besada, C., Navarro, P., and Bermejo, A. (2021). Physico-chemical, sensorial and nutritional quality during the harvest season of 'Tango'mandarins grafted onto *Carrizo Citrange* and *Forner-Alcaide* no. 5. *Food Chem.* 339, 127781. doi: 10.1016/j.foodchem.2020.127781

Nićiforović, N., and Abramovič, H. (2014). Sinapic acid and its derivatives: natural sources and bioactivity. *Compr. Rev. Food Sci. Food Saf.* 13, 34–51. doi: 10.1111/1541-4337.12041

Ordóñez-Díaz, J. L., Hervalejol, A., Pereira-Carol, G., Muñoz-Redondo, J. M., Romero-Rodríguez, E., and Arenas-Arenas, F. J. (2020). & Moreno-Rojas, J.M. Effect of rootstock and harvesting period on the bioactive compounds and antioxidant activity of two orange cultivars ('Salustiana'and 'Sanguinelli') widely used in juice industry. *Processes* 8, 1212. doi: 10.3390/pr8101212

Ouma, G. (2012). Fruit thinning with specific reference to citrus species: A review. *Agric. Biol. J. N. Am.* 3, 175–191. doi: 10.5251/abjna.2012.3.4.175.191

Qureshi, M. A., Jaskani, M. J., Khan, A. S., Haider, M. S., Shafqat, W., Asif, M., et al. (2021). Influence of different rootstocks on physico-chemical quality attributes of Kinnow mandarin. *Pak. J. Agric. Sci.* 58, 929–935. doi: 10.21162/PAKJAS/21.348

Robbins, R. C. (1980). "Medical and nutritional aspects of citrus bioflavonoids," in *Citrus Nutrition and Quality* (Department of Food Science and Human Nutrition, University of Florida, Gainesville, ACS Symposium Series; American Chemical Society, Washington, DC), pp 43–pp 59. doi: 10.1021/bk-1980-0143.ch003

Saini, M. K., Capalash, N., Kaur, C., and Singh-Sukhvinder, P. (2019). Comprehensive metabolic profiling to decipher the influence of rootstocks on fruit juice metabolome of Kinnow (C. nobilis× *C. deliciosa*). *Sci. Hortic.* 257, 108673. doi: 10.1016/j.scienta.2019.108673

Sdiri, S., Salvador, A., Farhat, I., Navarro, P., and Besada, C. (2014). "Influence of postharvest handling on antioxidant compounds of Citrus fruits," in *Citrus: Molecular Phylogeny, Antioxidant Properties and Medicinal Uses*. Ed. K. Hayat (Nova Publisher Inc, New York, NY, USA), pp 73–pp 94.

Sheng, O., Song, S., Peng, S., and Deng, X. X. (2009). The effects of low boron on growth, gas exchange, boron concentration and distribution of 'Newhall'navel orange (*Citrus sinensis* Osb.) plants grafted on two rootstocks. *Sci. Hortic.* 121, 278–283. doi: 10.1016/j.scienta.2009.02.009

Shi, G., Kang, Z., Liu, H., Ren, F., and Zhou, Y. (2021). The effects of quercetin combined with nucleopolyhedrovirus on the growth and immune response in the silkworm (*Bombyx mori*). *Arch. Insect Biochem.* 108, e21839. doi: 10.1002/arch.21839

Shi, Q. W., Li, L. G., Huo, C. H., Zhang, M. L., and Wang, Y. F. (2010). Study on natural medicinal chemistry and new drug development. *Chine. Tradit. Herbal Drugs* 41, 1583–1589.

Sicari, V., Dorato, G., Giuffrè, A. M., Rizzo, P., and Albunia, A. R. (2017). The effect of different packaging on physical and chemical properties of oranges during storage. *J. Food Process* 41, e13168. doi: 10.1111/jfpp.13168

Silva, F. A. M., Borges, F., Guimar-aes, C., Lima, J. L. F. C., Matos, C., and Reis, S. (2000). Phenolic acids and derivatives: studies on the relationship among structure, radical scavenging activity, and physicochemical parameters. *J. Agric. Food Chem.* 48, 2122–2126. doi: 10.1021/jf9913110

Simmonds, M. S. J. (2003). Flavonoid–insect interactions: recent advances in our knowledge. *Phytochemistry* 64, 21–30. doi: 10.1016/s0031-9422(03)00293-0

Singh, S., Aulakh, P. S., and Gill, P. P. S. (2015). Physicochemical changes during fruit development and maturation in grapefruit (*Citrus paradisi* Macf.) cv. Star Ruby. *Ecoscan* 9, 17–20.

Singh, B., Singh, J. P., Kaur, A., and Singh, N. (2020). Phenolic composition, antioxidant potential and health benefits of citrus peel. *Food Res. Int.* 132, 109114. doi: 10.1016/j.foodres.2020.109114

Souza, J. D., de Andrade Silva, E. M., Coelho Filho, M. A., Morillon, R., Bonatto, D., Micheli, F., et al. (2017). Different adaptation strategies of two Citrus scion/rootstock combinations in response to drought stress. *PLoS One* 12, e0177993. doi: 10.1371/journal.pone.0177993

Tanaka, T., Kohno, H., Tsukio, Y., Honjo, S., Tanino, M., Miyake, M., et al. (2000). Citrus limonoids obacunone and limonin inhibit azoxymethane-induced colon carcinogenesis in rats. *BioFactors* 13, 213–218. doi: 10.1002/biof.5520130133

Tavarini, S., Gil, M. I., Tomas-Barberan, F. A., Buendia, B., Remorini, D., Massai, R., et al. (2011). Effects of water stress and rootstocks on fruit phenolic composition and physical/chemical quality in suncrest peach. *Ann. Appl. Biol.* 158, 226–233. doi: 10.1111/j.1744-7348.2010.00457.x

Tietel, Z., Srivastava, S., Fait, A., Tel-Zur, N., Carmi, N., and Raveh, E. (2020). Impact of scion/rootstock reciprocal effects on metabolomics of fruit juice and phloem sap in grafted *Citrus reticulata*. *PLoS One* 15, e0227192. doi: 10.1371/journal.pone.0227192

Wang, M., Chen, Y., Li, S., Yu, J. J., Yang, L., and Hong, L. (2024). Widely targeted metabolomic analysis provides new insights into the effect of rootstocks on citrus fruit quality. *Metabolites* 14, 242. doi: 10.3390/metabo14040242

Wu, W., Zeng, J. W., Zhu, C. Y., Zhang, R. M., and Huang, Y. J. (2021). Comparison of different rootstocks for orah and introduction performance of orah in Guangdong. *Guangdong Agric. Sci.* 48, 9. doi: 10.16768/j.issn.1004-874X.2021.11.005

Zandalinas, S. I., Sales, C., Beltrán, J., Gómez-Cadenas, A., and Arbona, V. (2017). Activation of secondary metabolism in citrus plants is associated to sensitivity to combined drought and high temperatures. *Front. Plant Sci.* 7. doi: 10.3389/fpls.2016.01954

Zhang, X., Breksa, A. P., Mishchuk, D. O., and Slupsky, C. M. (2011). Elevation, rootstock, and soil depth affect the nutritional quality of mandarin oranges. *J. Agr. Food Chem.* 59, 2672–2679. doi: 10.1021/jf104335z

Zhang, X. X., Li, Z. Y., Ma, Y. L., and Ma, S. C. (2015). Progress in research of traditional Chinese medicine Citrus aurantium. *China J. Chin. Mater. Med.* 40, 185–190. doi: 10.4268/cjcmm20150205

Zhu, C., Zhou, X., Long, C., Du, Y. X., Li, J. X., Yue, J. Q., et al. (2020). Variations of flavonoid composition and antioxidant properties among different cultivars, fruit tissues and developmental stages of citrus fruits. *Chem. Biodiver* 17, e1900690. doi: 10.1021/jf990916t

10.3389/fpls.2024.1382768

Appendix A

H Red orange *Citrus reticulata* Blanco cv. Red tangerine

X Ziyang xiangcheng (*Citrus junos* Sieb. ex Tanaka)

Z Trifoliate orange (*Poncirus trifoliata* L. Raf)

ZC Carrizo citrange (*Citrus.sinensis* Osb.×*P.trifoliate* Raf)

HP The peel of 'Orah' grafted on Red orange *Citrus reticulata* Blanco cv. Red tangerine

HR The pulp of 'Orah' grafted on Red orange *Citrus reticulata* Blanco cv. Red tangerine

XP The peel of 'Orah' grafted on Ziyang xiangcheng *Citrus junos* Sieb. ex Tanaka

XR The pulp of 'Orah' grafted on Ziyang xiangcheng *Citrus junos* Sieb. ex Tanaka

ZP The peel of 'Orah' grafted on Trifoliate orange *Poncirus trifoliata* L. Raf

ZR The pulp of 'Orah' grafted on Trifoliate orange *Poncirus trifoliata* L. Raf

ZCP The peel of 'Orah' grafted on Carrizo citrange *Citrus.sinensis* Osb.×*P.trifoliate* Raf

ZCR The pulp of 'Orah' grafted on Carrizo citrange *Citrus.sinensis* Osb.×*P.trifoliate* Raf

90d Fruit at 90d after flowering

120d Fruit at 120d after flowering

150d Fruit at 150d after flowering.

180d Fruit at 180d after flowering

210d Fruit at 210d after flowering

240d Fruit at 240d after flowering

VC Vitamin C

RTT ratio of TSS to TA

Frontiers in Plant Science

Cultivates the science of plant biology and its applications

The most cited plant science journal, which advances our understanding of plant biology for sustainable food security, functional ecosystems and human health.

Discover the latest Research Topics

See more →

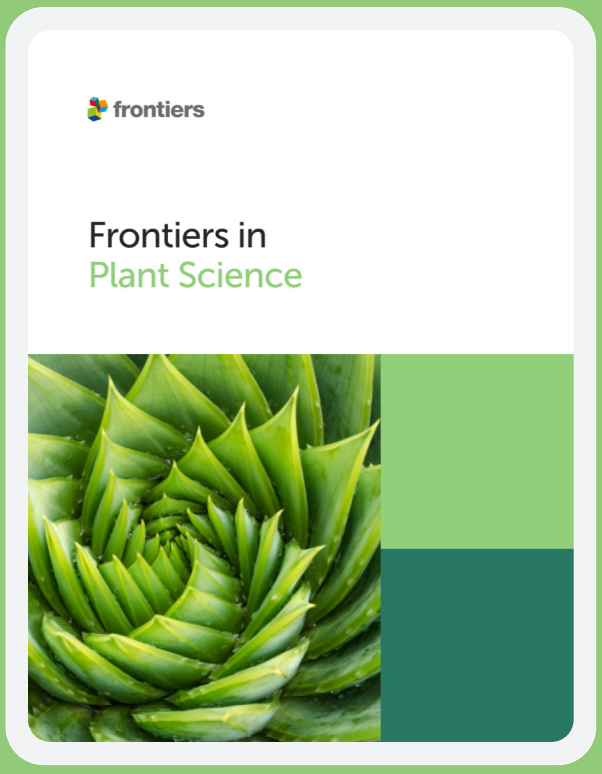

Frontiers

Avenue du Tribunal-Fédéral 34
1005 Lausanne, Switzerland
frontiersin.org

Contact us

+41 (0)21 510 17 00
frontiersin.org/about/contact